Oxidative Medicine and Cellular Longevity

# Oxidative Stress and Vascular Dysfunction in Myocardial Ischemia

Lead Guest Editor: Aleksandar Kibel
Guest Editors: Tatjana Bačun and Mallika Ghosh

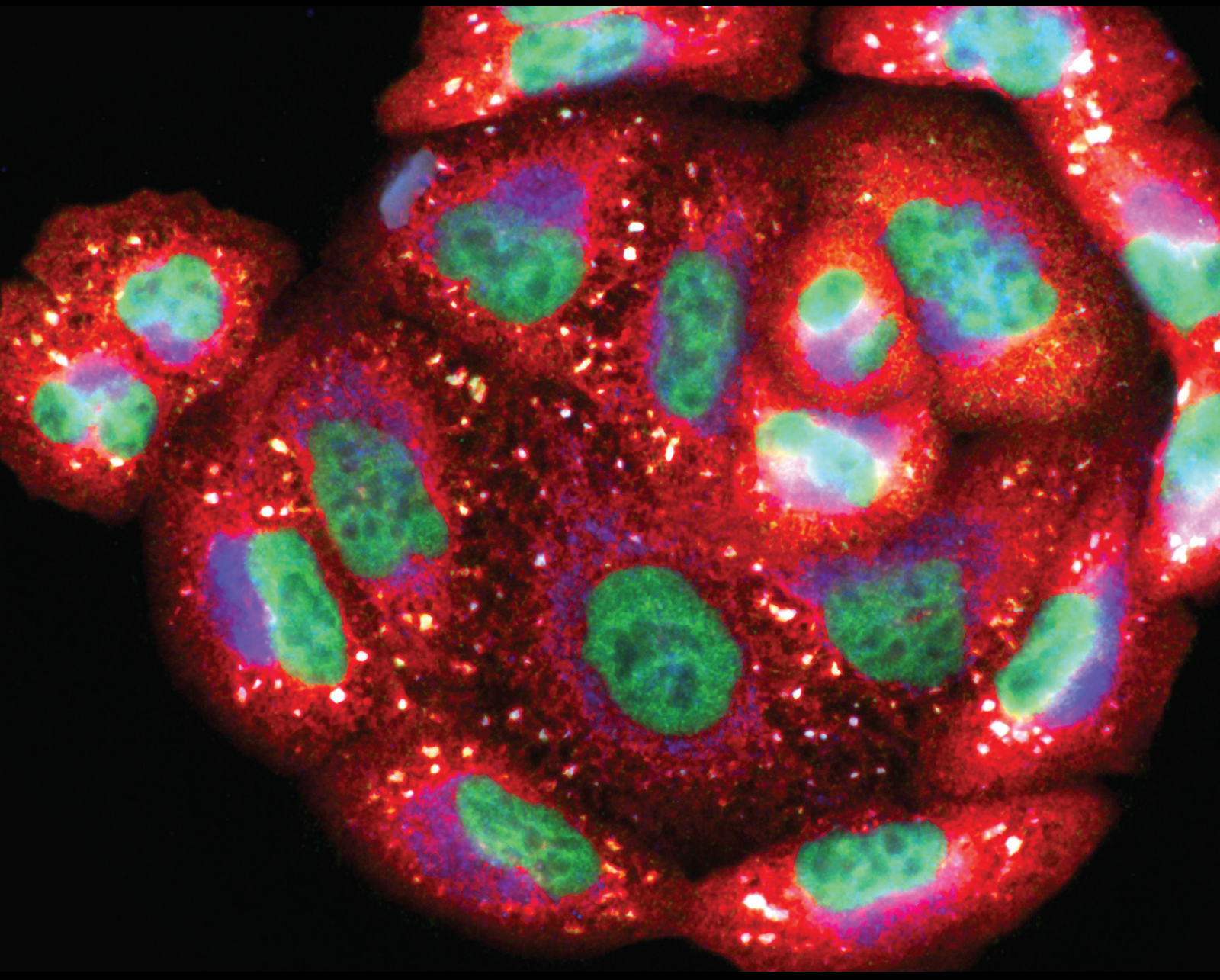

# Oxidative Stress and Vascular Dysfunction in Myocardial Ischemia

Oxidative Medicine and Cellular Longevity

# Oxidative Stress and Vascular Dysfunction in Myocardial Ischemia

Lead Guest Editor: Aleksandar Kibel
Guest Editors: Tatjana Bačun and Mallika Ghosh

# Contents

**Inhibitor 1 of Protein Phosphatase 1 Regulates $Ca^{2+}$/Calmodulin-Dependent Protein Kinase II to Alleviate Oxidative Stress in Hypoxia-Reoxygenation Injury of Cardiomyocytes**
Huiqin Luo, Shu Song, Yun Chen, Mengting Xu, Linlin Sun, Guoliang Meng, and Wei Zhang
Research Article (19 pages), Article ID 2193019, Volume 2019 (2019)

**Plin5/p-Plin5 Guards Diabetic CMECs by Regulating FFAs Metabolism Bidirectionally**
Jin Du, Juanni Hou, Juan Feng, Hong Zhou, Heng Zhao, Dachun Yang, De Li, Yongjian Yang, and Haifeng Pei
Research Article (15 pages), Article ID 8690746, Volume 2019 (2019)

Hindawi
Oxidative Medicine and Cellular Longevity
Volume 2022, Article ID 9891489, 2 pages
https://doi.org/10.1155/2022/9891489

*Corrigendum*

# Corrigendum to "Vanillic Acid Alleviates Acute Myocardial Hypoxia/Reoxygenation Injury by Inhibiting Oxidative Stress"

**Xiuya Yao,[1,2] Shoufeng Jiao,[3] Mingming Qin,[1] Wenfeng Hu,[1] Bo Yi,[4] and Dan Liu[1]**

[1]*Jiangxi Provincial Key Laboratory of Basic Pharmacology, Nanchang University, School of Pharmaceutical Science, Nanchang 330006, China*
[2]*Department of Pharmacy, Changzhou Maternal and Child Health Care Hospital, Changzhou 213000, China*
[3]*Department of Pharmacy, The First Affiliated Hospital of Nanchang University, Nanchang 330006, China*
[4]*Second Abdominal Surgery Department, Jiangxi Province Tumor Hospital, Nanchang 330029, China*

Correspondence should be addressed to Bo Yi; yibo790508@163.com and Dan Liu; liudan1201jx@163.com

Received 5 January 2022; Accepted 5 January 2022; Published 27 January 2022



In the article titled "Vanillic Acid Alleviates Acute Myocardial Hypoxia/Reoxygenation Injury by Inhibiting Oxidative Stress" [1], there was an error in Figure 8, where the VA+NC+H/R panel was duplicated as the VA+H/R panel.

The corrected figure with the correct VA+H/R panel is shown in Figure 8.

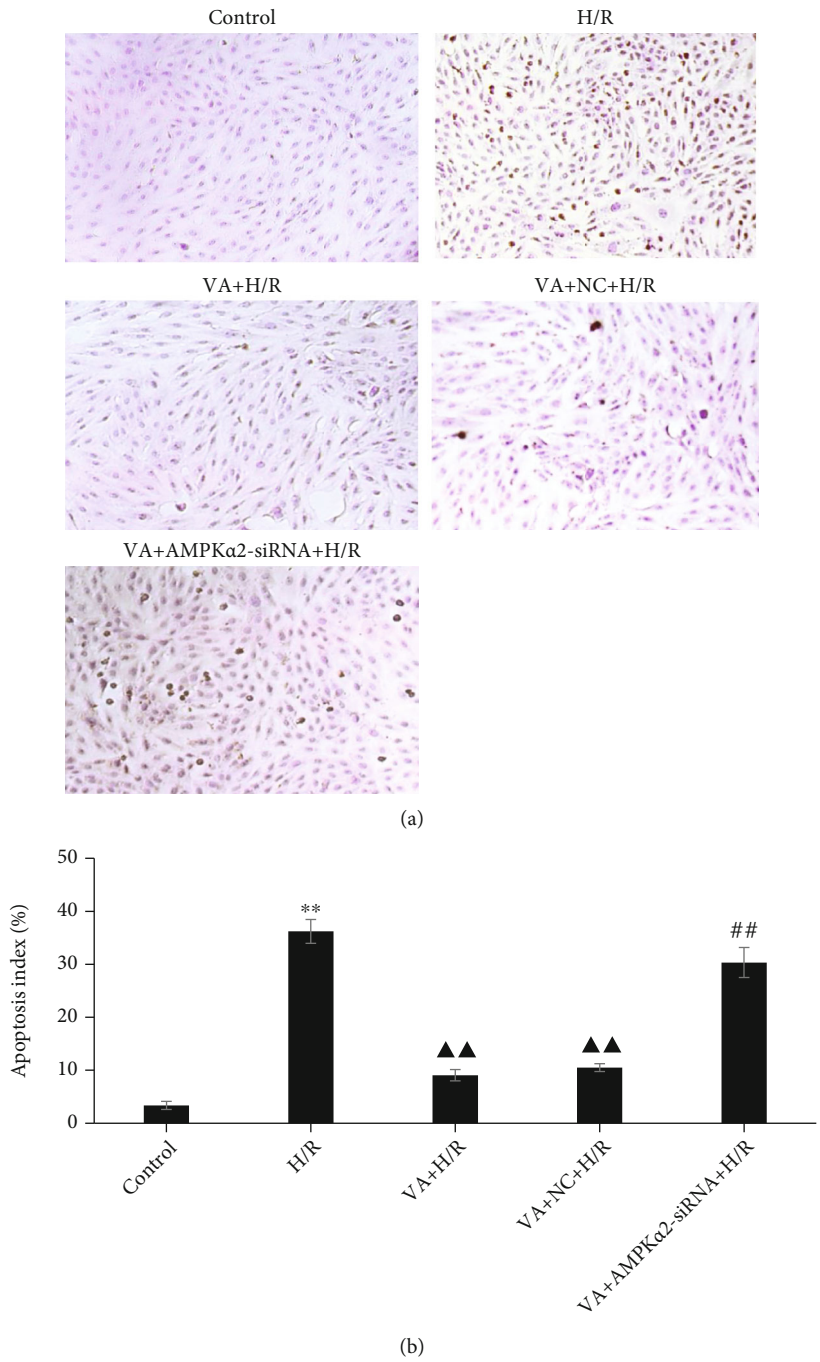


Figure 8: Vanillic acid (VA) pretreatment inhibits apoptosis in H9c2 cells exposed to hypoxia/reoxygenation (H/R), while AMPK$\alpha$2-siRNA abrogates this effect. (a) H9c2 cells were sectioned and analysed for apoptosis using TUNEL staining. The panels show representative histological images. (b) The number of apoptotic cells evaluated by TUNEL is expressed as a percentage. Data are expressed as the mean $\pm$ SEM, $n = 3$. $^{**}p < 0.01$ vs. control group; $^{\blacktriangle\blacktriangle}p < 0.01$ vs. H/R group; $^{\#\#}p < 0.01$ vs. VA+H/R group.

## References

[1] X. Yao, S. Jiao, M. Qin, W. Hu, B. Yi, and D. Liu, "Vanillic Acid Alleviates Acute Myocardial Hypoxia/Reoxygenation Injury by Inhibiting Oxidative Stress," *Oxidative Medicine and Cellular Longevity*, vol. 2020, Article ID 8348035, 12 pages, 2020.

Hindawi
Oxidative Medicine and Cellular Longevity
Volume 2020, Article ID 6627144, 30 pages
https://doi.org/10.1155/2020/6627144

*Review Article*

# Oxidative Stress in Ischemic Heart Disease

**Aleksandar Kibel**,[1,2] **Ana Marija Lukinac**,[3,4] **Vedran Dambic**,[4,5] **Iva Juric**,[1,6] **and Kristina Selthofer-Relatic**[1,6]

[1]*Department for Heart and Vascular Diseases, Osijek University Hospital, Osijek, Croatia*
[2]*Department of Physiology and Immunology, Faculty of Medicine, University J.J. Strossmayer in Osijek, Osijek, Croatia*
[3]*Department of Rheumatology and Clinical Immunology, Osijek University Hospital, Osijek, Croatia*
[4]*Faculty of Medicine, University J.J. Strossmayer in Osijek, Osijek, Croatia*
[5]*Department for Emergency Medical Services of the Osijek-Baranja county, Osijek, Croatia*
[6]*Department of Internal Medicine, Faculty of Medicine, University J.J. Strossmayer in Osijek, Osijek, Croatia*

Correspondence should be addressed to Aleksandar Kibel; aleksandar_mf@yahoo.com

Received 19 November 2020; Revised 27 November 2020; Accepted 7 December 2020; Published 29 December 2020

Academic Editor: Andreas Daiber



One of the novel interesting topics in the study of cardiovascular disease is the role of the oxidation system, since inflammation and oxidative stress are known to lead to cardiovascular diseases, their progression and complications. During decades of research, many complex interactions between agents of oxidative stress, oxidation, and antioxidant systems have been elucidated, and numerous important pathophysiological links to na number of disorders and diseases have been established. This review article will present the most relevant knowledge linking oxidative stress to vascular dysfunction and disease. The review will focus on the role of oxidative stress in endotheleial dysfunction, atherosclerosis, and other pathogenetic processes and mechanisms that contribute to the development of ischemic heart disease.

## 1. Introduction

Atherosclerosis is the most common form of large vessel pathology responsible for syndromes of vital organ ischemic damage like myocardial infarction [1].

The key pathophysiologic process of atherosclerosis is chronic inflammation, where oxidative stress plays an essential role in vascular homeostasis regulation including endothelial and smooth muscle cell growth, proliferation, and migration; angiogenesis; apoptosis; vascular tone; host defenses; and genomic stability. Imbalance in the oxidant/antioxidant mechanisms leads to oxidative stress and uncontrolled vascular injury [2–4].

The relation between heart failure and vascular disease is also marked by oxidative stress, caused by ischemia, left ventricular (LV) dysfunction, and neuroendocrinological activation. Reactive oxygen species (ROS) negatively affect myocardial calcium handling, cause arrhythmias, and contribute to cardiac remodeling by inducing hypertrophic signaling, apoptosis, and necrosis. Neurohumoral activation via the renin-angiotensin-aldosterone system (RAAS) and the sympathetic nervous system (SNS), combined with increased pre- and after-load, impose additional myocardial oxidative stress [5].

Ageing, traditional cardiovascular risk factors (arterial hypertension, dyslipidemia, diabetes mellitus and smoking), genetic predisposition, and environmental factors increase ROS generation and decrease endothelial nitric oxide (NO) production. Additional factors like mechanic vascular properties and geometry, hemodynamic forces, and endothelial gene regulation by biomechanical forces (atheroprone and atheroprotective phenotypes), disturbed flow in vascular regions like arches, branches, and bifurcations can promote vascular injury, ROS activity, coronary atherosclerosis, and ischemic heart failure development [6, 7]. The gut microbiota is involved in mediating metabolic processes associated with risk factors for coronary artery disease such as obesity, dyslipidemia, diabetes mellitus, and dyslipidemia. These

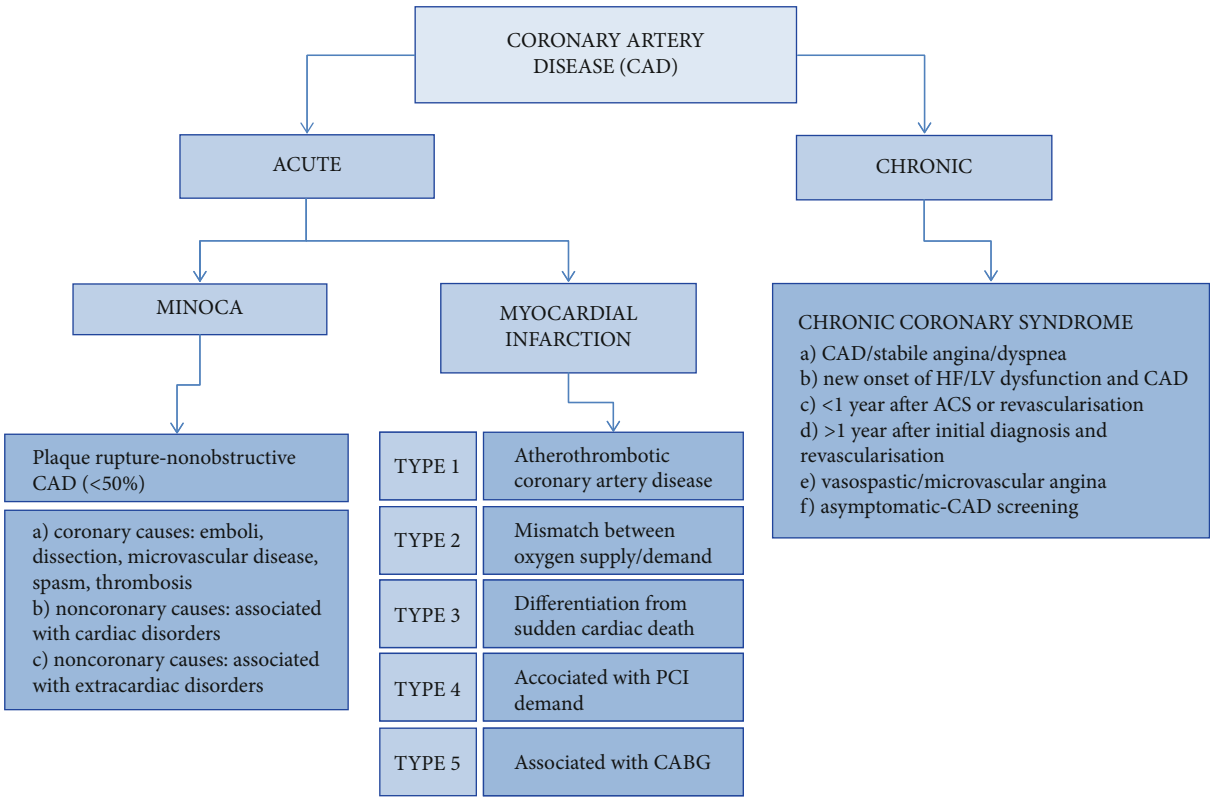


Figure 1: Acute and chronic coronary syndrome definitions and classification [14, 17].

comorbidities via its metabolites can induce development of atheroslerosis and aterosclerotic coronary artery disease. The main pathways for these processes are provided via oxidative stress, inflammation, cholesterol, and uric acid metabolism [8, 9].

The current therapeutic approach for atherosclerotic vascular plaque stabilization and disease includes RAAS inhibitors, statins, and acetylsalicylic acid, because of their pleiotropic antioxidative effects [10–12]. There is a need to elucidate oxidative stress physiology and pathophysiology, to identify novel therapeutic modalities for selective oxidative stress targeting in atherosclerosis [4].

## 2. Ischemic Heart Disease

Myocardial infarction (MI) is defined by clinical presentation, new ischemic electrocardiogram changes, and cardiac biomarkers elevation. The cause of MI is acute myocardial injury. Prolonged ischemia (a restriction in tissue blood supply, causing a deficiency of oxygen) can lead to myocardial necrosis and cell death. According to the Fourth Universal Definition of Myocardial Infarction 2018, MI can be divided into five categories (Figure 1).

MI type 1—caused by atherothrombotic coronary artery disease (CAD) and usually precipitated by atherosclerotic plaque disruption (rupture or erosion)

MI type 2—result of a mismatch between oxygen supply and demand: (a) reduced myocardial perfusion—coronary artery spasm, microvascular dysfunction, coronary embolism, coronary artery dissection, sustained bradyarrhythmia, hypotension or shock, respiratory failure, and severe anemia; (b) increased myocardial oxygen demand—sustained tachyarrhythmia and severe hypertension with or without LV hypertrophy

MI type 3—differentiation from sudden cardiac death

MI type 4—associated with percutaneous coronary intervention (PCI)

MI type 5—associated with coronary artery bypass grafting [7]

MINOCA (myocardial infarction with nonobstructive coronary arteries) can cause MI presenting with typical symptoms for acute coronary syndrome (ACS) and ST-segment elevation or equivalent. The underlying cause of disease may be nonobstructive (<50%) coronary artery disease stenosis, or mismatch between oxygen supply and demand, or secondary to myocardial disorders without involvement of the coronary arteries as myocarditis or Takotsubo syndrome [13].

Coronary artery disease (CAD) is a chronic, mostly progressive pathological process with predominant serious prognosis. This process can be modified by conservative and invasive treatment to achieve disease stabilization or regression [14]. Other cardiac conditions that are related to secondary myocardial injury are heart failure, myocarditis, any type of cardiomyopathy, Takotsubo syndrome, coronary revascularization procedure, cardiac procedure other than revascularization, catheter ablation, defibrillator shocks, cardiac contusion, systemic conditions, sepsis, infectious disease, chronic kidney disease, stroke, subarachnoid hemorrhage, pulmonary embolism, pulmonary hypertension,

infiltrative diseases, amyloidosis, sarcoidosis, chemotherapeutic agents, critically ill patients, and strenuous exercise [15].

The leading symptom that initiates the diagnostic and therapeutic cascade in patients with suspected ACS is chest pain. Two groups of patients should be differentiated based on the electrocardiogram (ECG): those with persistent ST-segment elevation and those without persistent ST-segment elevation (transient ST-segment elevation, persistent or transient ST-segment depression, T wave inversion, flat T waves or pseudonormalization of T waves, or with normal ECG). The pathological finding at the myocardial level is cardiomyocyte necrosis or myocardial ischemia without cell loss [16].

Criteria for type 1 MI and type 2 MI detection are rise and/or fall of upper reference limit (URL) values with at least one value above the 99th percentile URL, with at least one of the following criteria: acute myocardial ischemia symptoms, new ischemic ECG changes, pathological Q wave development, and imaging evidence of new loss of viable myocardium or new regional wall motion abnormality in a pattern consistent with an ischemic etiology. For type 1 MI identification of a coronary thrombus by angiography including intracoronary imaging or by autopsy is needed as a one of the criteria, while evidence of an imbalance between myocardial oxygen supply and demand unrelated to acute coronary atherothrombosis for type 2 MI is a part of key definition [15].

The dynamic nature of the CAD results in various clinical presentations, which can be categorized as acute and chronic coronary syndromes. The diagnostic approach and management for patients with dyspnea and suspected ACS include assessment of symptoms and signs of disease, evaluation of the patient's general condition and quality of life, comorbidities evaluation, basic testing and assessment of LV function, risk assessment of obstructive CAD, diagnostic testing for CAD, and further event risk determination and treatment [14].

Management—including diagnosis and treatment—of acute ACS starts from the point of first medical contact. Out- and in-hospital treatment in acute setting is obligatory: relief of pain, breathlessness, and anxiety; arrhythmia management; reperfusion with PCI alone or/with fibrinolysis strategy, and periprocedural pharmacologic and nonpharmacologic therapy in a coronary unit [13].

Long-term management following acute treatment includes life style intervention, risk factor control, blood pressure and dyslipidemia treatment, glucose lowering therapy, antithrombotic therapy in acute and long-term settings, possible heart failure treatment, and arrhythmia management. Cardiac rehabilitation should be recommended [13].

CAD is a chronic, progressive disease with a predominantly serious prognosis. The outcome of MINOCA strongly depends on the underlying cause, and its overall prognosis is serious, with a 1-year mortality of about 3.5% [13, 14].

## 3. Endothelial Dysfunction and Oxidative Stress

Endothelial dysfunction caused by oxidative stress is an early event in the pathogenesis of many cardiovascular diseases including atherosclerosis, dyslipidemia, hypertension, diabetes, chronic kidney disease, heart failure, and ischaemia/reperfusion injury [18–23], and it is a hallmark of vascular diseases. An imbalance between NO bioavailability and ROS, also called oxidative stress, promotes endothelial dysfunction [24, 25] which is characterized by an altered modulation of vasomotor tone and vascular growth, impaired anti-inflammatory and antithrombotic endothelial characteristics, and disturbances of vascular remodeling [26].

The endothelium is a simple squamous layer of cells that forms an interface between the circulating blood and the vascular wall. A healthy endothelium provides endothelium-dependent vasorelaxation in response to vascular stress, controls vascular permeability, and prevents platelet aggregation [27]. It is very reactive to mechanical stimuli, chemical factors, and humoral agents by producing several mediators, such as NO, to maintain vasomotor tone and structural integrity. NO has a major role in endogenous antioxidant defense because of its potent vasodilatory, anti-inflammatory, and antithrombotic characteristics [28, 29]. Most of the vascular NO is produced by endothelial nitric oxide synthase (eNOS), a cytochrome p450 reductase-like enzyme which uses tetrahydrobiopterin to form NO from *L*-arginine [19]. The main causes of reduced NO bioavailability include increased NO degradation caused by ROS, decreased expression of eNOS, deficiency of substrates or cofactors for eNOS, and an inappropriate activation of eNOS caused by impaired cellular signaling [19, 30, 31]. Also, previous studies examined the phenomenon called eNOS uncoupling, causing reduced NO bioavailability by eNOS switching its enzymatic activity to generate superoxide ($O_2^-$) and $H_2O_2$ instead of NO [32, 33]. This occurs, for example, in the absence of NOS substrate *L*-arginine or the cofactor tetrahydrobiopterin in that process [34, 35]. Besides eNOS, which is mostly expressed in endothelial cells, there are two more isoforms of NO synthase with other functions—neuronal NOS (nNOS) and inducible NOS (iNOS) [36], which can also be a subject to uncoupling [33].

ROS are the products of the normal cellular aerobic metabolism generated during the reduction of oxygen [19]. ROS include unstable free radicals such as superoxide anion ($O_2^-$), hydroxyl radical or lipid radicals, and nonfree radicals such as hydrogen peroxide ($H_2O_2$), hypoclorous acid, or peroxynitrite which also have oxidizing effects that contribute to oxidative stress [19]. At moderate concentrations, ROS exert some physiological roles such as signaling [19, 37], but increased production of ROS which exceeds endogenous antioxidant defense mechanisms causes oxidizing of DNA, proteins, carbohydrates, lipids, and other biological macromolecules, leading to oxidative stress [6]. Enzymatic sources of ROS that are important in the cardiovascular system are NADPH (reduced form of nicotinamide adenine dinucleotide phosphate) oxidase, xanthine oxidase, and uncoupled eNOS with an addition of the mitochondrial electron transport chain, cyclooxygenase, and lipoxygenase as additional possible sources [6, 19, 32, 37]. Furthermore, production of ROS may be enhanced by free radical chain reactions. Several studies showed a very important role of NADPH oxidase, including Nox family oxidases Nox1, Nox2, Nox4, and Nox5, in endothelial dysfunction [19, 32]. NADPH oxidase

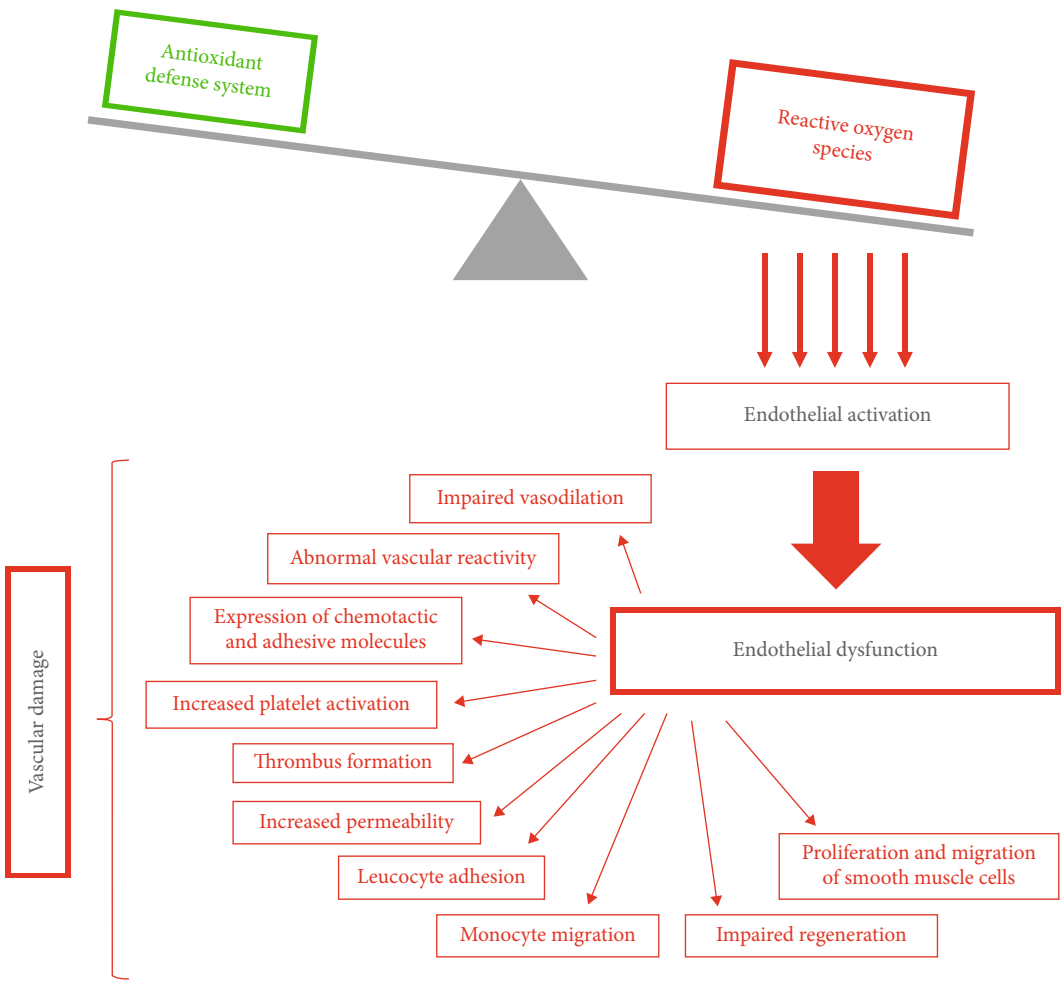


Figure 2: Endothelial dysfunction and development of vascular damage.

is an enzyme located in the membrane of endothelial cells, smooth muscle cells, and fibroblasts, and it is the most powerful source of $O_2^-$ production [38]. Angiotensin II, thrombin, platelet-derived growth factor, tumor growth factor-$\alpha$, and lactosylceramide upregulate this enzyme and cause excessive ROS production [19]. Previous studies regarding angiotensin II-induced hypertension, diabetes mellitus, and hypercholesterolemia demonstrated the important impact of NADPH oxidase [23, 38, 39]. Xanthine oxidase is an enzyme that has a role in oxidation of hypoxanthine and xanthine in the metabolism of purines, leading to production of $O_2^-$ and $H_2O_2$. The activity and expression of this enzyme are increased by interferon-$\gamma$ [19]. The role of xanthine oxidase in ROS production in hypertension and hypercholesterolemia has been discovered in previous research [40–42]. As mentioned before, all three isoforms of NOS can be a source of ROS when uncoupling occurs, and NOS starts producing $O_2^-$ and $H_2O_2$ instead of NO, but uncoupled eNOS products play a critical role in the pathogenetic processes of cardiovascular diseases [33]. This was shown in previous studies regarding hypertension, hypercholesterolemia, smoking, and diabetes mellitus [6, 43, 44]. Mitochondrial oxidative phosphorylation normally produces physiological levels of superoxide, which is converted to hydrogen peroxide and afterwards to water. Mitochondrial oxidative stress can be a consequence of excessive ROS production or insufficient ROS detoxification [39].

Excessive ROS production exceeding antioxidant defense systems leads to endothelial oxidative stress. The first step of endothelial dysfunction is called endothelial activation, which represents the expression of abnormal prothrombotic and proinflammatory characteristics of the endothelial cells, leading to other chronic changes [45]. Endothelial dysfunction includes impaired endothelium-mediated vasodilation; abnormal vascular reactivity and vasospasm; greater expression of chemotactic and adhesive molecules; increased platelet activation and thrombus formation; increased permeability of endothelium, leucocyte adhesion, and monocyte migration into the vascular wall; and impaired regeneration of endothelial cells with proliferation and migration of smooth muscle cells, leading to vascular damage [32, 46] (Figure 2).

Many studies have demonstrated an important role of oxidative stress in endothelial dysfunction under the conditions of excessive oxidative stress. Cardiovascular risk factors cause imbalances between NO and ROS, so prevention of

endothelial dysfunction by reducing oxidative stress and enhancement of endothelial NO production is seen as a reasonable therapeutic strategy in cardiovascular diseases [6, 46].

## 4. Oxidative Stress in Atherosclerosis

Atherosclerosis is a multisystemic, progressive, chronic inflammatory disease characterized by the interaction of immune and endothelial cells that is mediated by adhesion molecules on the surface of the vascular endothelium leading to the release of numerous proinflammatory mediators [47]. Specifically, it has been demonstrated that there is a close interaction between vascular endothelial inflammation and intense oxidative stress in triggering the atherosclerotic process [48].

The imbalance between the generation of excess reactive oxygen species (ROS) and the antioxidant mechanism leads to increased oxidative stress resulting in the formation of atherogenic oxidized low-density lipoprotein (Ox-LDL) which is a major determinant of atherogenesis [49].

Production of ROS from various sources (xanthine oxidase, lipoxygenase, nicotinamide adenine dinucleotide phosphate oxidase, eNOS, nNOs, and iNOS) leads to damage to mitochondrial capacity and to the development of mitochondrial dysfunction [50]. Free fatty acids in endothelial cells enter the tricarboxylic acid cycle during which oxidation results in the overformation of NADH, which is an important driver of ROS during oxidative phosphorylation [51]. Mitochondrial dysfunction leads to increased ROS formation and oxidative stress and thus plays a role in the initiation, formation, and progression of an atherosclerotic lesion [51].

Studies have shown that increasing ROS production in mitochondria is induced by age, obesity, smoking, hypertension, diabetes, and dyslipidemia [52]. Numerous studies have found that mitochondrial dysfunction significantly affects the regulation of inflammation, proliferation, and apoptosis in the onset and progression of atherosclerotic plaques [53–57].

During the atherosclerotic process, the accumulated neutrophils produced an additional amount of ROS [58]. ROS enhance the activation of poly (ADPribose) polymerase 1 (PARP1), which damages mtDNA and thus the mitochondrial transport chain, further enhancing ROS formation and further damaging endothelial cells [59]. The resulting ROS trigger the synthesis of inflammatory cytokines by different cellular pathways resulting in vascular inflammation and participating in the oxidation process of LDL [58]. Ox-LDL has a cytotoxic effect on vascular cells, and macrophage removal receptors can phagocytose them, forming foaming cells that deposit in the blood vessel wall forming an atherosclerotic plaque [60]. Ox-LDL exerts its various effects on cells such as endothelial cells, macrophages, platelets, fibroblasts, and smooth muscle cells through transmembrane glycoproteins such as SR-A, CD36, and LOX-1 [61]. The resulting Ox-LDL increases the NADPH oxidase activity, leading to an increase in ROS synthesis and to NO inactivation. It also causes eNOS dysfunction by displacing it from the alveolar membrane site and enhances the arginase II activity thereby reducing the amount of *L*-arginine cosubstrate for eNOS resulting in an additional decrease in NO synthesis [62]. Ox-LDL increases the synthesis of matrix metalloproteinases (MMP), namely MMP-1, MMP-3, and MMP-9, leading to a breakdown of the fibrotic cap and to a consequent rupture of the atherosclerotic plaque. LOX-1 is expressed on macrophages, vascular endothelial smooth muscle cells, cardiomyocytes, platelets, and fibroblasts. The binding of Ox-LDL to LOX-1 in macrophages and vascular smooth muscle cells results in the formation of foam cells [63]. The main inducers of the LOX-1 expression are tumor necrosis factor-alpha (TNF-$\alpha$), interleukin-1 (IL-1), interferon-gamma (IFN-$\gamma$), CRP, and modified lipoproteins such as glyxidized LDL, lysophosphatidylcholine, and ROS, while the mediators and conditions regulating the gene expression are numerous: angiotensin II, cytokines, glycation end products, diabetes mellitus, hypertension, dyslipidemia, ischemia reperfusion injury (IRI), heart failure, psychological stress, and HIV infection [61]. TNF-$\alpha$ and NF-kB increase $Ca^{2+}$ levels in the mitochondria and consequently increase ROS production. SR-A and CD36 take up 75% to 90% of LDL [64]. SR-A is expressed in the presence of oxidative stress and growth factors in endothelial and smooth muscle cells, while normally found only in myeloid cells [65]. CD36 is found on monocytes, macrophages, platelets, and adipocytes [63]. Human macrophages lacking CD36 have a 40% reduction in Ox-LDL binding and uptake [66]. Toll-like receptors (TLRs) constitute a major subset of pattern recognition receptors (PRRs) that are significantly expressed on different immune cells during atherogenesis in the coronary circulation [67]. TLR signaling cascades can be activated by a wide range of endogenous ligands associated with tissue damage, which plays a central role in the development of atherosclerotic plaques [67]. The main culprits involved in the immune response to oxLDL are TLR4 [67]. Ox-LDL has been shown to lead to increase the expression of TLR4 in macrophages, neutrophils, and dendritic cells with which it plays an important role in the development of atherosclerotic plaques in the coronary circulation by activating MAPK and NF-$\kappa$B pathways [68, 69]. Activation of MAPK and NF-$\kappa$B transcription factors results in enhanced activation of genes encoding proinflammatory cytokines and chemokines important for the progression of the atherosclerotic process, including TNF-$\alpha$, IL-1, and Il-6 [67]. miR-590 has antiapoptotic effects on endothelial cells attacked by the atherosclerotic process by inactivating the TLR4/NF-$\kappa$B pathway, which may be a potential therapeutic target [70]. TLR4 is required for Ox-LDL-induced differentiation of macrophages into foam cells in the early stages of atherosclerosis [71]. It plays a crucial role in plaque progression and rupture leading to occlusive thrombus formation in human coronary arteries [72]. Specific Ox-LDL derivatives act as TLR4 ligands by enhancing the MMP-9 expression [73]. Also, minimally modified low-density lipoproteins (mmLDL) via CD14 and TLR4 induce actin polymerization which together with MMP-9 leads to remodeling of the coronary artery wall, resulting in instability of atherosclerotic plaques and their rupture [74]. Cellular fibronectin (cFN) is an extracellular matrix protein (ECM) that is overexpressed only in chronically inflamed tissues and is synthesized by vascular smooth muscle cells and endothelial cells [75]. cFN activates

macrophages and platelets via TLR4 resulting in platelet aggregation and arterial thrombosis within atherosclerotic lesions in the coronary arteries [75]. TLR2 activation stimulates VSMC migration from the intima in an IL-6-dependent manner, regulates inflammatory processes and ROS production after vascular injury, and contributes to coronary endothelial dysfunction after ischemic-reperfusion injury by activating neutrophils and creating ROS [67]. Ox-LDL can induce the expression of mRNAs of Wnt5a (Wnt family of glycoproteins) that are coexpressed with TLR2 and TLR4 and play a key role in the formation of foam cells, especially in advanced atherosclerotic plaques, which correlates with the severity of atherosclerotic lesions in human studies [76, 77]. TLR9 is expressed in the endoplasmic reticulum and not on cell surfaces such as TLR2 and TLR4 [67]. TLR9 is activated by CpG motifs in nucleic acids released during vascular necrosis and stimulates the transformation of macrophages into foam cells in a manner dependent on NF-$\kappa$B and IRF7 (interferon regulatory factor 7) and stimulates the secretion of INF and increases cytotoxic activity CD4 + T cell versus coronary artery smooth muscle cells [78].

VSMCs are important components of atherosclerotic plaques that, under the influence of biostimulation or mechanical damage triggered by oxidative stress, change their phenotype and, through differentiation, become synthetic VSMCs that produce significantly less contractile proteins, increase proliferation and migration, and thus participate in the development of atherosclerosis [79]. Increased concentrations of Ox-LDL via LOX-1 cause smooth muscle cell apoptosis as they increase the expression of a proapoptotic protein such as the bcl-2-associated X protein (Bax) leading to instability and rupture of the atherosclerotic plaque. In addition, through inducers, CD147 can cause plaque instability by releasing extracellular MMP [52].

Oxidative stress caused by the production of ROS and RNS (nitric oxide (NO), peroxynitrite (ONOO−)) and S-nitrosothiol (RSNO)) can damage macromolecules because it reacts with specific amino acid residues and DNA and chromatin cause mutations or double-stranded breaks in a phenomenon overall known as "oxidative damage" [80]. The selenoprotein family is involved in the control of oxidative stress in the cardiovascular system by inhibiting oxidative stress, modulating inflammation, suppressing endothelial dysfunction, and protecting vascular cells from apoptosis and calcification [81]. Potent selenoproteins of particular importance to the cardiovascular system are glutathione peroxidase (GPX), thioredoxin reductase 1 (TXNRD), methionine sulfoxide reductase B1 (MSRB1), selenoprotein P (SELENOP), selenoprotein S (SELENOS), and selenoprotein T (SELENOT) [81]. Dysfunction of various selenoproteins can lead to congestive heart failure, coronary heart disease, and to damaged heart structure and function [80]. The main catalytic site of selenoprotein is called Sec [80]. GPXs are the major components of the antioxidant system that maintain oxidative homeostasis, using glutathione as a cofactor for catalyzing the reduction of hydrogen peroxide (H2O2) and/or phospholipid hydroperoxide [80]. GPX3 controls vascular tone and the thrombotic properties of vascular endothelium [80]. TXNRD, along with thioredoxin (Trx) and NADPH, represents the major disulfide reduction system in the cell [82]. MSRB1 acts synergistically with GPX and TXNRD primarily in the liver, kidneys, and heart [80]. Selenoprteins P, S, and T predominantly contribute to calcium ion ($Ca^{2+}$) signaling, protein folding, and ER-related degradation [80]. SELENOS, SELENOK, SELENOM, SELENON, SELENOF, and SELENOT are involved in maintaining the homeostasis of oxidative stress in the ER of cardiac myocytes [80]. Studies have shown that decreased selenoprotein levels are associated with the increased Nrf2 expression which may represent an important compensatory response to the maintenance of homeostasis [83]. Selenoproteins play an important role in embryogenesis, since it was found that mice that had a genetic disorder of cytosolic TXNRD1, mitochondrial TXNRD2, and GPX4 experienced embryonic mortality [84].

Polyunsaturated fatty acids (PUFAs) exert anti-inflammatory, antiatherogenic, and antioxidant properties on the cardiovascular system [85–87]. These important effects are achieved by competing with arachidonic acid (AA) for enzymes involved in the biosynthesis of proinflammatory mediator molecules, by suppressing proinflammatory NF-$\kappa$B by modulating TLR4 signaling, by activating PPAR-$\gamma$, and FFA4 receptors (before GPR120 d) in macrophages and metabolites such as esolvins, maresins, and protectins that have anti-inflammatory and antioxidant effects [88, 89]. The most studied molecular mechanisms are the activation of Nrf2 in the vascular tissue, leading to the production of antioxidant enzymes (HO-1, GPx) and the activation of FFA4 receptors, resulting in the preservation of $\kappa$B inhibitors (I$\kappa$B) and the prevention of NF-$\kappa$B nuclear translocation [90–93]. F2-isoprostanes are prostaglandin-like molecules formed as a result of peroxidation of ROS-mediated esterified arachidonic acid [94]. n-3 PUFAs reduce 8-isoprostane levels in macrophages and reduce oxidative stress [88]. The peroxidation products of $\omega$-3 PUFAs and $\omega$-6 PUFAs can also have toxic effects in oxidative stress, and a diet rich in PUFAs can lead to tissue hypersensitivity to lipid peroxidation induced by oxidative stress [95, 96]. Therefore, in the future, it will be necessary to investigate individually each potential PUFA that has been shown to be an important protective factor in oxidative stress.

The most important antioxidants are glutathion peroxidase (Gpx), glutathion reductase, catalase, and superoxide dismutase [97]. Numerous studies have shown that efficient elimination of ROS from cells reduces the formation and progression of atherosclerotic plaques [98, 99]. The role of antioxidants on the progression of an atherosclerotic lesion needs to be further investigated as there are studies that confirm that certain antioxidants have no effect on the development of an atherosclerotic lesion [100]. A transcriptional coactivator that regulates a gene involved in energy metabolism in mitochondria called peroxisome proliferator-activated receptor gamma coactivator 1-alpha (PGC-1$\alpha$) which is an important mitochondrial protector that promotes the synthesis of NO enzymes, mitochondrial protein 2 (UCP-2), and the antioxidant defense of mitochondria (manganese SOD, catalase, and thioredoxin 2), and this way limits endothelial dysfunction [52, 101]. PGC-1$\alpha$ also reduces the activity of the inflammatory factors NF-$\kappa$B and

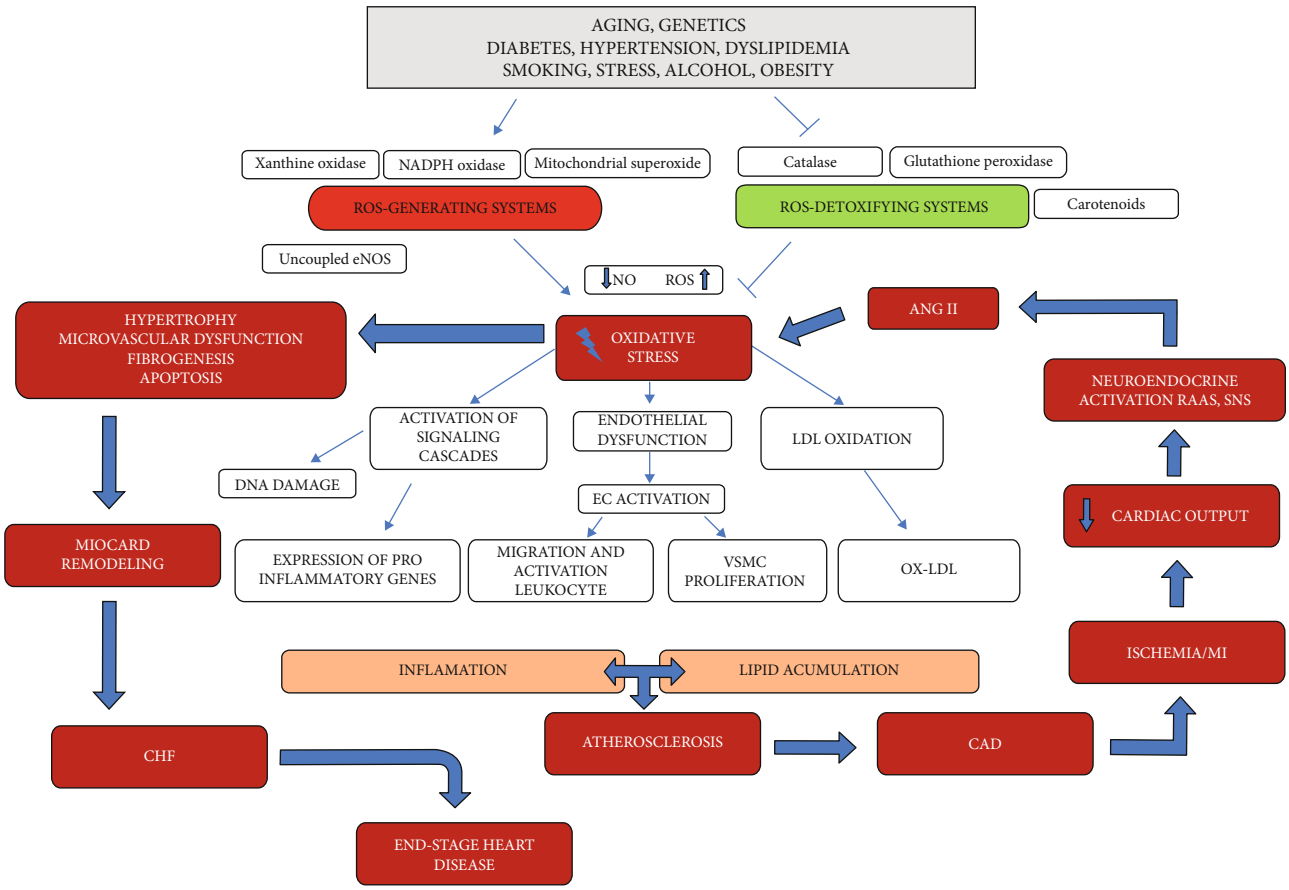


Figure 3: The role of oxidative stress in the onset of atherosclerosis and the pathophysiological implications of congestive heart failure. ANG II: angiotensin II; CAD: coronary artery disease; CHF: congestive heart failure; DNA: deoxyribonucleic acid; EC: endothelial cells; eNOS: endothelial nitric oxide synthase; LDL: low-density lipoprotein; MI: myocardial infarction; NO: nitric oxide; RAAS: renin–angiotensin–aldosterone system; ROS: reactive oxygen species; SNS: sympathetic nervous system; VSMC: vascular smooth muscle cells.

TNF-$\alpha$ and prevents the entry of Ox-LDL into cells [62, 102]. Twinkle mtDNA helicase plays a major role in stabilizing atheromatous plaques and reducing the development of atherosclerosis as it decreases apoptosis of VMSCs and macrophages [52]. Mitofusini 1 (Mfn1) is an important GTPase that regulates VMSC proliferation and apoptosis and acts as an important endogenous inhibitor of VSMC proliferation by inhibiting the Ras-Raf-ERK 1/2 pathway during the atherosclerotic process [103, 104]. Thus, prevention of vascular oxidative stress and improvement of NO production may be key future targets of new therapeutic strategies for the treatment of atherosclerosis [61]. Figure 3 summarizes the interactions of pathogenetic mechanisms linking oxidative stress to atherosclerosis, coronary artery disease, and consequently heart failure.

## 5. Oxidative Stress in Coronary Artery Disease

Dyslipidemia, as well as an imbalance between ROS production and enzymatic and nonenzymatic antioxidant protection systems, leads to endothelial dysfunction and atherosclerosis of the coronary arteries [1]. Numerous studies have shown impaired balance of prooxidants and antioxidants in patients with CAD [105–108]. Oxidative stress is today considered a new risk factor responsible for the development of CAD that affects the onset, prognosis, quality of life, and survival of patients [109].

In addition to being associated with atherosclerosis, oxidative stress can create oxidative modification or damage to lipid peroxidation at the level of deoxyribonucleic acids (DNA) and proteins with deleterious effects on the structure and function of the vascular system [110]. In addition to classical free oxygen radicals (superoxide radical (O2-), hydrogen peroxide (H2O2), hydroxyl (OH), peroxyl (RO), hydroperoxyl (HRO-)), reactive oxidative stress has also been shown to be involved in the oxidative stress process of nitrogen species (RNS), especially peroxynitrite (ONOO-) [111]. We know that ROS damages key molecules in signaling pathways involved in vascular inflammation, and it damages essential biomolecules in cells and participates in oxidative modification of lipids that make them atherogenic [112]. The most important sources of oxidative stress are the phagocytic isoform of NADPH oxidase (Nox2 and to a lesser extent Nox1) with its regulatory subunit p47phox, xanthine oxidase (XO), and dysregulated eNOS [113].

Common risk factors (hyperlipidemia, hyperglycemia, smoking, hypoxia, etc.) activate NADPH oxidase via different signaling pathways. It is now known that enhanced

release of reactive oxygen species (ROS) by NADPH oxidases and mitochondrial enzymes results in cardiomyocyte hypertrophy, fibrosis, and an increase in metalloproteinase. The most studied mechanism of NADPH activation is mediated by one of the mechanisms of the PKC$\alpha/\beta$2 signaling pathway in which protein kinase C plays a key role [114]. The p47phox subunit is the major Nox2 (gp91phox) regulatory subunit whose phosphorylation is required for Nox2 activation. The expression of p47phox was significantly increased in patients with CAD and overweight by about 60% and in obese patients with CAD by about 80%. So far, XO is known to be significantly elevated in CAD patients, and overweight is thought to be a potent driver of the enhanced XO expression [113].

In patients who have a BMI increase, suffer from CAD and will undergo CABG, increased ROS levels, increased expression of ROS-producing enzymes (P47phox, xanthine oxidase), decreased expression of antioxidant enzymes (mitochondrial aldehyde dehydrogenase, heme oxygenase-1, and eNOS), and increase in markers of inflammatory processes in serum and right atrial myocardial tissue (sVCAM-1 and CCL5/RANTES) have been demonstrated [115].

Endoplasmic reticulum stress (ERS) occurs in cardiac myocytes and cardiac tissue in response to various stressors, such as ischemia, hypoglycemia, hyperlipidemia, inflammation, and osmotic stress [116]. The resulting oxidative stress leads to changes in the redox status of the ER that interfere with the formation of protein disulfide and cause misfolding of the protein [116]. High cholesterol, fatty acids, and oxidative stress may induce ERS-induced apoptosis of macrophages and endothelial cells in atherosclerotic plaques [117]. ERS is associated with the development and progression of cardiac hypertrophy, ischemic heart disease, and heart failure [118]. The consequences of ERS are the accumulation of incorrectly posttranslationally modified secretory and transmembrane proteins that have important cellular functions [116]. During ERS, intracellular signaling pathways called *unfolded protein response* (UPR) are activated, restoring ER homeostasis, but if ERS persists chronically at high levels, terminal UPR activates cell apoptosis, which may be one of the important pathophysiological mechanisms for disease development [116]. Terminal UPR makes an important contribution to myocyte loss during myocardial infarction [119]. Also, it has been discovered that ER autophagy may be the last resort to restore ERS homeostasis [120]. There is also evidence that activation of UPR also activates Nrf2, which has been shown to be an important cardioprotective factor [121]. Improved understanding of the molecular mechanisms of regulated ERS in the future may lead to the discovery of new therapeutic targets [118].

ROS leads to the activation of the nuclear transcription factor kappa B (NF-$\kappa$B), which regulates key genes for the encoding of proinflammatory cytokines, chemokines, and leukocyte adhesion molecules. Two important transcription factors—nuclear factor erythroid 2-related factor 2 (Nrf2) and peroxisome proliferator-activated receptor-$\beta/\delta$ (PPAR$\beta/\delta$)—have been shown to protect coronary blood vessels from excessive exposure to oxidative stress. Oxidative stress and inflammation are thought to be major activators of these protective transcription factors [122]. Nrf2 stimulates genes for the synthesis of antioxidant and detoxifying enzymes and indirectly antagonizes the proinflammatory effects of NF-$\kappa$B by removing ROS [123–125]. PPAR$\beta/\delta$ is predominantly located in the heart and has cardioprotective effects by suppressing the activity of several transcription factors, including NF-$\kappa$B [126].

Bone marrow endothelial progenitor cells (EPCs) are responsible for neovascularization and reendothelialization after ischemia and/or tissue injury, and a decrease in EPC numbers and their function has been demonstrated in CAD patients [114, 127]. High levels of oxidative stress in CAD patients are thought to be closely related to the enhanced activation of NDPH oxidase mediated by the membrane component p47phox, which plays a major role in the regulation of the NADPH activity and thus reduced vascular capacity of EPCs in CAD patients [114]. Medications used today, such as AT blockers, ACE inhibitors, statins, and tazolidindiones, have a beneficial effect on the bioactivity of EPCs that maintain vascular homeostasis [2]. During oxidative stress, serum EPC levels drop significantly, suggesting that this may serve as a good biomarker of oxidative stress [128].

Cytotoxic products of the enzyme myeloperoxidase (MPO), such as hypochlorous acid, lead to oxidative damage to blood vessels. Human MPO is an important pathophysiological mediator and biomarker in CAD patients whose levels are significantly elevated, leading to the formation of dysfunctional lipoproteins with increased atherogenic potential, decreasing NO availability, weakening vasoreactivity, and leading to atherosclerotic plaque instability [129]. Malonyldialdehyde (MDA) is one of the last products of peroxidation of polyunsaturated fatty acids in cells whose levels increase significantly during oxidative stress. Therefore, the level of human MDA in blood plasma is a very important biomarker of ROS-induced lipid peroxidation [130]. In a study on 30 patients with angiographically defined CAD and 30 healthy control subjects, serum MDA levels were increased, although these values did not differ depending on the number of affected coronary vessels and were not correlated with the severity of vascular lesions [131]. The level of MDA and the percentage of MDA release were significantly elevated, while the level of glutathione (GSH), erythrocyte GPx activity, and total plasma antioxidant capacity (TAC) was significantly reduced in patients with acute coronary syndrome and with CAD, compared to healthy subjects ($n = 30$/group) [112]. The study thus found that in patients with CAD, there was a significant decrease in glutathione in erythrocytes and consequently elevated levels and increased release of MDA, confirming that the susceptibility of erythrocyte membranes to oxidative stress was significantly higher in patients with CAD than in healthy subjects. Also, the same study showed results in which the erythrocyte level and total antioxidant capacity (TAC) value were significantly lower compared to healthy controls [112].

Various study groups have reported significant decreases in the parameters of antioxidants in patients with CAD. It is important to emphasize that, according to current data, patients with multivessel coronary artery stenoses have significantly higher levels of MDA and significantly lower levels

of GSH, TAC, and GPx activity than patients with double and single coronary artery disease, which clearly leads to the conclusion that the greater the number of coronary artery stenoses, the higher the level of oxidative stress [112].

Abolhasani et al. conducted a study showing that the serum concentrations of high-sensitivity C-reactive protein (hs-CRP), sialic acid (SA), vitronectin (VN), plasminogen activator inhibitor-1 (PAI-1), Ox-LDL, and MDA were significantly elevated in patients with CAD relative to the healthy control group [132]. ROS-mediated lipid peroxidation leads to the formation of unsaturated aldehydes, including acrolein and MDA, which have toxic effects [112]. A study conducted by Yilmaz et al. showed that serum MDA was significantly higher, and TAC was significantly lower in CAD patients [133]. A study by Ninic et al. showed that the major lipid peroxidation product thiobarbiturate acid-reactive substances (TBARS) was significantly higher in patients with CAD than in the control group, while the antioxidant effect of many serum antioxidants was significantly lower [1]. TBARS leads to further formation of ROS and acts on proteins and DNA that exert proatherogenic and mutagenic effects [134]. Tumor necrosis factor-related apoptosis-inducing ligand (TRAIL) is a cytokine that acts as an apoptosis-inducing ligand, and research has shown that TRAIL levels are significantly reduced in animal CAD models, and that the unknown mechanism of TRAIL reduces oxidative stress and endothelial dysfunction [135].

Below, we present new insights into the numerous molecules, signaling pathways, and antioxidants involved in the highly complex development of oxidative stress in the coronary circulation. Iranian researchers have shown in a study that the increased expression of HSP27 mRNA in the peripheral blood mononuclear cell (PBMCs) is significantly associated with the severity of CAD and can serve as an important prognostic biomarker, indicating the degree of total oxidative stress [136]. A large study conducted by Khaper et al. showed that one week after acute myocardial infarction, the mRNA level for mitochondrial manganese superoxide dismutase (Mn SOD) decreased by 40% and after sixteen weeks by 73% compared with healthy subjects, an indicator of depleted antioxidant protection in patients with CAD [137].

In the animal model, the growth arrest-specific 5 (GAS5) overexpression in CAD rats has been shown to inhibit abnormal activation of the Wnt/$\beta$-catenin signaling pathway, leading to improvement of hyperlipidaemia, attenuation of myocardial injury, inhibition of cardiomyocyte apoptosis, and reduction of oxidative stress [138]. Decrease in leukocyte telomere length (TL) and mitochondrial DNA copy number (mtDNA-CN) are important indicators of the development of CAD, which are involved in the modulation of oxidative stress as independent risk factors, but this needs further investigation [139]. Polymorphisms in NRF2 and its target antioxidant genes: HMOX-1, NQO1, and MT significantly influence the level of oxidative stress in CAD formation [51, 140]. Inhibition of SAH hydrolase (SAHH) adenosine dialdehyde inhibitor in CAD patients leads to a significant increase in plasma S-adenosylhomocysteine (SAH) that promotes the production of free oxygen radicals and leads to endothelial dysfunction by epigenetic regulation of the oxidative stress pathway mediated by the p66shc gene promoter expression [141].

An antioxidant and an important component of the electron transport chain, coenzyme Q10 (CoQ10), has an effect on biomarkers of inflammation and oxidative stress, and the study found that CoQ10 significantly increased SOD and catalase (CAT) levels in CAD patients, significantly reduced MDA and dienes, and had significant effect on C-reactive protein (CRP), tumor necrosis factor-alpha (TNF-$\alpha$), interleukin-6 (IL-6), and GPx levels [142]. Supplementation with L-carnitine at a dose of 1000 mg/d after 12 weeks reduces oxidative stress (MDA level by 7%) and increases the activity of antioxidant enzymes (CAT by 16%, SOD by 47%, and GPx by 12%) in patients with CAD [143], while the administration of doses higher than 2000 mg/d showed a cardioprotective effect and reduced mortality rates in CAD patients [144].

Protein phosphatase and actin regulator 1 (PHACTR1), which regulates the reorganization of the actin cytoskeleton, is significantly expressed in atherosclerotic plaques of the coronary arteries. Inhibition of PHACTR1 synthesis led to a decrease in the Ox-LDL-induced expression of VCAM-1, ICAM-1, and VE-cadherin; attenuation of p47phox phosphorylation; and attenuation of the p65 and NF-$\kappa$B activity without affecting I$\kappa$B$\alpha$ and IKK$\alpha/\beta$ phosphorylation, all resulting in a decrease of intracellular oxidative stress [145].

Sirtuin 1 (SIRT1) is a protein that plays a role in mitochondrial biogenesis and deacetylation of proteins important for stimulating antioxidant defense. SIRT1 enhances the antioxidant enzyme activity and inhibits free radical-mediated oxidative injury by reducing NADPH oxidase activation, also reducing endothelial cell death caused by oxidative injury [146]. The main mechanism of its action is the inhibition of the LOX-1 expression by modulation of the LOX-1 promoter [147]. The SIRT1 expression level is suppressed, while the acetylated p53 expression levels are increased in monocytes of CAD patients. The mitochondrial function is significantly impaired in monocytes in patients with CAD, and it is thought that SIRT1 may increase the mitochondrial function. Also, a consequence of the decreased expression of SIRT1 is the increased adhesion of monocytes to endothelial cells [148].

We can conclude that oxidative stress plays a key role in the development and pathogenesis of CAD and the emergence of its complications [2]. By modulating very complex and numerous singular pathways and various biomolecules, oxidative stress can be reduced. In the future, there is a possibility and need to investigate more thoroughly all molecules involved in this highly complex biological process, which may open up new therapeutic targets and ultimately reduce the onset and complications of CAD.

## 6. Coronary Microvascular Dysfunction

Coronary microvascular dysfunction (CMD) is a disorder that leads to the development of myocardial ischemia, although there is no proven obstruction in coronary arteries on coronary angiography [149] (Figure 4). Risk factors that can trigger oxidative stress in coronary microvascular

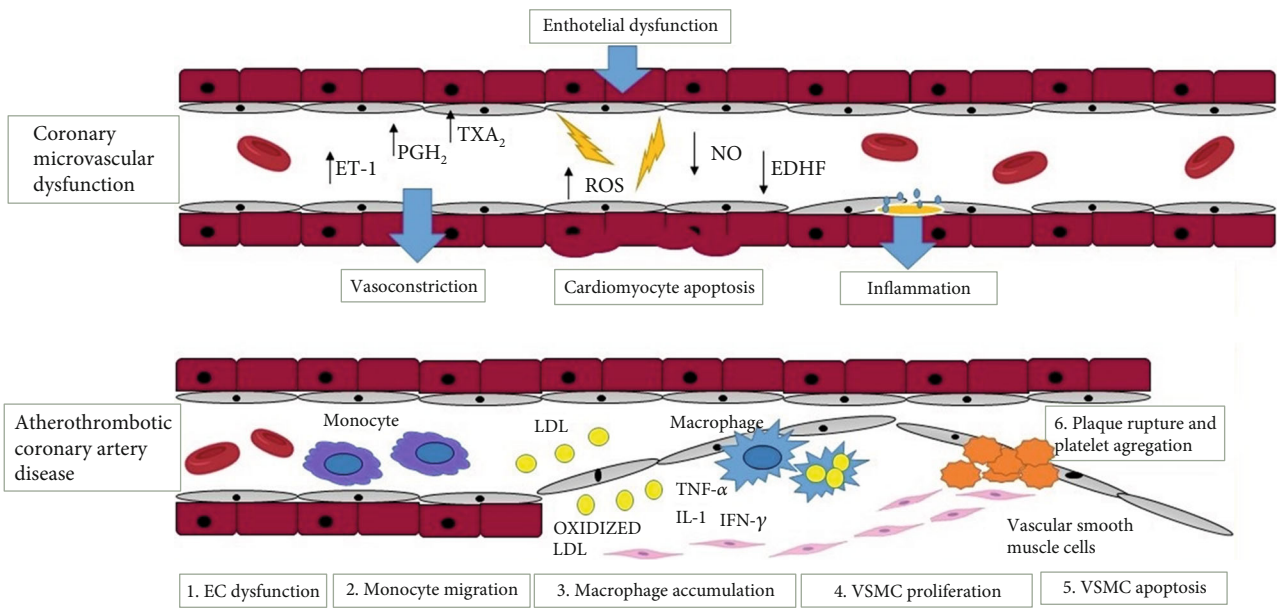


Figure 4: Difference between coronary microvascular dysfunction and atherothrombotic coronary artery disease. ET-1: endothelin -1; PGH2: prostaglandin H2; TXA2: thromboxane A2; ROS: reactive oxygen species; NO: nitric oxide; EDHF: endothelium-derived hyperpolarizing factor; LDL: low-density lipoprotein; TNF-$\alpha$: tumor necrosis factor – $\alpha$; IL-1: interleukin-1; IFN- $\gamma$:), interferon-gamma; VSMC: *vascular smooth muscle cells;* EC: endothelial cell.

dysfunction are obesity, dyslipidemia, diabetes, and the metabolic syndrome. Some disorders such as hypertrophic cardiomyopathy, hypertensive heart disease, myocarditis, and vasculitis are examples where myocardial ischemia can develop without the presence of coronary artery obstruction. In addition to these conditions, structural and functional alterations in the coronary microcirculation may be responsible for the occurrence of myocardial ischemia, in up to 20% of patients with acute coronary syndromes (ACS) and up to 50% of patients with chronic coronary syndromes (CCS) [150].

*6.1. CMD in Nonobstructive ACS.* MINOCA is a term that refers to myocardial infarction with nonobstructive coronary arteries [13]. Today, the pathophysiology of MINOCA is not very well understood. Some studies show that MINOCA has two causes: epicardial causes which are represented by coronary plaque disease, coronary dissection, coronary artery spasm and micorvascular causes such as coronary microvascular spasms, Takotsubo syndrome, myocarditis, or coronary embolism [17, 151]. Conditions such as myocarditis and Takotsubo syndrome are considered nonobstructive ACS, but cardiac nonischemic aetiologies [152, 153].

*6.2. CMD in Nonobstructive CCS.* INOCA is a term denoting ischemia with non-obstructive coronary arteries, where endothelial dysfunction is a key mediator in the pathogenesis of CMD [154, 155]. Studies have shown that INOCA is present in approximately one-third of men and two-thirds of women undergoing angiography for suspected ischemic heart disease [155, 156]. Some studies show that factors originating from the blood and endothelium, as well as metabolic and neurohumoral influences, affect the regulation of the coronary microvascular tone. These include the influence of passive mechanical factors (extravascular contraction of contracting myocardium, distension by intravascular pressure) as well as active changes in the smooth muscle tone by myogenic responses (in response to changes in perfusion pressure) [157, 158]. An important role in the development of this disorder is played by the vascular endothelium where if there is dysfunction, inadequate release of NOS would result in coronary artery vasoconstriction [149]. More specifically, reduced endothelial NO synthesis or increased inactivation will result in endothelial dysfunction and vasoconstriction of blood vessels [159–161]. Endothelial dysfunction is also present as an imbalance between the release of vasorelaxant substances, such as prostacyclin (PGI2), endothelium-derived hyperpolarizing factors (EDHF), and vasoconstricting substances, such as endothelin-1, superoxide, hydrogen peroxide, and thromboxanes [162]. Endothelin-1 (ET-1), as a potent vasoconstrictor, plays a significant role in the pathogenesis of coronary microvascular dysfunction by acting through endothelin A receptors located on coronary vascular smooth muscle cells. Also, ET-1 participates in the regulation of vascular tone via endothelin B receptors located on coronary vascular smooth muscle cells and on endothelial cells where it has an effect on NO release and vasodilation [163]. Endothelium-derived NO is produced from *L*-arginine using NO synthase and released to the vascular smooth muscle layer, ultimately causing vasodilation. NO occurs in response to an increase in shear stress [164]. Endothelial NO has an effect on mitochondrial metabolism, reducing the production of ROS and thus inhibiting inflammation. In addition, it inhibits myocyte hypertrophy by activating cGMP-dependent protein kinase (PKG). It also prevents thrombosis and vascular inflammation by inhibiting platelet activation. Therefore, in conditions such as ischemia and metabolic diseases, there is an increased release of ET-1,

thromboxane A2, and ROS, which ultimately results in increased cardiomyocyte apoptosis [165].

Corban et al. have combined numerous studies, pointing out that mutations of eNOS and ET-1 genes are crucial for the development of coronary microvascular dysfunction [162]. For example, an eNOS gene missense Glu298Asp variant is associated with reduced NO production and impaired endothelial cell response to physiological stimuli such as shear stress, then the T786 > C mutation in the eNOS gene compromises endothelial NO synthesis [166, 167].

Ford et al. conducted a multimodality investigation on patients with angina, investigating the role of ET-1 and the gene variant (rs9349379-G allele), chromosome 6 (PHACTR1/EDN1)] in the pathogenesis of CMD. Their goal was to investigate whether the G allele associates with noninvasive parameters of myocardial ischaemia. The second goal was to examine vascular mechanisms using isometric tension recordings in small peripheral resistance vessels isolated from patients according to genotype. In conclusion, peripheral small artery reactivity to endothelin-1 and ETA receptor antagonist affinity was conserved in the rs9349379-G allele group. Zibotentan tested at clinically relevant concentrations completely prevented the effect of endothelin-1. This study indicates that ETA receptor antagonism in this group of patients may have therapeutic benefits [168, 169].

Experimental studies conducted to date on large animal models such as swine, given that they show a remarkably similar cardiovascular anatomy as humans, have significantly helped in the understanding of the regulation of coronary microvascular function [170]. Experimental studies on animal models, with an emphasis on metabolic derangements as risk factors—in dogs, swine, rabbits, rats, and mice—today help to understand the pathophysiology of CMD. Metabolic derangements in animals are most commonly caused by a high-fat diet (HFD) and/or diabetes mellitus through an injection of alloxan or streptozotocin. There are also transgenic animal models in which metabolic derangements develop. All these animal models show disturbances in the function and structure of the coronary microvascular bed. Therefore, the application of these animal models will be useful in identifying novel therapeutic targets for the purpose of combating ischemic heart disease [171]. Experimental studies have shown that adipocytes, leptin, interleukin-6 (IL-6), and tumor necrosis factor-$\alpha$ (TNF-$\alpha$) are crucial in the development of oxidative stress [172, 173]. In patients with metabolic syndrome, the increased sympathetic activity produces exaggerated alpha-adrenergic coronary vasoconstriction and thus contributes to the development of coronary microvascular dysfunction [174]. Also, in patients with metabolic syndrome and prehypertension, the RAAS system is activated resulting in the formation of angiotensin II—causing vasoconstriction in the coronary circulation [175].

In spite of the conducted research efforts to date, there is still insufficient knowledge about the role of oxidative stress in the pathophysiology of coronary microvascular dysfunction, as a disorder leading to the development of myocardial ischemia despite a normal finding of coronary angiography.

## 7. The Impact of Environmental Factors on CAD

Research to date has shown that environmental factors may play an important role in the development of cardiovascular disease (CVD), but the mechanisms by which environmental factors affect CVD have not been fully explained [176]. Knowing how different environmental factors affect CVD risk would greatly improve the development of therapeutic and preventive strategies to combat CVD. In addition to the previously known fact that genetics, combined with environmental factors, is contributing to the development of CVD, the results of many studies have shown that environmental factors play a more dominant role, as many subjects have prevented CVD by maintaining a healthy lifestyle [177].

The study by Hill et al. investigated the influence of selected genetic and environmental factors on the clinical expression of heterozygous familial hypercholesterolemia. Men were shown to have a higher risk of developing CAD because they had lower high-density lipoprotein (HDL) cholesterol levels and were smokers. In women, CAD has been associated with elevated triglycerides and the presence of hypertension [178].

In order to understand how the environment affects CVD or how that risk is transmitted, we need to understand the complexity of the human environment. According to research, it has been shown that there is a mismatch between ancient human genes and the current human environment, and that the mismatch is the result of a rapid change in the human environment relative to genetic adaptation. First of all, the circadian rhythm is a fundamental feature of the natural environment and has an impact on the levels of neurohormones that regulate cardiovascular function, such as angiotensin II, renin, aldosterone, growth hormone, and atrial natriuretic peptide [179–181]. Therefore, an interesting link is that the frequency of adverse cardiovascular events varies with time. For example, myocardial infarction most commonly occurs between 6 a.m. and 12 p.m. and is more likely to occur early in the morning than at night [182, 183]. Also, a disturbed circadian rhythm increases the risk of diabetes mellitus, obesity, and hypertension [184–186].

The change of seasons has an impact on the development of CVD which is shown by research which found that in the northern and southern hemispheres, and the levels of blood pressure, HDL, LDL, and glucose are slightly higher in winter than in summer. More patients on statin therapy reach the target LDL level in summer than in winter [187–189]. Likewise, exposure to cold ambient temperature increases vascular resistance and blood pressure and can induce coronary vasospasm and lead to the development of myocardial infarction [190]. Also, heat waves, especially in the elderly who cannot adapt quickly to changes in temperature, can promote the development of CVD [191]. That high levels of sunlight early in life can delay CVD by 0.6 to 2.1 years has been shown by some studies [192, 193]. Vitamin D deficiency is associated with an increased risk of adverse cardiovascular events such as myocardial infarction, stroke, heart failure, and sudden cardiac death [194, 195].

Studies have shown that short-term irradiation of the whole body of healthy people with UVA has the effect of lowering blood pressure, on the principle of releasing NO, and increasing the level of S-nitrosoglutation, which reduces blood pressure [196–200]. Also, differences in solar exposure to UV radiation and synthesis of vitamin D increase at high altitudes [201]. Studies show that the proximity of vegetation is associated with lower levels of stress, diabetes mellitus, and CVD [202, 203]. Children who live in greener areas have lower levels of asthma, blood pressure, and insulin resistance [204, 205]. Socioeconomic conditions have an impact on CVD as evidenced by higher data on the incidence of the disease among the poor population. Which is also related to the supply of food and the availability of health care [206]. Exposure to synthetic chemicals and environmental pollutants can have an impact on the health of the population and is ubiquitous and unavoidable today [207]. There is evidence to suggest that chronic and persistent exposure to air pollution increases the progression of atherosclerotic lesions and has adverse effects on blood pressure regulation, peripheral thrombosis, endothelial function, and insulin sensitivity [201, 208–210]. Some studies have shown that constant exposure to noise induces stress and has an impact on cognitive function, autonomic homeostasis, and sleep, and that it increases the risk of CVD [211]. In animal models, chronic exposure to continuous noise (80-100 dB) has been shown to increase the heart rate and mean systemic arterial blood pressure, functional changes associated with increased plasma corticosterone, adrenaline, and endothelin-1 [212].

Smoking, as one of the environmental factors, has a great influence on the development of CVD. Data show that smoking reduces regional left ventricular function even in asymptomatic individuals and significantly (45% –80%) increases the risk of heart failure [213]. The reasons for the high vulnerability of cardiovascular tissue remain unclear, but may relate to poor xenobiotic metabolism in these tissues and their direct exposure to blood-borne toxins. Although the mechanisms by which smoking increases the risk of CVD are not fully known, they appear to affect CVD independently of other factors [214]. A meta-analysis of 54 different studies suggests that smoking increases LDL-C and decreases HDL, but lipid changes account for <10% of the excessive risk of CVD in smokers [215]. Similarly, although acute smoking affects blood pressure, smokers tend to maintain lower blood pressure. Smoking leads to coronary occlusion causes endothelial dysfunction and platelet adhesion to subintimal layers, thereby increasing lipid infiltration and platelet-derived growth factor- (PDGF-) mediated proliferation of smooth muscle cells [216].

Studies have shown that people with homocystinuria, which is one of the inherited recessive disorders in methionine metabolism, have a tendency to develop cardiovascular disease. Such persons have high levels of homocysteine in the circulation and urine, which has an impact on the development of atherosclerosis and in the coagulation system [217–219].

Also, patients with hyperuricemia have a tendency to develop CAD because serum uric acid levels are positively associated with arterial intima-media thickness, which is a precursor to atherosclerosis [220, 221]. In conclusion, we can greatly contribute to the prevention and severity of CVD by influencing environmental factors.

## 8. Pharmacological Therapeutic Possibilities

The therapeutic approach in patients with or without evidence of coronary atherosclerosis involves, first and foremost, lifestyle changes and the management of risk factors, including an effort to influence environmental factors. Beta-blockers are a class of medications that are used to protect the heart from a myocardial infarction because they may reduce myocardial oxygen consumption [222]. Potential therapeutic strategies are focused on the NO-cGMP (nitric oxide-cyclic guanosine monophosphate) pathway. Given that the NO-cGMP pathway has been implicated in the pathophysiology of heart failure, it is a promising target for therapy; although unfortunately, clinical data are not yet fully conclusive [222]. A beta-blocker such as nebivolol exerts its effect through beta-adrenoreceptors located on endothelial cells. In this way, it stimulates eNOS, which ultimately results in NO release and vasodilation. Data on the effect of nebivolol have been supported by studies such as the SENIORS (the Study of the Effects of Nebivolol Intervention on Outcomes and Rehospitalization in Seniors with Heart Failure) study conducted in elderly patients with heart failure [223–225].

Mihai et al. investigated the effect of vericiguat, a soluble guanylate cyclase (sGC) stimulator, on N-terminal prohormone of brain natriuretic peptide (NT-proBNP) levels in patients with chronic heart failure and reduced ejection fraction. The study concluded that among 351 patients with heart failure (HF) and reduced ejection fraction, compared with placebo, vericiguat did not have a statistically significant effect on NT-proBNP levels at 12 weeks. Therefore, the researchers suggested additional clinical trials of vericiguat based on the dose-response relationship to determine the potential role of this drug, and that phase III outcome trial is still ongoing [222]. Natriuretic peptides (NPs) via the natriuretic peptide receptor-A are known to increase intracellular cyclic guanosine monophosphate (cGMP) levels [226]. A drug such as sacubitril/valsartan that simultaneously inhibits neprilysin (neutral endopeptidase) via LBQ657 and the angiotensin II receptor has its effect in chronic heart failure with a reduced ejection fraction. The benefits of this drug are attributed to the increase in the amount of peptides that neprilysin breaks down, such as NPs, by LBQ657 and the simultaneous inhibition of the effects of angiotensin II by valsartan. NPs exert their effects by activating membrane-bound receptors paired with guanylate cyclase, which results in an increase in the second messenger cGMP and ultimately leads to vasodilation, natriuresis, diuresis, and decreased sympathetic activity. These insights are supported by the PARADIGM-HF administration trial [227]. Also, research such as PARAMOUNT, designed as a randomized, parallel-group, double-blind study in a phase II clinical trial of sacubitril/valsartan in the clinical syndrome of HF with preserved ejection fraction (HFpEF), suggested benefits in HFpEF at least in terms of NT-proBNP reduction [228].

Medication groups such as angiotensin-converting enzyme (ACE) inhibitors and statins are used in patients who have evidence of endothelial dysfunction and evidence of atherosclerosis. ACE inhibitors exert vasoprotective effects by inhibiting the renin-angiotensin axis. Statins, in addition to reducing cholesterol levels, also have an inhibitory effect on vascular inflammation, they upregulate eNOS, and enhance vascular NO bioavailability [229].

Studies to date have shown that antioxidants such as flavonoids and vitamins reduce the risk of stroke [230, 231]. Since ROS are known to occur during ischemia, reperfusion, and bleeding in the brain, several antioxidants of different chemical structures have been investigated as neuroprotective therapeutic agents for brain injuries. An example of this is the use of Vaccinium berries that have high antioxidant activity and that have been used in an animal model. They showed their neuroprotective effect due to the high total content of polyphenols [232–234]. It would be interesting to consider such antioxidants in ischemic heart disease, although conclusive evidence is lacking for now.

Resveratrol (chemical name: 3,5,4′-trihydroxy-trans-stilbene) is another polyphenol abundantly found in the skin and seeds of grapes [235, 236].

NXY-059 (chemical name: $\alpha$(2,4-disulfophenyl)-N-tert-butylnitrone) is a novel nitrone free radical trapping (antioxidant) agent. This compound is a stable form of NO, capable of inhibiting the reaction of O2 - and NO to produce ONOO-. This chemical agent might thus be able to neutralize ROS [237, 238].

Therapeutic options for CMD are limited. Some studies show that inhibition of Rho-kinase might constitute one of the treatment options in patients with CMD and vasospastic angina, but this has not yet been proved [239]. Some studies show that targeting of perivascular adipose tissue to stimulate the production of vasoactive factors such as hydrogen sulphide [240] and adiponectin could be of benefit [241].

Studies show that the use of platelet inhibitors such as aspirin may have an effect on treatment in CAD but they have not been sufficiently implicated in the treatment of CMD [241]. Studied of Zhang et al. showed aspirin provides a new potential strategy for regulating cardiac microcirculation, preventing heat stress- (HS-) induced heart failure. In this study, they used a heat stress model of rat cardiac microvascular endothelial cell cultures in vitro and investigated the cell injuries and molecular resistance mechanisms of cardiac microvascular endothelial cells (CMVECs) caused by heat stress. In conclusion, aspirin treatment of CMVECs induced a significant expression of heat shock proteins (Hsp90), which promoted both Akt and M2 isoform of pyruvate kinase (PKM2) signals, which are beneficial for relieving HS damage and for maintaining the function of CMVECs [242].

Clinical research on the use of ticagrelor for microcirculation protection is still ongoing [243]. Nitrates are effective in inducing vasodilatation, and they relieve angina symptoms, but not in patients with nonobstructive CAD [244]. *L*-arginine is as precursor of NO, with attempted use in subjects with nonobstructive CAD [245, 246], but its use is controversial. Zibotentan and atrasentan are ETA receptor antagonists, and there are studies that have suggested them to be a potential therapeutic option in patients with microvascular dysfunction [247, 248].

Drugs or substances that modify TLR4 signaling can be very useful in treating the atherosclerotic process in the coronary arteries [249]. Some already known cardiovascular drugs may have pleiotropic anti-inflammatory and antiatherosclerotic effects achieved through TLR4 (). The well-known statin atorvastatin [249] and angiotensin-converting enzyme (ACE) inhibitors fosinopril [250] showed their antiatherosclerotic properties because they reduced the expression of the TLR4 protein in atherosclerotic lesions. Furthermore, combination treatment with atorvastatin and telmisartan (angiotensin II receptor blocker) or atorvastatin and enalapril (ACE inhibitors) in human PBMCs (peripheral blood mononuclear cells) resulted in decreased TLR4 receptor expression in patients with CAD [251]. Some studies have shown that thiazolidinediones (TZDs), such as rosiglitanose and pioglitazone, can exert their antiatherogenic effect by inhibiting the TLR4 singular pathways [252–254]. Carvedilol, a third-generation beta-blocker, decreased the TLR4 expression in AIM-induced rats [255]. Paclitaxel, an anticancer drug, has also been shown to inhibit TLR4 signaling [256]. The anesthetic propofol and ketamine have the ability to reduce ROS production and suppress the NF-$\kappa$B expression and reduce IL-6 [256]. The exact mechanisms of action of these already known cardiological drugs remain to be explored in the future. Of course, there are a number of newly discovered potential TLR4 antagonists (eritoran, cyanobacterial product (CyP), EM-163, epigallocatechin-3-gallate, 6-shogaol, cinnamon extract, N-acetylcysteine, melatonin, molecular hydrogen, monoclonal antibody anti-hTLR4-IgG) which could be useful in preventing atherosclerosis in patients with CAD [257].

Also, epigenetic regulation (DNA methylation and histone acetylation) could become the most promising therapeutic target for the treatment of TLR4-mediated inflammatory disorders [258].

Tsai et al. conducted research in rat and in vitro models examining the role of IL-20 in the infarcted heart following ischemia/reperfusion injury, with the aim of discovering new therapeutic options in the treatment of ischemic heart disease. This study revealed that IL-20 and its receptors, IL-20R1 and IL-20R2, were increased in H2C2 cardiomyoblast cells and ventricular tissues subjected to prior hypoxia/reoxygenation (H/R) stimulation. The obtained results suggest that IL-20 causes an increase in $Ca^{2+}$ and activation of the PKC/NADPH oxidase pathway, leading to an increase in oxidase stress and a decrease in AKT regulation. Also, IL-20 can mediate H/R-induced apoptosis via PKC/NADPH oxidase/AKT signaling. Therefore, regulation of IL-20 may contribute to cardiomyocyte apoptosis, and this might be helpful in future considerations of new therapeutic targets in the treatment of ischemic heart disease [259]. In their work, Samakova et al. combined insights into the phosphatidylinositol-3-kinase-(phosphoinositide-3-kinase-) protein kinase B (serine-threonine protein kinase) (PI3k/Akt) pathway and the association with oxidative stress, angiogenesis, and mesenchymal stem cell survival in pathophysiologic conditions in ischemia [260].

Cell therapy has long been known to be one of the options for treating ischemic heart disease when, in 1974, Friedenstein and his associates first isolated and characterized the use of mesenchymal stem cells (MSC) [261, 262]. Since then, numerous studies have been conducted to improve the use of mesenchymal stem cells in regenerative therapy. Also, the influences of biologically active molecules such as cytokines, growth factors, and chemokines were found to be important for any attempts at successful cell therapies. In addition, the PI3K/Akt pathway was determined to be one of the mechanisms of intracellular signaling that plays a role in regulating cell proliferation, differentiation, apoptosis, and migration. Therefore, the aforementioned contributors emphasized that preconditioning of MSCs is an important process for the improvement of the efficiency of signaling mechanisms [260].

Some studies show that fisetin protects against cardiac cell death through reduction of ROS production and caspase activity. In vitro studies of mammalian cardiac cell models have shown that fisetin increases the vitality of rat cardiomyocytes after hypoxia or starvation or reoxygenation. It also reduces ROS formation, activates caspases, protects from DNA damage, and ultimately inhibits apoptosis. Fisetin is a very promising drug for protection against ischemic damage after myocardial infarction and for counteracting ischemia reperfusion injury because it can, in addition, activate genes involved in cell proliferation [263].

Experimental studies in rat models have shown that cocoa flavonoids reduce inflammation, oxidative stress, and myocardial apoptosis after acute coronary ischemia-reperfusion. In these studies, cocoa extract treatment reversed membrane peroxidation and nitro-oxidative stress as well as lead to reduction of inflammatory marker levels such as IL-6 and NF-$\kappa$B [264]. Verma et al. conducted an experimental study in rats that showed that morin, a bioflavonoid, has antioxidant and anti-inflammatory effects, and that it prevents apoptosis. It exerts its effects by regulating RISK/SAPK pathways. Extracellular regulated kinase (ERK), protein kinase A (Akt), and eNOS are involved in the RISK pathways. The p38 proteins and c-Jun N-terminal kinase (JNK) are involved in the SAPK pathway [265]. Syeda et al. in their study in mice investigated the cardioprotective potential of anthocyanidin against myocardial ischemia injury. In in vivo conditions, the left anterior descending coronary artery was ligated to induce myocardial ischemia in mice, whereas in in vitro conditions, neonatal mice cardiomyocytes were treated with $H_2O_2$ to induce oxidative stress. It was concluded that, in vivo and in vitro, anthocyanidin can induce a state of myocardial resistance against ischemic insult. Inhibition of the ROS/p-JNK/Bcl-2 pathway is the underlying mechanism of action of anthocyanidin [266]. Table 1 summarizes the discussed pharmacological therapeutic possibilities.

## 9. Biomarkers of Oxidative Stress in Ischemic Heart Disease

Many oxidative stress-related biomarkers have been recently proposed, reflecting different and independent pathways, including oxidative and antioxidant ones [267]. Some reliable and simple tests have been presented to estimate oxidative stress in vivo, and also a calculation of a global oxidative stress index (OSI) is described, which represents the ratio of total oxidant status to total antioxidant status [268], and it showed higher values in patients with CAD [269]. Some of the oxidative stress-related biomarkers seem promising for future clinical use in understanding the pathogenesis and predicting clinical outcomes of ischemic heart disease. Although there are a lot of common biological features between ACS and stable CAD, there are also many differences resulting in variation of levels of biomarkers included in different oxidative stress-related pathways [270].

Measurement of reactive oxygen metabolites (ROM) based on the conversion of hydroperoxides to alkoxyl and peroxyl radicals under acidic conditions in combination with estimation of total antioxidant capacity (OXY) can quantify oxidative stress levels [271, 272]. Previous studies evaluated levels of ROM and OXY in patients with cardiovascular disease in comparison with the general population and evaluated their prediction value in adverse CV events [268, 271, 273]. Lubrano et al. examined ROM and OXY levels during acute myocardial infarction (AMI) which showed a progressive increase and then decrease suggesting significant rise of oxidative stress level during AMI [270]. The level of ROM values was higher in stable CAD in comparison with ACS patients, indicating that this parameter reflects the chronic oxidative stress status [270]. OXY was progressively reduced in stable CAD and more in ACS compared with the control group, showing severe acute harm to the antioxidant system in ischemic disease, especially during myocardial reperfusion injury [270]. This fact is further enhanced by findings that different vitamins and antioxidant enzymes were also reduced during acute myocardial infarction [270, 274].

Low levels of NO are related to endothelial dysfunction and many CV events, but its direct quantification is difficult so it can be estimated by measurements of its stable metabolites—nitrite/nitrate (NOX) [275]. NOX are end-products of NO metabolism and a reliable index of NO production. In previous studies, there are controversial results regarding NOX levels in CV disease and CV risk. Some of them revealed higher levels of NOX in a group with CAD and AMI, which can be explained by the fact that increase in systemic NOX can be a consequence of activation of inducible NO synthase as a result of vascular injury, without restoration of endothelial NO release [276, 277]. Other studies showed reduced levels of NOX during acute myocardial infarction, pointing to deteriorated NO levels during an acute ischemic event. Further researches are needed to understand meaning of different levels of NOX [270].

Several studies suggested that Ox-LDL may play an important role in the pathogenesis of atherosclerosis, plaque rupture, and onset of ACS [278, 279]. Uptake of Ox-LDL by macrophages and activated smooth muscle cells probably transforms these cells into foam cells which are found in the atherosclerotic intima. Endothelial uptake of Ox-LDL depends on receptors expressed on the cell surface. LOX-1 is a major receptor for Ox-LDL, and its expression is induced by oxidative stress, hemodynamic stimuli, and inflammatory

Table 1: Discussed pharmacological therapeutic possibilities in ischemic heart disease.

| Reference | Study characteristic | Therapeutic options | Primary endpoint |
|---|---|---|---|
| Zhang X et al. [242] | Experimental study on animal models such as rat | Aspirin (platelet inhibitors) | Enhances the protection of Hsp90 from heat-stressed injury in cardiac microvascular endothelial cells through PI3K-Akt and PKM2 pathways |
| Rodius et al. [263] | In vitro studies of mammalian cardiac cell models | Fisetin (plant polyphenol from the flavonoid group) | Reduction of ROS production, protects from DNA damage |
| Verma et al. [265] | Experimental study on male albino Wistar rats | Morin (bioflavonoid) | Regulation of RISK/SAPK pathways |
| Syeda et al. [266] | Experimental study on mice | Anthocyanidins (plant pigments) | Inhibition of ROS/p-JNK/Bcl-2 pathway |
| Flather et al. Ambrosio et al. [223, 224] | Randomized trial in elderly patients with heart failure | Nebivolol (beta-1-selective blocker), beta(3)-adrenoreceptor agonistic effect | Stimulates eNOS, NO release, vasodilatation |
| Mihai et al. [222] | Randomized trial in patients with heart failure and reduced ejection fraction | Vericiguat (a soluble guanylate cyclase stimulator) | Changes in the NT-proBNP level have not been achieved, but the phase III trial is ongoing |
| McMurray et al. [226] | Randomized, double-blind trial in patients with heart failure and reduced ejection fraction | Sacubitril/valsartan (NP degradation inhibitor/angiotensin II receptor inhibitor) vs. enalapril | Increase cGMP, vasodilatation |
| Solomon et al. [227] | Randomized, double-blind study in a phase II trials, in patients with heart failure and reduced ejection fraction | Sacubitril/valsartan (NP degradation inhibitor/angiotensin II receptor inhibitor) vs. valsartan | Changes in NT-proBNP |
| Carmine et al. [228] | Randomized, prospective, single-blind, placebo-controlled fashion in patients who have chest pain and angiographically normal epicardial vessels | Ramipril (ACE inhibitor) and atorvastatin (statins) | Reduced SOD activity, low superoxide anion level |
| Amir et al. [245] | Randomized study, double- blind in patients with patients without significant CAD on coronary angiography | *L*-arginine (substrate for NO synthase) | Improve endothelial function, increase NO and NO inhibits the production of endothelin via cGMP pathway |
| Martin et al. [247] | Single-center, double-blind, randomized controlled trial in patients with CMD | Atrasentan (ETA receptor antagonist) | Supports the role of the endogenous endothelin system |

eNOS: endothelial nitric oxide synthase; NO: nitric oxide; NT-proBNP: N-terminal prohormone of brain natriuretic peptide; cGMP: cyclic guanosine monophosphate; ACE inhibitor: angiotensin converting enzyme inhibitors; SOD: superoxide dismutase; Hsp90: heat shock proteins 90; PI3K/Akt: phosphoinositide-3-kinase–protein kinase; PKM2: M2 isoform of pyruvate kinase; ETA receptor: endothelin-A receptor; CMD: coronary microvascular dysfunction; ROS: reactive oxygen species; RISK/SAPK pathway: extracellular regulated kinase (ERK), protein kinase A (Akt) and eNOS/p38 proteins, and c-Jun N-terminal kinase (JNK); ROS/p-JNK/Bcl-2 pathway: reactive oxygen species/stress-activated c-Jun N-terminal kinase/B-cell lymphoma.

cytokines, and it is related to development of atherosclerosis and plaque instability. It is highly expressed in luminal endothelial cells in the early stage of atherogenesis as well as in intimal neovascular endothelial cells of advanced plaques and released during plaque rupture, promising to be a good marker of plaque instability [280]. Soluble LOX-1 (sLOX-1) is proposed as a potential marker for identification of ACS in the early stage [281, 282] with the peak time being even earlier than troponin T [281]. Some studies suggest that levels of sLOX-1 might begin to rise before onset of ACS but that could be a subject of further research [282].

In addition to these biomarkers, there is a large cohort study that found an association of urinary oxidized guanine/guanosine (OxGua) and 8-isoprostane levels with CVD mortality prediction and with myocardial infarction incidence in obese subjects [283]. Other studies also showed that elevated plasmatic levels of 8-isoprostane are associated with acute myocardial infarction and also with the severity and extent of CAD [284, 285].

## 10. Epigenetic (Dys)regulation MicroRNA in CAD

Small noncoding RNAs (microRNAs or miRs) of 19–25 nucleotides (nt) regulate the expression of more than 30% of human genes at the posttranscriptional level [286]. They are involved in intracellular and intercellular signaling and circulate in the blood in stable forms due to packaging into apoptotic bodies, microvesicles (MV), exosomes, and lipoproteins (Lp) [287]. Each miR from RNA is transcribed by RNA polymerase II and, less frequently, by RNA polymerase III [288, 289]. First, Pri-miRNA is formed, containing a canonical hairpin structure, a 50 cap, and a 30 poly-A tail, which is processed in the nucleus by Drosha-DGCR8 (Di George Syndrome Critical Region Gene 8), then pre-miRNA is formed to a hairpin form which is exported to the cytoplasm via Exportin-5 and then further truncated by the RNase III enzyme complex Dicer/TRBP (TAR RNA-binding protein), yielding a mature duplex of miRNA (miRNA-5p and miRNA3p) [290]. Mature miRs bind at a specific site of the messenger RNA (mRNA) in the Argonaute protein multiprotein complex, known as RNA-induced attenuation complex (RISC), providing sequence-specific attenuation by degrading messenger RNA (mRNA) and/or inhibiting its translation [286]. Each miR can target several mRNAs that act in several important cellular functions such as differentiation, proliferation, and apoptosis in the cardiovascular system [291]. MicroRNAs that can regulate cellular homeostasis of oxidative stress by modulating the expression of antioxidant genes and the expression of enzymes that generate ROS are called redox sensitive micorRNAs or redoximiR [292]. RedoximiR achieves its oxidative or antioxidant effects by directly regulating the posttranscriptional level of the redox-sensitive nuclear factor Nrf2. Of course, there are also miRs that achieve their effects independently of Nrf2 [293]. Nrf is considered a major regulator of cell survival in oxidative stress because it controls the basal and induced expression of a number of important antioxidant genes via a *cis*-acting element, designated the antioxidant-response element (ARE), in the promoter of target genes [293]. Some of these genes are the genes for heme oxygenase-1 (HO-1), gamma-glutamylcysteine synthetase, thioredoxin reductase, glutathione-S-transferase, and NAD (P) H: quinone oxidoreductase [293]. Protein kinase C (PKC), mitogen-activated protein kinase (MAPK), and phosphotidylinositol 3-kinase (PI3K) are involved in the regulation of Nrf2/ARE signaling [293]. Numerous microRNAs participate in the regulation of Nrf2 via certain coregulatory proteins such as Kelch-like ECH-associated protein 1 (Keap1), BTB and CNC homolog 1 (Bach1), Parkinson's protein 7 (PARK7/DJ-1), and small masculoaponeurotic fibrosarcoma (Maf) proteins. Most miRs act by the downregulation mechanism Nrf2 (miR-153, miR-27a, miR-142-5p, miR144 miR-28, and miR-34a), while some act by the upregulation mechanism Nrf2 (miR 200-a, miR-136-3p, miR-128). Also, miRs regulate the expression of key enzymes that generate ROS which can lead to modification of the biogenesis of miRs. Cellular oxidative stress can alter miR biogenesis during processing in the nucleus and cytoplasm, altering its stability, functionality, and binding affinity for target promoter sites [292] (Figure 5).

The primary pathological process that causes CAD is atherosclerosis triggered by oxidative stress [291]. miR is involved in almost all steps of atherosclerosis and CAD, such as endothelial damage and endothelial dysfunction, oxidative enzyme expression, inflammatory molecule expression, monocyte invasion and activation, LDL oxidation, platelet function, vascular smooth muscle response, and angiogenesis [294]. The miRs involved in oxidative stress and associated with CAD are miR-155, miR34a, and miR-136-3p.

miR-155 was expressed in mononuclear and endothelial cells [295]. Ox-LDL can induce the expression of miR-155 [295]. miR-155 may inhibit the inflammatory response thereby reducing enhanced lipid oxidation in macrophages during oxidative stress [295]. Inhibition of endogenous miR-155 in THP-1 macrophages resulted in increased lipid uptake and release of several cytokines, including interleukin (IL)-6, -8, and tumor necrosis factor-$\alpha$ (TNF-$\alpha$) [296]. The overexpression of miR-155 may induce apoptosis of Ox-LDL attacked macrophages [295]. Levels of miR-155 were decreased in plasma and peripheral blood mononuclear cells (PBMCs) in patients with CAD. The study showed that miR-155 levels in peripheral blood mononuclear cells or plasma were inversely correlated with the severity of stenotic lesions in the coronary arteries [297]. miR-155 acts on the Nrf2 pathway whose activation of Nrf2 can reduce the degree of oxidative stress in mitochondria and can reduce oxidative stress and the inflammatory response of vascular endothelial cells [298]. Bach1 in association with the masculoaponeurotic fibrosarcoma (Maf) protein dominantly hides ARE sequences from Nrf2 binding of transcription factor [299, 300]. Oxidative stress and inflammation-induced tumor necrosis factor-$\alpha$ (TNF-$\alpha$) activate TNFR (tumor necrosis factor receptor) [301]. NF-$\kappa$B is in an inactive state bound to the inhibitor protein I$\kappa$B, and activation of TNFR leads to activation of I$\kappa$B kinases (IKKs) which by phosphorylation dislocates I$\kappa$B with NF-$\kappa$B [302]. Phosphorylated IB is degraded by the 26s proteasome [303]. Nuclear translocation of NF-$\kappa$B stimulates

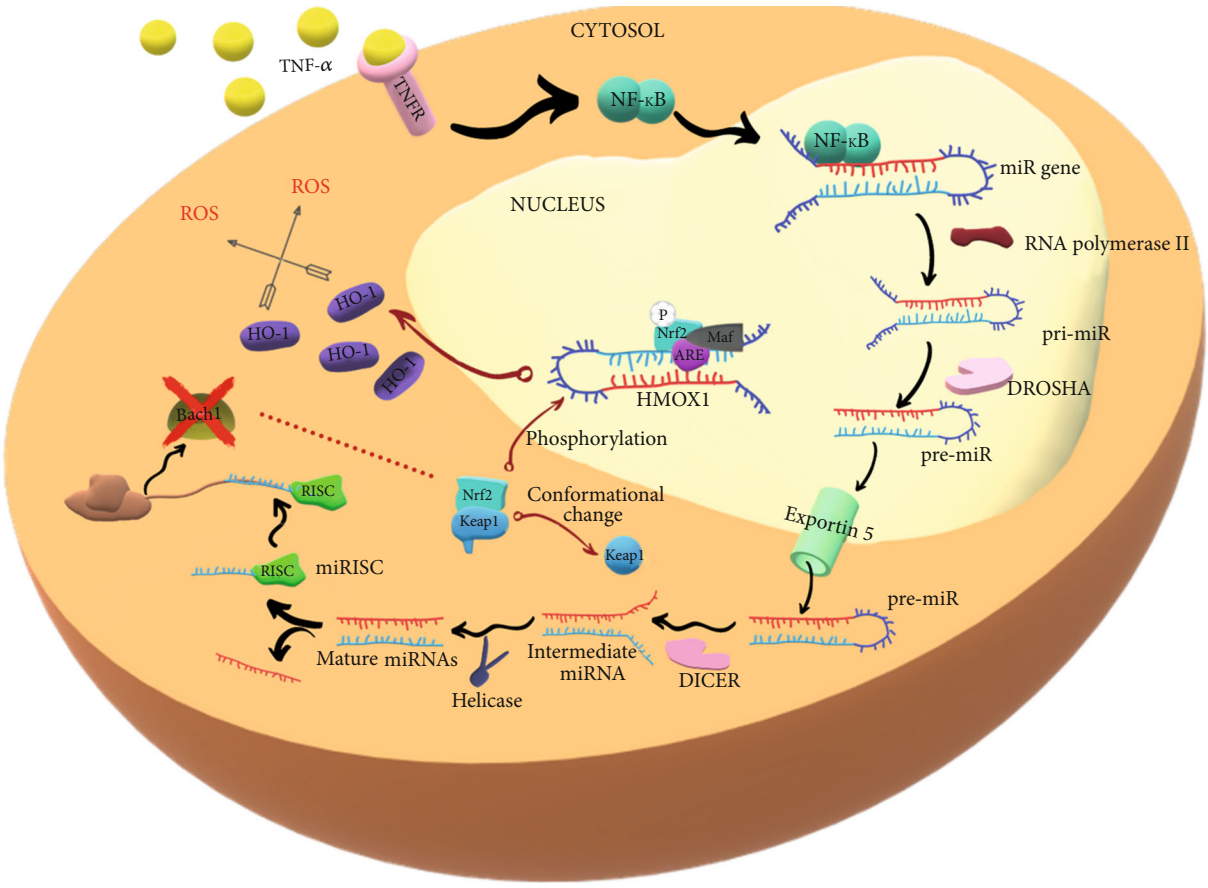


Figure 5: Biogenesis of miR-155. ARE: antioxidant responsive element; Bach 1: BTB domain and CNC homolog 1; DICER: ribonuclease DICER; DROSHA: ribonuclease DROSHA; HO-1: heme oxygenase-1; KEAP1: Kelch-like ECH-associated protein 1; MAF: musculoaponeurotic fibrosarcoma; miR: microRNA; NF-κB: nuclear factor kappa-light-chain-enhancer of activated B cells; NRF2: nuclear factor erythroid 2-related factor 2; RISC: RNA-induced silencing complex; ROS: reactive oxygen species; TNF-α: tumor necrosis factor-α; TNFR: tumor necrosis factor receptor.

the expression of miR-155 which inhibits the production of Bach1 protein, allowing the binding of the Nrf2 transcription factor to the ARE sequence [299]. Under normal physiological conditions, Nrf2 is bound to Kelch-like ECH-associated protein-1 (Keap1) within the cytoplasm [304].When the Bach1 expression is reduced and cells are attacked by oxidative stress, phosphorylation of Nrf2 via (MAPK), protein kinase C (PKC) and (phosphoinositide 3-kinase (PI3K) and its transport into the nucleus and binding to the ARE sequence together with Maf protein occurs [295]. Consequently, there is an increased synthesis of HO-1 (heme oxygenase-1) [299]. HO-1 is a microsomal enzyme induced in oxidative stress that metabolizes heme to biliverdin, carbon monoxide (CO), and iron, and CO has antiapoptotic and anti-inflammatory properties and may act as a vasodilator in atherogenesis when NO bioavailability is reduced due to ROS inactivation [305]. Numerous studies have shown a cardioprotective effect of HO-1 [306–308]. Thus, it is clear that suppression of the Bach1 protein expression alters cellular redox signaling and enhances the expression of antioxidant enzymes induced by Nrf2 [309].

miR-34a induced by oxidative stress via PI3K signaling in EPCs obtained from patients with CAD reduces the expression of the enzymes SIRT1 and SIRT6 involved in histone deacetylation and DNA repair [310, 311]. Silencing the entire miR-34 family may protect the heart from pathological myocardial remodeling [312]. miR-34a induces postacute MI, and inhibition of miR-34a improves recovery of cardiac contractile function after acute MI [313].

miR-136-3p can reduce oxidative stress and inflammatory response and consequent pathological damage to myocardial tissue by inhibiting the expression of the target EIF5A2 gene thereby blocking the Rho A/ROCK signaling pathway in the CAD rat myocardial tissue and models of cardiac microvascular endothelial cell (CMEC) injury [314].

Numerous studies have shown that miR can serve as an important biomarker for early detection of CAD, differentiation of patients with or without CAD, as well as patients with stable CAD or unstable CAD, and assessment of disease severity, as prognostic indicators and indicator of restenosis after stenting (in-stent restenosis, ISR) [291]. miRNAs are not specific because each miRNA can be elevated or decreased in different disease conditions, so this is a big challenge for researchers [291].

Increased levels of miR-31, miR-720, miR-181, and miR-208a may have potential roles for early CAD detection

[315–317]. miR-208a is a highly selective cardiac RNA that is overexpressed 3 hours after myocardial infarction (MI) and correlates with increased cardiac troponin (cTn) I levels [318]. MiR-208a has been shown to have superiority in early diagnosis of MI over cTn [318]. Devaux et al. argue that miR-499-5p which is myosin gene-regulated has higher diagnostic accuracy in correlation with cTN than miR-208a [319].

To distinguish CAD from non-CAD patients, numerous miRNAs were detected that were significantly increased in patients with CAD (miR-149, miR-765, miR-424, miR-133a miR-206, miR-574-5p, miR-135a, miRNA-24, miRNA-33, miRNA-103a, miRNA-122). On the other hand, levels of miRNA-23a, miR-19a, miR-484, miR155, miR-222, miR-145, miR-29a, miR-378, miR-342, miR-181d, miR-150, and miR-30e-5p were found to be reduced in the blood of patients with CAD compared to healthy controls [320]. Faccin et al. state that the combination of three miRNAs (miRNA-155, -145, and flight-7c) has better classification power than just one miRNA [321]. Two studies have shown that increased plasma levels of miRNA-133a, miR-126, and miR-1 are useful for the diagnosis of unstable CAD [322, 323]. MiR-145 is significantly elevated in unstable angina compared to stable angina, but so far, no miR or cascade of miR has been detected in the blood of patients by which we will distinguish these two types of angina [287]. Another study showed that miR-134, miR-198, and miR-370 were increased in unstable versus stable angina pectoris [324]. Li suggested that six microRNAs (miR-1/134/186/208a and 208b/233/499-5p) have increased sensitivity and specificity in MI detection, although miR208 and miR499 were significantly higher in patients with pecotris angina compared to IM [325]. Ward et al. demonstrated that myocardial infarction miRNA-25-3p, miRNA-221-3p, and miRNA-374b-5p are highly present in the blood of patients with STEMI and miRNA 221-3p and 483-5 in patient with NSTEMI [326].

To assess the severity of coronary artery disease, miR-133a was presented as a potential biomarker showing the presence of coronary artery stenosis and is a better indicator of assessing the severity of CAD compared to cTn1 [327]. Other miRNA-208a, miRNA-155, and miRNA-223 strongly correlated with the CAD severity assessment [291]. Levels of miRNA-92a lipoprotein-2 (HDL-2) HDL-2 miRNA-92a, and HDL-3 miRNA-486 could be signals of severe CAD and threatened myocardial infarction [328]. Oxidative stress-induced microRNA-92a (miR-92a) leads to endothelial dysfunction caused by activation of sirtuin 1, Krüppel-like factor 2, and Krüppel-like factor 4, leading to NOD-like receptor family pyrin domain-containing 3 inflammasome activation and endothelial nitric oxide synthase inhibition [329]. The expression of miRNA-21 in the macrophages of uncalcified coronary artery lesions was significantly higher than in calcified lesions [330]. miR-100 can be released into the coronary circulation from sensitive coronary plaques and can therefore be useful as a biomarker of plaque vulnerability [331].

Some vascular miRs may have a prognostic potential for coronary artery disease. The increased expression of miRNA-126 and miRNA-199a in circulating microvesicles is associated with a lower cardiovascular mortality rate [332]. Also, elevated levels of miRNA-197, miRNA-223, miRNA-133a, and miRNA-208b were significantly associated with higher mortality rates in patients with CAD [333, 334]. In obese patients, miR-181a levels within polymorphonuclear cells are increased, which is associated with an increased risk of developing CAD [316].

As new noninvasive potential biomarkers for assessing the occurrence of ISR, levels of circulating miRNA-143, miRNA-145, and miRNA-181b and increased levels of miRNA-185 and miRNA-155 were reduced compared to non-ISR [335, 336].

During the development and progression of atherosclerotic plaques, miR-92a, miR-100, miR-126, miR-127, and miR-145 are mostly released as a result of vascular damage. The miRNAs released from myeloid cells involved in the formation of atherosclerotic lesions are miR-155 and miR-223. During myocardial injury in patients with CAD, miR-133a, miR-208a, and miR-499 are mostly released into the coronary circulation [337].

RedoximiR is an important regulator of the cellular redox status and new valuable biomarkers that constitute a key step in the pathogenesis of CAD. Due to their cell-type specificity, abundance, and stability in most solid and liquid clinical specimens, they provide the opportunity for further study to expand our understanding of CAD pathogenesis and open up new innovative diagnostic and therapeutic approaches. For now, the following therapeutic strategies are being studied: inhibition of premicroRNA export from the nucleus, inhibition of premicroRNA transcription into mature microRNAs, or competitive inhibition via complementary binding to specific microRNAs [287]. Whether we can block or prevent the progression of atherosclerosis and CAD development in the future remains to be patiently awaited.

## 11. Final Remarks

This review article discussed evidence associating oxidative stress with the pathogenesis and occurrence of ischemic heart disease. Since oxidative stress is an important group of processes in a number of disorders connected with vascular structure and function, it is not surprising that there are many indications that some of the factors implicated in oxidative stress play roles in vascular disease mechanisms. From this review, however, it is likewise clear that the interactions of the many factors of oxidative stress that contribute to vascular disease mechanisms in ischemic heart disease are very complex and not yet clearly nor completely understood. At the same time, it would be desirable and interesting to therapeutically target oxidative stress, in hopes of developing better therapeutic strategies for ischemic heart disease, which after many years of various treatment approaches and strategy changes is still not managed optimally and with satisfactory results in a large number of affected patients. The main prerequisite for the development of such therapeutic strategies targeting oxidative stress is, however, a much better understanding of all the specific roles of ROS in specific pathophysiological mechanisms, as well as the interactions of ROS with other signaling systems. Only then can a targeted therapeutic approach be successful, effective, and with a

limited spectrum of adverse effects. To achieve such an understanding of the roles of oxidative stress in ischemic heart disease, more research in this area is warranted.

## Conflicts of Interest

The authors have no conflict of interest to declare.

## References


[1] M. A. Gimbrone Jr. and G. García-Cardeña, "Vascular endothelium, hemodynamics, and the pathobiology of atherosclerosis," *Cardiovascular Pathology*, vol. 22, no. 1, pp. 9–15, 2013.

[2] A. Ninić, N. Bogavac-Stanojević, M. Sopić et al., "Superoxide dismutase isoenzymes gene expression in peripheral blood mononuclear cells in patients with coronary artery disease," *Journal of Medical Biochemistry*, vol. 38, no. 3, pp. 284–291, 2019.

[3] C. P. Lin, F. Y. Lin, P. H. Huang et al., "Endothelial progenitor cell dysfunction in cardiovascular diseases: role of reactive oxygen species and inflammation," *BioMed Research International*, vol. 2013, Article ID 845037, 10 pages, 2013.

[4] A. J. Kattoor, N. V. K. Pothineni, D. Palagiri, and J. L. Mehta, "Oxidative stress in atherosclerosis," *Current Atherosclerosis Reports*, vol. 19, no. 11, 2017.

[5] T. Münzel, G. G. Camici, C. Maack, N. R. Bonetti, V. Fuster, and J. C. Kovacic, "Impact of oxidative stress on the heart and vasculature: part 2 of a 3-part series," *Journal of the American College of Cardiology*, vol. 70, no. 2, pp. 212–229, 2017.

[6] U. Förstermann, N. Xia, and H. Li, "Roles of vascular oxidative stress and nitric oxide in the pathogenesis of atherosclerosis," *Circulation Research*, vol. 120, no. 4, pp. 713–735, 2017.

[7] K. Thygesen, J. S. Alpert, A. S. Jaffe et al., "Fourth universal definition of myocardial infarction (2018)," *Circulation*, vol. 138, no. 20, pp. e618–e651, 2018.

[8] H. Liu, J. Zhuang, P. Tang, J. Li, X. Xiong, and H. Deng, "The role of the gut microbiota in coronary heart disease," *Current Atherosclerosis Reports*, vol. 22, no. 12, 2020.

[9] E. Sanchez-Rodriguez, A. Egea-Zorrilla, J. Plaza-Díaz et al., "The gut microbiota and its implication in the development of atherosclerosis and related cardiovascular diseases," *Nutrients*, vol. 12, no. 3, 2020.

[10] A. R. Amin, M. G. Attur, M. Pillinger, and S. B. Abramson, "The pleiotropic functions of aspirin: mechanisms of action," *Cellular and Molecular Life Sciences*, vol. 56, no. 3-4, pp. 305–312, 1999.

[11] S. G. Chrysant and G. S. Chrysant, "The pleiotropic effects of angiotensin receptor blockers," *The Journal of Clinical Hypertension*, vol. 8, no. 4, pp. 261–268, 2006.

[12] E. Profumo, B. Buttari, L. Saso, and R. Rigano, "Pleiotropic effects of statins in atherosclerotic disease: focus on the antioxidant activity of atorvastatin," *Current Topics in Medicinal Chemistry*, vol. 14, no. 22, pp. 2542–2551, 2014.

[13] B. Ibanez, S. James, S. Agewall et al., "2017 ESC Guidelines for the management of acute myocrdial infarction in patients presenting with ST-segment elevation: The Task Force for the management of acute myocardial infarction in patients presenting with ST-segment elevation of the European Society of Cardiology (ESC)," *European Heart Journal*, vol. 39, no. 2, pp. 119–177, 2018.

[14] J. Knuuti, W. Wijns, A. Saraste et al., "2019 ESC Guidelines for the diagnosis and management of chronic coronary syndromes," *European Heart Journal*, vol. 41, no. 3, pp. 407–477, 2020.

[15] K. Thygesen, J. S. Alpert, A. S. Jaffe et al., "Fourth universal definition of myocardial infarction (2018)," *European Heart Journal*, vol. 40, no. 3, pp. 237–269, 2019.

[16] M. Roffi, C. Patrono, J. P. Collet et al., "2015 ESC Guidelines for the management of acute coronary syndromes in patients presenting without persistent ST-segment elevation: Task Force for the Management of Acute Coronary Syndromes in Patients Presenting without Persistent ST-Segment Elevation of the European Society of Cardiology (ESC)," *European Heart Journal*, vol. 37, no. 3, pp. 267–315, 2016.

[17] S. Agewall, J. F. Beltrame, H. R. Reynolds et al., "ESC working group position paper on myocardial infarction with nonobstructive coronary arteries," *European Heart Journal*, vol. 38, no. 3, pp. 143–153, 2017.

[18] C. Urso and G. Caimi, "Oxidative stress and endothelial dysfunction," *Minerva Medica*, vol. 102, no. 1, pp. 59–77, 2011.

[19] H. Cai and D. G. Harrison, "Endothelial dysfunction in cardiovascular diseases: the role of oxidant stress," *Circulation Research*, vol. 87, no. 10, pp. 840–844, 2000.

[20] K. M. Channon, H. S. Qian, and S. E. George, "Nitric oxide synthase in atherosclerosis and vascular Injury," *Arteriosclerosis, Thrombosis, and Vascular Biology*, vol. 20, no. 8, pp. 1873–1881, 2000.

[21] J. A. Panza, C. E. García, C. M. Kilcoyne, A. A. Quyyumi, and R. O. Cannon III, "Impaired endothelium-dependent vasodilation in patients with essential hypertension: evidence that nitric oxide abnormality is not localized to a single signal transduction pathway," *Circulation*, vol. 91, no. 6, pp. 1732–1738, 1995.

[22] E. L. Schiffrin, M. L. Lipman, and J. F. Mann, "Chronic kidney disease: effects on the cardiovascular system," *Circulation*, vol. 116, no. 1, pp. 85–97, 2007.

[23] U. Hink, H. Li, H. Mollnau et al., "Mechanisms underlying endothelial dysfunction in diabetes mellitus," *Circulation Research*, vol. 88, no. 2, pp. E14–E22, 2001.

[24] Y. Higashi, T. Maruhashi, K. Noma, and Y. Kihara, "Oxidative stress and endothelial dysfunction: clinical evidence and therapeutic implications," *Trends in Cardiovascular Medicine*, vol. 24, no. 4, pp. 165–169, 2014.

[25] M. A. Gimbrone Jr., "Vascular endothelium: an integrator of pathophysiologic stimuli in atherosclerosis," *The American Journal of Cardiology*, vol. 75, no. 6, pp. 67B–70B, 1995.

[26] H. Drexler, "Endothelial dysfunction: clinical implications," *Progress in Cardiovascular Diseases*, vol. 39, no. 4, pp. 287–324, 1997.

[27] G. A. Mensah, "Healthy endothelium: the scientific basis for cardiovascular health promotion and chronic disease prevention," *Vascular Pharmacology*, vol. 46, no. 5, pp. 310–314, 2007.

[28] D. X. Zhang and D. D. Gutterman, "Mitochondrial reactive oxygen species-mediated signaling in endothelial cells," *American Journal of Physiology. Heart and Circulatory Physiology*, vol. 292, no. 5, pp. H2023–H2031, 2007.

[29] L. J. Ignarro, G. M. Buga, K. S. Wood, R. E. Byrns, and G. Chaudhuri, "Endothelium-derived relaxing factor produced

and released from artery and vein is nitric oxide," *Proceedings of the National Academy of Sciences*, vol. 84, no. 24, pp. 9265–9269, 1987.

[30] J. N. Wilcox, R. R. Subramanian, C. L. Sundell et al., "Expression of multiple isoforms of nitric oxide synthase in normal and atherosclerotic vessels," *Arteriosclerosis, Thrombosis, and Vascular Biology*, vol. 17, no. 11, pp. 2479–2488, 1997.

[31] D. G. Harrison, "Endothelial function and oxidant stress," *Clinical Cardiology*, vol. 20, no. S2, pp. II-11–II-17, 1997.

[32] A. C. Montezano and R. M. Touyz, "Reactive oxygen species and endothelial function–role of nitric oxide synthase uncoupling and Nox family nicotinamide adenine dinucleotide phosphate oxidases," *Basic & Clinical Pharmacology & Toxicology*, vol. 110, no. 1, pp. 87–94, 2012.

[33] S. Luo, H. Lei, H. Qin, and Y. Xia, "Molecular mechanisms of endothelial NO synthase uncoupling," *Current Pharmaceutical Design*, vol. 20, no. 22, pp. 3548–3553, 2014.

[34] T. Munzel, A. Daiber, V. Ullrich, and A. Mulsch, "Vascular consequences of endothelial nitric oxide synthase uncoupling for the activity and expression of the soluble guanylyl cyclase and the cGMP-dependent protein kinase," *Arteriosclerosis, Thrombosis, and Vascular Biology*, vol. 25, no. 8, pp. 1551–1557, 2005.

[35] U. Forstermann and T. Munzel, "Endothelial nitric oxide synthase in vascular disease," *Circulation*, vol. 113, no. 13, pp. 1708–1714, 2006.

[36] U. Förstermann and W. C. Sessa, "Nitric oxide synthases: regulation and function," *European Heart Journal*, vol. 33, no. 7, pp. 829–837, 2012.

[37] S. A. Sanders, R. Eisenthal, and R. Harrison, "NADH oxidase activity of human xanthine oxidoreductase–generation of superoxide anion," *European Journal of Biochemistry*, vol. 245, no. 3, pp. 541–548, 1997.

[38] T. J. Guzik, N. E. West, E. Black et al., "Vascular superoxide production by NAD (P) H oxidase: association with endothelial dysfunction and clinical risk factors," *Circulation Research*, vol. 86, no. 9, pp. E85–E90, 2000.

[39] J. B. Laursen, S. Rajagopalan, Z. Galis, M. Tarpey, B. A. Freeman, and D. G. Harrison, "Role of superoxide in angiotensin II–induced but not catecholamine-induced hypertension," *Circulation*, vol. 95, no. 3, pp. 588–593, 1997.

[40] K. Nakazono, N. Watanabe, K. Matsuno, J. Sasaki, T. Sato, and M. Inoue, "Does superoxide underlie the pathogenesis of hypertension?," *Proceedings of the National Academy of Sciences*, vol. 88, no. 22, pp. 10045–10048, 1991.

[41] H. Suzuki, A. Swei, B. W. Zweifach, and G. W. Schmid-Schonbein, "In vivo evidence for microvascular oxidative stress in spontaneously hypertensive rats: hydroethidine microfluorography," *Hypertension*, vol. 25, no. 5, pp. 1083–1089, 1995.

[42] Y. Ohara, T. E. Peterson, and D. G. Harrison, "Hypercholesterolemia increases endothelial superoxide anion production," *The Journal of Clinical Investigation*, vol. 91, no. 6, pp. 2546–2551, 1993.

[43] S. Kerr, M. J. Brosnan, M. McIntyre, J. L. Reid, A. F. Dominiczak, and C. A. Hamilton, "Superoxide anion production is increased in a model of genetic hypertension: role of the endothelium," *Hypertension*, vol. 33, no. 6, pp. 1353–1358, 1999.

[44] T. Heitzer, C. Brockhoff, B. Mayer et al., "Tetrahydrobiopterin improves endothelium-dependent vasodilation in chronic smokers: evidence for a dysfunctional nitric oxide synthase," *Circulation Research*, vol. 86, no. 2, pp. E36–E41, 2000.

[45] M. A. Incalza, R. D'Oria, A. Natalicchio, S. Perrini, L. Laviola, and F. Giorgino, "Oxidative stress and reactive oxygen species in endothelial dysfunction associated with cardiovascular and metabolic diseases," *Vascular Pharmacology*, vol. 100, pp. 1–19, 2018.

[46] U. Förstermann, "Nitric oxide and oxidative stress in vascular disease," *Pflügers Archiv - European Journal of Physiology*, vol. 459, no. 6, pp. 923–939, 2010.

[47] P. Sima, L. Vannucci, and V. Vetvicka, "Atherosclerosis as autoimmune disease," *Annals of Translational Medicine*, vol. 6, no. 7, 2018.

[48] K. Malekmohammad, R. D. E. Sewell, and M. Rafieian-Kopaei, "Antioxidants and atherosclerosis: mechanistic aspects," *Biomolecules*, vol. 9, no. 8, 2019.

[49] A. J. Kattoor, A. Goel, and J. L. Mehta, "LOX-1: regulation, signaling and its role in atherosclerosis," *Antioxidants*, vol. 8, no. 7, 2019.

[50] H. L. Yeh, L. T. Kuo, F. C. Sung, and C. C. Yeh, "Association between polymorphisms of antioxidant gene (MnSOD, CAT, and GPx1) and risk of coronary artery disease," *BioMed Research International*, vol. 2018, Article ID 5086869, 8 pages, 2018.

[51] M. Tibaut and D. Petrovi|, "Oxidative stress genes, antioxidants and coronary artery disease in type 2 diabetes mellitus," *Cardiovascular & Hematological Agents in Medicinal Chemistry*, vol. 14, no. 1, pp. 23–38, 2016.

[52] W. Peng, G. Cai, Y. Xia et al., "Mitochondrial dysfunction in atherosclerosis," *DNA and Cell Biology*, vol. 38, no. 7, pp. 597–606, 2019.

[53] E. Yu, P. A. Calvert, J. R. Mercer et al., "Mitochondrial DNA damage can promote atherosclerosis independently of reactive oxygen species through effects on smooth muscle cells and monocytes and correlates with higher-risk plaques in humans," *Circulation*, vol. 128, no. 7, pp. 702–712, 2013.

[54] E. P. K. Yu, J. Reinhold, H. Yu et al., "Mitochondrial respiration is reduced in atherosclerosis, promoting necrotic core formation and reducing relative fibrous cap thickness," *Arteriosclerosis, Thrombosis, and Vascular Biology*, vol. 37, no. 12, pp. 2322–2332, 2017.

[55] S. Y. Ahn, Y. S. Choi, H. J. Koo et al., "Mitochondrial dysfunction enhances the migration of vascular smooth muscles cells via suppression of Akt phosphorylation," *Biochimica et Biophysica Acta*, vol. 1800, no. 3, pp. 275–281, 2010.

[56] Z. Zhang, P. Meng, Y. Han et al., "Mitochondrial DNA-LL-37 complex promotes atherosclerosis by escaping from autophagic recognition," *Immunity*, vol. 43, no. 6, pp. 1137–1147, 2015.

[57] D. A. Chistiakov, T. P. Shkurat, A. A. Melnichenko, A. V. Grechko, and A. N. Orekhov, "The role of mitochondrial dysfunction in cardiovascular disease: a brief review," *Annals of Medicine*, vol. 50, no. 2, pp. 121–127, 2018.

[58] C. Ruan, "Endothelial progenitor cells and atherosclerosis," *Frontiers in Bioscience*, vol. 18, no. 4, pp. 1194–1201, 2013.

[59] L. Virag, "Structure and function of poly (ADP-ribose) polymerase-1: role in oxidative stress-related pathologies," *Current Vascular Pharmacology*, vol. 3, no. 3, pp. 209–214, 2005.

[60] X. Le Guezennec, A. Brichkina, Y. F. Huang, E. Kostromina, W. Han, and D. V. Bulavin, "Wip1-dependent regulation of

autophagy, obesity, and atherosclerosis," *Cell Metabolism*, vol. 16, no. 1, pp. 68–80, 2012.

[61] I. Perrotta and S. Aquila, "The role of oxidative stress and autophagy in atherosclerosis," *Oxidative Medicine and Cellular Longevity*, vol. 2015, Article ID 130315, 10 pages, 2015.

[62] M. A. Kluge, J. L. Fetterman, and J. A. Vita, "Mitochondria and endothelial function," *Circulation Research*, vol. 112, no. 8, pp. 1171–1188, 2013.

[63] A. Plüddemann, C. Neyen, and S. Gordon, "Macrophage scavenger receptors and host-derived ligands," *Methods*, vol. 43, no. 3, pp. 207–217, 2007.

[64] V. V. Kunjathoor, M. Febbraio, E. A. Podrez et al., "Scavenger receptors class A-I/II and CD36 are the principal receptors responsible for the uptake of modified low density lipoprotein leading to lipid loading in macrophages," *The Journal of Biological Chemistry*, vol. 277, no. 51, pp. 49982–49988, 2002.

[65] M. F. Linton and S. Fazio, "Class A scavenger receptors, macrophages, and atherosclerosis," *Current Opinion in Lipidology*, vol. 12, no. 5, pp. 489–495, 2001.

[66] S. Nozaki, H. Kashiwagi, S. Yamashita et al., "Reduced uptake of oxidized low density lipoproteins in monocyte-derived macrophages from CD36-deficient subjects," *Journal of Clinical Investigation*, vol. 96, no. 4, pp. 1859–1865, 1995.

[67] M. H. Roshan, A. Tambo, and N. P. Pace, "The role of TLR2, TLR4, and TLR9 in the pathogenesis of atherosclerosis," *International Journal of Inflammation*, vol. 2016, Article ID 1532832, 11 pages, 2016.

[68] J. E. Cole, E. Georgiou, and C. Monaco, "The expression and functions of toll-like receptors in atherosclerosis," *Mediators of Inflammation*, vol. 2010, Article ID 393946, 18 pages, 2010.

[69] S. Ghosh, M. J. May, and E. B. Kopp, "NF-κB and rel proteins: evolutionarily conserved mediators of immune responses," *Annual Review of Immunology*, vol. 16, no. 1, pp. 225–260, 1998.

[70] L. Yang and C. Gao, "MiR-590 Inhibits endothelial cell apoptosis by inactivating the TLR4/NF-κB pathway in atherosclerosis," *Yonsei Medical Journal*, vol. 60, no. 3, pp. 298–307, 2019.

[71] K. W. Howell, X. Meng, D. A. Fullerton, C. Jin, T. B. Reece, and J. C. Cleveland, "Toll-like receptor 4 mediates oxidized LDL-induced macrophage differentiation to foam cells," *Journal of Surgical Research*, vol. 171, no. 1, pp. e27–e31, 2011.

[72] Y. Ishikawa, M. Satoh, T. Itoh, Y. Minami, Y. Takahashi, and M. Akamura, "Local expression of Toll-like receptor 4 at the site of ruptured plaques in patients with acute myocardial infarction," *Clinical Science*, vol. 115, no. 4, pp. 133–140, 2008.

[73] S. Gargiulo, P. Gamba, G. Testa et al., "Relation between TLR4/NF-κB signaling pathway activation by 27-hydroxycholesterol and 4-hydroxynonenal, and atherosclerotic plaque instability," *Aging Cell*, vol. 14, no. 4, pp. 569–581, 2015.

[74] Y. I. Miller, S. Viriyakosol, C. J. Binder, J. R. Feramisco, T. N. Kirkland, and J. L. Witztum, "Minimally modified LDL binds to CD14, induces macrophage spreading via TLR4/MD-2, and inhibits phagocytosis of apoptotic cells," *The Journal of Biological Chemistry*, vol. 278, no. 3, pp. 1561–1568, 2003.

[75] P. Prakash, P. Kulkarni, S. R. Lentz, and A. K. Chauhan, "Cellular fibronectin containing extra domain A promotes arterial thrombosis in mice through platelet Toll-like receptor 4," *Blood*, vol. 125, no. 20, pp. 3164–3172, 2015.

[76] P. M Bhatt, "Increased Wnt5a mRNA expression in advanced atherosclerotic lesions, and oxidized LDL treated human monocyte-derived macrophages," *The Open Circulation and Vascular Journal*, vol. 5, no. 1, pp. 1–7, 2012.

[77] I. Ackers, C. Szymanski, K. J. Duckett, K. McCall, and R. Malgor, "Wnt 5a signaling in atherosclerosis, its effect on OxLDL uptake and foam cell differentiation," *The FASEB Journal*, vol. 29, supplement 1, 2015.

[78] R. Sorrentino, S. Morello, E. Bonavita, and A. Pinto, "The activation of liver X receptors inhibits toll-like receptor-9-induced foam cell formation," *Journal of Cellular Physiology*, vol. 223, no. 1, 2009.

[79] A. L. Durham, M. Y. Speer, M. Scatena, C. M. Giachelli, and C. M. Shanahan, "Role of smooth muscle cells in vascular calcification: implications in atherosclerosis and arterial stiffness," *Cardiovascular Research*, vol. 114, no. 4, pp. 590–600, 2018.

[80] C. Rocca, T. Pasqua, L. Boukhzar, Y. Anouar, and T. Angelone, "Progress in the emerging role of selenoproteins in cardiovascular disease: focus on endoplasmic reticulum-resident selenoproteins," *Cellular and Molecular Life Sciences*, vol. 76, no. 20, pp. 3969–3985, 2019.

[81] H. Liu, H. Xu, and K. Huang, "Selenium in the prevention of atherosclerosis and its underlying mechanisms," *Metallomics*, vol. 9, no. 1, pp. 21–37, 2017.

[82] F. Ursini, M. Maiorino, R. Brigelius-Flohé et al., "[5] Diversity of glutathione peroxidases," *Methods in Enzymology*, vol. 252, pp. 38–53, 1995.

[83] T. Suzuki, V. P. Kelly, H. Motohashi et al., "Deletion of the selenocysteine tRNA gene in macrophages and liver results in compensatory gene induction of cytoprotective enzymes by Nrf2," *The Journal of Biological Chemistry*, vol. 283, no. 4, pp. 2021–2030, 2008.

[84] M. Conrad, "Transgenic mouse models for the vital selenoenzymes cytosolic thioredoxin reductase, mitochondrial thioredoxin reductase and glutathione peroxidase 4," *Biochimica et Biophysica Acta*, vol. 1790, no. 11, pp. 1575–1585, 2009.

[85] K. Casós, M. C. Zaragozá, N. Zarkovic et al., "A fish oil-rich diet reduces vascular oxidative stress in apoE–/–mice," *Free Radical Research*, vol. 44, no. 7, pp. 821–829, 2010.

[86] M. Penumetcha, M. Song, N. Merchant, and S. Parthasarathy, "Pretreatment with n-6 PUFA protects against subsequent high fat diet induced atherosclerosis–potential role of oxidative stress-induced antioxidant defense," *Atherosclerosis*, vol. 220, no. 1, pp. 53–58, 2012.

[87] R. A. Siddiqui, K. A. Harvey, N. Ruzmetov, S. J. Miller, and G. P. Zaloga, "n-3 fatty acids prevent whereastrans-fatty acids induce vascular inflammation and sudden cardiac death," *The British Journal of Nutrition*, vol. 102, no. 12, pp. 1811–1819, 2009.

[88] L. T. Meital, M. T. Windsor, M. Perissiou et al., "Omega-3 fatty acids decrease oxidative stress and inflammation in macrophages from patients with small abdominal aortic aneurysm," *Scientific Reports*, vol. 9, no. 1, article 12978, 2019.

[89] A. Ishikado, K. Morino, Y. Nishio et al., "4-Hydroxy hexenal derived from docosahexaenoic acid protects endothelial cells via Nrf2 activation," *PLoS One*, vol. 8, no. 7, article e69415, 2013.

[90] E. J. Anderson, K. Thayne, M. Harris, K. Carraway, and S. R. Shaikh, "Aldehyde stress and up-regulation of Nrf2-mediated antioxidant systems accompany functional adaptations in cardiac mitochondria from mice fed n−3 polyunsaturated fatty acids," *The Biochemical Journal*, vol. 441, no. 1, pp. 359–366, 2012.

[91] Y. C. Yang, C. K. Lii, Y. L. Wei et al., "Docosahexaenoic acid inhibition of inflammation is partially via cross-talk between Nrf2/heme oxygenase 1 and IKK/NF-κB pathways," *The Journal of Nutritional Biochemistry*, vol. 24, no. 1, pp. 204–212, 2013.

[92] D. Y. Oh, S. Talukdar, E. J. Bae et al., "GPR120 is an omega-3 fatty acid receptor mediating potent anti-inflammatory and insulin-sensitizing effects," *Cell*, vol. 142, no. 5, pp. 687–698, 2010.

[93] J. G. Farías, C. Carrasco-Pozo, R. Carrasco Loza et al., "Polyunsaturated fatty acid induces cardioprotection against ischemia-reperfusion through the inhibition of NF-kappaB and induction of Nrf2," *Experimental Biology and Medicine*, vol. 242, no. 10, pp. 1104–1114, 2016.

[94] J. D. Morrow, J. A. Awad, H. J. Boss, I. A. Blair, and L. J. Roberts, "Non-cyclooxygenase-derived prostanoids (F2-isoprostanes) are formed in situ on phospholipids," *Proceedings of the National Academy of Sciences of the United States of America*, vol. 89, no. 22, pp. 10721–10725, 1992.

[95] M. Di Nunzio, V. Valli, and A. Bordoni, "PUFA and oxidative stress. Differential modulation of the cell response by DHA," *International Journal of Food Sciences and Nutrition*, vol. 67, no. 7, pp. 834–843, 2016.

[96] S. O'Farrell and M. J. Jackson, "Dietary polyunsaturated fatty acids, vitamin E and hypoxia/reoxygenation- induced damage to cardiac tissue," *Clinica Chimica Acta*, vol. 267, no. 2, pp. 197–211, 1997.

[97] E. Naik and V. M. Dixit, "Mitochondrial reactive oxygen species drive proinflammatory cytokine production," *The Journal of Experimental Medicine*, vol. 208, no. 3, pp. 417–420, 2011.

[98] J. R. Mercer, E. Yu, N. Figg et al., "The mitochondria-targeted antioxidant MitoQ decreases features of the metabolic syndrome in $ATM^{+/-}/ApoE^{-/-}$ mice," *Free Radical Biology and Medicine*, vol. 52, no. 5, pp. 841–849, 2012.

[99] Y. Wang, L. Li, W. Zhao et al., "Targeted therapy of atherosclerosis by a broad-spectrum reactive oxygen species scavenging nanoparticle with intrinsic anti-inflammatory activity," *ACS Nano*, vol. 12, no. 9, pp. 8943–8960, 2018.

[100] K. J. Williams and E. A. Fisher, "Oxidation, lipoproteins, and atherosclerosis: which is wrong, the antioxidants or the theory?," *Current Opinion in Clinical Nutrition and Metabolic Care*, vol. 8, no. 2, pp. 139–146, 2005.

[101] A. O. Kadlec, D. S. Chabowski, K. Ait-Aissa, and D. D. Gutterman, "Role of PGC-1α in vascular regulation," *Arteriosclerosis, Thrombosis, and Vascular Biology*, vol. 36, no. 8, pp. 1467–1474, 2016.

[102] S. Stein, C. Lohmann, C. Handschin et al., "ApoE−/− PGC-1α−/− mice display reduced IL-18 levels and do not develop enhanced atherosclerosis," *PLoS One*, vol. 5, article e13539, no. 10, 2010.

[103] K. H. Chen, X. Guo, D. Ma et al., "Dysregulation of HSG triggers vascular proliferative disorders," *Nature Cell Biology*, vol. 6, no. 9, pp. 872–883, 2004.

[104] X. Guo, K.-H. Chen, Y. Guo, H. Liao, J. Tang, and R.-P. Xiao, "Mitofusin 2 triggers vascular smooth muscle cell apoptosis via mitochondrial death pathway," *Circulation Research*, vol. 101, no. 11, pp. 1113–1122, 2007.

[105] C. Kunsch and R. M. Medford, "Oxidative stress as a regulator of gene expression in the vasculature," *Circulation Research*, vol. 85, no. 8, pp. 753–766, 1999.

[106] N. R. Madamanchi, S.-K. Moon, Z. S. Hakim et al., "Differential activation of mitogenic signaling pathways in aortic smooth muscle cells deficient in superoxide dismutase isoforms," *Arteriosclerosis, Thrombosis, and Vascular Biology*, vol. 25, no. 5, pp. 950–956, 2005.

[107] A. K. Shrivastava, H. V. Singh, A. Raizada, and S. K. Singh, "C-reactive protein, inflammation and coronary heart disease," *The Egyptian Heart Journal*, vol. 67, no. 2, pp. 89–97, 2015.

[108] T. Wronska-Nofer, J.-R. Nofer, J. Stetkiewicz et al., "Evidence for oxidative stress at elevated plasma thiol levels in chronic exposure to carbon disulfide ($CS_2$) and coronary heart disease," *Nutrition, Metabolism and Cardiovascular Diseases*, vol. 17, no. 7, pp. 546–553, 2007.

[109] X. Yang, T. He, S. Han et al., "The role of traditional chinese medicine in the regulation of oxidative stress in treating coronary heart disease," *Oxidative Medicine and Cellular Longevity*, vol. 2019, Article ID 3231424, 13 pages, 2019.

[110] J. A. Leopold and J. Loscalzo, "Oxidative risk for atherothrombotic cardiovascular disease," *Free Radical Biology and Medicine*, vol. 47, no. 12, pp. 1673–1706, 2009.

[111] A. C. Roberts and K. E. Porter, "Cellular and molecular mechanisms of endothelial dysfunction in diabetes," *Diabetes & Vascular Disease Research*, vol. 10, no. 6, pp. 472–482, 2013.

[112] A. Bastani, S. Rajabi, A. Daliran, H. Saadat, and F. Karimi-Busheri, "Oxidant and antioxidant status in coronary artery disease," *Biomedical Reports*, vol. 9, no. 4, pp. 327–332, 2018.

[113] J. El-Benna, P. M.-C. Dang, and M.-A. Gougerot-Pocidalo, "Priming of the neutrophil NADPH oxidase activation: role of p47phox phosphorylation and NOX2 mobilization to the plasma membrane," *Seminars in Immunopathology*, vol. 30, no. 3, pp. 279–289, 2008.

[114] J. Zhang, M. Wang, Z. Li et al., "NADPH oxidase activation played a critical role in the oxidative stress process in stable coronary artery disease," *American Journal of Translational Research*, vol. 8, no. 12, pp. 5199–5210, 2016.

[115] Y. Gramlich, A. Daiber, K. Buschmann et al., "Oxidative stress in cardiac tissue of patients undergoing coronary artery bypass graft surgery: the effects of overweight and obesity," *Oxidative Medicine and Cellular Longevity*, vol. 2018, Article ID 6598326, 13 pages, 2018.

[116] S. A. Oakes and F. R. Papa, "The role of endoplasmic reticulum stress in human pathology," *Annual Review of Pathology*, vol. 10, no. 1, pp. 173–194, 2015.

[117] T. A. Seimon, M. J. Nadolski, X. Liao et al., "Atherogenic lipids and lipoproteins trigger CD36-TLR2-dependent apoptosis in macrophages undergoing endoplasmic reticulum stress," *Cell Metabolism*, vol. 12, no. 5, pp. 467–482, 2010.

[118] S. Wang, P. Binder, Q. Fang et al., "Endoplasmic reticulum stress in the heart: insights into mechanisms and drug targets," *British Journal of Pharmacology*, vol. 175, no. 8, pp. 1293–1304, 2018.

[119] O. Yamaguchi, Y. Higuchi, S. Hirotani et al., "Targeted deletion of apoptosis signal-regulating kinase 1 attenuates left ventricular remodeling," *Proceedings of the National Academy of Sciences of the United States of America*, vol. 100, no. 26, pp. 15883–15888, 2011.

[120] Z. Qi and L. Chen, "Endoplasmic Reticulum Stress and Autophagy," *Advances in Experimental Medicine and Biology*, vol. 1206, pp. 167–177, 2019.

[121] L. Cominacini, C. Mozzini, U. Garbin et al., "Endoplasmic reticulum stress and Nrf2 signaling in cardiovascular diseases," *Free Radical Biology and Medicine*, vol. 88, no. Part B, pp. 233–242, 2015.

[122] J. E. Barbosa, M. B. Stockler-Pinto, B. O. da Cruz et al., "Nrf2, NF-$\kappa$B and PPAR$\beta/\delta$ mRNA expression profile in patients with coronary artery disease," *Arquivos Brasileiros de Cardiologia*, vol. 113, no. 6, pp. 1121–1127, 2019.

[123] C. Mozzini, A. F. Pasini, U. Garbin et al., "Increased endoplasmic reticulum stress and Nrf2 repression in peripheral blood mononuclear cells of patients with stable coronary artery disease," *Free Radical Biology and Medicine*, vol. 68, pp. 178–185, 2014.

[124] H. Zhu, Z. Jia, L. Zhang et al., "Antioxidants and phase 2 enzymes in macrophages: regulation by Nrf2 signaling and protection against oxidative and electrophilic stress," *Experimental Biology and Medicine*, vol. 233, no. 4, pp. 463–474, 2008.

[125] A. J. Collins, R. N. Foley, B. Chavers et al., "United States Renal Data System 2011 Annual Data Report: Atlas of chronic kidney disease & end-stage renal disease in the United States," *American Journal of Kidney Diseases*, vol. 59, no. 1, 2012Supplement 1, 2012.

[126] S. Visvikis-Siest, J.-B. Marteau, A. Samara, H. Berrahmoune, B. Marie, and M. Pfister, "Peripheral blood mononuclear cells (PBMCs): a possible model for studying cardiovascular biology systems," *Clinical Chemistry and Laboratory Medicine*, vol. 45, no. 9, pp. 1154–1168, 2007.

[127] E. Shantsila, T. Watson, and G. Y. Lip, "Endothelial progenitor cells in cardiovascular disorders," *Journal of the American College of Cardiology*, vol. 49, pp. 741–752, 2007.

[128] T. Watson, P. K. Y. Goon, and G. Y. H. Lip, "Endothelial progenitor cells, endothelial dysfunction, inflammation, and oxidative stress in hypertension," *Antioxidants & Redox Signaling*, vol. 10, no. 6, pp. 1079–1088, 2008.

[129] G. Ndrepepa, "Myeloperoxidase – a bridge linking inflammation and oxidative stress with cardiovascular disease," *Clinica Chimica Acta*, vol. 493, pp. 36–51, 2019.

[130] F. Nielsen, B. B. Mikkelsen, J. B. Nielsen, H. R. Andersen, and P. Grandjean, "Plasma malondialdehyde as biomarker for oxidative stress: reference interval and effects of life-style factors," *Clinical Chemistry*, vol. 43, no. 7, pp. 1209–1214, 1997.

[131] U. Mutlu-Türkoğlu, Z. Akalin, E. Ilhan et al., "Increased plasma malondialdehyde and protein carbonyl levels and lymphocyte DNA damage in patients with angiographically defined coronary artery disease," *Clinical Biochemistry*, vol. 38, no. 12, pp. 1059–1065, 2005.

[132] S. Abolhasani, S. V. Shahbazloo, H. M. Saadati, N. Mahmoodi, and N. Khanbabaei, "Evaluation of serum levels of inflammation, fibrinolysis and oxidative stress markers in coronary artery disease prediction: a cross-sectional study," *Arquivos Brasileiros de Cardiologia*, vol. 113, 2019.

[133] M. Yılmaz, C. Altın, A. Özyıldız, and H. Müderrisoğlu, "Are oxidative stress markers helpful for diagnosing the disease and determining its complexity or extent in patients with stable coronary artery disease?," *Türk Kardiyoloji Derneği Arşivi*, vol. 45, no. 7, pp. 599–605, 2017.

[134] M. Ghaffarzadeh, H. Ghaedi, B. Alipoor et al., "Association of MiR-149 (RS2292832) Variant with the Risk of Coronary Artery Disease," *Journal of Medical Biochemistry*, vol. 36, no. 3, pp. 251–258, 2017.

[135] P. Manuneedhi Cholan, S. P. Cartland, L. Dang et al., "TRAIL protects against endothelial dysfunction in vivo and inhibits angiotensin-II-induced oxidative stress in vascular endothelial cells in vitro," *Free Radical Biology and Medicine*, vol. 126, pp. 341–349, 2018.

[136] A. R. Abaspour, M. Taghikhani, S. M. R. Parizadeh et al., "HSP27 expression in the human peripheral blood mononuclear cells as an early prognostic biomarker in coronary artery disease patients," *Diabetes and Metabolic Syndrome: Clinical Research and Reviews*, vol. 13, no. 3, pp. 1791–1795, 2019.

[137] N. Khaper, K. Kaur, T. Li, F. Farahmand, and P. Singal, "Antioxidant enzyme gene expression in congestive heart failure following myocardial infarction," *Molecular and Cellular Biochemistry*, vol. 251, pp. 9–15, 2003.

[138] X. Li, L. Hou, Z. Cheng, S. Zhou, J. Qi, and J. Cheng, "Overexpression of GAS5 inhibits abnormal activation of Wnt/$\beta$-catenin signaling pathway in myocardial tissues of rats with coronary artery disease," *Journal of Cellular Physiology*, vol. 234, no. 7, pp. 11348–11359, 2019.

[139] X. B. Wang, N. H. Cui, S. Zhang, Z. J. Liu, and J. F. Ma, "Leukocyte telomere length, mitochondrial DNA copy number, and coronary artery disease risk and severity: a two-stage case-control study of 3064 Chinese subjects," *Atherosclerosis*, vol. 284, pp. 165–172, 2019.

[140] I. Sarutipaiboon, N. Settasatian, N. Komanasin, U. Kukongwiriyapan, K. Sawanyawisuth, and P. Intraraphet, "Association of genetic variations in NRF2, NQO1, HMOX1, and MT with severity of coronary artery disease and related risk factors," *Cardiovascular Toxicology*, vol. 20, no. 2, pp. 176–189, 2020.

[141] Y. Xiao, J. Xia, J. Cheng, H. Huang, and Y. Zhou, "Inhibition of S-adenosylhomocysteine hydrolase induces endothelial dysfunction via epigenetic regulation of p66shc-mediated oxidative stress pathway," *Circulation*, vol. 139, no. 19, pp. 2260–2277, 2019.

[142] M. V. Jorat, R. Tabrizi, F. Kolahdooz, M. Akbari, and M. Salami, "The effects of coenzyme Q10 supplementation on biomarkers of inflammation and oxidative stress in among coronary artery disease: a systematic review and meta-analysis of randomized controlled trials," *Inflammopharmacology*, vol. 27, no. 2, pp. 233–248, 2019.

[143] B. J. Lee, J. S. Lin, Y. C. Lin, and P. T. Lin, "Effects of L-carnitine supplementation on oxidative stress and antioxidant enzymes activities in patients with coronary artery disease: a randomized, placebo-controlled trial," *Nutrition Journal*, vol. 13, no. 1, 2014.

[144] A. R. Guby, "Nutrition treatments for acute myocardial infarction," *Alternative Medicine Review*, vol. 15, pp. 113–123, 2010.

[145] Z. Zhang, F. Jiang, L. Zeng, X. Wang, and S. Tu, "PHACTR1 regulates oxidative stress and inflammation to coronary artery endothelial cells via interaction with NF-$\kappa$B/p65," *Atherosclerosis*, vol. 278, pp. 180–189, 2018.

[146] M. J. Zarzuelo, R. Lopez-Sepulveda, M. Sanchez et al., "SIRT1 inhibits NADPH oxidase activation and protects endothelial function in the rat aorta: implications for vascular aging," *Biochemical Pharmacology*, vol. 85, no. 9, pp. 1288–1296, 2013.

[147] C. H. Hung, S. H. Chan, P. M. Chu, and K. L. Tsai, "Homocysteine facilitates LOX-1 activation and endothelial death through the PKC$\beta$ and SIRT1/HSF1 mechanism: relevance to human hyperhomocysteinaemia," *Clinical Science*, vol. 129, no. 6, pp. 477–487, 2015.

[148] S. H. Chan, C. H. Hung, J. Y. Shih et al., "SIRT1 inhibition causes oxidative stress and inflammation in patients with coronary artery disease," *Redox Biology*, vol. 13, pp. 301–309, 2017.

[149] V. R. Taqueti and M. F. Di Carli, "Coronary microvascular disease pathogenic mechanisms and therapeutic options: JACC state-of-the-art review," *Journal of the American College of Cardiology*, vol. 72, no. 21, pp. 2625–2641, 2018.

[150] T. Padro, O. Manfrini, R. Bugiardini et al., "ESC working group on coronary pathophysiology and microcirculation position paper on 'coronary microvascular dysfunction in cardiovascular disease'," *Cardiovascular Research*, vol. 116, no. 4, pp. 741–755, 2020.

[151] G. Niccoli, G. Scalone, and F. Crea, "Acute myocardial infarction with no obstructive coronary atherosclerosis: mechanisms and management," *European Heart Journal*, vol. 36, no. 8, pp. 475–481, 2015.

[152] F. Crea, P. G. Camici, and C. N. Bairey Merz, "Coronary microvascular dysfunction: an update," *European Heart Journal*, vol. 35, pp. 1101–1111, 2014.

[153] N. R. Smilowitz, A. M. Mahajan, M. T. Roe et al., "Mortality of myocardial infarction by sex, age, and obstructive coronary artery disease status in the ACTION Registry–GWTG (Acute Coronary Treatment and Intervention Outcomes Network Registry–Get With the Guidelines)," *Circulation Cardiovascular Quality and Outcomes*, vol. 10, article e003443, 2017.

[154] S. M. Bradley, T. M. Maddox, M. A. Stanislawski et al., "Normal coronary rates for elective angiography in the Veterans Affairs Healthcare System: insights from the VA CART program (veterans affairs clinical assessment reporting and tracking)," *Journal of the American College of Cardiology*, vol. 63, pp. 417–426.10, 2014.

[155] L. Jespersen, A. Hvelplund, S. Z. Abildstrom et al., "Stable angina pectoris with no obstructive coronary artery disease is associated with increased risks of major adverse cardiovascular events," *European Heart Journal*, vol. 33, pp. 734–744, 2012.

[156] B. Sharaf, T. Wood, L. Shaw et al., "Adverse outcomes among women presenting with signs and symptoms of ischemia and no obstructive coronary artery disease: findings from the National Heart, Lung, and Blood Institute–sponsored Women's Ischemia Syndrome Evaluation (WISE) angiographic core laboratory," *American Heart Journal*, vol. 166, pp. 134–141, 2013.

[157] P. Meier, S. Gloekler, R. Zbinden et al., "Beneficial effect of recruitable collaterals. A 10- year follow-up study in patients with stable coronary artery disease undergoing quantitative collateral measurements," *Circulation*, vol. 116, pp. 975–983, 2007.

[158] P. Elsman, A. W. van't Hof, M. J. de Boer et al., "Role of collateral circulation in the acute phase of ST-segment-elevation myocardial infarction treated with primary coronary intervention," *European Heart Journal*, vol. 25, pp. 854–858, 2004.

[159] J. Loscalzo, "What we know and don't know about Larginine and NO," *Circulation*, vol. 101, pp. 2126–2129, 2000.

[160] I. Tritto and G. Ambrosio, "The multi-faceted behavior of nitric oxide in vascular "inflammation": catchy terminology or true phenomenon?," *Cardiovascular Research*, vol. 63, no. 1, pp. 1–4, 2004.

[161] H. Y. Small, S. Migliarino, M. Czesnikiewicz-Guzik, and T. J. Guzik, "Hypertension: focus on autoimmunity and oxidative stress," *Free Radical Biology and Medicine*, vol. 125, pp. 104–115, 2018.

[162] M. T. Corban, L. O. Lerman, and A. Lerman, "Endothelin-1 in coronary microvascular dysfunction: a potential new therapeutic target once again," *European Heart Journal*, vol. 41, no. 34, pp. 3252–3254, 2020.

[163] D. Bonderman, A. Teml, J. Jakowitsch et al., "Coronary no-reflow is caused by shedding of active tissue factor from dissected atherosclerotic plaque," *Blood*, vol. 99, pp. 2794–2800, 2002.

[164] N. Lim, M. J. Dubois, D. De Backer, and J.-L. Vincent, "Do all nonsurvivors of cardiogenic shock die with a low cardiac index?," *Chest*, vol. 124, no. 5, pp. 1885–1891, 2003.

[165] M. S. Joshi, C. Mineo, P. W. Shaul, and J. A. Bauer, "Biochemical consequences of the NOS3 Glu298Asp variation in human endothelium: altered caveolar localization and impaired response to shear," *The FASEB Journal*, vol. 21, pp. 2655–2663, 2007.

[166] Y. Shimasaki, H. Yasue, M. Yoshimura et al., "Association of the missense Glu298Asp variant of the endothelial nitric oxide synthase gene with myocardial infarction," *Journal of the American College of Cardiology*, vol. 31, no. 7, pp. 1506–1510, 1998.

[167] M. Nakayama, H. Yasue, M. Yoshimura et al., "T −786→C mutation in the 5′-flanking region of the endothelial nitric oxide synthase gene is associated with coronary spasm," *Circulation*, vol. 99, pp. 2864–2870, 1999.

[168] T. J. Ford, D. Corcoran, S. Padmanabhan et al., "Genetic dysregulation of endothelin-1 is implicated in coronary microvascular dysfunction," *European Heart Journal*, vol. 41, no. 34, pp. 3239–3252, 2020.

[169] M. Dorobantu and L. Badimon, *Microcirculation: From Bench to Bedside*, Springer Nature, 2020.

[170] O. Sorop, J. van de Wouw, S. Chandler et al., "Experimental animal models of coronary microvascular dysfunction," *Cardiovascular Research*, vol. 116, no. 4, pp. 756–770, 2020.

[171] L. Badimon, R. Bugiardini, E. Cenko et al., "Position paper of the European Society of Cardiology–working group of coronary pathophysiology and microcirculation: obesity and heart disease," *European Heart Journal*, vol. 38, pp. 1951–1958, 2017.

[172] Z. Bagi, A. Feher, and J. Cassuto, "Microvascular responsiveness in obesity: implications for therapeutic intervention," *British Journal of Pharmacology*, vol. 165, pp. 544–560, 2012.

[173] G. Grassi, G. Seravalle, F. Quarti-Trevano et al., "Excessive sympathetic activation in heart failure with obesity and metabolic syndrome: characteristics and mechanisms," *Hypertension*, vol. 49, pp. 535–541, 2007.

[174] S. Kachur, R. Morera, A. D. Schutter, and C. J. Lavie, "Cardiovascular risk in patients with prehypertension and the metabolic syndrome," *Current Hypertension Reports*, vol. 20, p. 15, 2018.

[175] L. Kalinowski, L. W. Dobrucki, M. Szczepanska-Konkel et al., "Third-Generation $\beta$-blockers stimulate nitric oxide release from endothelial cells through ATP Efflux," *Circulation*, vol. 107, pp. 2747–2752, 2003.

[176] E. S. Ford, U. A. Ajani, J. B. Croft et al., "Explaining the decrease in U.S. deaths from coronary disease, 1980-2000," *The New England Journal of Medicine*, vol. 356, pp. 2388–2398, 2007.

[177] M. J. Stampfer, F. B. Hu, J. E. Manson, E. B. Rimm, and W. C. Willett, "Primary Prevention of Coronary Heart Disease in Women through Diet and Lifestyle," *The New England Journal of Medicine*, vol. 343, pp. 16–22, 2000.

[178] J. S. Hill, M. R. Hayden, J. Frohlich, and P. H. Pritchard, "Genetic and environmental factors affecting the incidence of coronary artery disease in heterozygous familial hypercholesterolemia," *Arteriosclerosis and Thrombosis: A Journal of Vascular Biology*, vol. 11, no. 2, pp. 290–297, 1991.

[179] T. Martino, S. Arab, M. Straume et al., "Day/night rhythms in gene expression of the normal murine heart," *Journal of Molecular Medicine*, vol. 82, pp. 256–264, 2004.

[180] P. McNamara, S. B. Seo, R. D. Rudic, A. Sehgal, D. Chakravarti, and G. A. Fitz Gerald, "Regulation of CLOCK and MOP4 by nuclear hormone receptors in the vasculature," *Cell*, vol. 105, pp. 877–889, 2001.

[181] T. A. Martino and M. J. Sole, "Molecular time: an often overlooked dimension to cardiovascular disease," *Circulation Research*, vol. 105, pp. 1047–1061, 2009.

[182] J. E. Muller, P. H. Stone, Z. G. Turi et al., "Circadian variation in the frequency of onset of acute myocardial infarction," *The New England Journal of Medicine*, vol. 313, pp. 1315–1322, 1985.

[183] M. C. Cohen, K. M. Rohtla, C. E. Lavery, J. E. Muller, and M. A. Mittleman, "Meta-analysis of the morning excess of acute myocardial infarction and sudden cardiac death," *The American Journal of Cardiology*, vol. 79, pp. 1512–1516, 1997.

[184] K. L. Knutson, A. M. Ryden, B. A. Mander, and E. Van Cauter, "Role of sleep duration and quality in the risk and severity of type 2 diabetes mellitus," *Archives of Internal Medicine*, vol. 166, pp. 1768–1774, 2006.

[185] N. D. Kohatsu, R. Tsai, T. Young et al., "Sleep duration and body mass index in a rural population," *Archives of Internal Medicine*, vol. 166, pp. 1701–1705, 2006.

[186] J. E. Gangwisch, S. B. Heymsfield, B. Boden-Albala et al., "Short sleep duration as a risk factor for hypertension: analyses of the first National Health and Nutrition Examination Survey," *Hypertension*, vol. 47, pp. 833–839, 2006.

[187] H. Marti-Soler, C. Gubelmann, S. Aeschbacher et al., "Seasonality of cardiovascular risk factors: an analysis including over 230 000 participants in 15 countries," *Heart*, vol. 100, no. 19, pp. 1517–1523, 2014.

[188] P. Tung, S. D. Wiviott, C. P. Cannon, S. A. Murphy, C. H. McCabe, and C. M. Gibson, "Seasonal variation in lipids in patients following acute coronary syndrome on fixed doses of pravastatin (40 mg) or atorvastatin (80 mg) (from the Pravastatin or Atorvastatin Evaluation and Infection Therapy–Thrombolysis In Myocardial Infarction 22 [PROVE IT-TIMI 22] Study)," *The American Journal of Cardiology*, vol. 103, pp. 1056–1060, 2009.

[189] P. M. Laplaud, L. Beaubatie, and D. Maurel, "A spontaneously seasonal hyper-cholesterolemic animal: plasma lipids and lipoproteins in the European badger (Meles meles L.)," *Journal of Lipid Research*, vol. 21, pp. 724–738, 1980.

[190] B. Marchant, K. Ranjadayalan, R. Stevenson, P. Wilkinson, and A. D. Timmis, "Circadian and seasonal factors in the pathogenesis of acute myocar-dial infarction: the influence of environmental temperature," *British Heart Journal*, vol. 69, pp. 385–387, 1993.

[191] D. R. Gold and M. A. Mittleman, "New insights into pollution and the cardiovascular system: 2010 to 2012," *Circulation*, vol. 127, pp. 1903–1913, 2013.

[192] L. Yang, M. Lof, M. B. Veierød, S. Sandin, H. O. Adami, and E. Weiderpass, "Ultraviolet exposure and mortality among women in Sweden," *Cancer Epidemiology, Biomarkers & Prevention*, vol. 20, pp. 683–690, 2011.

[193] P. G. Lindqvist, E. Epstein, K. Nielsen, M. Landin-Olsson, C. Ingvar, and H. Olsson, "Avoidance of sun exposure as a risk factor for major causes of death: a competing risk analysis of the Melanoma in Southern Sweden cohort," *Journal of Internal Medicine*, vol. 280, pp. 375–387, 2016.

[194] T. J. Wang, "Vitamin D and cardiovascular disease," *Annual Review of Medicine*, vol. 67, pp. 261–272, 2016.

[195] S. Pilz, N. Verheyen, M. R. Grübler, A. Tomaschitz, and W. März, "Vitamin D and cardiovascular disease prevention," *Nature Reviews Cardiology*, vol. 13, pp. 404–417, 2016.

[196] S. De Mendoza, H. Nucete, E. Ineichen, E. Salazar, A. Zerpa, and C. J. Glueck, "Lipids and Lipoproteins in Subjects at 1,000 and 3, 500 Meter Altitudes," *Archives of Environmental Health*, vol. 34, pp. 308–311, 1979.

[197] S. Sharma, "Clinical, biochemical, electrocardiographic and noninvasive hemodynamic assessment of cardiovascular status in natives at high to ex-treme altitudes (3000m-5500m) of the Himalayan region," *Indian Heart Journal*, vol. 42, pp. 375–379, 1990.

[198] S. Mohanna, R. Baracco, and S. Seclén, "Lipid profile, waist circumference, and body mass index in a high altitude population," *High Altitude Medicine & Biology*, vol. 7, pp. 245–255, 2006.

[199] S. Domínguez Coello, A. Cabrera De León, F. Bosa Ojeda, L. I. Pérez Méndez, L. Díaz González, and A. J. Aguirre-Jaime, "High density lipoprotein cholesterol increases with living altitude," *International Journal of Epidemiology*, vol. 29, pp. 65–70, 2000.

[200] A. Cabrera de Leon, D. A. Gonzalez, L. I. Mendez et al., "Leptin and altitude in the cardiovascular diseases," *Obesity Research*, vol. 12, pp. 1492–1498, 2004.

[201] M. F. Holick, T. C. Chen, Z. Lu, and E. Sauter, "Vitamin D and skin physiology: a D-lightful story," *Journal of Bone and Mineral Research*, vol. 22, no. S2, pp. V28–V33, 2007.

[202] P. Dadvand, X. Bartoll, X. Basagaña et al., "Green spaces and General Health: Roles of mental health status, social support, and physical activity," *International Journal of Environmental Research and Public Health*, vol. 14, no. 11, p. 1411, 2017.

[203] P. James, R. F. Banay, J. E. Hart, and F. Laden, "A review of the health benefits of greenness," *Current Epidemiology Reports*, vol. 2, pp. 131–142, 2015.

[204] G. S. Lovasi, J. W. Quinn, K. M. Neckerman, M. S. Perzanowski, and A. Rundle, "Children living in areas with more street trees have lower prevalence of asthma," *Journal of Epidemiology and Community Health*, vol. 62, pp. 647–649, 2008.

[205] I. Markevych, E. Thiering, E. Fuertes et al., "A cross-sectional analysis of the effects of residential greenness on blood pressure in 10-year old children: results from the GINIplus and

LISAplus studies," *BMC Public Health*, vol. 14, article 477, 2014.

[206] B. Chaix, "Geographic life environments and coronary heart disease: a literature review, theoretical contributions, methodological updates, and a research agenda," *Annual Review of Public Health*, vol. 30, pp. 81–105, 2009.

[207] T. Hartung, "Toxicology for the twenty-first century," *Nature*, vol. 460, pp. 208–212, 2009.

[208] K. E. Cosselman, A. Navas-Acien, and J. D. Kaufman, "Environmental factors in cardiovascular disease," *Nature Reviews. Cardiology*, vol. 12, pp. 627–642, 2015.

[209] A. Bhatnagar, "Environmental cardiology: studying mechanistic links between pollution and heart disease," *Circulation Research*, vol. 99, pp. 692–705, 2006.

[210] R. D. Brook, S. Rajagopalan, C. A. Pope et al., "Particulate matter air pollution and cardiovas-cular disease: an update to the scientific statement from the American Heart Association," *Circulation*, vol. 121, pp. 2331–2378, 2010.

[211] T. Münzel, T. Gori, W. Babisch, and M. Basner, "Cardiovascular effects of envi-ronmental noise exposure," *European Heart Journal*, vol. 35, pp. 829–836, 2014.

[212] M. A. Said and O. A. El-Gohary, "Effect of noise stress on cardiovascular system in adult male albino rat: implication of stress hormones, endothelial dysfunction and oxidative stress," *General Physiology and Biophysics*, vol. 35, pp. 371–377, 2016.

[213] R. E. Schane, P. M. Ling, and S. A. Glantz, "Health effects of light and intermittent smoking: a review," *Circulation*, vol. 121, pp. 1518–1522, 2010.

[214] S. M. Grundy, G. J. Balady, M. H. Criqui et al., "Primary prevention of coronary heart disease: guidance from Framingham: a statement for healthcare professionals from the AHA Task Force on Risk Reduction. American Heart Association," *Circulation*, vol. 97, pp. 1876–1887, 1998.

[215] T. E. O'Toole, D. J. Conklin, and A. Bhatnagar, "Environmental risk factors for heart disease," *Reviews on Environmental Health*, vol. 23, pp. 167–202, 2008.

[216] A. K. Malakar, D. Choudhury, B. Halder, P. Paul, A. Uddin, and S. Chakraborty, "A review on coronary artery disease, its risk factors, and therapeutics," *Journal of Cellular Physiology*, vol. 234, no. 10, pp. 16812–16823, 2019.

[217] S. H. Mudd, F. Skovby, H. L. Levy et al., "The natural history of homocystinuria due tocystathionine $\beta$-synthase deficiency," *American Journal of Human Genetics*, vol. 37, no. 1, pp. 1–31, 1985.

[218] K. S. McCully, "Vascular pathology of homocysteinemia: Implica-tions for the pathogenesis of arteriosclerosis," *The American Journal of Pathology*, vol. 56, no. 1, pp. 111–128, 1969.

[219] M. R. Malinow, "Homocyst(e)ine and arterial occlusive diseases," *Journal of Internal Medicine*, vol. 236, no. 6, pp. 603–617, 1994.

[220] J. Dawson, T. Quinn, and M. Walters, "Uric acid reduction: a new paradigm in the management of cardiovascular risk?," *Current Medicinal Chemistry*, vol. 14, no. 17, pp. 1879–1886, 2007.

[221] T. Montalcini, G. Gorgone, C. Gazzaruso, G. Sesti, F. Perticone, and A. Pujia, "Relation between serum uric acid and carotid intima-media thickness in healthy postmenopausal women," *Internal and Emergency Medicine*, vol. 2, no. 1, pp. 19–23, 2007.

[222] M. Gheorghiade, S. J. Greene, J. Butler et al., "Effect of vericiguat, a soluble guanylate cyclase stimulator, on natriuretic peptide levels in patients with worsening chronic heart failure and reduced ejection fraction," *JAMA*, vol. 314, no. 21, pp. 2251–2262, 2015.

[223] M. D. Flather, M. C. Shibata, A. J. S. Coats et al., "Randomized trial to determine the effect of nebivolol on mortality and cardiovascular hospital admission in elderly patients with heart failure (seniors)," *European Heart Journal*, vol. 26, no. 3, pp. 215–225, 2005.

[224] G. Ambrosio, M. D. Flather, M. Bohm et al., "$\beta$-Blockade with nebivolol for prevention of acute ischaemic events in elderly patients with heart failure," *Heart*, vol. 97, no. 3, pp. 209–214, 2011.

[225] T. Nishikimi, N. Maeda, and H. Matsuoka, "The role of natriuretic peptides in cardioprotection," *Cardiovascular Research*, vol. 69, no. 2, pp. 318–328, 2006.

[226] M. M. JJ, M. Packer, A. S. Desai et al., "Angiotensin-neprilysin inhibition versus enalapril in heart failure," *The New England Journal of Medicine*, vol. 371, no. 11, pp. 993–1004, 2014.

[227] S. D. Solomon, M. Zile, B. Pieske et al., "The angiotensin receptor neprilysin inhibitor LCZ696 in heart failure with preserved ejection fraction: a phase 2 double-blind randomised controlled trial," *The Lancet*, vol. 380, no. 9851, pp. 1387–1395, 2012.

[228] C. Pizzi, O. Manfrini, F. Fontana, and R. Bugiardini, "Angiotensin-converting enzyme inhibitors and 3-hydroxy-3-methylglutaryl coenzyme A reductase in cardiac Syndrome X: role of superoxide dismutase activity," *Circulation*, vol. 109, no. 1, pp. 53–58, 2004.

[229] K. Ohyama, Y. Matsumoto, K. Takanami et al., "Coronary adventitial and perivascular adipose tissue inflammation in patients with vasospastic angina," *Journal of the American College of Cardiology*, vol. 71, no. 4, pp. 414–425, 2018.

[230] S. O. Keli, M. G. Hertog, E. J. Feskens, and D. Kromhout, "Dietary flavonoids, antioxidant vitamins, and incidence of stroke," *Archives of Internal Medicine*, vol. 156, no. 6, pp. 637–642, 1996.

[231] A. R. Ness, J. W. Powles, and K. T. J. Khaw, "Vitamin C and cardiovascular disease: a systematic review," *Cardiovascular Risk*, vol. 3, p. 513, 1996.

[232] H. Wang, G. Cao, and R. L. Prior, "Total Antioxidant Capacity of Fruits," *Journal of Agricultural and Food Chemistry*, vol. 44, no. 3, pp. 701–705, 1996.

[233] W. Kalt, C. F. Forney, A. Martin, and R. L. Prior, "Antioxidant capacity, vitamin C, phenolics, and anthocyanins after fresh storage of small fruits," *Journal of Agricultural and Food Chemistry*, vol. 47, no. 11, pp. 4638–4644, 1999.

[234] S. Sellappan and C. C. Akoh, "Flavonoids and antioxidant capacity of Georgia-grown Vidalia onions," *Journal of Agricultural and Food Chemistry*, vol. 50, no. 19, pp. 5338–5342, 2002.

[235] S. Doré, "Unique properties of polyphenol stilbenes in the brain: more than direct antioxidant actions; gene/protein regulatory activity," *Neurosignals*, vol. 14, no. 1-2, pp. 61–70, 2005.

[236] G. J. Soleas, E. P. Diamandis, and D. M. Goldberg, "Wine as a biological fluid: history, production, and role in disease prevention," *Journal of Clinical Laboratory Analysis*, vol. 11, no. 5, pp. 287–313, 1997.

[237] S. Kuroda, R. Tsuchidate, M.-L. Smith, K. R. Maples, and B. K. Siesjö, "Neuroprotective effects of a novel nitrone, NXY-059, after transient focal cerebral ischemia in the rat," *Journal of Cerebral Blood Flow & Metabolism*, vol. 19, no. 7, pp. 778–787, 1999.

[238] S. G. Sydserff, A. R. Borelli, A. R. Green, and A. J. Cross, "Effect of NXY-059 on infarct volume after transient or permanent middle cerebral artery occlusion in the rat; studies on dose, plasma concentration and therapeutic time window," *British Journal of Pharmacology*, vol. 135, no. 1, pp. 103–112, 2002.

[239] A. S. Antonopoulos, M. Margaritis, S. Verheule et al., "Mutual regulation of epicardial adipose tissue and myocardial redox state by PPAR-$\gamma$/Adiponectin signalling," *Circulation Research*, vol. 118, no. 5, pp. 842–855, 2016.

[240] G. Wójcicka, A. Jamroz-Wiśniewska, P. Atanasova, G. N. Chaldakov, B. Chylińska-Kula, and J. Bełtowski, "Differential effects of statins on endogenous $H_2S$ formation in perivascular adipose tissue," *Pharmacological Research*, vol. 63, no. 1, pp. 68–76, 2011.

[241] A. Samim, L. Nugent, P. K. Mehta, C. Shufelt, and C. N. Bairey Merz, "Treatment of angina and microvascular coronary dysfunction," *Current Treatment Options in Cardiovascular Medicine*, vol. 12, no. 4, pp. 355–364, 2010.

[242] X. Zhang, B. Chen, J. Wu et al., "Aspirin enhances the protection of Hsp 90 from heat-stressed injury in cardiac microvascular endothelial cells Through PI3K-Akt and PKM2 pathways," *Cells*, vol. 9, no. 1, p. 243, 2020.

[243] G. Vilahur, M. Gutiérrez, L. Casani et al., "Protective effects of ticagrelor on myocardial injury after infarction," *Circulation*, vol. 134, no. 22, pp. 1708–1719, 2016.

[244] R. Bugiardini, A. Borghi, A. Pozzati, F. Ottani, G. L. Morgagni, and P. Puddu, "The paradox of nitrates in patients with angina pectoris and angiographically normal coronary arteries," *The American Journal of Cardiology*, vol. 72, no. 3, pp. 343–347, 1993.

[245] A. Lerman, J. C. Burnett, S. T. Higano, L. J. McKinley, and D. R. Holmes, "Long-term l-arginine supplementation improves small-vessel coronary endothelial function in humans," *Circulation*, vol. 97, no. 21, pp. 2123–2128, 1998.

[246] J. Herrmann, J. C. Kaski, and A. Lerman, "Coronary microvascular dysfunction in the clinical setting: from mystery to reality," *European Heart Journal*, vol. 33, no. 22, pp. 2771–2783, 2012.

[247] M. Reriani, E. Raichlin, A. Prasad et al., "Long-term administration of endothelin receptor antagonist improves coronary endothelial function in patients with early atherosclerosis," *Circulation*, vol. 122, no. 10, pp. 958–966, 2010.

[248] S. A. Nasser and M. M. El-Mas, "Endothelin $ET_A$ receptor antagonism in cardiovascular disease," *European Journal of Pharmacology*, vol. 737, pp. 210–213, 2014.

[249] D. Fang, S. Yang, W. Quan, H. Jia, Z. Quan, and Z. Qu, "Atorvastatin suppresses Toll-like receptor 4 expression and NF-$\kappa$B activation in rabbit atherosclerotic plaques," *European Review for Medical and Pharmacological Sciences*, vol. 18, no. 2, pp. 242–246, 2014.

[250] S. Yang, R. Li, L. Tang et al., "TLR4-mediated anti-atherosclerosis mechanisms of angiotensin-converting enzyme inhibitor - Fosinopril," *Cellular Immunology*, vol. 285, no. 1-2, pp. 38–41, 2013.

[251] Y. Takahashi, M. Satoh, Y. Minami, T. Tabuchi, T. Itoh, and M. Nakamura, "Expression of miR-146a/b is associated with the Toll-like receptor 4 signal in coronary artery disease: effect of renin-angiotensin system blockade and statins on miRNA-146a/b and Toll-like receptor 4 levels," *Clinical Science (London, England)*, vol. 119, no. 9, pp. 395–405, 2010.

[252] Y. Ji, J. Liu, Z. Wang, N. Liu, and W. Gou, "PPAR $\gamma$ agonist, rosiglitazone, regulates angiotensin II-induced vascular inflammation through the TLR4-dependent signaling pathway," *Laboratory Investigation*, vol. 89, no. 8, pp. 887–902, 2009.

[253] C.-Z. Wang, Y. Zhang, X.-D. Li et al., "PPAR$\gamma$ agonist suppresses TLR4 expression and TNF-$\alpha$ production in LPS stimulated monocyte leukemia cells," *Cell Biochemistry and Biophysics*, vol. 60, no. 3, pp. 167–172, 2011.

[254] A. E. Ferreira, F. Sisti, F. Sônego et al., "PPAR-$\gamma$/IL-10 axis inhibits MyD88 Expression and ameliorates murine polymicrobial sepsis," *The Journal of Immunology*, vol. 192, no. 5, pp. 2357–2365, 2014.

[255] Y. Xu, Y. Huang, C. Wu, J. Zhang, and Q. Liu, "Effect of carvedilol on cardiomyocyte apoptosis in a rat model of myocardial infarction: a role for toll-like receptor 4," *Indian Journal of Pharmacology*, vol. 45, no. 5, pp. 458–463, 2013.

[256] D. Zhang, Y. Li, Y. Liu, X. Xiang, and Z. Dong, "Paclitaxel ameliorates Lipopolysaccharide-Induced kidney injury by binding myeloid differentiation protein-2 to block Toll-Like receptor 4-mediated nuclear Factor-$\kappa$B activation and cytokine production," *Journal of Pharmacology and Experimental Therapeutics*, vol. 345, no. 1, pp. 69–75, 2013.

[257] K. Lucas and M. Maes, "Role of the Toll Like receptor (TLR) radical cycle in chronic inflammation: possible treatments targeting the TLR4 pathway," *Molecular Neurobiology*, vol. 48, no. 1, pp. 190–204, 2013.

[258] S. J. Jia, P. P. Niu, J. Z. Cong, B. K. Zhang, and M. Zhao, "TLR4 signaling: a potential therapeutic target in ischemic coronary artery disease," *International Immunopharmacology*, vol. 23, no. 1, pp. 54–59, 2014.

[259] K.-L. Tsai, P.-L. Hsieh, W.-C. Chou et al., "IL-20 promotes hypoxia/reoxygenation-induced mitochondrial dysfunction and apoptosis in cardiomyocytes by upregulating oxidative stress by activating the PKC/NADPH oxidase pathway," *Biochimica et Biophysica Acta (BBA)-Molecular Basis of Disease*, vol. 1866, no. 5, p. 165684, 2020.

[260] A. Samakova, A. Gazova, N. Sabova, S. Valaskova, M. Jurikova, and J. Kyselovic, "The pi 3k/Akt pathway is associated with angiogenesis, oxidative stress and survival of mesenchymal stem cells in pathophysiologic condition in ischemia," *Physiological Research*, vol. 68, no. 2, pp. S131–S138, 2019.

[261] A. Friedenstein, R. Chailakhjan, and K. Lalykina, "The development of fibroblast colonies in monolayer cultures of guinea-pig bone marrow and spleen cells," *Cell and Tissue Kinetics*, vol. 3, no. 4, pp. 393–403, 1970.

[262] A. J. Friedenstein, R. K. Chailakhyan, N. V. Latsinik, A. F. Panasyuk, and I. V. Keiliss-Borok, "Stromal cells responsible for transferring the microenvironment of the hemopoietic tissues. Cloning in vitro and retransplantation in vivo," *Transplantation*, vol. 17, no. 4, pp. 331–340, 1974.

[263] S. Rodius, N. de Klein, C. Jeanty et al., "Fisetin protects against cardiac cell death through reduction of ROS production and caspases activity," *Scientific Reports*, vol. 10, no. 1, 2020.

[264] S. Ahmed, N. Ahmed, A. Rungatscher et al., "Cocoa flavonoids reduce inflammation and oxidative stress in a myocardial schemia-reperfusion experimental model," *Antioxidants*, vol. 9, no. 2, p. 167, 2020.

[265] V. K. Verma, S. Malik, E. Mutneja, A. K. Sahu, J. Bhatia, and D. S. Arya, "Attenuation of ROS-mediated myocardial ischemia–reperfusion injury by morin via regulation of RISK/-SAPK pathways," *Pharmacological Reports*, vol. 72, no. 4, pp. 877–889, 2020.

[266] M. Z. Syeda, M. B. Fasae, E. Yue et al., "Anthocyanidin attenuates myocardial ischemia induced injury via inhibition of ROS-JNK-Bcl-2 pathway: New mechanism of anthocyanidin action," *Phytotherapy Research*, vol. 33, no. 12, pp. 3129–3139, 2019.

[267] V. Cristina, "Oxidative stress and cardiovascular risk prediction: The long way towards a "radical" perspective," *International Journal of Cardiology*, vol. 273, pp. 252-253, 2018.

[268] C. Vassalle, "An easy and reliable automated method to estimate oxidative stress in the clinical setting," *Methods in Molecular Biology*, vol. 477, pp. 31–39, 2008.

[269] C. Vassalle, L. Pratali, C. Boni, A. Mercuri, and R. Ndreu, "An oxidative stress score as a combined measure of the pro-oxidant and anti- oxidant counterparts in patients with coronary artery disease," *Clinical Biochemistry*, vol. 41, no. 14-15, pp. 1162–1167, 2008.

[270] V. Lubrano, A. Pingitore, I. Traghella et al., "Emerging biomarkers of oxidative stress in acute and stable coronary artery disease: levels and determinants," *Antioxidants*, vol. 8, no. 5, p. 115, 2019.

[271] L. Iamele, R. Fiocchi, and A. Vernocchi, "Evaluation of an automated spectrophotometric assay for reactive oxygen metabolites in serum," *Clinical Chemistry and Laboratory Medicine*, vol. 40, no. 7, pp. 673–676, 2002.

[272] C. Vassalle, S. Maffei, C. Boni, and G. C. Zucchelli, "Gender-related differences in oxidative stress levels among elderly patients with coronary artery disease," *Fertility and Sterility*, vol. 89, pp. 608–613, 2008.

[273] Y. Hirata, E. Yamamoto, T. Tokitsu et al., "Reactive oxygen metabolites are closely associated with the diagnosis and prognosis of coronary artery disease," *Journal of the American Heart Association*, vol. 4, no. 2, 2015.

[274] R. Rodrigo, M. Libuy, F. Feliú, and D. Hasson, "Oxidative stress-related biomarkers in essential hypertension and ischemia-reperfusion myocardial damage," *Disease Markers*, vol. 35, no. 6, p. 790, 2013.

[275] J. A. Chirinos, S. R. Akers, L. Trieu et al., "Heart failure, left ventricular remodeling, and circulating nitric oxide metabolites," *Journal of the American Heart Association*, vol. 5, no. 10, 2016.

[276] K. Akiyama, A. Kimura, H. Suzuki et al., "Production of oxidative products of nitric oxide in infarcted human heart," *Journal of the American College of Cardiology*, vol. 32, no. 2, pp. 373–379, 1998.

[277] H. Higashino, M. Tabuchi, S. Yamagata et al., "Serum nitric oxide metabolite levels in groups of patients with various diseases in comparison of healthy control subjects," *Journal of Medical Sciences*, vol. 10, pp. 1–11, 2009.

[278] L. Cominacini, A. Rigoni, A. F. Pasini et al., "The binding of oxidized low density lipoprotein (ox-LDL) to ox-LDL receptor-1 reduces the intracellular concentration of nitric oxide in endothelial cells through an increased production of superoxide," *The Journal of Biological Chemistry*, vol. 276, no. 17, pp. 13750–13755, 2001.

[279] J. L. Mehta, J. Chen, P. L. Hermonat, F. Romeo, and G. Novelli, "Lectin-like, oxidized low-density lipoprotein receptor-1 (LOX-1): a critical player in the development of atherosclerosis and related disorders," *Cardiovascular Research*, vol. 69, no. 1, pp. 36–45, 2006.

[280] H. Kataoka, N. Kume, S. Miyamoto et al., "Expression of Lectinlike oxidized low-density lipoprotein receptor-1 in human atherosclerotic lesions," *Circulation*, vol. 99, no. 24, pp. 3110–3117, 1999.

[281] K. Hayashida, N. Kume, T. Murase et al., "Serum soluble lectin-like oxidized low-density lipoprotein receptor-1 levels are elevated in acute coronary syndrome: a novel marker for early diagnosis," *Circulation*, vol. 112, no. 6, pp. 812–818, 2005.

[282] A. Ueda, N. Kume, K. Hayashida et al., "ELISA for soluble form of lectin-like oxidized LDL receptor-1, a novel marker of acute coronary syndrome," *Clinical Chemistry*, vol. 52, no. 6, pp. 1210-1211, 2006.

[283] Y. Xuan, X. Gào, B. Holleczek, H. Brenner, and B. Schöttker, "Prediction of myocardial infarction, stroke and cardiovascular mortality with urinary biomarkers of oxidative stress: Results from a large cohort study," *International Journal of Cardiology*, vol. 273, pp. 223–229, 2018.

[284] A. A. Elesber, P. J. Best, R. J. Lennon et al., "Plasma 8-isoprostaglandin F2alpha, a marker of oxidative stress, is increased in patients with acute myocardial infarction," *Free Radical Research*, vol. 40, no. 4, pp. 385–391, 2009.

[285] C. Vassalle, N. Botto, M. G. Andreassi, S. Berti, and A. Biagini, "Evidence for enhanced 8-isoprostane plasma levels, as index of oxidative stress in vivo, in patients with coronary artery disease," *Coronary Artery Disease*, vol. 14, no. 3, pp. 213–218, 2003.

[286] M. Fierro-Fernández, V. Miguel, and S. Lamas, "Role of redoximi Rs in fibrogenesis," *Redox Biology*, vol. 7, pp. 58–67, 2016.

[287] E. K. Economou, E. Oikonomou, G. Siasos et al., "The role of microRNAs in coronary artery disease: from pathophysiology to diagnosis and treatment," *Atherosclerosis*, vol. 241, no. 2, pp. 624–633, 2015.

[288] Y. Lee, M. Kim, J. Han et al., "MicroRNA genes are transcribed by RNA polymerase II," *The EMBO Journal*, vol. 23, no. 20, pp. 4051–4060, 2004.

[289] G. M. Borchert, W. Lanier, and B. L. Davidson, "RNA polymerase III transcribes human microRNAs," *Nature Structural & Molecular Biology*, vol. 13, no. 12, pp. 1097–1101, 2006.

[290] K. Okamura, A. Ishizuka, H. Siomi, and M. C. Siomi, "Distinct roles for Argonaute proteins in small RNA-directed RNA cleavage pathways," *Genes & Development*, vol. 18, no. 14, pp. 1655–1666, 2004.

[291] T. Melak and H. W. Baynes, "Circulating microRNAs as possible biomarkers for coronary artery disease: a narrative review," *EJIFCC*, vol. 30, no. 2, pp. 179–194, 2019.

[292] X. Cheng, C.-H. Ku, and R. C. M. Siow, "Regulation of the Nrf2 antioxidant pathway by microRNAs: New players in micromanaging redox homeostasis," *Free Radical Biology & Medicine*, vol. 64, pp. 4–11, 2013.

[293] G. E. Mann, J. Niehueser-Saran, A. Watson et al., "Nrf2/ARE regulated antioxidant gene expression in endothelial and

smooth muscle cells in oxidative stress: implications for atherosclerosis and preeclampsia," *Sheng Li Xue Bao*, vol. 59, no. 2, pp. 117–127, 2007.

[294] N. Papageorgiou, D. Tousoulis, M. Charakida et al., "Prognostic role of miRNAs in coronary artery disease," *Current Topics in Medicinal Chemistry*, vol. 13, no. 13, pp. 1540–1547, 2013.

[295] Y. H. Zhang, L. H. Xia, J. M. Jin, M. Zong, M. Chen, and B. Zhang, "Expression level of miR-155 in peripheral blood," *Asian Pacific Journal of Tropical Medicine*, vol. 8, no. 3, pp. 214–219, 2015.

[296] R. S. Huang, G. Q. Hu, B. Lin, Z. Y. Lin, and C. C. Sun, "MicroRNA-155 silencing enhances inflammatory response and lipid uptake in oxidized low-density lipoprotein-stimulated human THP-1 macrophages," *Journal of Investigative Medicine*, vol. 58, no. 8, pp. 961–967, 2015.

[297] G. F. Zhu, L. X. Yang, R. W. Guo et al., "microRNA-155 is inversely associated with severity of coronary stenotic lesions calculated by the Gensini score," *Coronary Artery Disease*, vol. 25, no. 4, pp. 304–310, 2014.

[298] M. Zhang, H. Pan, Y. Xu, X. Wang, Z. Qiu, and L. Jiang, "Allicin decreases lipopolysaccharide-induced oxidative stress and inflammation in human umbilical vein endothelial cells through suppression of mitochondrial dysfunction and activation of Nrf2," *Cellular Physiology and Biochemistry*, vol. 41, no. 6, pp. 2255–2267, 2017.

[299] K. H. Pulkkinen, S. Yla-Herttuala, and A. L. Levonen, "Heme oxygenase 1 is induced by miR-155 via reduced BACH1 translation in endothelial cells," *Free Radical Biology & Medicine*, vol. 51, no. 11, pp. 2124–2131, 2011.

[300] J. F. Reichard, G. T. Motz, and A. Puga, "Heme oxygenase-1 induction by NRF2 requires inactivation of the transcriptional repressor BACH1," *Nucleic Acids Research*, vol. 35, pp. 7074–7086, 2007.

[301] J. Alam and J. L. Cook, "How many transcription factors does it take to turn on the heme oxygenase-1 gene?," *American Journal of Respiratory Cell and Molecular Biology*, vol. 36, pp. 166–174, 2007.

[302] K. Igarashi and J. Sun, "The heme-Bach 1 pathway in the regulation of oxidative stress response and erythroid differentiation," *Antioxidants & Redox Signaling*, vol. 8, pp. 107–118, 2006.

[303] W. Xiao, "Advances in NF-kappa B signaling transduction and transcription," *Cellular & Molecular Immunology*, vol. 1, pp. 425–435, 2004.

[304] X. Zhang, Y. Yu, H. Lei et al., "The Nrf-2/HO-1 signaling axis: a ray of hope in cardiovascular diseases," *Cardiology Research and Practice*, vol. 2020, Article ID 5695723, 2020.

[305] R. C. Siow, H. Sato, and G. E. Mann, "Heme oxygenase-carbon monoxide signalling pathway in atherosclerosis: anti-atherogenic actions of bilirubin and carbon monoxide?," *Cardiovascular Research*, vol. 41, pp. 385–394, 1999.

[306] X. Jin, Z. Xu, J. Cao et al., "HO-1/EBP interaction alleviates cholesterol-induced hypoxia through the activation of the AKT and Nrf2/mTOR pathways and inhibition of carbohydrate metabolism in cardiomyocytes," *International Journal of Molecular Medicine.*, vol. 39, no. 6, pp. 1409–1420, 2017.

[307] D. Chen, Z. Jin, J. Zhang et al., "HO-1 protects against hypoxia/reoxygenation-induced mitochondrial dysfunction in H9c2 cardiomyocytes," *PLoS One*, vol. 11, no. 5, 2016.

[308] S. W. Jin, Y. P. Hwang, C. Y. Choi et al., "Protective effect of rutaecarpine against _t_ -BHP-induced hepatotoxicity by upregulating antioxidant enzymes via the CaMKII-Akt and Nrf2/ARE pathways," *Food and Chemical Toxicology*, vol. 100, pp. 138–148, 2017.

[309] H. K. Bryan, A. Olayanju, C. E. Goldring, and B. K. Park, "The Nrf2 cell defence pathway: Keap1-dependent and -independent mechanisms of regulation," *Biochemical Pharmacology*, vol. 85, no. 6, pp. 705–717, 2013.

[310] J. R. Baker, C. Vuppusetty, T. Colley et al., "Oxidative stress dependent microRNA-34a activation via PI3K$\alpha$ reduces the expression of sirtuin-1 and sirtuin-6 in epithelial cells," *Scientific Reports*, vol. 6, no. 1, 2016.

[311] T. Tabuchi, M. Satoh, T. Itoh, and M. Nakamura, "MicroRNA-34a regulates the longevity-associated protein SIRT1 in coronary artery disease: effect of statins on SIRT1 and microRNA-34a expression," *Clinical Science (London, England)*, vol. 123, no. 3, pp. 161–171, 2012.

[312] B. C. Bernardo, X.-M. Gao, C. E. Winbanks et al., "Therapeutic inhibition of the miR-34 family attenuates pathological cardiac remodeling and improves heart function," *Proceedings of the National Academy of Sciences of the United States of America*, vol. 109, no. 43, pp. 17615–17620, 2012.

[313] K. Iekushi, F. Seeger, B. Assmus, A. M. Zeiher, and S. Dimmeler, "Regulation of cardiac microRNAs by bone marrow mononuclear cell therapy in myocardial infarction," *Circulation*, vol. 125, no. 14, pp. 1765–1773, 2012.

[314] Y. Lin, H. Dan, and J. Lu, "Overexpression of microRNA-136-3p alleviates myocardial injury in coronary artery disease via the Rho A/ROCK signaling pathway," *Kidney & Blood Pressure Research*, vol. 45, no. 3, pp. 477–496, 2020.

[315] H.-W. Wang, T.-S. Huang, H.-H. Lo et al., "Deficiency of the microRNA-31-microRNA-720 pathway in the plasma and endothelial progenitor cells from patients with coronary artery disease," *Arteriosclerosis, Thrombosis, and Vascular Biology*, vol. 34, no. 4, pp. 857–869, 2014.

[316] M. Hulsmans, P. Sinnaeve, B. Van der Schueren, C. Mathieu, S. Janssens, and P. Holvoet, "Decreased miR-181a expression in monocytes of obese patients is associated with the occurrence of metabolic syndrome and coronary artery disease," *The Journal of Clinical Endocrinology and Metabolism*, vol. 97, no. 7, pp. E1213–E1218, 2012.

[317] S. Białek, D. Górko, A. Zajkowska et al., "Release kinetics of circulating miRNA-208a in the early phase of myocardial infarction," *Kardiologia polska*, vol. 73, no. 8, pp. 613–619, 2015.

[318] G.-K. Wang, J.-Q. Zhu, J.-T. Zhang et al., "Circulating microRNA: a novel potential biomarker for early diagnosis of acute myocardial infarction in humans," *European Heart Journal*, vol. 31, no. 6, pp. 659–666, 2010.

[319] Y. Devaux, M. Vausort, E. Goretti et al., "Use of circulating microRNAs to diagnose acute myocardial infarction," *Clinical Chemistry*, vol. 58, no. 3, pp. 559–567, 2012.

[320] M. Weber, M. B. Baker, R. S. Patel, A. A. Quyyumi, G. Bao, and C. D. Searles, "MicroRNA expression profile in CAD patients and the impact of ACEI/ARB," *Cardiology Research and Practice*, vol. 2011, Article ID 532915, 5 pages, 2011.

[321] J. Faccini, J.-B. Ruidavets, P. Cordelier et al., "Circulating miR-155, miR-145 and let-7c as diagnostic biomarkers of

the coronary artery disease," *Scientific Reports*, vol. 7, no. 1, 2017.

[322] Y. D'Alessandra, M. C. Carena, L. Spazzafumo et al., "Diagnostic potential of plasmatic microRNA signatures in stable and unstable angina," *PLoS ONE*, vol. 8, no. 11, 2013.

[323] Y. D'Alessandra, G. Pompilio, and M. C. Capogrossi, "MicroRNAs and myocardial infarction," *Current Opinion in Cardiology*, vol. 27, no. 3, pp. 228–235, 2012.

[324] J. Ren, J. Zhang, N. Xu et al., "Signature of circulating microRNAs as potential biomarkers in vulnerable coronary artery disease," *PLoS One*, vol. 8, no. 12, article e80738, 2013.

[325] C. Li, Z. Fang, T. Jiang et al., "Serum microRNAs profile from genome-wide serves as a fingerprint for diagnosis of acute myocardial infarction and angina pectoris," *BMC Medical Genomics*, vol. 6, no. 1, 2013.

[326] J. A. Ward Nada Esa, "Circulating Cell and Plasma microRNA Profiles Differ between Non-STSegment and ST-Segment-Elevation Myocardial Infarction," *Family medicine & medical science research*, vol. 2, no. 2, 2013.

[327] F. Wang, G. Long, C. Zhao et al., "Plasma microRNA-133a is a new marker for both acute myocardial infarction and underlying coronary artery stenosis," *Journal of Translational Medicine*, vol. 11, no. 1, p. 222, 2013.

[328] C. F. SN, "Piazza impact of bifurcation lesions on angiographic characteristics and procedural success in primary percutaneous coronary intervention for ST-segment elevation myocardial infarction," *Archives of Cardiovascular Diseases*, vol. 104, no. 4, pp. 234–241, 2011.

[329] Z. Chen, L. Wen, M. Martin et al., "Oxidative stress activates endothelial innate immunity via sterol regulatory element binding protein 2 (SREBP2) transactivation of microRNA-92a," *Circulation*, vol. 131, no. 9, pp. 805–814, 2015.

[330] X. Fan, E. Wang, X. Wang, X. Cong, and X. Chen, "MicroRNA-21 is a unique signature associated with coronary plaque instability in humans by regulating matrix metalloproteinase-9 via reversion-inducing cysteine-rich protein with Kazal motifs," *Experimental and Molecular Pathology*, vol. 96, no. 2, pp. 242–249, 2014.

[331] T. Soeki, K. Yamaguchi, T. Niki et al., "Plasma microRNA-100 is associated with coronary plaque vulnerability," *Circulation Journal*, vol. 79, no. 2, pp. 413–418, 2015.

[332] F. Jansen, X. Yang, S. Proebsting et al., "MicroRNA expression in circulating microvesicles predicts cardiovascular events in patients with coronary artery disease," *Journal of the American Heart Association*, vol. 3, no. 6, p. e001249, 2014.

[333] C. Schulte, S. Molz, S. Appelbaum et al., "miRNA-197 and miRNA-223 predict cardiovascular death in a cohort of patients with symptomatic coronary artery disease," *PLoS ONE*, vol. 10, no. 12, article e0145930, 2015.

[334] C. Widera, S. K. Gupta, J. M. Lorenzen et al., "Diagnostic and prognostic impact of six circulating microRNAs in acute coronary syndrome," *Journal of Molecular and Cellular Cardiology*, vol. 51, no. 5, pp. 872–875, 2011.

[335] M. He, Y. Gong, J. Shi et al., "Plasma microRNAs as potential noninvasive biomarkers for instent restenosis," *PLoS One*, vol. 9, no. 11, article e112043, 2014.

[336] Z. Fejes, Z. Czimmerer, T. Szük et al., "Endothelial cell activation is attenuated by everolimus via transcriptional and post-transcriptional regulatory mechanisms after drug-eluting coronary stenting," *PLoS One*, vol. 13, no. 6, article e0197890, 2018.

[337] S. Fichtlscherer, S. De Rosa, H. Fox et al., "Circulating microRNAs in patients with coronary artery disease," *Circulation Research*, vol. 107, no. 5, pp. 677–684, 2010.

Hindawi
Oxidative Medicine and Cellular Longevity
Volume 2020, Article ID 4957238, 16 pages
https://doi.org/10.1155/2020/4957238

*Research Article*

# Diazoxide Protects against Myocardial Ischemia/Reperfusion Injury by Moderating ERS via Regulation of the miR-10a/IRE1 Pathway

**Lin Zhang,[1] Shuang Cai,[2] Song Cao,[1,3] Jia Nie,[3] Wenjing Zhou,[1] Yu Zhang,[1] Ke Li,[4] Haiying Wang,[3] Shouyang Yu,[1,2] and Tian Yu[1,2]**

[1]*Guizhou Key Laboratory of Anesthesia and Organ Protection, Affiliated Hospital of Zunyi Medical University, 563000 Zunyi, China*
[2]*Key Laboratory of Brain Science, Zunyi Medical University, 563000 Zunyi, China*
[3]*Department of Anesthesiology, Affiliated Hospital of Zunyi Medical University, 563000 Zunyi, China*
[4]*Department of Anesthesiology, Hospital of Stomatology, Zunyi Medical University, 563000 Zunyi, China*

Correspondence should be addressed to Shouyang Yu; yushouyang@foxmail.com and Tian Yu; dllyutian@163.com

Received 9 December 2019; Revised 16 June 2020; Accepted 17 July 2020; Published 8 September 2020

Guest Editor: Aleksandar Kibel



Nowadays, reperfusion is still the most effective treatment for ischemic heart disease. However, cardiac reperfusion therapy would lead to reperfusion injury, which may have resulted from endoplasmic reticulum stress (ERS) during reperfusion. Diazoxide (DZ) is a highly selective mitochondrial adenosine triphosphate-sensitive potassium channel opener. Its protective effect on I/R injury has been confirmed in many organs such as the heart and brain. However, the mechanism of its protective effect has not been fully elucidated. MicroRNAs (miRNAs) are widely involved in pathologies of heart disease. In this study, we found that miR-10a expression was highly upregulated in the myocardial I/R groups, and DZ treatment significantly reduced the expression of miR-10a. More importantly, we found that DZ treatment can moderate ERS via regulation of the miR-10a/IRE1 pathway in the I/R and H/R models, thereby protecting myocardial H/R injury.

## 1. Introduction

The timely opening of infarct-related arteries and the recovery of blood supply to the ischemic myocardium are key to saving the dying cardiac muscle [1]. However, studies have found that recovery of blood perfusion after a period of ischemia in the myocardium would lead to increased damage to myocardial structure and function and decreased cardiac function and malignant arrhythmia, resulting in myocardial ischemia/reperfusion (I/R) injury [2]. At present, I/R injury is still a major problem in the treatment of cardiac ischemia. So, it is of great clinical significance to study how to reduce or even eliminate the occurrence of I/R injury on the basis of early recovery of coronary blood flow.

Diazoxide (DZ) has been demonstrated to inhibit apoptosis to limit myocardial or cerebral I/R injury. DZ is a kind of $K^+$ channel agonist, and the mitochondrial ATP-dependent $K^+$ (mKATP) channels have been suggested to mediate neuroprotective effects [3]. In the rat and mouse models of I/R injury, DZ preconditioning reduced the volume of brain infarcts induced by middle cerebral artery occlusion [4, 5]. On a subcellular level, the stabilization of the mitochondrial membrane potential and the preservation of mitochondrial integrity may contribute to the antiapoptotic actions of DZ in neurons [6–8]. On a molecular level, the protective effects of DZ may be mediated by the inhibition of caspase-3 activation [9, 10]. Although the protective effects of DZ have been demonstrated previously, the detailed cellular mechanisms underlying its actions against I/R-induced myocardial injury remain to be elucidated.

MicroRNAs (miRNAs) are endogenous, noncoding, single-stranded small molecules that are composed of 22-23 bases and function to regulate gene expression posttranscriptionally, [11, 12]. More and more studies have found that

miRNA expression is tissue-specific. miR-21, miR-1, and miR-296 are specifically expressed in cardiomyocytes, which are involved in pathological and physiological processes such as cardiac development, myocardial apoptosis, myocardial remodeling, and heart failure [13, 14]. In recent years, the regulatory effect of miRNAs in myocardial I/R injury has received increasing attention. This study analyzed a subset of miRNAs that were differentially expressed during and after myocardial I/R injury, with miR-10a being the most variable. The miR-10 family is involved in cell growth and development. In neuroblastoma cells [15] or smooth muscle cells [16], overexpression of miR-10a/10b reduces cell proliferation and promotes differentiation. Overexpression of miR-10 in pancreatic cancer and malignant breast cancer promotes tumor invasion and metastasis [17, 18]. In addition, overexpression of miR-10b also inhibits angiogenesis by inhibiting the expression of BDNF [19]. miR-10a/10b promotes vascular growth by regulating the behavior of sophisticated cells [20]. However, whether miR-10a participates in the development of myocardial I/R injury and its mechanism of action is not clearly reported.

The endoplasmic reticulum (ER) is one of the most important organelles in eukaryotic cells regulating protein folding, $Ca^{2+}$ homeostasis, and stress response, which is very sensitive to stress stimuli [21]. Stress factors including ischemia/hypoxia, disulfide bond formation disorders, and protein transport abnormalities can lead to dysfunction of the endoplasmic reticulum, which is endoplasmic reticulum stress (ERS) [22]. When ERS occurs, the ER protein cannot be correctly folded and thus retained in large quantities, stimulating the signaling between the ER, the Golgi, and the nucleus, leading to inhibition of protein synthesis and initiation of transcription of related genes. ERS induces upregulation of ER chaperones such as glucose regulatory proteins (GRPs), folding enzymes, and calreticulin, enhancing the ability of the ER to treat unfolded proteins and promoting the recovery of ER function [23]. When ERS persists or is at a high level, it will induce the activation of proapoptotic factors, trigger related apoptosis pathways, and induce cell apoptosis. ERS is closely related to the occurrence and development of I/R injury [24].

In this study, a rat model of myocardial I/R injury was established to observe the changes of miRNA in myocardial I/R injury. DZ treatment was performed before reperfusion to verify the protective effect of DZ on myocardial I/R injury. The effect of ERS on the development of myocardial I/R injury was discussed by further analysis of miR-10a with significant differences in changes. Furthermore, the possible molecular mechanism of miR-10a regulating ERS was explored, which provided a theoretical basis for clinical treatment of the myocardial I/R injury.

## 2. Materials and Methods

*2.1. Animals.* Sprague Dawley rats (20 ± 3 D, male and female unlimited, 60 ± 5 g) were obtained from the animal center of Third Military Medical University. All rats were kept on a 12 h light-dark cycle individually ventilated cage in 75°F with free access to food and water before the experiment. All rats were treated according to the Guide for the Care and Use of Laboratory Animals published by the US National Institutes of Health (NAP, 8th edition, Dec. 2010), and the study was approved by the Institutional Laboratory Animal Care and Use Committee of Zunyi Medical University.

*2.2. Construction of Myocardial I/R Models.* The myocardial I/R models were performed as described previously [25]. Briefly, sodium pentobarbital (45 mg/kg) was used to anesthetize rats firstly; then, thoracotomy was performed. The aorta was removed, and the heart was placed in 4°C KH buffer, cannulated through the aorta, connected to the Langendorff system, and perfused at 37°C via the aorta by 95% $O_2$ and 5% $CO_2$ gas fully saturated KH solution. Rats were randomly divided into 3 groups. The control group was aerobically perfused with KH solution for 120 min. The heart of the I/R group rats was hypoxia-perfused for 30 min and reperfused for 60 min after 30 min of aerobic equilibration perfusion. The DZ group was treated the same as the I/R group but perfused with 50 $\mu$m DZ for 5 min before reperfusion. The DZ dissolved in DMSO solution.

*2.3. TTC Staining.* Heart samples were collected after the rats were sacrificed and placed into a refrigerator (-80) for 8 min, then cut into slices with a thickness of about 2~3 mm each. Slices were immersed for 30 min into 2% triphenyltetrazolium chloride (TTC) solution at 37°C in the dark. Stained slices were fixed in 4% paraformaldehyde for 30 min. Images were taken by the FSX100 microscope (Olympus, Shenzhen, China), and sizes of different stained areas were measured with the image analysis software Image-Pro Plus 6.0. The ratios of the infarct area to the left ventricular area were calculated.

*2.4. Histological Examination.* Myocardial samples were collected after the rats were sacrificed. After 4% paraformaldehyde-fixed, the heart samples were dehydrated and embedded in paraffin; hematoxylin-eosin (HE) staining was conducted. Images of stained sections were obtained by the FSX100 microscope (Olympus, Shenzhen, China).

*2.5. miRNA Profiling.* The aberrant miRNA expressions of the myocardial samples were analyzed by miRNA sequencing as previously described [26, 27] Briefly, total RNA of the tissues was extracted to prepare the small RNA sequencing library by using the NEBNext Multiplex Small RNA Library Prep Set for Illumina (NEB, USA) according to the manufacturer's instruction. The libraries were finally sequenced, and the Solexa CHASTITY quantity filtered reads were harvested as clean reads. For data analysis, differentially expressed miRNA profiles between two groups were compared, and fold change and $p$ value were calculated and used to identify significant differentially expressed miRNAs, and hierarchical clustering was performed. The selected miRNAs verified the change of the expression by qRT-PCR.

*2.6. Isolation and Purification of Rat Primary Cardiomyocytes.* After being sacrificed, the rats were sterilized with 75% ethanol; the chest skin was cut and disinfected once. The surgical instrument was then replaced, and the heart was extracted

and placed in a large dish containing PBS. After removing the large blood vessels attached to the surface of the heart and the atria, tissues were mixed with 5 ml collagenase and 2.5 ml 0.05% trypsin, digested at 37°C for 10 min. The supernatant was collected and resuspended in DMEM containing 10% fetal bovine serum. Cells were placed in the incubator for 2 to 3 hours until the fibroblasts were attached. The supernatant was collected and resuspended in DMEM containing 10% calf serum and BrdU (10 mM) (1 : 80), and cardiomyocytes were obtained. Obtained cardiomyocytes were identified by immunofluorescence. Cardiomyocytes were cultured in a humidified incubator at 37°C and 5% $CO_2$.

*2.7. Cardiomyocyte Hypoxia/Reoxygenation (H/R) Model.* Cardiomyocytes were divided into different groups. The normal group was continuously cultured in a cell incubator under normoxic conditions (95% $CO_2$+5% $O_2$) until the end of the experiment. The H/R group was hypoxic for 4 hours (5% $CO_2$+1% $O_2$+94% $N_2$) and reoxygenated (95% CO2+5% O2) for 24 h. 100 $\mu$mol/l DZ was added into DMEM and incubated with cardiomyocytes for 5 min at the beginning of reoxygenation in the DZ group.

*2.8. In Vivo and In Vitro Transfection.* The miR-10a mimic, miR-10a inhibitor, and negative control oligonucleotides were purchased from Synthgene (Nanjing, China). Lipofectamine 2000 (Invitrogen, USA) was utilized to transfect the miR-10a mimic, miR-10a inhibitor, and negative control oligonucleotides (NC) according to the manufacturer's instructions. The concentration of the miR-10a mimic, miR-10a inhibitor, and NC used for transfection was 100 nM in this study. The miR-10a and IRE1 adenovirus were designed by Obio Technology (Shanghai, China) and injected into the tail vein of the experimental rat before one week of the operation.

*2.9. MTT Assay and LDH Analysis.* 3-(4,5-Dimethylthiazol-2-yl)-2,5-diphenyltetrazolium bromide (MTT) assay and lactate dehydrogenase (LDH) cytotoxicity assay (Beyotime, Nanjing, China) were used to detect cardiomyocytes proliferation and lactate dehydrogenase release in the different groups according to the manufacturer's instructions. For MTT assay, cardiomyocytes were harvested at 48 h, after which 200 $\mu$l of MTT solution was added to each well. After 4 h of incubation at 37°C, the MTT solution was carefully aspirated and 200 $\mu$l of DMSO was added per well. The optical density of each well at 490 nm was read with a microplate reader (Molecular Devices, USA). The cell viability was calculated as follows: $[(\text{experimental release} - \text{spontaneous release})/(\text{maximum release} - \text{spontaneous release})] \times 100$.
For LDH assay, the supernatants of cells were collected for the measurement of LDH release by a commercial LDH cytotoxicity assay kit (Beyotime, Nanjing, China). The absorbance at 490 nm was read using a microplate reader (BioTek Instruments, Inc.).

*2.10. Real-Time PCR.* Total RNA was extracted from cardiomyocytes and rat myocardial tissues using total RNA extraction reagent (Synthgene, Nanjing, China) according to the manufacturer's instructions. For the analysis of miRNA expression, TaqMan probes (Thermo Fisher Scientific, Shanghai, China) were used according to the manufacturer's instructions. qPCR reaction was performed for 40 cycles (95°C, 30 s; 72°C, 30 s) after an initial denaturation step (95°C, 5 min) on the CFX96 system of Bio-Rad. Quantitative measurements were determined with the $2^{-\Delta\Delta CT}$ method; the small U6 RNA expression was used as the internal control. For the analysis of mRNA expression, qPCR was performed using an SYBR Green qPCR Mix (Vazyme, Nanjing, China) on an Applied Biosystems 7300 sequence detection system (Applied Biosystems). GAPDH was used as the internal control. The reactions were performed in a 96-well plate at 95°C for 10 min, followed by 40 cycles of 95°C for 15 s, 56°C for 15 s, and 72°C for 30 s. PCR primers were as follows: IRE1$\alpha$ FP: 5′-TAGTCAGTTCTGCGTCCGCT-3′; IRE1$\alpha$ RP: 5′-TTCCAAAAATCCCGAGGCCG-3′; GRP78 FP: 5′-GAACGTCTGATTGGCGATGC-3′; GRP78 RP: 5′-TCAAAGACCGTGTTCTCGGG-3′; XBP-1 FP: 5′-CTGAGTCCGCAGCAGGTG-3′; XBP-1 RP: 5′-GTCCAGAATGCCCAACAGGA-3′; GAPDH FP: 5′-GATATTGTTGACATCAATGAC-3′; GAPDH RP: 5′-TTGATTTTGGAGGGATCTCG-3′.

*2.11. Western Blot Analysis.* Total protein was extracted using RIPA lysis buffer containing 1 mM PMSF (Synthgene, Nanjing, China) from rat myocardial tissues or transfected cardiomyocytes. The rat myocardial tissues included normal control, I/R injury, and I/R injury or DZ treatment rat myocardial tissues injected miR-10a and IRE1 adenovirus. The cardiomyocytes included normal, I/R, I/R and DZ treatment cells that transfected the NC, miR-10a mimic, and miR-10a inhibitor separately. Protein concentration was measured by the BCA protein assay kit (Thermo Fisher Scientific, Waltham, China) according to the manufacturer's instructions. The experimental procedure was carried out according to the previously published protocol [28]. The extracted protein was loaded onto a 10% Bis-Tris gel (50 $\mu$g per cell) and electrophoresed for 1 h at 150 V, transferred to PVDF membranes, and blocked with 5% skimmed milk at room temperature for 2 h, followed by incubation with IRE1, XBP1, and GRP78 primary antibody, respectively (1 : 1000 dilution, Proteintech, Wuhan, China) at 4°C for overnight; then, membranes were incubated with HRP-conjugated secondary antibody (1 : 3000 dilution, Proteintech, Wuhan, China) for 2 h. ECL Western blotting substrate (Synthgene, Nanjing, China) was applied to detect PVDF membranes.

*2.12. Pull-Down Assay.* The pull-down assay was carried out according to a previously described protocol [29]. Briefly, cardiomyocytes were transfected with biotinylated miR-10a (miR-10a probe) and control probe that were purchased from Synthgene (Nanjing, China). A total of $10^7$ cells were harvested and lysed by using lysis buffer. Total RNA was pretreated with DNase I and then heated at 65°C for 5 min, followed by an instant ice bath. Then, the probes were incubated with streptavidin-coated magnetic beads (New England Biolabs, USA) at 4°C for 4 h. After incubation, beads were washed and treated with TRIzol reagent to extract RNA.

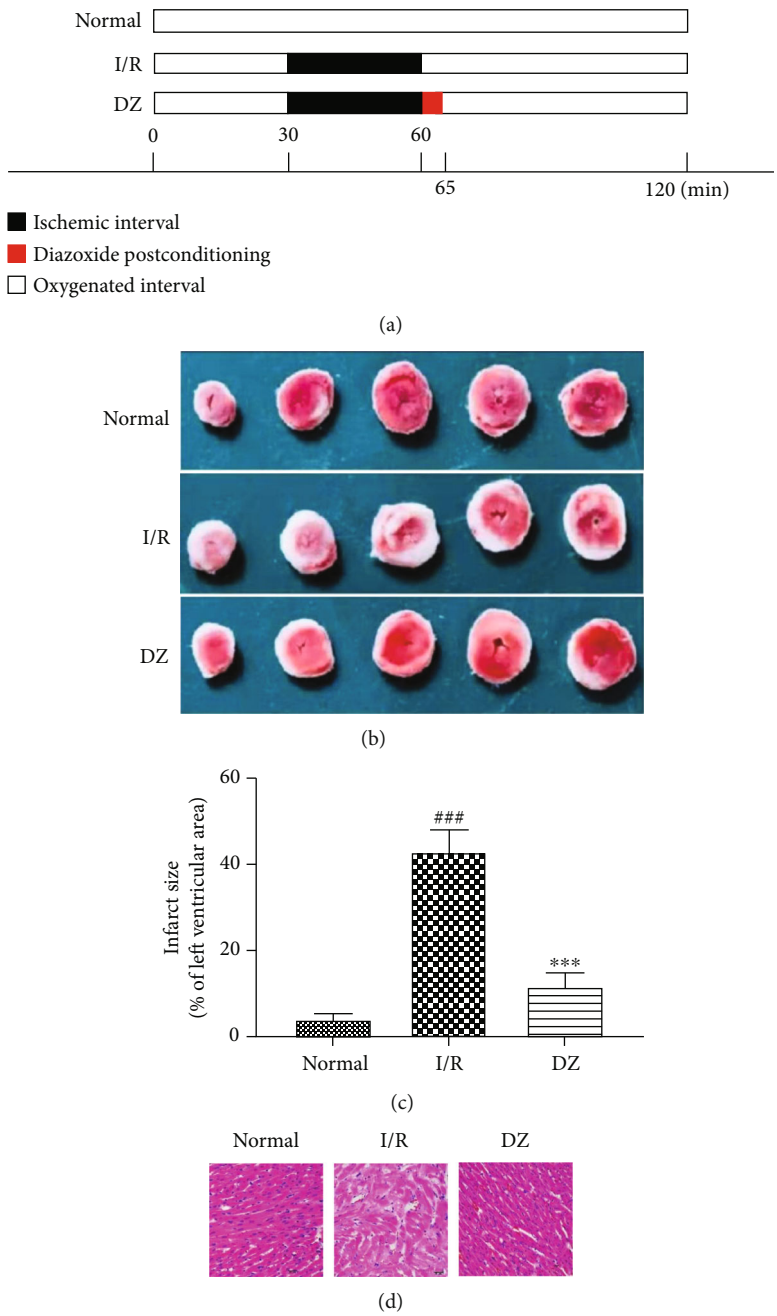


Figure 1: Continued.

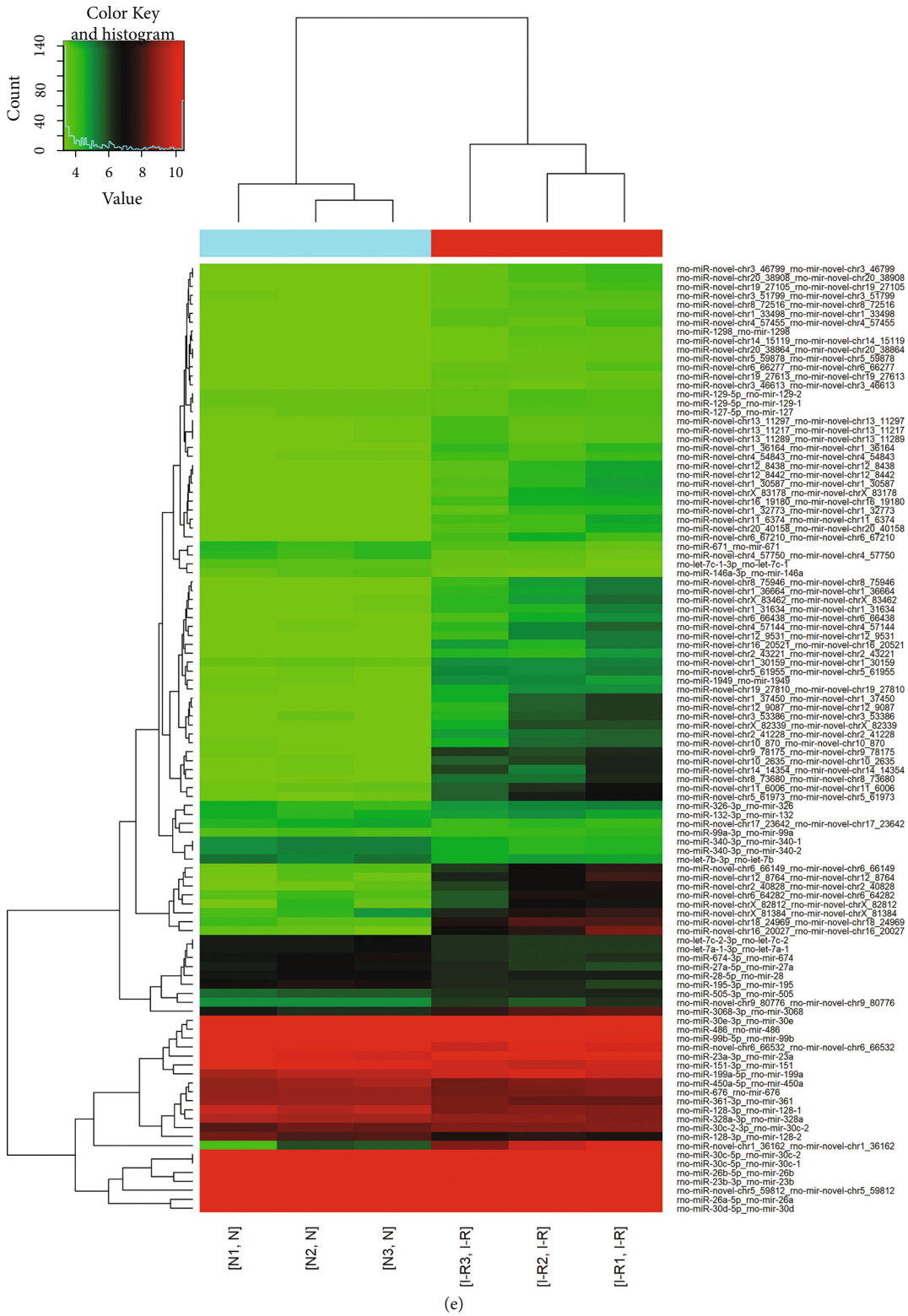


(e)

Figure 1: Continued.

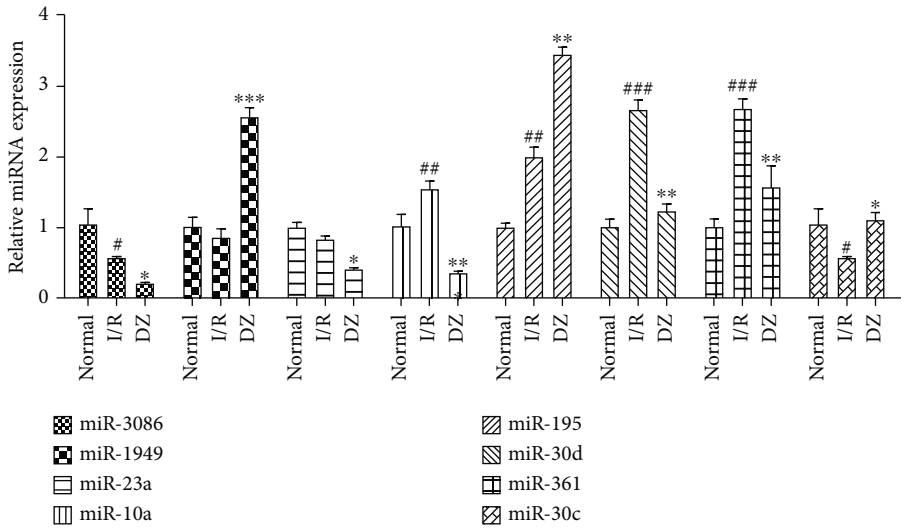


(f)

Figure 1: Effects of I/R injury and DZ treatment on the expression of miRNAs in rat myocardial tissue. (a) The schematic diagram of the established myocardial I/R injury rat model. (b, c) Representative images of hearts from the NC, I/R, and DZ rats, hearts were stained with TTC to reveal infarcted tissue, the red area represents the viable myocardium, and the white area represents ischemic dead tissue. Scale bar = 1 mm. (d) Rat myocardial tissues in different groups were detected by HE staining. Scale bar = 20 $\mu$m. (e) RNA sequencing detects the miRNA expression difference in normal and I/R injury myocardial tissues. (f) miRNA screening: miRNA expression in the myocardium was assessed by qRT-PCR. Data were expressed as mean ± SD ($n = 6$). $^{\#}p < 0.05$, $^{\#\#}p < 0.01$, and $^{\#\#\#}p < 0.001$, compared to the normal group; $^{*}p < 0.05$, $^{**}p < 0.01$, and $^{***}p < 0.001$, compared to the I/R group.

*2.13. Luciferase Reporter Analysis.* $1 \times 10^5$ HEK 293T cells were seeded in triplicate in 6-well plates and allowed to settle for 24 h. Wild-type/mutant luciferase plasmid pGL3-IRE1-3′ UTR, control luciferase plasmid, and pRL-TK Renilla plasmid were constructed by Synthgene (Nanjing, China). Plasmids were transfected into HEK 293T cells using Lipofectamine 2000 according to the manufacturer's instructions. Luciferase assays were performed 48 hours after transfection using the Dual-Luciferase Reporter Assay System (Promega, Beijing, China).

*2.14. Immunofluorescence Analysis.* For immunofluorescence staining, cardiomyocytes were blocked by incubation with 4% ($w/v$) BSA, incubated overnight with GRP78 primary antibody or ACTA1 primary antibody, separately. After incubation with Alexa Fluor 488 or 594 labeled secondary antibody and staining with DAPI, cardiomyocytes were observed under a confocal microscope (Leica, Shanghai, China).

*2.15. Statistical Analysis.* Results are collected from three independent experiments. All the results are presented as mean ± SD. Results were analyzed with one-way ANOVA and $t$-test using GraphPad Prism 6.0; $p < 0.05$ is considered statistic significant.

## 3. Results

*3.1. Effects of I/R Injury and DZ Treatment on the Expression of miRNAs in Rat Myocardial Tissue.* To investigate the effects of I/R injury and DZ treatment on the expression of miRNAs in rat myocardial tissue, we established a rat model of myocardial I/R injury; the process is shown in Figure 1(a). I/R injury can induce myocardial infarction (MI), TTC staining was used as a confirmation of consistent induction of MI, the red area represents the viable myocardium, and the white area represents ischemic dead tissue. Compared with the sham group, the infarct size of the I/R group increased significantly, but DZ can protect cardiomyocytes from MI and reduced infarct size (Figures 1(b) and 1(c)). According to the results of HE staining, we found that the sham group has strict rules of myofilament and complete sarcomere morphology (Figure 1(d)). In the I/R group, the myofilament is confused and cardiomyocytes rupture, together with sarcomere contracture deformation and sarcoplasmic reticulum expansion. In the DZ group, the damage was alleviated compared to the I/R group, and the myofilament was arranged neatly. The results show that the model was successfully established. Afterward, in order to conform DZ effect I/R injury through miRNA, we used sequencing and qPCR to detect the expression of miRNAs in myocardial tissue (Figures 1(e) and 1(f)). The difference in miR-10a was most pronounced among all miRNAs tested. Compared with the sham group, the expression of miR-10a was significantly increased in the I/R group, and the expression of miR-10a was significantly inhibited after treatment with DZ. Based on these findings, diazoxide protects against myocardial ischemia/reperfusion injury, possibly by regulating miR-10a.

*3.2. Upregulation of miR-10a Is Involved in H/R-Induced Cardiomyocyte Injury.* I/R can significantly increase the expression of miR-10a in myocardial tissue. To further explore the role of miR-10a in myocardial injury, we established an H/R injury model using rat primary cardiomyocytes. Rat primary cardiomyocytes were isolated from rat

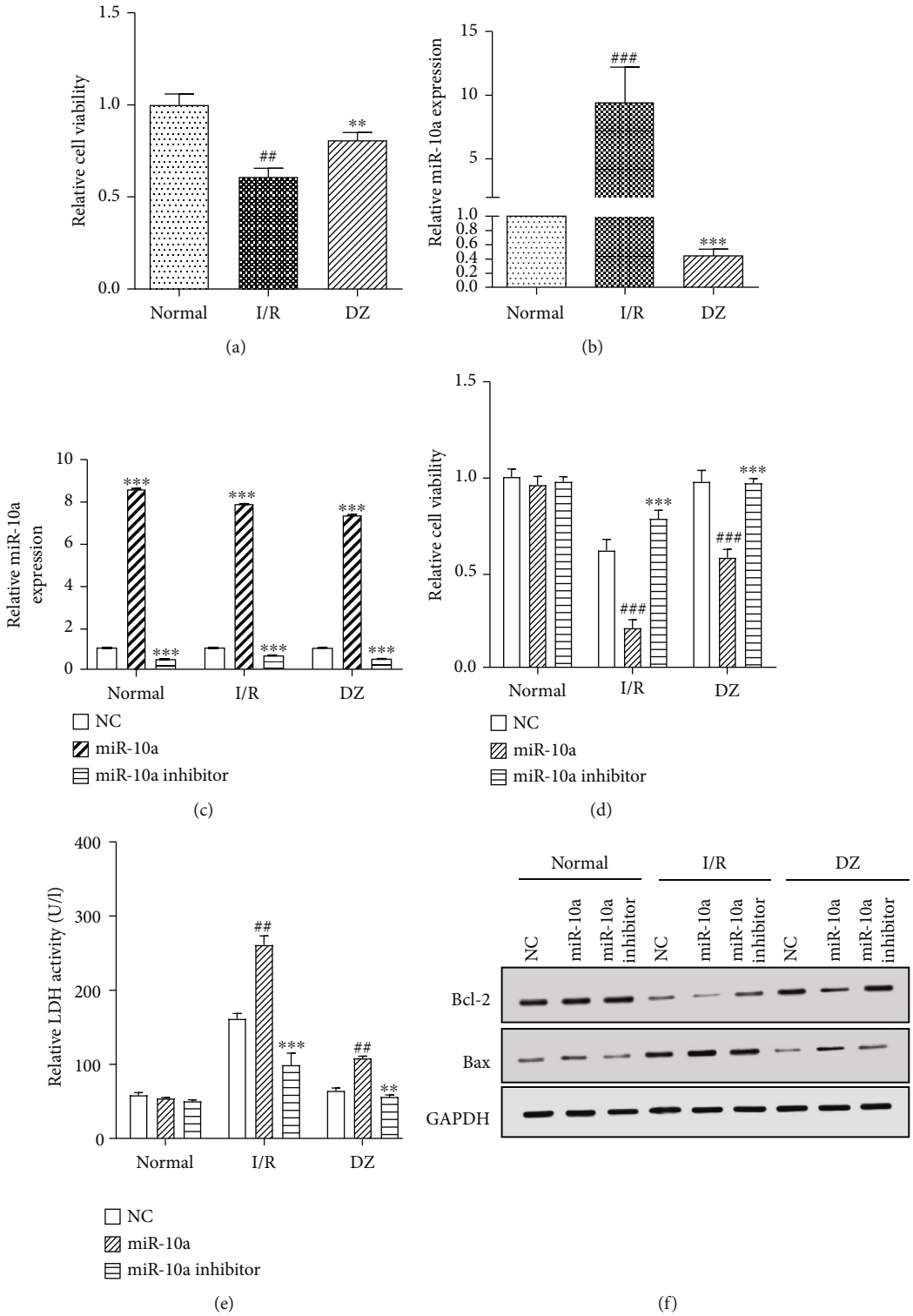


Figure 2: Continued.

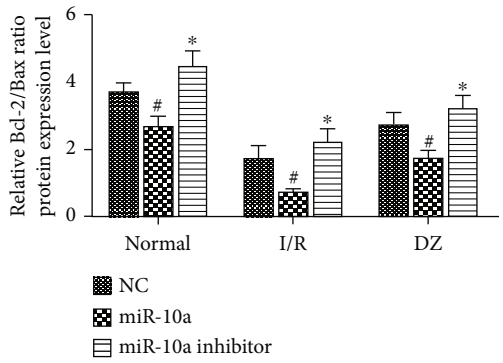


(g)

Figure 2: Upregulation of miR-10a is involved in H/R-induced cardiomyocyte injury. (a) MTT assay was used to detect the cell viability of each group. (b) miR-10a expression in cardiomyocytes was assessed by qRT-PCR. (c) The transfection efficiency of the miR-10a mimic and miR-10a inhibitor was detected by qRT-PCR in cardiomyocytes. (d) The effect of the miR-10a mimic and miR-10a inhibitor on cell viability of each group was detected by MTT analysis. (e) The effect of the miR-10a mimic and miR-10a inhibitor on LDH release of each group was detected by LDH analysis. (f) Protein expressions of Bcl-2 and Bax were detected using Western blot. (g) Quantitative analysis of (f). Data were expressed as mean ± SD in three independent experiments. For (a) and (b), $^{\#\#}p < 0.01$ and $^{\#\#\#}p < 0.001$, compared to the normal group; $^{**}p < 0.01$ and $^{***}p < 0.001$, compared to the I/R group. For (c), $^{***}p < 0.001$, compared to the NC group. For (d)–(f), $^{\#}p < 0.05$, $^{\#\#}p < 0.01$, and $^{\#\#\#}p < 0.001$, compared to the NC group; $^{*}p < 0.05$, $^{**}p < 0.01$, and $^{***}p < 0.001$, compared to the miR-10a group.

cardiac tissue and identified by immunofluorescence. The identification results were shown in the supplementary data. The immunofluorescence results confirmed the cells were rat cardiomyocytes. As shown in Figure 2(a), the cell viability of the H/R group was significantly inhibited as compared with the control group, and the cell viability of the DZ group was increased compared with the H/R group. Next, we examined the expression of miR-10a. As a result (Figure 2(b)), the expression of miR-10a was significantly increased in the H/R group compared with the control group, and the expression of miR-10a was restored in the DZ group, which was consistent in rat myocardial tissue. To further investigate the cardiomyocyte injury of miR-10a, we transfected the miR-10a mimic and miR-10a inhibitor in cardiomyocytes and detected the transfection efficiency. The transfection efficiency results are shown in Figure 2(c). Then, we detected myocardial cell function-related indicators after treatment. MTT (Figure 2(d)) and LDH test results (Figure 2(e)) showed that, compared with the control group, H/R was able to inhibit cell viability and increase the level of LDH in the cardiomyocyte culture supernatant; DZ treatment could restore the cell viability and LDH expression level, indicating that the model was successfully constructed. In addition, the miR-10a mimic can cause cell damage and LDH can increase cardiomyocytes in the H/R group and DZ group; DZ treatment alleviates the effect of miR-10a on cell damage and LDH release. However, the H/R damage effect can be reversed by the miR-10a inhibitor. The miR-10a inhibitor can protect cardiomyocytes from H/R injury, that is, increase myocardial cell viability and reduce LDH levels in the supernatant. At the same time, we examined the protein expression levels of Bcl-2 and Bax by Western blot (Figure 2(f)) and quantitatively analyzed the Bcl-2 and Bax expression ratio (Figure 2(g)). It was found that the H/R injury caused a decrease in the expression ratio of Bcl-2 and Bax, the miR-10a mimic aggravated this phenomenon, and the miR-10a inhibitor reversed the decrease of the Bcl-2 and Bax expression ratio. DZ slows down miR-10a mimic or inhibitor effects on Bcl-2 and Bax expression in H/R group cells. In conclusion, upregulation of miR-10a is involved in H/R injury in cardiomyocytes, and diazoxide protects against myocardial ischemia/reperfusion injury by regulating miR-10a.

*3.3. ERS Is Involved in I/R Injury.* After successfully establishing the model of I/R in rat primary cardiomyocytes, we also examined changes in ERS-related protein expression (Figure 3(a)). Compared with the control group, the expression of ERS marker proteins GRP78, IRE1, and XBP1 in the H/R group was significantly downregulated, and DZ treatment rescued the expression of ERS marker proteins (Figure 3(b)). The results indicated that ERS is inhibited in the early stage of myocardial H/R injury. At the same time, we transfected the miR-10a mimic and miR-10a inhibitor in the H/R group and DZ group cardiomyocytes, respectively. Then, we detected the expression of ERS-related proteins (Figure 3(c)). Compared with the NC group, the miR-10a mimic significantly reduced the expression of ERS-related proteins GRP78, IRE1, and XBP1, while the miR-10a inhibitor reversed the inhibitory effect of miR-10a. DZ diminished the effect of miR-10a on ERS-related proteins expression compared with the H/R group cells (Figure 3(d)). In combination, the effect of the miR-10a mimic is similar to that of H/R injury, which can inhibit moderate ERS and cause damage to cardiomyocytes.

*3.4. IRE1 Is the Target Gene of miR-10a in Cardiomyocytes.* To explore the relationship between miR-10a and ERS-related proteins, we designed an affinity purification method to determine the target gene for miR-10a. Cells were transfected with biotinylated synthetic miRNAs and lysed after incubation, and miRNA and its mRNA were screened by streptavidin-coated magnetic beads (Figure 4(a)). As shown in Figure 4(b), IRE1 expression levels were higher than other ERS-related proteins including XBP1 and GRP78. We further examined the relationship between miR-10a and IRE1

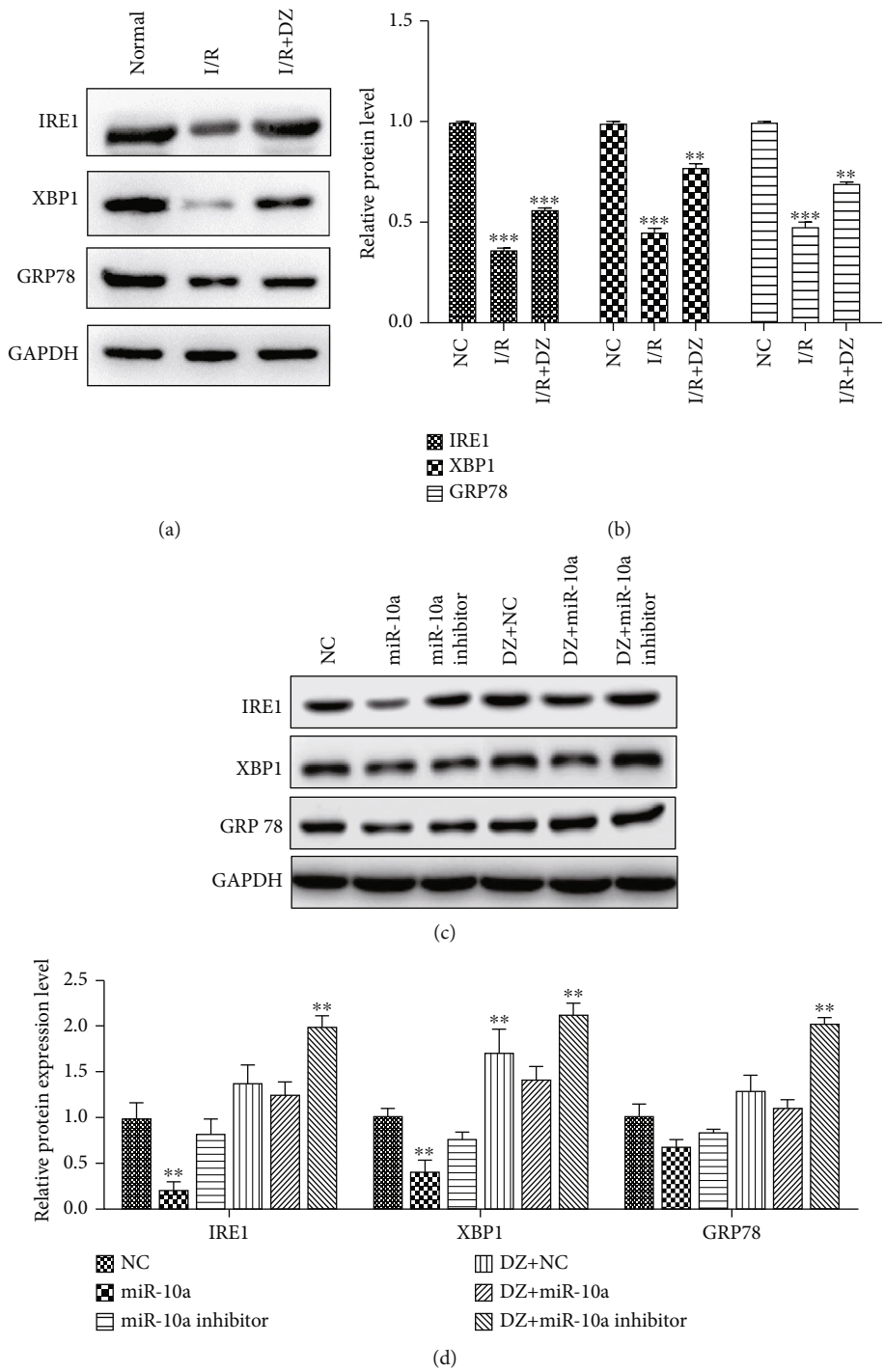


Figure 3: ERS is involved in I/R injury. (a) The effects of I/R and DZ treatment on protein expressions of GRP78, IRE1, and XBP1 were detected using Western blot. (b) Histogram summarizing results in (a). (c) The effects of the miR-10a mimic, miR-10a inhibitor, and DZ treatment separately or simultaneously on protein expressions of GRP78, IRE1, and XBP1 were detected using Western blot. (d) Histogram summarizing results in (c). Data were expressed as mean ± SD in three independent experiments. $^{**}p < 0.01$ and $^{***}p < 0.001$, compared to the NC group.

by Western blot (Figure 4(c)). It was found that miR-10a significantly inhibited the protein expression of IRE1, while the miR-10a inhibitor reversed its inhibitory effect and promoted IRE1 protein expression (Figure 4(d)). Furthermore, qPCR detection of IRE1 mRNA expression revealed that IRE1 mRNA expression was not affected, suggesting that IRE1 is regulated by posttranscriptional regulation of miR-10a (Figure 4(e)). To further clarify that miR-10a directly regulates the transcriptional activity of IRE1, we constructed luciferase reporter gene plasmid of wild-type and mutant IRE1 separately, and the mutation pattern is shown in Figure 4(f). The results showed that the miR-10a mimic

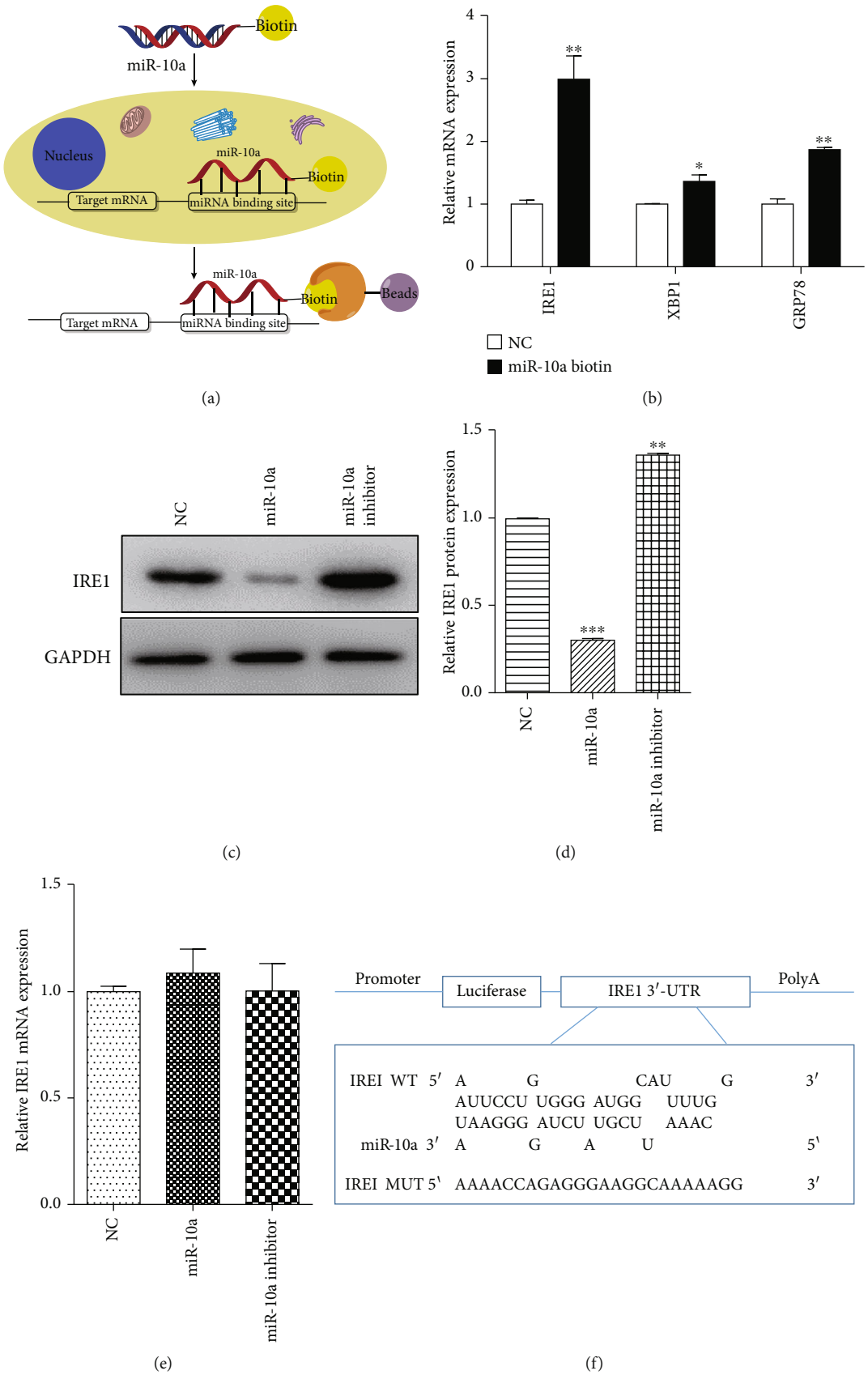


Figure 4: Continued.

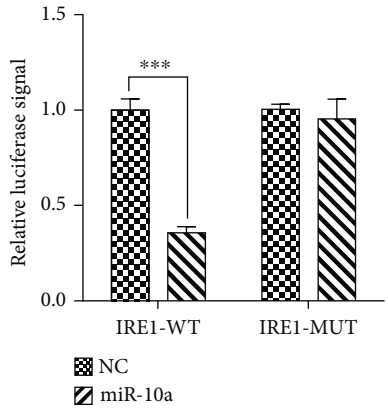


(g)

Figure 4: IRE1 is the target gene of miR-10a in cardiomyocytes. (a) Schematic representation of the biotinylated miRNA pull-down method. (b) The relative mRNA expression of IRE1, XBP1, and GRP78 using the biotinylated miRNA pull-down method. (c, d) The effect of the miR-10a mimic and miR-10a inhibitor on protein expression of IRE1 was detected using Western blot. (e) The effect of the miR-10a mimic and miR-10a inhibitor on mRNA expression of IRE1 was detected using qPCR. (f) Mutant sequence of IRE1 mRNA 3′UTR. (g) The effect of the miR-10a mimic on transcriptional activity of IRE1 using luciferase activity assay. Data were expressed as mean ± SD in three independent experiments. $^{**}p < 0.01$ and $^{***}p < 0.001$, compared to the NC group.

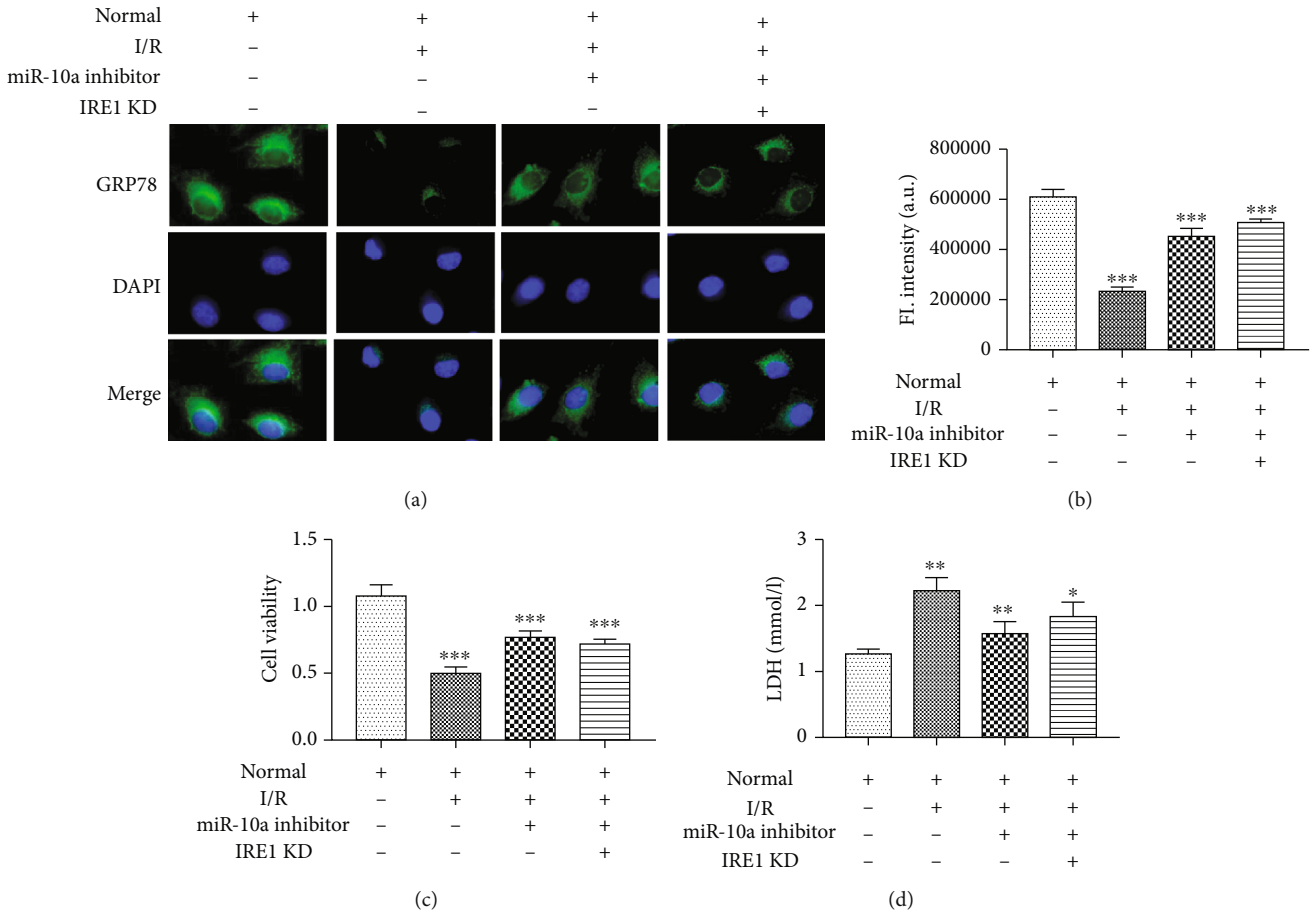


Figure 5: Regulation of ERS by miR-10a in cardiomyocytes. (a) The effect of the miR-10a inhibitor and knockdown IRE1 on expression of GRP78 was detected by immunofluorescence. Scale bar = 20 $\mu$m. (b) Fluorescence intensity of each group in (a). (c) The effect of the miR-10a inhibitor and knockdown IRE1 on cell viability of each group was detected by MTT analysis. (d) The effect of the miR-10a inhibitor and knockdown IRE1 on LDH release of each group was detected by LDH analysis. Data were expressed as mean ± SD in three independent experiments. $^{**}p < 0.01$ and $^{***}p < 0.001$, compared to the NC group.

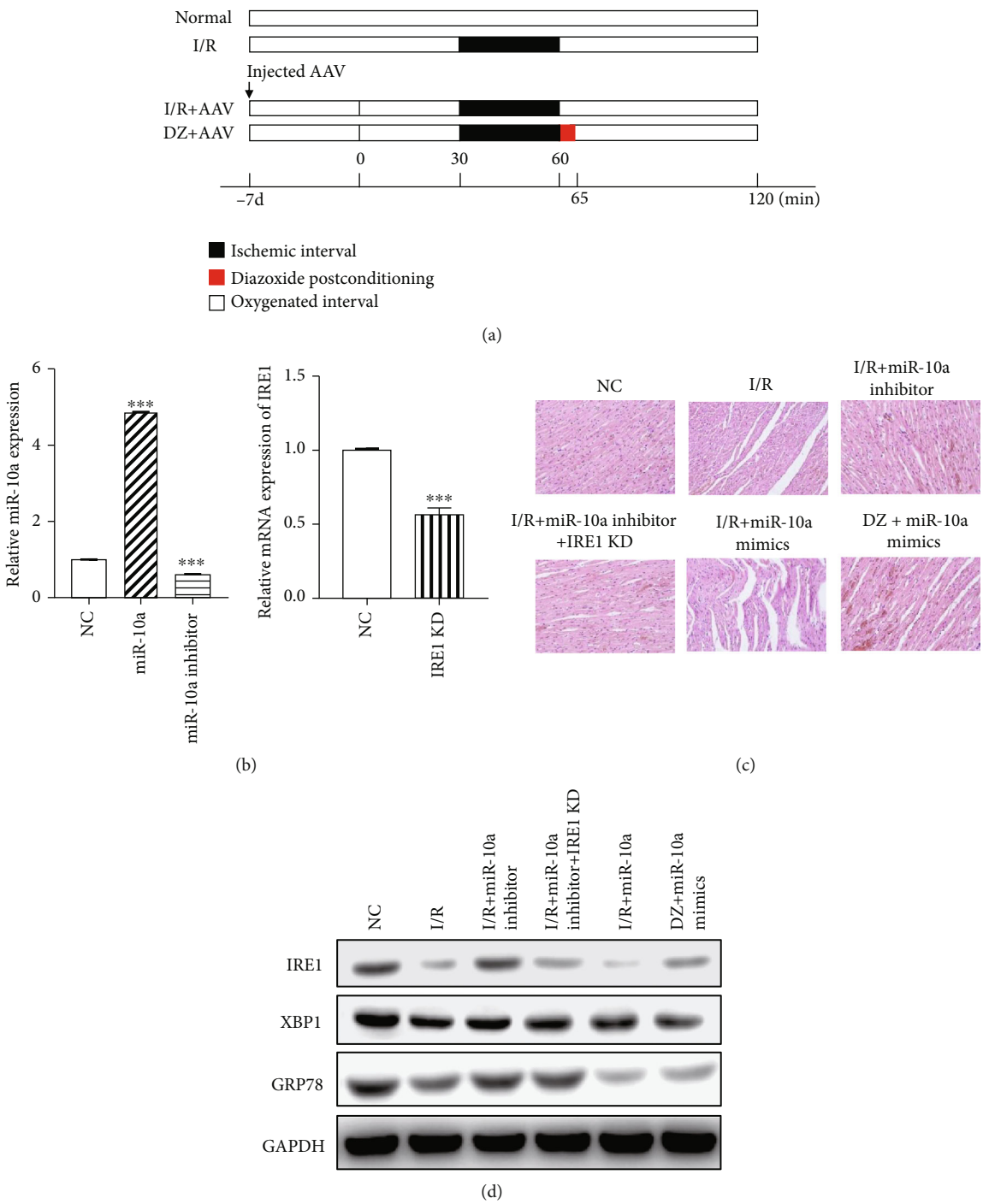


Figure 6: Continued.

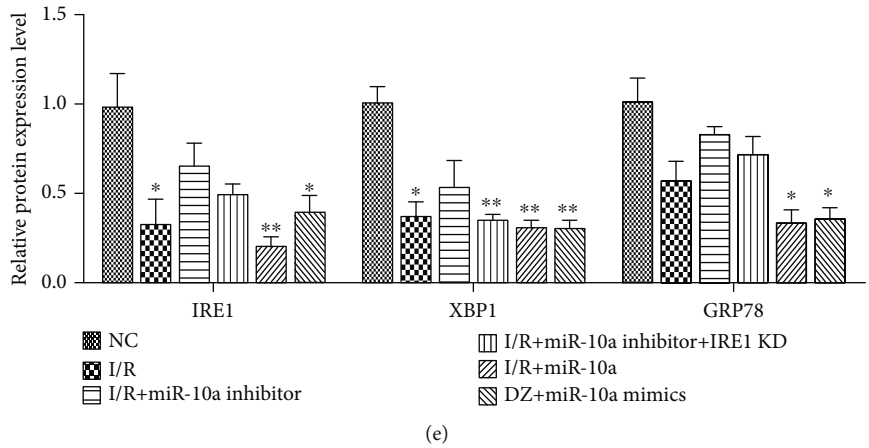


Figure 6: Regulation of ERS by the miR-10a inhibitor in rat myocardial tissue. (a) The schematic diagram of the established myocardial I/R injury rat model and injected AAV. (b) qRT-PCR was used to detect the miR-10a and IRE1 expression. (c) Rat myocardial tissues in different groups were detected by HE staining. Scale bar = 20 $\mu$m. (d) The effects of the miR-10a inhibitor on protein expressions of GRP78, IRE1, and XBP1 were detected using Western blot. (e) Histogram summarizing results in (d). Data were expressed as mean ± SD ($n = 6$). $^{**}p < 0.01$ and $^{***}p < 0.001$, compared to the NC group.

significantly reduced the transcriptional activity of wild-type IRE1 compared to the control group (Figure 4(g)). Combined with the above results, we confirmed that miR-10a directly inhibited the expression of IRE1.

*3.5. Regulation of ERS by miR-10a in Cardiomyocytes.* After confirming that miR-10a targets IRE1, we further explored its effects on ERS in cardiomyocytes. We detected the expression of the ERS marker protein GRP78 by fluorescence (Figure 5(a)). By measuring the fluorescence intensity, we found that when I/R occurs, the expression of GRP78 in cardiomyocytes is significantly inhibited, the miR-10a inhibitor will increase the expression of GRP78 on the basis of H/R injury, and the GRP78 expression increase could be inhibited when IRE1 expression is inhibited. (Figure 5(b)). The results further indicated that miR-10a inhibits moderate ERS and played the roles through IRE1 gene. In addition, we also examined cardiomyocyte viability by MTT and LDH analyses (Figures 5(c) and 5(d)). The results showed that the miR-10a inhibitor attenuated the damage of H/R on cell viability, and knockdown IRE1 can reverse myocardial cell viability.

*3.6. Regulation of ERS by the miR-10a Inhibitor in the Rat Myocardium.* At the cellular level, we have verified the regulation circuitry of DZ against myocardial I/R injury. We found that the miR-10a inhibitor can promote moderate ERS and reduce the effect of I/R injury on myocardial cell viability, thus protecting cardiomyocytes. We further verified this conclusion in the rat I/R model, as shown in Figure 6(a). The miR-10a and IRE1 expression change was determined by qRT-PCR (Figure 6(b)). As shown by the HE results, the miR-10a inhibitor was used on the basis of the I/R model, and the sarcomere morphology was relatively intact, and the myofilament was arranged neatly compared with the I/R group. Downregulation of IRE1 in the I/R rats attenuates the effect of the miR-10a inhibitor. miR-10a mimics impact the sarcomere morphology, and the arrangement of the myofilament is contrary to the miR-10a inhibitor. DZ also slows down the effect of miR-10a mimics in myocardial tissues (Figure 6(c)). Subsequently, we examined the expression of ERS-related proteins by Western blot (Figure 6(d)). The results indicated that the miR-10a inhibitor reverses the decrease in ERS-related protein expression caused by I/R injury, and reduced IRE1 expression could retard the effect of the miR-10a inhibitor in ERS-related protein expression. miR-10a mimics further decrease the ERS-related protein expression; DZ reverses the decrease in ERS-related protein expression by miRNA mimics transfected (Figure 6(e)). This part of the results confirmed that DZ protects myocardial tissue through miR-10a expression inhibition; the miR-10a inhibitor can reverse myocardial damage caused by I/R injury and protect myocardial tissue by promoting moderate ERS.

## 4. Discussion

Ischemic cardiomyopathy is one of the most common life-threatening diseases. Studies have shown that oxygen free radicals and intracellular calcium overload during reperfusion may be an important path of myocardial I/R injury [30–32]. Diazoxide (DZ) has been demonstrated to limit myocardial or cerebral I/R injury and apoptosis. However, the specific mechanism has not been fully elucidated. In this study, the rat model of myocardial I/R injury and myocardial H/R model were established to detect the changes of miRNA and the expression of ERS-related molecules to investigate the effect of DZ on myocardial I/R injury.

The ER is an important place for protein synthesis, folding, modification, and storage of $Ca^{2+}$, which is of great significance for maintaining normal physiological functions. Pathological factors could induce an imbalance of ER homeostasis and dysfunction, leading to the ERS state [33]. Studies have shown that moderate ERS is a protective mechanism for cells to cope with various stresses. ERS could reduce cell damage by treating abnormal proteins, regulating calcium concentration, and restoring homeostasis. However,

persistent or excessive ERS can cause cell death by a series of cascades of activation-related factors [34].

GRP78 is a marker protein of ERS and mediates the processing and maturation of nascent proteins. GRP78 is a key regulatory protein that promotes cell protein maturation, cell function, and life under normal growth conditions [35]. IRE1 is a type I transmembrane protein localized on the ER membrane with both kinase and endonuclease activities. Under normal physiological conditions, IRE1 binds to GRP78 and is inactive, but when ERS occurs, they are separated from each other and become activated [36]. The IRE1-XBP1 signaling pathway plays an important role in the ERS reaction [37, 38]. Western blot and HE results in the present studies showed that I/R could significantly downregulate the expression of IRE1 and XBP1 in the early stage the of I/R group compared with the sham operation group, indicating that I/R can inhibit the occurrence of ERS at the early stage. Diazoxide (DZ) is a highly selective mitochondrial adenosine triphosphate-sensitive potassium channel opener [39]. Its protective effect on I/R injury has been confirmed in many organs such as the heart and brain [40, 41]. Myocardial I/R injury studies have shown that DZ treatment can induce moderate ERS and reduce myocardial damage. The results of this study showed that the myocardial damage in the DZ +I/R group was significantly lower than that in the I/R group, and the ultrastructural damage of the myocardium was smaller, indicating that DZ treatment could reduce myocardial I/R injury. At the same time, among the several miRNAs treated with DZ, the change of miR-10a was the most significant, and the expression level was significantly inhibited. We found that the expression of miR-10a under I/R conditions was significantly increased, and it exerted I/R damage effects both in vitro and in vivo. In vitro studies found that when the expression of miR-10a was inhibited, the damage was reversed, which resulted in a similar effect of DZ treatment. At the same time, it was found that the miR-10a inhibitor and DZ may inhibit the release of Bcl-2, inhibit the opening of the mitochondrial permeability transition pore, and reduce the release of cytochrome in mitochondria of myocardial cells during I/R injury, thereby inhibiting cardiomyocyte apoptosis induced by I/R to play a protective role.

The effects of apoptosis and apoptosis-related gene expression preliminarily confirmed the protective effects of diazoxide and miR-10a inhibitors on cardiomyocyte apoptosis induced by H/R. Further study on the effect of miR-10a on pathomorphology and ERS of myocardial I/R injury clarified that miR-10a promoted myocardial I/R injury by downregulating ERS-related proteins IRE1, thereby inhibiting the IREl-XBP1 signaling pathway to aggravate myocardial I/R injury. This study explored the protective mechanism of DZ in myocardial I/R injury and provided a theoretical basis for clinical application of drug preconditioning to prevent myocardial I/R injury.

## Data Availability

All processed data and models used during the study are available from the corresponding authors by request. But the raw data required to reproduce these findings cannot be shared at this time as the data also forms part of an ongoing study.

## Conflicts of Interest

The authors declare that the research was conducted in the absence of any commercial or financial relationships that could be construed as a potential conflict of interest.

## Authors' Contributions

The contributions of the authors involved in this study are as follows: conceptualization: Song Cao and Shouyang Yu; data curation: Lin Zhang, Shuang Cai, Jia Nie, and Wenjing Zhou; formal analysis: Song Cao; funding acquisition: Lin Zhang, Haiying Wang, and Tian Yu; investigation: Haiying Wang; methodology: Wenjing Zhou and Yu Zhang; supervision: Tian Yu; writing–original draft: Shuang Cai; and writing–review and editing: Shouyang Yu. Lin Zhang, Shuang Cai, and Song Cao are co-first authors.

## Acknowledgments

This study was supported by National Natural Science Foundation Committee of China (NSFC) under grant nos. 81560593, 81860062, and 81760097.

## Supplementary Materials

Rat primary cardiomyocytes were isolated from rat cardiac tissue and identified by ACTA1 immunofluorescence. *(Supplementary materials)*

## References

[1] O. Takasu, J. P. Gaut, E. Watanabe et al., "Mechanisms of cardiac and renal dysfunction in patients dying of sepsis," *American Journal of Respiratory and Critical Care Medicine*, vol. 187, no. 5, pp. 509–517, 2013.

[2] S. He, X. Wang, and A. Chen, "Myocardial ischemia/reperfusion injury: the role of adaptor proteins Crk," *Perfusion*, vol. 32, no. 5, pp. 345–349, 2017.

[3] U. Dirnagl, R. P. Simon, and J. M. Hallenbeck, "Ischemic tolerance and endogenous neuroprotection," *Trends in Neurosciences*, vol. 26, no. 5, pp. 248–254, 2003.

[4] D. Liu, C. Lu, R. Wan, W. W. Auyeung, and M. P. Mattson, "Activation of mitochondrial ATP-dependent potassium channels protects neurons against ischemia-induced death by a mechanism involving suppression of Bax translocation and CytochromecRelease," *Journal of Cerebral Blood Flow and Metabolism*, vol. 22, no. 4, pp. 431–443, 2016.

[5] K. Shimizu, Z. Lacza, N. Rajapakse, T. Horiguchi, J. Snipes, and D. W. Busija, "MitoK(ATP) opener, diazoxide, reduces neuronal damage after middle cerebral artery occlusion in the rat," *American Journal of Physiology. Heart and Circulatory Physiology*, vol. 283, no. 3, pp. H1005–H10011, 2002.

[6] D. J. Hausenloy, D. M. Yellon, S. Mani-Babu, and M. R. Duchen, "Preconditioning protects by inhibiting the mitochondrial permeability transition," *American Journal of Physiology. Heart and Circulatory Physiology*, vol. 287, no. 2, pp. H841–H849, 2004.

[7] L. Wu, F. Shen, L. Lin, X. Zhang, I. C. Bruce, and Q. Xia, "The neuroprotection conferred by activating the mitochondrial ATP-sensitive K+ channel is mediated by inhibiting the mitochondrial permeability transition pore," *Neuroscience Letters*, vol. 402, no. 1-2, pp. 184–189, 2006.

[8] D. W. Busija, P. Katakam, N. C. Rajapakse et al., "Effects of ATP-sensitive potassium channel activators diazoxide and BMS-191095 on membrane potential and reactive oxygen species production in isolated piglet mitochondria," *Brain Research Bulletin*, vol. 66, no. 2, pp. 85–90, 2005.

[9] X. He, X. Mo, H. Gu et al., "Neuroprotective effect of diazoxide on brain injury induced by cerebral ischemia/reperfusion during deep hypothermia," *Journal of the Neurological Sciences*, vol. 268, no. 1-2, pp. 18–27, 2008.

[10] L. Wang, Q. L. Zhu, G. Z. Wang et al., "The protective roles of mitochondrial ATP-sensitive potassium channels during hypoxia-ischemia-reperfusion in brain," *Neuroscience Letters*, vol. 491, no. 1, pp. 63–67, 2011.

[11] K. U. Tüfekci, M. G. Öner, R. L. J. Meuwissen, and Ş. Genç, "The role of microRNAs in human diseases," in *miRNomics: MicroRNA Biology and Computational Analysis*, pp. 33–50, Humana Press, Totowa, NJ, 2014.

[12] M. Bhaskaran and M. Mohan, "MicroRNAs: history, biogenesis, and their evolving role in animal development and disease," *Veterinary Pathology*, vol. 51, no. 4, pp. 759–774, 2013.

[13] B. Duygu, L. J. de Windt, and P. A. da Costa Martins, "Targeting microRNAs in heart failure," *Trends in Cardiovascular Medicine*, vol. 26, no. 2, pp. 99–110, 2016.

[14] T. Thum, P. Galuppo, C. Wolf et al., "MicroRNAs in the human heart: a clue to fetal gene reprogramming in heart failure," *Circulation*, vol. 116, no. 3, pp. 258–267, 2007.

[15] N. H. Foley, I. Bray, K. M. Watters et al., "MicroRNAs 10a and 10b are potent inducers of neuroblastoma cell differentiation through targeting of nuclear receptor corepressor 2," *Cell Death and Differentiation*, vol. 18, no. 7, pp. 1089–1098, 2011.

[16] H. Huang, C. Xie, X. Sun, R. P. Ritchie, J. Zhang, and Y. E. Chen, "miR-10a contributes to retinoid acid-induced smooth muscle cell differentiation," ***Journal of Biological Chemistry***, vol. 285, no. 13, pp. 9383–9389, 2010.

[17] M. V. Yigit, S. K. Ghosh, M. Kumar et al., "Context-dependent differences in miR-10b breast oncogenesis can be targeted for the prevention and arrest of lymph node metastasis," *Oncogene*, vol. 36, no. 18, p. 2628, 2017.

[18] M. Bloomston, W. L. Frankel, F. Petrocca et al., "MicroRNA expression patterns to differentiate pancreatic adenocarcinoma from normal pancreas and chronic pancreatitis," *JAMA*, vol. 297, no. 17, pp. 1901–1908, 2007.

[19] K. Varendi, A. Kumar, M. A. Harma, and J. O. Andressoo, "miR-1, miR-10b, miR-155, and miR-191 are novel regulators of BDNF," ***Cellular and Molecular Life Sciences***, vol. 71, no. 22, pp. 4443–4456, 2014.

[20] X. Wang, C. C. Ling, L. Li et al., "MicroRNA-10a/10b represses a novel target gene mib1 to regulate angiogenesis," *Cardiovascular Research*, vol. 110, no. 1, pp. 140–150, 2016.

[21] D. S. Schwarz and M. D. Blower, "The endoplasmic reticulum: structure, function and response to cellular signaling," *Cellular and Molecular Life Sciences*, vol. 73, no. 1, pp. 79–94, 2016.

[22] S. A. Oakes and F. R. Papa, "The role of endoplasmic reticulum stress in human pathology," *Annual Review of Pathology*, vol. 10, no. 1, pp. 173–194, 2015.

[23] S. Nishikawa, J. L. Brodsky, and K. Nakatsukasa, "Roles of molecular chaperones in endoplasmic reticulum (ER) quality control and ER-associated degradation (ERAD)," *Journal of Biochemistry*, vol. 137, no. 5, pp. 551–555, 2005.

[24] F. R. Sari, K. Watanabe, B. Widyantoro et al., "Sex differences play a role in cardiac endoplasmic reticulum stress (ERS) and ERS-initiated apoptosis induced by pressure overload and thapsigargin," *Cardiovascular Pathology*, vol. 20, no. 5, pp. 281–290, 2011.

[25] J. Li, W. Zhou, W. Chen, H. Wang, Y. Zhang, and T. Yu, "Mechanism of the hypoxia inducible factor 1/hypoxic response element pathway in rat myocardial ischemia/diazoxide post-conditioning," *Molecular Medicine Reports*, vol. 21, no. 3, pp. 1527–1536, 2020.

[26] D. Wang, Y. Chen, M. Liu et al., "The long noncoding RNA Arrl1 inhibits neurite outgrowth by functioning as a competing endogenous RNA during neuronal regeneration in rats," *The Journal of Biological Chemistry*, vol. 295, no. 25, pp. 8374–8386, 2020.

[27] Y. Qin, B. Zheng, G. S. Yang et al., "Tanshinone IIA inhibits VSMC inflammation and proliferation _in vivo_ and _in vitro_ by downregulating miR-712-5p expression," *European Journal of Pharmacology*, vol. 880, article 173140, 2020.

[28] X. P. Peng, L. Huang, and Z. H. Liu, "miRNA-133a attenuates lipid accumulation via TR4-CD36 pathway in macrophages," *Biochimie*, vol. 127, pp. 79–85, 2016.

[29] Y. Liu, R. Liu, F. Yang et al., "miR-19a promotes colorectal cancer proliferation and migration by targeting TIA1," *Molecular Cancer*, vol. 16, no. 1, 2017.

[30] T. Kalogeris, C. P. Baines, M. Krenz, and R. J. Korthuis, "Ischemia/reperfusion," *Comprehensive Physiology*, vol. 7, no. 1, pp. 113–170, 2016.

[31] Y. Meng, W. Z. Li, Y. W. Shi, B. F. Zhou, R. Ma, and W. P. Li, "Danshensu protects against ischemia/reperfusion injury and inhibits the apoptosis of H9c2 cells by reducing the calcium overload through the p-JNK-NF-$\kappa$B-TRPC6 pathway," *International Journal of Molecular Medicine*, vol. 37, no. 1, pp. 258–266, 2016.

[32] X. B. Wang, X. M. Huang, T. Ochs et al., "Effect of sulfur dioxide preconditioning on rat myocardial ischemia/reperfusion injury by inducing endoplasmic reticulum stress," *Basic Research in Cardiology*, vol. 106, no. 5, pp. 865–878, 2011.

[33] L. B. Agellon and M. Michalak, "The endoplasmic reticulum and the cellular reticular network," *Advances in Experimental Medicine and Biology*, vol. 981, pp. 61–76, 2017.

[34] Y. Yu, L. Zhang, Q. Liu, L. Tang, H. Sun, and H. Guo, "Endoplasmic reticulum stress preconditioning antagonizes low-density lipoprotein-induced inflammation in human mesangial cells through upregulation of XBP1 and suppression of the IRE1$\alpha$/IKK/NF-$\kappa$B pathway," *Molecular Medicine Reports*, vol. 11, no. 3, pp. 2048–2054, 2015.

[35] L. Zhang, Z. Tian, W. Li, X. Wang, Z. Man, and S. Sun, "Inhibitory effect of quercetin on titanium particle induced endoplasmic reticulum stress related apoptosis and in vivo osteolysis," *Bioscience Reports*, vol. 37, no. 4, 2017.

[36] Y. Chen and F. Brandizzi, "IRE1: ER stress sensor and cell fate executor," *Trends in Cell Biology*, vol. 23, no. 11, pp. 547–555, 2013.

[37] M. Zhang, N. Han, Y. Jiang et al., "EGFR confers radioresistance in human oropharyngeal carcinoma by activating endoplasmic reticulum stress signaling PERK-eIF2$\alpha$-GRP94 and

IRE1$\alpha$-XBP1-GRP78," *Cancer Medicine*, vol. 7, no. 12, pp. 6234–6246, 2018.

[38] X. Cao, Y. He, X. Li, Y. Xu, and X. Liu, "The IRE1$\alpha$-XBP1 pathway function in hypoxia-induced pulmonary vascular remodeling, is upregulated by quercetin, inhibits apoptosis and partially reverses the effect of quercetin in PASMCs," *American Journal of Translational Research*, vol. 11, no. 2, pp. 641–654, 2019.

[39] J. Koch-Weser, "Diazoxide," *The New England Journal of Medicine*, vol. 294, no. 23, pp. 1271–1274, 1976.

[40] H. Dong, S. Wang, Z. Zhang, A. Yu, and Z. Liu, "The effect of mitochondrial calcium uniporter opener spermine on diazoxide against focal cerebral ischemia–reperfusion injury in rats," *Journal of Stroke and Cerebrovascular Diseases*, vol. 23, no. 2, pp. 303–309, 2014.

[41] X. Lei, L. Lei, Z. Zhang, and Y. Cheng, "Diazoxide inhibits of ER stress-mediated apoptosis during oxygen-glucose deprivation in vitro and cerebral ischemia-reperfusion in vivo," *Molecular Medicine Reports*, vol. 17, no. 6, pp. 8039–8046, 2018.

Hindawi
Oxidative Medicine and Cellular Longevity
Volume 2020, Article ID 8418407, 19 pages
https://doi.org/10.1155/2020/8418407

*Research Article*

# Exosomal CircHIPK3 Released from Hypoxia-Induced Cardiomyocytes Regulates Cardiac Angiogenesis after Myocardial Infarction

**Yan Wang,[1] Ranzun Zhao,[1] Changyin Shen,[2] Weiwei Liu,[1] Jinson Yuan,[1] Chaofu Li,[1] Wenwen Deng,[1] Zhenglong Wang,[1] Wei Zhang,[1] Junbo Ge,[3] and Bei Shi[1]**

[1]*Department of Cardiology, Affiliated Hospital of Zunyi Medical University, Zunyi 563000, China*
[2]*Department of Cardiology, The Second Affiliated Hospital of Zunyi Medical University, Zunyi 563000, China*
[3]*Department of Cardiology, Shanghai Institute of Cardiovascular Diseases, Zhongshan Hospital, Fudan University, Shanghai 200032, China*

Correspondence should be addressed to Bei Shi; shibei2147@163.com

Received 24 February 2020; Revised 27 April 2020; Accepted 1 June 2020; Published 14 July 2020

Guest Editor: Tatjana Bačun



Exosomes play critical roles in mediating cell-to-cell communication by delivering noncoding RNAs (including miRNAs, lncRNAs, and circRNAs). Our previous study found that cardiomyocytes (CMs) subjected to hypoxia released circHIPK3-rich exosomes to regulate oxidative stress damage in cardiac endothelial cells. However, the role of exosomes in regulating angiogenesis after myocardial infarction (MI) remains unknown. The aim of this study was to establish the effects of exosomes derived from hypoxia-induced CMs on the migration and angiogenic tube formation of cardiac endothelial cells. Here, we reported that hypoxic exosomes (HPC-exos) can effectively reduce the infarct area and promote angiogenesis in the border surrounding the infarcted area. HPC-exos can also promote cardiac endothelial cell migration, proliferation, and tube formation in vitro. However, these effects were weakened after silencing circHIPK3 in hypoxia-induced CMs. We further verified that silencing and overexpressing circHIPK3 changed cardiac endothelial cell proliferation, migration, and tube formation in vitro by regulating the miR-29a expression. In addition, exosomal circHIPK3 derived from hypoxia-induced CMs first led to increased VEGFA expression by inhibiting miR-29a activity and then promoted accelerated cell cycle progression and proliferation in cardiac endothelial cells. Overexpression of miR-29a mimicked the effect of silencing circHIPK3 on cardiac endothelial cell activity in vitro. Thus, our study provides a novel mechanism by which exosomal circRNAs are involved in the communication between CMs and cardiac endothelial cells.

## 1. Introduction

It is important to regulate and maintain cardiac function by ensuring sufficient blood supply to deprived areas after myocardial infarction (MI) [1]. The maintenance of anatomic and functional integrity of the microvasculature after MI is dependent on the proliferation and migration of cardiac endothelial cells and neovascularization. It is well recognized that there is a direct path of communication between cardiomyocytes (CMs) and cardiac endothelial cells in the mammalian heart [2]. We and others have observed that exosomes derived from CMs contain a variety of miRNAs, circRNAs and proteins, which may be transferred to adjacent endothelial cells and consequently regulate their function [3, 4].

Exosomes are involved in regulating the function of target cells by releasing their contents into the target cells [5]. Therefore, exosomes can induce completely different outcomes in recipient cells since the composition of exosomes changes depending on the physiological state of the producing cell [6, 7]. CMs, as well as many other types of cells, can release exosomes [8, 9]. Recently, CM-derived exosomes were found to promote angiogenesis by delivering miR-222 under ischemic conditions [10]. In this context, we demonstrated that exosomes derived from CMs cultured under

hypoxic conditions are able to protect endothelial cells from $H_2O_2$-induced apoptosis and that this effect was dependent on the delivery of circHIPK3 [11]. However, the effect of exosomal circHIPK3 released by hypoxia-induced CMs on the proliferation and migration cardiac endothelial cells and neovascularization remains to be elucidated.

As one of the most abundant circRNAs in the heart [12], circHIPK3 has previously been confirmed to be involved in mediating a wide range of physiological and pathological processes, such as cell survival, autophagy, proliferation, and angiogenesis, by sponging different miRNAs [13–16]. In the present study, we demonstrated in vitro and in vivo that the exosomal circHIPK3 released by hypoxia-induced CMs stimulates cardiac angiogenesis in MI via miR-29a-mediated regulation of VEGFA.

## 2. Materials and Methods

*2.1. Animals.* This study conforms to the Guide for the Care and Use of Laboratory Animals in China. All experimental procedures were in accordance with the protocols approved by the Institutional Animal Care and Use Committee of Zunyi Medical University. Three-week-old wild-type (WT) C57BL/6J mice were procured from Zunyi Medical University (Zunyi, China).

*2.2. Hypoxic Preconditioning of CMs.* Mouse CMs were cultured as we previously described [11]. Briefly, neonatal mice were sacrificed after heparinization and were sterilized. Trypsin (0.03%, Sigma) and collagenase type II (0.04%, Sigma) were used to digest the ventricle fragments. Subsequently, mouse CMs were purified by differential attachment culture to remove cardiac fibroblasts. Afterwards, CMs were subjected to hypoxia. Approximately $5 \times 10^6$ CMs were incubated in complete Dulbecco's modified Eagle medium supplemented with 10% fetal calf serum (FBS) under a 94% $N_2$, 5% $CO_2$, and 1% $O_2$ gas mixture in an incubator (Galaxy Corporation, USA) at 37°C for 12 h.

*2.3. Cardiac Endothelial Cell Culture and Establishment of the $H_2O_2$ Oxidative Stress Model.* The isolation of cardiac endothelial cells was performed according to a previously published protocol [17]. Briefly, mice were euthanized by an overdose of Avertin (200 mg/kg). LV tissue was dissected into ≈1 $mm^3$ pieces and subsequently digested in 450 U/mL collagenase I, 60 U/mL DNase I, and 60 U/mL hyaluronidase (Sigma-Aldrich) for 1 h at 37°C under agitation (750 rpm). The cells were then filtered through a 40 $\mu$m nylon mesh (BD Falcon), washed, and centrifuged (8 min, 300 × g, 4°C). A magnetic bead separation assay with $CD31^+$ beads was used to isolate cardiac endothelial cells, and the purity of the cell population was confirmed by FACS analysis of $CD31^+$ (clone 390) cells. To establish an oxidative stress model for subsequent experiments, these cells were exposed to 200 $\mu$M $H_2O_2$ for 3 h as previously described [18].

*2.4. Isolation and Internalization of Exosomes.* The extraction of CM-derived exosomes was performed as previously described [19]. After CMs were subjected to normoxic or hypoxic conditions for 12 h, the media were collected to obtain exosomes by ultracentrifugation (Beckman Coulter SW 41 Ti rotor and an XPN-100 ultracentrifuge). Then, the exosomes were added to cardiac endothelial cells for update [7] by incubating 300 $\mu$g/mL exosomes with cardiac endothelial cells for 24 h [11].

*2.5. CircRNA-miRNA Interaction.* Interactions between circHIPK3 and miR-29a were predicted using proprietary miRNA target prediction software from Arraystar based on miRanda and TargetScan. Our previous study confirmed that circHIPK3 and miR-29a colocalize in the cytoplasm and have binding sites to each other [11].

*2.6. Cell Transfection.* CircHIPK3, small interfering RNAs (siRNAs) against circHIPK3, the linear HIPK3 gene, and siRNAs against HIKP3 were transfected into CMs or cardiac endothelial cells using a lentiviral construct according to the manufacturer's protocol (Hanbio, China) and performed as previously published [11]. In addition, miR-29a mimic, inhibitor, or their corresponding negative controls (RiboBio, China) were transfected into cardiac endothelial cells with Lipofectamine 3000 (Invitrogen, USA) according to the kit's instructions. At 48 h after transfection, qPCR was used to evaluate the gene expression in cardiac endothelial cells.

*2.7. Real-Time qPCR.* The relative expression of circHIPK3, miR-29a, and VEGFA mRNA was measured as previously described [11]. TRIzol reagent (Life Technologies, Carlsbad, CA) was used to isolate total RNA from cell lysates, after which 500 ng of RNA was subjected to reverse transcription with a PrimeScript RT Master Mix (Takara, Dalian, China) to synthesize cDNAs from circHIPK3, miR29a, and VEGFA mRNA. qPCR analyses of the cDNAs were performed with SYBR Premix Ex Taq II (Takara). RNase R treatment was used for circRNA detection as before. The amount of miRNA was detected using Stem-loop qPCR TaqMan MicroRNA assays (Life Technologies), and GAPDH and U6 were used as the internal reference for mRNA and miRNA expression, respectively. The $2^{-\Delta\Delta Ct}$ method was used to quantify gene expression. All primer sequences are listed in Table 1 and were designed and synthesized by RiboBio (Guangzhou, China).

*2.8. Western Blot.* The protein levels in cardiac endothelial cells were analyzed by Western blot as previously described. Protein extracts were separated by SDS-PAGE and transferred onto PVDF membranes. After the membranes were blocked overnight in BSA solution, they were probed with primary antibodies against VEGFA, CyclinD1, PCNA, and $\beta$-actin. Next, GAPDH and horseradish peroxidase-conjugated secondary antibodies were incubated with the PVDF membranes for 1 h, and then, an enhanced chemiluminescence reagent (Amersham Biosciences, USA) was incubated on the PVDF membranes before the protein band intensities were detected with a ChemiDoc MP system.

*2.9. Cardiac Endothelial Cell Proliferation, Migration, and Tube Formation Assays.* Cell migration was determined using Transwell assays as previously described [20]. A total of 100 $\mu$L of cell suspension ($1 \times 10^5$ cells/mL) was added to

Table 1: The sequences of primers used for PCR.

| Primer sequence | |
|---|---|
| CircHIPK3 | Forward 5′- GGATCGGCCAGTCATGTATC-3′<br>Reverse 5′-ACCGCTTGGCTCTACTTTGA-3′ |
| HIPK3 mRNA | Forward 5′- GTGATCCGGCCTGTTCTTCA-3′<br>Reverse 5′- TGACTGGCCGATCCAAAGTC-3′ |
| GAPDH mRNA | Forward 5′-GTCAAGGCTGAGAACGGGAA-3′<br>Reverse 5′-AAATGAGCCCCAGCCTTCTC-3′ |
| $\beta$-Actin mRNA | Forward 5′-TTGTTACAGGAAGTCCCTTGCC-3′<br>Reverse 5′-ATGCTATCACCTCCCCTGTGTG-3′ |
| VEGFA mRNA | F: 5′-ATGATTCTGCCCTCCTCCTT-3′<br>R: 5′-CCTTGCTGCTCTACC TCCAC-3′ |
| miR-29a | RT: 5′-GTCGTATCCAGTGCGTGTCGTGGAGTCGGCAATTGCACTGGA TACGACTAACCGAT-3′<br>F: 5′-ACACTCCAGCTGGGTAGCACCATCTGAAAT-3′<br>R: 5′-TGGTGTCGTGGAGTCG-3′ |
| U6 | RT: 5′-AACGCTTCACGAATTTGCGT-3′<br>F: 5′-CTCGCTTCGGCAGCACA-3′<br>R: 5′-AACGCTTCACGAATTTGCGT-3′ |

the upper chamber, and 600 $\mu$L of complete medium was added to the lower chamber. After 24 h, cells that did not migrate to the lower chamber were removed. Subsequently, the chamber was fixed in 4% paraformaldehyde for 30 min and dyed with 1% crystal violet for another 15 min. Five randomly selected fields in each chamber were imaged with an inverted microscope (magnification 10x) to determine the number of migrated cells.

Cell proliferation was detected with the Cell-Light 5-Ethynyl-20-deoxyuridine (EdU) Kit (RiboBio, China) according to the manufacturer's protocol. After cells were incubated with EdU for 2 h, they were stained with Apollo Dye Solution for 30 min followed by Hoechst 33342 staining. EdU-positive cells in five randomly selected fields were imaged and counted under an Olympus FSX100 microscope (Olympus, Tokyo, Japan).

Cardiac endothelial cells ($1 \times 10^5$ cells/mL) were plated on 120 $\mu$L of Matrigel (BD Falcon) in a 48-well plate and incubated at 37°C in an atmosphere of 5% CO2 for 16 h. The gels were observed under an inverted microscope (4x magnification) (Nikon TS100), and the numbers of branch points and tubes formed for each unique tube structure were counted in each image.

*2.10. Cell Cycle Assay.* Cardiac endothelial cells were harvested and then washed with ice-cold phosphate-buffered saline (PBS). The cells were fixed in 70% ethanol for 24 h before they were resuspended in 500 $\mu$L of PBS containing 10 $\mu$g/mL RNase A, 50 $\mu$g/mL propidium iodide (Sigma), 0.1% Triton X-100, and 0.1% sodium citrate. The suspensions were incubated for 15 min at room temperature in the dark and then immediately analyzed on a flow cytometer (Millipore Guava).

*2.11. MI Induction and Exosome Delivery.* Mice underwent inhalational anesthesia with 2% isoflurane and were subjected to MI via ligation of the left anterior descending coronary artery (LAD) as described previously [21, 22]. Immediately after LAD ligation, the mice received an intramyocardial injection of either 1 $\mu$g/g exosomes or PBS ($n = 10$) in a total volume of 20 $\mu$L at 5 different sites in the peri-infarct area. All mice were followed up at 4 weeks post-MI to evaluate both LV functional changes using echocardiography and structural remodeling.

*2.12. Echocardiography.* Echocardiography was performed on mice before MI (baseline) and at 4 weeks post-MI using a Vevo 770 imaging system (VisualSonics, Toronto, Canada) equipped with a 30 MHz transducer. The mice underwent inhalational anesthesia with a mixture of 1.5% isoflurane and oxygen (1 L/min). The internal diameter of the LV was measured in the short-axis view from M-mode recordings, and the ejection fraction (EF) and left ventricular end diastolic diameter (LVIDd) were calculated using corresponding formulas as previously described [23].

*2.13. Morphometric Studies.* Mice were euthanized by an overdose of Avertin (200 mg/kg). The hearts were fixed with 10% buffered formalin and paraffin embedded. Morphometric analysis was performed on tissue sections prepared with Masson's trichrome and hematoxylin/eosin staining using ImageJ software. The fibrotic area was measured to determine the percentage of fibrosis [17].

*2.14. Histology.* Immunofluorescence staining of tissue sections was performed as described previously [24]. The formation of a new capillary network was assessed by CD31 (Abcam) staining as described before [17]. Nuclei were

counterstained with 4,6-diamidino-2-phenylindole (Sigma-Aldrich, St. Louis, MO), and 10 randomly selected fields in each sample were imaged under a fluorescence microscope (Olympus, Tokyo, Japan).

*2.15. Statistical Analysis.* Analyses were conducted with the SPSS 21.0 statistical package (IBM, Armonk, NY, USA). The data were normally distributed and are expressed as the mean ± SD. Comparisons among multiple groups were performed with one-way analysis of variance (ANOVA). In addition, a $P$ value $< 0.05$ was considered statistically significant.

## 3. Results

*3.1. HPC-Exos Promote Angiogenesis following MI In Vivo.* To evaluate the beneficial function of exosomes released from hypoxic CMs, normoxic exosomes (Nor-exos), or hypoxic exosomes (HPC-exos) were delivered to the border area of MI at the moment of injury. Four weeks after MI, mice administered with HPC-exos tended to have an increased EF and decreased LVIDd (Figures 1(a)–1(c)). Most importantly, the myocardial vascular density was increased in the infarcted region in mice in the HPC-exo group, as shown by the increase in CD31-stained cells (Figures 1(d) and 1(e)). CM-derived exosomes may also reduce cardiac fibrosis and improve ventricular remodeling after MI [10]. Masson's and hematoxylin-eosin staining showed a substantial decrease in myocardial fibrosis after HPC-exo treatment compared with PBS treatment in mice subjected to MI (Figures 1(f)–1(h)). Altogether, these results indicated that the exosomes produced by hypoxic CMs promote neovascularization after MI and ameliorate myocardial fibrosis.

*3.2. HPC-Exos Promote Cardiac Endothelial Cell Migration, Proliferation, and Tube Formation.* As a multistep physiological process, angiogenesis comprises several sequential steps involving the proliferation, migration, and morphogenesis of cardiac endothelial cells. Therefore, we tested whether CM-derived exosomes impact the behavior and angiogenic potential capacity of cardiac endothelial cells in vitro. $H_2O_2$ (200 $\mu$M for 3 h) was used to pretreat cardiac endothelial cells to simulate the microenvironment of oxidative stress in vitro. The results demonstrated that, compared with the normal group, the $H_2O_2$ group showed decreased proliferation, migration, and tube formation (Figures 2(a)–2(i)). Furthermore, compared with Nor-exos, HPC-exos promoted cardiac endothelial cell proliferation and migration after 24 h of treatment, as indicated by the EdU and Transwell assays (Figures 2(a)–2(d)). CyclinD1 and PCNA are proliferation markers and are required for regulating the cell cycle of proliferating endothelial cells at G1 phase [25]. Western blot assays also indicated that cyclinD1 and PCNA were upregulated in the HPC-exo group compared with the Nor-exo group (Figures 2(h)–2(i)). Moreover, compared to Nor-exos, HPC-exos exhibited an increased capacity to induce tube formation, as demonstrated by the presence of more branch points and tube-like segments in the Matrigel assay (Figures 2(e)–2(g)). Taken together, these results provide credible evidence that HPC-exos promote cardiac endothelial cell migration, proliferation, and tube formation, which are the cardinal features of angiogenesis.

*3.3. HPC-Exosomal CircHIPK3 Is Involved in Promoting the Cell Cycle and Accelerating Migration in Cardiac Endothelial Cells.* The above data indicated that exosomes derived from CMs subjected to hypoxia have a greater capacity to promote cardiac endothelial cell proliferation than exosomes derived from CMs under normoxic conditions. Exosomes facilitate the communication between adjacent cells by transferring circRNAs [26], and circRNA expression is dynamically regulated after cells are exposed to hypoxia [27]. In a previous study, we demonstrated that circHIPK3 was enriched in exosomes derived from CMs cultured under hypoxic conditions [11]. This prompted us to further investigate the function of exosomal circHIPK3 on the proliferation and migration of cardiac endothelial cells and neovascularization. To understand the role of exosomal circHIPK3 in cardiovascular biology, we first detected circHIPK3 expression in cardiac endothelial cells incubated with HPC-exos or Nor-exos by using qPCR. The results indicate that compared with the control group, the $H_2O_2$ group exhibited significantly downregulated levels of circHIPK3. Compared with $H_2O_2$ treatment alone, exosome pretreatment significantly rescued circHIPK3 levels, and circHIPK3 expression was higher in the HPC-exo group than the Nor-exo group (Figure 3(a)).

To investigate the role of circHIPK3 alone in cardiac endothelial cells, we generated lentiviral vectors that expressed ectopic circHIPK3 or siRNA targeting circHIPK3 (sicircHIPK3) and transfected these vectors into mouse cardiac endothelial cells for 48 h. The impact of linear HIPK3 was also determined by conducting gain- and loss-of-function analyses. Cell proliferation resulting from altered cell cycle progression is a main event in neovascularization. In cardiac endothelial cells under oxidative conditions, circHIPK3 overexpression significantly promoted the cell cycle, as evidenced by an accelerated G1/S transition in cells assessed by flow cytometry. Suppressing circHIPK3 arrested the cell cycle at G0/G1 phase (Figures 3(b)–3(e)). Furthermore, the migration ability of cells was significantly increased in the circHIPK3 overexpression group and further decreased in the circHIPK3 suppression group compared with the $H_2O_2$ group (Figures 3(f)–3(i)). In addition, the levels of cyclinD1 and PCNA were upregulated in cells overexpressing circHIPK3 but downregulated in cells with circHIPK3 suppression (Figures 3(j)–3(m)). However, neither overexpressing nor inhibiting linear HIPK3 expression had a significant effect on cell proliferation and migration (Figures 3(a)–3(m)).

To further verify whether the effects of HPC-exos on cardiac endothelial cells were dependent on circHIPK3 but not linear HIPK3, we overexpressed and inhibited both circHIPK3 and linear HIPK3 in hypoxia-induced CMs by transfecting them with HIPK3 siRNA, linear HIPK3, circHIPK3, or circHIPK3 siRNA for 48 h and then culturing them under hypoxic conditions for 12 h. Their exosomes (HPCHIPK3-exos, HPC-circHIPK3-exos, HPC-siHIPK3-

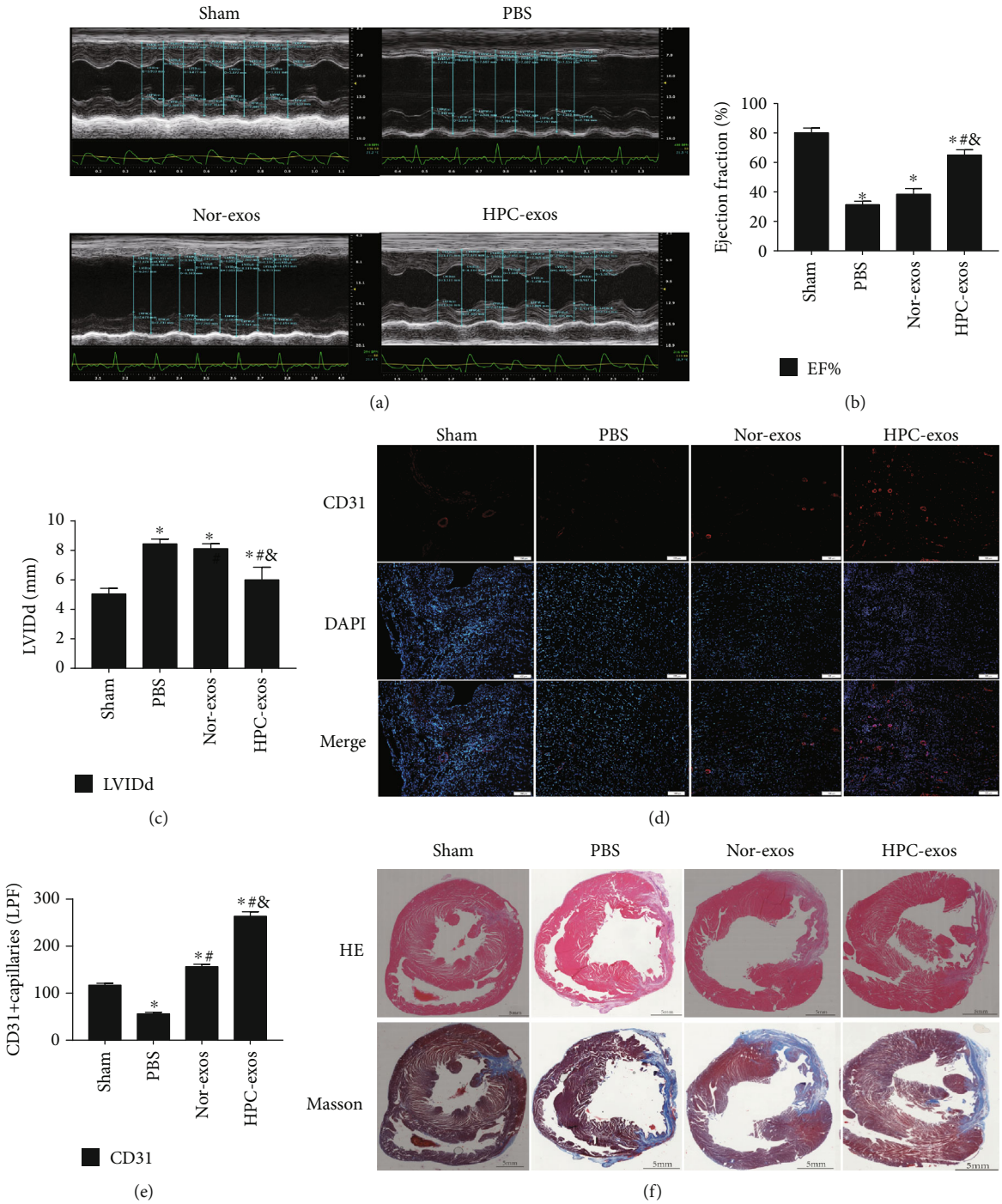


Figure 1: Continued.

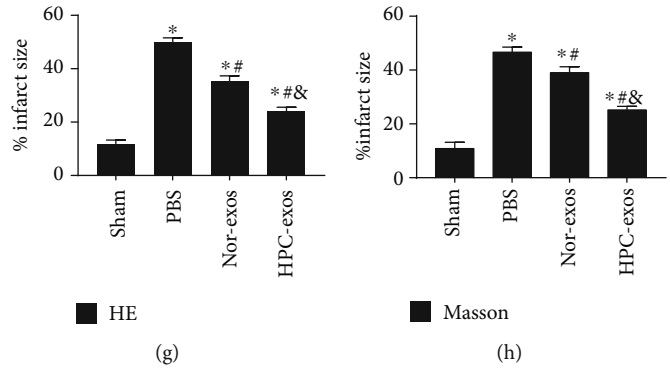


Figure 1: HPC-exos stimulate neovascularization and improve cardiac function at 4 weeks following MI. PBS, Nor-exos, and HPC-exos were delivered to the border area of MI at the moment of injury. Four weeks following MI, the neovascularization density, cardiac function, and fibrosis levels were evaluated. (a) Representative echocardiographic images. The LVEF% (b) and LVIDd (c) were calculated in various groups as indicated ($n = 5$ for the PBS group and $n = 6$ for the Nor-exo and HPC-exo groups). (d) CD31 immunolabeling in the infarcted area. (e) Quantification of CD31-positive cells. (f) Representative cross-sectional images of hearts subjected to hematoxylin-eosin staining and Masson's trichrome staining 4 weeks after exosome transplantation. The blue color indicates fibrosis, and the red color indicates myocardial fibers. (g, h) HPC-exo transplantation reduced the fibrotic area (mean ± SD, $n = 3$; $^{*}P < 0.05$, compared with the sham group, $^{\#}P < 0.05$ compared with the PBS group, and $^{\&}P < 0.05$ compared with the Nor-exo group).

exos, and HPC-sicircHIPK3-exos, respectively) were cocultured with cardiac endothelial cells. There is no doubt that HPC-exos significantly induced increases in cyclinD1 and PCNA and promoted cell cycle progression and cell migration (Figures 3(j)–3(m)). HPC-exos derived from CMs with circHIPK3 overexpression induced enhanced cell cycle progression and migration of cardiac endothelial cells (Figures 3(b)–3(i)). However, HPC-exos derived from CMs with inhibited circHIPK3 expression resulted in reduced levels of cell cycle progression and migration in cardiac endothelial cells (Figures 3(b)–3(i)). The overexpression or inhibition of linear HIPK3 did not change the effects of HPC-exos on the cell cycle or migration (Figures 3(b)–3(i)). The use of HPC-exos is a potential strategy for promoting cell cycle progression and migration of cardiac endothelial cells under oxidative stress conditions by rescuing downregulated circHIPK3 expression.

*3.4. miR-29a Is Upregulated in Cardiac Endothelial Cells and Suppresses Cell Proliferation and Migration by Targeting VEGF In Vitro.* Previous studies have shown that circHIPK3 can regulate cell growth by acting as a miR-29a inhibitor [28]. In our earlier work, we verified that miR-29 and circHIPK3 colocalize in the cytoplasm in cardiac endothelial cells and can directly bind to each other to regulate cell function. miR-29a was shown to be upregulated in endothelial cells under oxidative stress, which subsequently promoted apoptosis. Thus, the effect of miR-29a could be effectively inhibited by overexpressing circHIPK3 in cells.

To investigate the role of miR-29a in cardiac endothelial cells, we treated cells with miR-29a mimic or inhibitor and evaluated their effects on angiogenesis. The data showed that compared with the $H_2O_2$ group, the miR-29a mimic group showed decreased proliferation and migration, as determined by the EdU and Transwell assays, respectively (Figures 4(a)–4(d)). By contrast, inhibiting miR-29a significantly promoted proliferation and migration of cardiac endothelial cells, even under oxidative stress conditions (Figures 4(a)–4(d)). The relative quantities of cyclinD1 and PCNA were also analyzed by Western blotting. CyclinD1 and PCNA were substantially decreased in the miR-29a mimic group compared with the $H_2O_2$ group, while they were substantially increased in the miR-29a inhibitor group (Figures 4(e) and 4(f)). In addition, we also evaluated tube formation. The results showed that the relative tube formation and numbers of branch points were decreased in the miR-29a mimic group compared with the $H_2O_2$ group, while they were increased in the miR-29a inhibitor group compared with the $H_2O_2$ group (Figures 4(g) and 4(h)).

Subsequently, upon searching the miRanda database, we found that the 3′-UTR of VEGFA contains a binding site of miR-29a. Angiogenesis is mediated via activation of VEGFR2 by its primary ligand, VEGFA; VEGFR2 is then phosphorylated (p-VEGFR2) and translocates to the nucleus [29]. In addition, miR-29a has been shown to play a key antiangiogenic role within the tumor microenvironment by suppressing the expression of VEGFA [30]. Dual-luciferase reporter assays were used to confirm that VEGFA is a target gene of miR-29a in cardiac endothelial cells (Figure 4(j)). In addition, the miR-29a mimics effectively increased miR-29a expression in cardiac endothelial cells whereas the miR-29a inhibitor effectively reduced it (Figure 4(k)). We also found that VEGFA mRNA levels were significantly reduced in the miR-29a mimic group, whereas the miR-29a inhibitor group showed the opposite trend (Figure 4(l)). Western blot analysis revealed that the miR-29a inhibitor effectively promoted VEGFA expression, while the miR-29a mimics clearly reduced VEGFA levels (Figures 4(m) and 4(n)). These results suggested that miR-29a targets VEGFA and inhibits its expression. Therefore, the effects of miR-29a on inhibiting the proliferation, migration, and tube formation of cardiac endothelial cells were partially mediated by targeting VEGFA.

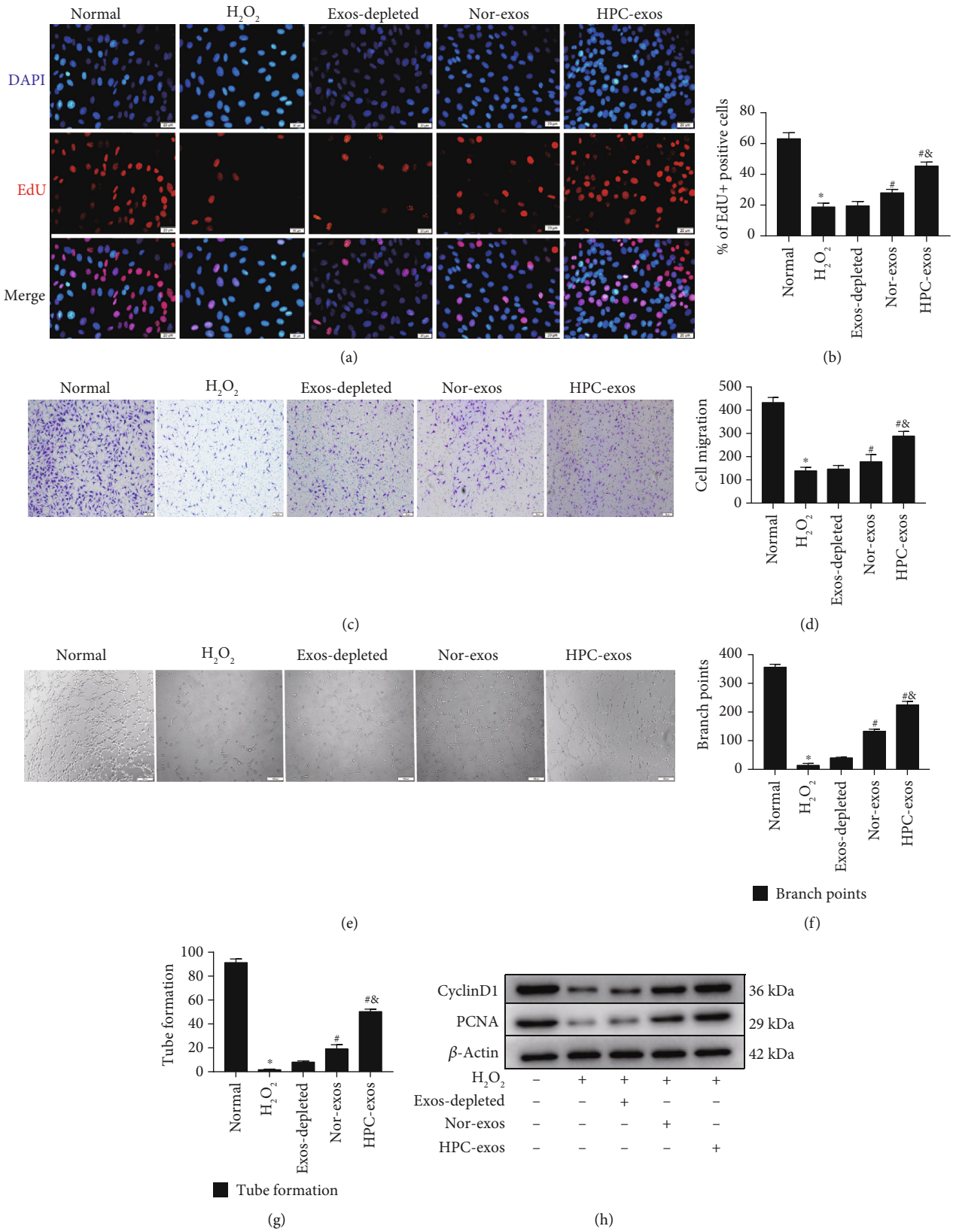


Figure 2: Continued.

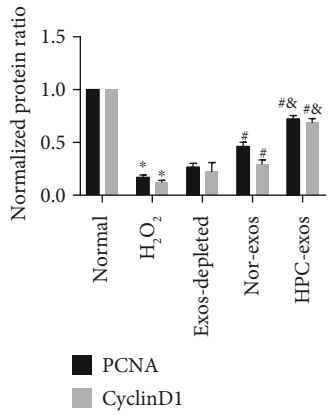


(i)

Figure 2: HPC-exos promote cardiac endothelial cell migration, proliferation, and tube formation. Cardiac endothelial cells were incubated with depleted exos, Nor-exos, or HPC-exos for 24 h after exposure to 200 $\mu$M $H_2O_2$ for 3 h. (a) Cell proliferation was detected by using the EdU assay. (b) Quantification of the data presented in (a). (c) The migration ability of cardiac endothelial cells was measured by Transwell assay (original magnification, ×200). (d) Quantification of the data presented in (c). (e) Tube formation in Matrigel was assessed. (f, g) Quantitative assessment of the number of branch points and tubes formed. (h) The protein expression levels of cyclinD1 and PCNA were determined using Western blot analysis. (i) Quantification of the relative expression levels of cyclinD1 and PCNA. The results are normalized to the control (mean ± SD, $n = 3$; $^{*}P < 0.05$, compared with the normal group; $^{\#}P < 0.05$ compared with the $H_2O_2$ group; and $^{\&}P < 0.05$ compared with the Nor-exo group).

*3.5. HPC-Exosomal CircHIPK3 Induces Cell Proliferation, Migration, and Tube Formation via miR-29a/VEGFA in Cardiac Endothelial Cells.* To investigate whether HPC-exos mediated angiogenesis in cardiac endothelial cells by targeting VEGFA via inhibition of miR-29a, cardiac endothelial cells were transfected with miR-29a mimics for 48 h and then exposed to HPC-exos for 24 h. EdU and Transwell assays revealed that the miR-29a mimics reversed the effects of HPC-exos on the levels of proliferation and migration in cardiac endothelial cells (Figures 5(a)–5(d)). In addition, flow cytometry showed that the facilitated G1/S transition induced by HPC-exos was also reversed by miR-29a mimics (Figures 5(e) and 5(f)). Moreover, transfection of miR-29a mimic in cardiac endothelial cells could also partly block the HPC-exo-induced increase in tube formation capacity and the expression of the proliferation-related proteins cyclin D1 and PCNA (Figures 5(g) and 5(h)). Western blot analysis also showed that in the HPC-exo+mimic+VEGFA group, miR-29a significantly inhibited VEGFA expression, while VEGFA overexpression strikingly reversed the reduced VEGFA levels (Figures 5(l) and 5(m)). In addition, we observed that exogenous VEGFA could partially reverse the repressive effect of miR-29a on the cell proliferation, migration, and tube formation of cardiac endothelial cells (Figures 5(a)–5(k)). In conclusion, in cardiac endothelial cells, HPC-exos promoted angiogenesis by regulating the cell cycle, cell proliferation, and migration through circHIPK3/-miR-29a/VEGFA signaling axes in vitro and in vivo.

## 4. Discussion

It is well established that there is tightly regulated crosstalk among the different cell types via CM-derived exosomes. For example, exosomes secreted by CMs subjected to ischemia promote cardiac angiogenesis by delivering miRNA-222 and miRNA-143 [10]. The regulatory effect of CM-derived exosomes in endothelial cells is relatively well studied. However, the role of a few exosomal circRNAs in this interplay remains unknown. CircRNAs can be enriched in exosomes under certain pathological conditions; their capture by neighboring cells regulate the function of these target cells [31]. In our previous study, we found that exosomal circHIPK3 released from hypoxia-induced CMs could inhibit miR-29a activity and then regulate oxidative damage in cardiac endothelial cells in the microvasculature, thus leading to increased IGF-1 expression in vitro [11]. In the current study, we revealed that the exogenous delivery of exosomes secreted by CMs subjected to hypoxia can play an important role in promoting angiogenesis after MI in vitro and in vivo. At the same time, we also confirmed that circHIPK3 was the most enriched circRNA in HPC-exos, inducing the angiogenic process.

Hypoxia could increase myocardial tolerance as an adaptive response to prevent endoplasmic reticulum stress and apoptosis [32]. However, hypoxic preconditioning enhanced the benefits of cell-derived exosomes in an animal MI model and led to an increase in the proangiogenic effect of exosomes [33]. In this study, we also observed that exosomes released from hypoxic CMs could promote angiogenesis after an acute MI and improve myocardial fibrosis. It was verified that HPC-exos promote migration, proliferation, and tube formation of cardiac endothelial cell in vitro; however, the exact mechanism is unclear.

Exosomes are vectors of circRNAs, lncRNAs, and miRNAs; they serve as a mechanism that allows cell-to-cell communication [20, 31]. CircRNAs can compete for miRNA- or protein-binding sites to regulate several diseases [34]. Interestingly, some circRNAs are differentially expressed in cells subjected to hypoxic conditions [27].

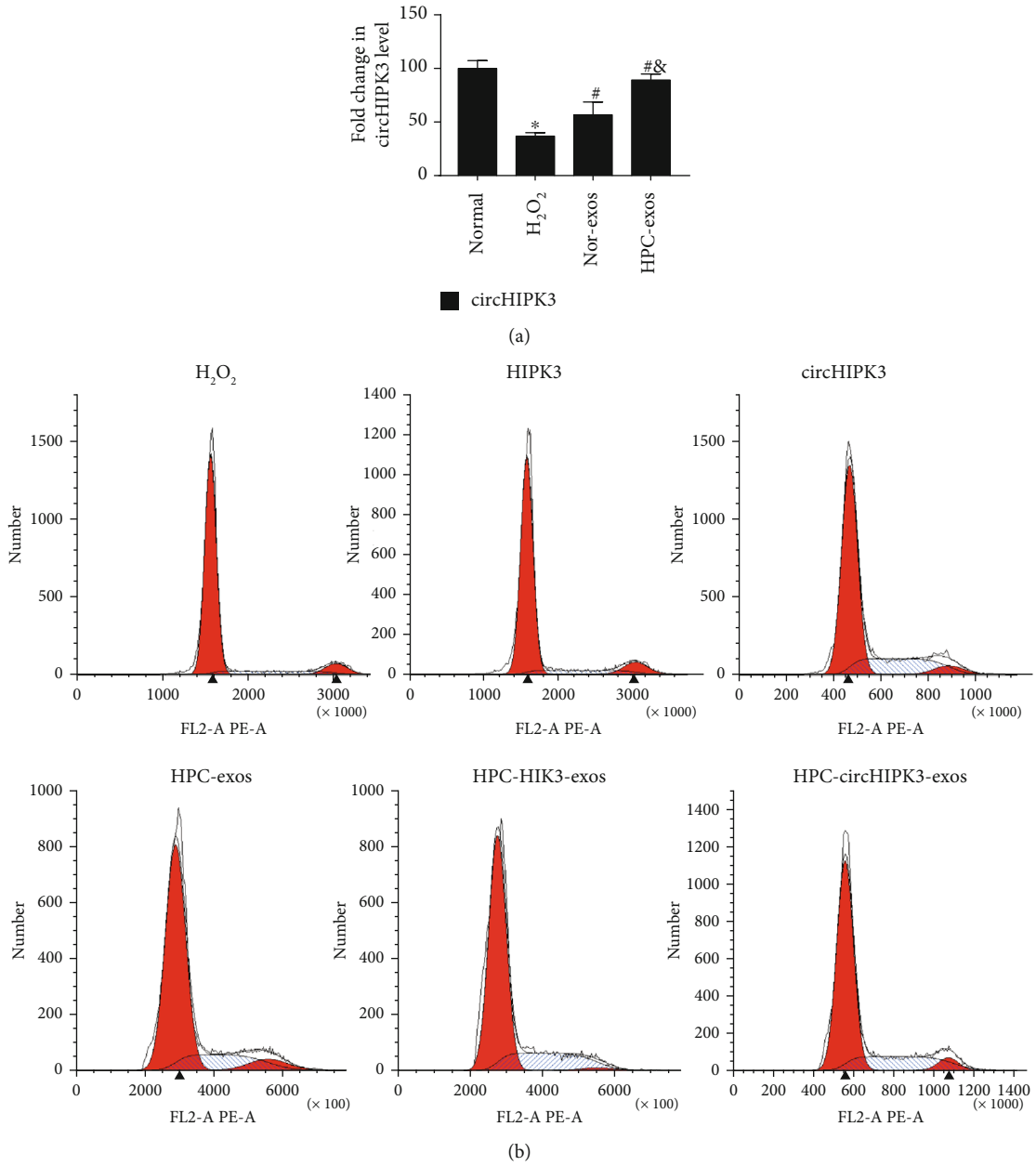


Figure 3: Continued.

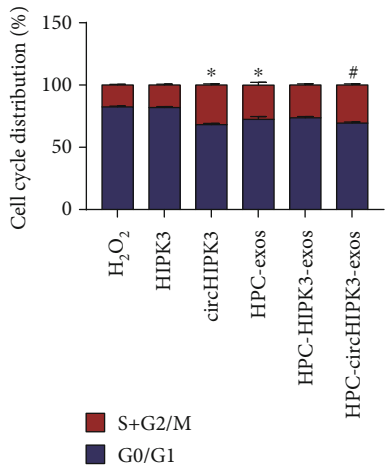


(c)

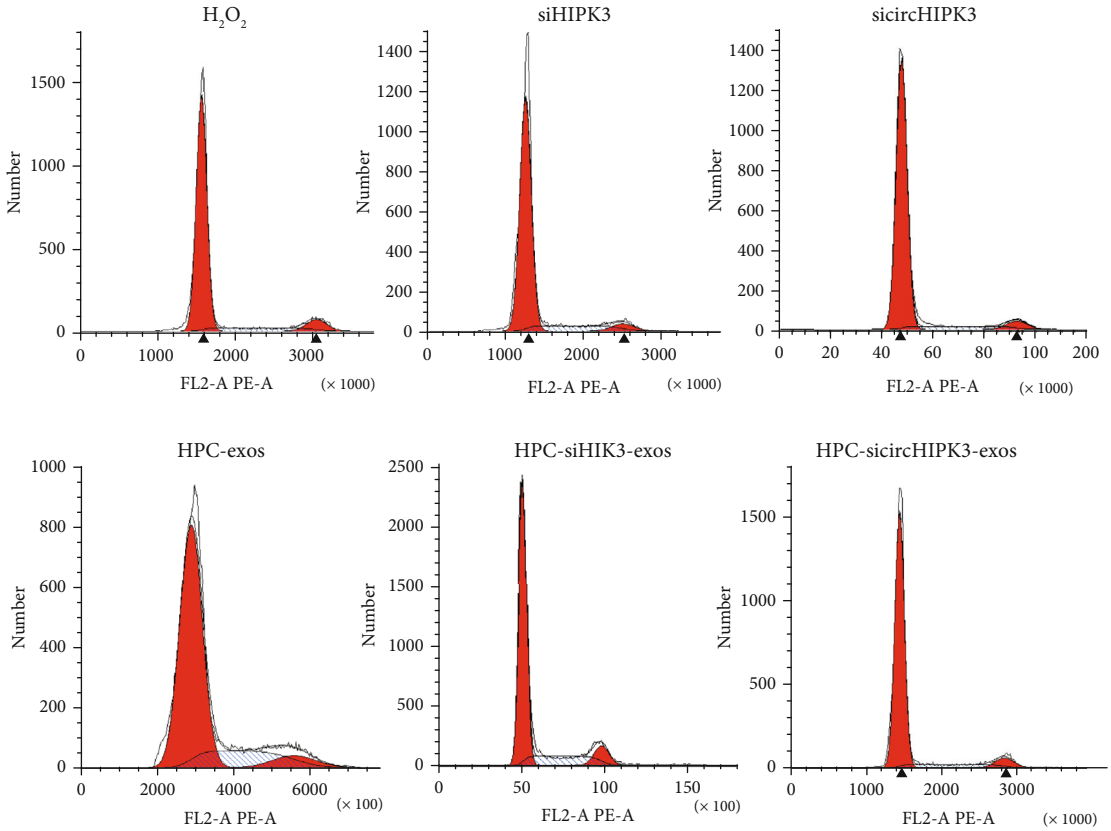


(d)

Figure 3: Continued.

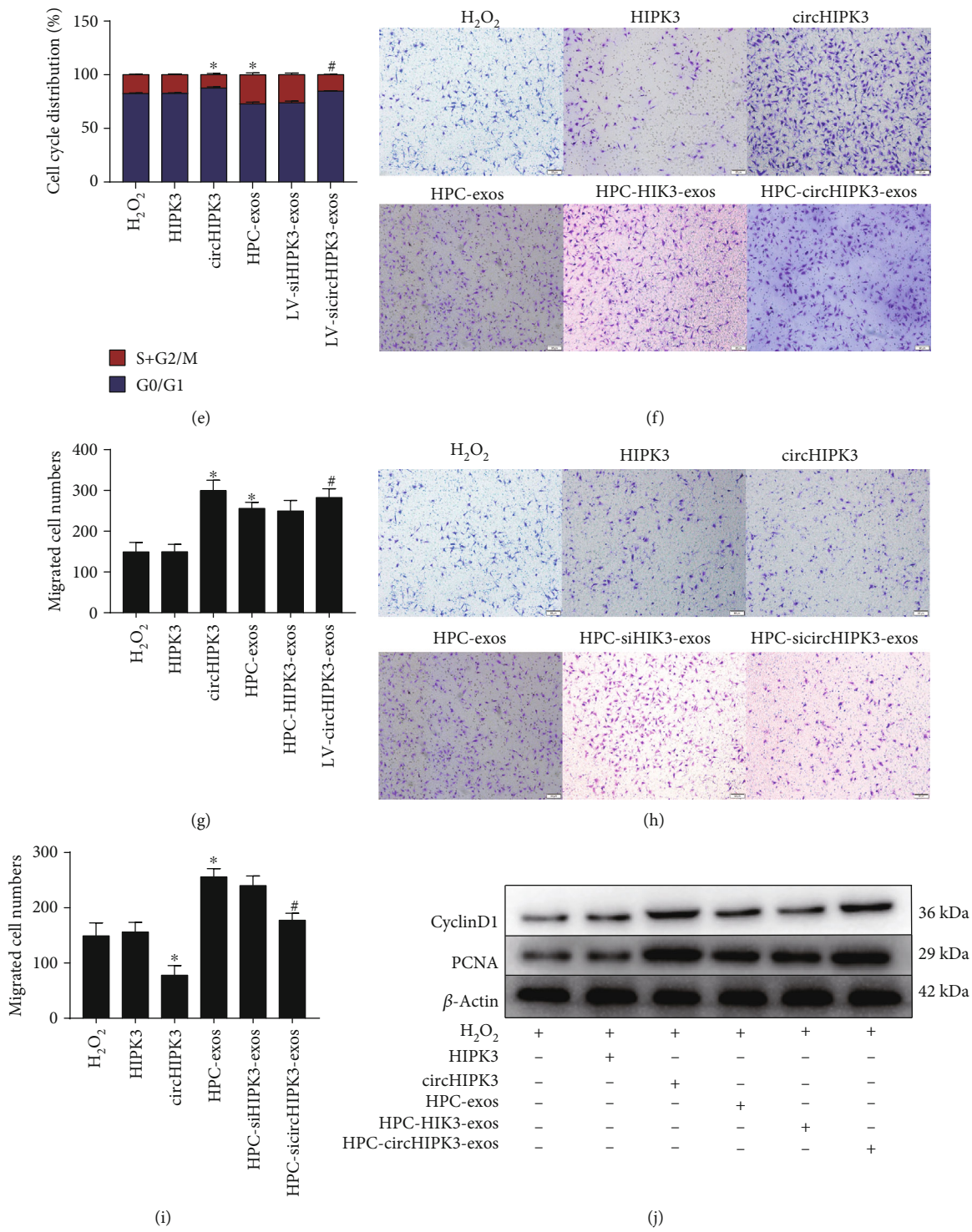


Figure 3: Continued.

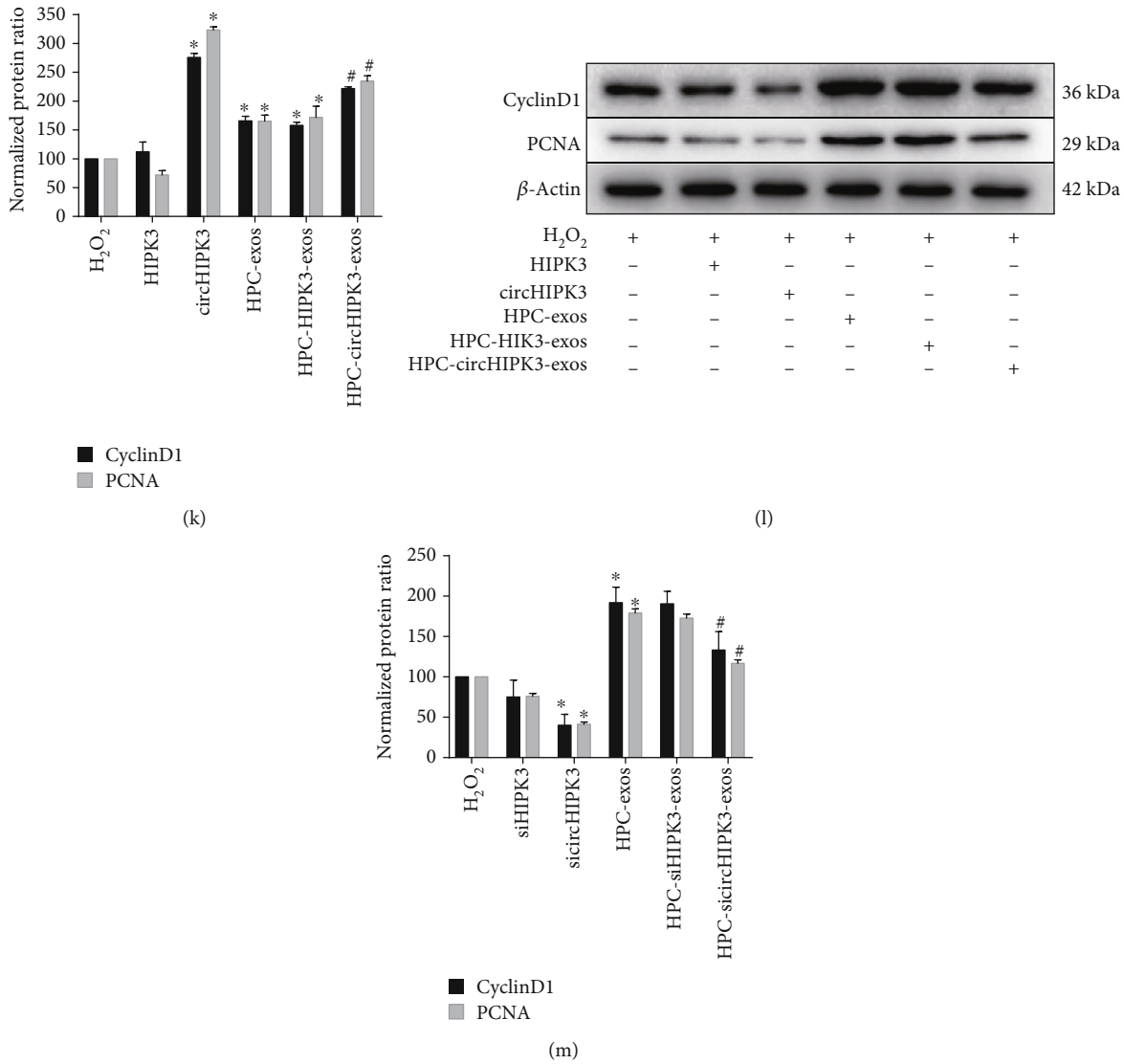


Figure 3: HPC-exosomal circHIPK3 accelerates cell cycle progression and migration of cardiac endothelial cells. circHIPK3, circHIPK3 siRNA, linear HIPK3, or linear HIPK3 siRNA was transfected into cardiac endothelial cells for 48 h to evaluate cell proliferation and migration. Furthermore, cardiac endothelial cells were incubated with HPC-HIPK3-exos, HPC-circHIPK3-exos, HPC-siHIPK3-exos, or HPC-sicircHIPK3-exos to understand the role of exosomal circHIPK3. (a) circHIPK3 expression in cardiac endothelial cells subjected to different treatments was analyzed with qPCR. (b, d) Flow cytometry was performed to analyze the distribution of cells in the cell cycle. (c, e) Representative quantification of the data from (b) and (d), respectively. (f, h) Cell migration among the six groups as confirmed by the Transwell assay (lower, bars = 50 $\mu$m). (g, i) The number of migrated cells per field was determined. (j, l) Western blot analyses were performed. (k, m) Quantification of the relative protein levels of cyclinD1 and PCNA in cardiac endothelial cells was performed (means ± SD, $n = 3$, $^{*}P < 0.05$, compared with the $H_2O_2$ group, $^{\#}P < 0.05$ compared with the HPC-exo group).

CircHIPK3 is expressed in endothelial cells and can increase cell proliferation and improve vascular dysfunction [16]. Our previous study found that circHIPK3 within HPC-exos could regulate the oxidative stress damage of cardiac endothelial cells in the microvasculature through the miR-29a/IGF-1 axis [11]. However, another study showed that circHIPK3 overexpression had the opposite effect [13]. On the basis of our previous results and those of others, we hypothesized that circHIPK3 released from HPC-exos affects cardiac endothelial cells, resulting in angiogenesis. In the present study, we observed upregulated levels of circHIPK3 in cardiac endothelial cells treated with exosomes from MCs cultured under oxidative conditions. We also showed that overexpression of circHIPK3 alone, but not of linear HIPK3, promoted the proliferation, migration, and tube formation of cardiac endothelial cells. Knocking down circHIPK3 but not linear HIPK3 mRNA suppressed the proliferation, migration, and tube formation of cardiac endothelial cells. Moreover, when circHIPK3 was overexpressed in CMs subjected to hypoxic conditions, the results suggested that HPC-exos from these CMs enhanced the cell cycle progression and migration of cells. However, HPC-exos derived from CMs with inhibition of circHIPK3 reduced the cell cycle progression and migration. The overexpression or

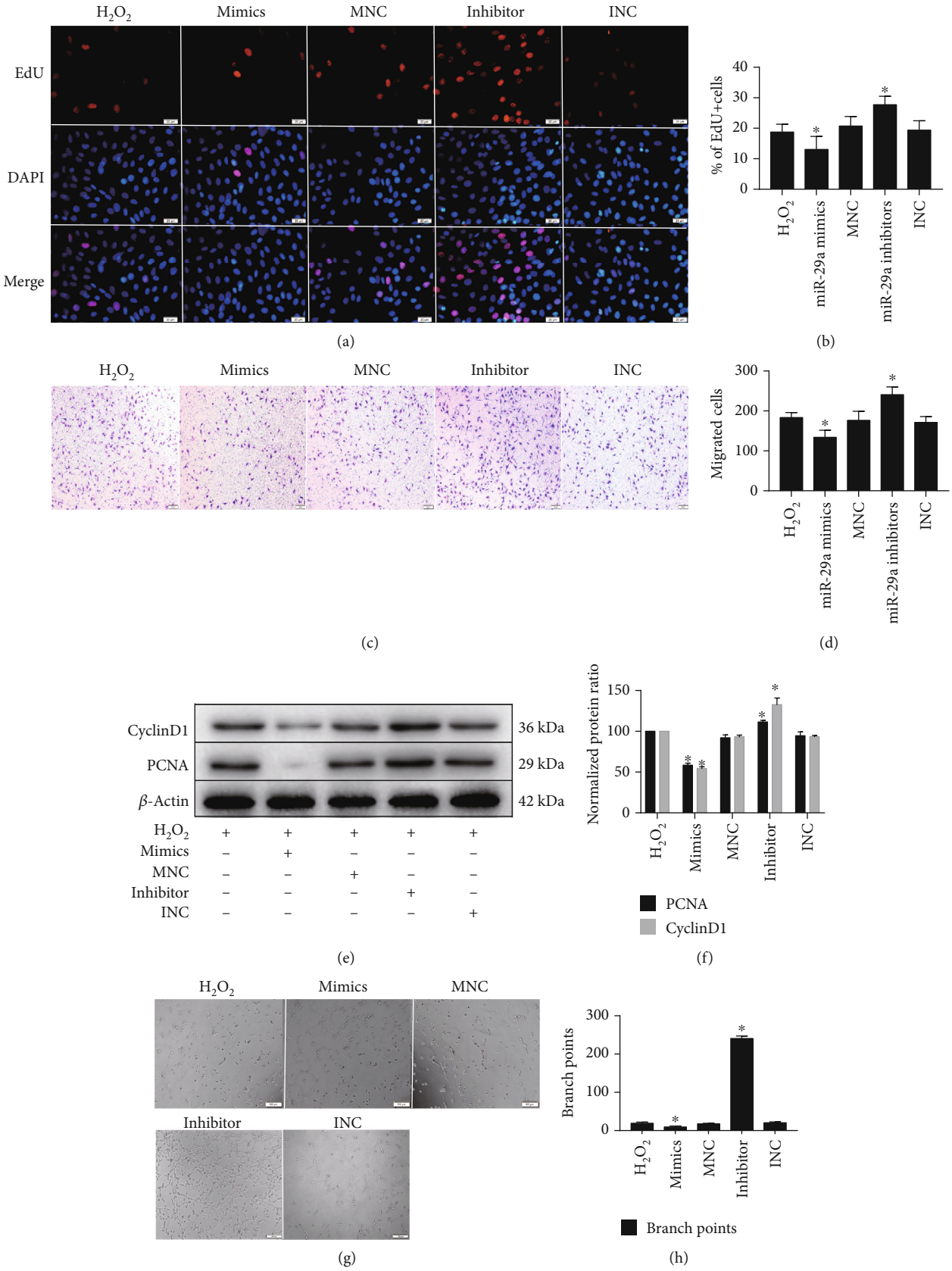


Figure 4: Continued.

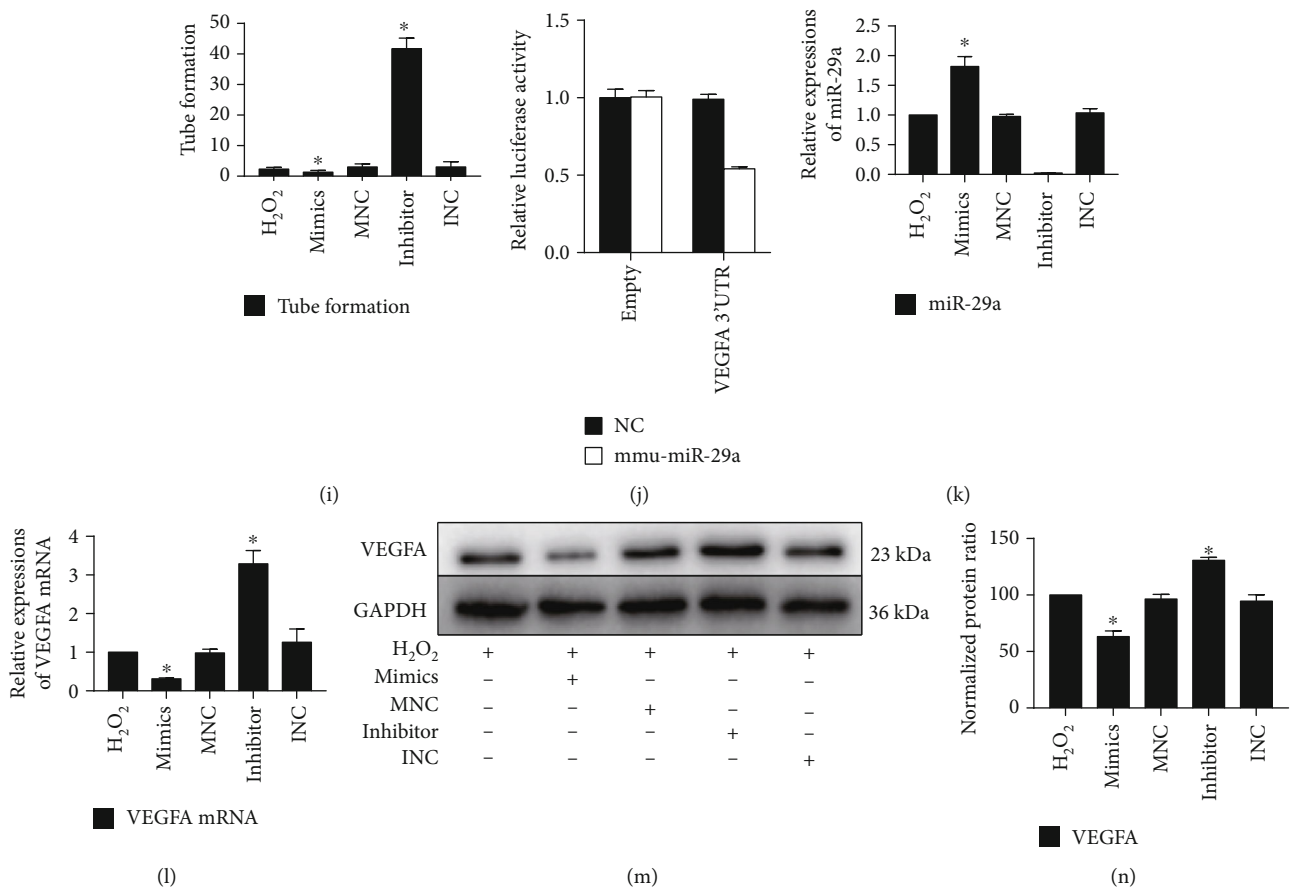


Figure 4: miR-29a regulated the proliferation, migration, and tube formation of cardiac endothelial cells by targeting VEGFA. miR-29a mimics or inhibitors were transfected into cardiac endothelial cells via Lipofectamine 2000; 48 h later, an oxidative stress model was established with the cardiac endothelial cells to investigate the effects of miR-29a. (a) Cell proliferation of cardiac endothelial cells as determined by EdU assays. (b) Quantitative analysis of (a). (c) Migration of cardiac endothelial cells was measured by Transwell migration assays (scale bar = 50 $\mu$m). (d) The number of migrated cells per field was determined. (e) Western blot analyses were performed. (f) Relative protein levels of cyclinD1 and PCNA in cardiac endothelial cells were determined. (g) Representative images of cardiac endothelial cells in Matrigel. (h, i) Quantitative assessment of the total number of meshes and branch points. (j) The dual-luciferase activity was verified by cotransfecting either miR-29a mimics or miR-29a-NC and the luciferase reporter vectors pmiRGLO-VEGFA-Mut or pmiRGLO-VEGFA-WT. (k) Relative miR-29a expression in different groups of cardiac endothelial cells was detected via qPCR analysis. (l) VEGFA mRNA expression in cardiac endothelial cells in different groups was also detected by using qPCR analysis. (m) Western immunoblotting was used to detect the relative protein expression of VEGFA. (n) Quantitative analysis of relative VEGFA protein expression (mean ± SD, $n = 3$; $^*P < 0.05$, compared with the $H_2O_2$ group).

inhibition of linear HIPK3 mRNA in HPC-exos did not change the effect of HPC-exos on either cell cycle or migration. Taken together, the results suggest that circHIPK3 from HPC-exos derived from CMs mediates cardiac endothelial cell angiogenesis.

In corroboration with a recent study suggesting that some circRNAs have miRNA binding sites and thus can sequester homologous miRNAs using these sites [35], our previous studies stated that circHIPK3 and miR-29a are colocalized in the cytoplasm of cardiac microvascular endothelial cells and that circHIPK3 interacts with miR-29a and decreases miR-29a stability [11]. Based on this, we also assessed the effect of miR-29a on cardiac endothelial cell angiogenesis by establishing the miR-29a gain-of-function and loss-of-function models. Our data showed that the miR-29a inhibitor effectively accelerated cell cycle progression and increased the migration of cardiac endothelial cells and followed by enhanced tube formation. Moreover, these effects were strikingly similar to the effects of circHIPK3 overexpression.

Canonically, miRNAs can decrease the expression of a target protein by either inhibiting translation or inducing the degradation of its mRNA [36]. Many target mRNAs of miR-29a, including but not limited to VEGFA in gastric carcinoma [30] and IGF-1 in cardiac endothelial cells [11], have been discovered. We investigated VEGFA, which has been shown to play a primary role in various cellular processes, including cell cycle progression and angiogenesis [37]. Moreover, cardiac-specific deletion of VEGFA in mice resulted in hypovascular hearts with basal contractile dysfunction [38]. We also found that upregulated miR-29a levels effectively decreased the expression of VEGFA mRNA and protein by

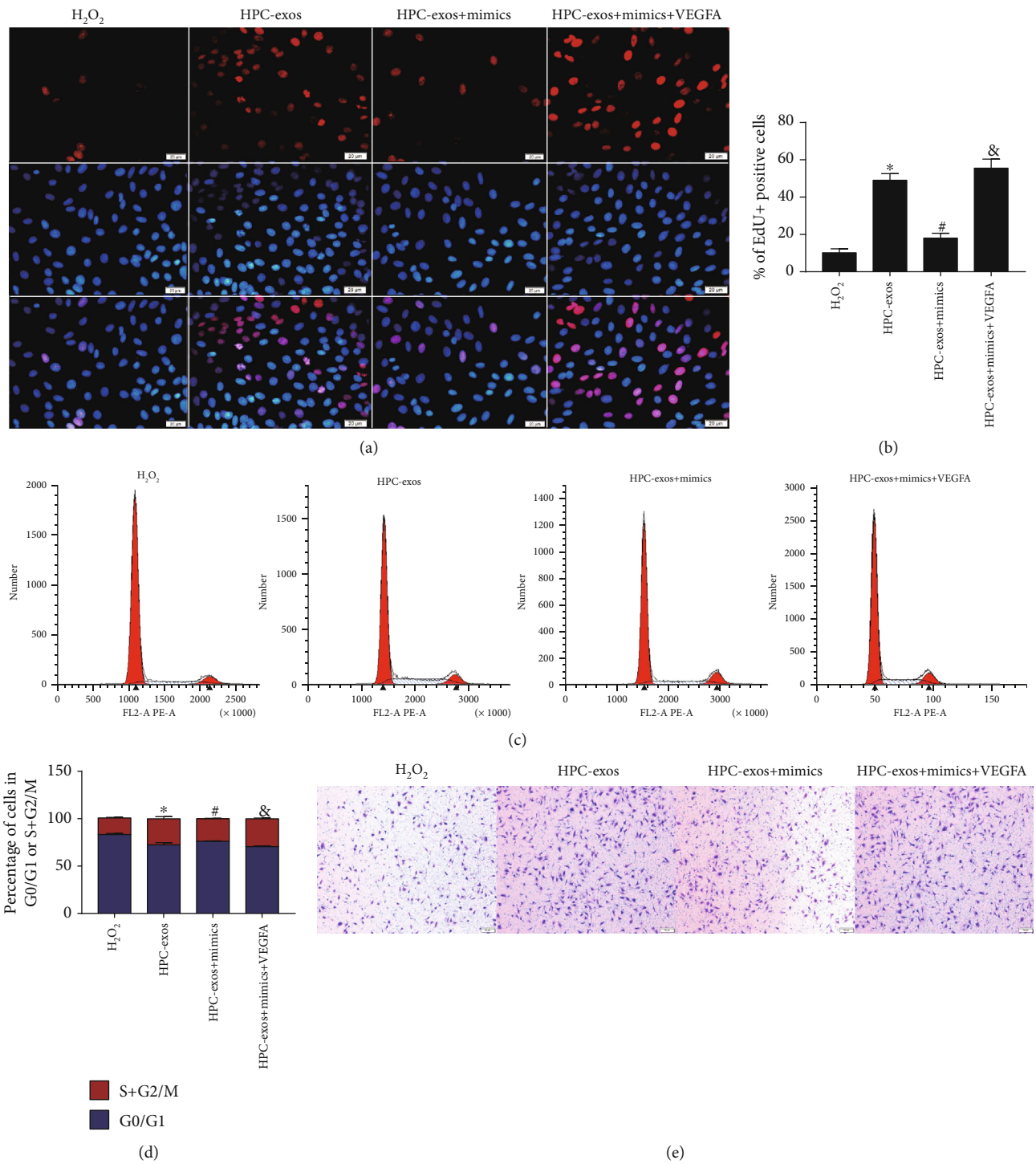


Figure 5: Continued.

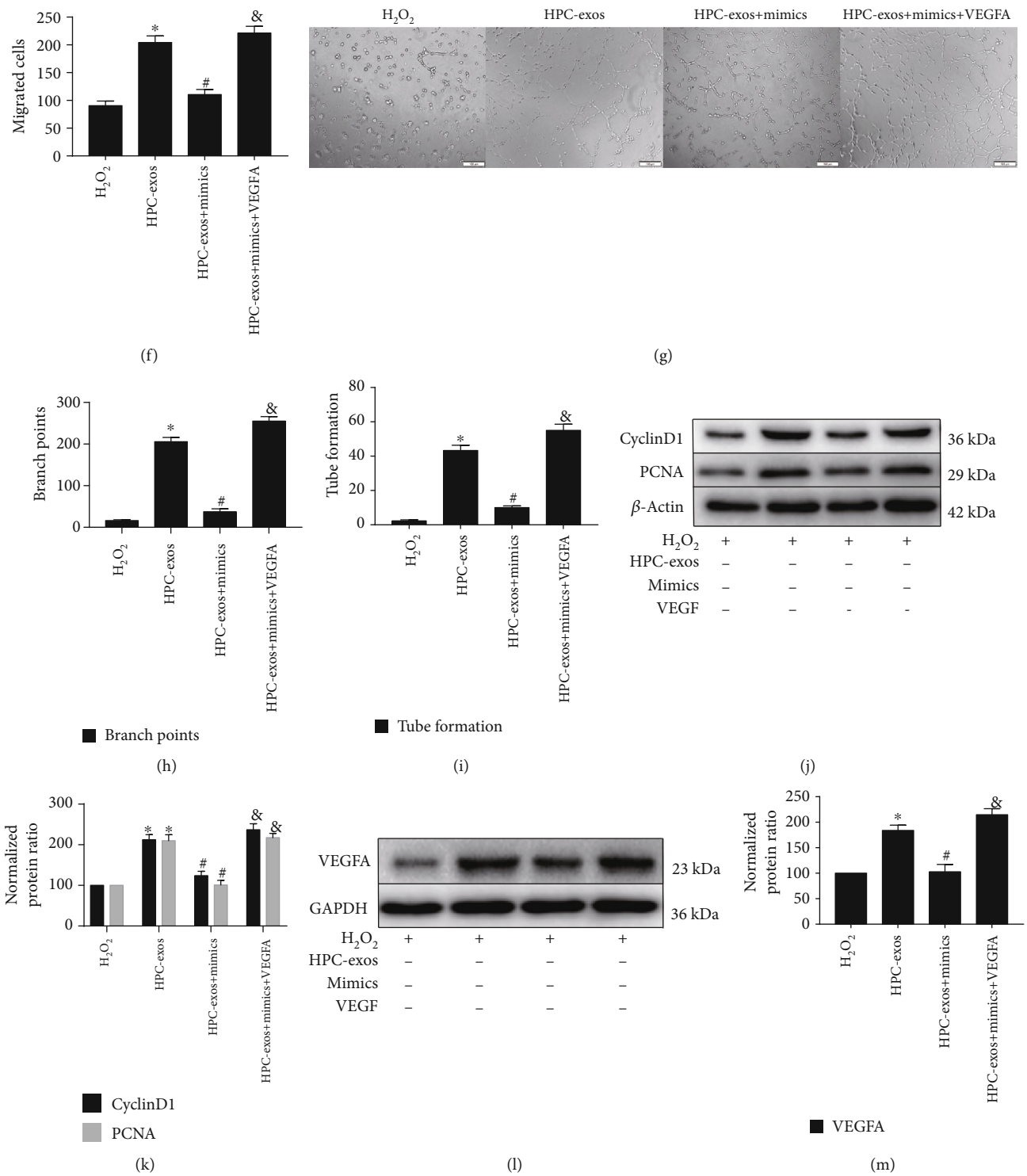


Figure 5: Exosomal circHIPK3 induces cell proliferation, migration, and tube formation via the miR-29a/VEGFA axis in cardiac endothelial cells. To further investigate the role of HPC-exosomal circHIPK3, miR-29a or VEGFA was transfected into cardiac endothelial cells. (a) Proliferation of cardiac endothelial cells was determined by EdU assays. (b) Quantitative analysis of (a). (c) Flow cytometry was performed to analyze the cell cycle distribution. (d) Representative histograms are shown. (e) Migration of cardiac endothelial cells was measured by Transwell migration assays (scale bar = 50 $\mu$m). (f) The number of migrated cells per field was determined. (g) Representative images of cardiac endothelial cells in Matrigel. (h, i) The total number of meshes and branch points were evaluated with a quantitative analysis method. (j) Western blot analyses were performed. (k) Relative protein levels of cyclinD1 and PCNA in cardiac endothelial cells were determined. (l) VEGFA protein expression was detected by immunoblotting. (m) VEGFA protein relative expression was evaluated with quantitative analysis method (mean ± SD, $n = 3$, $^*P < 0.05$, compared with the $H_2O_2$ group).

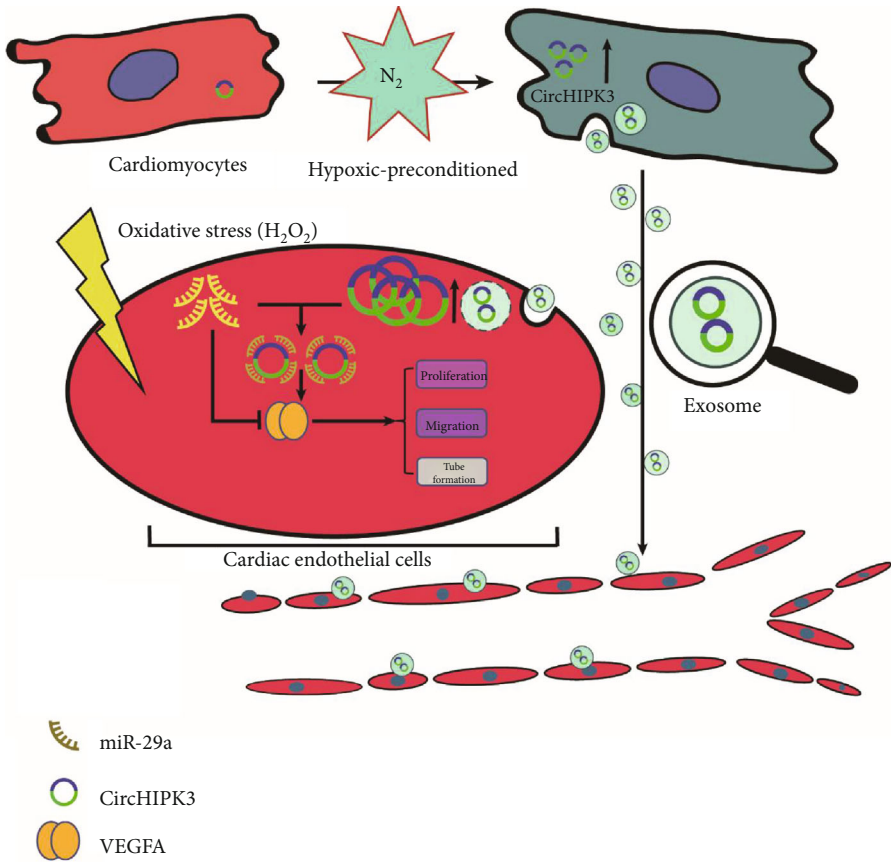


Figure 6: A schematic cartoon of the circHIPK3/miR-29g/VEGFA axis in cardiac endothelial cells. CircHIPK3 is upregulated in CMs subjected to hypoxia and released to the extracellular space by exosomes. Subsequently, adjacent cardiac endothelial cells internalize these exosomes, which causes circHIPK3 levels to increase in cardiac endothelial cells. CircHIPK3 could inhibit miR-29a activity and then regulate angiogenesis in cardiac endothelial cells by increasing VEGFA expression.

binding to the 3′-UTR of VEGFA mRNA. miR-29a mimics abrogated the HPC-exo-mediated protective effects by decreasing cell proliferation and migration under oxidative conditions. By contrast, overexpression of VEGFA significantly increased proliferation and migration in cardiac endothelial cells transfected with miR-29a mimics. The modulation of miR-29a levels in our study revealed a crucial role of HPC-exosomal circHIPK3/miR-29a in the regulation of VEGFA levels, suggesting that exosomal circHIPK3 is a molecular regulator of cardiac function via miR-29a/VEGFA signaling.

In summary, our data demonstrate that HPC-exos derived from CMs exhibit cardioprotective effects by enhancing neovascularization, limiting the infarct size, and preserving post-MI cardiac endothelial cell function and integrity in part through the miR-29a/VEGFA signaling axis (Figure 6). To the best of our knowledge, we show that the use of HPC-exos derived from CMs is a feasible approach to limit ischemic injury.

## Data Availability

The data used to support the findings of this study are included within the article.

## Conflicts of Interest

The authors declare that there are no conflicts of interest regarding the publication of this paper.

## Authors' Contributions

Yan Wang, Ranzun Zhao, and Changyin Shen contributed equally to this work.

## Acknowledgments

This work is supported by a grant from the National Natural Science Foundation of China (Grant no. 81860061 and Grant no. 81760042). The study is also supported by a scientific research project from the Science and Technology Department of Guizhou Province (LH(2017)7107) and a high-level person-time training project of Guizhou Province ((2015)4025).

## References

[1] C. Seiler, M. Stoller, B. Pitt, and P. Meier, "The Human Coronary Collateral Circulation: Development And Clinical Importance," *European Heart Journal*, vol. 34, no. 34, pp. 2674–2682, 2013.

[2] A. P.-L. Chiu, A. Wan, N. Lal et al., "Cardiomyocyte VEGF regulates endothelial cell GPIHBP1 to relocate lipoprotein lipase to the coronary lumen during diabetes mellitus," *Arteriosclerosis, Thrombosis, and Vascular Biology*, vol. 36, no. 1, pp. 145–155, 2016.

[3] X. Wang, W. Huang, G. Liu et al., "Cardiomyocytes mediate anti-angiogenesis in type 2 diabetic rats through the exosomal transfer of miR-320 into endothelial cells," *Journal of Molecular and Cellular Cardiology*, vol. 74, pp. 139–150, 2014.

[4] N. A. Garcia, J. Moncayo-Arlandi, P. Sepulveda, and A. Diez-Juan, "Cardiomyocyte exosomes regulate glycolytic flux in endothelium by direct transfer of GLUT transporters and glycolytic enzymes," *Cardiovascular Research*, vol. 109, no. 3, pp. 397–408, 2016.

[5] C. Braicu, C. Tomuleasa, P. Monroig, A. Cucuianu, I. Berindan-Neagoe, and G. A. Calin, "Exosomes as divine messengers: are they the Hermes of modern molecular oncology?," *Cell Death and Differentiation*, vol. 22, no. 1, pp. 34–45, 2015.

[6] S. M. Davidson, J. A. Riquelme, Y. Zheng, J. M. Vicencio, S. Lavandero, and D. M. Yellon, "Endothelial cells release cardioprotective exosomes that may contribute to ischaemic preconditioning," *Scientific Reports*, vol. 8, no. 1, p. 15885, 2018.

[7] B. Shi, Y. Wang, R. Zhao, X. Long, W. Deng, and Z. Wang, "Bone marrow mesenchymal stem cell-derived exosomal miR-21 protects C-kit+ cardiac stem cells from oxidative injury through the PTEN/PI3K/Akt axis," *PLoS One*, vol. 13, no. 2, article e0191616, 2018.

[8] D. Chistiakov, A. Orekhov, and Y. Bobryshev, "Cardiac Extracellular Vesicles in Normal and Infarcted Heart," *International Journal of Molecular Sciences*, vol. 17, no. 1, p. 63, 2016.

[9] X. Loyer, I. Zlatanova, C. Devue et al., "Intra-cardiac release of extracellular vesicles shapes inflammation following myocardial infarction," *Circulation Research*, vol. 123, no. 1, pp. 100–106, 2018.

[10] T. M. Ribeiro-Rodrigues, T. L. Laundos, R. Pereira-Carvalho et al., "Exosomes secreted by cardiomyocytes subjected to ischaemia promote cardiac angiogenesis," *Cardiovascular Research*, vol. 113, no. 11, pp. 1338–1350, 2017.

[11] Y. Wang, R. Zhao, W. Liu et al., "Exosomal circHIPK3 released from hypoxia-pretreated cardiomyocytes regulates oxidative damage in cardiac microvascular endothelial cells via the miR-29a/IGF-1 pathway," *Oxidative Medicine and Cellular Longevity*, vol. 2019, 28 pages, 2019.

[12] D. Liang and J. E. Wilusz, "Short intronic repeat sequences facilitate circular RNA production," *Genes & Development*, vol. 28, no. 20, pp. 2233–2247, 2014.

[13] Y. Li, F. Zheng, X. Xiao et al., "CircHIPK3 sponges miR-558 to suppress heparanase expression in bladder cancer cells," *EMBO reports*, vol. 18, no. 9, pp. 1646–1659, 2017.

[14] N. Liu, J. Zhang, L. Y. Zhang, and L. Wang, "CircHIPK3 is upregulated and predicts a poor prognosis in epithelial ovarian cancer," *European Review for Medical and Pharmacological Sciences*, vol. 22, no. 12, pp. 3713–3718, 2018.

[15] X. Liu, B. Liu, M. Zhou et al., "Circular RNA HIPK3 regulates human lens epithelial cells proliferation and apoptosis by targeting the miR-193a/CRYAA axis," *Biochemical and Biophysical Research Communications*, vol. 503, no. 4, pp. 2277–2285, 2018.

[16] K. Shan, C. Liu, B.-H. Liu et al., "Circular Noncoding RNA HIPK3 Mediates Retinal Vascular Dysfunction in Diabetes Mellitus," *Circulation*, vol. 136, no. 17, pp. 1629–1642, 2017.

[17] V. N. S. Garikipati, S. K. Verma, Z. Cheng et al., "Circular RNA CircFndc3b modulates cardiac repair after myocardial infarction via FUS/VEGF-A axis," *Nature Communications*, vol. 10, no. 1, p. 4317, 2019.

[18] W. Xuan, B. Wu, C. Chen et al., "Resveratrol improves myocardial ischemia and ischemic heart failure in mice by antagonizing the detrimental effects of fractalkine*," *Critical Care Medicine*, vol. 40, no. 11, pp. 3026–3033, 2012.

[19] Y. Wang, R. Zhao, D. Liu et al., "Exosomes derived from miR-214-enriched bone marrow-derived mesenchymal stem cells regulate oxidative damage in cardiac stem cells by targeting CaMKII," *Oxidative Medicine and Cellular Longevity*, vol. 2018, 21 pages, 2018.

[20] X. Zhang, B. Sai, F. Wang et al., "Hypoxic BMSC-derived exosomal miRNAs promote metastasis of lung cancer cells via STAT3-induced EMT," *Molecular Cancer*, vol. 18, no. 1, p. 40, 2019.

[21] M. Hu, G. Guo, Q. Huang et al., "The harsh microenvironment in infarcted heart accelerates transplanted bone marrow mesenchymal stem cells injury: the role of injured cardiomyocytes-derived exosomes," *Cell Death & Disease*, vol. 9, no. 3, p. 357, 2018.

[22] X. Wang, H. Gu, W. Huang et al., "Hsp20-Mediated Activation of Exosome Biogenesis in Cardiomyocytes Improves Cardiac Function and Angiogenesis in Diabetic Mice," *Diabetes*, vol. 65, no. 10, pp. 3111–3128, 2016.

[23] A. Kubota, M. Juanola-Falgarona, V. Emmanuele et al., "Cardiomyopathy and altered integrin-actin signaling in Fhl1 mutant female mice," *Human Molecular Genetics*, vol. 28, no. 2, pp. 209–219, 2019.

[24] J. Guarnerio, M. Bezzi, J. C. Jeong et al., "Oncogenic role of fusion-circRNAs derived from cancer-associated chromosomal translocations," *Cell*, vol. 166, no. 4, pp. 1055-1056, 2016.

[25] B. Liao, R. Chen, F. Lin et al., "Long noncoding RNA HOTTIP promotes endothelial cell proliferation and migration via activation of the Wnt/$\beta$-catenin pathway," *Journal of Cellular Biochemistry*, vol. 119, no. 3, pp. 2797–2805, 2018.

[26] E. Lasda and R. Parker, "Circular RNAs co-precipitate with extracellular vesicles: a possible mechanism for circRNA clearance," *PLoS One*, vol. 11, no. 2, article e0148407, 2016.

[27] J. N. Boeckel, N. Jaé, A. W. Heumüller et al., "Identification and characterization of hypoxia-regulated endothelial circular RNA," *Circulation Research*, vol. 117, no. 10, pp. 884–890, 2015.

[28] Q. Zheng, C. Bao, W. Guo et al., "Circular RNA profiling reveals an abundant circHIPK3 that regulates cell growth by sponging multiple miRNAs," *Nature Communications*, vol. 7, no. 1, 2016.

[29] I. Domingues, J. Rino, J. A. A. Demmers, P. de Lanerolle, and S. C. R. Santos, "VEGFR2 translocates to the nucleus to regulate its own transcription," *PLoS One*, vol. 6, no. 9, article e25668, 2011.

[30] H. Zhang, M. Bai, T. Deng et al., "Cell-derived microvesicles mediate the delivery of miR-29a/c to suppress angiogenesis in gastric carcinoma," *Cancer Letters*, vol. 375, no. 2, pp. 331–339, 2016.

[31] X. Dai, C. Chen, Q. Yang et al., "Exosomal circRNA_100284 from arsenite-transformed cells, via microRNA-217 regulation of EZH2, is involved in the malignant transformation of human hepatic cells by accelerating the cell cycle and

promoting cell proliferation," *Cell Death & Disease*, vol. 9, no. 5, p. 454, 2018.

[32] J. C. Chang, W. F. Hu, W. S. Lee et al., "Intermittent hypoxia induces autophagy to protect cardiomyocytes from endoplasmic reticulum stress and apoptosis," *Frontiers in Physiology*, vol. 10, p. 995, 2019.

[33] H. Namazi, E. Mohit, I. Namazi et al., "Exosomes secreted by hypoxic cardiosphere-derived cells enhance tube formation and increase pro-angiogenic miRNA," *Journal of Cellular Biochemistry*, vol. 119, no. 5, pp. 4150–4160, 2018.

[34] Z. Zhong, M. Huang, M. Lv et al., "Circular RNA MYLK as a competing endogenous RNA promotes bladder cancer progression through modulating VEGFA/VEGFR2 signaling pathway," *Cancer Letters*, vol. 403, pp. 305–317, 2017.

[35] K. Zeng, X. Chen, M. Xu et al., "CircHIPK3 promotes colorectal cancer growth and metastasis by sponging miR-7," *Cell Death & Disease*, vol. 9, no. 4, p. 417, 2018.

[36] D. de Rie, T. F. A. N. T. O. M. Consortium, I. Abugessaisa et al., "An integrated expression atlas of miRNAs and their promoters in human and mouse," *Nature Biotechnology*, vol. 35, no. 9, pp. 872–878, 2017.

[37] M. Shibuya, "Vascular Endothelial Growth Factor (VEGF) and Its Receptor (VEGFR) Signaling in Angiogenesis: A Crucial Target for Anti- and Pro-Angiogenic Therapies," *Genes & cancer*, vol. 2, no. 12, pp. 1097–1105, 2011.

[38] F. J. Giordano, H.-P. Gerber, S.-P. Williams et al., "A cardiac myocyte vascular endothelial growth factor paracrine pathway is required to maintain cardiac function," *Proceedings of the National Academy of Sciences*, vol. 98, no. 10, pp. 5780–5785, 2001.

Hindawi
Oxidative Medicine and Cellular Longevity
Volume 2020, Article ID 1412696, 11 pages
https://doi.org/10.1155/2020/1412696

*Research Article*

# Hydrogen Sulfide Promotes Cardiomyocyte Proliferation and Heart Regeneration *via* ROS Scavenging

**Jianqiu Pei, Fang Wang, Shengqiang Pei, Ruifeng Bai, Xiangfeng Cong, Yu Nie, and Xi Chen**

*State Key Laboratory of Cardiovascular Disease, Fuwai Hospital, National Center for Cardiovascular Disease, Chinese Academy of Medical Sciences and Peking Union Medical College, Beijing 100037, China*

Correspondence should be addressed to Yu Nie; nieyu@fuwaihospital.org and Xi Chen; chenxifw@pumc.edu.cn

Received 12 January 2020; Revised 26 February 2020; Accepted 27 April 2020; Published 22 May 2020

Guest Editor: Aleksandar Kibel



Neonatal mouse hearts can regenerate completely in 21 days after cardiac injury, providing an ideal model to exploring heart regenerative therapeutic targets. The oxidative damage by Reactive Oxygen Species (ROS) is one of the critical reasons for the cell cycle arrest of cardiomyocytes (CMs), which cause mouse hearts losing the capacity to regenerate in 7 days or shorter after birth. As an antioxidant, hydrogen sulfide ($H_2S$) plays a protective role in a variety of diseases by scavenging ROS produced during the pathological processes. In this study, we found that blocking $H_2S$ synthesis by PAG ($H_2S$ synthase inhibitor) suspended heart regeneration and CM proliferation with ROS deposition increase after cardiac injury (myocardial infarction or apex resection) in 2-day-old mice. NaHS (a $H_2S$ donor) administration improved heart regeneration with CM proliferation and ROS elimination after myocardial infarction in 7-day-old mice. NaHS protected primary neonatal mouse CMs from $H_2O_2$-induced apoptosis and promoted CM proliferation *via* SOD2-dependent ROS scavenging. The oxidative DNA damage in CMs was reduced with the elimination of ROS by $H_2S$. Our results demonstrated for the first time that $H_2S$ promotes heart regeneration and identified NaHS as a potent modulator for cardiac repair.

## 1. Introduction

Cardiovascular disease, the leading cause of death in humans, poses serious threats to life and is a heavy economic burden. Loss of cardiomyocyte (CM) induced by cardiac injury is the main cause of heart failure which is of awful prognosis [1]. Studies in recent decades have shown that lower vertebrate such as zebrafish maintains a heart-regenerating ability throughout their lives [2], while mammals, such as pig [3, 4], mouse [5], and even human [6, 7], have a transient ability to regenerate the heart when they were neonates. With postnatal development, mammals lose heart regeneration ability soon after birth. Mice lose this regenerative capacity by postnatal day (P)7 [5, 8], and pig can keep this potency just one day after birth [3, 4].

Recently, lineage tracing studies have found that newly generated CMs are mainly the result of division of preexisting CMs [9, 10]. For this reason, efforts have been made to identify the molecular mechanisms underlying postnatal cardiac cell cycle arrest. Researchers have found that the upstream signal triggering CMs to exit the proliferative cycle is related to reactive oxygen species (ROS) produced by oxidative metabolism [11, 12]. High levels of ROS are harmful to many processes; for example, they oxidize membrane lipids and amino acid residues of proteins, which may alter cell function and integrity [13]. ROS production associated with metabolism-induced DNA damage is a major cause of cell cycle arrest [14–16]. How to remove these metabolic byproducts safely and effectively is a key question in myocardial regeneration.

Hydrogen sulfide ($H_2S$), like nitric oxide (NO) and carbon monoxide (CO), is an endogenous gas signaling molecule. After synthesis, $H_2S$ can spread into the environment surrounding cells or be stored in cells. In mammalian tissues, $H_2S$ is produced by both nonenzymatic and enzymatic catalysis, with cystathionine-$\beta$-synthase (CBS) and cystathionine-$\gamma$-lyase (CSE) enzyme catalysis being dominant [17]. $H_2S$ has been widely accepted to exhibit protective properties in many organs [18, 19], especially in the heart in the context of

damage such as that from myocardial infarction (MI), ischemia-reperfusion (I/R), arrhythmia, cardiac hypertrophy, myocardial fibrosis, and heart failure [20, 21]. However, whether $H_2S$ plays an essential role during heart regeneration is still unknown.

We previously established neonatal mouse MI and apex resection (AR) models to study heart regeneration [22–25]. Employing the neonatal mouse heart regeneration model, here, we explored the role of $H_2S$ signaling in heart regeneration. The results showed that $H_2S$ improved CM cell cycle progression by scavenging ROS, thereby promoting heart regeneration. During this process, $H_2S$-mediated ROS elimination was mainly SOD2-dependent.

## 2. Methods and Materials

*2.1. Mice.* The mice were provided by the National Center of Cardiovascular Disease. All experiments with mice were conducted according to the "Regulation to the Care and Use of Experimental Animals" of the Beijing Council on Animal Care (1996). The protocol was approved by the Fuwai Hospital Animal Care and Use Committee.

*2.2. MI Model.* The MI model was created in neonatal C57BL/6 mice (P2 or P7) through ligation of the left anterior descending coronary artery (LAD), as previously described [26]. Briefly, each mouse was anesthetized on ice for 2-4 min, and the chest was opened to expose the heart. The LAD in the left ventricle was ligated with 8-0 suture, and the chest was then closed with 8-0 nonabsorbable silk suture. The same procedure was performed for the sham-operated group except that the LAD was not ligated. Then, the mice were rewarmed under a heating lamp at 37°C for recovery. After surgery, cardiac function was assessed by echocardiography using a VisualSonics Vevo 2100 ultrasound system (VisualSonics, Inc.) At specific time points, the animals were sacrificed, and the hearts were dissected and processed for histological and other analyses.

*2.3. Apex Resection.* The neonatal mouse heart apex resection model was performed as described previously [24]. Briefly, neonatal C57BL/6J mice at postnatal day (P)2 were anesthetized by hypothermia and embedded in ice for 2 min. The skin was cut open with a micro scissors in the fourth intercostal space on the left side. The mouse's thorax was gently pressed, and the apex was pushed out; the apex was then resected using iridectomy scissors, and the chest and skin were sewn up with 8-0 nonabsorbable silk suture. For sham controls, the same procedures were performed without removing the heart apex. After surgery, mice were waked up under a heating pad.

*2.4. ROS Measurement.* The production of ROS was evaluated by analyzing the fluorescence intensity that resulted from dihydroethidium (DHE) (Invitrogen D11347) staining. In brief, frozen mouse hearts were cut into 5 $\mu$m sections. Serial heart sections were stained with 5 $\mu$M DHE at 37°C for 30 min and then measured by fluorescence microscopy (excitation at 490 nm, emission at 610 nm).

*2.5. CM Isolation.* CMs were isolated from the hearts of neonatal mice at P1 using a Neonatal Heart Dissociation Kit with a gentleMACS™ Octo Dissociator (Miltenyi Biotec, Teterow, Germany) according to the manufacturer's instructions and cultured in DMEM supplemented with 10% FBS at 37°C and 5% $CO_2$.

*2.6. In Vitro Oxidative Stress Induction.* To induce oxidative stress injury, primary CMs ($1.5 \times 10^4$ per well) were differentiated in 96-well plates. The cells were treated with 500 $\mu$M $H_2O_2$ in serum-free DMEM for 12 h in a 5% $CO_2$ incubator at 37°C. $H_2O_2$ was obtained from AppliChem GmbH (Darmstadt, Germany). NaHS was purchased from Sigma-Aldrich Chemie GmbH (Taufkirchen, Germany).

*2.7. Knockdown of Mn-SOD.* Mn-SOD was knocked down with siRNA (Thermo AM16708). Ambion® Silencer® Negative Control #2 siRNA (Thermo AM 4613), which has no significant sequence similarity to mouse, rat, or human gene sequences, was used as the negative control. CMs were seeded into 12-well plates ($1.0 \times 10^6$ cells/well) for 24 h and then transfected with siRNA using Lipofectamine 3000 (Invitrogen, Waltham, USA) according to the manufacturer's instructions. The cells were collected 48 h after transfection.

*2.8. Quantitative Real-Time PCR (qRT-PCR).* Total RNA was extracted from cells using TRIzol reagent and then quantified using a NanoDrop 2000 spectrophotometer. cDNA was generated from the total RNA (1 $\mu$g) using M-MLV reverse transcriptase and oligo(dT)15 primers. qRT-PCR was performed using SYBR Green PCR Master Mix and an Applied Biosystems 7500 instrument (ABI, Foster City, CA, USA). The primer pairs used were as follows: SOD2—5′-CAGACCTGC CTTACGACTATGG-3′ (forward) and 5′-CTCGGTGGC GTTGAGATTGTT-3′ (reverse); $\beta$-actin—5′-AGCCAT GTACGTAGCCATCC-3′ (forward) and 5′-CTCTCAGCT GTGGTGGTGAA-3′ (reverse).

*2.9. Histology.* The hearts were harvested, fixed in 4% paraformaldehyde at room temperature for 24 h, dehydrated in ethanol and xylene, and then embedded in paraffin. For the MI model, the hearts were longitudinally embedded and sectioned at 5 $\mu$m thickness. With standard procedures, Masson's trichrome staining was performed. The thickness of the left ventricle anterior wall (LVAW) was calculated by Image-Pro Plus.

*2.10. Immunostaining.* Deparaffinization, antigen retrieval with 1 mM EDTA (pH 9.0) in boiling water, and blocking of nonspecific binding sites were performed. The sections were then incubated with primary antibodies overnight at 4°C, washed three times with PBS, and incubated with fluorescence-labeled secondary antibodies for 1 h at 25°C in the dark. The slides were washed three times in PBS, counterstained with DAPI (Sigma-Aldrich, St. Louis, MO, USA), and mounted with VECTASHIELD (Vector Labs, CA, USA). The primary antibodies used were as follows: anti-phospho Histone H3 Ser10 (Millipore #06-570, 1 : 100), anti-Ki67 (Abcam, ab16667, 1 : 200), anti-Aurora B (1 : 100; ab2254, Abcam), and anti-Sarcomeric Alpha

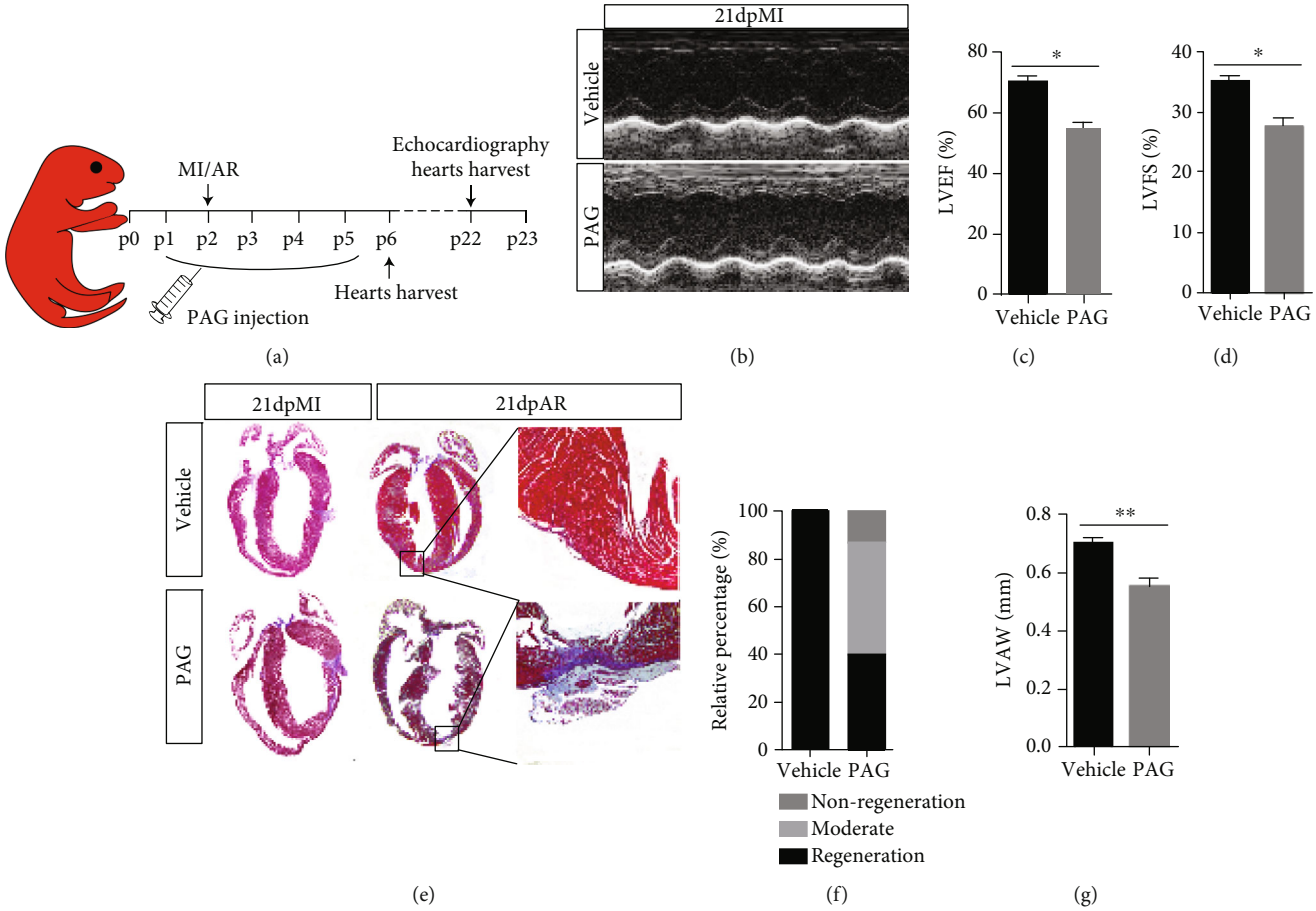


Figure 1: Inhibition of $H_2S$ synthase with PAG impairs heart regeneration. (a) Schema of the animal experiment. (b–d) Representative images and statistics of echo analysis 21 days post MI. LVEF: left ventricular ejection fraction; LVFS: left ventricular fractional shortening. (e) Representative images of Masson's trichrome-stained heart sections from mice 21 days post MI or AR. (f) Statistics of neonatal mouse heart regeneration. (g) LVAWd: left ventricular anterior wall diastolic thickness. Vehicle: $n = 6$; PAG: $n = 15$. The data are presented as the mean ± SEM. $^{*}p < 0.05$ and $^{**}p < 0.01$ by Student's $t$-test.

Actinin (Abcam, ab9465, 1 : 500). The anti-rabbit Alexa Fluor 488-conjugated (1 : 500; A-21206) and anti-mouse Alexa Fluor 594-conjugated (1 : 500; A-21203) secondary antibodies were from Invitrogen. Fluorescence was observed under a ZEISS LSM800 confocal laser scanning microscope (Carl Zeiss, Inc., Jena, Germany).

*2.11. Western Blot Analysis.* CMs were lysed in a RIPA buffer that contained protease inhibitors (Roche, Basel, Switzerland). After centrifugation (15000 × $g$, 10 min, 4°C), the cell lysate protein concentrations were determined by BCA Protein Assay (Beyotime Institute of Biotechnology, Beijing, China). The membranes were blotted with the indicated antibodies. Some membranes were stripped and reblotted with an actin antibody. Monoclonal primary antibodies against phosphorylated-Ataxia Telangiectasis Mutated (pATM) (1 : 1000; Santa Cruz sc-47739), Mn-SOD (1 : 1000; Millipore Millipore-06-984), phosphorylated checkpoint kinase 1 (p-Chk1) (Ser296) (1 : 1000; CST #90178), phosphorylated checkpoint kinase 2 (p-Chk2) (Thr68) (1 : 1000; CST #2197), and GAPDH (1 : 5000; Sigma G9545) were used.

## 3. Results

*3.1. Inhibition of $H_2S$ Impairs Mouse Neonatal Heart Regeneration.* Endogenous $H_2S$ is derived from the catalytic activity of two enzymes: CBS, which is particularly expressed in the central nervous system, and CSE, which is primarily in the cardiovascular system. Therefore, to determine the functional significance of $H_2S$ signaling in heart regeneration, CSE in neonatal mice was inhibited with propargylglycine (PAG). The mice were subjected to permanent LAD ligation or AR at P2, the time point associated with a strong heart regenerative capability. The experimental schedule is shown in Figure 1(a). After 21 days, echocardiography revealed that heart function was significantly deteriorated in the PAG-treated group compared with the vehicle-treated group (Figures 1(b)–1(d)). Additionally, the hearts of the vehicle group were completely regenerated with little scarring, while those of the PAG-treated group showed large fibrotic scars (Figure 1(e)) and suppressed regenerative ability (Figure 1(f)).

*3.2. PAG Reduces Proliferative Capability of Cardiomyocytes in Neonatal Mice.* To determine whether PAG treatment

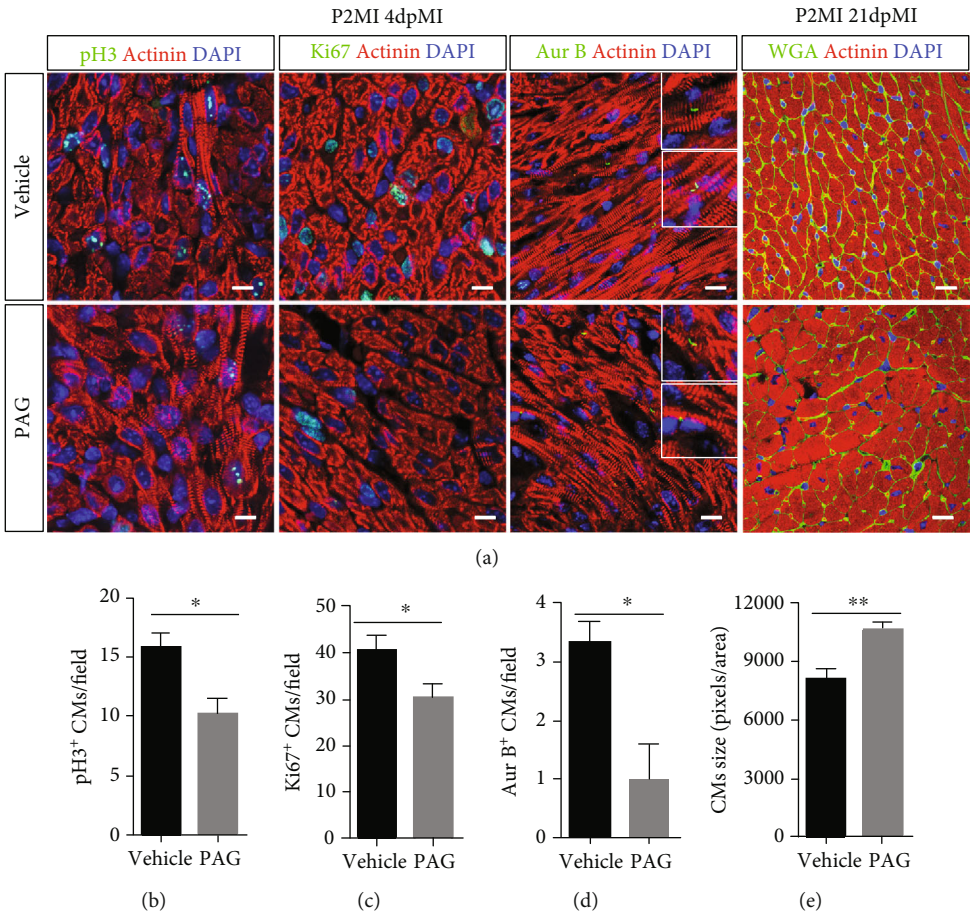


Figure 2: Inhibition of $H_2S$ synthase with PAG impedes CM proliferation. (a–d) Representative images and related statistical results of CM mitosis and cytokinesis, as analyzed by pH3, Ki67, and Aurora B staining. Actinin was used to label CMs, and DAPI was used to label nuclei. Scale bar =50 $\mu$m. Vehicle: $n = 4$; PAG: $n = 5$. (a, e) Cell size was measured by WGA staining. Actinin was used to label CMs, and DAPI was used to label nuclei. Scale bar = 20 $\mu$m. Vehicle: $n = 3$; PAG: $n = 5$. The data are presented as the mean ± SEM. $^{*}p < 0.05$ and $^{**}p < 0.01$ by Student's $t$-test.

impeded CM proliferation during neonatal heart regeneration, we examined CM proliferation with the mitosis markers pH3 and Ki67, and cytokinesis marker Aurora B, at 4 days postsurgery. PAG treatment decreased the numbers of proliferative myocytes in the injured myocardium (Figures 2(a)–2(d)). Wheat germ agglutinin (WGA) staining for cell size assessment with ImageJ revealed a significantly decreased CM size in PAG-treated mouse hearts compared with vehicle-treated mouse hearts (Figures 2(a) and 2(e)), suggesting that inhibition of $H_2S$ signaling impairs CM proliferative capability in neonatal mouse hearts following injury.

*3.3. NaHS Promotes Heart Regeneration and CM Proliferation.* Although mice exhibit a strong heart regenerative capability during the neonatal stage, the window closes at P7 [5, 8, 27]. To further investigate the effect of $H_2S$ on heart regeneration, we treated neonatal mice with NaHS (a donor of $H_2S$) daily for 10 days after birth and subject them to LAD ligation at P7 (Figure 3(a)). The mice underwent echocardiographic measurement of left ventricular function 21 days after cardiac injury (Figures 3(b)–3(d)). Masson trichrome staining showed that the NaHS-treated hearts had smaller scars, less fibrosis with collagen deposition (Figure 3(e)), and enhanced regeneration (Figure 3(f)) compared with the vehicle group. There was a significant improvement in the LVAW thickness in the NaHS-treated group (Figure 3(g)), which implies that NaHS does have a positive role in heart regeneration. To confirm this, we examined CM proliferation in NaHS-treated heart tissues. Immunofluorescence staining for pH3, Ki67, and Aurora B revealed that there were more proliferative CMs in NaHS-treated hearts than in vehicle hearts (Figures 3(h)–3(k)). WGA staining for cell size assessment revealed that CMs were smaller in NaHS-treated mouse hearts than in vehicle mouse hearts (Figures 3(h) and 3(l)). Taken together, these results indicate that $H_2S$ promotes heart regeneration and improves heart function after MI in P7 mice by enhancing CM proliferation.

*3.4. $H_2S$ Mitigates DNA Damage-Mediated Cell Cycle Arrest.* To determine whether ROS scavenging is involved in $H_2S$-mediated heart regeneration, we examined ROS

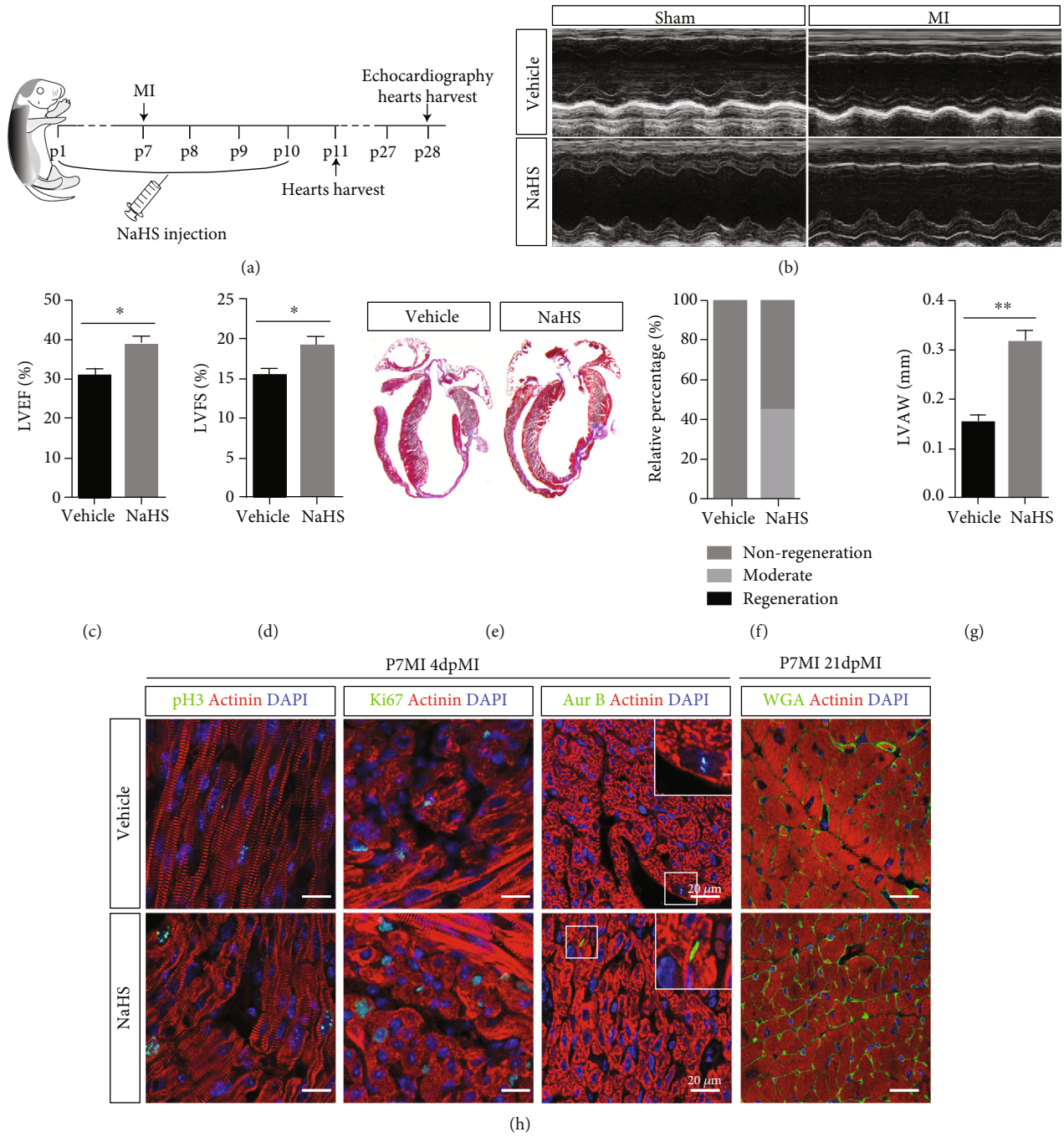


Figure 3: Continued.

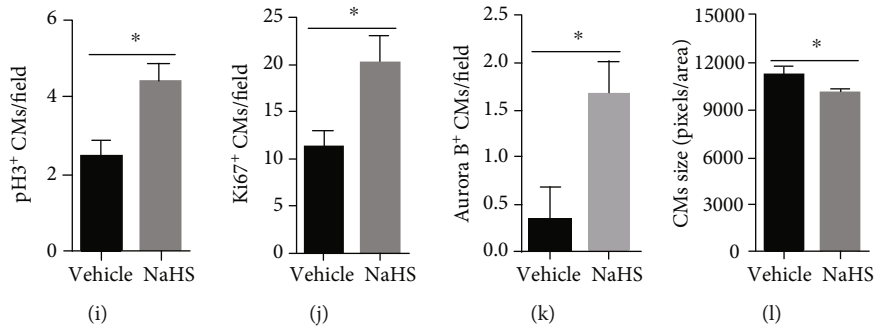


Figure 3: NaHS promotes heart regeneration related to CM proliferation. (a) Schema of the animal experiment. (b–d) Representative images and statistics of echo analysis 21 days post MI. LVEF: left ventricular ejection fraction; LVFS: left ventricular fraction shortening. (e) Representative images of Masson's trichrome-stained heart sections from mice 21 days post MI. (f) Neonatal mouse heart regeneration percentages. (g) LVAWd: left ventricular anterior wall diastolic thickness. Vehicle: $n = 8$; NaHS: $n = 15$. (h–k) Representative images and related statistical results of CM mitosis and cytokinesis, as indicated by pH3, Ki67, and Aurora B staining. Actinin was used to label CMs, and DAPI was used to label nuclei. Vehicle: $n = 4$; PAG: $n = 5$. Scale bar = 50 $\mu$m. (l) Cell size was measured by WGA staining. Actinin was used to label CMs, and DAPI was used to label nuclei. Scale bar = 20 $\mu$m. Vehicle: $n = 3$; PAG: $n = 5$. The data are presented as the mean ± SEM. $^{*}p < 0.05$ and $^{**}p < 0.01$ by Student's $t$-test.

deposition levels in frozen sections using DHE staining. We found that there were significantly greater ROS levels in PAG-treated mouse hearts than in vehicle-treated mouse hearts 3 days post MI (Figures 4(a) and 4(c)). In contrast, the ROS levels were lower in NaHS-treated mouse hearts (Figures 4(b) and 4(d)). These findings indicate that $H_2S$-mediated promotion of CM proliferation during heart regeneration may be correlated with ROS scavenging.

ROS deposition is a major cause of oxidative DNA damage. Once a cell suffers DNA damage, the cell cycle checkpoint is activated, causing the cell to become arrested in the G1 or G2 phase [28, 29]. Here, we assessed the expression of pATM, Chk1, and Chk2, important markers of the DNA damage response. The results showed increased expression of pATM, p-Chk1, and p-Chk2 in PAG-treated mice but decreased expression of these proteins in NaHS-treated mice compared with vehicle-treated mice. Consistent with these findings, a crucial antioxidant enzyme, Mn-SOD (SOD2), was downregulated in the PAG-treated group but upregulated in the NaHS group compared with the vehicle-treated group (Figures 4(e) and 4(f)). These results reveal that $H_2S$ signaling can attenuate the DNA damage response during cell cycle progression.

*3.5. $H_2S$ Suspends the ROS-Caused Cell Cycle Arrest in Primary CM.* $H_2O_2$ treatment reduced the proliferative capacity of CMs, as quantified by pH3 and Ki67 immunohistochemistry assays, while NaHS treatment attenuated this reduction (Figures 5(a) and 5(b)). In addition, Aurora B staining showed a tendency of proliferation promotion, although not significant (Figure 5(c)). We also studied the protective effect of $H_2S$ on cardiomyocytes under oxidative stress (Supplement Figure 1). Overall, these findings imply that $H_2S$ signaling can reduce barriers to CM proliferation.

*3.6. SOD2 Is Required for $H_2S$-Mediated CM Proliferation.* In mitochondria, a variety of antioxidant enzymes are important in determining ROS levels and maintaining cardiac function [30, 31]. Among them, SOD2 plays a critical role in ROS scavenging. Previous results have shown that PAG treatment reduces the expression of SOD2. To explore whether $H_2S$-induced CM proliferation is mediated by SOD2, we knocked down SOD2 in primary CMs with siRNA. qRT-PCR revealed that SOD2 siRNA dramatically suppressed the expression of SOD2 (Figure 6(a)). Immunostaining revealed that downregulation of SOD2 impaired CM proliferation. Under siSOD2 treatment, CM proliferation was not greater in the $H_2S$ group than in the control group, as indicated by pH3, Ki67, and Aurora B immunofluorescence staining (Figures 6(b)-6(e)). These results indicate that SOD2 is required for $H_2S$-mediated CM proliferation.

## 4. Discussion

In this study, we demonstrated that $H_2S$ signaling exerts a protective effect in the heart and plays a role in maintaining CM proliferation and heart regeneration after injury, with neonatal mouse heart regeneration AR and MI models. Inhibition of the $H_2S$ synthase CSE with PAG caused structural and functional defects in neonatal mouse hearts with decreased CM proliferation. In contrast, treatment with NaHS, a donor of $H_2S$, promoted heart repair, increasing CM proliferation and decreasing ROS deposition and fibrosis. $H_2O_2$-mediated CM injury was mitigated by NaHS, and NaHS treatment improved CM proliferation capacity by attenuating ROS-induced cellular DNA damage, which may cause cell cycle arrest.

$H_2S$ regulates a variety of cellular signals and is involved in the regulation of cell death, differentiation, and proliferation [19]. It has been widely accepted that $H_2S$ is not only a secondary reaction product but also a critical mediator of the pathophysiological processes of many diseases. Over the past few years, a broad range of studies has shown that $H_2S$ plays important roles in renal ischemic injury repair [32]

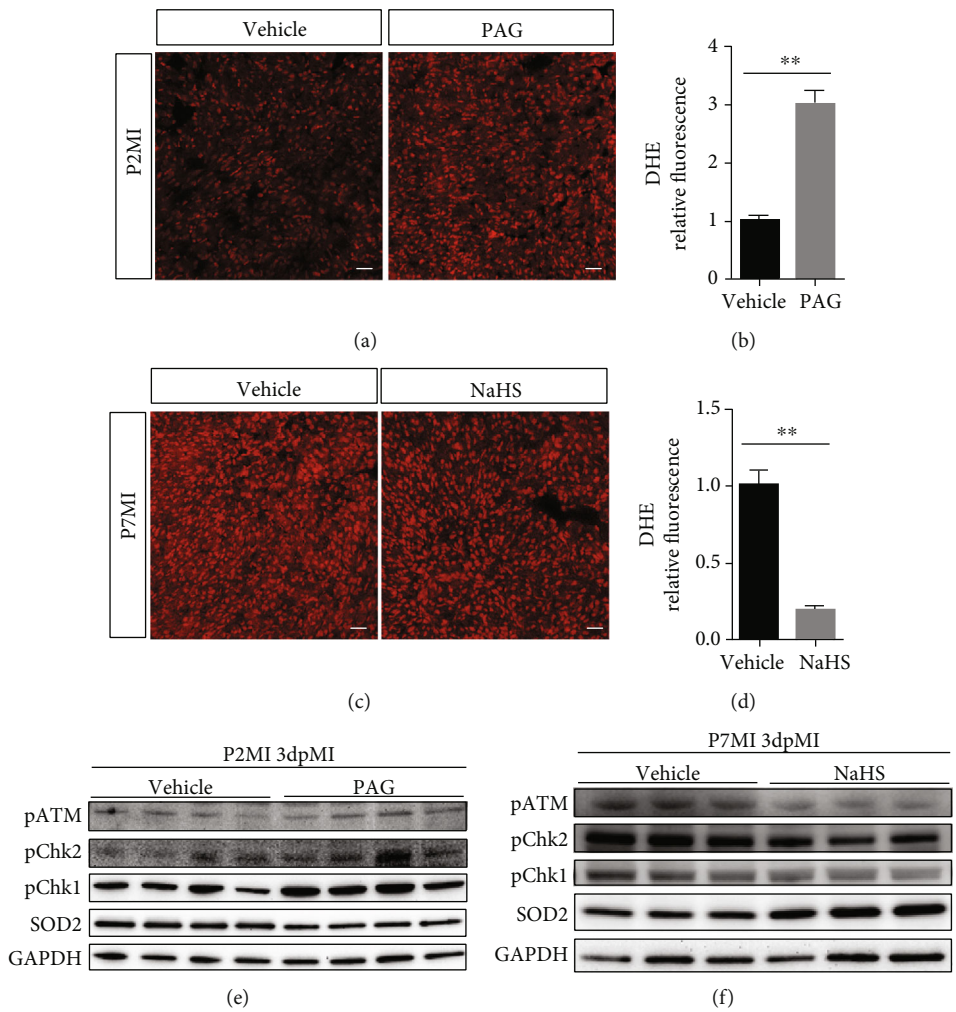


Figure 4: $H_2S$ is correlated with ROS scavenging and DNA damage during heart regeneration. (a–d) ROS levels in hearts after injury. (a, c) Representative images of DHE-stained heart sections from mice 1 day post MI. Scale bar = 20 $\mu$m. (b, d) Relative index of DHE fluorescence. $n = 3$ per group. (e) DNA damage during oxidative stress was detected with western blotting (WB) in PAG-treated mouse hearts 3 days after MI. (f) DNA damage during oxidative stress was detected with WB in NaHS-treated mouse hearts 3 days after MI. The data are presented as the mean ± SEM. $^{**}p < 0.01$ by Student's $t$-test.

and renal fibrosis alleviation [33], lung disease repair [34], burn healing [35], and bone damage repair and bone regeneration [19]. In particular, the effects of $H_2S$ in cardiac ischemia injury repair and function preservation have been well studied.

Inhibition of CSE with PAG has been shown to increase infarct size in an *ex vivo* I/R study [36]. Confirming this finding, CSE knockout aggravates heart damage after I/R in mice [37]. Conversely, $H_2S$ produced endogenously through cardiac-specific overexpression of CSE significantly limits the extent of injury after MI [38]. All of the above findings have shown that $H_2S$ signaling has protective effects on adult mouse and rat hearts. In accord with these reports, our results showed that $H_2S$ signaling could promote heart regeneration and preserve heart function, further demonstrating the protective role of $H_2S$ in a neonatal mouse heart.

Immediate reperfusion of the occluded coronary artery is the gold standard method for treating MI and reducing associated mortality. However, re-recovery of blood flow in the ischemic myocardium often leads to the loss of function or even the death of myocardial cells, causing cardiac reperfusion injury [39]. A large number of mechanistic studies have shown that this damage may be related to intracellular calcium overload and the formation of ROS [40, 41]. ROS can cause lipid peroxidation, leading to destruction of the cell membrane structure and thus causing cell swelling. Many studies have confirmed that blocking the production of or scavenging oxygen free radicals such as ROS can improve cardiac function after cardiac I/R and reduce myocardial damage [42, 43].

Mammalian CMs, as terminally differentiated cells, lose their proliferative capacity soon after birth. Studies have found that mammals, such as mice, are in a hyperoxic environment after birth, and their metabolic patterns change from anaerobic glycolysis to mitochondrial oxidative phosphorylation [11]. The electron leakage of the electron

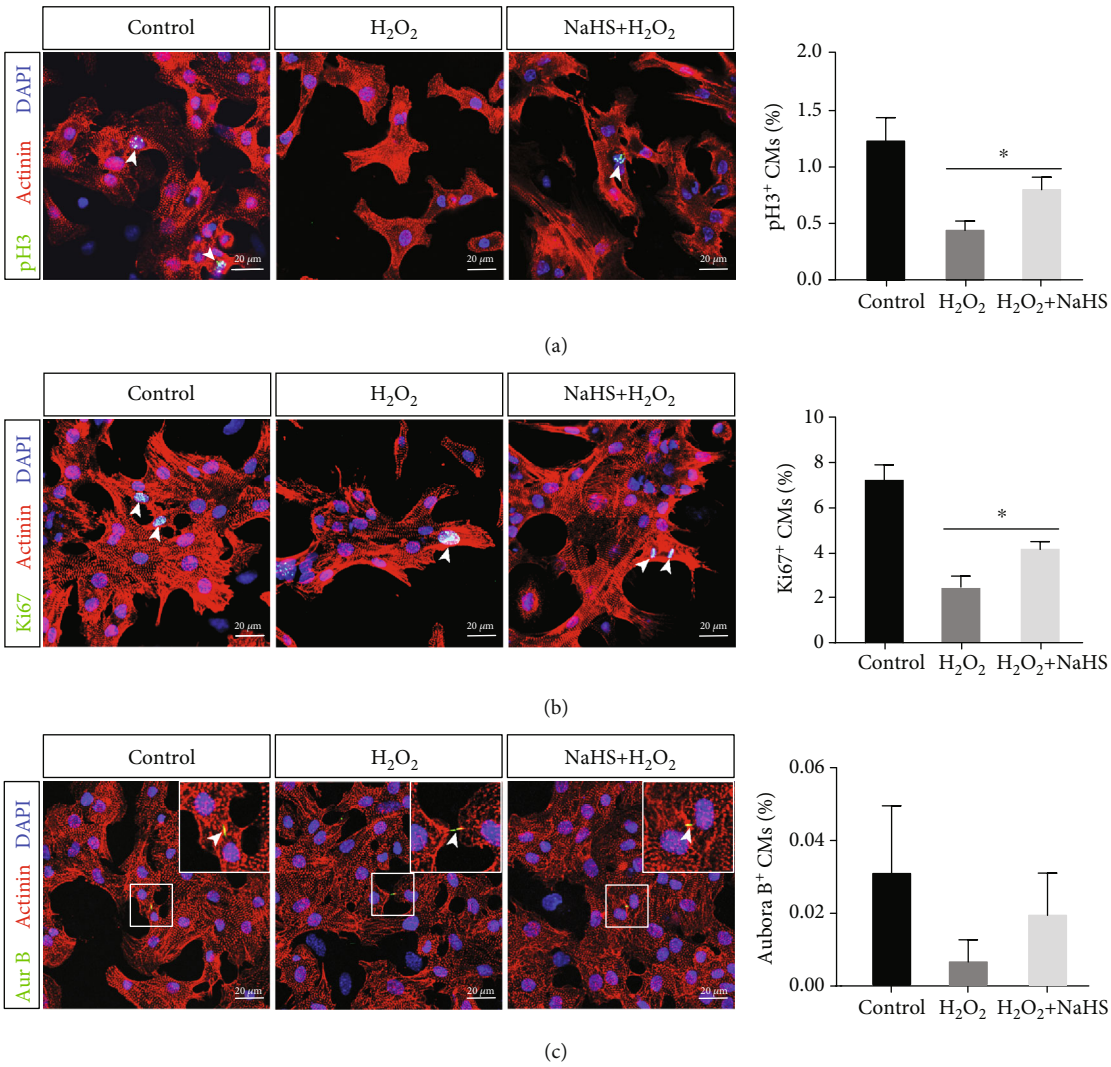


Figure 5: $H_2S$ exerts proliferative effects on CMs in vitro under conditions of $H_2O_2$ stimulation. Primary CMs from neonatal mice were cultured under $H_2O_2$ stimulation. (a, b) Representative images of pH3 and Ki67 immunofluorescence staining. And quantification of CM proliferation, as indicated by pH3 and Ki67 positive staining. (c) Representative images of Aurora B immunofluorescence staining and statistical results. Actinin was used to label CMs, and DAPI was used to label nuclei. Scale bar = 20 $\mu$m. The data are presented as the mean ± SEM. $^*p < 0.05$ by Student's $t$-test.

transport chain during oxidative phosphorylation causes ROS production and accumulation, and ROS accumulation gradually increases with growth and development [44]. Excessive ROS can cause DNA damage, leading to the cell cycle arrest of CMs; this arrest causes CMs to exit the proliferative cycle, making the mammalian heart nonrenewable after injury. Consistent with the above results, we found that $H_2S$ can clear ROS, thereby promoting the reentry of CMs into the proliferative cycle.

$H_2S$, a major antioxidant in mammalian tissues and cells, is usually present at low concentrations ranging from 10 to 30 nM [45–47]; however, its concentrations are 20- to 100-fold higher in the heart and aorta [48], implying a prominent regulatory role in the cardiovascular system. Studies have reported that $H_2S$ is involved in myocardial protection during I/R injury and that this protective effect is mainly derived from the antioxidative, anti-inflammatory, and antiapoptotic properties of $H_2S$ [49–51]. $H_2S$ can be used directly as an antioxidant to scavenge superoxide anions such as ROS. Many kinds of antioxidant enzymes can scavenge superoxide anions, and SOD is one of the most important candidates. Of the three types of SOD, SOD2 is mainly located in the mitochondria, which is consistent with the location of ROS produced from oxidative respiration. It has been reported that NaHS treatment can increase the expression of SOD2 and improve the activity of SOD1 in kidney tissues [32]. This study also found that NaHS treatment can increase the expression of SOD2 in the myocardium in neonatal mice and that SOD2 plays a role in ROS clearance and promotes CM proliferation. Furthermore, we found that $H_2S$ signaling-mediated ROS clearance reduces myocardial cell

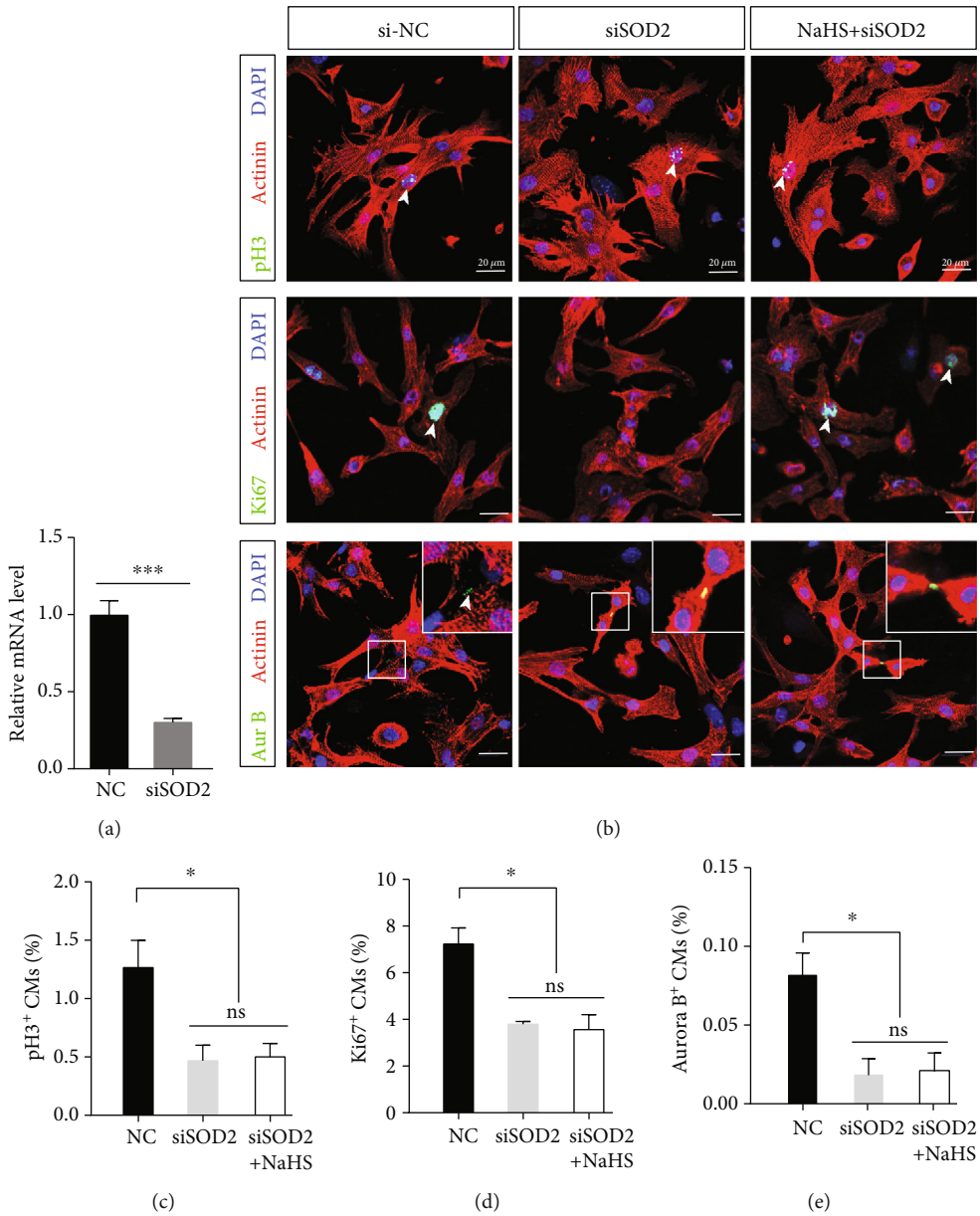


Figure 6: SOD2 is crucial to CM proliferation under physiological conditions. Primary CMs from P1 mice were treated with siSOD2 and NaHS. (a) Knockdown efficiency of siSOD2. $^{***}p < 0.001$ by Student's $t$-test. (b) Representative images of pH3 and Ki67 immunofluorescence staining. Actinin was used to label CMs, and DAPI was used to label nuclei. Scale bar = 20 $\mu$m. (c–e) Quantification of CM proliferation, as indicated by pH3, Ki67, and Aurora B positive staining. The data are presented as the mean ± SEM. $^{*}p < 0.05$; ns: not significant, by one-way ANOVA with Bonferroni's multiple comparison test.

size. This finding is consistent with a previous study by Luo et al. showing that angiotensin II treatment increases ROS accumulation in myocardial tissue, which can cause hypertrophy of CMs [52].

## 5. Conclusions

In this study, we have shown, for the first time, that NaHS, an $H_2S$ donor, has the ability to promote heart regeneration by scavenging ROS to reduce ROS-induced DNA damage, thus promoting CM reentry into the cell cycle. This study revealed the potential benefits of NaHS in heart regeneration, and identifying $H_2S$ may be a potential target for myocardial injury therapy in clinical applications.

## Data Availability

All data used to support the findings of this study are included within the article. Raw data used to generate the figures are available from the corresponding author upon request.

## Conflicts of Interest

The authors declare that they have no conflicts of interest.

## Authors' Contributions

Xi Chen, Yu Nie, and Jianqiu Pei were responsible for the study conception and design. Experiments were performed by Jianqiu Pei and Shengqiang Pei. Ruifeng Bai, Fang Wang, and Jianqiu Pei analyzed the data. Advice for the project was received from Xiangfeng Cong, and Xi Chen, Yu Nie, and Jianqiu Pei wrote the manuscript and revised it critically for important intellectual content. All authors read and approved the manuscript.

## Acknowledgments

This work was supported by CAMS Innovation Fund for Medical Sciences (CIFMS: 2016-I2M-1-015 and 2017-I2M-3-003), the National Natural Science Foundation of China (NSFC: 81770304, 81970243, and 81770308), and the National Key Research and Development Project of China (2019YFA0801500). We would like to thank Jian Meng (State Key Laboratory of Cardiovascular Disease, National Center for Cardiovascular Disease) with the pathological studies.

## Supplementary Materials

Supplement Figure 1: $H_2S$ exerts protective effects on CMs. Primary CMs from neonatal mice were cultured under $H_2O_2$ stimulation. (A) Apoptosis was tested by Hoechst 33258 staining. Scale bar = 50 $\mu$m. (B) Cell viability was measured by CCK-8 assay. (C) Representative images of TUNEL staining from CM and related statistical results. (D) Flow cytometric analysis of apoptosis in CMs subjected to $H_2O_2$ and quantification of CM apoptosis by Annexin V and PI flow cytometry assay. (E) Representative images of TUNEL immunofluorescence staining from heart. Actinin was used to label CMs, and DAPI was used to label nuclei. Vehicle: $n = 5$, NaHS: $n = 5$. Scale bar =50 $\mu$m. The data are presented as the mean ± SEM; ns: not significant. $^*p < 0.05$ by Student's $t$-test. *(Supplementary Materials)*

## References

[1] E. J. Benjamin, M. J. Blaha, S. E. Chiuve et al., "Heart Disease and Stroke Statistics-2017 update: a report from the American Heart Association," *Circulation*, vol. 135, no. 10, pp. e146–e603, 2017.

[2] K. D. Poss, L. G. Wilson, and M. T. Keating, "Heart regeneration in zebrafish," *Science*, vol. 298, no. 5601, pp. 2188–2190, 2002.

[3] W. Zhu, E. Zhang, M. Zhao et al., "Regenerative potential of neonatal porcine hearts," *Circulation*, vol. 138, no. 24, pp. 2809–2816, 2018.

[4] L. Ye, G. D'Agostino, S. J. Loo et al., "Early Regenerative Capacity in the Porcine Heart," *Circulation*, vol. 138, no. 24, pp. 2798–2808, 2018.

[5] E. R. Porrello, A. I. Mahmoud, E. Simpson et al., "Transient regenerative potential of the neonatal mouse heart," *Science*, vol. 331, no. 6020, pp. 1078–1080, 2011.

[6] B. J. Haubner, J. Schneider, U. Schweigmann et al., "Functional recovery of a human neonatal heart after severe myocardial infarction," *Circulation research.*, vol. 118, no. 2, pp. 216–221, 2016.

[7] M. Mollova, K. Bersell, S. Walsh et al., "Cardiomyocyte proliferation contributes to heart growth in young humans," *Proceedings of the National Academy of Sciences of the United States of America*, vol. 110, no. 4, pp. 1446–1451, 2013.

[8] E. R. Porrello, B. A. Johnson, A. B. Aurora et al., "MiR-15 family regulates postnatal mitotic arrest of cardiomyocytes," *Circulation research.*, vol. 109, no. 6, pp. 670–679, 2011.

[9] Q. Xiao, G. Zhang, H. Wang et al., "A p53-based genetic tracing system to follow postnatal cardiomyocyte expansion in heart regeneration," *Development*, vol. 144, no. 4, pp. 580–589, 2017.

[10] C. Jopling, E. Sleep, M. Raya, M. Martí, A. Raya, and J. C. I. Belmonte, "Zebrafish heart regeneration occurs by cardiomyocyte dedifferentiation and proliferation," *Nature*, vol. 464, no. 7288, pp. 606–609, 2010.

[11] B. N. Puente, W. Kimura, S. A. Muralidhar et al., "The oxygen-rich postnatal environment induces cardiomyocyte cell-cycle arrest through DNA damage response," *Cell*, vol. 157, no. 3, pp. 565–579, 2014.

[12] Y. Nakada, D. C. Canseco, S. Thet et al., "Hypoxia induces heart regeneration in adult mice," *Nature*, vol. 541, no. 7636, pp. 222–227, 2017.

[13] A. Negre-Salvayre, P. Guerby, S. Gayral, M. Laffargue, and R. Salvayre, "Role of reactive oxygen species in atherosclerosis: Lessons from murine genetic models," *Free Radical Biology & Medicine*, vol. 149, pp. 8–22, 2020.

[14] K. Ito and T. Suda, "Metabolic requirements for the maintenance of self-renewing stem cells," *Nature Reviews. Molecular Cell Biology*, vol. 15, no. 4, pp. 243–256, 2014.

[15] W. Kimura, S. Muralidhar, D. C. Canseco et al., "Redox signaling in cardiac renewal," *Antioxidants & Redox Signaling*, vol. 21, no. 11, pp. 1660–1673, 2014.

[16] C. C. Zhang and H. A. Sadek, "Hypoxia and metabolic properties of hematopoietic stem cells," *Antioxidants & Redox Signaling*, vol. 20, no. 12, pp. 1891–1901, 2014.

[17] X. Chen, K.-H. Jhee, and W. D. Kruger, "Production of the neuromodulator H2S by cystathionine $\beta$-Synthase via the condensation of cysteine and homocysteine," *The Journal of biological chemistry.*, vol. 279, no. 50, pp. 52082–52086, 2004.

[18] R. Guan, J. Wang, Z. Cai et al., "Hydrogen sulfide attenuates cigarette smoke-induced airway remodeling by upregulating SIRT1 signaling pathway," *Redox Biology*, vol. 28, p. 101356, 2020.

[19] L. Gambari, B. Grigolo, and F. Grassi, "Hydrogensulfide in regeneration and Repair:state of the and Perspectives," *International Journal of Molecular Sciences*, vol. 20, no. 20, p. 5231, 2019.

[20] E. Donnarumma, R. K. Trivedi, and D. J. Lefer, "Protective Actions of H2S in Acute Myocardial Infarction and Heart Failure," *Comprehensive Physiology*, vol. 7, no. 2, pp. 583–602, 2017.

[21] V. Citi, E. Piragine, L. Testai, M. C. Breschi, V. Calderone, and A. Martelli, "The role of hydrogen sulfide and H2S-donors in myocardial protection against ischemia/reperfusion injury," *Current Medicinal Chemistry*, vol. 25, no. 34, pp. 4380–4401, 2018.

[22] J. Wang, X. Chen, D. Shen et al., "A long noncoding RNA NR_045363 controls cardiomyocyte proliferation and cardiac

repair," *Journal of Molecular and Cellular Cardiology*, vol. 127, pp. 105–114, 2019.

[23] Z. Yue, J. Chen, H. Lian et al., "PDGFR-$\beta$ Signaling Regulates Cardiomyocyte Proliferation and Myocardial Regeneration," *Cell reports*, vol. 28, no. 4, pp. 966–978.e4, 2019.

[24] C. Han, Y. Nie, H. Lian et al., "Acute inflammation stimulates a regenerative response in the neonatal mouse heart," *Cell Research*, vol. 25, no. 10, pp. 1137–1151, 2015.

[25] Y. Li, H. Li, J. Pei, S. Hu, and Y. Nie, "Transplantation of murine neonatal cardiac macrophage improves adult cardiac repair," *Cellular & Molecular Immunology*, vol. 2020, 2020.

[26] J. N. Blom, X. Lu, P. Arnold, and Q. Feng, "Myocardial Infarction in Neonatal Mice, A Model of Cardiac Regeneration," *Journal of Visualized Experiments*, vol. 111, no. 111, 2016.

[27] L. Rui, N. Yu, L. Hong et al., "Extending the time window of mammalian heart regeneration by thymosin beta 4," *Journal of Cellular and Molecular Medicine*, vol. 18, no. 12, pp. 2417–2424, 2014.

[28] S. J. Elledge, "Cell cycle checkpoints: preventing an identity crisis," *Science*, vol. 274, no. 5293, pp. 1664–1672, 1996.

[29] A. Barzilai and K.-I. Yamamoto, "DNA damage responses to oxidative stress," *DNA Repair (Amst)*, vol. 3, no. 8-9, pp. 1109–1115, 2004.

[30] T. Loch, O. Vakhrusheva, I. Piotrowska et al., "Different extent of cardiac malfunction and resistance to oxidative stress in heterozygous and homozygous manganese-dependent superoxide dismutase-mutant mice," *Cardiovascular Research*, vol. 82, no. 3, pp. 448–457, 2009.

[31] D.-F. Dai, P. S. Rabinovitch, and Z. Ungvari, "Mitochondria and cardiovascular aging," *Circulation research.*, vol. 110, no. 8, pp. 1109–1124, 2012.

[32] S. J. Han, J. I. Kim, J.-W. Park, and K. M. Park, "Hydrogen sulfide accelerates the recovery of kidney tubules after renal ischemia/reperfusion injury," *Nephrology, Dialysis, Transplantation*, vol. 30, no. 9, pp. 1497–1506, 2015.

[33] S. J. Han, M. R. Noh, J.-M. Jung et al., "Hydrogen sulfide-producing cystathionine $\gamma$-lyase is critical in the progression of kidney fibrosis," *Free Radical Biology & Medicine*, vol. 112, pp. 423–432, 2017.

[34] N. Bazhanov, M. Ansar, T. Ivanciuc, R. P. Garofalo, and A. Casola, "Hydrogen sulfide: a novel player in airway development, pathophysiology of respiratory diseases, and antiviral defenses," *American Journal of Respiratory Cell and Molecular Biology*, vol. 57, no. 4, pp. 403–410, 2017.

[35] F. Akter, "The role of hydrogen sulfide in burns," *Burns*, vol. 42, no. 3, pp. 519–525, 2016.

[36] M. Bliksøen, M.-L. Kaljusto, J. Vaage, and K. O. Stensløkken, "Effects of hydrogen sulphide on ischaemia-reperfusion injury and ischaemic preconditioning in the isolated, perfused rat heart," *European Journal of Cardio-Thoracic Surgery*, vol. 34, no. 2, pp. 344–349, 2008.

[37] A. L. King, D. J. Polhemus, S. Bhushan et al., "Hydrogen sulfide cytoprotective signaling is endothelial nitric oxide synthase-nitric oxide dependent," *Proceedings of the National Academy of Sciences of the United States of America*, vol. 111, no. 8, pp. 3182–3187, 2014.

[38] J. W. Elrod, J. W. Calvert, J. Morrison et al., "Hydrogen sulfide attenuates myocardial ischemia-reperfusion injury by preservation of mitochondrial function," *Proceedings of the National Academy of Sciences of the United States of America*, vol. 104, no. 39, pp. 15560–15565, 2007.

[39] D. L. Carden and D. N. Granger, "Pathophysiology of ischaemia-reperfusion injury," *The Journal of Pathology*, vol. 190, no. 3, pp. 255–266, 2000.

[40] R. B. Jennings, "Historical perspective on the pathology of myocardial ischemia/reperfusion injury," *Circulation research.*, vol. 113, no. 4, pp. 428–438, 2013.

[41] D. J. Hausenloy and D. M. Yellon, "Myocardial ischemia-reperfusion injury: a neglected therapeutic target," *The Journal of clinical investigation*, vol. 123, no. 1, pp. 92–100, 2013.

[42] A. Rakotovao, S. Tanguy, M.-C. Toufektsian et al., "Selenium status as determinant of connexin-43 dephosphorylation in ex vivo ischemic/reperfused rat myocardium," *Journal of Trace Elements in Medicine and Biology*, vol. 19, no. 1, pp. 43–47, 2005.

[43] C. Barandier, S. Tanguy, S. Pucheu, F. Boucher, and J. Leiris, "Effect of antioxidant trace elements on the response of cardiac tissue to oxidative Stressa," *Annals of the New York Academy of Sciences*, vol. 874, no. 1 HEART IN STRE, pp. 138–155, 1999.

[44] W. J. H. Koopman, L. G. J. Nijtmans, C. E. J. Dieteren et al., "Mammalian mitochondrial complex I: biogenesis, regulation, and reactive oxygen species generation," *Antioxidants & Redox Signaling*, vol. 12, no. 12, pp. 1431–1470, 2010.

[45] V. Vitvitsky, O. Kabil, and R. Banerjee, "High turnover rates for hydrogen sulfide allow for rapid regulation of its tissue concentrations," *Antioxidants & Redox Signaling*, vol. 17, no. 1, pp. 22–31, 2012.

[46] J. Furne, A. Saeed, and M. D. Levitt, "Whole tissue hydrogen sulfide concentrations are orders of magnitude lower than presently accepted values," *American Journal of Physiology. Regulatory, Integrative and Comparative Physiology*, vol. 295, no. 5, pp. R1479–R1485, 2008.

[47] N. L. Whitfield, E. L. Kreimier, F. C. Verdial, N. Skovgaard, and K. R. Olson, "Reappraisal of H2S/sulfide concentration in vertebrate blood and its potential significance in ischemic preconditioning and vascular signaling," *American Journal of Physiology. Regulatory, Integrative and Comparative Physiology*, vol. 294, no. 6, pp. R1930–R1937, 2008.

[48] M. D. Levitt, M. S. Abdel-Rehim, and J. Furne, "Free and acid-labile hydrogen sulfide concentrations in mouse tissues: anomalously high free hydrogen sulfide in aortic tissue," *Antioxidants & Redox Signaling*, vol. 15, no. 2, pp. 373–378, 2011.

[49] B. Geng, J. Yang, Y. Qi et al., "H2S generated by heart in rat and its effects on cardiac function," *Biochemical and Biophysical Research Communications*, vol. 313, no. 2, pp. 362–368, 2004.

[50] A. Sivarajah, M. Collino, M. Yasin et al., "Anti-apoptotic and anti-inflammatory effects of hydrogen sulfide in a rat model of regional myocardial I/R," *Shock*, vol. 31, no. 3, pp. 267–274, 2009.

[51] G. Yang, L. Wu, B. Jiang et al., "H2S as a physiologic vasorelaxant: hypertension in mice with deletion of cystathionine gamma-lyase," *Science*, vol. 322, no. 5901, pp. 587–590, 2008.

[52] Y.-X. Luo, X. Tang, X.-Z. An et al., "SIRT4 accelerates Ang II-induced pathological cardiac hypertrophy by inhibiting manganese superoxide dismutase activity," *European heart journal.*, vol. 38, no. 18, pp. 1389–1398, 2017.

Hindawi
Oxidative Medicine and Cellular Longevity
Volume 2020, Article ID 8348035, 12 pages
https://doi.org/10.1155/2020/8348035

*Research Article*

# Vanillic Acid Alleviates Acute Myocardial Hypoxia/Reoxygenation Injury by Inhibiting Oxidative Stress

**Xiuya Yao,[1,2] Shoufeng Jiao,[3] Mingming Qin,[1] Wenfeng Hu,[1] Bo Yi,[4] and Dan Liu[1]**

[1]*Jiangxi Provincial Key Laboratory of Basic Pharmacology, Nanchang University, School of Pharmaceutical Science, Nanchang 330006, China*
[2]*Department of Pharmacy, Changzhou Maternal and Child Health Care Hospital, Changzhou 213000, China*
[3]*Department of Pharmacy, The First Affiliated Hospital of Nanchang University, Nanchang 330006, China*
[4]*Second Abdominal Surgery Department, Jiangxi Province Tumor Hospital, Nanchang 330029, China*

Correspondence should be addressed to Bo Yi; yibo790508@163.com and Dan Liu; liudan1201jx@163.com

Received 25 November 2019; Accepted 23 March 2020; Published 21 April 2020

Guest Editor: Aleksandar Kibel



Oxidative stress is an important factor of myocardial hypoxia/reoxygenation (H/R) injury. Our research focuses on how to reduce the cardiac toxicity caused by oxidative stress through natural plant extracts. Vanillic acid (VA) is a phenolic compound found in edible plants and rich in the roots of *Angelica sinensis*. Experimental studies have provided evidence for this compound's effectiveness in cardiovascular diseases; however, its mechanism is still unclear. In this study, molecular mechanisms related to the protective effects of VA were investigated in H9c2 cells in the context of H/R injury. The results showed that pretreatment with VA significantly increased cell viability and decreased the percentage of apoptotic cells, as well as lactate dehydrogenase and creatine phosphokinase activity, in the supernatant, accompanied by reduced levels of reactive oxygen species and reduced caspase-3 activity. VA pretreatment also restored mitochondrial membrane potentials. Moreover, preincubation with VA significantly attenuated mitochondrial permeability transition pore activity. VA administration upregulated adenosine monophosphate-activated protein kinase $\alpha 2$ (AMPK$\alpha 2$) protein expression, and interestingly, pretreatment with AMPK$\alpha 2$-siRNA lentivirus effectively attenuated the cardioprotective effects of VA in response to H/R injury.

## 1. Introduction

Myocardial hypoxia/reoxygenation (H/R) injury leads to significant morbidity and mortality [1], and oxidative stress is one of the most important factors causing cardiac toxicity. Natural plant extracts have the advantages of few side effects and easy access. Therefore, our research focuses on the use of natural plant extracts to protect the heart against oxidative stress, thereby reducing cardiac toxicity caused by I/R injury. Vanillic acid (VA) is a phenolic compound found in secondary plant products with the molecular formula $C_8H_8O_4$. VA is widely used in the food industry as flavouring agent, food additive, and preservative. We detected VA in various foods, such as herbs, tea, coffee, wine, and beer [2–7]. VA possesses powerful antioxidant functions, antihypotensive effects, cardioprotective effects, hepatoprotective effects, and antiapoptotic activities [8–11].

Adenosine monophosphate-activated protein kinase (AMPK) is a stress responsive kinase that modulates a number of physiologically and metabolically significant pathways, including apoptosis, energy dynamic balance, and cellular metabolism [12]. AMPK ameliorates cellular antioxidant enzyme systems, such as manganese superoxide dismutase (Mn-SOD) and catalase, consequently reducing oxidant-induced injury [13].

Accordingly, we hypothesized that VA exerts a protective effect against hypoxia/reoxygenation (H/R) injury, which might be related to the AMPK signalling pathway. Therefore, the present study is aimed at addressing the following aims: (1) determine whether VA pretreatment protects H9c2

cells from hypoxia/reoxygenation (H/R) injury and (2) explore the underlying protective mechanisms of VA on hypoxia/reoxygenation (H/R) injury in H9c2 cells.

## 2. Materials and Methods

*2.1. Reagents.* VA (purity: >98%) was purchased from Sigma Chemical Co. (St. Louis, MO, USA). The AMPK$\alpha$2-siRNA lentivirus was purchased from Genechem Co. (Shanghai, China).

*2.2. Cell Culture.* Embryonic rat heart-derived H9c2 cells were purchased from the Chinese Academy of Sciences cell bank. H9c2 cells were incubated at 37°C in a 5% $CO_2$ incubator (Forma™ 310, Thermo Fisher, USA) with high glucose (4.5 g/l glucose) DMEM (Solarbio, Beijing, China) by adding 13% FBS (foetal bovine serum, WISENT, Canada) and antibiotics (100 U/ml penicillin and 100 $\mu$g/ml streptomycin, Solarbio, Beijing, China). The hypoxia/reoxygenation (H/R) cell model was set up to imitate an ischaemia/reperfusion (I/R) model in vitro [14–17]. Briefly, after different pretreatments, H9c2 cells were cultured in hypoxic solution (sodium lactate 40 mM, $NaH_2PO_4$ 0.9 mM, $NaHCO_3$ 6 mM, $MgSO_4$ 1.2 mM, HEPES 20 mM, $CaCl_2$ 1.8 mM, NaCl 98.5 mM, KCl 10 mM, pH 6.8) and incubated at 37°C with 5% $CO_2$ and 0.1% $O_2$ in a hypoxic chamber (Proox model C21, BioSpherix Ltd., USA) for 3 h. H9c2 cells were subsequently cultured in reoxygenation solution (glucose 5.5 mM, $NaH_2PO_4$ 0.9 mM, $NaHCO_3$ 20 mM, $MgSO_4$ 1.2 mM, HEPES 20 mM, $CaCl_2$ 1.8 mM, NaCl 129.5 mM, KCl 5 mM, pH 7.4) and incubated at 37°C and 95% $O_2$/5% $CO_2$ in a reoxygenation chamber for 2 h. All experiments were performed in triplicate.

*2.3. Experimental Protocol.* Cultured H9c2 cells were randomly divided into the following experimental groups:

(1) Control group comprised H9c2 cells that were maintained in normoxic conditions with 95% air and 5% $CO_2$ in complete medium for 5 h

(2) H/R group comprised conditions described in Section 2.2

(3) VA+H/R group comprised H9c2 cells that were pretreated with 1.00 mM VA 24 h before H/R treatment

(4) VA+NC+H/R group included H9c2 cells that were pretreated with 1.00 mM VA 24 h before H/R treatment and the negative lentivirus 48 h before H/R treatment

(5) VA+AMPK$\alpha$2-siRNA+H/R group comprised H9c2 cells that were pretreated with 1.00 mM VA 24 h before H/R treatment and the lentivirus AMPK$\alpha$2-siRNA 48 h before H/R treatment

*2.4. Cell Viability Assays.* The viability of H9c2 cells was determined using the 3-(4,5-dimethylthiazol-2-yl)-5-(3-carboxymethoxyphenyl)-2-(4-sulfophenyl)-2H-tetrazolium (MTS) kit. MTS (Promega, USA) produces a dark blue formazan product when incubated with living cells. H9c2 cells were trypsinized, counted, and seeded in 96-well plates at a density of $1 \times 10^4$ cells per well. Following incubation and different treatments, H9c2 cells were treated with 20 $\mu$l MTS (5 mg/ml) in 100 $\mu$l medium for 2 h at 37°C. After 2 h, the optical density (OD) of each well was determined at a wavelength of 490 nm using a microplate reader (Bio-Rad 680, USA). H9c2 cell viability is indicated as a percentage of controls.

*2.5. Assessment of LDH and CPK Activities.* Lactate dehydrogenase (LDH) and creatine phosphate kinase (CPK) activities were determined using LDH and CPK commercial assay kits (Jiancheng Bioengineering Institute, Nanjing, China) according to the manufacturer's instructions [18]. H9c2 cell supernatants were collected after different treatments, and optical density (OD) was determined at a wavelength of 440 nm and 660 nm to measure LDH and CPK activities, respectively, using a microplate reader (Bio-Rad 680, USA).

*2.6. Western Blot Analysis.* H9c2 cells were washed using cold phosphate-buffered saline (PBS) three times, followed by lysis with Radio Immunoprecipitation Assay (RIPA) and phenylmethanesulfonyl fluoride (PMSF) buffer on ice for 10 min. To remove insoluble material, extracts were centrifuged at 12,000 rpm for 15 min at 4°C. Total protein content was subsequently measured using the Bradford protein assay kit (Beyotime, Shanghai, China). Equal amounts of protein were electrophoresed on 10% sodium dodecyl sulfate polyacrylamide gel electrophoresis (SDS-PAGE) using a gel apparatus (Bio-Rad, USA). Gels were cut according to a prestained, dual color protein molecular weight marker followed by transfer to polyvinylidene fluoride (PVDF) membranes (Solarbio, Beijing, China) which were blocked with 5% nonfat milk in TBST (Tris-Buffer Saline, 0.25% Tween-20) for 2 h. Membranes were incubated with antibodies (1 : 500 dilution) for AMPK$\alpha$2 (Abcam, USA) and $\beta$-actin (ZSGB-BIO, Beijing, China) overnight at 4°C. Next, membranes were washed nine times for 10 min each in TBST (Tris-Buffer Saline, 0.25% Tween-20). Then, the membranes were incubated with HRP-labelled IgG secondary antibodies for AMPK$\alpha$2 (1 : 5000 dilution) (ZSGB-BIO, Beijing, China) and $\beta$-actin (1 : 2000 dilution) with shaking at room temperature for 2 h. Next, membranes were washed six times for 10 min each in TBST. To detect the immune complexes, the enhanced chemiluminescence (ECL) method was used. To measure protein expression, densitometry analysis was employed using Image Lab software (Bio-Rad, USA). We used the ratio of the grey value of the target protein and the corresponding beta-actin protein for quantification and statistical analysis.

*2.7. Determination of Reactive Oxygen Species (ROS) Levels.* The fluorescence probe DCFH-DA (2,7-dichlorofluorescein diacetate) is converted to $DCFH_2$ which is oxidized to DCF by ROS. DCF emits a green fluorescent signal that can be measured by flow cytometry. This assay was used according to the manufacturer's instructions. H9c2 cells were collected and incubated in a serum-free medium with a final concentration of 10 $\mu$M DCFH-DA (KeyGEN BioTECH, Nanjing, China) at 37°C for 30 min in the dark. Fluorescence intensity

of dichlorofluorescin (DCF) was measured by flow cytometry (Beckman Coulter, USA) at 488 nm excitation and at 525 nm emission. A.U. is the abbreviation for arbitrary units.

*2.8. Measurement of Mitochondrial Membrane Potential ($\Delta\Psi_m$).* JC-1 (5,5′,6,6′-tetrachloro-1,1′,3,3′-tetraethylbenzimidazolo carbocyanine iodide) is a dye that changes color from green to red when $\Delta\psi_m$ increases. Mitochondrial membrane potential was measured using JC-1 (KeyGEN BioTECH, Nanjing, China) staining following the manufacturer's instructions. After washing twice with ice-cold PBS, H9c2 cells were harvested and incubated with JC-1 solution at a final concentration of 200 $\mu$M at 37°C for 20 min in the dark. Fluorescence was detected by flow cytometry (Beckman Coulter, USA) at excitation and emission wavelengths (ex/em) of 488/630 nm (red) and 488/530 nm (green). $\Delta\psi_m$ was calculated as the red/green fluorescence ratio.

*2.9. $Ca^{2+}$-Induced Mitochondria Swelling.* After different treatments, H9c2 cell mitochondria were extracted using the cell mitochondria isolation kit (KeyGEN BioTECH, Nanjing, China). Next, purified mitochondria were treated with swelling buffer (120 mM KCl, 5 mM $KH_2PO_4$, 20 mM MOPS, and 10 mM Tris-HCl (pH 7.4)). The mPTP open level was assessed using a $Ca^{2+}$-induced mitochondria swelling assay [19]. After adding 200 $\mu$M $CaCl_2$ to the mitochondria, the opening of the mitochondrial permeability transition pore leads to mitochondrial swelling causing a stable decline in mitochondrial optical density. Due to the ability of the mitochondria to dilate, optical density (OD) was recorded using a microplate reader at 520 nm (Bio-Rad 680, USA). Mitochondrial swelling was recorded as the optical density ($OD_1$) at 520 nm, and a second optical density ($OD_2$) was recorded 20 min after induction. The optical density at 520 nm was continuously recorded over 20 min. mPTP activity was calculated as $\Delta OD(OD_1 - OD_2)/\min \times 1000$.

*2.10. Measurement of Caspase-3 Activity.* Caspase-3 activity was measured using a caspase-3 activity assay kit (Beyotime, Shanghai, China) following the manufacturer's instructions. H9c2 cells were lysed in lysis buffer on ice for 15 min and then collected and centrifuged at 16,000g for 15 min at 4°C to obtain the supernatant. Protein concentration was determined using the bicinchoninic acid (BCA) protein assay kit (Beyotime, Shanghai, China). After adding detection buffer and Ac-DEVD-pNA and incubating at 37°C for 18 h, optical density was detected at 405 nm. Caspase-3 activity was measured using a microplate reader (Bio-Rad 680, USA). A.U. is the abbreviation for arbitrary units.

*2.11. Analysis of Apoptosis by Flow Cytometry.* We previously published methods for measuring apoptosis [20]. Briefly, apoptosis was assessed by flow cytometry using an Annexin V-FITC/PI apoptosis kit (KeyGEN BioTECH, Nanjing, China) following the manufacturer's instructions. Briefly, H9c2 cells were collected and washed three times with ice-cold PBS. Next, collected H9c2 cells were resuspended in 1x Binding Buffer at a final concentration of $5 \times 10^5$ cells/ml. After the addition of 5 $\mu$l Annexin V-FITC and 5 $\mu$l PI, H9c2 cells were incubated in the dark for 15 min at room temperature. Cellular fluorescence was analysed by flow cytometry (ex 488 nm; em 530 nm, Beckman Coulter, USA).

*2.12. Assessment of Apoptosis by TUNEL Staining.* Apoptotic H9c2 cells were analysed by optical microscopy using the terminal deoxynucleotidyl transferase-mediated nick end labelling (TUNEL) staining method, which was performed using a TUNEL Apoptosis Detection kit (Promega, USA) [21]. Apoptotic H9c2 cells are stained brown, identifying them as TUNEL positive. Then, apoptotic H9c2 cells were subsequently observed on a microscope (Olympus, Japan). The number of TUNEL-positive H9c2 cells/the total number of H9c2 cells represents the apoptotic index.

*2.13. Statistical Analysis.* All values are presented as the mean ± SEM. ANOVA was applied to measure the significance of examined data across different groups, followed by *post hoc* analysis to determine individual differences. $p$ values $\leq 0.05$ were considered statistically significant.

## 3. Results

*3.1. Pretreatment with VA Ameliorates the Viability of H9c2 Cells and Reduces Levels of LDH and CPK in H9c2 Cells after H/R.* To measure the effects of VA on H9c2 cells undergoing hypoxia/reoxygenation (H/R), MTS assay was performed on H9c2 cells that were pretreated with different concentrations of VA 24 h prior to H/R. H9c2 cell viability decreased markedly in response to H/R (Figure 1(a), $p < 0.01$ vs. control group). We demonstrated that VA significantly increased H9c2 cell viability. Pretreatment with different concentrations of VA progressively increased viability of H9c2 cell in a concentration-dependent manner. H9c2 cell viability peaked at 1.00 mM VA ($p < 0.05$ vs. 0.50 mM VA+H/R group). However, H9c2 cells pretreated with concentrations of VA higher than 2.00 mM exhibited a significant reduction in cell viability, illustrating that higher VA concentrations cause toxicity. Thus, 1.00 mM VA was selected as the optimal pretreatment concentration for subsequent experiments. In addition, in Figure 1(b), our results show that AMPK$\alpha$2-siRNA caused significantly reduced cell viability ($p < 0.05$ vs. VA+H/R group). Thus, we hypothesized that VA protects H9c2 cells from H/R injury through the AMPK signalling pathway.

To measure injury to H9c2 cell membranes in response to H/R, we evaluated levels of LDH and CPK in the supernatant after H/R treatment. The levels of both LDH and CPK were increased in the H/R group ($p < 0.01$ vs. control group) and markedly decreased in the VA+H/R group ($p < 0.01$ vs. H/R group). Furthermore, the VA+AMPK$\alpha$2-siRNA+H/R group significantly increased the levels of LDH and CPK ($p < 0.01$ vs. VA+H/R group) (Figure 1(c)).

*3.2. Pretreatment with VA Upregulates AMPK$\alpha$2 Protein Levels in H9c2 Cells Undergoing H/R.* To verify whether the AMPK$\alpha$2 protein was associated with observed cardioprotective activity and optimal pretreatment concentration of VA, we assessed protein levels of AMPK$\alpha$2 by western blot. We pretreated H9c2 cells with different concentrations (0.25,

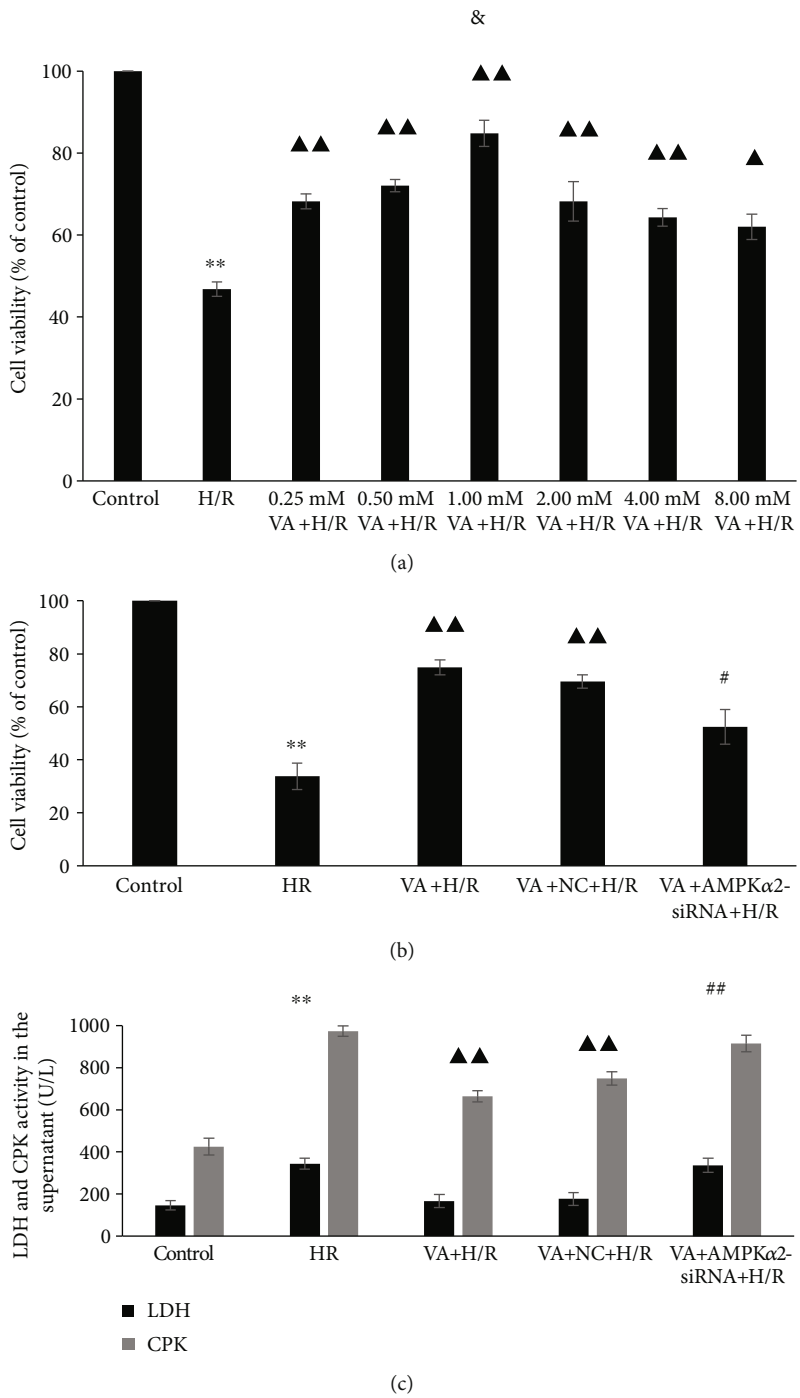


Figure 1: Effects of vanillic acid (VA) on the activities of creatine phosphate kinase (CPK) and lactate dehydrogenase (LDH) activities in the supernatant and cell viability in H9c2 cells subjected to hypoxia/reoxygenation (H/R) injury. (a) $^{**}p < 0.01$ vs. control group; $^{\blacktriangle\blacktriangle}p < 0.01$ vs. H/R group; $^{\blacktriangle}p < 0.05$ vs. H/R group; $^{\&}p < 0.05$ vs. 0.50 mM VA+H/R group. (b) $^{**}p < 0.01$ vs. control group; $^{\blacktriangle\blacktriangle}p < 0.01$ vs. H/R group; $^{\#}p < 0.05$ vs. VA+H/R group. Data are expressed as the mean ± SEM, $n = 3$. M: mol/l. (c) $^{**}p < 0.01$ vs. control group; $^{\blacktriangle\blacktriangle}p < 0.01$ vs. H/R group; $^{\#\#}p < 0.01$ vs. VA+H/R group. Data are expressed as the mean ± SEM, $n = 3$.

0.50, 1.00, 2.00, 4.00, and 8.00 mM) of VA for 24 h before H/R. In Figure 2(a), most of VA-pretreated groups exhibited upregulated levels of AMPKα2 protein relative to those of control and H/R groups, and the 1.00 mM VA+H/R group exhibited the highest levels of AMPKα2 protein ($p < 0.05$ vs. 0.50 mM VA+H/R group). The optimal pretreatment concentration was consistent with that observed by MTS. However, levels of AMPKα2 protein were markedly decreased in the VA+AMPKα2-siRNA+H/R group relative to those in the VA+H/R group ($p < 0.01$) (Figure 2(b)). Thus, our data indicate that VA exhibits cardioprotective effects against H/R by upregulating AMPKα2 protein levels.

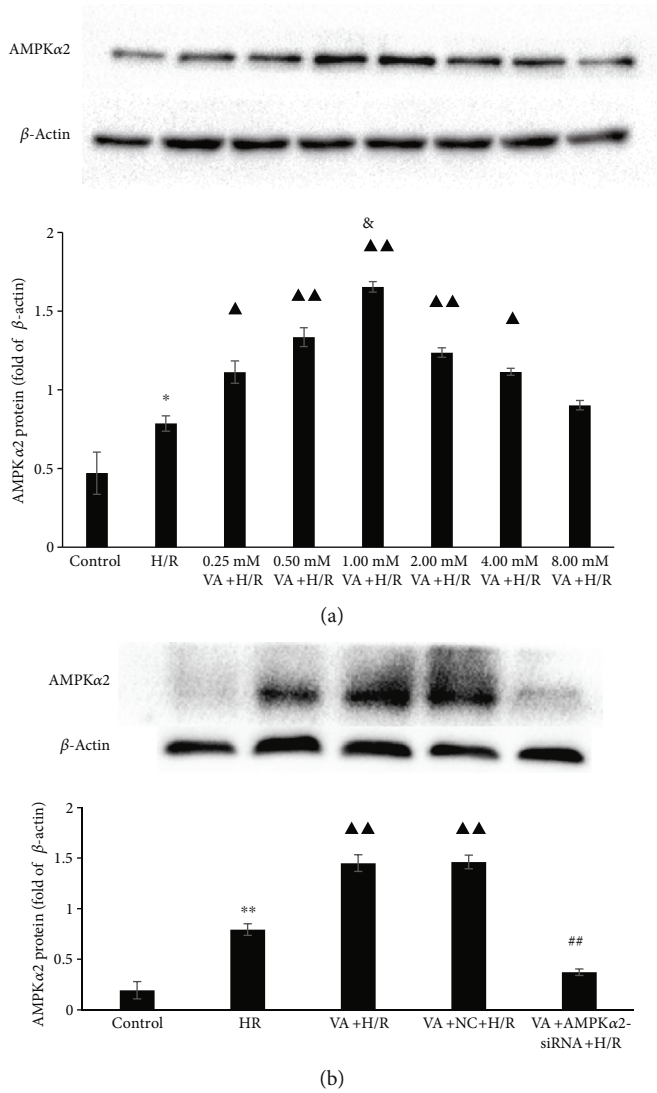


Figure 2: The effect of vanillic acid (VA) on the expression of AMPK$\alpha$2 in H9c2 cells exposed to hypoxia/reoxygenation (H/R) injury. AMPK$\alpha$2 expression was evaluated by western blot, and $\beta$-actin was used as an internal control. (a) $^{*}p < 0.05$ vs. control group; $^{\blacktriangle\blacktriangle}p < 0.01$ vs. H/R group; $^{\blacktriangle}p < 0.05$ vs. H/R group; $^{\&}p < 0.05$ vs. 0.50 mM VA+H/R group. (b) $^{**}p < 0.01$ vs. control group; $^{\blacktriangle\blacktriangle}p < 0.01$ vs. H/R group; $^{\#\#}p < 0.01$ vs. VA+H/R group. Data are expressed as the mean ± SEM, $n = 3$. M: mol/l.

*3.3. Pretreatment with VA Reduces ROS Generation Induced by H/R.* Relevant experiments were performed to evaluate ROS levels using the DCFH-DA fluorescence probe. ROS levels increased significantly in the H/R group ($p < 0.01$ vs. control group), whereas there was a striking decrease in ROS levels in the VA+H/R and VA+NC+H/R groups ($p < 0.01$ vs. H/R group). As expected, ROS levels markedly increased in the VA+AMPK$\alpha$2-siRNA+H/R group ($p < 0.01$ vs. VA+H/R group and VA+NC+H/R group). These results confirmed that VA reduces ROS generation associated with the AMPK signalling pathway (Figure 3).

*3.4. Pretreatment with VA Restores $\Delta\psi_m$ in H9c2 Cells Exposed to H/R.* To determine $\Delta\psi_m$ in H9c2 cells after H/R injury, a JC-1 fluorescent probe assay was performed. We used the fluorescence ratio of the upper right quadrant and lower right quadrant to verify $\Delta\psi_m$. The results demonstrated that $\Delta\psi_m$ decreased in response to H/R ($p < 0.01$ vs. control group) (Figure 4). However, pretreatment with VA markedly reduced the loss of $\Delta\psi_m$ in the VA+H/R group ($p < 0.01$ vs. H/R group). In contrast, a disruption in $\Delta\psi_m$ was observed when the AMPK$\alpha$2 gene was knocked down ($p < 0.01$ vs. VA+H/R group), demonstrating that AMPK$\alpha$2-siRNA effectively abrogates the cardioprotective effects of VA against H/R injury.

*3.5. Pretreatment with VA Prevents Opening of the mPTP Induced by H/R.* $Ca^{2+}$-induced mitochondria swelling was used to examine the effects of VA on mPTP opening. We determined the degree of mPTP opening by recording varied optical density values at 520 nm/min (OD/min) over a period of time. As shown in Figure 5, there was a significant increase in $\Delta$OD/min in the H/R group ($p < 0.01$ vs. control group); however, pretreatment of H9c2 cells with VA delayed mPTP

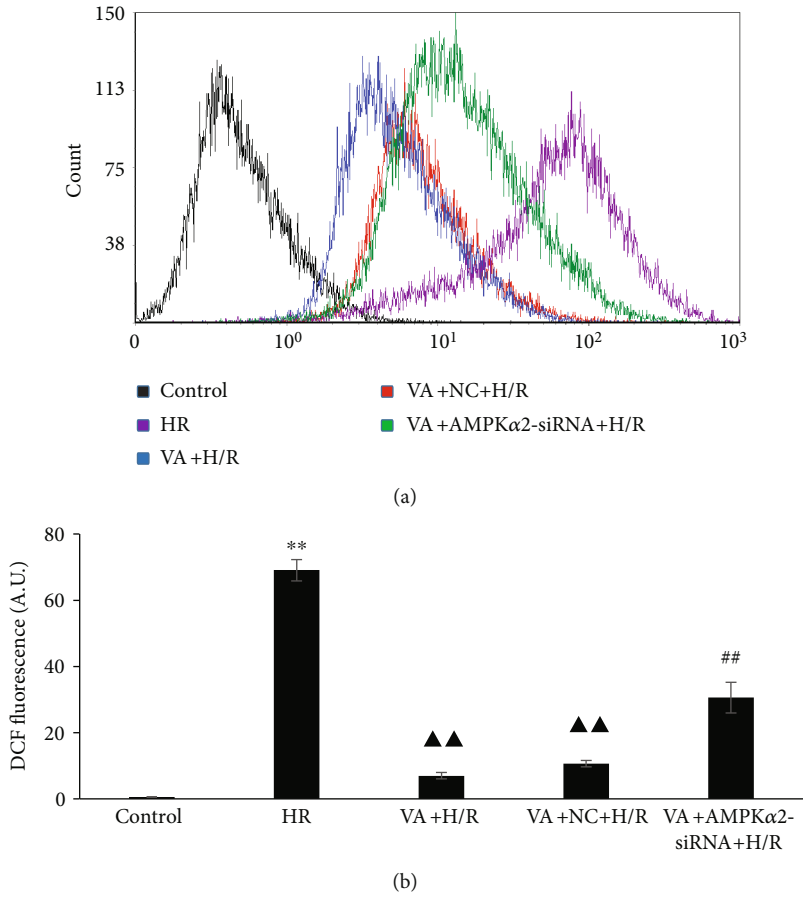


Figure 3: Vanillic acid (VA) pretreatment decreases ROS production in H9c2 cells exposed to hypoxia/reoxygenation (H/R). (a) Flow cytometry analysis of DCF fluorescence. (b) Column bar graph of cell fluorescence for DCF. Data are expressed as the mean ± SEM, $n = 3$. $^{**}p < 0.01$ vs. control group; $^{▲▲}p < 0.01$ vs. H/R group; $^{\#\#}p < 0.01$ vs. VA+H/R group. A.U. is the abbreviation for arbitrary unit.

opening ($p < 0.01$ vs. H/R group). AMPKα2 gene knockdown using AMPKα2-siRNA lentivirus abolished the cardioprotective effects of VA against H/R injury with respect to inhibiting mPTP opening ($p < 0.05$ vs. VA+H/R group).

*3.6. Pretreatment with VA Attenuates Caspase-3 Activity in response to H/R.* To examine the cardioprotective effects of VA on H/R-induced injury, levels of caspase-3 activity were estimated using a colorimetric method. Figure 6 shows a significant increase in caspase-3 activity in the H/R group ($p < 0.01$ vs. control group), yet VA pretreatment strikingly decreased caspase-3 activity ($p < 0.01$ vs. H/R group). Furthermore, in line with previous results, a significant increase in caspase-3 activity was observed in the VA+AMPKα2-siRNA+H/R group ($p < 0.01$ vs. VA+H/R group).

*3.7. Pretreatment with VA Decreases H9c2 Cell Apoptosis in response to H/R.* Apoptosis was assessed by flow cytometry using an Annexin V-FITC/PI apoptosis kit. As shown in Figure 7, H9c2 cell apoptotic rates increased markedly in the H/R group ($p < 0.01$ vs. control group), while progressively decreasing in the VA+H/R group ($p < 0.01$ vs. H/R group). Moreover, H9c2 cell apoptotic rates increased again in the VA+AMPKα2-siRNA+H/R group ($p < 0.01$ vs. VA+H/R group).

To further confirm the VA-induced cardioprotective effect against H/R injury, we scored the number of TUNEL-positive H9c2 cells by optical microscopy. As shown in Figure 8, H/R caused a significant increase in the number of TUNEL-positive H9c2 cells in the H/R group ($p < 0.01$ vs. control group). In contrast, the pretreatment of H9c2 cells with VA resulted in significantly reduced TUNEL-positive H9c2 cells ($p < 0.01$ vs. H/R group). In agreement with previous results, the cardioprotective effects of VA were abrogated after AMPKα2 gene knockdown using the AMPKα2-siRNA lentivirus.

## 4. Discussion

Vanillic acid (VA) is a phenolic compound in edible plants that is enriched in the roots of *Angelica sinensis*. VA exhibits powerful antioxidant functions and possesses cardioprotective, antihypotensive, antiapoptotic, and hepatoprotective activities [8–11]. Experimental studies have provided evidence of this compound's efficacy in cardiac toxicity.

In this study, we found that H9c2 cells pretreated with 1.00 mM VA 24 h prior to H/R significantly increased the viability of H9c2 cells and reduced the levels of LDH and CPK. And our data further confirmed VA pretreatment

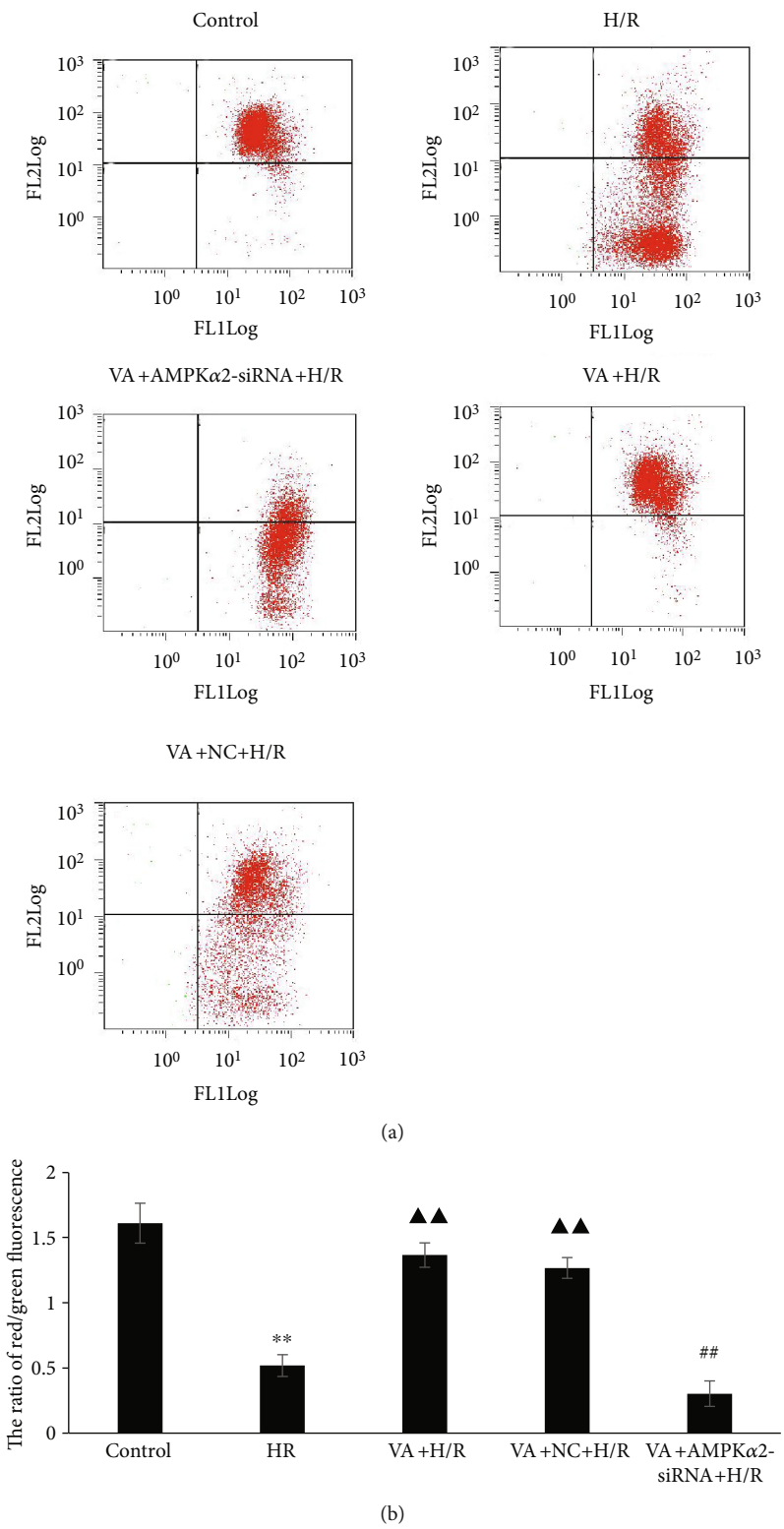


Figure 4: Vanillic acid (VA) pretreatment alleviates loss of $\Delta\Psi_m$ in H9c2 cells exposed to hypoxia/reoxygenation (H/R), while AMPKα2-siRNA abrogates this effect. (a) Representative dot plots of flow cytometry. (b) $\Delta\Psi_m$ was calculated with the ratio of red/green fluorescence obtained by flow cytometry. The ratio of fluorescence in the upper right quadrant and lower right quadrant was used to evaluate levels of $\Delta\Psi_m$. Data are expressed as the mean ± SEM, $n = 3$. $^{**}p < 0.01$ vs. control group; $^{▲▲}p < 0.01$ vs. H/R group; $^{\#\#}p < 0.01$ vs. VA+H/R group. JC-1 FL1: JC-1 fluorescence channel 1; JC-1 FL2: JC-1 fluorescence channel 2.

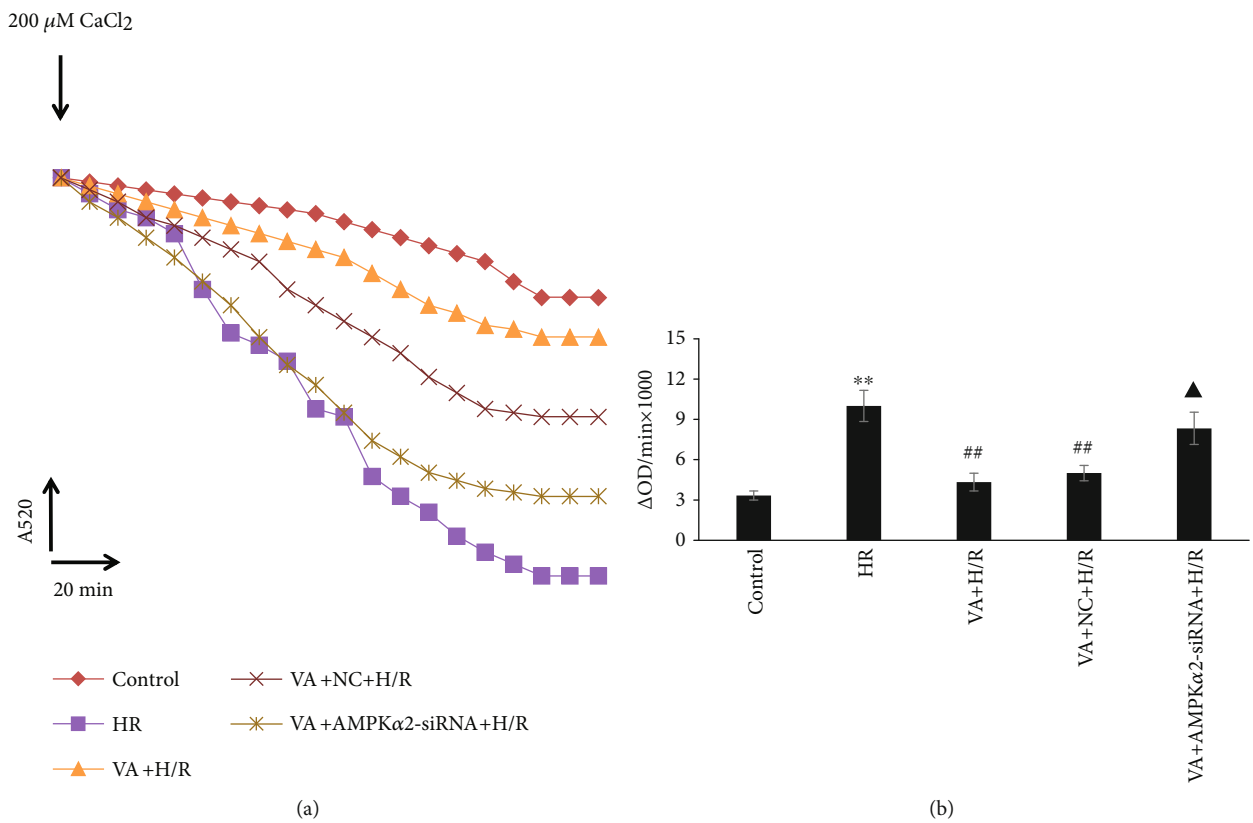


Figure 5: Vanillic acid (VA) preconditioning limited mPTP opening in response to hypoxia/reoxygenation (H/R) in H9c2 cells, while AMPK$\alpha$2-siRNA attenuates this effect. (a) After the addition of 200 $\mu$M $CaCl_2$, the absorbance value at A520 was monitored over 20 min to reflect the opening of mitochondrial permeability transition pore (mPTP). (b) Changes in absorbance values at 520 nm/min ($\Delta$ODmin$^{-1}$) were used to express the extent of mPTP opening ($\Delta OD = A520_{0\ min} - A520_{20\ min}$). Data are expressed as the mean ± SEM, $n = 3$. $^{**}p < 0.01$ vs. control group; $^{\#\#}p < 0.01$ vs. H/R group; $^{\blacktriangle}p < 0.05$ vs. VA+H/R group.

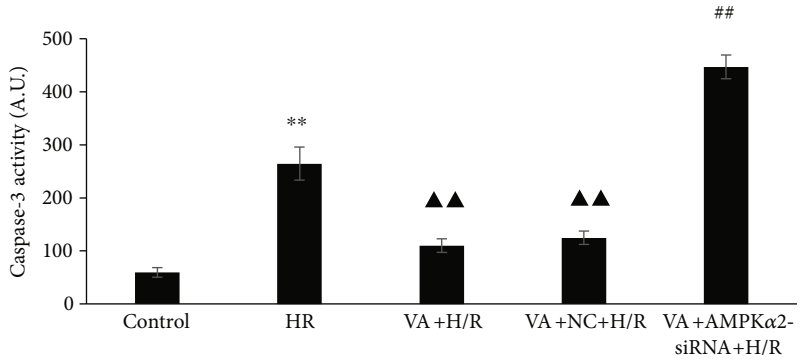


Figure 6: Vanillic acid (VA) pretreatment influences the activity of caspase-3 induced by hypoxia/reoxygenation (H/R) injury, while AMPK$\alpha$2-siRNA abrogates this effect. The column bar graph represents the activity of caspase-3 in the different groups. Data are expressed as the mean ± SEM, $n = 3$. $^{**}p < 0.01$ vs. control group; $^{\blacktriangle\blacktriangle}p < 0.01$ vs. H/R group; $^{\#\#}p < 0.01$ vs. VA+H/R group. A.U. is the abbreviation for absorbance unit.

could inhibit cardiomyocyte apoptosis and protect them against H/R injury.

The cardioprotective effect of VA was extensively investigated, and the potential mechanisms might be associated with countering oxidative stress caused by energy metabolism imbalance, but the mechanism remains to be fully elucidated. AMPK plays an important role in the balance of energy dynamics and is implicated in various diseases [22]. Studies including those from our group have shown that AMPK may be an oxidative stress sensor and redox regulator in addition to its traditional role as an energy sensor and regulator [23, 24]. Moreover, AMPK activation is believed to enhance cellular antioxidant capacity [25, 26]. These findings all led us to hypothesize that VA protects H9c2 cells against

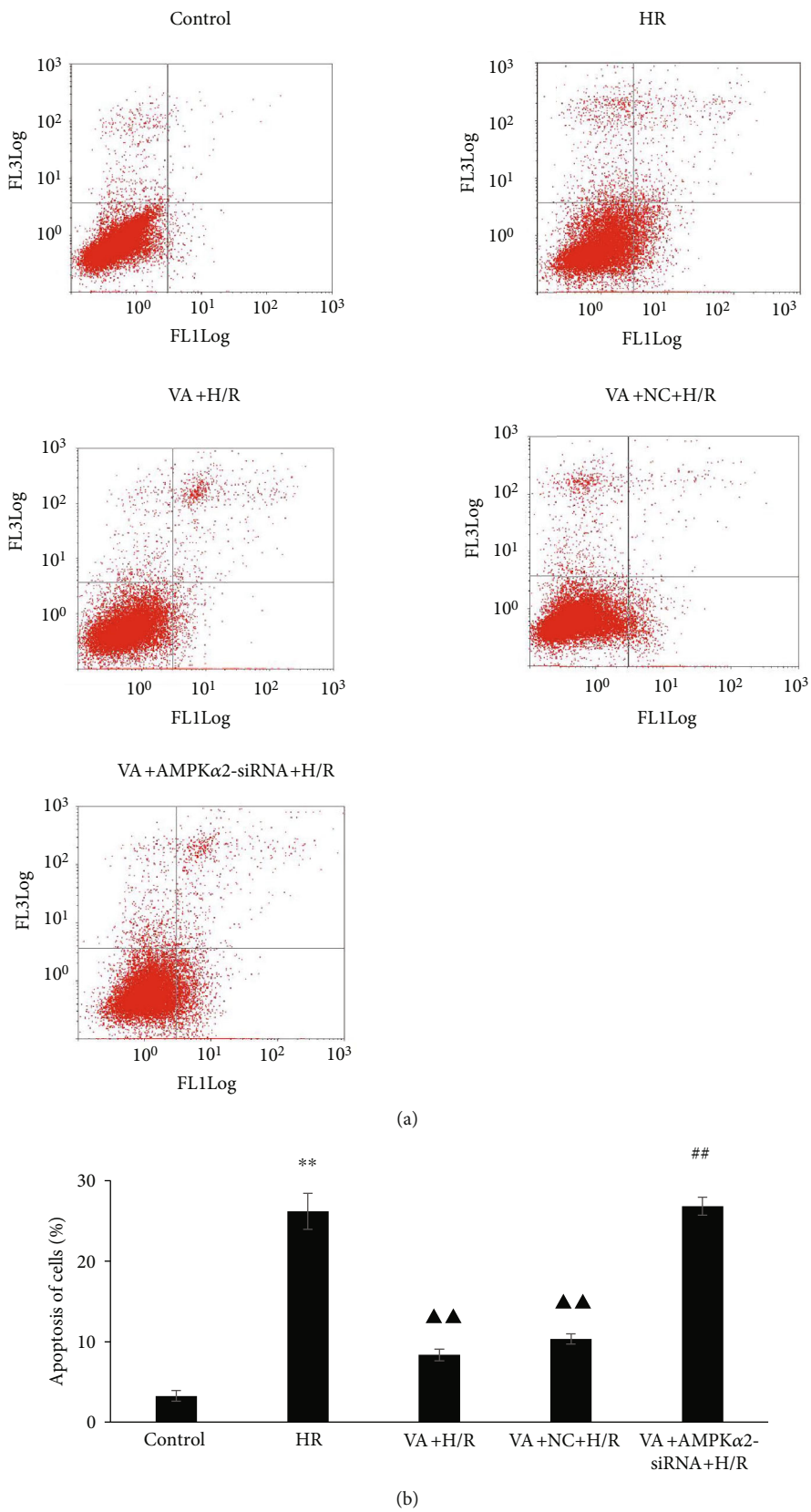


Figure 7: Vanillic acid (VA) pretreatment inhibits apoptosis in H9c2 cells exposed to hypoxia/reoxygenation (H/R), while AMPK$\alpha$2-siRNA abrogates this effect. (a) Representative dot plots of flow cytometry ($x$-axis and $y$-axis represent Annexin V and PI staining, respectively). (b) Evaluation of apoptotic cell populations. Data are expressed as the mean ± SEM, $n = 3$. $^{**}p < 0.01$ vs. control group; $^{\blacktriangle\blacktriangle}p < 0.01$ vs. H/R group; $^{\#\#}p < 0.01$ vs. VA+H/R group.

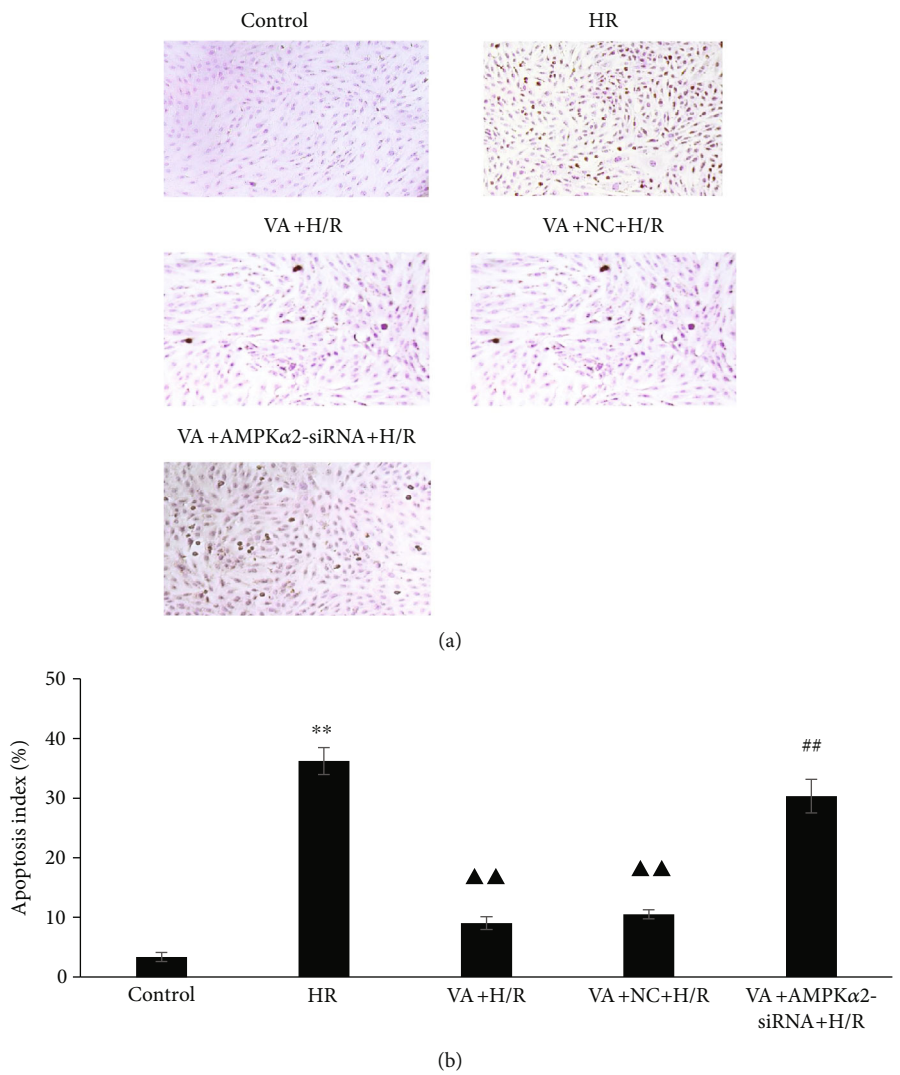


Figure 8: Vanillic acid (VA) pretreatment inhibits apoptosis in H9c2 cells exposed to hypoxia/reoxygenation (H/R), while AMPKα2-siRNA abrogates this effect. (a) H9c2 cells were sectioned and analysed for apoptosis using TUNEL staining. The panels show representative histological images. (b) The number of apoptotic cells evaluated by TUNEL is expressed as a percentage. Data are expressed as the mean ± SEM, $n = 3$. $^{**}p < 0.01$ vs. control group; $^{▲▲}p < 0.01$ vs. H/R group; $^{\#\#}p < 0.01$ vs. VA+H/R group.

H/R injury through antioxidant stress mediated by the AMPK signalling pathway. Therefore, we attempted to detect the expression level of AMPKα2 in the treatment of H9c2 anti-H/R injury with different concentrations of vanillic acid and found that the expression level trend of AMPKα2 was consistent with the concentration trend of vanillic acid against H/R injury, as shown in Figures 1(a) and 2(a). H9c2 cells pretreated with 1.00 mM VA 24 h before H/R exhibited the highest AMPKα2 protein levels. AMPKα2 is known to be sensitive to hypoxia and can be activated by increases in AMP. Once H9c2 cells are subjected to H/R damage, they inevitably increase the expression of the AMPKα2 protein as an emergency response. However, the increase in AMPKα2 protein levels induced by H/R damage is very limited and does not have a protective effect. Our results showed that vanillic acid induces H9c2 cells to produce large quantities of AMPKα2 protein and plays a protective role against H/R injury (Figures 1 and 2). So in the following studies, we focused on whether the protective effect of VA against H/R injury was associated with AMPKα2.

To verify whether the AMPKα2 protein was associated with the cardioprotective activity induced by vanillic acid, we used knockdown of AMPKα2 by its specific siRNA. In the recent years, a number of siRNAs have been successfully used in experimental models [27–29]. We specifically suppressed AMPKα2 expression using RNA interference, which selectively silenced gene expression by delivering double-stranded RNA molecules into cells, and western blot analysis showed that the expression of target protein AMPKα2 could be reduced, as shown in Figure 2(b). Once the expression of AMPKα2 was inhibited, the protective effect of vanillic acid pretreatment against H/R injury in H9c2 cells was eliminated. These findings confirmed that VA-induced cardioprotective effects on H/R are associated with the AMPKα2 signalling pathway.

Electron transport chain injury results in the production of mitochondrial ROS and oxidative stress damage due to

anoxia/reoxygenation [30]. ROS bursts lead to mPTP opening and trigger cellular energetic signals in response to ATP depletion and alterations in ion dynamic balance, ultimately resulting in plasma membrane breach and cell death [31, 32]. It has been demonstrated that mPTP is the central factor in different preconditioning protective mechanisms, and mPTP opening is thought to be important in the interim reperfusion injury [33]. H9c2 cells exposed to H/R injury demonstrated the increased production of ROS, the opening of the mPTP, and the loss of $\Delta\Psi_m$. In contrast, pretreatment with VA attenuated ROS production, the opening of the mPTP, and the loss of $\Delta\Psi_m$.

Oxidative stress damage results in a cellular apoptotic signalling cascade [34]. Caspase-3 is one of the key effectors in this mitochondria-mediated apoptosis pathway. The results showed increased caspase-3 activity in response to H/R injury. In contrast, pretreatment with VA attenuated this effect. Furthermore, pretreatment with VA markedly decreased apoptosis in response to H/R injury in H9c2 cells. To further verify the protective effect of VA against H/R-induced injury, the apoptosis was detected using two methods. The apoptosis results of flow cytometry and TUNEL were consistent, indicating that VA significantly protects H9c2 cells exposed to H/R. It is noteworthy that the protective effect of VA disappeared in response to AMPK$\alpha$2 downregulation.

Our study has proven that VA protects H9c2 cells against H/R-induced injury via reducing the generation of ROS, stabilizing mitochondrial membrane potential, limiting the opening of mPTP, decreasing caspase-3 activity, and ultimately inhibiting cardiomyocyte apoptosis. Furthermore, all protective effects were abrogated by the knockdown of AMPK$\alpha$2-siRNA. Therefore, our findings confirm that VA-induced cardioprotective effects on H/R injury are associated with the AMPK$\alpha$2 protein.

## Data Availability

Interested readers can reproduce our results by using our algorithm.

## Conflicts of Interest

The authors report no conflicts of interests.

## Authors' Contributions

Xiuya Yao and Shoufeng Jiao contributed equally to this work.

## Acknowledgments

This work was supported by the Natural Science Foundation of China (Nos. 81460551, 81760587, 81460371, and 81760731), the Graduate Student Innovation Special Foundation of Nanchang University (No. cx2016299), and the Jiangxi Province Technology Support and Social Development Projects (No. 2010BSA13900).

## References

[1] X. He, S. Li, B. Liu et al., "Major contribution of the 3/6/7 class of TRPC channels to myocardial ischemia/reperfusion and cellular hypoxia/reoxygenation injuries," *Proceedings of the National Academy of Sciences of the United States of America*, vol. 114, no. 23, pp. E4582–E4591, 2017.

[2] W. Zheng and S. Y. Wang, "Antioxidant activity and phenolic compounds in selected herbs," *Journal of Agricultural and Food Chemistry*, vol. 49, no. 11, pp. 5165–5170, 2001.

[3] W. R. Russell, L. Scobbie, A. Labat, and G. G. Duthie, "Selective bio-availability of phenolic acids from Scottish strawberries," *Molecular Nutrition & Food Research*, vol. 53, Suppplement 1, pp. S85–S91, 2009.

[4] M. Gitzinger, C. Kemmer, D. A. Fluri, M. Daoud el-Baba, W. Weber, and M. Fussenegger, "The food additive vanillic acid controls transgene expression in mammalian cells and mice," *Nucleic Acids Research*, vol. 40, no. 5, article e37, 2012.

[5] H. I. Jun, G. S. Song, E. I. Yang, Y. Youn, and Y. S. Kim, "Antioxidant activities and phenolic compounds of pigmented rice bran extracts," *Journal of Food Science*, vol. 77, no. 7, pp. C759–C764, 2012.

[6] H. Palafox-Carlos, E. M. Yahia, and G. A. González-Aguilar, "Identification and quantification of major phenolic compounds from mango (Mangifera indica, cv. Ataulfo) fruit by HPLC–DAD–MS/MS-ESI and their individual contribution to the antioxidant activity during ripening," *Food Chemistry*, vol. 135, no. 1, pp. 105–111, 2012.

[7] V. G. Alves, A. G. Souza, L. U. R. Chiavelli et al., "Phenolic compounds and anticancer activity of commercial sugarcane cultivated in Brazil," *Anais da Academia Brasileira de Ciências*, vol. 88, no. 3, pp. 1201–1209, 2016.

[8] A. Itoh, K. Isoda, M. Kondoh et al., "Hepatoprotective effect of syringic acid and vanillic acid on concanavalin a-induced liver injury," *Biological & Pharmaceutical Bulletin*, vol. 32, no. 7, pp. 1215–1219, 2009.

[9] T. H. Chou, H. Y. Ding, W. J. Hung, and C. H. Liang, "Antioxidative characteristics and inhibition of alpha-melanocyte-stimulating hormone-stimulated melanogenesis of vanillin and vanillic acid from Origanum vulgare," *Experimental Dermatology*, vol. 19, no. 8, pp. 742–750, 2010.

[10] S. Kumar, P. Prahalathan, and B. Raja, "Antihypertensive and antioxidant potential of vanillic acid, a phenolic compound in L-NAME-induced hypertensive rats: a dose-dependence study," *Redox Report*, vol. 16, no. 5, pp. 208–215, 2011.

[11] P. S. Prince, K. Dhanasekar, and S. Rajakumar, "Preventive effects of vanillic acid on lipids, bax, bcl-2 and myocardial infarct size on isoproterenol-induced myocardial infarcted rats: a biochemical and in vitro study," *Cardiovascular Toxicology*, vol. 11, no. 1, pp. 58–66, 2011.

[12] V. G. Zaha, D. Qi, K. N. Su et al., "AMPK is critical for mitochondrial function during reperfusion after myocardial ischemia," *Journal of Molecular and Cellular Cardiology*, vol. 91, pp. 104–113, 2016.

[13] S. B. Wu, Y. T. Wu, T. P. Wu, and Y. H. Wei, "Role of AMPK-mediated adaptive responses in human cells with mitochondrial dysfunction to oxidative stress," *Biochimica et Biophysica Acta (BBA) - General Subjects*, vol. 1840, no. 4, pp. 1331–1344, 2014.

[14] H. Huang, S. Lai, Q. Wan, W. Qi, and J. Liu, "Astragaloside IV protects cardiomyocytes from anoxia/reoxygenation injury by upregulating the expression of Hes1 protein," *Canadian*

*Journal of Physiology and Pharmacology*, vol. 94, no. 5, pp. 542–553, 2016.

[15] T. Koyama, K. Temma, and T. Akera, "Reperfusion-induced contracture develops with a decreasing $[Ca^{2+}]_i$ in single heart cells," *American Journal of Physiology-Heart and Circulatory Physiology*, vol. 261, no. 4, pp. H1115–H1122, 1991.

[16] M. Xu, Y. Wang, K. Hirai, A. Ayub, and M. Ashraf, "Calcium preconditioning inhibits mitochondrial permeability transition and apoptosis," *American Journal of Physiology-Heart and Circulatory Physiology*, vol. 280, no. 2, pp. H899–H908, 2001.

[17] D. Ren, X. Wang, T. Ha et al., "SR-A deficiency reduces myocardial ischemia/reperfusion injury; involvement of increased microRNA-125b expression in macrophages," *Biochimica et Biophysica Acta (BBA) - Molecular Basis of Disease*, vol. 1832, no. 2, pp. 336–346, 2013.

[18] M. Zhu, W. Deng, S. di, M. Qin, D. Liu, and B. Yi, "Gastrodin protects cardiomyocytes from anoxia/reoxygenation injury by 14-3-3$\eta$," *Oxidative Medicine and Cellular Longevity*, vol. 2018, Article ID 3685391, 11 pages, 2018.

[19] Z. Guo, Z. Liao, L. Huang, D. Liu, D. Yin, and M. He, "Kaempferol protects cardiomyocytes against anoxia/reoxygenation injury via mitochondrial pathway mediated by SIRT1," *European Journal of Pharmacology*, vol. 761, pp. 245–253, 2015.

[20] D. Liu, B. Yi, Z. Liao et al., "14-3-3$\gamma$ protein attenuates lipopolysaccharide-induced cardiomyocytes injury through the Bcl-2 family/mitochondria pathway," *International Immunopharmacology*, vol. 21, no. 2, pp. 509–515, 2015.

[21] Z. Liao, H. He, G. Zeng et al., "Delayed protection of Ferulic acid in isolated hearts and cardiomyocytes: upregulation of heat-shock protein 70 via NO-ERK1/2 pathway," *Journal of Functional Foods*, vol. 34, pp. 18–27, 2017.

[22] G. R. Steinberg and B. E. Kemp, "AMPK in health and disease," *Physiological Reviews*, vol. 89, no. 3, pp. 1025–1078, 2009.

[23] S. M. Jeon, "Regulation and function of AMPK in physiology and diseases," *Experimental & Molecular Medicine*, vol. 48, no. 7, article e245, 2016.

[24] S. Wang, P. Song, and M. H. Zou, "AMP-activated protein kinase, stress responses and cardiovascular diseases," *Clinical Science*, vol. 122, no. 12, pp. 555–573, 2012.

[25] W. Sun, C. Yan, B. Frost et al., "Pomegranate extract decreases oxidative stress and alleviates mitochondrial impairment by activating AMPK-Nrf2 in hypothalamic paraventricular nucleus of spontaneously hypertensive rats," *Scientific Reports*, vol. 6, no. 1, article 34246, 2016.

[26] X. Han, H. Tai, X. Wang et al., "AMPK activation protects cells from oxidative stress-induced senescence via autophagic flux restoration and intracellular $NAD^+$ elevation," *Aging Cell*, vol. 15, no. 3, pp. 416–427, 2016.

[27] H. Dana, G. M. Chalbatani, H. Mahmoodzadeh et al., "Molecular mechanisms and biological functions of siRNA," *International Journal of Biomedical Science*, vol. 13, no. 2, pp. 48–57, 2017.

[28] Y. Ishibashi and Y. Hirabayashi, "AMP-activated protein kinase suppresses biosynthesis of glucosylceramide by reducing intracellular sugar nucleotides," *Journal of Biological Chemistry*, vol. 290, no. 29, pp. 18245–18260, 2015.

[29] X. Chen, X. Li, W. Zhang et al., "Activation of AMPK inhibits inflammatory response during hypoxia and reoxygenation through modulating JNK-mediated NF-$\kappa$B pathway," *Metabolism*, vol. 83, pp. 256–270, 2018.

[30] W. J. Li, S. P. Nie, Y. Chen et al., "Ganoderma atrum polysaccharide protects cardiomyocytes against anoxia/reoxygenation-induced oxidative stress by mitochondrial pathway," *Journal of Cellular Biochemistry*, vol. 110, no. 1, pp. 191–200, 2010.

[31] E. J. Griffiths, "Mitochondria and heart disease," *Advances in Experimental Medicine and Biology*, vol. 942, pp. 249–267, 2012.

[32] D. B. Zorov, M. Juhaszova, and S. J. Sollott, "Mitochondrial reactive oxygen species (ROS) and ROS-induced ROS release," *Physiological Reviews*, vol. 94, no. 3, pp. 909–950, 2014.

[33] D. Morin, R. Assaly, S. Paradis, and A. Berdeaux, "Inhibition of mitochondrial membrane permeability as a putative pharmacological target for cardioprotection," *Current Medicinal Chemistry*, vol. 16, no. 33, pp. 4382–4398, 2009.

[34] N. Moorjani, S. Westaby, J. Narula et al., "Effects of left ventricular volume overload on mitochondrial and death-receptor-mediated apoptotic pathways in the transition to heart failure," *The American Journal of Cardiology*, vol. 103, no. 9, pp. 1261–1268, 2009.

Hindawi
Oxidative Medicine and Cellular Longevity
Volume 2020, Article ID 1645249, 19 pages
https://doi.org/10.1155/2020/1645249

*Research Article*

# The Long Noncoding RNA Hotair Regulates Oxidative Stress and Cardiac Myocyte Apoptosis during Ischemia-Reperfusion Injury

**Kai Meng, Jiao Jiao, Rui-Rui Zhu, Bo-Yuan Wang, Xiao-Bo Mao, Yu-Cheng Zhong, Zheng-Feng Zhu, Kun-Wu Yu, Yan Ding, Wen-Bin Xu, Jian Yu, Qiu-Tang Zeng, and Yu-Dong Peng**

*Department of Cardiology, Union Hospital, Tongji Medical College, Huazhong University of Science and Technology, Wuhan 430022, China*

Correspondence should be addressed to Yu-Dong Peng; am-penicillin@163.com

Received 16 December 2019; Revised 3 February 2020; Accepted 17 February 2020; Published 12 March 2020

Guest Editor: Tatjana Bačun



Oxidative stress and subsequent cardiac myocyte apoptosis play central roles in the initiation and progression of myocardial ischemia-reperfusion (I/R) injury. Homeobox transcript antisense intergenic RNA (*Hotair*) was previously implicated in various heart diseases, yet its role in myocardial I/R injury has not been clearly demonstrated. Mice with cardiac-restricted knockdown or overexpression of *Hotair* were exposed to I/R surgery. H9c2 cells were cultured and subjected to hypoxia/reoxygenation (H/R) stimulation to further verify the role and underlying mechanisms of *Hotair* in vitro. Histological examination, molecular detection, and functional parameters were determined in vivo and in vitro. In response to I/R or H/R treatment, *Hotair* expression was increased in a bromodomain-containing protein 4-dependent manner. Cardiac-restricted knockdown of *Hotair* exacerbated, whereas *Hotair* overexpression prevented I/R-induced oxidative stress, cardiac myocyte apoptosis, and cardiac dysfunction. Mechanistically, we observed that *Hotair* exerted its beneficial effects via activating AMP-activated protein kinase alpha (AMPK$\alpha$). Further detection revealed that *Hotair* activated AMPK$\alpha$ through regulating the enhancer of zeste homolog 2/microRNA-451/calcium-binding protein 39 (EZH2/*miR-451*/Cab39) axis. We provide the evidence that endogenous lncRNA *Hotair* is an essential negative regulator for oxidative stress and cardiac myocyte apoptosis in myocardial I/R injury, which is dependent on AMPK$\alpha$ activation via the EZH2/*miR-451*/Cab39 axis.

## 1. Introduction

Acute myocardial infarction (AMI) is the leading cause of death worldwide due to the induction of congestive heart failure and life-threatening arrhythmias [1]. The survival and long-term prognosis in patients after AMI largely depend on the extent of cardiac myocyte death in ischemic myocardium. Percutaneous coronary intervention (PCI) is an effective therapeutic intervention to restore coronary blood flow and preserve the viable cardiac myocytes [2]. However, revascularization by PCI can cause additional ischemia-reperfusion (I/R) damage, which hampers myocardial salvage and diminishes the maximum potential benefit of this intervention [3]. Therefore, an extensive dissection about the molecular basis for myocardial I/R injury and the identification of novel therapeutic targets are scientifically and clinically important.

Despite multiple events, including inflammation, endoplasmic reticulum stress, autophagy, and intracellular $Ca^{2+}$ overload, have been reported to be involved in the pathogenesis of I/R injury, emerging evidences suggest that oxidative stress and subsequent cardiac myocyte apoptosis play central roles in the initiation and progression of myocardial I/R injury [4, 5]. Mitochondria are the major source of reactive species oxygen (ROS) within the myocardium [6]. However, their normal structure and physiologic function are markedly compromised during cardiac ischemia, which then drive excessive ROS generation and elicit oxidative damage after the rapid restoration of coronary perfusion [7]. In addition, the expression of antioxidant enzymes in murine hearts is

notably downregulated by I/R injury, which further aggravates I/R-triggered oxidative damage to the heart. Unstrained ROS accumulation induces oxidative damage to biological macromolecules, including DNA, lipids, and proteins, eventually resulting in cell apoptosis. Conversely, suppression of ROS overproduction significantly prevents I/R-induced cardiac myocyte apoptosis and cardiac dysfunction [8, 9]. AMP-activated protein kinase alpha (AMPK$\alpha$), a highly conserved eukaryotic serine/threonine protein kinase, is proved to have beneficial effects in multiple cardiac pathophysiological conditions, including endoplasmic reticulum stress, energetic homeostasis, cellular calcium handling, cardiac hypertrophy, and fibrogenesis [10–13]. Russell et al. previously verified that AMPK$\alpha$ was responsible for the activation of glucose uptake and glycolysis during I/R-injured hearts, and prevented I/R-induced cardiac myocyte damage [14]. Besides, AMPK$\alpha$ was also implicated in regulating oxidative stress and cell survival in cardiac diseases [8, 15]. Wang et al. recently found that AMPK$\alpha$ overexpression could provoke efficient mitophagy to eliminate damaged mitochondria, thereby preventing ROS overproduction and cardiac myocyte apoptosis in the development of heart failure [16]. Moreover, numerous studies determined that AMPK$\alpha$ activation could attenuate myocardial I/R injury via blocking oxidative damage and cell apoptosis, whereas AMPK$\alpha$-deficient mice exhibited increased ROS generation and cell apoptosis in response to myocardial I/R injury [15, 17, 18]. Therefore, targeting AMPK$\alpha$ may be of great therapeutic interest for treating I/R-induced injury.

Long noncoding RNAs (lncRNAs) are identified as kinds of non-protein-coding RNAs with the length longer than 200 nucleotides. Despite initially considered as the nonfunctional byproducts of RNA polymerase II transcripts, lncRNAs are now verified to participate in regulating numerous pathophysiological processes, ranging from cell proliferation, differentiation, senescence, to cell death [19, 20]. Recently, lncRNAs have attacked increasing attentions for their critical roles in the progression of cardiovascular diseases, especially myocardial I/R injury [21]. Homeobox transcript antisense intergenic RNA (*Hotair*) is a 2148 nucleotide lncRNA located in the HOXC cluster on chromosome 12 in humans [22, 23]. Previous studies showed that *Hotair* was implicated in the pathogenesis of various heart diseases, such as cardiac hypertrophy, myocardial infarction, diabetic cardiomyopathy, and sepsis-related cardiac injury [24–27]. Data from Lai et al. indicated that *Hotair* overexpression reduced cell surface area and the expression of hypertrophic markers via sponging microRNA-19 (*miR-19*) [25]. In a septic mouse model, Wu et al. found that *Hotair* was significantly upregulated in cardiomyocytes from septic mice, and *Hotair* silence reduced inflammatory response and improved sepsis-related cardiac dysfunction [26]. Consistently, *Hotair* expression was found to be increased in heart tissues subjected to AMI surgery, which then promoted myocardial inflammation and malfunction after AMI [27]. In contrast, results from Zhang lab verified *Hotair* overexpression alleviated AMI or hypoxia-induced inflammation and cardiac myocyte apoptosis [28]. And a recent study by Gao et al. further confirmed that *Hotair* knockdown increased, whereas cardiomyocyte-specific *Hotair* overexpression decreased inflammation, oxidative stress, and cardiac myocyte death in diabetic mice [24]. However, the role and potential molecular basis of *Hotair* in myocardial I/R injury have not been clearly clarified. The complex function of *Hotair* in cardiac diseases prompted us to investigate its credible role in myocardial I/R injury.

## 2. Materials and Methods

*2.1. Animals and Treatments.* Male C57BL/6 mice (6-10 weeks; 22-27 g) were obtained from HFK Bioscience Co., Ltd. (Beijing, China) and were bred in a specific pathogen-free laboratory environment at the Animal Center of Tongji Medical College of Huazhong University of Science and Technology. All animal experiments were consistent with the principles of the Care and Use of Laboratory Animals (NIH publication no. 85–23, revised 1996), which were also approved by the Animal Care and Use Committee of the Union Hospital of Huazhong University of Science and Technology. Cardiac-restricted knockdown or overexpression of *Hotair* was achieved by the adeno-associated virus 9 (AAV9) system as previously described [29, 30]. Briefly, mice were injected with AAV9 carrying *Hotair* (AAV9-*Hotair*, *Hotair*) or short hairpin RNA against *Hotair* (AAV9-sh*Hotair*, sh*Hotair*) under the cTnT promoter via the tail vein at a dose of $1 \times 10^{11}$ viral genome particles per mice 4 weeks before I/R surgery to overexpress or knock down *Hotair* in the myocardium, respectively, whereas the mice assigned to the control group were injected with AAV9-*Ctrl* (*Ctrl*) or AAV9-sh*Ctrl* (sh*Ctrl*). The *Hotair* full genome (NR_003716.3) was cloned into pAAV-cTNT-MCS-ZsGreen carrier and amplified with the Stbl3 Escherichia coli to generate AAV9-*Hotair* virus. The AAV9-sh*Hotair* was cloned from the interfering sequence of *Hotair* (#n397142, Thermo Fisher Scientific).

Myocardial I/R injury mouse model was generated as previously described [4, 9]. Briefly, mice were injected with pentobarbital sodium (50 mg/kg, i.p.) and ventilated via intubation for anesthetization. Murine hearts were exposed by a left thoracotomy incision and then a slipknot was made around the left anterior descending coronary artery (LAD) against a PE10 tubing by an 8-0 Prolene suture. Animals assigned to sham-operated groups received the same procedure, except the snare was left untied. After 30 minute ligation, the occlusion was released to allow reperfusion for additional 24 hours except for specific annotations in Figure 1. During the surgical processes, the mice were kept warm on the heating pad. To verify the role of AMPK$\alpha$, the mice were pretreated with compound C (CpC, 20 mg/kg, every other day) for 2 weeks before I/R surgery [11]. In addition, the mice were pretreated with JQ1 intraperitoneally at the indicated dosage 24 hours prior to I/R surgery to clarify the role of bromodomain-containing protein 4 (BRD4) in vivo.

*2.2. Echocardiography Measurements.* Transthoracic echocardiography was performed to measure left ventricle ejection fraction (LVEF) and left ventricle end-systolic

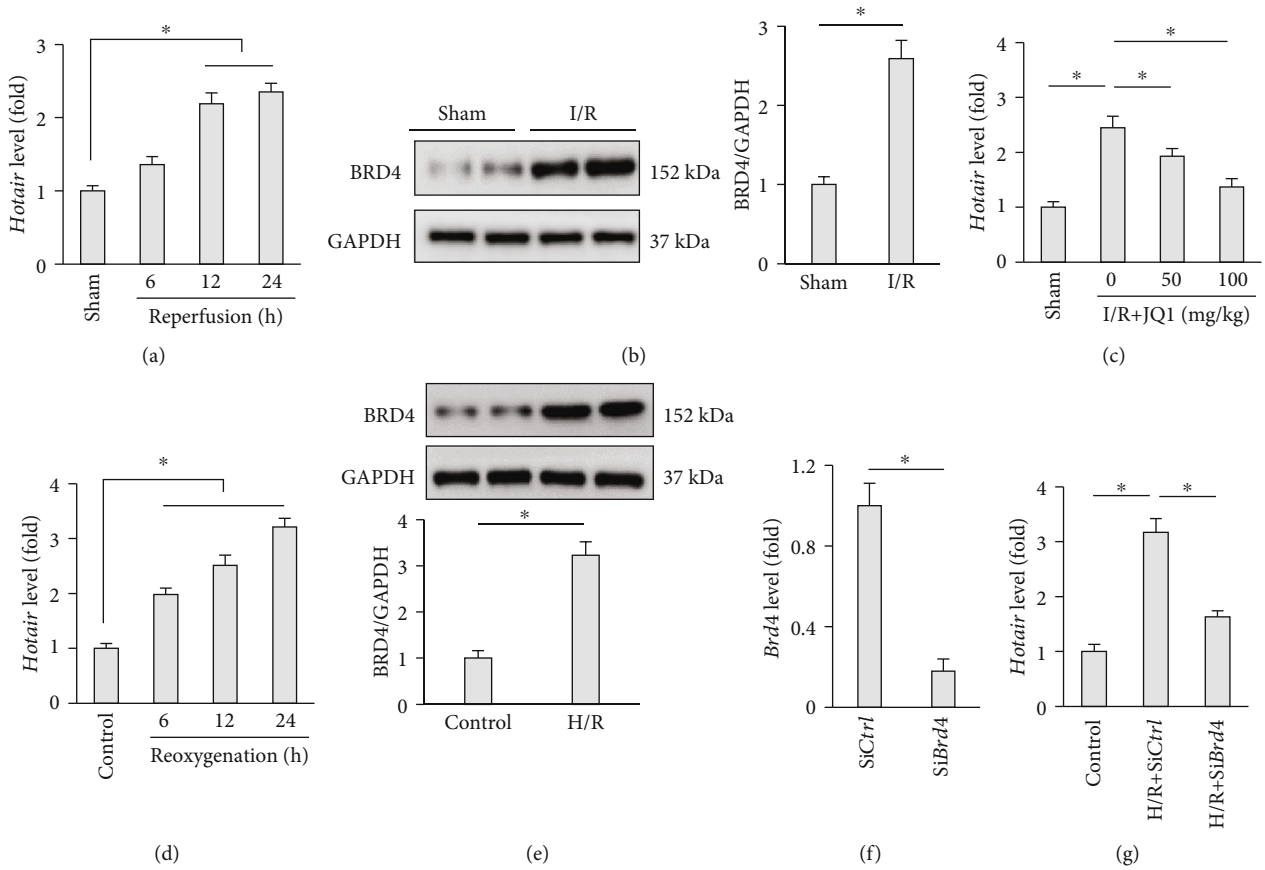


Figure 1: *Hotair* expression is increased by BRD4 in response to I/R stimulation. (a) *Hotair* expression within the reperfused myocardium in the indicated time points ($n = 8$). (b) Western blot images and the quantitative data of BRD4 in hearts subjected to ischemia for 30 minutes and reperfusion for additional 24 hours (I/R) ($n = 6$). (c) *Hotair* expression in murine hearts after I/R injury with or without JQ1 treatment ($n = 8$). (d) *Hotair* expression in H9c2 cells subjected to hypoxia for 2 hours and reoxygenation for the indicated time points ($n = 8$). (e) Western blot images and the quantitative data of BRD4 in H9c2 cells subjected to hypoxia for 2 hours and reoxygenation for additional 24 hours (H/R) ($n = 6$). (f) The efficiency of small interfering RNA against BRD4 (si*Brd4*) detected by PCR data ($n = 8$). (g) *Hotair* expression in H9c2 cells after H/R stimulation with or without si*Brd4* ($n = 8$). Data are presented as mean ± standard deviation (SD). $^*P < 0.05$ versus the matched group.

dimension (LVESD) using the Vevo 1100 ultrasound system (Visual Sonics, Toronto, Canada) equipped with 30 MHz linear transducer according to our previous study [31]. Briefly, the mice were anesthetized by 2% isoflurane and then were exposed to the two-dimensional (2D) imaging echocardiography at the parasternal short axis to observe papillary muscles and septal wall. After that, M-mode imaging was recorded to measure the cardiac morphology and contractility. Echocardiography images were analyzed using the echo work station, and the functional parameters were calculated and averaged from six continuous cardiac cycles. All data acquisition and subsequent analysis were performed in a blinded manner.

*2.3. Determination on the Size of Area at Risk (AAR) and Infarction Area (IA).* After reperfusion for 24 hours, the left coronary artery was reoccluded at the same position, and then 1% Evans blue was injected into the left ventricular chamber to calculate the AAR. Next, murine hearts were quickly excised, frozen at -20°C for 30 minutes, and subsequently cut into 5 short-axis slices, which were incubated in 1% 2,3,5-triphenyltetrazolium chloride (TTC, Sigma) at 37°C for 15 minutes to delineate the infarcted myocardium. All slices were photographed by a digital camera (Nikon Corp., Tokyo, Japan), and AAR (nonblue, including viable myocardium and infarcted area) together with IA (pale) was quantified by computerized planimetry using ImageJ software (NIH, Bethesda, MD, USA) [4, 9]. The AAR was expressed as percent of the total left ventricular area, whereas IA was expressed as percent of the AAR.

*2.4. Western Blot Analysis.* Total proteins were isolated from cultured cells or freshly removed left ventricles as previously described [32]. Briefly, the myocardial homogenates or cell lysates were prepared in a RIPA lysis buffer with protease inhibitor cocktail (Roche), which were then subjected to scraping, sonication, and centrifugation. After that, the protein concentration was determined by bicinchoninic acid (BCA) reagents (Pierce biotechnology, Rockford, IL), and equal amounts of protein samples were separated by sodium dodecyl sulfate polyacrylamide gel electrophoresis (SDS-PAGE). Next, the proteins were transferred to polyvinylidene

fluoride (PVDF; EMD Millipore, USA) membranes, followed by the incubation with 5% skim milk at room temperature for 0.5 hour and the indicated antibodies at 4°C overnight. Next day, the membranes were incubated with the secondary antibodies at room temperature for 1.5 hours and then were scanned by the ChemiDoc™ XRS+ System (Bio-Rad Laboratories, Inc.). The primary antibodies for western blot analysis were provided as follows: BRD4 (Abcam; #ab128874, 1 : 1000 dilution), glyceraldehyde-3-phosphate dehydrogenase (GAPDH; Cell Signaling Technology; #2118, 1 : 3000 dilution), Mn-superoxide dismutase (MnSOD; Abcam; #ab13533, 1 : 1000 dilution), catalase (CAT; Abcam; #ab52477, 1 : 1000 dilution), B cell lymphoma-2 (BCL-2; Abcam; #ab59348, 1 : 1000 dilution), BCL-2 associated X (BAX; Cell Signaling Technology; #2772, 1 : 1000 dilution), NADPH oxidase 2 (NOX2; Abcam; #ab129068, 1 : 1000 dilution) phosphorylated protein kinase B (p-AKT; Cell Signaling Technology; #4060, 1 : 1000 dilution), total-AKT (t-AKT; Cell Signaling Technology; #2920, 1 : 1000 dilution), sirtuin1 (SIRT1; Abcam; #ab110304; 1 : 1000 dilution), p-AMPK$\alpha$ (Cell Signaling Technology; #2535, 1 : 1000 dilution), t-AMPK$\alpha$ (Cell Signaling Technology; #5831, 1 : 1000 dilution), p-acetyl coenzyme A carboxylase (p-ACC; Cell Signaling Technology; #3661, 1 : 1000 dilution), t-ACC (Cell Signaling Technology; #3676, 1 : 1000 dilution), calcium-binding protein 39 (Cab39; Abcam; #ab51132, 1 : 1000 dilution), and zeste homolog 2 (EZH2; Cell Signaling Technology; #5246; 1 : 1000 dilution).

*2.5. RNA Extraction and Transcript Analysis.* Total RNA was extracted from heart tissue or cultured cells by TRIZOL reagent (Takara Biotechnology, Dalian, China) and converted to cDNA using the PrimeScript RT reagent kit (Takara Biotechnology, Dalian, China). Quantitative real-time PCR was performed using the ABI PRISM 7900 Sequence Detector system (Applied Biosystems, Foster City, CA). Gene expressions were calculated using the $\Delta\Delta$Ct methods. The relative mRNA levels were normalized to GAPDH, whereas relative lncRNA or miRNA levels were normalized to the U6 expression according to previous studies [31, 32].

*2.6. Measurement of Cardiac Troponin I (cTnI), N-Terminal B-Type Natriuretic Peptide (NT-proBNP), and Creatine Kinase (CK) in Serum.* Serum levels of cTnI, NT-proBNP, and CK were measured by an automatic biochemical analyzer (Cobas 8000, Roche) as previously described [33].

*2.7. Cell Culture and Treatments.* H9c2 cells were purchased from ATCC (Manassas, VA, USA) and cultured in Dulbecco's modified Eagle's medium (DMEM) containing 10% fetal bovine serum (FBS). To imitate the I/R injury in vitro, H9c2 cells were preincubated in Krebs buffer with pyruvate (5 $\mu$M) and sodium sulfite (50 $\mu$M) in the humidified incubator (5% $CO_2$/95% $N_2$, 37°C) for 2 hours, which were then replaced with fresh DMEM containing 10% FBS under normoxic conditions (5% $CO_2$/95% air, 37°C) for additional 24 hours to generate hypoxia/reoxygenation (H/R) cell model according to previous studies with a little modifications [34, 35]. To notify the role of BRD4 in vitro, H9c2 cells were incubated with small interfering RNA against BRD4 (si*Brd4*, 50 nM; #RSS338226, Thermo Fisher Scientific) using Lipofectamine RNAiMAX (Invitrogen) for 24 hours before H/R stimulation [32]. To knock down the expression of *Hotair* in vitro, H9c2 cells were infected with adenovirus carrying sh*Hotair* (Adsh*Hotair*) at the multiplicity of infection (MOI) of 150 in serum-free DMEM medium for 4 hours or Adsh*Ctrl* as the control. Cells were preinfected with adenovirus carrying *Hotair* (Ad*Hotair*, MOI = 60) for 4 hours to overexpress *Hotair* in H9c2 cells or Ad*Ctrl* as the negative control. After adenoviral delivery experiments, the cells were cultured in normal medium for additional 48 hours before the H/R stimulation. To inhibit AMPK$\alpha$ in vitro, cells were preincubated with CpC (10 $\mu$M) for 30 minutes before the adenoviral infection [34]. To verify the involvement of *miR-451* and EZH2, cells were pretreated with *miR-451* inhibitor (50 nM; #AM17000, Thermo Fisher Scientific) or si*Ezh2* (50 nM; #RSS319678, Thermo Fisher Scientific) using Lipofectamine RNAiMAX (Invitrogen) for 24 hours.

*2.8. Biochemical Analysis.* The levels of malondialdehyde (MDA), 4-hydroxynonenal (4-HNE) and 3-nitrotyrosine (3-NT) in freshly removed left ventricles and cultured cells were detected by the commercial kits (Abcam, UK) according to the instructions [33]. Protein carbonylations (PCs) were measured spectrophotometrically at 360 nm as previously described [36]. Enzymatic activities of superoxide dismutase (SOD) and catalase (CAT) were detected using the commercial kits (Nanjing Jiancheng Bioengineering Institute, China) by a microplate reader (Synergy HT, BioTek, USA) according to the manufacturer's instructions.

*2.9. Assessment of Cardiac Myocyte Apoptosis.* Terminal deoxynucleotidyl transferase-mediated dUTP nick end-labeling (TUNEL) staining was performed to detect cell apoptosis in vivo and in vitro using a commercial kit (Millipore, USA) as previously described [37]. To quantify the apoptotic cells in the myocardium, more than 15 high power fields (×400 magnification) per heart were included in a blinded manner. Apoptotic index was calculated as the ration between TUNEL-positive cardiac myocyte nuclei and the total number of nuclei. Cell counting kit-8 (CCK-8) was used to further determine cell viability in vitro [32]. Moreover, supernatants derived from the cell lysates of murine hearts or cultured cells were collected for the assessment of caspase3 activity by using peptide-based DEVD-pNA as substrate [38].

*2.10. 2′,7′-Dichlorodihydrofluorescein Diacetate (DCFH-DA) Staining.* DCFH-DA staining was performed to evaluate ROS generation in H9c2 cells via referring to previous studies [39]. In brief, cells were incubated with DMEM medium containing 10 $\mu$mol/L DCFH-DA (Beyotime Biotechnology, China) for half an hour at 37°C, and then the images were captured by an Olympus IX53 fluorescence microscope in a blinded manner.

*2.11. Statistical Analysis.* Results were shown as mean ± standard deviation (SD). Comparisons between two groups were performed using two-tailed Student's *t*-test, whereas multigroup comparisons were performed by one-way

ANOVA analysis (SPSS 22.0). A $P$ value less than 0.05 was considered statistically significant.

## 3. Results

*3.1. Hotair Expression Is Increased by BRD4 in Response to I/R Stimulation.* To explore the possible role of *Hotair* in myocardial I/R injury, we first detected the expression of *Hotair* in response to I/R injury in murine hearts. As shown in Figure 1(a), myocardial *Hotair* expression was significantly upregulated during heart reperfusion. Then, we investigated the underlying mechanism for the alteration of *Hotair* expression during I/R injury. Proteins of BRD family are epigenetic modulators that have been identified to play critical roles in regulating cardiovascular diseases and oxidative stress [40, 41]. Previous studies verified that BRD4 was abundantly expressed within the myocardium and it could directly bind to the *Hotair* promoter, thereby promoting *Hotair* expression in glioblastoma cells [42]. Intriguingly, we found that BRD4 protein level was also increased by myocardial I/R injury, and the inhibition of BRD4 by JQ1 notably abolished I/R-induced upregulation of *Hotair* in murine hearts (Figures 1(b) and 1(c)). To further confirm the observation, we established H/R models in H9c2 cells, and the data proved that *Hotair* expression together with BRD4 protein level were both increased by H/R stimulation (Figures 1(d) and 1(e)). BRD4 knockdown markedly decreased *Hotair* expression in H9c2 cells after H/R stimulation (Figures 1(f) and 1(g)). Collectively, these data demonstrated that *Hotair* expression was increased by BRD4 in response to I/R stimulation, suggesting that *Hotair* might be implicated in the pathogenesis of myocardial I/R injury.

*3.2. Hotair Prevents Myocardial Injury Caused by I/R.* To examine the role of endogenous *Hotair* in I/R-mediated myocardial injury and dysfunction, we knocked down *Hotair* expression in murine hearts via the AAV9 system. As shown in Figure 2(a), *Hotair* expression within the I/R-injured myocardium was attenuated by sh*Hotair* injection. In response to myocardial I/R injury, *Hotair*-insufficient mice exhibited markedly decreased LVEF and elevated LVESD compared with that in control groups (Figure 2(b)). Furthermore, *Hotair* knockdown significantly increased the ischemia area (IA) without affecting the size of area at risk (AAR) after I/R, as evidenced by the AAR/LV and IA/AAR (Figure 2(c)). In addition, serum levels of biomarkers related to myocardial injury, including cTnI, NT-proBNP, and CK, were further elevated in mice after *Hotair* knockdown (Figure 2(d)). Collectively, these data indicated that *Hotair* knockdown exacerbated I/R-induced myocardial injury and the resultant heart dysfunction.

To further clarify the role of *Hotair*, mice were injected with AAV9-*Hotair* to overexpress *Hotair* in murine hearts or AAV9-*Ctrl* as the negative control 4 weeks prior to I/R surgery, and *Hotair* overexpression within the I/R-injured myocardium was validated in Figure 2(e). As shown in Figures 2(f) and 2(g), mice with *Hotair* overexpression exhibited a notable alleviation of cardiac dysfunction and the size of ischemia area was also reduced. Consistently, serum levels of myocardial injury biomarkers were also drastically suppressed in *Hotair*-overexpressed mice (Figure 2(h)). Interestingly, neither *Hotair* overexpression nor knockdown markedly affected the cardiac function under basal conditions compared with their matched controls. Taken together, these gain- and loss-of-function studies verified that *Hotair* was essential for the pathogenesis of I/R-induced myocardial injury.

*3.3. Hotair Protects against I/R-Induced Oxidative Stress and Cardiac Myocyte Apoptosis.* Previous studies confirmed that oxidative stress and subsequent cardiac myocyte apoptosis play central roles in the initiation and progression of myocardial I/R injury [9, 35]. We then assessed the role of *Hotair* in I/R-induced oxidative stress and cardiac myocyte apoptosis. As shown in Figure 3(a), lipid peroxidation was enhanced in mice subjected to I/R injury, which was further aggravated by *Hotair* knockdown, as confirmed by the increased levels of MDA and 4-HNE. Protein oxidative damage is another key event for oxidative stress that contributes to I/R-induced myocardial injury. Correspondingly, we found that myocardial 3-NT and PCs were upregulated in mice assigned to I/R injury, which were notably augmented in *Hotair*-insufficient mice (Figures 3(b) and 3(c)). Superoxide-$H_2O_2$ have been identified as the key component of ROS and contributed to the development of I/R-induced cardiac dysfunction [43, 44]. MnSOD is the key enzyme to catalyze the conversion of superoxide anion to $H_2O_2$, which were then scavenged by the CAT. We thus detected MnSOD and CAT expressions and activities in I/R-injured murine hearts. In line with previous studies, the activities of SOD and CAT in murine hearts were notably suppressed by I/R surgery, and *Hotair* knockdown further decreased the capacity of endogenous cellular antioxidant defenses (Figure 3(d)). Further detection about the expressions of MnSOD and CAT verified that *Hotair* knockdown promoted oxidative stress induced by I/R operation (Figures 3(e) and 3(f)). ROS is primarily generated by NOX, among which NOX2 is the key isoform with the myocardium. We therefore examined NOX2 expression and observed that *Hotair* knockdown made no alteration on NOX2 expression in response to myocardial I/R injury (Figure S1A). Unstrained oxidative stress directly induces oxidative damage to biological macromolecules and causes cell apoptosis. Accordingly, I/R surgery caused increased cell apoptosis in the myocardium, which was further enhanced in *Hotair*-insufficient mice (Figure 3(g)). Besides, western blot analysis revealed that mice with *Hotair* knockdown exhibited markedly elevated BAX/BCL-2 in comparison with the control mice (Figure 3(h)). Consistent with the above data, we found that caspase3 activity was markedly increased in murine hearts after *Hotair* knockdown in response to I/R insult (Figure 3(i)).

In line with the functional phenotype in *Hotair*-overexpressed mice, oxidative stress was drastically alleviated by *Hotair* overexpression in response to I/R operation, as indicated by the decreased myocardial MDA, 4-HNE, 3-NT, and PCs (Figure S1B-D). On the other hand, I/R-triggered inhibition on endogenous antioxidants was also derepressed in *Hotair*-overexpressed murine hearts, as revealed by

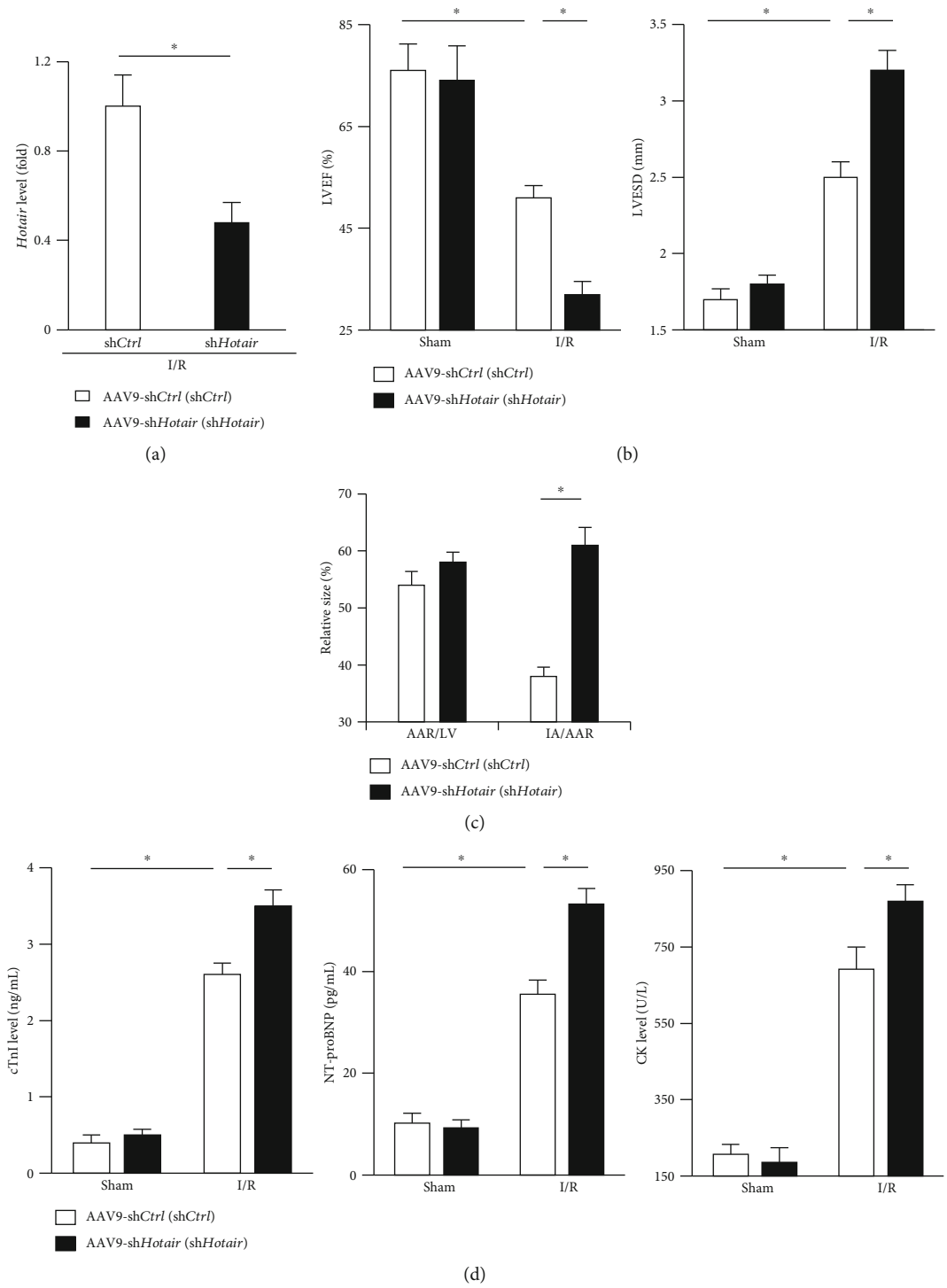


Figure 2: Continued.

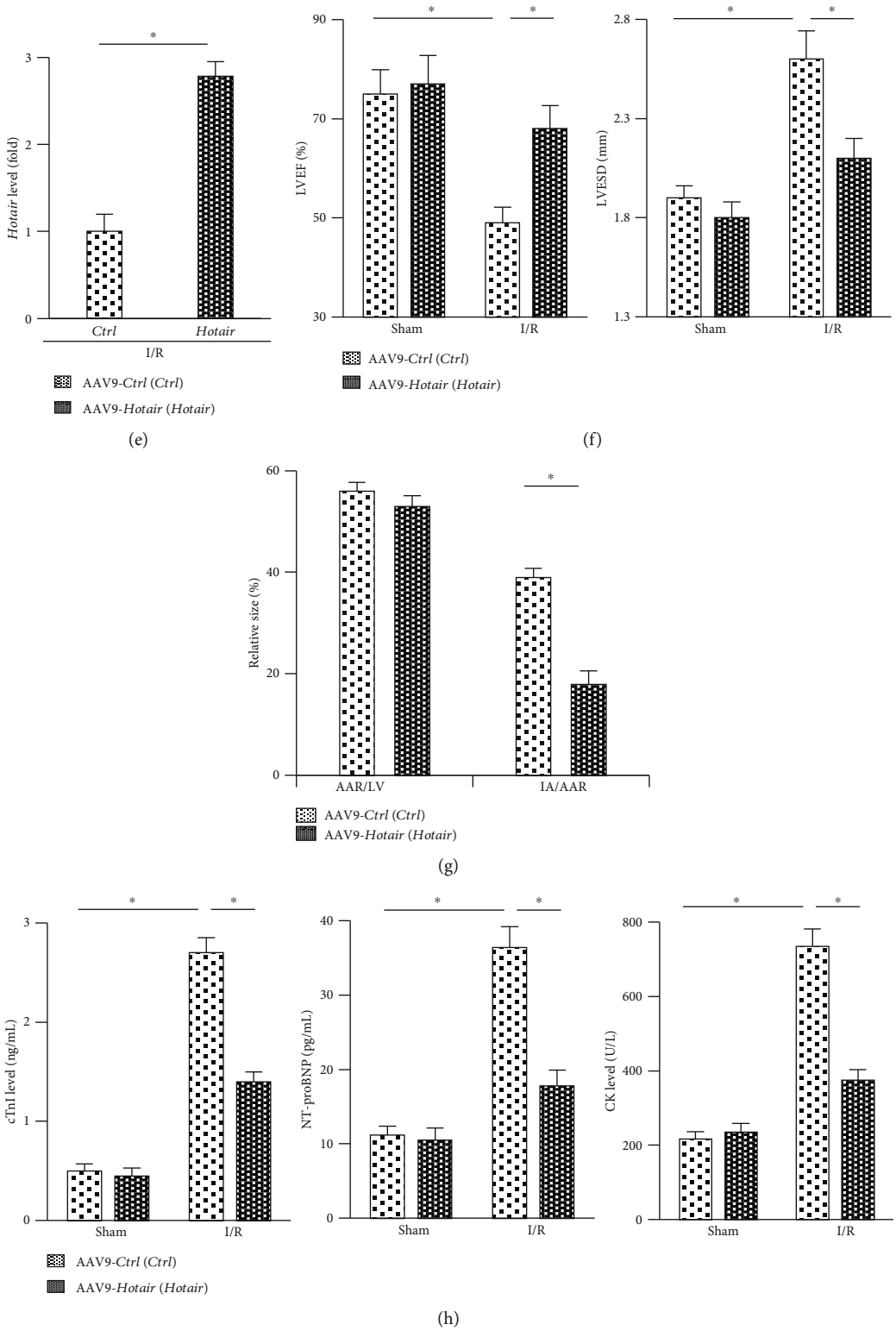


Figure 2: *Hotair* prevents myocardial injury caused by I/R. (a) *Hotair* expression in murine hearts in the indicated groups ($n = 8$). (b) Left ventricular ejection fraction (LVEF) and end-systolic diameter (LVESD) in mice subjected to I/R injury with or without *Hotair* knockdown ($n = 10$). (c) Morphometric analysis of the size of the area at risk (AAR) and infarction area (IA) in I/R-treated mice injected with AAV9-sh*Ctrl* or AAV9-sh*Hotair* ($n = 8$). (d) Serum biomarkers related to cardiac injury in mice subjected to I/R injury with or without *Hotair* knockdown ($n = 8$). (e) The efficiency of *Hotair* overexpression in I/R-injured murine hearts by AAV9-*Hotair* ($n = 8$). (f) Functional parameters in mice subjected to I/R injury with or without *Hotair* overexpression ($n = 10$). (g) Morphometric analysis of AAR and IA in I/R-treated murine hearts with or without AAV9-*Hotair* treatment ($n = 8$). (h) Serum biomarkers related to cardiac injury in mice subjected to I/R injury with or without *Hotair* overexpression ($n = 8$). Data are presented as mean ± SD. $^*P < 0.05$ versus the matched group.

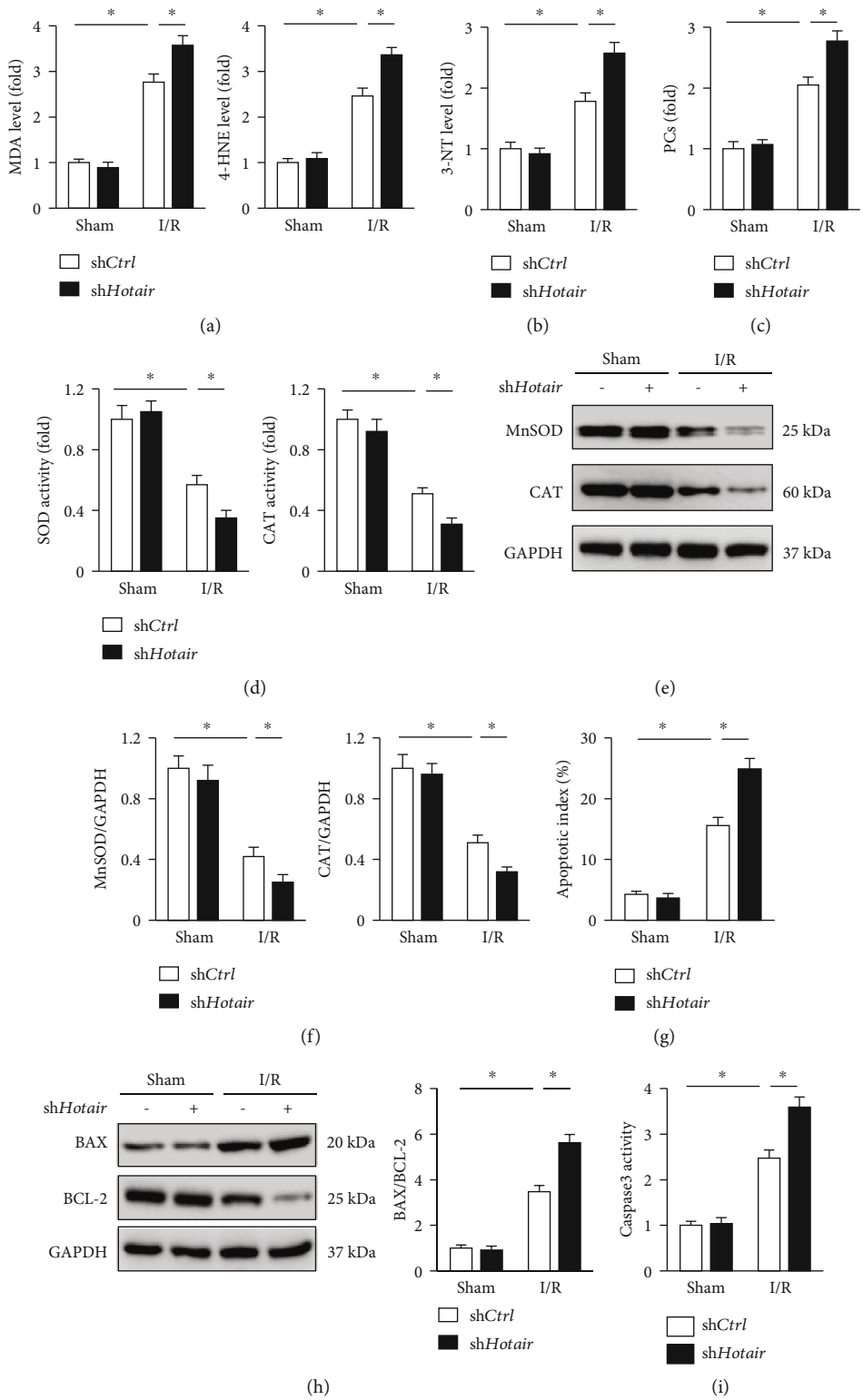


Figure 3: *Hotair* knockdown aggravates I/R-induced oxidative stress and cardiac myocyte apoptosis. (a–c) Myocardial malondialdehyde (MDA), 4-hydroxynonenal (4-HNE), 3-nitrotyrosine (3-NT), and protein carbonylation (PC) levels in mice with or without *Hotair* knockdown after I/R injury ($n = 6$). (d) Enzymatic activities of superoxide dismutase (SOD) and catalase (CAT) in murine hearts ($n = 6$). (e, f) MnSOD and CAT expression changes were evaluated by western blot in *Hotair*-inhibited murine hearts or their negative controls subjected to I/R ($n = 6$). (g) Cardiac myocyte apoptosis index detected by TUNEL staining ($n = 8$). (h) BAX and BCL-2 protein levels in murine hearts from the indicated groups ($n = 6$). (i) Myocardial caspase3 activity in *Hotair*-insufficient mice or their negative controls subjected to I/R surgery ($n = 8$). Data are presented as mean ± SD. $^*P < 0.05$ versus the matched group.

the increased activities and expressions of MnSOD and CAT (Figure S1E-G). Western blot analysis also demonstrated that *Hotair* overexpression attenuated I/R-induced upregulation of BAX and downregulation of BCL-2, and decreased BAX/BCL-2 (Figure S1H). In addition, we confirmed that the increased caspase3 activity and the induction of cell apoptosis were both improved in *Hotair*-overexpressed hearts (Figure S1I-J). Therefore, we concluded that *Hotair* knockdown exacerbated, whereas *Hotair* overexpression ameliorated I/R-induced oxidative stress and cardiac myocyte apoptosis in murine hearts.

*3.4. Hotair Prevents Oxidative Stress and Cardiac Myocyte Apoptosis in Response to H/R In Vitro.* To further verify the role of *Hotair* in vitro, we knocked down the endogenous *Hotair* expression in H9c2 cells and then the cells were subjected to H/R stimulation. The efficiency was clarified by the PCR data (Figure 4(a)). DCFH-DA staining suggested that *Hotair* knockdown significantly increased ROS generation after H/R (Figure 4(b)). Correspondingly, H9c2 cells infected with Adsh*Hotair* exhibited enhanced MDA and 3-NT production (Figure 4(c)). The antioxidant enzymes, SOD, and CAT activities together with protein levels were further decreased in *Hotair*-insufficient cells (Figures 4(d) and 4(e)). Conversely, BAX/BCL-2 and caspase3 activity were notably increased in H9c2 cells after *Hotair* knockdown in the presence of H/R stimulation (Figures 4(f)–4(h)). Consistent with the molecular alteration, we observed that *Hotair* silence notably decreased cell viability and augmented H/R-induced cardiac myocyte apoptosis (Figures 4(i) and 4(j)).

H9c2 cells were also infected with Ad*Hotair* to overexpress *Hotair* before H/R stimulation, which caused ~6.9 fold increase of *Hotair* expression (Figure S2A). As shown in Figure S2B-C, H/R stimulation led to increased ROS generation and caused oxidative stress in Ad*Ctrl*-infected cells, which were markedly attenuated in cells with *Hotair* overexpression, as shown by the DCFH-DA staining and decreased MDA, 3-NT levels. The decreased activities and protein levels of SOD and CAT were both preserved in Ad*Hotair*-treated H9c2 cells compared with that infected with Ad*Ctrl* (Figure S2D-F). Protein analysis also revealed that the upregulation of BAX/BCL-2 was notably attenuated in cells with *Hotair* overexpression (Figure S2G). Further detection confirmed that *Hotair* overexpression improved H/R-induced cardiac myocyte apoptosis, as evidenced by the decreased caspase3 activity and increased cell viability (Figure S2H-I). The in vitro experiments clearly validated a beneficial role of *Hotair* in the pathogenesis of H/R-induced oxidative stress and cardiac myocyte apoptosis.

*3.5. Hotair Alleviates H/R-Induced Oxidative Stress and Cardiac Myocyte Apoptosis via Activating AMPKα.* Next, we investigated the molecular mechanisms underlying the protective effects of *Hotair* in vitro. Given the capacity of *Hotair* to regulate AKT and the involvement of AKT pathway in I/R-induced myocardial injury, we first detected the level of AKT phosphorylation in cultured H9c2 cells. However, despite the markedly inhibition on AKT activation induced by H/R stimulation, we observed no significant alterations in AKT phosphorylated levels by *Hotair* overexpression (Figures 5(a) and 5(b)). We then investigated the potential role of SIRT1, which was well identified as the downstream target of *Hotair* in heart. Western blot result showed that Ad*Hotair* did not affect SIRT1 expression in response to H/R stimulation in vitro (Figures 5(a) and 5(b)). Inspiringly, we observed that H/R-triggered inhibition of AMPKα pathway was prevented in Ad*Hotair*-infected H9c2 cells, as verified by the increased phosphorylation of AMPKα and ACC (Figures 5(c) and 5(d)). To address whether AMPKα activation was essential for Ad*Hotair*-mediated beneficial effects in vitro, we co-treated H9c2 cells with CpC to inhibit AMPKα. The data showed that Ad*Hotair*-mediated inhibition on MDA and 3-NT production was blunted in cells with AMPKα suppression (Figure 5(e)). Consistently, *Hotair* overexpression significantly increased the activities of SOD and CAT in H9c2 cells, but not in that pretreated with CpC (Figure 5(f)). Notably, CpC incubation also largely blunted the protective effect of Ad*Hotair* on cardiac myocyte apoptosis, which was confirmed by the increased caspase3 activity and decreased cell viability (Figures 5(g) and 5(h)). Taken together, these data suggested that AMPKα activation appeared to be essential for *Hotair* overexpression-mediated protective effects in vitro.

*3.6. Hotair Overexpression Loses Its Beneficial Effects in AMPKα-Inhibited Mice.* Consistent with the in vitro data, we found that *Hotair* overexpression significantly preserved AMPKα activation in murine hearts after I/R injury, and conversely, AMPKα and ACC phosphorylation were further decreased in *Hotair*-inhibited murine hearts (Figures 6(a)–6(d)). As shown in Figure 6(e), *Hotair* overexpression markedly decreased MDA and 3-NT production in murine hearts after I/R surgery but had no protective effects in that treated with CpC. In addition, *Hotair* overexpression-mediated inhibitory effect on caspase3 activity was also abrogated by AMPKα inhibition (Figure 6(f)). Accordingly, we observed that the improvement on ischemia area and myocardial injury provided by *Hotair* overexpression was retarded with AMPKα suppression (Figures 6(g) and 6(h)). Echocardiographic measurements showed that *Hotair* overexpression caused a significant alleviation on cardiac contractile dysfunction, reflected by the increased LVEF, yet this was lost in mice with AMPKα suppression (Figure 6(i)). Therefore, it could be reasonably deduced that AMPKα activation was responsible for *Hotair* overexpression-mediated beneficial effects on myocardial I/R injury.

*3.7. EZH2/miR-451/Cab39 Axis Is Involved in AMPKα Activation Caused by Hotair.* We then sought to determine the possible way through which *Hotair* activated AMPKα. Previous studies determined that lncRNAs can act on miRNA to regulate protein-coding gene expression, and *Hotair* was involved in various pathophysiological processes via negatively regulating miRNAs [45]. We then detected the level of *miR-19*, *miR-125*, and *miR-34a* in H9c2 cells, which have been verified to mediate the regulatory effects of *Hotair* on cardiac function [24, 25, 46]. As shown in Figure 7(a), we found that *Hotair* overexpression did not

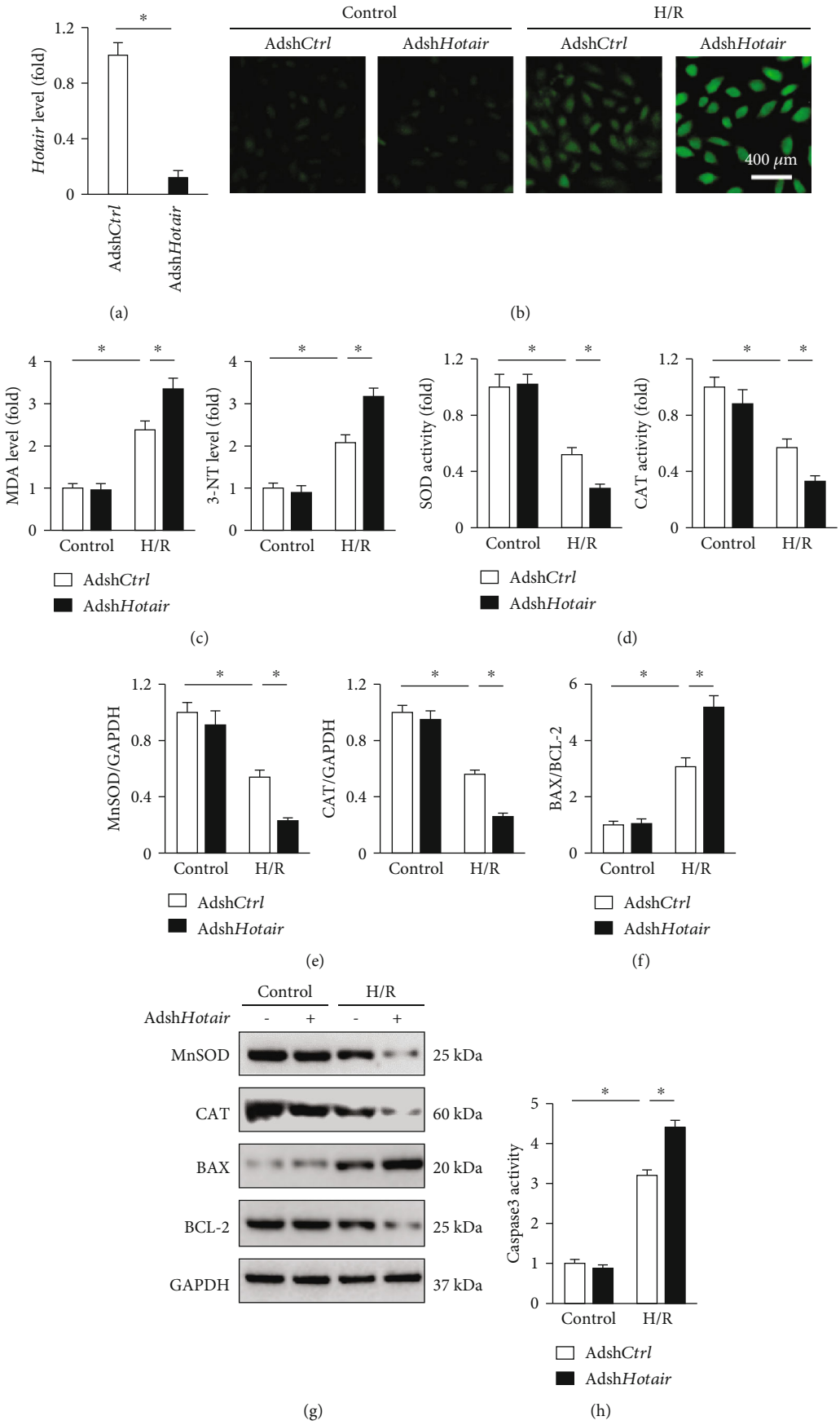


Figure 4: Continued.

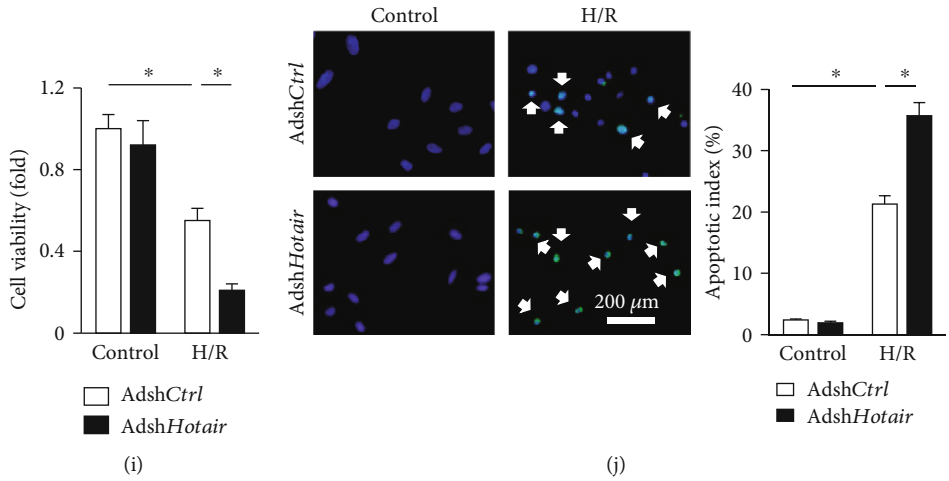


Figure 4: *Hotair* knockdown exacerbates oxidative stress and cardiac myocyte apoptosis in response to H/R in vitro. (a) *Hotair* expression in H9c2 cells infected with Adsh*Ctrl* or Adsh*Hotair* ($n = 6$). (b) Representative images of DCFH-DA in H9c2 cells with or without *Hotair* knockdown after H/R stimulation ($n = 8$). (c) MDA and 3-NT levels in H9c2 cells ($n = 6$). (d) Enzymatic activities of SOD and CAT in H9c2 cells ($n = 6$). (e–g) MnSOD, CAT, BAX, and BCL-2 expression changes in H/R-stimulated H9c2 cells with or without Adsh*Hotair* treatment ($n = 6$). (h) Caspase3 activity in H9c2 cells ($n = 6$). (i) Cell viability assessed by the CCK-8 assay ($n = 6$). (j) TUNEL staining and the statistical result in H9c2 cells; white arrows indicate TUNEL-positive nuclei ($n = 8$). Data are presented as mean ± SD. $^*P < 0.05$ versus the matched group.

affect the level of *miR-19*, *miR-125*, and *miR-34a* in H/R-stimulated H9c2 cells yet markedly decreased *miR-451* expression in H9c2 cells after H/R stimulation. And *Hotair* silence notably increased *miR-451* expression in H/R-stimulated H9c2 cells (Figure 7(b)). Cab39 was shown to form a heterotrimeric complex with ste20-related adaptor (STRAD) and served as a scaffold protein for liver kinase B1 (LKB1), an upstream kinase of AMPK$\alpha$, to stabilize its activity [47]. It is well-accepted that *miR-451* plays an essential role in modulating AMPK$\alpha$ pathway via directly targeting Cab39; we thus detected Cab39 protein expression in sh*Hotair*-treated murine hearts [48]. As shown in Figure S3A, we found that Cab39 was downregulated in *Hotair*-deficient murine hearts after I/R surgery. To notify the involvement of *miR-451* in *Hotair*-mediated regulation on Cab39/AMPK$\alpha$, we treated H9c2 cells with *miR-451* inhibitor. As expected, we found that Adsh*Hotair*-mediated inhibition on Cab39 mRNA and protein was markedly reversed by the *miR-451* inhibitor (Figures 7(c) and 7(d), Figure S3B). Correspondingly, AMPK$\alpha$ dephosphorylation and the augmented oxidative stress as well as cardiac myocyte apoptosis induced by *Hotair* knockdown were all abolished in the presence of a *miR-451* inhibitor, as confirmed by the decreased MDA, 3-NT level, caspase3 activity, and increased cell viability (Figures 7(e)–7(i)).

We finally aimed to elucidate the regulatory mechanism between *Hotair* and *miR-451* in the context of I/R injury. Previous data showed that *Hotair* functioned as a molecular sponge on *miR-19*, *miR-125*, and *miR-34a* to regulate cardiac pathophysiology; however, we observed no alteration of these miRNAs in the present study, which implied the existence of a distinct modulation. Emerging evidences suggested that *Hotair* could recruit polycomb repressive complex 2 (PRC2) and lead to epigenetic silence of target genes. Furthermore, Cheng et al. recently clarified that *Hotair* suppressed *miR-122* expression in hepatocellular carcinoma by an epigenetic mechanism [49]. EZH2, an important component of PRC2, was reported to be responsible for the downregulation of many miRNAs. We therefore tried to ascertain whether EZH2 contributed to *Hotair*-mediated *miR-451* inhibition after H/R stimulation. As shown in Figures 7(j) and 7(k), Ad*Hotair*-stimulated downregulation on *miR-451* was abolished by EZH2 silence. Subsequently, Cab39/AMPK$\alpha$ activation in Ad*Hotair*-infected cells was suppressed after EZH2 knockdown (Figures 7(l)–7(n)). In line with the molecular alteration, we found that *Hotair* overexpression-elicited beneficial effect on H/R-induced oxidative damage and cardiac myocyte apoptosis was completely retarded in si*Ezh2*-infected cells (Figures 7(o)–7(q)). Thus, we concluded that EZH2/*miR-451*/Cab39 axis was involved in AMPK$\alpha$ activation caused by *Hotair*.

## 4. Discussion

In the present study, we found that *Hotair* was upregulated in response to I/R injury via a BRD4-dependent manner. Cardiac-restricted knockdown of *Hotair* exacerbated, whereas *Hotair* overexpression prevented I/R-induced oxidative stress, cardiac myocyte apoptosis, and cardiac dysfunction. Further detection showed that *Hotair* exerted the protective effects via regulating EZH2/*miR-451*/Cab39/AMPK$\alpha$ axis. Taken together, our preclinical studies identified *Hotair* as a potential therapeutic target for treating myocardial I/R injury.

Ischemic heart disease causes great morbidity and mortality worldwide that results in tremendous burden to individuals, families, and the whole society. Early restoration of the blood supply based either on pharmacological thrombolysis or on PCI is identified as the cornerstone in coronary heart disease therapy. However, reperfusion itself could cause a second wave of insult to the ischemic myocardium, which

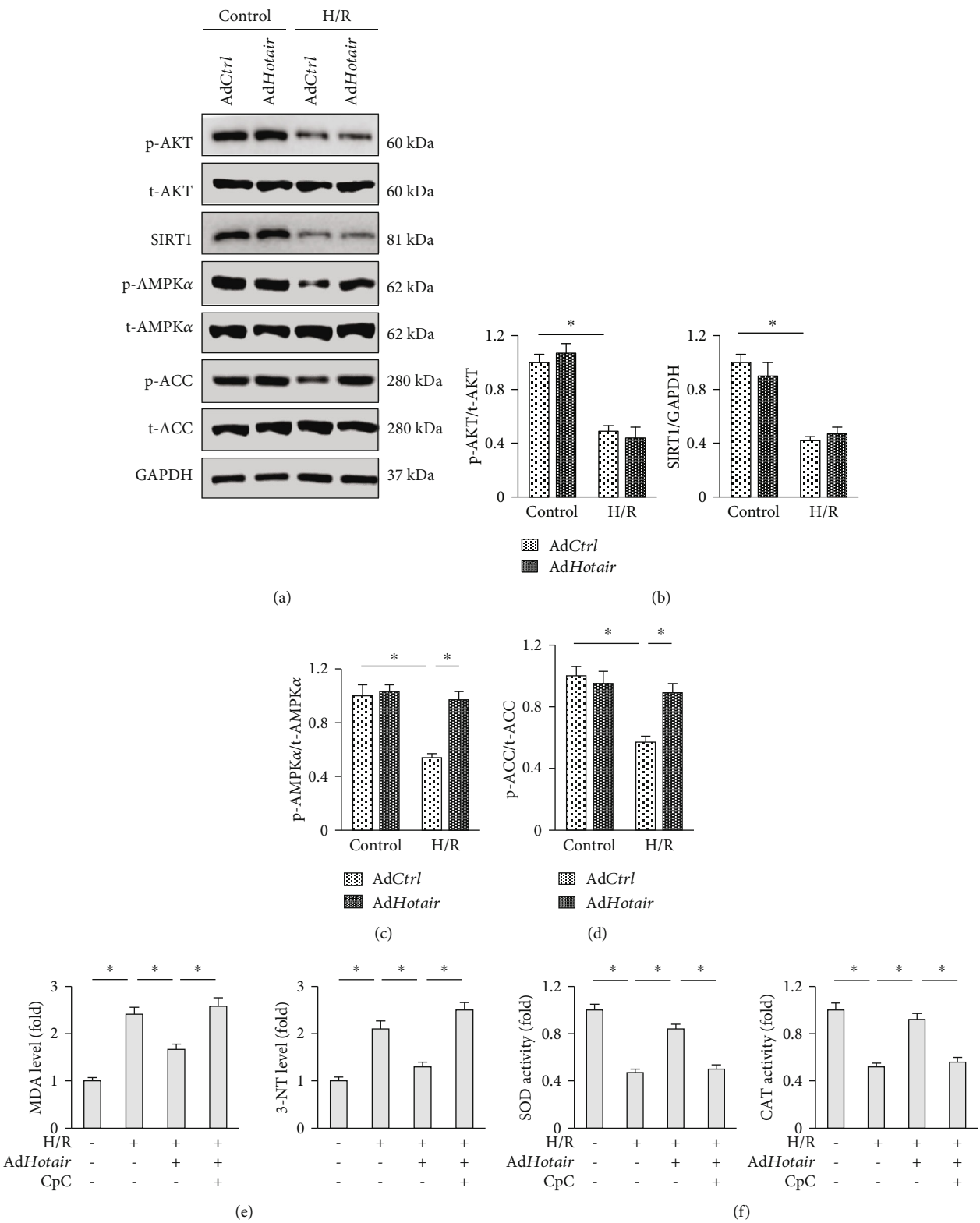


Figure 5: Continued.

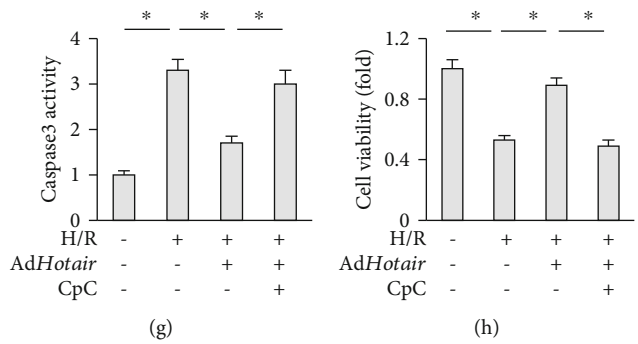


Figure 5: *Hotair* alleviates H/R-induced oxidative stress and cardiac myocyte apoptosis via activating AMPK$\alpha$. (a–d) Representative western blot images and the quantitative data ($n = 6$). (e) MDA and 3-NT levels in H9c2 cells ($n = 6$). (f) Enzymatic activities of SOD and CAT in H9c2 cells ($n = 6$). (g) Caspase3 activity in H9c2 cells ($n = 6$). (h) Cell viability assessed by the CCK-8 assay ($n = 6$). Data are presented as mean ± SD. $^*P < 0.05$ versus the matched group.

has been estimated to contribute to about half of the overall functional loss of the infarcted heart [1–3]. So far, there is no effective therapeutic regimen against myocardial I/R injury. Intriguingly, our data suggested that lncRNA *Hotair* in cardiac myocytes was instrumental for the heart to counteract I/R-induced injury and dysfunction. Numerous studies have been performed to explore the role of *Hotair* in cardiovascular diseases, including the ischemic damage, yet the exact role of *Hotair* in oxidative stress and cardiac myocyte apoptosis during I/R injury remains delusive. Lu et al. previously observed that *Hotair* overexpression promoted the synthesis and release of inflammatory cytokines from hypoxia-induced H9c2 cells, which is in line with a previous study found that high *Hotair* level promoted the onset of cerebral infarct and dysfunction [27, 50]. In contrast, data from other studies indicated that *Hotair* overexpression suppressed hypoxia- or oxidative stress-induced cardiac myocyte injury [46, 51]. Even so, the role of *Hotair* in ischemic hearts cannot be transposed to the myocardial I/R injury condition. Besides, several studies identified *Hotair* expression was decreased in myocytes exposed to hypoxia/oxidative damage and in the serum from AMI patients [46, 51]. Yet, we herein found that *Hotair* was upregulated in murine hearts subjected to I/R surgery and H9c2 cells exposed to H/R stimulation. The different expression pattern during myocardial ischemia and I/R implied a distinct role for *Hotair* in the progression of myocardial I/R injury. In the present study, gain- and loss-of-function studies clearly corroborated *Hotair* overexpression has a beneficial effect on I/R-triggered oxidative stress, apoptosis, and cardiac dysfunction in vivo and in vitro. Previous studies implied that the same intervention might cause diametrically opposite outcome in different disease models, and more importantly, a study from Zhai et al. defined differential roles of GSK3$\beta$ in myocardial ischemia and I/R injury [52–54]. Matsui et al. further proved that the pathophysiologic mechanism might be distinctly different during myocardial ischemia and I/R [55]. Collectively, our data elucidated the distinctly beneficial role of *Hotair* in myocardial I/R injury.

Accumulation of ROS within the myocardium has been verified as the central mechanism of myocardial I/R injury [9]. Nutrient deficit and oxygen deprivation due to coronary artery occlusion elicit distinct alterations in intracellular signaling axis and metabolic status. As a consequence, free fatty acid oxidation is inhibited and glycolysis becomes the predominant means of energy production. However, the sudden influx of nutrients together with the restoration of oxygen supply reconstructs the oxidative phosphorylation in cardiac myocytes for more efficient ATP generation, which meanwhile leads to ROS overproduction via the disrupted electron transport chain [56]. Fulminant oxygen free radicals directly modify proteins via posttranslational methods, including nitration and carbonylation, which subsequently destroy protein functions and cause cell apoptosis [9]. The abnormal expression of lncRNAs has been identified to be involved in oxidative stress and cell apoptosis and was responsible for the occurrence of myocardial I/R injury. Li et al. recently found that lncRNA H19 functioned as a competing endogenous RNA of *miR-877-3p* and alleviated cardiac myocyte apoptosis and myocardial I/R damage [57]. Su and colleagues proved that lncRNA TUG1 inhibition upregulated *miR-142-3p* and ameliorated myocardial injury in I/R-stimulated hearts [21]. Results from Wang et al. also revealed that lncRNA NRF directly repressed *miR-873* expression and regulated cardiac myocyte necrosis and myocardial I/R injury in mice [58]. In the current study, we clarified that lncRNA *Hotair* overexpression prevented oxidative stress, cardiac myocyte apoptosis, and cardiac malfunction after I/R surgery via activating AMPK$\alpha$. AMPK$\alpha$ is commonly regarded as the endogenous energy sensor and maintains energy homoeostasis via regulating cellular ATP levels [10]. In addition to sensing energy deficit, AMPK$\alpha$ also plays essential roles in the pathogenesis of heart diseases. Zhang et al. found that activation of AMPK$\alpha$ prevented cardiac fibrosis following long-term pressure overload [12]. Besides, a recent study also confirmed that AMPK$\alpha$ activation notably alleviated oxidative stress and cardiac myocyte apoptosis in doxorubicin-treated murine hearts, thereby preventing doxorubicin-induced cardiac impairment [8]. Moreover, Wang et al. observed that mice with cardiac-specific inhibition of AMPK$\alpha$ exhibited increased oxidative stress and cardiac myocyte apoptosis in response to myocardial I/R injury, indicating AMPK$\alpha$ as a cardioprotective factor against I/R-induced cardiac injury and malfunction [15]. Our current

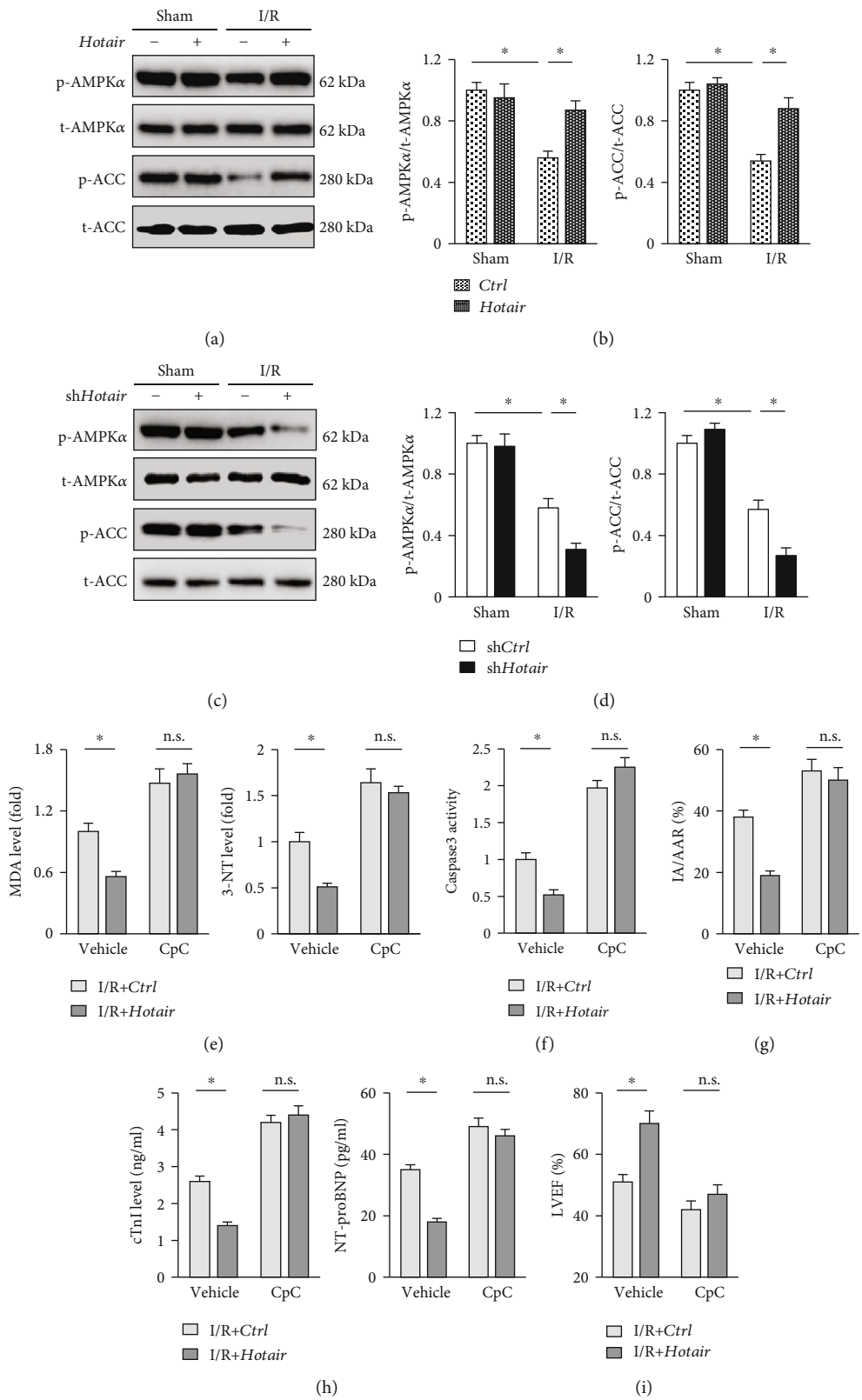


Figure 6: *Hotair* overexpression loses its beneficial effects in AMPKα-inhibited mice. (a, b) Representative western blot images and the quantitative data in I/R-treated murine hearts with or without *Hotair* overexpression ($n = 6$). (c, d) Representative western blot images and the quantitative data in murine hearts subjected to I/R surgery ($n = 6$). (e) MDA and 3-NT levels in murine hearts ($n = 6$). (f) Caspase3 activity in murine hearts ($n = 6$). (g) Morphometric analysis of IA in I/R-treated murine hearts ($n = 8$). (h) Serum biomarkers related to cardiac injury in mice ($n = 8$). (i) Echocardiographic parameters of murine hearts ($n = 8$). Data are presented as mean ± SD. $^*P < 0.05$ versus the matched group.

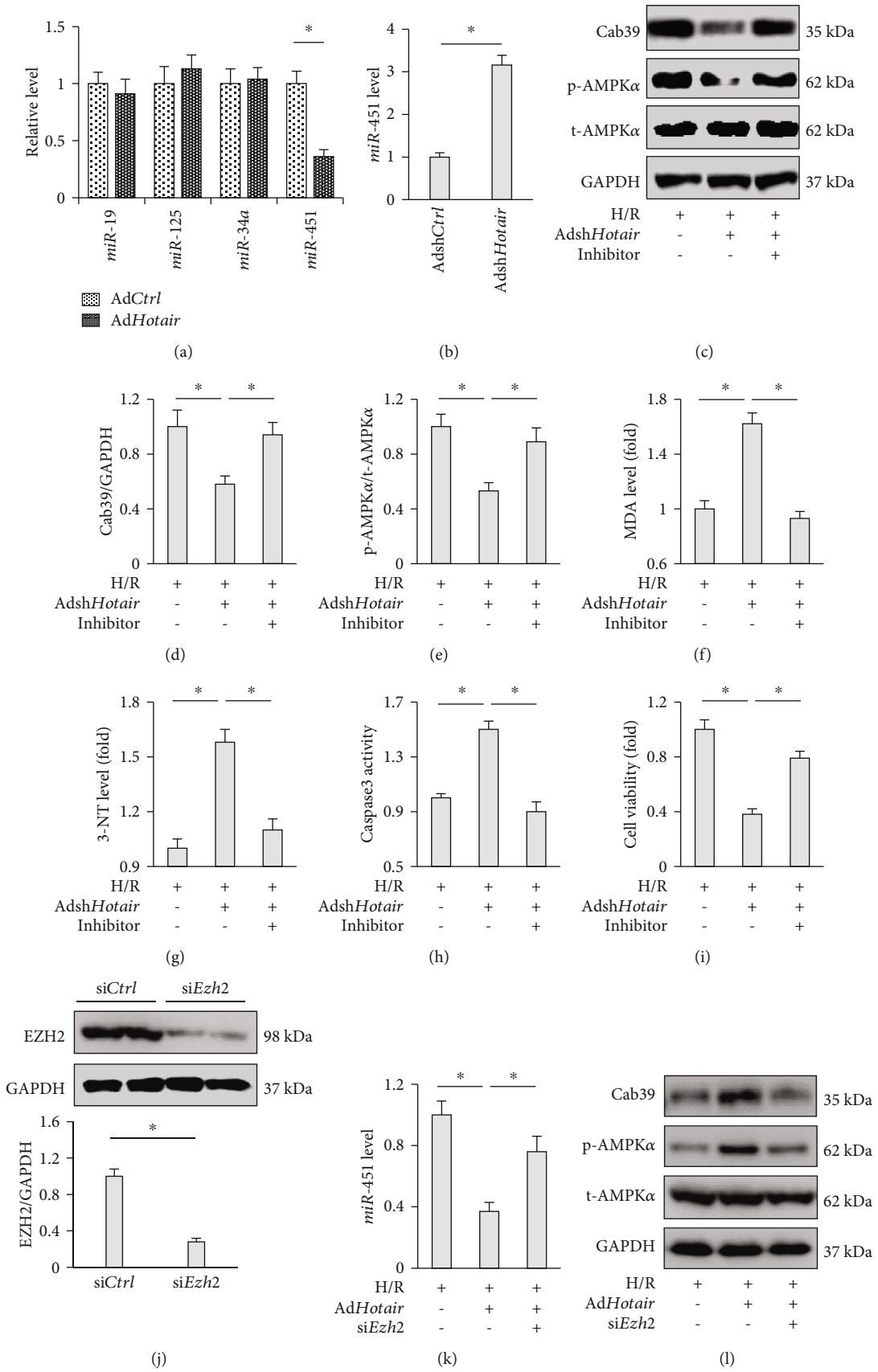


Figure 7: Continued.

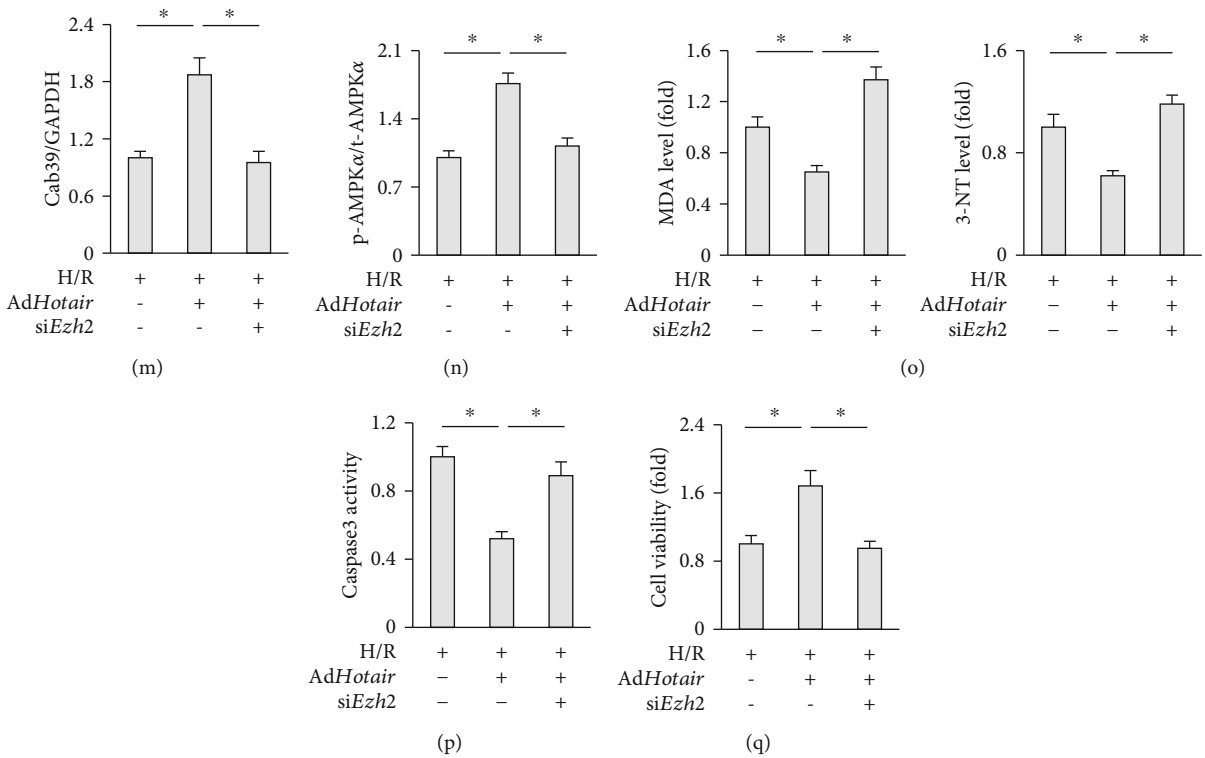


Figure 7: The EZH2/*miR-451*/Cab39 axis is involved in AMPK$\alpha$ activation caused by *Hotair*. (a) Expression of microRNAs (miRs) in H9c2 cells subjected to H/R injury with or without Ad*Hotair* incubation ($n = 6$). (b) The level of *miR-451* in H9c2 cells with or without *Hotair* knockdown after H/R stimulation ($n = 6$). (c–e) Representative western blot images and the quantitative data ($n = 6$). (f, g) MDA and 3-NT levels in H9c2 cells ($n = 6$). (h) Caspase3 activity in H9c2 cells ($n = 6$). (i) Cell viability assessed by the CCK-8 assay ($n = 6$). (j) The efficiency of si*Ezh2* determined by western blot in H9c2 cells ($n = 6$). (k) The level of *miR-451* in H9c2 cells in the indicated groups after H/R stimulation ($n = 6$). (l–n) Representative western blot images and the quantitative data ($n = 6$). (o) MDA and 3-NT levels in H9c2 cells ($n = 6$). (p) Caspase3 activity in H9c2 cells ($n = 6$). (q) Cell viability assessed by the CCK-8 assay ($n = 6$). Data are presented as mean ± SD. $^*P < 0.05$ versus the matched group.

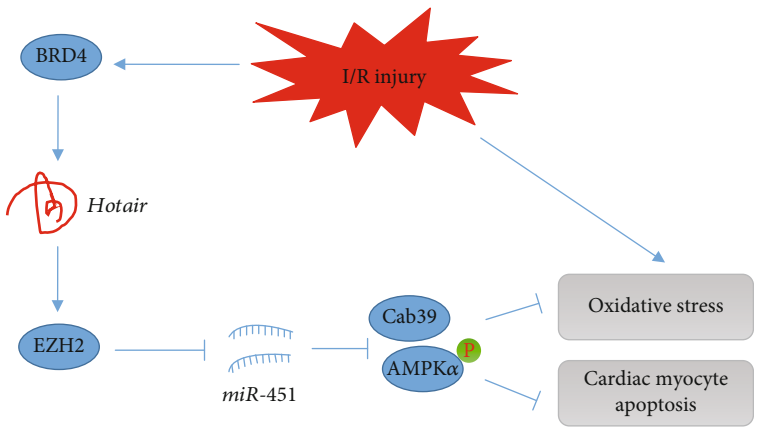


Figure 8: The proposed model of the role of Hotair in myocardial I/R injury. *Hotair* was upregulated in response to I/R stimuli. *Hotair* exerted a protective effect on oxidative stress and cardiac myocyte apoptosis via regulating the enhancer of zeste homolog 2/microRNA-451/calcium-binding protein 39/AMP-activated protein kinase alpha (EZH2/*miR-451*/Cab39/AMPK$\alpha$) axis.

data suggested that AMPK$\alpha$ was responsible for the protective effects of *Hotair* against myocardial I/R injury.

We finally investigated the possible mechanism through which *Hotair* activated AMPK$\alpha$. Previous studies determined that lncRNAs can act on miRNAs to regulate protein-coding gene expression and *Hotair* has been shown to regulate cardiac pathophysiology via *miR-19*, *miR-125*, and *miR-34a*. Unexpectedly, we found that *Hotair* manipulation did not

affect these miRNAs in the context of myocardial I/R injury but caused *miR-451* alteration. Cab39 was shown to form a heterotrimeric complex with STRAD and contributed to the stabilization of LKB1 activity [47]. Previous studies proved that *miR-451* inactivated AMPK$\alpha$ pathway via directly targeting Cab39 [48]. In line with these data, we observed that Cab39 expression was decreased in *Hotair*-deficient cardiac myocytes or heart samples, which was prevented by the treatment of a *miR-451* inhibitor. Generally, lncRNAs functioned as a molecular sponge of miRNAs, and the modulation of *Hotair* on *miR-19*, *miR-125*, and *miR-34a* was also related to the sponge function. Intensive studies showed that individual lncRNAs can also act as the interface between DNA and specific chromatin remodeling activities. Data from Chang lab previously determined that *Hotair* overexpression in epithelial cancer cells could trigger genome-wide retargeting of PRC2 within genomic loci [22]. Further detection revealed that *Hotair* bound to both PRC2 and lysine-specific demethylase 1 (LSD1) complex, which subsequently resulted in a silent chromatin state and transcriptional repression [59]. EZH2, a histone 3 lysine 27 (H3K27) methyltransferase, is an important component of PRC2 and plays critical roles in regulating miRNAs silence. In accordance with previous studies, we found *Hotair* inhibited *miR-451* via EZH2, and *Ezh2* deficiency abrogated the inhibitory effect of *Hotair* in vitro.

In summary, we provide the evidence that endogenous lncRNA *Hotair* is an essential negative regulator for the progression of myocardial I/R injury, which is dependent on AMPK$\alpha$ activation via the EZH2/*miR-451*/Cab39 axis (Figure 8). Therefore, targeting *Hotair* might provide novel insight into developing effective therapeutic strategies for the treatment of myocardial I/R injury.

## Data Availability

The data that support the findings of this study are available from the corresponding author upon reasonable request.

## Conflicts of Interest

The authors declare that there are no conflicts of interests.

## Authors' Contributions

Kai Meng, Jiao Jiao, and Yu-Dong Peng contributed to the conception and design of the experiment. Kai Meng, Jiao Jiao, Rui-Rui Zhu, and Bo-Yuan Wang performed the study and acquired the data. Xiao-Bo Mao, Yu-Cheng Zhong, Zheng-Feng Zhu, and Kun-Wu Yu performed the study and conducted data analysis. Yan Ding, Wen-Bin Xu, and Jian Yu contributed to the data interpretation and revised the manuscript. Kai Meng and Rui-Rui Zhu drafted the manuscript. Qiu-Tang Zeng and Yu-Dong Peng revised it critically for important intellectual content. Each author had participated sufficiently in the work. Kai Meng and Jiao Jiao contributed equally to this work.

## Acknowledgments

This work was supported by the National Natural Science Foundation of China (grant numbers 81600231 and 81800439).

## Supplementary Materials

Figure S1: Hotair overexpression protected against I/R-induced oxidative stress and cardiac myocyte apoptosis. Figure S2: Hotair overexpression prevented oxidative stress and cardiac myocyte apoptosis in response to H/R in vitro. Figure S3: the expression of Cab39 in vivo and in vitro. A. Cab39 protein level in Hotair-deficient murine hearts after I/R injury ($n = 6$). B. Cab39 mRNA level in H/R-stimulated H9c2 cells in the indicated groups ($n = 6$). Data are presented as mean ± SD ($^*P < 0.05$ versus the matched group). *(Supplementary Materials)*

## References

[1] T. Nestelberger, J. Boeddinghaus, D. Wussler et al., "Predicting major adverse events in patients with acute myocardial infarction," *Journal of the American College of Cardiology*, vol. 74, no. 7, pp. 842–854, 2019.

[2] G. M. Fröhlich, P. Meier, S. K. White, D. M. Yellon, and D. J. Hausenloy, "Myocardial reperfusion injury: looking beyond primary PCI," *European Heart Journal*, vol. 34, no. 23, pp. 1714–1722, 2013.

[3] S. M. Davidson, P. Ferdinandy, I. Andreadou et al., "Multitarget strategies to reduce myocardial ischemia/reperfusion injury: JACC review topic of the week," *Journal of the American College of Cardiology*, vol. 73, no. 1, pp. 89–99, 2019.

[4] H. Zhou, P. Zhu, J. Wang, H. Zhu, J. Ren, and Y. Chen, "Pathogenesis of cardiac ischemia reperfusion injury is associated with CK2alpha-disturbed mitochondrial homeostasis via suppression of FUNDC1-related mitophagy," *Cell Death and Differentiation*, vol. 25, no. 6, pp. 1080–1093, 2018.

[5] L. Y. Zhou, M. Zhai, Y. Huang et al., "The circular RNA ACR attenuates myocardial ischemia/reperfusion injury by suppressing autophagy via modulation of the Pink1/ FAM65B pathway," *Cell Death and Differentiation*, vol. 26, no. 7, pp. 1299–1315, 2019.

[6] F. Fan, Y. Duan, F. Yang et al., "Deletion of heat shock protein 60 in adult mouse cardiomyocytes perturbs mitochondrial protein homeostasis and causes heart failure," *Cell Death & Differentiation*, vol. 27, no. 2, pp. 587–600, 2019.

[7] S. B. Ong, S. Subrayan, S. Y. Lim, D. M. Yellon, S. M. Davidson, and D. J. Hausenloy, "Inhibiting mitochondrial fission protects the heart against ischemia/reperfusion injury," *Circulation*, vol. 121, no. 18, pp. 2012–2022, 2010.

[8] C. Hu, X. Zhang, W. Wei et al., "Matrine attenuates oxidative stress and cardiomyocyte apoptosis in doxorubicin-induced cardiotoxicity via maintaining AMPKalpha/UCP2 pathway," *Acta Pharmaceutica Sinica B*, vol. 9, no. 4, pp. 690–701, 2019.

[9] R. J. Vagnozzi, G. J. Gatto, L. S. Kallander et al., "Inhibition of the cardiomyocyte-specific kinase TNNI3K limits oxidative stress, injury, and adverse remodeling in the ischemic heart," *Science Translational Medicine*, vol. 5, no. 207, article 207ra141, 2013.

[10] D. G. Hardie, F. A. Ross, and S. A. Hawley, "AMPK: a nutrient and energy sensor that maintains energy homeostasis," *Nature Reviews Molecular Cell Biology*, vol. 13, no. 4, pp. 251–262, 2012.

[11] Z. G. Ma, J. Dai, W. B. Zhang et al., "Protection against cardiac hypertrophy by geniposide involves the GLP-1 receptor / AMPKalpha signalling pathway," *British Journal of Pharmacology*, vol. 173, no. 9, pp. 1502–1516, 2016.

[12] X. Zhang, Z. G. Ma, Y. P. Yuan et al., "Rosmarinic acid attenuates cardiac fibrosis following long-term pressure overload via AMPKalpha/Smad3 signaling," *Cell Death & Disease*, vol. 9, no. 2, p. 102, 2018.

[13] M. Harada, A. Tadevosyan, X. Qi et al., "Atrial fibrillation activates AMP-dependent protein kinase and its regulation of cellular calcium handling: potential role in metabolic adaptation and prevention of progression," *Journal of the American College of Cardiology*, vol. 66, no. 1, pp. 47–58, 2015.

[14] R. R. Russell III, J. Li, D. L. Coven et al., "AMP-activated protein kinase mediates ischemic glucose uptake and prevents postischemic cardiac dysfunction, apoptosis, and injury," *The Journal of Clinical Investigation*, vol. 114, no. 4, pp. 495–503, 2004.

[15] Y. Wang, E. Gao, L. Tao et al., "AMP-activated protein kinase deficiency enhances myocardial ischemia/reperfusion injury but has minimal effect on the antioxidant/antinitrative protection of adiponectin," *Circulation*, vol. 119, no. 6, pp. 835–844, 2009.

[16] B. Wang, J. Nie, L. Wu et al., "AMPKalpha2 protects against the development of heart failure by enhancing mitophagy via PINK1 phosphorylation," *Circulation Research*, vol. 122, no. 5, pp. 712–729, 2018.

[17] R. Shibata, K. Sato, D. R. Pimentel et al., "Adiponectin protects against myocardial ischemia-reperfusion injury through AMPK- and COX-2-dependent mechanisms," *Nature Medicine*, vol. 11, no. 10, pp. 1096–1103, 2005.

[18] Y. Zhang, Y. Wang, J. Xu et al., "Melatonin attenuates myocardial ischemia-reperfusion injury via improving mitochondrial fusion/mitophagy and activating the AMPK-OPA1 signaling pathways," *Journal of Pineal Research*, vol. 66, no. 2, article e12542, 2019.

[19] Y. Liang, X. Chen, Y. Wu et al., "LncRNA CASC9 promotes esophageal squamous cell carcinoma metastasis through upregulating LAMC2 expression by interacting with the CREB-binding protein," *Cell Death and Differentiation*, vol. 25, no. 11, pp. 1980–1995, 2018.

[20] R. A. Boon, N. Jaé, L. Holdt, and S. Dimmeler, "Long noncoding RNAs: from clinical genetics to therapeutic targets?," *Journal of the American College of Cardiology*, vol. 67, no. 10, pp. 1214–1226, 2016.

[21] Q. Su, Y. Liu, X. W. Lv et al., "Inhibition of lncRNA TUG1 upregulates miR-142-3p to ameliorate myocardial injury during ischemia and reperfusion via targeting HMGB1- and Rac1-induced autophagy," *Journal of Molecular and Cellular Cardiology*, vol. 133, pp. 12–25, 2019.

[22] R. A. Gupta, N. Shah, K. C. Wang et al., "Long non-coding RNA HOTAIR reprograms chromatin state to promote cancer metastasis," *Nature*, vol. 464, no. 7291, pp. 1071–1076, 2010.

[23] C. Battistelli, G. Sabarese, L. Santangelo et al., "The lncRNA HOTAIR transcription is controlled by HNF4alpha-induced chromatin topology modulation," *Cell Death and Differentiation*, vol. 26, no. 5, pp. 890–901, 2019.

[24] L. Gao, X. Wang, S. Guo et al., "LncRNA HOTAIR functions as a competing endogenous RNA to upregulate SIRT1 by sponging miR-34a in diabetic cardiomyopathy," *Journal of Cellular Physiology*, vol. 234, no. 4, pp. 4944–4958, 2019.

[25] Y. Lai, S. He, L. Ma et al., "HOTAIR functions as a competing endogenous RNA to regulate PTEN expression by inhibiting miR-19 in cardiac hypertrophy," *Molecular and Cellular Biochemistry*, vol. 432, no. 1-2, pp. 179–187, 2017.

[26] H. Wu, J. Liu, W. Li, G. Liu, and Z. Li, "LncRNA-HOTAIR promotes TNF-alpha production in cardiomyocytes of LPS-induced sepsis mice by activating NF-kappaB pathway," *Biochemical and Biophysical Research Communications*, vol. 471, no. 1, pp. 240–246, 2016.

[27] W. Lu, L. Zhu, Z. B. Ruan, M. X. Wang, Y. Ren, and W. Li, "HOTAIR promotes inflammatory response after acute myocardium infarction by upregulating RAGE," *European Review for Medical and Pharmacological Sciences*, vol. 22, no. 21, pp. 7423–7430, 2018.

[28] D. Zhang, B. Wang, M. Ma, K. Yu, Q. Zhang, and X. Zhang, "lncRNA HOTAIR protects myocardial infarction rat by sponging miR-519d-3p," *Journal of Cardiovascular Translational Research*, vol. 12, no. 3, pp. 171–183, 2019.

[29] X. Zhang, C. Hu, C. Y. Kong et al., "FNDC5 alleviates oxidative stress and cardiomyocyte apoptosis in doxorubicin-induced cardiotoxicity via activating AKT," *Cell Death & Differentiation*, vol. 27, no. 2, article 372, pp. 540–555, 2019.

[30] C. Wahlquist, D. Jeong, A. Rojas-Muñoz et al., "Inhibition of *miR-25* improves cardiac contractility in the failing heart," *Nature*, vol. 508, no. 7497, pp. 531–535, 2014.

[31] R. Zhu, H. Sun, K. Yu et al., "Interleukin-37 and dendritic cells treated with interleukin-37 plus troponin I ameliorate cardiac remodeling after myocardial infarction," *Journal of the American Heart Association*, vol. 5, no. 12, 2016.

[32] Y. Peng, K. Meng, L. Jiang et al., "Thymic stromal lymphopoietin-induced HOTAIR activation promotes endothelial cell proliferation and migration in atherosclerosis," *Bioscience Reports*, vol. 37, no. 4, 2017.

[33] H. Wei, H. Li, S. P. Wan et al., "Cardioprotective effects of malvidin against isoproterenol-induced myocardial infarction in rats: a mechanistic study," *Medical Science Monitor*, vol. 23, pp. 2007–2016, 2017.

[34] X. X. Wang, X. L. Wang, M. M. Tong et al., "SIRT6 protects cardiomyocytes against ischemia/reperfusion injury by augmenting FoxO3alpha-dependent antioxidant defense mechanisms," *Basic Research in Cardiology*, vol. 111, no. 2, p. 13, 2016.

[35] B. Wu, J. Y. Feng, L. M. Yu et al., "Icariin protects cardiomyocytes against ischaemia/reperfusion injury by attenuating sirtuin 1-dependent mitochondrial oxidative damage," *British Journal of Pharmacology*, vol. 175, no. 21, pp. 4137–4153, 2018.

[36] P. Efentakis, A. Varela, E. Chavdoula et al., "Levosimendan prevents doxorubicin-induced cardiotoxicity in time- and dose-dependent manner: implications for inotropy," *Cardiovascular Research*, 2019.

[37] X. Zhang, J. X. Zhu, Z. G. Ma et al., "Rosmarinic acid alleviates cardiomyocyte apoptosis via cardiac fibroblast in doxorubicin-induced cardiotoxicity," *International Journal of Biological Sciences*, vol. 15, no. 3, pp. 556–567, 2019.

[38] B. S. Sixt, C. Núñez-Otero, O. Kepp, R. H. Valdivia, and G. Kroemer, "*Chlamydia trachomatis* fails to protect its growth

niche against pro- apoptotic insults," *Cell Death and Differentiation*, vol. 26, no. 8, pp. 1485–1500, 2019.

[39] S. Qi, L. Guo, S. Yan, R. J. Lee, S. Yu, and S. Chen, "Hypocrellin A-based photodynamic action induces apoptosis in A549 cells through ROS-mediated mitochondrial signaling pathway," *Acta Pharmaceutica Sinica B*, vol. 9, no. 2, pp. 279–293, 2019.

[40] Q. Duan, S. McMahon, P. Anand et al., "BET bromodomain inhibition suppresses innate inflammatory and profibrotic transcriptional networks in heart failure," *Science Translational Medicine*, vol. 9, no. 390, p. eaah5084, 2017.

[41] N. Chatterjee, M. Tian, K. Spirohn, M. Boutros, and D. Bohmann, "Keap1-independent regulation of Nrf2 activity by protein acetylation and a BET bromodomain protein," *PLoS Genetics*, vol. 12, no. 5, article e1006072, 2016.

[42] C. Pastori, P. Kapranov, C. Penas et al., "The bromodomain protein BRD4 controls HOTAIR, a long noncoding RNA essential for glioblastoma proliferation," *Proceedings of the National Academy of Sciences*, vol. 112, no. 27, pp. 8326–8331, 2015.

[43] M. D. Brand, R. L. Goncalves, A. L. Orr et al., "Suppressors of superoxide-H2O2 production at site IQ of mitochondrial complex I protect against stem cell hyperplasia and ischemia-reperfusion injury," *Cell Metabolism*, vol. 24, no. 4, pp. 582–592, 2016.

[44] V. P. M. van Empel, A. T. Bertrand, R. J. van Oort et al., "EUK-8, a superoxide dismutase and catalase mimetic, reduces cardiac oxidative stress and ameliorates pressure overload-induced heart failure in the harlequin mouse mutant," *Journal of the American College of Cardiology*, vol. 48, no. 4, pp. 824–832, 2006.

[45] W. M. Fu, X. Zhu, W. M. Wang et al., "Hotair mediates hepatocarcinogenesis through suppressing miRNA-218 expression and activating P14 and P16 signaling," *Journal of Hepatology*, vol. 63, no. 4, pp. 886–895, 2015.

[46] L. Li, M. Zhang, W. Chen et al., "LncRNA-HOTAIR inhibition aggravates oxidative stress-induced H9c2 cells injury through suppression of MMP2 by miR-125," *Acta Biochimica et Biophysica Sinica*, vol. 50, no. 10, pp. 996–1006, 2018.

[47] J. Boudeau, A. F. Baas, M. Deak et al., "MO25alpha/beta interact with STRADalpha/beta enhancing their ability to bind, activate and localize LKB1 in the cytoplasm," *The EMBO Journal*, vol. 22, no. 19, pp. 5102–5114, 2003.

[48] Y. Kuwabara, T. Horie, O. Baba et al., "MicroRNA-451 exacerbates lipotoxicity in cardiac myocytes and high-fat diet-induced cardiac hypertrophy in mice through suppression of the LKB1/AMPK pathway," *Circulation Research*, vol. 116, no. 2, pp. 279–288, 2015.

[49] D. Cheng, J. Deng, B. Zhang et al., "LncRNA HOTAIR epigenetically suppresses miR-122 expression in hepatocellular carcinoma via DNA methylation," *eBioMedicine*, vol. 36, pp. 159–170, 2018.

[50] L. Yang and Z. N. Lu, "Long non-coding RNA HOTAIR promotes ischemic infarct induced by hypoxia through up-regulating the expression of NOX2," *Biochemical and Biophysical Research Communications*, vol. 479, no. 2, pp. 186–191, 2016.

[51] L. Gao, Y. Liu, S. Guo et al., "Circulating long noncoding RNA HOTAIR is an essential mediator of acute myocardial infarction," *Cellular Physiology and Biochemistry*, vol. 44, no. 4, pp. 1497–1508, 2017.

[52] M. Appari, A. Breitbart, F. Brandes et al., "C1q-TNF-related protein-9 promotes cardiac hypertrophy and failure," *Circulation Research*, vol. 120, no. 1, pp. 66–77, 2017.

[53] Y. Sun, W. Yi, Y. Yuan et al., "C1q/tumor necrosis factor-related protein-9, a novel adipocyte-derived cytokine, attenuates adverse remodeling in the ischemic mouse heart via protein kinase A activation," *Circulation*, vol. 128, 11 Suppl 1, pp. S113–S120, 2013.

[54] P. Zhai, S. Sciarretta, J. Galeotti, M. Volpe, and J. Sadoshima, "Differential roles of GSK-3beta during myocardial ischemia and ischemia/reperfusion," *Circulation Research*, vol. 109, no. 5, pp. 502–511, 2011.

[55] Y. Matsui, H. Takagi, X. Qu et al., "Distinct roles of autophagy in the heart during ischemia and reperfusion: roles of AMP-activated protein kinase and Beclin 1 in mediating autophagy," *Circulation Research*, vol. 100, no. 6, pp. 914–922, 2007.

[56] X. Bi, G. Zhang, X. Wang et al., "Endoplasmic reticulum chaperone GRP78 protects heart from ischemia/reperfusion injury through Akt activation," *Circulation Research*, vol. 122, no. 11, pp. 1545–1554, 2018.

[57] X. Li, S. Luo, J. Zhang et al., "lncRNA H19 alleviated myocardial I/RI via suppressing miR-877-3p/Bcl-2-mediated mitochondrial apoptosis," *Molecular Therapy-Nucleic Acids*, vol. 17, pp. 297–309, 2019.

[58] K. Wang, F. Liu, C. Y. Liu et al., "The long noncoding RNA NRF regulates programmed necrosis and myocardial injury during ischemia and reperfusion by targeting miR-873," *Cell Death and Differentiation*, vol. 23, no. 8, pp. 1394–1405, 2016.

[59] L. Li, B. Liu, O. L. Wapinski et al., "Targeted disruption of Hotair leads to homeotic transformation and gene derepression," *Cell Reports*, vol. 5, no. 1, pp. 3–12, 2013.

Hindawi
Oxidative Medicine and Cellular Longevity
Volume 2019, Article ID 9084643, 9 pages
https://doi.org/10.1155/2019/9084643

*Research Article*

# Intragastric Application of Aspirin, Clopidogrel, Cilostazol, and BPC 157 in Rats: Platelet Aggregation and Blood Clot

**Sanja Konosic,[1] Mate Petricevic,[1] Visnja Ivancan,[1] Lucija Konosic,[1] Eleonora Goluza,[1] Branimir Krtalic,[1] Domagoj Drmic,[2] Mirjana Stupnisek,[3] Sven Seiwerth,[4] and Predrag Sikiric[2]**

[1]*University Hospital Centre Zagreb, Zagreb, Croatia*
[2]*Department of Pharmacology, School of Medicine, University of Zagreb, Zagreb, Croatia*
[3]*Department of Pharmacology, Faculty of Medicine, J.J. Strossmayer University of Osijek, Osijek, Croatia*
[4]*Department of Pathology, School of Medicine, University of Zagreb, Zagreb, Croatia*

Correspondence should be addressed to Predrag Sikiric; sikiric@mef.hr

Received 13 June 2019; Revised 24 September 2019; Accepted 11 December 2019; Published 31 December 2019

Guest Editor: Aleksandar Kibel



We suggest that the stable gastric pentadecapeptide BPC 157 may rescue thrombocyte function. We focused on the antithrombotic agent aspirin, clopidogrel, and cilostazol application in rats; arachidonic acid, ADP, collagen, and arachidonic acid/PGE1 platelet aggregation (aggregometry) and blood clot viscoelastic properties (thromboelastometry); and the pentadecapeptide BPC 157. Rats received intragastrically for three days once daily treatment with antithrombotic agents—aspirin (10 mg/kg) or clopidogrel (10 mg/kg) or cilostazol (10 mg/kg). Medication (BPC 157 (10 $\mu$g/kg) or an equal volume of saline (5 ml/kg)) was given intragastrically, immediately after each antithrombotic agent application. For multiple electrode aggregometry and modified rotational thromboelastometry studies, blood sampling was at 2 h after last application. Adenosine diphosphate (ADP test 6.5 $\mu$M), arachidonic acid (ASPI test 0.5 mM), a combination of arachidonic acid and prostaglandin E1 (ASPI test 0.5 mM and PGE1-test 30 nM), and collagen (COL test 3.2 $\mu$g/ml) were used as aggregation agonists. Given with aspirin, clopidogrel, or cilostazol in rats, BPC 157 counteracted their inhibitory effects on aggregation activated by arachidonic acid, ADP, collagen, and arachidonic acid/PGE1. Specifically, this includes recovery of the aggregation induced by arachidonic acid (*vs.* aspirin, *vs.* clopidogrel, and *vs.* cilostazol), arachidonic acid/PGE1 (*vs.* cilostazol), ADP (*vs.* clopidogrel), or collagen (*vs.* clopidogrel). Contrarily, there is no effect on the used tests (extrinsic/intrinsic hemostasis system, the fibrin part of the clot) EXTEM, INTEM, and FIBTEM; clotting time; clot formation time; alpha-angle; maximum clot firmness; lysis index after 30 minutes; and maximum lysis. In conclusion, we revealed that BPC 157 largely rescues thrombocyte function.

## 1. Introduction

We focused on the inhibitory effect of the stable gastric pentadecapeptide BPC 157 (used in trials: ulcerative colitis; now, multiple sclerosis) [1–13] on the antithrombotic agents (i.e., aspirin, inhibitor of thromboxane A2 (TXA2) production; clopidogrel, $P2Y_{12}$ subtype of adenosine-diphosphate (ADP) receptor antagonist; and cilostazol, phosphodiesterase type 3 ($PDE_3$) inhibitor [14]). The effect on platelet aggregation and viscoelastic properties of the blood clot was investigated using multiple electrode aggregometry and modified rotational thromboelastometry (ROTEM) studies [15–20].

Recently, BPC 157 therapy (for review, see [1–13]) approaches solving of the vascular occlusion disturbances [21–25]. The rapid activation of the bypassing loop occurs in the rats with infrarenal occlusion of the inferior caval vein (and thereby resolved Virchow, venous lesion and thrombosis, caval hypertension, aortal hypotension, and consequent thrombocytopenia), much like in the rats with ischemic/-reperfusion colitis, duodenal venous congestion lesions, perforated cecum, bile duct ligation-induced liver cirrhosis, and portal hypertension [21–25]. Previously, BPC 157, as a prototype antiulcer agent with potent cytoprotective capability [1–13], thereby exerting innate endothelium protection,

counteracted abdominal anastomosis-induced thrombosis [26] and prolonged bleeding and thrombocytopenia after amputation and/or anticoagulant (heparin, warfarin), aspirin, and NO-agents (L-NAME/L-arginine) [27, 28] and largely interacts with NO-system in various models and species [1–13]. While having no effect on noninjured rats or on coagulation parameters, BPC 157 in heparin-treated rats decreased prolonged activated partial thromboplastin time (APTT) but did not influence heparin activity (anti-Xa test) [27].

Thus, we further studied how BPC 157 may influence platelet aggregation and viscoelastic properties of the blood clot. Therefore, these outcomes were carried out using ex vivo and in vitro studies, using impedance aggregometry and ROTEM studies. Rats received intragastrically for three days once daily treatment with antithrombotic agents—-aspirin or clopidogrel or cilostazol. Medication (BPC 157 (regular dose of the 10 $\mu$g/kg) or saline (controls)) was given intragastrically, immediately after each antithrombotic agent application. In aggregometry studies, arachidonic acid, ADP, collagen, and arachidonic acid/PGE1 were used as aggregation agonists [15–17]. ROTEM studies include CT (clotting time), CFT (clot formation time), and alpha-angle, to indicate the rate of fibrin formation; MCF (maximum clot firmness) to show the platelet contribution to clot formation; Ly30 (lysis index after 30 minutes) and ML (maximum lysis) to show the percentage of lost clot stability; EXTEM test (a screening test for the (extrinsic) hemostasis system); INTEM test (intrinsic pathway is being tested); and FIBTEM (isolates fibrinogen function) [18, 19].

## 2. Materials and Methods

*2.1. Animals.* Male albino Wistar rats, 200 g b.w., were randomly assigned; 6 rats per each group were used for the experiments, approved by the Local Ethics Committee at School of Medicine (University of Zagreb, Zagreb, Croatia). The medication procedure was performed on rats, which had food and water ad libitum before the procedure and until the end of the experiment, and was assessed by the observer unaware about the treatment.

*2.2. Drugs and Protocol.* Pentadecapeptide Gly-Glu-Pro-Pro-Pro-Gly-Lys-Pro-Ala-Asp-Asp-Ala-Gly-Leu-Val, M.W. 1419, named BPC 157, a part of the sequence of human gastric juice protein, coded BPC, freely soluble in water at pH 7.0 and in saline, was prepared (Diagen, Slovenia) as described previously [1–13]. L-NAME and L-arginine were commercially purchased (Sigma, USA).

Aspirin (Andol, Pliva, Croatia), clopidogrel (Zyllt, Krka Ltd., Slovenia), and cilostazol (PLETAL, Otsuka Pharmaceutical Ltd., UK) were used.

Rats received intragastrically for three days once daily treatment with antithrombotic agents—aspirin (10 mg/kg) or clopidogrel (10 mg/kg) or cilostazol (10 mg/kg). Medication (BPC 157 (10 $\mu$g/kg) or an equal volume of saline (5 ml/kg)) was given intragastrically, immediately after each antithrombotic agent application. The rats were then sacrificed at 2 h after the last application.

*2.3. Blood Sampling.* In deeply anaesthetized rats (with ketamine (20 mg/kg, Ketanest, Parke Davis GmbH, Germany) and diazepam (10 mg/kg, Normabel, Belupo, Croatia)), a median sternotomy was performed. By direct puncture to the right atrium using a 20G needle, blood was collected into 2.6 ml S-Monovette tubes (Sarsted Ltd., Germany) (final hirudin concentration 25 $\mu$g/ml) for aggregometric measurements, and 1.8 ml into 3.8% citrate Vacuette tubes (Greiner Bio-One Ltd., Austria) for thromboelastometric measurements.

*2.4. Measurements.* Platelet aggregation was determined in whole blood by multiple electrode aggregometry (MEA) on Multiplate® Analyzer (Tem International GmbH, Germany). Technical details have already been described in previous literature [15–17]. To put it briefly, MEA is based on the principle that activated platelets stick on the test cell sensor wires and then enhance the electrical resistance between them, which is continuously recorded and expressed as 3 parameters: aggregation (AGG) (highest increase in impedance between the electrodes measured in aggregation units (AU)), area under the curve (AUC) (determined by the height of the aggregation curve and the slope measured in U = AU/min (1 U = 10 AU/min)), and velocity (VEL) (maximum slope of aggregation measured in AU/minute). Measurements were executed according to the manufacturer's instructions, using equipment and kits provided by Dynabyte, Munich, Germany. Four test cells were loaded with 300 $\mu$l of normal saline and 300 $\mu$l of whole blood, followed by three-minute incubation at 37°C. After the incubation, 20 $\mu$l of the agonist was added to each respective cell: via ADP receptors by ADP (ADP test 6.5 $\mu$M) [17]; by arachidonic acid, the substrate of cyclooxygenase (COX), which subsequently forms the potent platelet activator TXA2 (ASPI test 0.5 mM) [17]; by a combination of arachidonic acid and prostaglandin E1 (ASPI test 0.5 mM and PGE1 test 30 nM), where PGE1 does not affect arachidonic acid-induced platelet aggregation per se but potentiates the inhibitory effects of cilostazol on platelet aggregation in *in vitro* studies [20]; and by collagen via the collagen receptor, which leads to a release of endogenous arachidonic acid and TXA2 (COL test 3.2 $\mu$g/ml) [17]. After six minutes of measurement, AUC, AGG, and VEL were recorded.

Viscoelastic properties of the blood were assessed using modified rotational thromboelastometry (TEM) on ROTEM® delta analyzer (Tem International GmbH, Germany). A detailed description of the ROTEM technology has been published previously [18, 19]. In short, TEM measures elasticity and strength of the developing clot in whole blood via a pin suspended in a cup. Changes in the movement of the pin are converted by digital data processing to create graphical and numerical output. Typical parameters obtained are the time from the beginning of measurement until the clot starts to form (CT); the time needed for the clot to reach an amplitude of 20 mm (CFT); alpha-angle, angle of tangent at 2 mm amplitude; the maximum amplitude of the curve during 60 minutes of measurement (MCF); clot lysis at 30 minutes (Ly30); and maximum lysis (ML), which describes the percentage of the maximum lost clot firmness

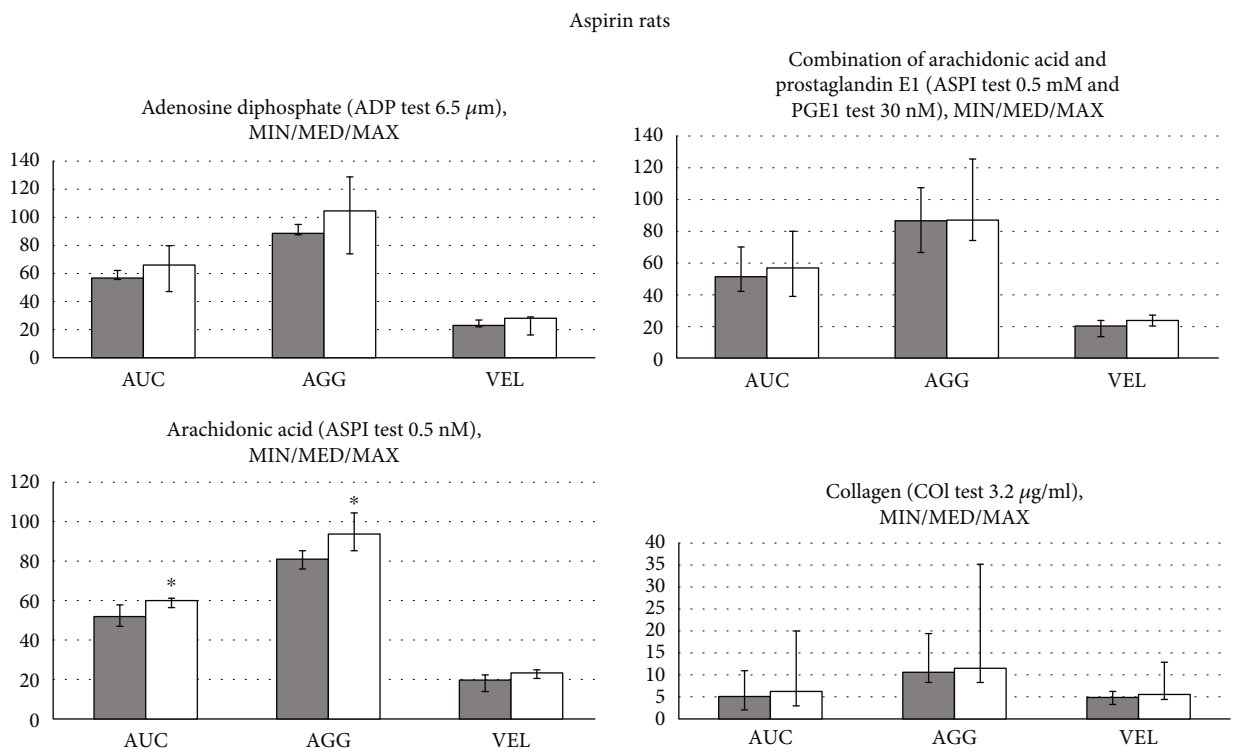


Figure 1: Rats which underwent antithrombotic agent aspirin (10 mg/kg intragastrically, once daily for three days) received immediately thereafter BPC 157 (10 $\mu$g/kg intragastrically, once daily for three days) (white bars) or an equal volume of saline (5 ml/kg, intragastrically, once daily for three days) (gray bars); they were sacrificed at 2 h after the last application. Platelet aggregation was determined in whole blood by multiple electrode aggregometry (MEA) on Multiplate® Analyzer (aggregation (AGG)) (highest increase in impedance between the electrodes measured in aggregation units (AU)), area under the curve (AUC) (determined by the height of the aggregation curve and the slope measured in U = AU/min (1 U = 10 AU/min)), and velocity (VEL) (maximum slope of aggregation measured in AU/minute). After the incubation, 20 $\mu$l of the agonist was added to each respective cell: adenosine diphosphate (ADP test 6.5 $\mu$M), arachidonic acid (ASPI test 0.5 mM), a combination of arachidonic acid and prostaglandin E1 (ASPI test 0.5 mM and PGE1 test 30 nM), and collagen (COL test 3.2 $\mu$g/ml). After six minutes of measurement, AUC, AGG, and VEL were recorded. $^*P < 0.05$, *vs.* control, at least.

relative to MCF. Following standard analyzer set-up and reagents provided by Tem International GmbH, Germany, 300 $\mu$l of citrated whole blood was firstly recalcified with 20 $\mu$l of $CaCl_2$ 0.2 mol/l (STARTEM). Coagulation was then initiated by adding 20 $\mu$l of activator through EXTEM, INTEM, or FIBTEM. After 60 minutes CT, CFT, alpha-angle, MCF, Ly30, and ML were recorded.

*2.5. Statistical Methods.* The normality of the distribution was tested using the Kolmogorov-Smirnov test. The differences between parameters were analyzed using the Kruskal-Wallis test and post hoc analysis using the Mann-Whitney *U* test with Bonferroni correction. All *P* values less than 0.05 were considered significant. In data analysis, StatsDirect statistical software (http://www.statsdirect.com; England: StatsDirect Ltd. 2013) 3.0.171 version was employed.

## 3. Results

*3.1. Aggregometry Studies.* BPC 157, given immediately after antithrombotic agents in rats (aspirin, inhibitor of TXA2 synthesis; clopidogrel, ADP receptor antagonist; and cilostazol, selective $PDE_3$ inhibitor), counteracted their inhibitory effects on aggregation activated by arachidonic acid, ADP, collagen, and arachidonic acid/PGE1, which were used as aggregation agonists (Figures 1–3).

In general, while aggregation responses to arachidonic acid, ADP, collagen, and arachidonic acid/PGE1 were observed in all animals, some particularities consistently appear. Maximal AUC, AGG, and VEL values obtained with collagen were lower in the aspirin rats (Figure 1) and in the clopidogrel rats (Figure 2) than in the cilostazol rats (Figure 3). Maximal AUC, AGG, and VEL values obtained with arachidonic acid or arachidonic acid and prostaglandin E1 were lower in the clopidogrel rats (Figure 2) and in the aspirin rats (Figure 1) than in the cilostazol rats (Figure 3). The platelet agonist ADP-induced maximal AUC, AGG, and VEL values were comparable in the aspirin rats (Figure 1), clopidogrel rats (Figure 2), and cilostazol rats (Figure 3), and ADP is therefore considered as a most common agonist.

*3.1.1. Aspirin Rats.* It is likely indicative that BPC 157 reversed the aspirin effect on the arachidonic acid-induced platelet aggregation (maximal AUC and AGG), since arachidonic acid-induced platelet aggregation is typically inhibited by aspirin. However, the rescuing effect on the maximal AUC, AGG, and VEL induced by ADP, arachidonic acid

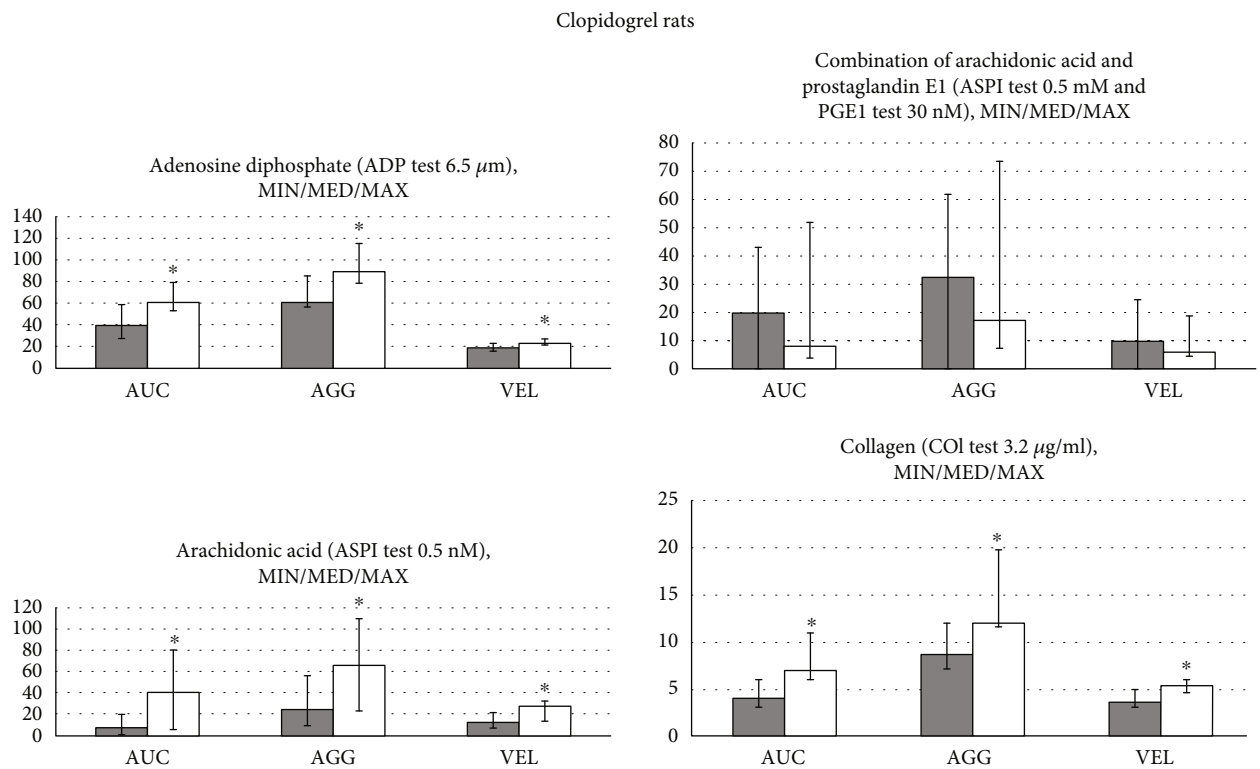


Figure 2: Rats which underwent antithrombotic agent clopidogrel (10 mg/kg intragastrically, once daily for three days) received immediately thereafter BPC 157 (10 $\mu$g/kg intragastrically, once daily for three days) (white bars) or an equal volume of saline (5 ml/kg, intragastrically, once daily for three days) (gray bars); they were sacrificed at 2 h after the last application. Platelet aggregation was determined in whole blood by multiple electrode aggregometry (MEA) on Multiplate® Analyzer (aggregation (AGG)) (highest increase in impedance between the electrodes measured in aggregation units (AU)), area under the curve (AUC) (determined by the height of the aggregation curve and the slope measured in U = AU/min (1 U = 10 AU/min)), and velocity (VEL) (maximum slope of aggregation measured in AU/minute). After the incubation, 20 $\mu$l of the agonist was added to each respective cell: adenosine diphosphate (ADP test 6.5 $\mu$M), arachidonic acid (ASPI test 0.5 mM), a combination of arachidonic acid and prostaglandin E1 (ASPI test 0.5 mM and PGE1 test 30 nM), and collagen (COL test 3.2 $\mu$g/ml). After six minutes of measurement, AUC, AGG, and VEL were recorded. $^*P < 0.05$, *vs.* control, at least.

and prostaglandin E1, and collagen did not reach the level of the significance (Figure 1).

*3.1.2. Clopidogrel Rats.* It is likely indicative that BPC 157 reversed the effect of clopidogrel on the ADP-induced platelet aggregation since ADP-induced platelet aggregation is typically inhibited by clopidogrel. Interestingly, BPC 157 reversed also the effect of clopidogrel on the maximal AUC, AGG, and VEL induced by arachidonic acid or collagen. The rescuing effect on the arachidonic acid and prostaglandin E1 did not reach the level of the significance (Figure 2).

*3.1.3. Cilostazol Rats.* It is likely indicative that BPC 157 reversed the effect of cilostazol on the arachidonic acid- and arachidonic acid and prostaglandin E1-induced platelet aggregation. Namely, arachidonic acid- and arachidonic acid and prostaglandin E1-induced platelet aggregation is typically inhibited by cilostazol. The rescuing effect on the ADP and collagen did not reach the level of the significance (Figure 3).

*3.2. Rotational Thromboelastometry.* By contrast, neither of the used tests, EXTEM, INTEM, and FIBTEM, found any effect on CT, CFT, alpha-angle, MCF, Ly30, and ML (Figures 4–6).

Thus, these studies demonstrated in the thrombocytes after antithrombotic agents' application, with distinctive targets (TXA2 inhibition-ADP receptor inhibition-selective $PDE_3$ inhibition), distinctive failures in the particular functions (as may be seen with distinctive aggregation responses to arachidonic acid, ADP, collagen, and arachidonic acid/-PGE1) (Figures 1–3). Having no effect on the coagulation pathways (Figures 4–6), BPC 157 corroborates vice versa with typical antithrombotic agents' targets (TXA2 inhibition-ADP receptor inhibition-selective $PDE_3$ inhibition) (Figures 1–3) rescuing the aggregation activated by the arachidonic acid, ADP, collagen, and arachidonic acid/PGE1.

## 4. Discussion

We demonstrated that BPC 157 medication [1–13], given immediately after antithrombotic agents in rats, aspirin, clopidogrel, and cilostazol, counteracted their inhibitory effects on the aggregation activated by the arachidonic acid, ADP, collagen, and arachidonic acid/PGE1 used as aggregation agonists [15–17, 20]. Contrarily, BPC 157 does not affect

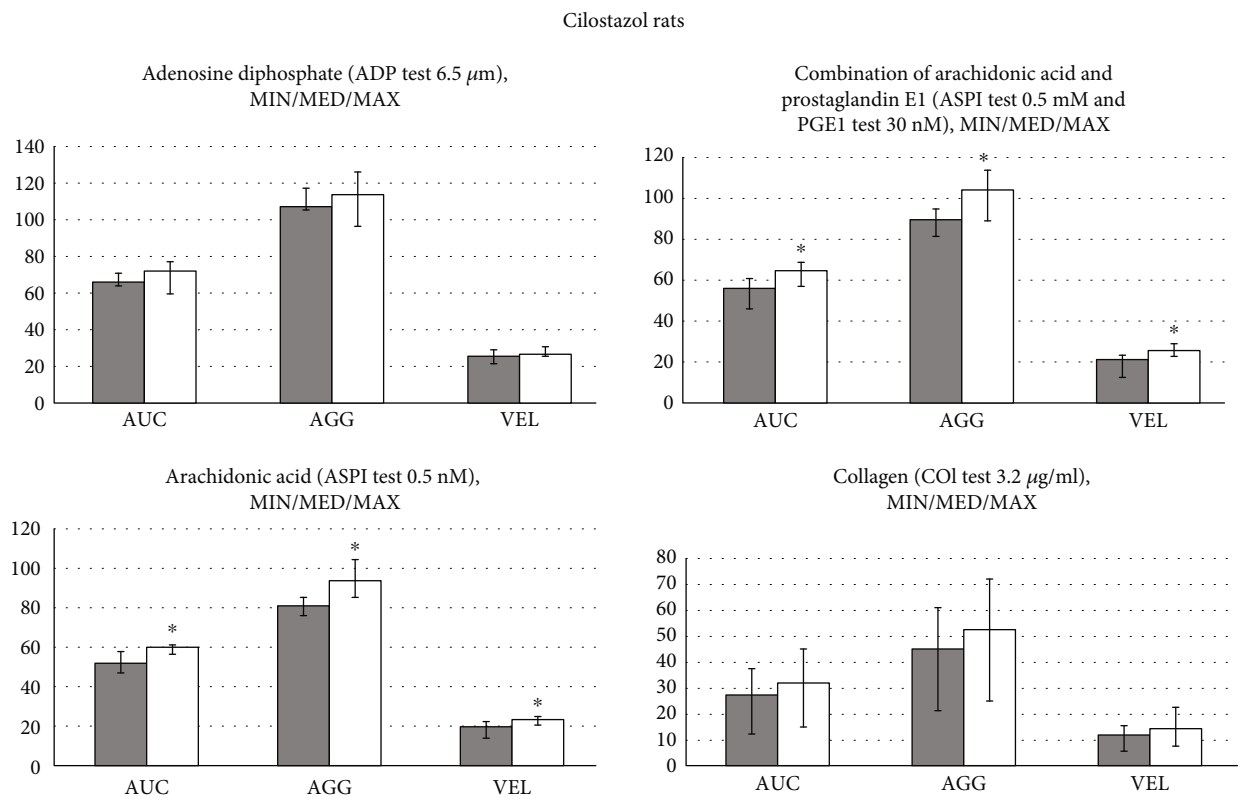


Figure 3: Rats which underwent antithrombotic agent cilostazol (10 mg/kg intragastrically, once daily for three days) received immediately thereafter BPC 157 (10 $\mu$g/kg intragastrically, once daily for three days) (white bars) or an equal volume of saline (5 ml/kg, intragastrically, once daily for three days) (gray bars); they were sacrificed at 2 h after the last application. Platelet aggregation was determined in whole blood by multiple electrode aggregometry (MEA) on Multiplate® Analyzer (aggregation (AGG)) (highest increase in impedance between the electrodes measured in aggregation units (AU)), area under the curve (AUC) (determined by the height of the aggregation curve and the slope measured in U = AU/min (1 U = 10 AU/min)), and velocity (VEL) (maximum slope of aggregation measured in AU/minute). After the incubation, 20 $\mu$l of the agonist was added to each respective cell: adenosine diphosphate (ADP test 6.5 $\mu$M), arachidonic acid (ASPI test 0.5 mM), a combination of arachidonic acid and prostaglandin E1 (ASPI test 0.5 mM and PGE1 test 30 nM), and collagen (COL test 3.2 $\mu$g/ml). After six minutes of measurement, AUC, AGG, and VEL were recorded. $^*P < 0.05$, *vs.* control, at least.

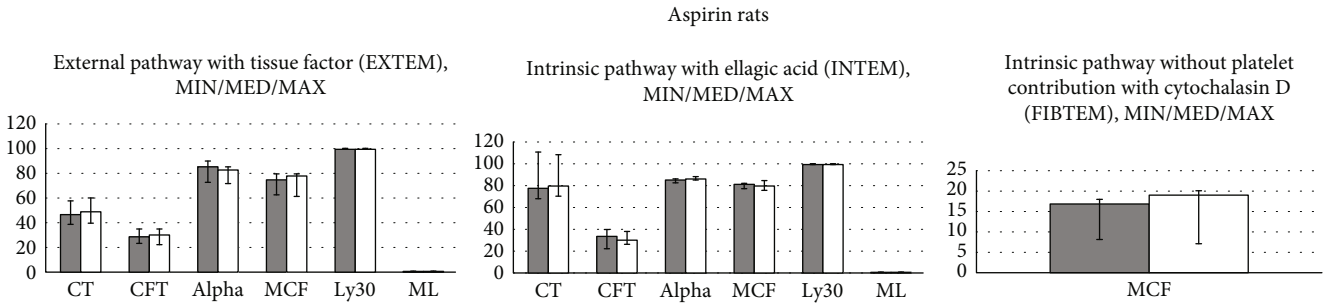


Figure 4: Rats which underwent antithrombotic agent aspirin (10 mg/kg intragastrically, once daily for three days) received immediately thereafter BPC 157 (10 $\mu$g/kg intragastrically, once daily for three days) (white bars) or an equal volume of saline (5 ml/kg, intragastrically, once daily for three days) (gray bars); they were sacrificed at 2 h after the last application. Viscoelastic properties of the blood were assessed using modified rotational thromboelastometry (TEM) on ROTEM® delta analyzer (Tem International GmbH, Germany). Typical parameters obtained are clotting time (CT), the time from the beginning of measurement until the clot starts to form; clot formation time (CFT), the time needed for the clot to reach an amplitude of 20 mm; alpha-angle, angle of tangent at 2 mm amplitude; maximum clot firmness (MCF), the maximum amplitude of the curve during 60 minutes of measurement; Ly30, clot lysis at 30 minutes; and maximum lysis (ML) which describes the percentage of the maximum lost clot firmness relative to MCF. We analyzed the external pathway with tissue factor (EXTEM), an intrinsic pathway with ellagic acid (INTEM), or without platelet contribution with cytochalasin D (FIBTEM). After 60 minutes, CT, CFT, alpha-angle, MCF, Ly30, and ML were recorded. $P > 0.05$, *vs.* control.

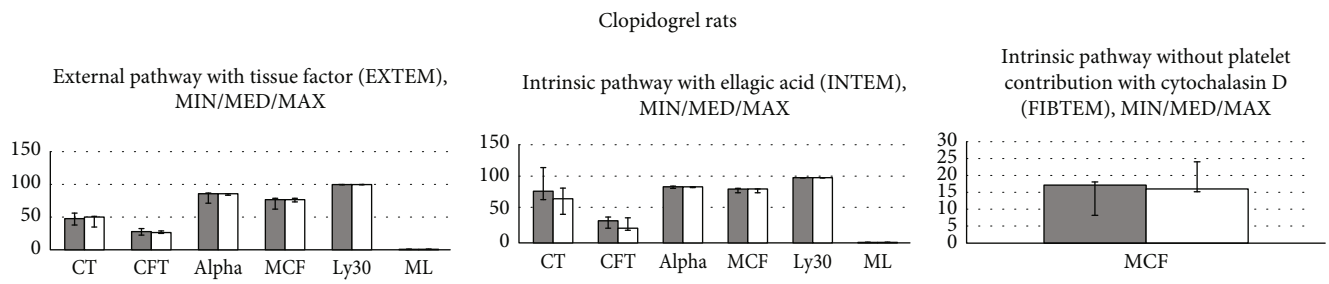


Figure 5: Rats which underwent antithrombotic agent clopidogrel (10 mg/kg intragastrically, once daily for three days) received immediately thereafter BPC 157 (10 $\mu$g/kg intragastrically, once daily for three days) (white bars) or an equal volume of saline (5 ml/kg, intragastrically, once daily for three days) (gray bars); they were sacrificed at 2 h after the last application. Viscoelastic properties of the blood were assessed using modified rotational thromboelastometry (TEM) on ROTEM® delta analyzer (Tem International GmbH, Germany). Typical parameters obtained are clotting time (CT), the time from the beginning of measurement until the clot starts to form; clot formation time (CFT), the time needed for the clot to reach an amplitude of 20 mm; alpha-angle, angle of tangent at 2 mm amplitude; maximum clot firmness (MCF), the maximum amplitude of the curve during 60 minutes of measurement; Ly30, clot lysis at 30 minutes; and maximum lysis (ML) which describes the percentage of the maximum lost clot firmness relative to MCF. We analyzed external pathway with tissue factor (EXTEM), an intrinsic pathway with ellagic acid (INTEM); or without platelet contribution with cytochalasin D (FIBTEM). After 60 minutes, CT, CFT, alpha-angle, MCF, Ly30, and ML were recorded. $P > 0.05$, *vs.* control.

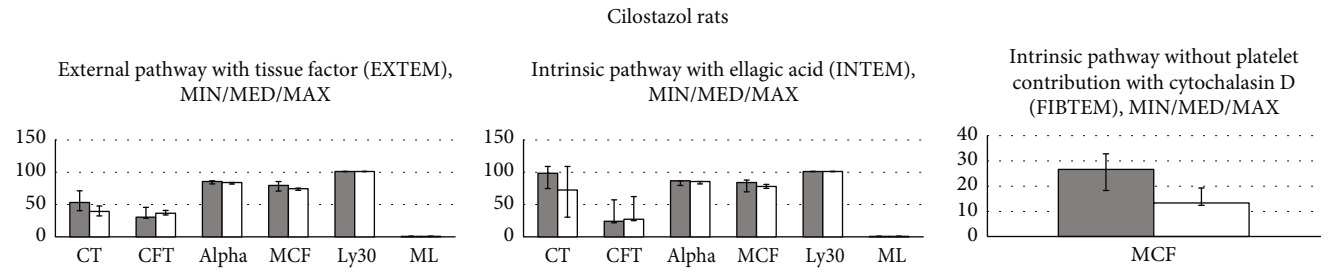


Figure 6: Rats which underwent antithrombotic agent cilostazol (10 mg/kg intragastrically, once daily for three days) received immediately thereafter BPC 157 (10 $\mu$g/kg intragastrically, once daily for three days) (white bars) or an equal volume of saline (5 ml/kg, intragastrically, once daily for three days) (gray bars); they were sacrificed at 2 h after the last application. Viscoelastic properties of the blood were assessed using modified rotational thromboelastometry (TEM) on ROTEM® delta analyzer (Tem International GmbH, Germany). Typical parameters obtained are clotting time (CT), the time from the beginning of measurement until the clot starts to form; clot formation time (CFT), the time needed for the clot to reach an amplitude of 20 mm; alpha-angle, angle of tangent at 2 mm amplitude; maximum clot firmness (MCF), the maximum amplitude of the curve during 60 minutes of measurement; Ly30, clot lysis at 30 minutes; and maximum lysis (ML) which describes the percentage of the maximum lost clot firmness relative to MCF. We analyzed external pathway with tissue factor (EXTEM), an intrinsic pathway with ellagic acid (INTEM), or without platelet contribution with cytochalasin D (FIBTEM). After 60 minutes CT, CFT, alpha-angle, MCF, Ly30, and ML were recorded. $P > 0.05$, *vs.* control.

coagulation pathways; neither of the used tests, EXTEM, INTEM, and FIBTEM, did find any effect on CT, CFT, alpha-angle, MCF, Ly30, and ML. Thus, this suggests a particular pleiotropic effect, likely a direct effect, on thrombocyte function. This may follow since BPC 157 counteracted abdominal aorta anastomosis or inferior caval vein occlusion-induced thrombosis [21, 26], prolonged bleeding and thrombocytopenia after amputation and/or anticoagulant (heparin, warfarin), aspirin, and NO-agents (L-NAME/L-arginine), or prolonged venous occlusion [21, 27, 28]. This may be particularly important considering the effectiveness with intragastric application, as a general follow-up of its cytoprotection background (i.e., antiulcer peptide, native and stable in human gastric juice more than 24 h) [1–13]. On the other hand, AUC is affected by both velocity and maximum aggregation and is considered as the best parameter to reflect overall platelet aggregation [17], and results are dependent on both platelet count and platelet function [17]. Therefore, there are distinctive presentations of the arachidonic acid-, ADP-, arachidonic acid/PGE1-, and collagen-induced aggregation in the aspirin, clopidogrel, and cilostazol rats. Consequently, we suggest typical distinction (TXA2 inhibition-ADP receptor inhibition-selective $PDE_3$ inhibition), which results with distinctive platelet dysfunctions, depending on the typical antithrombotic agent use, aspirin, clopidogrel, or cilostazol, and vice versa, on the applied therapy effect.

Namely, considering the BPC 157-aspirin counteracting relation (rescued arachidonic acid aggregation), if BPC 157 is given, thrombocyte function may resist against the effect of aspirin, which otherwise irreversibly blocks the formation of $TXA_2$ in platelets [14]. Therefore, in the aspirin rats cured with BPC 157 application, there is the viability of the thromboxane pathway. Much like this, with respect to

BPC 157-clopidogrel counteracting relation, with BPC 157, thrombocytes may function despite the effect of clopidogrel, which otherwise specifically and irreversibly inhibits the $P2Y_{12}$ subtype of ADP receptor [14]. Therefore, ADP likely binds to two G protein-coupled receptors P2Y1 and P2Y12 and initiates primary wave platelet aggregation through calcium mobilization [14]. This may allow in the BPC 157-clopidogrel rat collagen-induced platelet aggregation as a complex multistep process that is dependent on the release of ADP and thromboxane from platelets to amplify the response [29]. Similarly, with respect to the BPC 157-cilostazol counteracting relation, BPC 157 rescues thrombocyte function against cilostazol action and thereby against selective inhibition of $PDE_3$, an increase in cAMP, as well as against an increase in the active form of protein kinase A (PKA), which is directly related to an inhibition in platelet aggregation [14]. Therefore, we demonstrated in the BPC 157-cilostazol rats that arachidonic acid-induced platelet aggregation appears, otherwise most effectively inhibited by cilostazol ex vivo in previous reports [30, 31]. Moreover, in these BPC 157-cilostazol rats, rescue of the arachidonic acid and PGE1 aggregation also occurs, where PGE1 would otherwise potentiate the inhibitory effects of cilostazol on platelet aggregation in in vitro studies [32]. These beneficial effects on the typical targets of the antithrombotic agents may be present despite the other particular platelet function which may be still disturbed. Illustratively, in the aspirin rats, there is no significant rescue of the maximal AUC, AGG, and VEL induced by ADP, arachidonic acid and prostaglandin E1, and collagen. In clopidogrel rats, no significant rescue of the arachidonic acid and prostaglandin E1 occurs. In cilostazol rats, there is no significant rescue of the ADP and collagen.

In support, while the complete BPC 157 mechanisms remain to be fully determined (several molecular pathways affected, in particular VEGFR2-receptors) [2, 21, 33–38], BPC 157 may consolidate prostaglandin system function [1–13]. This may be also a follow-up of Robert's cytoprotection concept general understanding and applicability (i.e., epithelium/endothelium maintenance *vs.* prostaglandin-system inhibition by NSAIDs) [39] and BPC 157 role as the novel cytoprotection mediator [1–13]. It is therefore also logical to expect that thrombocyte function will be also maintained. BPC 157 largely reversed various NSAID-toxicities, after both COX 1 and COX 2 inhibitors, also gastrointestinal, liver, and brain lesions that appeared after their overdose(s) application(s) [8, 40–43], and has its own particular anti-inflammatory effect (BPC 157 counteracts the increase of the proinflammatory and procachectic cytokines [2]), and may both prevent and reverse adjuvant arthritis in rats [44]. Furthermore, BPC 157/NO-relationship is established in various experimental models and species, providing that it might interfere with the effects of either NOS-blockade or NOS-substrate agent application [1–12], and thereby consolidate NO-system toward better healing effect, thus maintaining platelet function along with the endothelium maintenance. Likely, such balanced thrombocyte function may also contribute to the beneficial effect obtained in the rats with occluded blood vessels [21–25]. Rapid activation of the bypassing loop occurs with BPC 157 therapy in the rats with the infrarenal occlusion of the inferior caval vein (and thereby resolved Virchow, venous lesion and thrombosis, caval hypertension, aortal hypotension, and consequent thrombocytopenia) [21]. It occurs much like in the rats with ischemic/reperfusion colitis, duodenal venous congestion lesions, perforated cecum, bile duct ligation-induced liver cirrhosis, and portal hypertension [22–25].

In conclusion, BPC 157 may exert a particular effect on thrombocyte function, being a promising agent in further application. This should be however seen with known limitations (i.e., the effect of acetylsalicylic acid and clopidogrel does not have any influence on thromboelastometry/thromboelastography, as well [45]).

## Data Availability

The data used to support the findings of manuscript 9084643 titled "Intragastric Application of Aspirin, Clopidogrel, Cilostazol, and BPC 157 in Rats: Platelet Aggregation and Blood Clot" are included within the article.

## Conflicts of Interest

All authors declare that they have no conflict of interest.

## Acknowledgments

This study was funded by the Ministry of Science, Education and Sports, Republic of Croatia (Grant No. 108-1083570-3635).

## References

[1] P. Sikiric, K. B. Hahm, A. B. Blagaic et al., "Stable gastric pentadecapeptide BPC 157, Robert's stomach cytoprotection/-adaptive cytoprotection/organoprotection, and Selye's stress coping response: progress, achievements, and the future," *Gut Liver*, vol. 13, 2019.

[2] E. A. Kang, Y. M. Han, J. M. An et al., "BPC157 as potential agent rescuing from cancer cachexia," *Current Pharmaceutical Design*, vol. 24, no. 18, pp. 1947–1956, 2018.

[3] S. Seiwerth, L. Brcic, L. Vuletic et al., "BPC 157 and blood vessels," *Current Pharmaceutical Design*, vol. 20, no. 7, pp. 1121–1125, 2014.

[4] S. Seiwerth, R. Rucman, B. Turkovic et al., "BPC 157 and standard angiogenic growth factors, gastrointestinal tract healing, lessons from tendon, ligament, muscle and bone healing," *Current Pharmaceutical Design*, vol. 24, no. 18, pp. 1972–1989, 2018.

[5] P. Sikiric, S. Seiwerth, L. Brcic et al., "Revised Robert's cytoprotection and adaptive cytoprotection and stable gastric pentadecapeptide BPC 157. Possible significance and implications for novel mediator," *Current Pharmaceutical Design*, vol. 16, no. 10, pp. 1224–1234, 2010.

[6] P. Sikiric, S. Seiwerth, R. Rucman et al., "Stable gastric pentadecapeptide BPC 157: novel therapy in gastrointestinal tract," *Current Pharmaceutical Design*, vol. 17, no. 16, pp. 1612–1632, 2011.

[7] P. Sikiric, S. Seiwerth, R. Rucman et al., "Focus on ulcerative colitis: stable gastric pentadecapeptide BPC 157," *Current Medicinal Chemistry*, vol. 19, no. 1, pp. 126–132, 2012.

[8] P. Sikiric, S. Seiwerth, R. Rucman et al., "Toxicity by NSAIDs. Counteraction by stable gastric pentadecapeptide BPC 157," *Current Pharmaceutical Design*, vol. 19, no. 1, pp. 76–83, 2012.

[9] P. Sikiric, S. Seiwerth, R. Rucman et al., "Stable gastric pentadecapeptide BPC 157-NO-system relation," *Current Pharmaceutical Design*, vol. 20, no. 7, pp. 1126–1135, 2014.

[10] P. Sikiric, S. Seiwerth, R. Rucman et al., "Brain-gut axis and pentadecapeptide BPC 157: theoretical and practical implications," *Current Neuropharmacology*, vol. 14, no. 8, pp. 857–865, 2016.

[11] P. Sikiric, S. Seiwerth, R. Rucman et al., "Stress in gastrointestinal tract and stable gastric pentadecapeptide BPC 157. Finally, do we have a solution?," *Current Pharmaceutical Design*, vol. 23, no. 27, pp. 4012–4028, 2017.

[12] P. Sikiric, R. Rucman, B. Turkovic et al., "Novel cytoprotective mediator, stable gastric pentadecapeptide BPC 157. Vascular recruitment and gastrointestinal tract healing," *Current Pharmaceutical Design*, vol. 24, no. 18, pp. 1990–2001, 2018.

[13] D. Gwyer, N. M. Wragg, and S. L. Wilson, "Gastric pentadecapeptide body protection compound BPC 157 and its role in accelerating musculoskeletal soft tissue healing," *Cell and Tissue Research*, vol. 377, no. 2, pp. 153–159, 2019.

[14] X. R. Xu, N. Carrim, M. A. D. Neves et al., "Platelets and platelet adhesion molecules: novel mechanisms of thrombosis and anti-thrombotic therapies," *Thrombosis Journal*, vol. 14, no. S1, p. 29, 2016.

[15] O. Tóth, A. Calatzis, S. Penz, H. Losonczy, and W. Siess, "Multiple electrode aggregometry: a new device to measure platelet aggregation in whole blood," *Thrombosis and Haemostasis*, vol. 96, no. 6, pp. 781–788, 2006.

[16] M. Defontis, S. Cote, M. Stirn, and D. Ledieu, "Optimization of Multiplate(®) whole blood platelet aggregometry in the Beagle dog and Wistar rat for ex vivo drug toxicity testing," *Experimental and Toxicologic Pathology*, vol. 65, no. 5, pp. 637–644, 2013.

[17] A. A. Hanke, K. Roberg, E. Monaca et al., "Impact of platelet count on results obtained from multiple electrode platelet aggregometry (Multiplate)," *European Journal of Medical Research*, vol. 15, no. 5, pp. 214–219, 2010.

[18] R. J. Luddington, "Thrombelastography/thromboelastometry," *Clinical and Laboratory Haematology*, vol. 27, no. 2, pp. 81–90, 2005.

[19] R. C. Franz, "ROTEM analysis: a significant advance in the field of rotational thrombelastography," *South African Journal of Surgery*, vol. 47, no. 1, pp. 2–6, 2009.

[20] K. Satoh, I. Fukasawa, K. Kanemaru et al., "Platelet aggregometry in the presence of PGE(1) provides a reliable method for cilostazol monitoring," *Thrombosis Research*, vol. 130, no. 4, pp. 616–621, 2012.

[21] J. Vukojević, M. Siroglavić, K. Kašnik et al., "Rat inferior caval vein (ICV) ligature and particular new insights with the stable gastric pentadecapeptide BPC 157," *Vascular Pharmacology*, vol. 106, pp. 54–66, 2018.

[22] A. Duzel, J. Vlainic, M. Antunovic et al., "Stable gastric pentadecapeptide BPC 157 in the treatment of colitis and ischemia and reperfusion in rats: new insights," *World Journal of Gastroenterology*, vol. 23, no. 48, pp. 8465–8488, 2017.

[23] A. Z. Sever, M. Sever, T. Vidovic et al., "Stable gastric pentadecapeptide BPC 157 in the therapy of the rats with bile duct ligation," *European Journal of Pharmacology*, vol. 847, pp. 130–142, 2019.

[24] D. Drmic, M. Samara, T. Vidovic et al., "Counteraction of perforated cecum lesions in rats: effects of pentadecapeptide BPC 157, L-NAME and L-arginine," *World Journal of Gastroenterology*, vol. 24, no. 48, pp. 5462–5476, 2018.

[25] F. Amic, D. Drmic, Z. Bilic et al., "Bypassing major venous occlusion and duodenal lesions in rats, and therapy with the stable gastric pentadecapeptide BPC 157, L-NAME and L-arginine," *World Journal of Gastroenterology*, vol. 24, no. 47, pp. 5366–5378, 2018.

[26] M. Hrelec, R. Kliček, L. Brčić et al., "Abdominal aorta anastomosis in rats and stable gastric pentadecapeptide BPC 157, prophylaxis and therapy," *Journal of Physiology and Pharmacology*, vol. 60, no. S7, pp. 161–165, 2009.

[27] M. Stupnisek, S. Franjic, D. Drmic et al., "Pentadecapeptide BPC 157 reduces bleeding time and thrombocytopenia after amputation in rats treated with heparin, warfarin or aspirin," *Thrombosis Research*, vol. 129, no. 5, pp. 652–659, 2012.

[28] M. Stupnisek, A. Kokot, D. Drmic et al., "Pentadecapeptide BPC 157 reduces bleeding and thrombocytopenia after amputation in rats treated with heparin, warfarin, L-NAME and L-arginine," *PLoS One*, vol. 10, no. 4, p. e0123454, 2015.

[29] Z. M. Ruggeri, "Platelets in atherothrombosis," *Nature Medicine*, vol. 8, no. 11, pp. 1227–1234, 2002.

[30] K. Yasunaga and K. Mase, "Antiaggregatory effect of oral cilostazol and recovery of platelet aggregability in patients with cerebrovascular disease," *Arzneimittel-Forschung*, vol. 35, no. 7A, pp. 1189–1192, 1985.

[31] Y. Ikeda, M. Kikuchi, H. Murakami et al., "Comparison of the inhibitory effects of cilostazol, acetylsalicylic acid and ticlopidine on platelet functions ex vivo. Randomized, double-blind cross-over study," *Arzneimittel-Forschung*, vol. 37, no. 5, pp. 563–566, 1987.

[32] J. W. Eikelboom, G. J. Hankey, J. Thom et al., "Enhanced antiplatelet effect of clopidogrel in patients whose platelets are least inhibited by aspirin: a randomized crossover trial," *Journal of Thrombosis and Haemostasis*, vol. 3, no. 12, pp. 2649–2655, 2005.

[33] M. J. Hsieh, H. T. Liu, C. N. Wang et al., "Therapeutic potential of pro-angiogenic BPC 157 is associated with VEGFR2 activation and up-regulation," *Journal of Molecular Medicine*, vol. 95, no. 3, pp. 323–333, 2017.

[34] T. Huang, J. Gu, K. Zhang et al., "Body protective compound-157 enhances alkali-burn wound healing in vivo and promotes proliferation, migration, and angiogenesis in vitro," *Drug Design, Development and Therapy*, vol. 9, pp. 2485–2499, 2015.

[35] C. H. Chang, W. C. Tsai, Y. H. Hsu, and J. H. Pang, "Pentadecapeptide BPC 157 enhances the growth hormone receptor expression in tendon fibroblasts," *Molecules*, vol. 19, no. 11, pp. 19066–19077, 2014.

[36] C. H. Chang, W. C. Tsai, M. S. Lin, Y. H. Hsu, and J. H. S. Pang, "The promoting effect of pentadecapeptide BPC 157 on tendon healing involves tendon outgrowth, cell survival, and cell migration," *Journal of Applied Physiology*, vol. 110, no. 3, pp. 774–780, 2011.

[37] V. Cesarec, T. Becejac, M. Misic et al., "Pentadecapeptide BPC 157 and the esophagocutaneous fistula healing therapy,"

*European Journal of Pharmacology*, vol. 701, no. 1-3, pp. 203–212, 2013.

[38] V. I. Tkalčević, S. Čužić, K. Brajša et al., "Enhancement by PL 14736 of granulation and collagen organization in healing wounds and the potential role of *egr-1* expression," *European Journal of Pharmacology*, vol. 570, no. 1-3, pp. 212–221, 2007.

[39] A. Robert, "Cytoprotection by prostaglandins," *Gastroenterology*, vol. 77, 4 Part 1, pp. 761–767, 1979.

[40] S. Ilic, D. Drmic, K. Zarkovic et al., "Ibuprofen hepatic encephalopathy, hepatomegaly, gastric lesion and gastric pentadecapeptide BPC 157 in rats," *European Journal of Pharmacology*, vol. 667, no. 1-3, pp. 322–329, 2011.

[41] S. Ilic, D. Drmic, S. Franjic et al., "Pentadecapeptide BPC 157 and its effects on a NSAID toxicity model: diclofenac-induced gastrointestinal, liver, and encephalopathy lesions," *Life Sciences*, vol. 88, no. 11-12, pp. 535–542, 2011.

[42] S. Ilic, D. Drmic, K. Zarkovic et al., "High hepatotoxic dose of paracetamol produces generalized convulsions and brain damage in rats. A counteraction with the stable gastric pentadecapeptide BPC 157 (PL 14736)," *Journal of Physiology and Pharmacology*, vol. 61, no. 2, pp. 241–250, 2010.

[43] D. Drmic, D. Kolenc, S. Ilic et al., "Celecoxib-induced gastrointestinal, liver and brain lesions in rats, counteraction by BPC 157 or L-arginine, aggravation by L-NAME," *World Journal of Gastroenterology*, vol. 23, no. 29, pp. 5304–5312, 2017.

[44] P. Sikiric, S. Seiwerth, Z. Grabarevic et al., "Pentadecapeptide BPC 157 positively affects both non-steroidal anti-inflammatory agent-induced gastrointestinal lesions and adjuvant arthritis in rats," *Journal of Physiology*, vol. 91, no. 3-5, pp. 113–122, 1997.

[45] T. Lang and M. von Depka, "Possibilities and limitations of thrombelastometry/-graphy," *Hämostaseologie*, vol. 26, 3 Suppl 1, pp. S20–S29, 2006.

Hindawi
Oxidative Medicine and Cellular Longevity
Volume 2019, Article ID 2193019, 19 pages
https://doi.org/10.1155/2019/2193019

*Research Article*

# Inhibitor 1 of Protein Phosphatase 1 Regulates $Ca^{2+}$/Calmodulin-Dependent Protein Kinase II to Alleviate Oxidative Stress in Hypoxia-Reoxygenation Injury of Cardiomyocytes

**Huiqin Luo,[1] Shu Song,[1] Yun Chen,[1,2] Mengting Xu,[1] Linlin Sun,[1] Guoliang Meng,[1,2] and Wei Zhang[1,2]**

[1]*Department of Pharmacology, School of Pharmacy, Nantong University, Key Laboratory of Inflammation and Molecular Drug Target of Jiangsu Province, Nantong, Jiangsu, China*
[2]*School of Medicine, Nantong University, Nantong, Jiangsu, China*

Correspondence should be addressed to Guoliang Meng; mengguoliang@ntu.edu.cn and Wei Zhang; zhangw@ntu.edu.cn

Received 5 August 2019; Revised 20 September 2019; Accepted 13 November 2019; Published 7 December 2019

Guest Editor: Mallika Ghosh



$Ca^{2+}$/calmodulin-dependent protein kinase II (CaMKII), regulated by inhibitor 1 of protein phosphatase 1 (I1PP1), is vital for maintaining cardiovascular homeostasis. However, the role and mechanism of I1PP1 against hypoxia-reoxygenation (H/R) injury in cardiomyocytes remain a question. In our study, after I1PP1 overexpression by adenovirus infection in the neonatal cardiomyocytes followed by hypoxia for 4 h and reoxygenation for 12 h, the CaMKII$\delta$ alternative splicing subtype, ATP content, and lactate dehydrogenase (LDH) release were determined. CaMKII activity was evaluated by phosphoprotein phosphorylation at Thr17 (p-PLB Thr17), CaMKII phosphorylation (p-CaMKII), and CaMKII oxidation (ox-CaMKII). Reactive oxygen species (ROS), mitochondrial membrane potential, dynamin-related protein 1 (DRP1), and optic atrophy 1 (OPA1) expressions were assessed. Our study verified that I1PP1 overexpression attenuated the CaMKII$\delta$ alternative splicing disorder; suppressed PLB phosphorylation at Thr17, p-CaMKII, and ox-CaMKII; decreased cell LDH release; increased ATP content; attenuated ROS production; increased mitochondrial membrane potential; and decreased DRP1 expression but increased OPA1 expression in the cardiomyocytes after H/R. Contrarily, CaMKII$\delta$ alternative splicing disorder, LDH release, ATP reduction, and ROS accumulation were aggravated after H/R injury with the I1PP1 knockdown. Collectively, I1PP1 overexpression corrected disorders of CaMKII$\delta$ alternative splicing, inhibited CaMKII phosphorylation, repressed CaMKII oxidation, suppressed ROS production, and attenuated cardiomyocyte H/R injury.

## 1. Introduction

Myocardial ischemia-reperfusion injury (MIRI) is a phenomenon wherein the myocardial function is not improved but aggravated immediately after blood perfusion is restored in the ischemic myocardium [1–4]. MIRI is often accompanied by cardiac and vascular adverse events such as arrhythmia, enlarged infarct size, persistent ventricular systolic dysfunction, or even no reflow, which seriously impair the prognosis of myocardial ischemia [5–7]. MIRI is a complex pathophysiological process involving multiple factors, such as oxygen-free radicals, calcium overload, inflammation, apoptosis, and endothelial cell homeostasis imbalance [8–10], in which excess of oxygen-free radicals is the critical factor for reperfusion injury [11]. Moreover, MIRI is a common cause of early cardiac dysfunction after cardiac surgery, which is a difficult problem to limit the treatment and prognosis of ischemic heart disease [12].

Calcium/calmodulin-dependent protein kinase II (CaMKII) is one serine-threonine protein kinase with multifunctions, which is abundant in the myocardium and other excitable tissues [13, 14]. Four isoforms of CaMKII$\delta$ ($\alpha$, $\beta$, $\gamma$, and $\delta$) have been found as of now. CaMKII$\delta$ is the most abundant subtype in the myocardium [15]. In the presence of alternative splicing, CaMKII$\delta$ is capable of producing three splicing variants of $\delta$A, $\delta$B, and $\delta$C

with the action of splicing factors [8–10]. Three different subtypes of CaMKII$\delta$ play diverse roles in the cardiovascular system. CaMKII$\delta$A was critical for cardiac systolic and diastolic function [16]. CaMKII$\delta$B regulated myocardial hypertrophy and progenitor cell survival in the myocardium [17]. CaMKII$\delta$C was closely related to cardiomyocyte apoptosis during myocardial remodeling [18].

Besides $Ca^{2+}$/calmodulin, CaMKII could also be activated by phosphorylation and oxidation [19–21]. Sustained excessive CaMKII activation has adverse effects on a variety of heart diseases [22, 23]. Some studies have found that CaMKII activity bloomed at the beginning of MIRI, which promoted calcium extravasation of the sarcoplasmic reticulum and aggravated myocardial dysfunction and injury [24, 25]. Alleviation of CaMKII activity is beneficial to attenuate the degree of MIRI, reduce the excessive production of reactive oxygen species (ROS) [26], and inhibit apoptosis and necrosis, which is advantageous for the recovery of the myocardial function [27]. In addition, CaMKII is also one of the key mediators for myocardial necroptosis [28]. Therefore, CaMKII is commonly regarded as the core signal in cardiomyocytes [14]. Although there were several common CaMKII inhibitors such as KN93 or AIP, the specificity and potency of these compounds limit their application due to some other effects unrelated to CaMKII inhibition [29]. Moreover, as an inhibitor of CaMKII, KN93 competitively inhibits the binding of calmodulin to kinase, but not the autonomic activity of CaMKII [29]. Altogether, CaMKII activity regulation might be a potential method to alleviate MIRI.

Protein phosphatase 1 (PP1) is regulated by intracellular calcium fluctuations in the heart to change the phosphorylation level of multiple proteins [30–33]. Studies have shown that PP1 is upregulated in the heart of patients suffering from cardiac hypertrophy, cardiac dysfunction, and heart failure [34–36]. Lack of PP1 protected against arrhythmias and myocardial hypertrophy [37]. Moreover, PP1 promoted CaMKII$\delta$ splicing. When PP1 increased, the ratio of CaMKII$\delta$ alternative splicing products could be imbalanced, resulting in an enhancement of CaMKII$\delta$C variants but a reduction of CaMKII$\delta$B and CaMKII$\delta$A variants [33]. Therefore, the pharmacological targeting of PP1 activity is believed to be useful in therapy and interventions for a variety of cardiomyopathies such as MIRI [38–41]. As far as we know, inhibitor 1 of protein phosphatase 1 (I1PP1) is an endogenous inhibitor to decrease PP1 activity or to inhibit PP1 expression [42]. I1PP1 upregulation accelerated $Ca^{2+}$ cycling, improved cardiac function, and alleviated cell injury [43, 44].

Therefore, hypoxia-reoxygenation (H/R) of cardiomyocytes in vitro was used to verify the effect of I1PP1 overexpression on CaMKII activity and alternative splicing. The detailed mechanism of I1PP1 overexpression against H/R injury was also explored. It is beneficial to provide a new strategy for MIRI.

## 2. Methods and Materials

*2.1. Cell Culture and Hypoxia-Reoxygenation Injury Model.* Neonatal cardiomyocytes were extracted from Sprague-Dawley (SD) rats aging 1-3 days by trypsin (Beyotime, Shanghai, China) digestion. After culturing for 2-3 days, the cells were incubated with the DMEM medium (Gibco, Carlsbad, CA) containing 1 g/L glucose and 0.5% FBS (Gibco, Carlsbad, CA) and cultured in the incubator with 94% $N_2$, 1% $O_2$, and 5% $CO_2$ to induce hypoxia. Four hours later, the medium was changed into 5.5 g/L glucose and 10% FBS and incubated in an incubator with 5% $CO_2$ and normal air. After another 12 h for reoxygenation, the cardiomyocytes were collected for further experiments. CaMKII inhibitor KN93 (1 $\mu$M, MedChemExpress, Monmouth Junction, NJ) was preincubated for 1 h before hypoxia and reoxygenation.

The present experiment strictly complied with guidelines for the Care and Use of Laboratory Animals from the Institute for Laboratory Animal Research, National Research Council, Washington, D.C., National Academy Press, 2011, and any updates. The detailed protocols were also approved by a specific committee in Nantong University (NTU-20161210).

*2.2. I1PP1 Adenovirus Infection.* Rat full length of I1PP1 (Gene ID, 58977, $1 \times 10^{11}$ PFU/mL) or vector ($1 \times 10^{11}$ PFU/mL) recombinant adenovirus solution (Hanbio Biotechnology Co., Ltd., Shanghai, China) with MOI value of 100 was infected into the cardiomyocytes. After 4 h, the adenovirus solution were washed out and DMEM medium with 10% FBS was replaced. Vector ($1 \times 10^{11}$ PFU/mL) recombinant adenovirus was applied as a negative control. Then, the cells were subjected to immunofluorescent staining, western blot, or hypoxia-reoxygenation injury.

*2.3. RNA Interference.* Three antisense oligodeoxynucleotides against rat I1PP1 mRNA (#1, 5′-AGACAATGGTTGAACA TCA-3′; #2, 5′-GCAGAATCCAAACCCAAGA-3′; #3, 5′-TCAGCGTCAAGGCCAGATA′-3′) and nonspecific control siRNA (NC siRNA) were commercially obtained (RiboBio, Guangzhou, China).

After serum deprivation for 24 h, the above siRNA was transfected into the cardiomyocytes with Lipofectamine 2000 (Invitrogen, Carlsbad, CA) and subjected to hypoxia-reoxygenation injury.

*2.4. Lactate Dehydrogenase (LDH) Measurement.* The level of LDH in the medium was detected by a commercial LDH-Cytotoxic Assay Kit (Beyotime, Shanghai, China). The cardiomyocytes were cultured in a 24-well plate with a density about 80%. After I1PP1 recombinant adenovirus infection followed by hypoxia for 4 h and reoxygenation for 12 h, the supernatant of 120 $\mu$L was taken into a 96-well plate after centrifugation, and 60 $\mu$L of the test solution was mixed into each well. Then, the plate was placed without light for 30 min at 25°C. LDH release into the medium was calculated according to the absorbance at 490 nm, which was normalized by the value in the control group.

*2.5. ATP Measurement.* The content of ATP in the cardiomyocytes was detected by a commercial ATP Assay Kit (Beyotime, Shanghai, China). After treatment and equilibration, 100 $\mu$L of a CellTiter-Lumi™ luminescence assay

Table 1: The sequences of the primers for real-time PCR.

| Gene | Forward primers | Reverse primers |
|---|---|---|
| CaMKIIδA | 5′-CGAGAAATTTTTCAGCAGCC-3′ | 5′-ACAGTAGTTTGGGGCTCCAG-3′ |
| CaMKIIδB | 5′-CGAGAAATTTTTCAGCAGCC-3′ | 5′-GCTCTCAGTTGACTCCATCATC-3′ |
| CaMKIIδC | 5′-CGAGAAATTTTTCAGCAGCC-3′ | 5′-CTCAGTTGACTCCTTTACCCC-3′ |
| 18S | 5′-AGTCCCTGCCCTTTGTACACA-3′ | 5′-CGATCCGAGGGCCTCACTA-3′ |

Table 2: The primary antibodies for western blot.

| Protein | Dilution | Company |
|---|---|---|
| I1PP1 | 1 : 5000 | Abcam, Cambridge, UK |
| OPA1 | 1 : 1000 | Abcam, Cambridge, UK |
| CaMKII | 1 : 1000 | Abcam, Cambridge, UK |
| PP1 | 1 : 1000 | Santa Cruz Biotechnology, Santa Cruz, CA, USA |
| PLB | 1 : 1000 | Santa Cruz Biotechnology, Santa Cruz, CA, USA |
| p-PLB Thr17 | 1 : 1000 | Santa Cruz Biotechnology, Santa Cruz, CA, USA |
| DRP1 | 1 : 1000 | Cell Signaling Technology, Danvers, MA, USA |
| p-CaMKII | 1 : 1000 | Thermo Fisher Scientific, Rockford, IL, USA |
| ox-CaMKII | 1 : 1000 | Millipore, Billerica, MA, USA |
| GAPDH | 1 : 5000 | Sigma-Aldrich, St. Louis, MO, USA |
| $\beta$-Tubulin | 1 : 3000 | CMCTAG, Milwaukee, WI, USA |

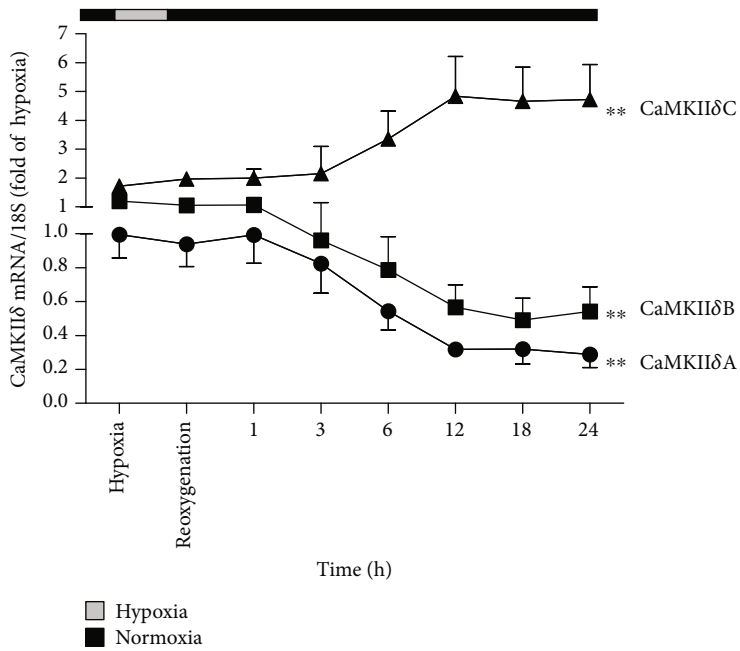


Figure 1: CaMKIIδ variants disordered in cardiomyocytes during H/R injury. After culture in 94% $N_2$, 1% $O_2$, and 5% $CO_2$ for 4 h, the cardiomyocytes were changed into 95% air and 5% $CO_2$. The mRNA levels of CaMKIIδA, CaMKIIδB, and CaMKIIδC of the cardiomyocytes at the start of the hypoxia and different times after reoxygenation were detected by quantitative real-time PCR. 18S was serviced as a housekeeping mRNA. Plots represent the mean ± SEM; $n = 6$. Statistical significance: $^{**}P < 0.01$ compared with "the start of the hypoxia."

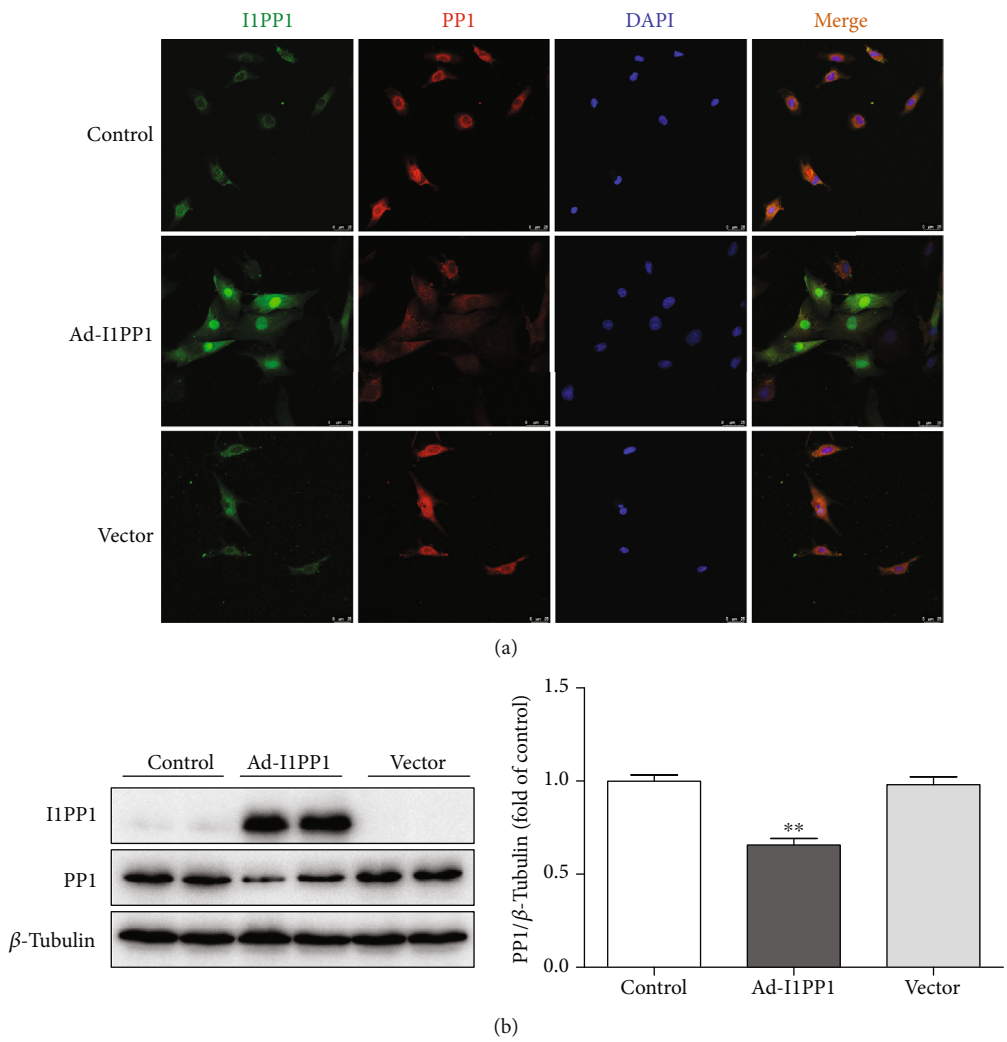


Figure 2: Recombinant adenovirus infection increased I1PP1 but decreased PP1 expression in cardiomyocytes. (a) After the recombinant adenovirus solution carrying the I1PP1 gene or vector was infected into the cardiomyocytes, I1PP1 and PP1 were immunofluorescence stained using Alexa Fluor 488- (green) or Cy3- (red) conjugated IgG. The nuclei were stained using DAPI (blue). Bar = 100 $\mu$m. (b) Expression of the I1PP1 and PP1 protein was quantified in the cardiomyocytes by western blot. $\beta$-Tubulin was used as a loading control. Plots represent the mean ± SEM; $n = 6$. Statistical significance: $^{**}P < 0.01$ compared with the control.

reagent was completely mixed with the medium. Then, the luminescence intensity was obtained with a spectrophotometer (BioTek Instruments, Inc., USA). The relative ATP level was calculated and normalized by the value in the control group.

*2.6. ROS Measurement.* After incubation with dihydroethidium (DHE, 2 $\mu$M, Beyotime, Shanghai, China) at 37°C for 30 min, the superoxide production, considered as the DHE fluorescence intensity, in the cardiomyocytes was assessed with a laser confocal microscope (Leica, Wetzlar, Germany) and quantified using ImageJ software.

After incubation with MitoTracker Green (100 nM, Beyotime, Shanghai, China) and MitoSOX (5 $\mu$M, YEASEN, Shanghai, China) at 37°C for 20 min, mitochondrial ROS, considered as the MitoSOX fluorescence intensity, in the cardiomyocytes was assessed with a laser confocal microscope at 490/516 nm wavelengths for MitoTracker Green and 510/580 nm wavelengths for MitoSOX, respectively, which was quantified using ImageJ software.

*2.7. Mitochondrial Membrane Potential ($\Delta\psi m$) Detection.* After incubation with JC-1 staining solution (Beyotime, Shanghai, China) for 20 min, $\Delta\psi m$, considered as the fluorescence intensity, in the cardiomyocytes was assessed with a laser confocal microscope at 495/519 nm wavelengths for the J-monomer and 550/570 nm wavelengths for the J-aggregates, which was quantified using ImageJ software.

*2.8. Immunofluorescent Staining.* After incubation with primary anti-optic atrophy 1 (OPA1, 1 : 50) or anti-dynamin-related protein 1 (DRP1, 1 : 50) antibodies for 12 h at 4°C, the cardiomyocytes were incubated with IgG conjugated with Cy3 or Alexa Fluor 488 (1 : 500; Beyotime, Shanghai, China) for 2 h. The protein expression which is considered as the fluorescence intensity was assessed.

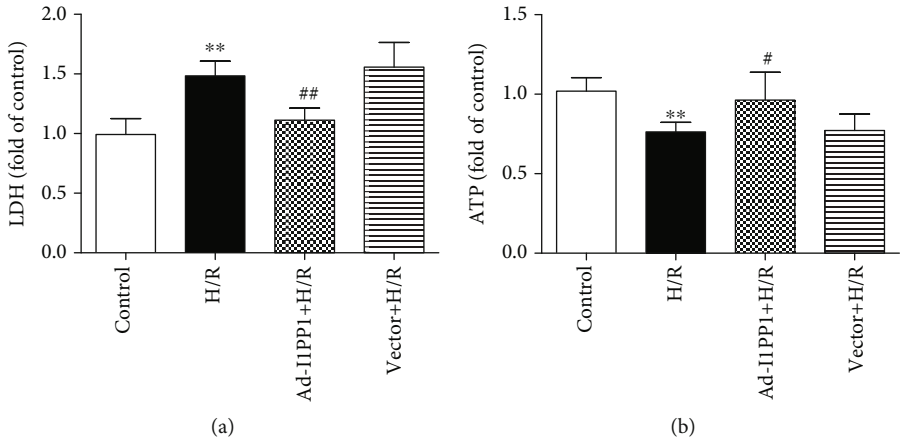


Figure 3: I1PP1 overexpression reduced the LDH release but increased the ATP level in cardiomyocytes after H/R injury. After infection of I1PP1 recombinant adenovirus, the cardiomyocytes were subjected to hypoxia for 4 h followed by 12 h reoxygenation. (a) LDH release in the culture medium was measured. (b) ATP level of the cardiomyocytes was measured. Plots represent the mean ± SEM; $n = 6$. Statistical significance: $^{**}P < 0.01$ compared with the control; $^{\#}P < 0.05$ and $^{\#\#}P < 0.01$ compared with H/R.

*2.9. Real-Time PCR.* After extraction of total RNA with TRIzol from the cardiomyocytes, 1 $\mu$L RNA sample, 2 $\mu$L 5x reaction buffer, and 7 $\mu$L DEPC water were mixed in the RNase-free tube. The procedure for reverse transcription was set up: incubation at 37°C for 15 minutes and 85°C for 5 s, and preservation at 4°C. Reversed cDNA was added into the SYBR Green qPCR mix for amplification (ABI, Carlsbad, CA, USA). The primer sequences (Table 1) of CaMKII$\delta$ and housekeeping mRNA were synthesized by Sangon Biotech Co., Ltd. (Shanghai, China). Quantitative real-time PCR analyses were performed three times for each group of DNA. The relative mRNA level was calculated by the comparative delta-delta cycle threshold (CT) method.

*2.10. Western Blot.* The proteins of about 50 $\mu$g were separated by sodium dodecyl sulfate-polyacrylamide gel electrophoresis (SDS-PAGE) and transferred to a polyvinylidene fluoride (PVDF) membrane. Next, the membrane was blocked by 5% milk without fat for 2 h followed by incubation with primary antibodies (Table 2) [45–47] at 4°C overnight. After washing, the membrane was incubated by horseradish peroxidase- (HRP-) conjugated IgG (Beyotime, Shanghai, China) for another 2 h. Enhanced chemiluminescence (ECL, Thermo Fisher Scientific Inc., Rockford, IL, USA) was dropped on the membrane to visualize the protein bands.

*2.11. Statistical Analysis.* The data were expressed as mean ± Standard Error of the Mean (SEM), which were analyzed by one-way ANOVA followed by Bonferroni post hoc test. $P$ values lower than 0.05 were regarded as a significant difference.

## 3. Results

*3.1. CaMKII$\delta$ Variants Disordered in Cardiomyocytes during Hypoxia-Reoxygenation Injury.* Because antibodies for CaMKII$\delta$ variants were unavailable, CaMKII$\delta$A, CaMKII$\delta$B, and CaMKII$\delta$C expressions were measured by quantitative real-time PCR at the start of hypoxia and different times after reoxygenation. There was no significant change on CaMKII$\delta$ variants after hypoxia for 4 h. Both CaMKII$\delta$A and CaMKII$\delta$B expressions were reduced, while the CaMKII$\delta$C expression increased after reoxygenation for 6 h, which was most obvious at 12 h. The data suggested that cardiomyocyte H/R injury induced a significant disorder on CaMKII$\delta$ variants (Figure 1).

*3.2. I1PP1 Overexpression Reduced LDH Release but Increased ATP Level in Cardiomyocytes after H/R Injury.* However, whether the correction of the CaMKII$\delta$ variant disorder was beneficial to attenuate H/R injury remains unknown. Next, the recombinant adenovirus technology was applied to induce I1PP1 overexpression in our study. PP1 antibody against PP1$\alpha$ was applied for detection of PP1 family catalytic subunits. We found that I1PP1 expression increased while PP1 expression decreased after recombinant adenovirus infection (Figure 2).

After infection, hypoxia-reoxygenation was performed in the cardiomyocytes. There was more LDH in the medium after H/R, suggesting that H/R induced more serious injury. Moreover, I1PP1 overexpression in the cardiomyocytes significantly reduced LDH release (Figure 3(a)).

Dysfunction of energy metabolism is an important mechanism of myocardial ischemia-reperfusion injury [48]. ATP production was also detected to evaluate H/R injury in the cardiomyocytes. The data showed that ATP production was blocked after H/R in the cardiomyocytes, which was restored by I1PP1 overexpression (Figure 3(b)).

*3.3. I1PP1 Overexpression Regulated CaMKII Activity and CaMKII$\delta$ Alternative Splicing in Cardiomyocytes after H/R Injury.* Previous researches verified that PLB phosphorylation at Thr17 was a robust marker for CaMKII activity, which was commonly used for CaMKII activity assessment [33]. Our present study confirmed that I1PP1

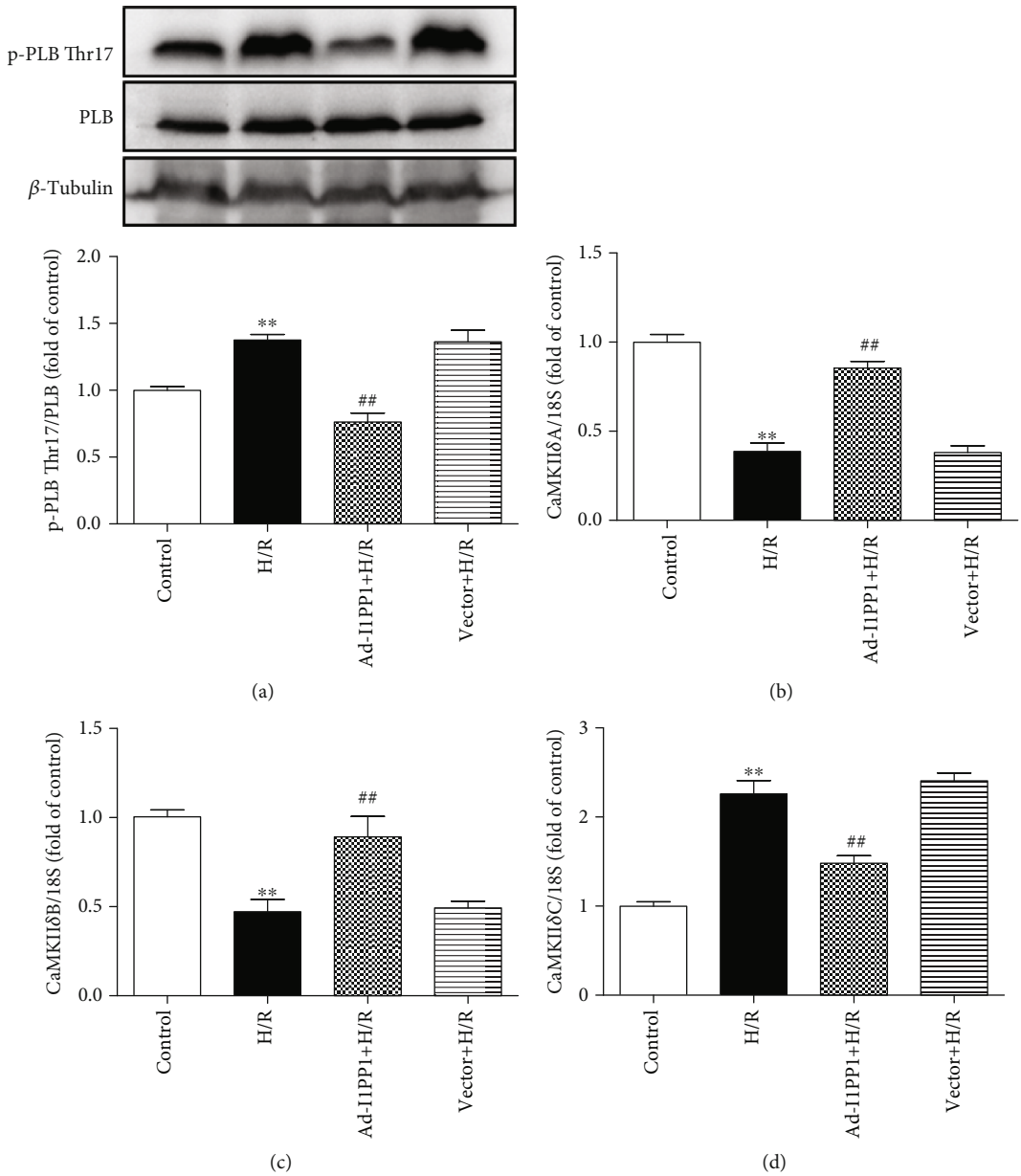


Figure 4: I1PP1 overexpression regulated CaMKII activity and CaMKII$\delta$ alternative splicing in cardiomyocytes after H/R injury. After infection of the I1PP1 recombinant adenovirus, the cardiomyocytes were subjected to hypoxia for 4 h followed by 12 h reoxygenation. (a) Expression of p-PLB Thr17 and PLB in the cardiomyocytes was quantified by western blot. $\beta$-Tubulin was used as a loading control. (b–d) The mRNA levels of CaMKII$\delta$A, CaMKII$\delta$B, and CaMKII$\delta$C in the cardiomyocytes were detected by quantitative real-time PCR. 18S was serviced as a housekeeping mRNA. Plots represent the mean ± SEM; $n = 6$. Statistical significance: $^{**}P < 0.01$ compared with the control; $^{\#\#}P < 0.01$ compared with H/R.

overexpression significantly inhibited PLB phosphorylation at Thr17 after H/R, suggesting that CaMKII activity was weakened due to a high level of I1PP1 (Figure 4(a)). It was also noted that CaMKII$\delta$A and CaMKII$\delta$B splicing variants significantly decreased, while CaMKII$\delta$C significantly increased after H/R. Moreover, I1PP1 overexpression increased CaMKII$\delta$A and CaMKII$\delta$B but decreased CaMKII$\delta$C expression (Figures 4(b)–4(d)). All these data suggested that both CaMKII activity and CaMKII$\delta$ alternative splicing disorder were corrected by I1PP1 overexpression after H/R.

*3.4. I1PP1 Overexpression Inhibited ROS but Elevated Mitochondrial Membrane Potential in Cardiomyocytes after H/R Injury.* Excessive ROS production was considered as one critical mechanism for myocardial I/R injury [49, 50]. Therefore, ROS production in the global cell and the mitochondria was detected with DHE and MitoSOX staining, respectively. The results indicated that there was stronger fluorescence intensity of DHE and MitoSOX after H/R, which was significantly attenuated by I1PP1 overexpression (Figures 5(a) and 5(b)).

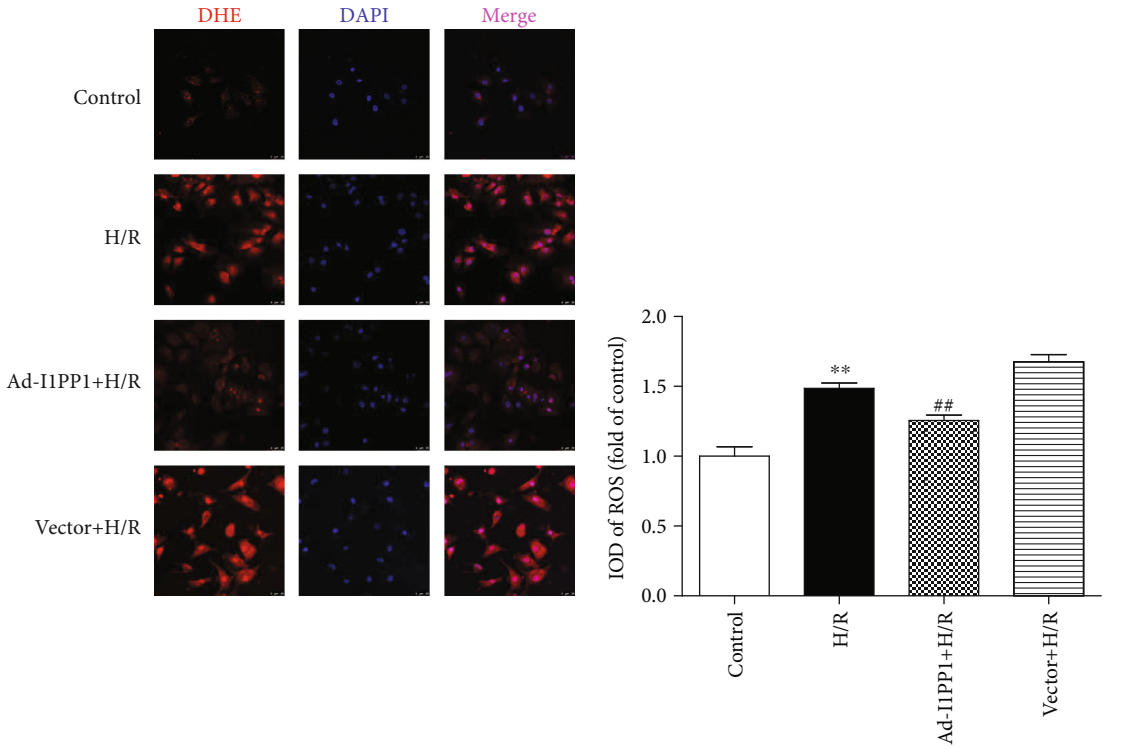


(a)

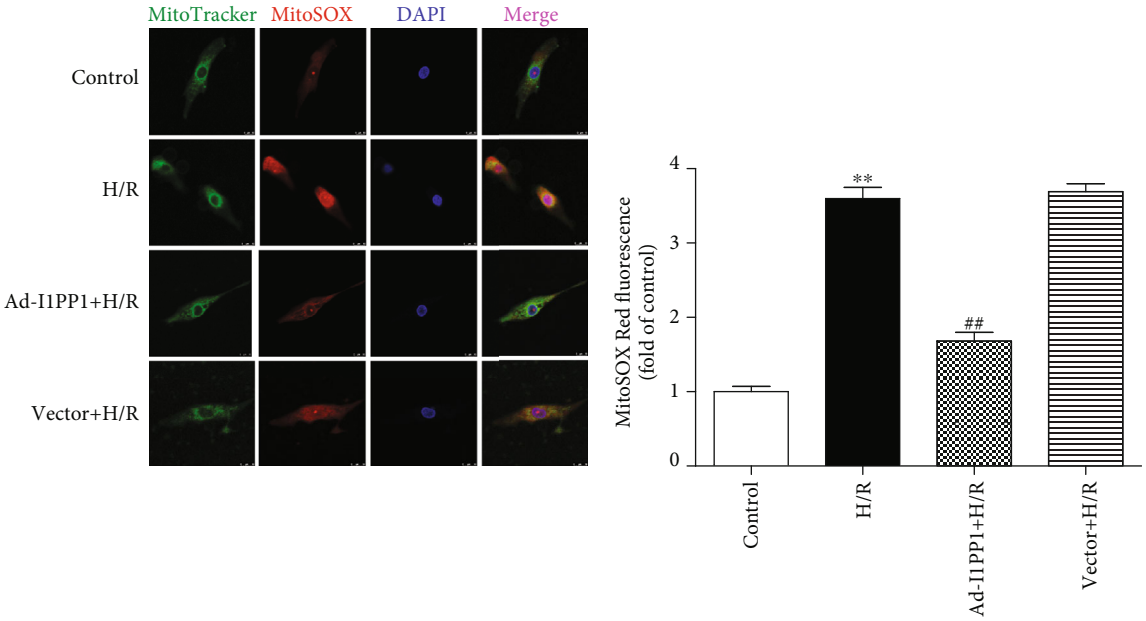


(b)

Figure 5: Continued.

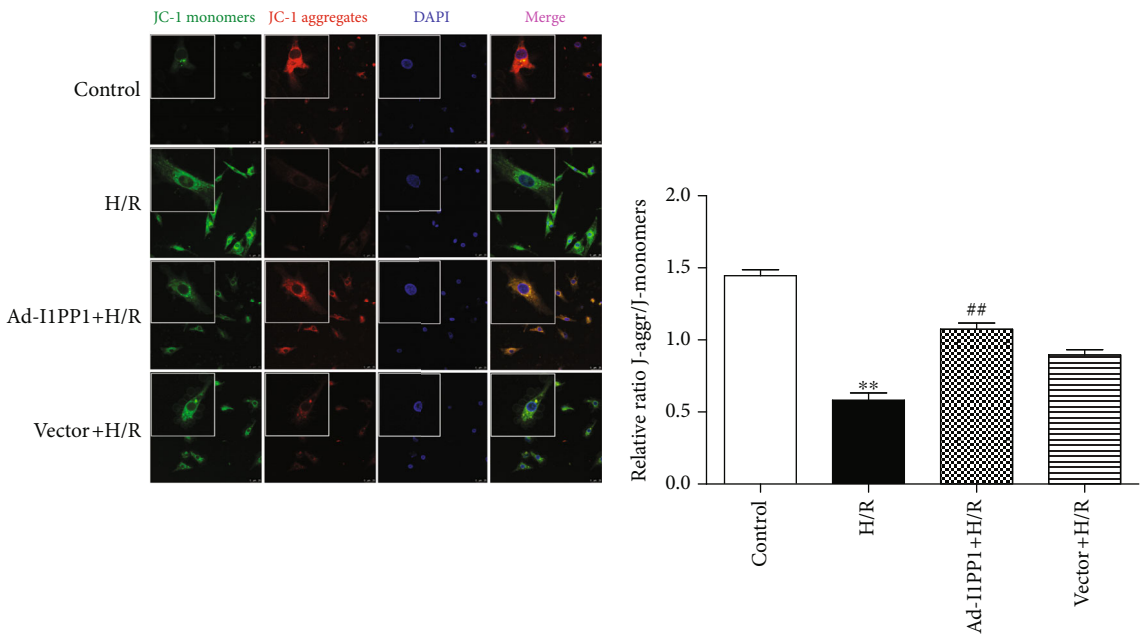


(c)

Figure 5: I1PP1 overexpression inhibited ROS but elevated mitochondrial membrane potential in cardiomyocytes after H/R injury. After infection of the I1PP1 recombinant adenovirus, the cardiomyocytes were subjected to hypoxia for 4 h followed by 12 h reoxygenation. (a) Superoxide production in the cardiomyocytes was detected using a fluorescence microscope with DHE fluorescent probe and quantified using ImageJ analysis software. Bar = 25 $\mu$m. (b) Mitochondrial ROS was measured using MitoSOX. Mitochondrial localization of MitoSOX signal was confirmed by colocalization with MitoTracker Green and quantified using ImageJ analysis software. Bar = 10 $\mu$m. (c) Mitochondrial membrane potential ($\Delta\psi$m) was measured by JC-1 staining and quantified using ImageJ analysis software. Bar = 25 $\mu$m. Plots represent the mean ± SEM; $n = 6$. Statistical significance: $^{**}P < 0.01$ compared with the control; $^{\#\#}P < 0.01$ compared with H/R.

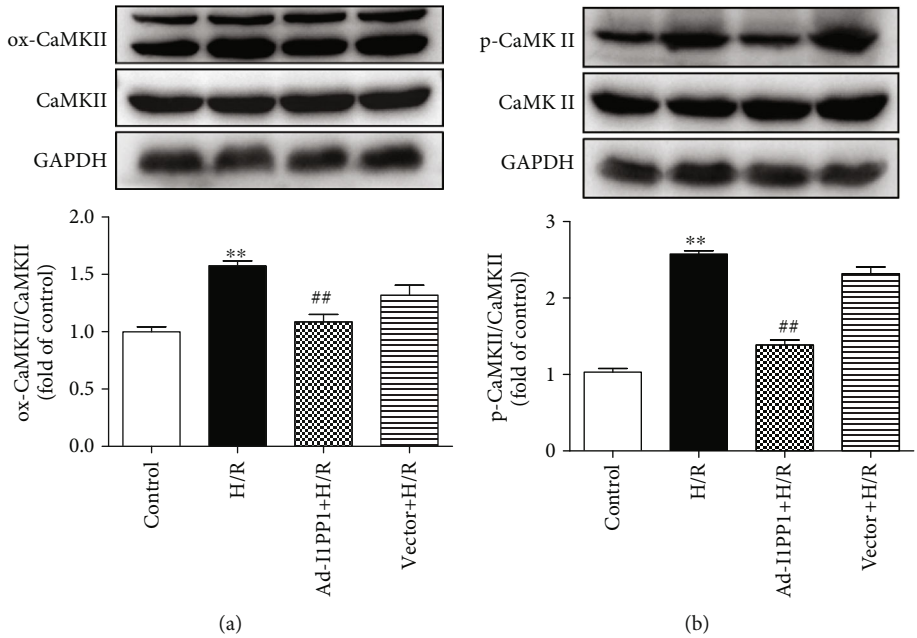


Figure 6: I1PP1 overexpression alleviated CaMKII oxidation and phosphorylation in cardiomyocytes after H/R injury. After infection of the I1PP1 recombinant adenovirus, the cardiomyocytes were subjected to hypoxia for 4 h followed by 12 h reoxygenation. (a) Expressions of CaMKII oxidation (ox-CaMKII) and total CaMKII in cardiomyocytes after H/R injury were quantified by western blot. GAPDH was used as a loading control. (b) Expression of CaMKII phosphorylation (p-CaMKII) and total CaMKII in cardiomyocytes after H/R injury was quantified by western blot. GAPDH was used as a loading control. Plots represent the mean ± SEM; $n = 6$. Statistical significance: $^{**}P < 0.01$ compared with the control; $^{\#\#}P < 0.01$ compared with H/R.

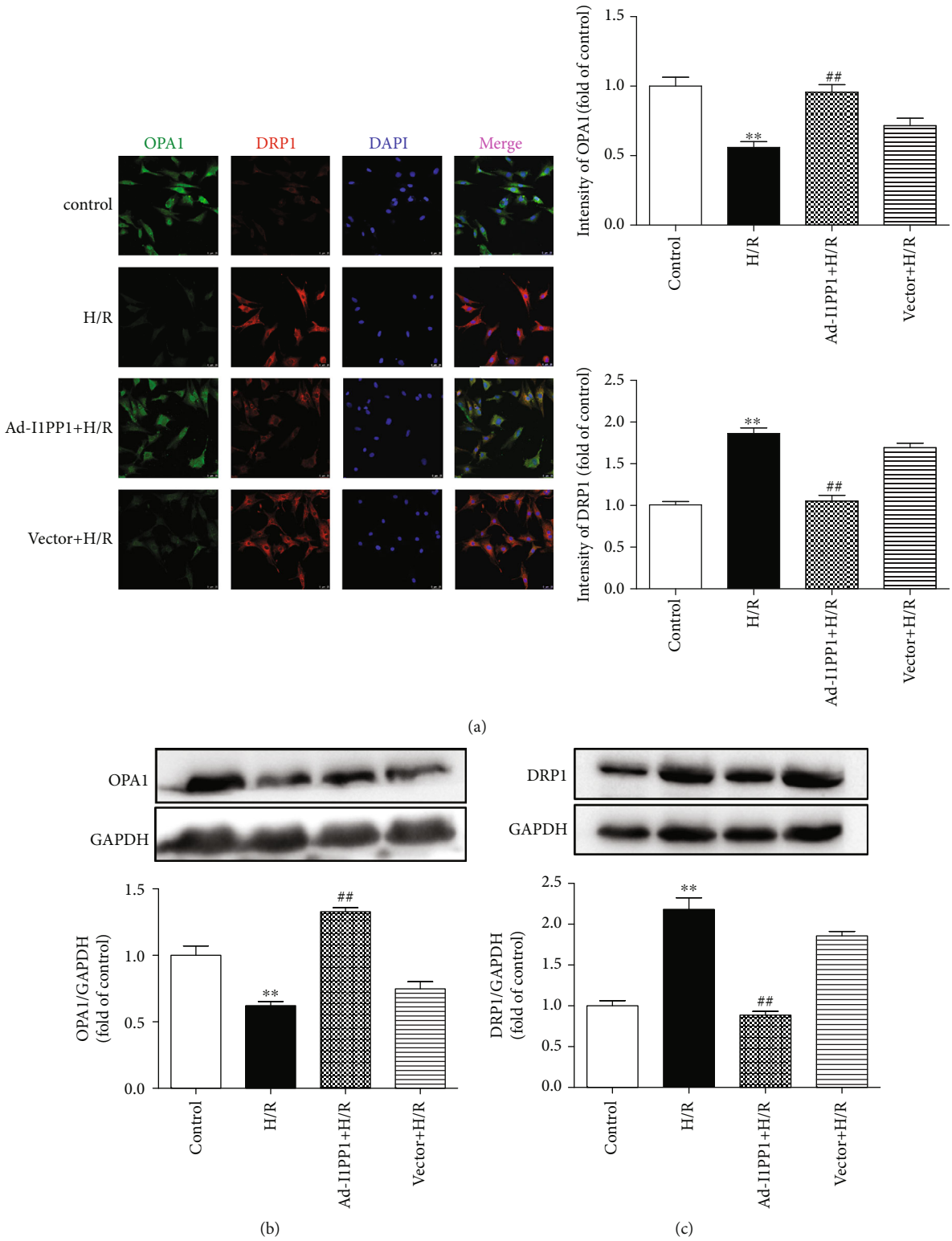


Figure 7: I1PP1 overexpression regulated mitochondrial OPA1 and DRP1 expression in cardiomyocytes after H/R injury. After infection of the I1PP1 recombinant adenovirus, the cardiomyocytes were subjected to hypoxia for 4 h followed by 12 h reoxygenation. (a) OPA1 and DRP1 were immunofluorescence stained using Cy3- (red) or Alexa Fluor 488- (green) conjugated IgG and quantified using ImageJ analysis software. The nuclei were stained using DAPI (blue). Bar = 10 $\mu$m. (b, c) Expressions of OPA1 and DRP1 in the cardiomyocytes were quantified by western blot. GAPDH was used as a loading control. Plots represent the mean ± SEM; $n = 6$. Statistical significance: $^{**}P < 0.01$ compared with the control; $^{\#\#}P < 0.01$ compared with H/R.

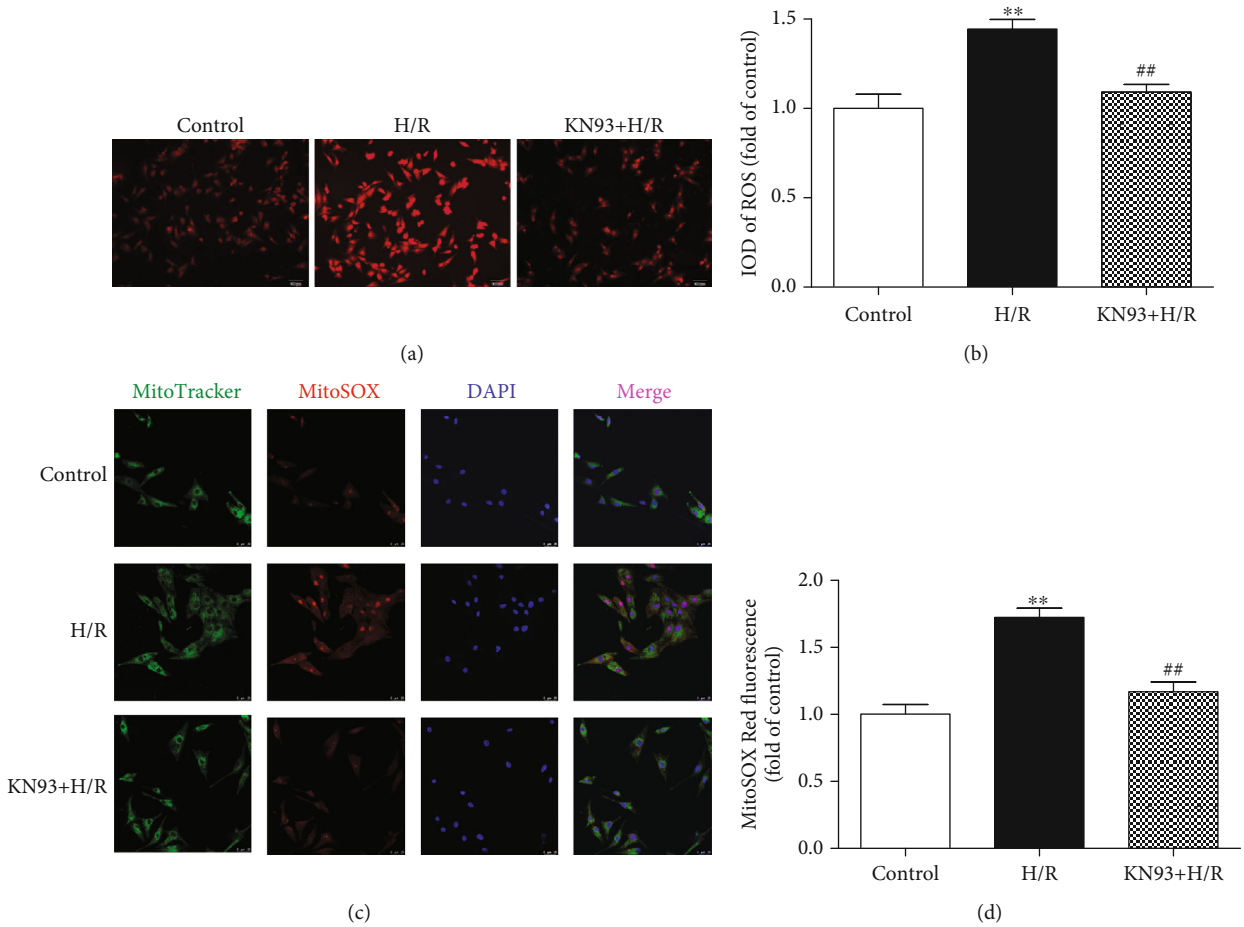


Figure 8: KN93 attenuated oxidative stress in cardiomyocytes after H/R injury. After CaMKII inhibitor KN93 (1 $\mu$M) preadministration for 1 h, the cardiomyocytes were subjected to hypoxia for 4 h followed by 12 h reoxygenation. (a, b) Superoxide production in the cardiomyocytes was detected using a fluorescence microscope with a DHE fluorescent probe and quantified using ImageJ analysis software. Bar = 100 $\mu$m. (c, d) Mitochondrial ROS was measured using MitoSOX. Mitochondrial localization of the MitoSOX signal was confirmed by colocalization with MitoTracker Green and quantified using ImageJ analysis software. Bar = 10 $\mu$m. Plots represent the mean ± SEM; $n = 6$. Statistical significance: $^{**}P < 0.01$ compared with the control; $^{\#\#}P < 0.01$ compared with H/R.

Studies have shown that decrease of mitochondrial membrane potential ($\Delta\psi$m) might lead to ROS accumulation and cell damage. Our study found that the green fluorescence intensity of JC-1 monomers, suggesting the impaired mitochondrial membrane potential, increased after H/R. Meanwhile, red fluorescence intensity of JC-1 aggregates, suggesting the normal membrane potential, decreased. Moreover, I1PP1 overexpression inhibited green but enhanced red fluorescence intensity. The data demonstrated that I1PP1 overexpression in the cardiomyocytes elevated mitochondrial membrane potential after H/R (Figure 5(c)).

*3.5. I1PP1 Overexpression Alleviated CaMKII Oxidation and Phosphorylation in Cardiomyocytes after H/R Injury.* CaMKII oxidation and phosphorylation, as two main activation forms of CaMKII, are favorable to accelerate the deterioration of cardiac function after MIRI [28]. The study verified that both oxidation and phosphorylation of CaMKII were heightened in cardiomyocytes after H/R injury, while I1PP1 overexpression in the cardiomyocytes diminished CaMKII oxidation and phosphorylation after H/R injury (Figures 6(a) and 6(b)).

*3.6. I1PP1 Overexpression Regulated Mitochondrial OPA1 and DRP1 Expression in Cardiomyocytes after H/R Injury.* OPA1 and DRP1 are mitochondrial fusion- and fission-associated proteins, respectively [51, 52]. The dynamic balance of OPA1 and DRP1 maintains mitochondrial structures and functions [53, 54]. We found that H/R injury significantly inhibited OPA1 but elevated DRP1 expression. I1PP1 overexpression in the cardiomyocytes increased OPA1 but decreased DRP1 after H/R injury, which was beneficial to maintaining the balance of OPA1 and DRP1 (Figures 7(a)–7(c)).

*3.7. I1PP1 Overexpression Combining with CaMKII Inhibitor KN93 Attenuated Oxidative Stress in Cardiomyocytes after H/R Injury.* In order to confirm the above protective effect of I1PP1 overexpression against oxidative stress during H/R

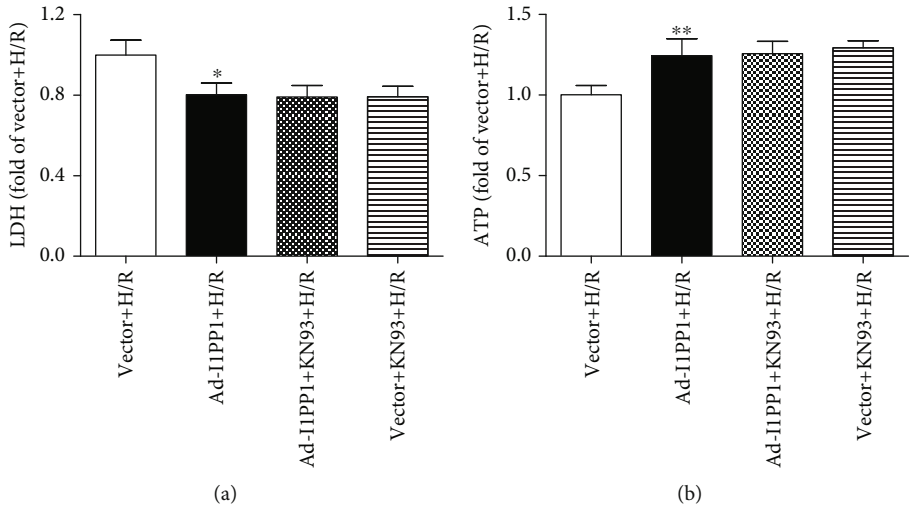


Figure 9: Effects of I1PP1 overexpression and KN93 on LDH release and ATP level in cardiomyocytes after H/R injury. After infection of the I1PP1 recombinant adenovirus, the cardiomyocytes with or without CaMKII inhibitor KN93 incubation for 1 h were subjected to hypoxia for 4 h followed by 12 h reoxygenation. (a) LDH release in the culture medium was measured. (b) ATP level of the cardiomyocytes was measured. Plots represent the mean ± SEM; $n = 6$. Statistical significance: $^{*}P < 0.05$ and $^{**}P < 0.01$ compared with vector+H/R.

injury was ascribed to CaMKII inhibition, the global cellular ROS and mitochondrial ROS were further measured. The study found that CaMKII inhibitor KN93 preadministration significantly inhibited ROS accumulation after H/R injury (Figures 8(a)–8(d)).

Moreover, both I1PP1 overexpression and I1PP1 overexpression combining with KN93 similarly decreased LDH release (Figure 9(a)) and enhanced ATP production (Figure 9(b)), weakened ROS production (Figure 10), and increased mitochondrial membrane potential (Figure 11) in cardiomyocytes after H/R. Furthermore, no significant difference appeared between the above two groups. These data indicated that I1PP1 overexpression alleviated cell damage, inhibited ROS production, and elevated mitochondrial membrane potential in cardiomyocytes after H/R injury via inhibition of CaMKII activation.

*3.8. I1PP1 Knockdown Exacerbated CaMKIIδ Alternative Splicing Disorder, Cell Injury, and Oxidative Stress in Cardiomyocytes after H/R Injury.* Contrarily, we also assessed the effect of I1PP1 knockdown with siRNA technology in cardiomyocytes under H/R injury. We found that all three siRNA significantly reduced I1PP1 expression, and there was the least expression of I1PP1 after siRNA#2 transfection. Therefore, siRNA#2 was applied in a further study (Figure 12(a)). Next, we found that the CaMKIIδ alternative splicing disorder (Figure 12(b)), LDH release (Figure 12(c)), ATP reduction (Figure 12(d)), and ROS accumulation (Figure 12(e)) in cardiomyocytes were aggravated after H/R in the cardiomyocytes with I1PP1 knockdown. However, there was no evidence regarding CaMKII activation in neonatal cardiomyocytes after I1PP1was knocked down. Altogether, I1PP1 knockdown exacerbated the CaMKIIδ alternative splicing disorder, cell injury, and oxidative stress in neonatal cardiomyocytes after H/R injury.

## 4. Discussion

Although reperfusion is essential for blood flow recovery in the myocardium, it might result in serious damage to the heart during myocardium ischemia and reperfusion. Thus, how to attenuate MIRI has been a very difficult problem in the clinic.

CaMKII is capable of integrating $\beta$-adrenergic, ROS, Gq-coupled receptors, hyperglycemia, and proapoptotic cytokine signals to induce oxidative stress in the myocardium [14]. The excessive activation of CaMKII exacerbates cardiomyocyte damage and accelerates the progression of cardiovascular disease. Previous research indicated that CaMKII was crucial in the pathogenesis of MIRI [55–59], and CaMKIIδ was the most vital isoform in the myocardium. Our present results showed that hypoxia-reoxygenation caused a disorder of CaMKIIδ alternative splicing in the cardiomyocytes, which was characterized by decreased expression of the δA and δB subtypes but increased expression of δC. On the other hand, levels of ox-CaMKII and p-CaMKII, as well as expression of p-PLB Thr17 representing CaMKII activity, also increased. Previous study found that PLB phosphorylation increased in the heart of I1PP1 transgenic mice in the basal state. I1PP1 elevated PLB phosphorylation after global ischemia for 40 min followed by reperfusion, whereas there were no differences at 60 min postreperfusion [43]. I1PP1 also increased PLB phosphorylation in the heart of pigs in the basal state [60]. In the present study, we found that I1PP1 significantly inhibited PLB phosphorylation after H/R in cardiomyocytes. The divergent effects on PLB phosphorylation may be explained by different types of cells or animals used in such studies, different ischemia or reperfusion times, different times for measurement, or a combination of these factors. To our knowledge, ROS oxidizes the methionine residue site

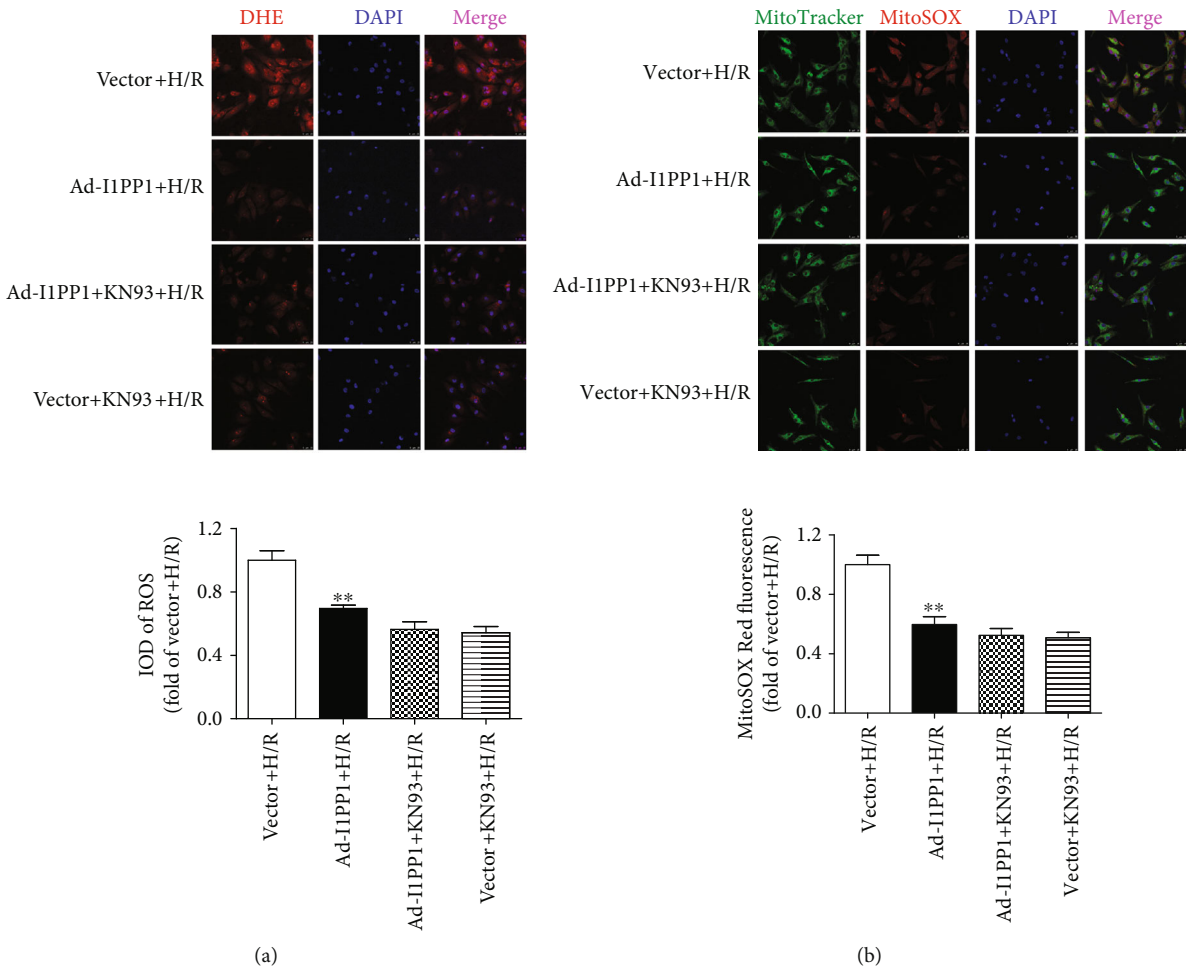


Figure 10: Effects of I1PP1 overexpression and KN93 on oxidative stress in cardiomyocytes after H/R injury. After infection of the I1PP1 recombinant adenovirus, the cardiomyocytes with or without CaMKII inhibitor KN93 incubation for 1 h were subjected to hypoxia for 4 h followed by 12 h reoxygenation. (a) Superoxide production in the cardiomyocytes was detected using a fluorescence microscope with DHE fluorescent probe and quantified using ImageJ analysis software. Bar = 25 $\mu$m. (b) Mitochondrial ROS was measured using MitoSOX. Mitochondrial localization of the MitoSOX signal was confirmed by colocalization with MitoTracker Green and quantified using ImageJ analysis software. Bar = 25 $\mu$m. Plots represent the mean ± SEM; $n = 6$. Statistical significance: $^{**}P < 0.01$ compared with vector+H/R.

of Met281/282 to promote CaMKII oxidation. CaMKII was able to be phosphorylated by itself. However, whether restoring the above abnormalities of CaMKII is able to alleviate H/R injury is not well known.

PP1 is able to alter the splicing factor phosphorylation and regulate CaMKII alternative splicing in the heart. A previous study found that hypoxia (but without reoxygenation) decreased the activity of PP1 in the cardiomyocytes [61], in the skeletal muscle of frogs [62], in the eukaryotic cells [63], and in the hippocampus [64]. A previous study found that enhanced PP1 activity was involved in $Ca^{2+}$ cycling, augmenting during H/R in the adult heart [43]. Moreover, previous research found that inducible overexpression of I1PP1 enhanced basal cardiac function and protected against ischemia-reperfusion injury [43], which was consistent with our results that I1PP1 overexpression attenuated cardiomyocyte H/R injury. Our research also confirmed that I1PP1 corrected the disorder of CaMKII$\delta$ splicing, reduced LDH release, but enhanced ATP production to alleviate cell injury. Contrarily, I1PP1 knockdown exacerbated the CaMKII$\delta$ alternative splicing disorder and aggravated cell injury after H/R injury. The protective effect of I1PP1 overexpression may be ascribed to the regulation of CaMKII alternative splicing and inhibition of CaMKII activity and ox-CaMKII as well as p-CaMKII. These data indicated that I1PP1 had a negative regulatory effect on H/R injury of cardiomyocytes through CaMKII regulation.

The protective mechanism of the attenuating effect on H/R damage by I1PP1 overexpression might be related to ROS inhibition. As far as we know, excessive ROS usually resulted in several types of pathological damage including myocardial hypertrophy [65, 66], liver injury or fibrosis [67, 68], pulmonary damage [69], and neuronal apoptosis [70]. The unsaturated fatty acids were vital for maintaining mitochondrial integrity and function, which is extremely susceptible to oxidative injury. The increase of oxidized unsaturated fatty acids directly impaired the function of the mitochondrial electron transport chain, thereby further

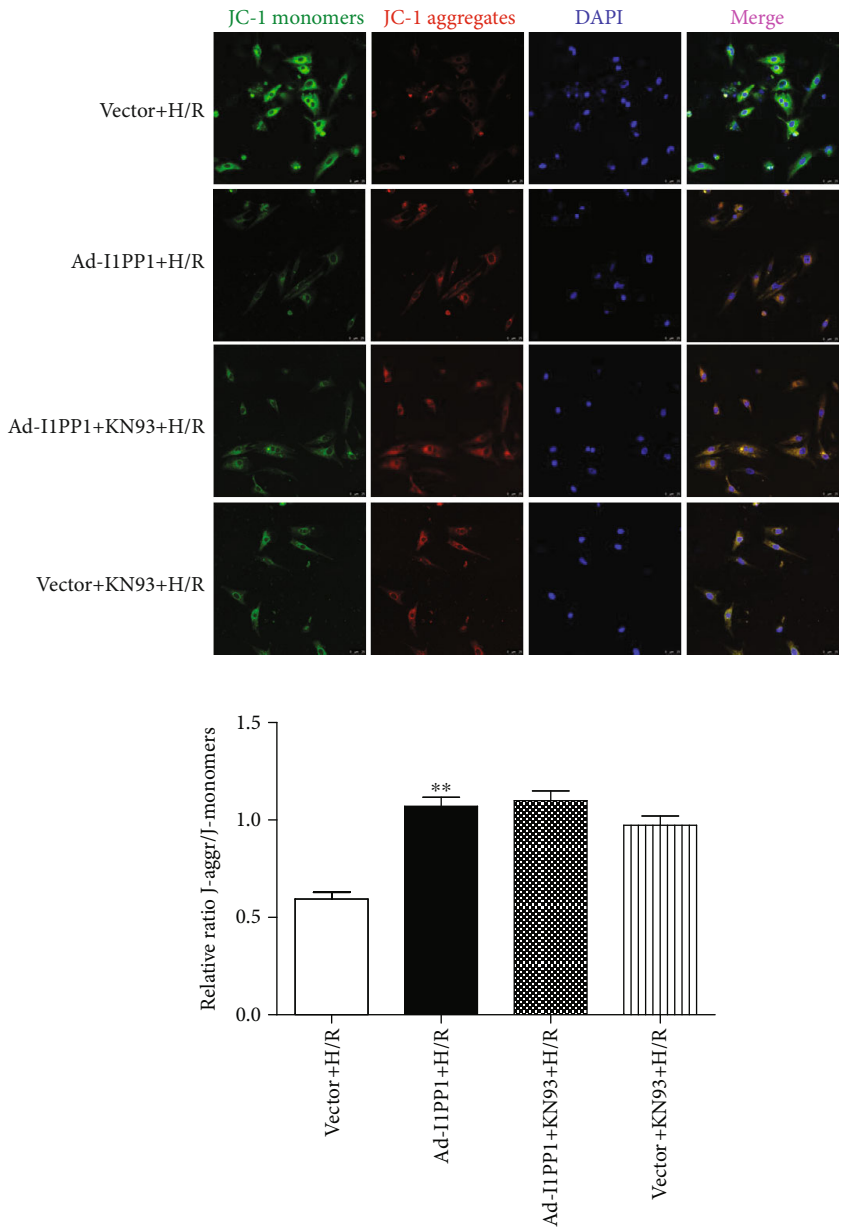


Figure 11: Effects of I1PP1 overexpression and KN93 on mitochondrial membrane potential in cardiomyocytes after H/R injury. After infection of the I1PP1 recombinant adenovirus, the cardiomyocytes with or without CaMKII inhibitor KN93 incubation for 1 h were subjected to hypoxia for 4 h followed by 12 h reoxygenation. Mitochondrial membrane potential ($\Delta\psi$m) was measured by JC-1 staining and quantified using ImageJ analysis software. Bar = 25 $\mu$m. Plots represent the mean ± SEM; $n = 6$. Statistical significance: $^{**}P < 0.01$ compared with vector+H/R.

promoting more ROS generation in mitochondria [71]. During H/R, ROS also induced the transformation of mitochondrial permeability by opening several small pores in the mitochondria immediately at the beginning of reperfusion [72], which resulted in mitochondrial matrix swelling and outer membrane integrity destruction. Besides, mitochondrial damage also directly blocks the production and storage of cellular ATP. Therefore, maintaining normal structure and function of mitochondria is critical for cell survive [73, 74]. Our present results showed that H/R decreased the mitochondrial membrane potential and promoted ROS accumulation. After I1PP1 successfully inhibited PP1 expression, the CaMKII pathway, cell damage, ATP production, and mitochondrial membrane potential as well as ROS accumulation were restored significantly. Moreover, CaMKII-specific inhibitor KN93 was further applied to clarify the causal relationship between negative regulation of CaMKII and the protective effect on cardiomyocytes. Our data indicated that KN93 was capable of attenuating both global intracellular and mitochondrial ROS after H/R. We also found that I1PP1 overexpression with or without CaMKII inhibition by KN93 similarly decreased LDH release, weakened ROS production, and increased mitochondrial membrane potential in cardiomyocytes after H/R. Altogether, it suggested that

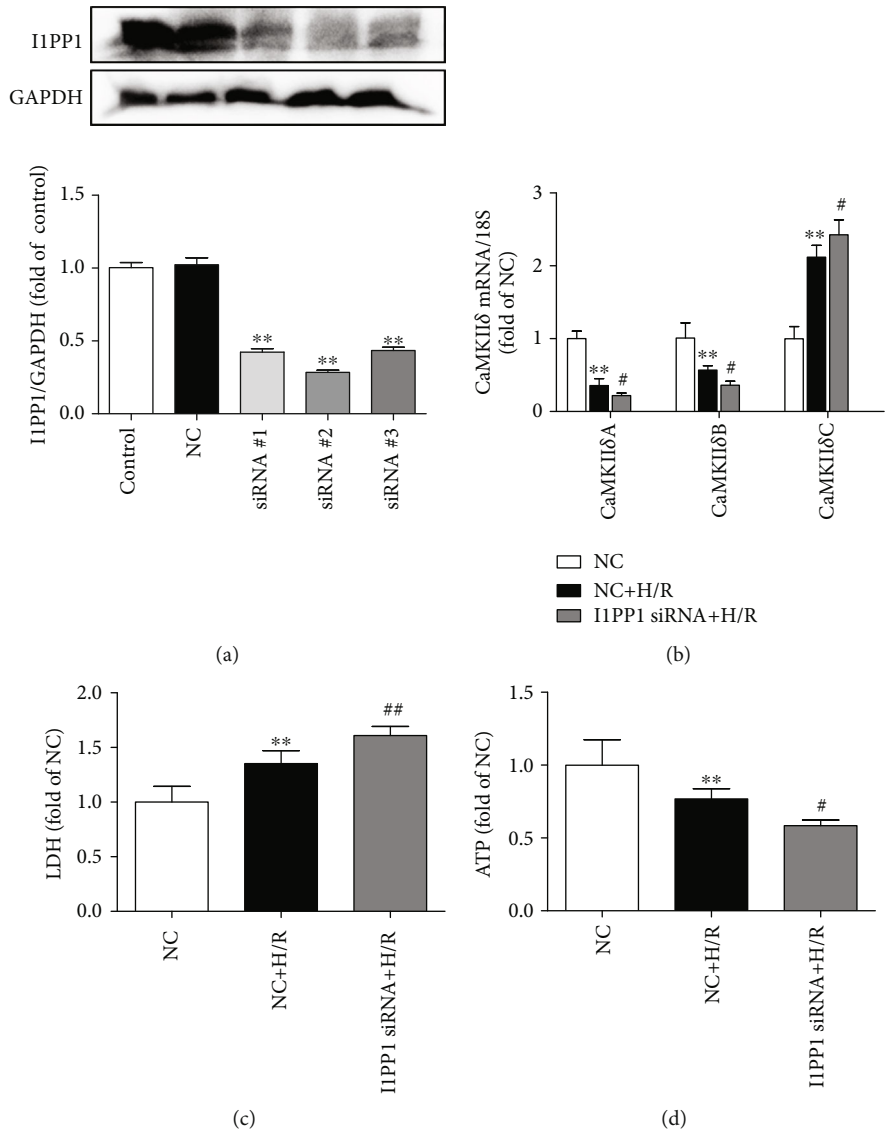


Figure 12: Continued.

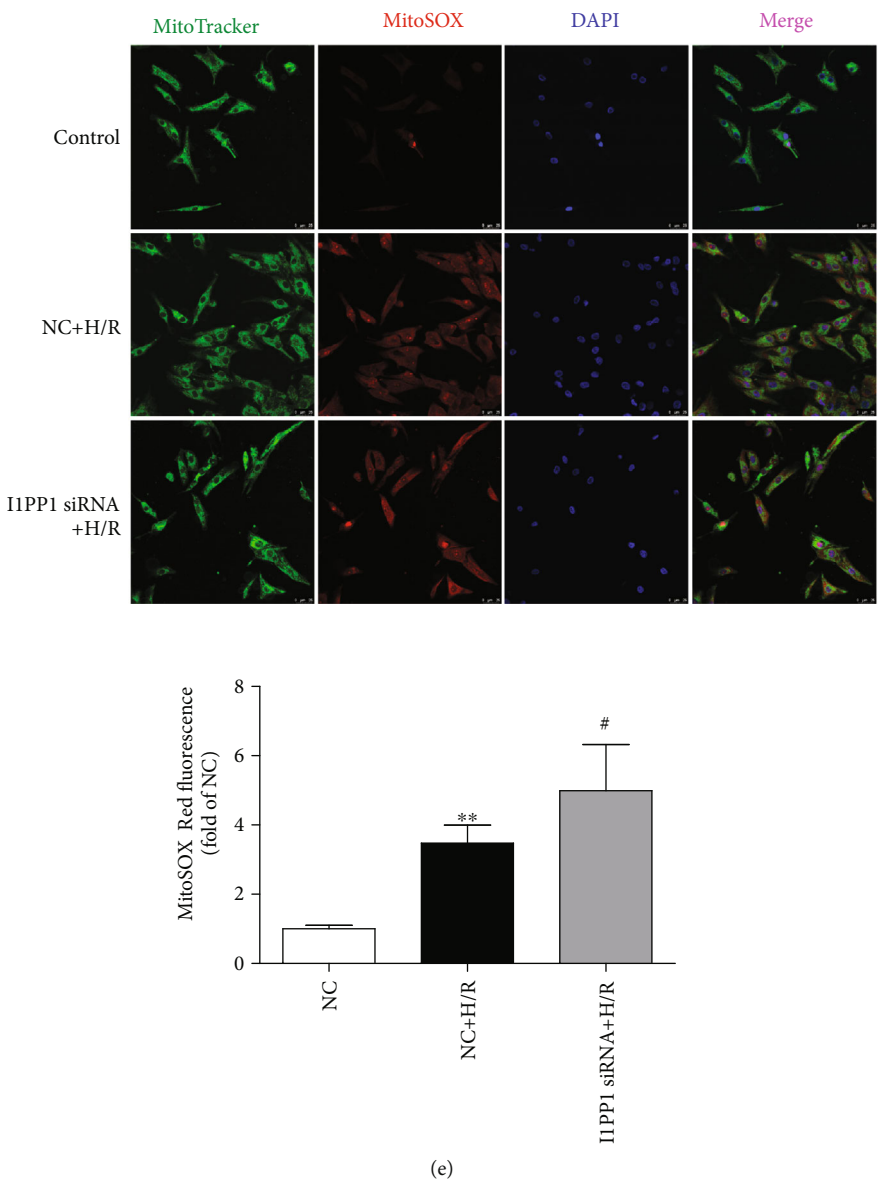


Figure 12: Effects of I1PP1 knockdown on CaMKIIδ alternative splicing disorder, cell injury, and oxidative stress in cardiomyocytes after H/R injury. (a) After I1PP1 siRNA or NC siRNA was transfected into neonatal rat cardiomyocytes, expressions of I1PP1 in the cardiomyocytes were quantified by western blot. GAPDH was used as a loading control. (b) After I1PP1 siRNA or NC siRNA was transfected into neonatal rat cardiomyocytes, cells were subjected to hypoxia for 4 h followed by 12 h reoxygenation. The mRNA levels of CaMKIIδA, CaMKIIδB, and CaMKIIδC of the cardiomyocytes after reoxygenation were detected by quantitative real-time PCR. 18S was serviced as a housekeeping mRNA. (c) LDH release in the culture medium was measured. (d) ATP level of the cardiomyocytes was measured. (e) Mitochondrial ROS was measured using MitoSOX. Mitochondrial localization of the MitoSOX signal was confirmed by colocalization with MitoTracker Green and quantified using ImageJ analysis software. Bar = 25 $\mu$m. Plots represent the mean ± SEM; $n = 6$. Statistical significance: $^{**}P < 0.01$ compared with NC; $^{\#}P < 0.05$ and $^{\#\#}P < 0.01$ compared with NC+H/R.

I1PP1 overexpression attenuated cardiomyocyte injury under stress conditions via inhibiting CaMKII activation.

Dynamic fusion and fission is beneficial to maintaining mitochondrial structure and function to appropriately respond to frequent changing environmental conditions [75]. OPA1 localizes on the mitochondrial inner membrane (IMM) and membrane gap to control IMM fusion and sputum structure [76]. OPA1 deficiency promoted mitochondrial fragmentation and abnormal sputum remodeling to suppress respiratory ability and inhibit mitochondria-dependent cell metabolism [77, 78]. Besides, OPA1 also prevented cytochrome C redistribution and release to inhibit cell injury [54]. Contrarily, DRP1 has been verified to mediate mitochondrial fission [79]. In our present study, hypoxia-reoxygenation caused the imbalance of OPA1 and DRP1 in cardiomyocytes, which would cause fatal damage to the morphology and function of mitochondria. Overexpression of I1PP1 reversed the imbalance of proportions between OPA1 and DRP1 which is normal to maintain the mitochondrial homeostasis.

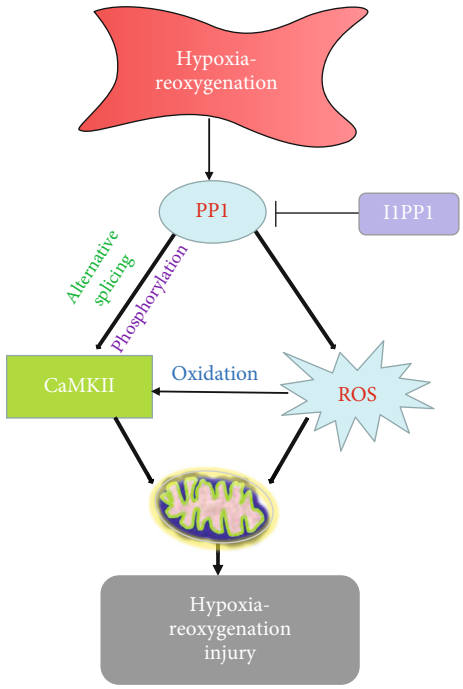


Figure 13: I1PP1 overexpression corrected CaMKIIδ alternative splicing disorders, inhibited CaMKII phosphorylation, repressed CaMKII oxidation, suppressed ROS production, and attenuated hypoxia-reoxygenation injury in the cardiomyocytes.

However, there are several limitations in our present study. Firstly, the use of human cardiomyocytes and measurement of CaMKII levels will greatly benefit extending the significance of the study, which will directly demonstrate the real impact of I1PP1 overexpression on cardiomyocytes for humans. However, human cardiomyocytes are unavailable in the present study. Secondly, due to the experimental strategy that mainly relies on the overexpression of I1PP1, it is unclear whether endogenous I1PP1 has a significant role under H/R injury in neonatal cardiomyocytes. The knockdown approach was performed in addition to overexpression of I1PP1. However, detection of CaMKII activity and CaMKII phosphorylation as well as PP1 levels was unavailable in the present study, which will be a great benefit to validate the effect and mechanism of I1PP1 on H/R injury in cardiomyocytes.

Collectively, I1PP1 overexpression corrected disorders of CaMKIIδ alternative splicing, inhibited CaMKII phosphorylation, repressed CaMKII oxidation, suppressed ROS production, and attenuated H/R injury in the cardiomyocytes (Figure 13). The present study is helpful to provide new biological targets for prevention and treatment of myocardial ischemia-reperfusion injury in the clinic.

## Data Availability

The data used to support the findings of this study are available from the corresponding authors upon request.

## Conflicts of Interest

The authors declare that there is no conflict of interests regarding the publication of this paper.

## Authors' Contributions

Huiqin Luo, Shu Song, and Yun Chen contributed equally to this study.

## Acknowledgments

The work was funded by grants 81670243, 81873470, and 81770279 from the National Natural Science Foundation of China, grant BK20151276 from the Natural Science Foundation of Jiangsu Province, a major project of the Natural Science Research of Jiangsu Higher Education Institutions of China (18KJA310005), the Six Talent Peaks Project in Jiangsu Province (2018-WSN-062), grants from the China Postdoctoral Science Foundation (2017M610342 and 2019T120449), the Jiangsu Planned Projects for Postdoctoral Research Funds (1701050A), the Graduate Research and Innovation Projects of Jiangsu Province (KYCX18_2401), and the Nantong University Cooperative Innovation Program of Small Molecular Compound R&D (NTU2016-1).

## References

[1] D. J. Hausenloy and D. M. Yellon, "Myocardial ischemia-reperfusion injury: a neglected therapeutic target," *Journal of Clinical Investigation*, vol. 123, no. 1, pp. 92–100, 2013.

[2] D. M. Muntean, A. Sturza, M. D. Dănilă, C. Borza, O. M. Duicu, and C. Mornoş, "The role of mitochondrial reactive oxygen species in cardiovascular injury and protective strategies," *Oxidative Medicine and Cellular Longevity*, vol. 2016, Article ID 8254942, 19 pages, 2016.

[3] T. Kalogeris, Y. Bao, and R. J. Korthuis, "Mitochondrial reactive oxygen species: a double edged sword in ischemia/-reperfusion vs preconditioning," *Redox Biology*, vol. 2, pp. 702–714, 2014.

[4] D. J. Hausenloy, H. E. Botker, T. Engstrom et al., "Targeting reperfusion injury in patients with ST-segment elevation myocardial infarction: trials and tribulations," *European Heart Journal*, vol. 38, no. 13, pp. 935–941, 2017.

[5] D. J. Hausenloy and D. M. Yellon, "Ischaemic conditioning and reperfusion injury," *Nature Reviews Cardiology*, vol. 13, no. 4, pp. 193–209, 2016.

[6] G. Heusch, "The coronary circulation as a target of cardioprotection," *Circulation Research*, vol. 118, no. 10, pp. 1643–1658, 2016.

[7] B. Ibanez, G. Heusch, M. Ovize, and F. WerfVan de, "Evolving therapies for myocardial ischemia/reperfusion injury," *Journal of the American College of Cardiology*, vol. 65, no. 14, pp. 1454–1471, 2015.

[8] T. Sun, Y. Zhang, S. Zhong et al., "*N*-n-Butyl haloperidol iodide, a derivative of the anti-psychotic haloperidol, antagonizes hypoxia/reoxygenation injury by inhibiting an Egr-1/ROS positive feedback loop in h9c2 cells," *Frontiers in Pharmacology*, vol. 9, p. 19, 2018.

[9] A. Mokhtari-Zaer, N. Marefati, S. L. Atkin, A. E. Butler, and A. Sahebkar, "The protective role of curcumin in myocardial

ischemia-reperfusion injury," *Journal of Cellular Physiology*, vol. 234, no. 1, pp. 214–222, 2018.

[10] H. H. Geng, R. Li, Y. M. Su et al., "Curcumin protects cardiac myocyte against hypoxia-induced apoptosis through upregulating miR-7a/b expression," *Biomedicine & Pharmacotherapy*, vol. 81, pp. 258–264, 2016.

[11] K. Raedschelders, D. M. Ansley, and D. D. Chen, "The cellular and molecular origin of reactive oxygen species generation during myocardial ischemia and reperfusion," *Pharmacology & Therapeutics*, vol. 133, no. 2, pp. 230–255, 2012.

[12] A. Frank, M. Bonney, S. Bonney, L. Weitzel, M. Koeppen, and T. Eckle, "Myocardial ischemia reperfusion injury: from basic science to clinical bedside," *Seminars in Cardiothoracic and Vascular Anesthesia*, vol. 16, no. 3, pp. 123–132, 2012.

[13] B. D. Westenbrink, H. Ling, A. S. Divakaruni et al., "Mitochondrial reprogramming induced by CaMKII$\delta$ mediates hypertrophy decompensation," *Circulation Research*, vol. 116, no. 5, pp. e28–e39, 2015.

[14] N. Feng and M. E. Anderson, "CaMKII is a nodal signal for multiple programmed cell death pathways in heart," *Journal of Molecular and Cellular Cardiology*, vol. 103, pp. 102–109, 2017.

[15] M. Y. Mollova, H. A. Katus, and J. Backs, "Regulation of CaMKII signaling in cardiovascular disease," *Frontiers in Pharmacology*, vol. 6, p. 178, 2015.

[16] E. D. Luczak and M. E. Anderson, "CaMKII oxidative activation and the pathogenesis of cardiac disease," *Journal of Molecular and Cellular Cardiology*, vol. 73, pp. 112–116, 2014.

[17] P. Quijada, N. Hariharan, J. D. Cubillo et al., "Nuclear calcium/calmodulin-dependent protein kinase II signaling enhances cardiac progenitor cell survival and cardiac lineage commitment," *Journal of Biological Chemistry*, vol. 290, no. 42, pp. 25411–25426, 2015.

[18] R. J. Liao, L. J. Tong, C. Huang et al., "Rescue of cardiac failing and remodelling by inhibition of protein phosphatase 1$\gamma$ is associated with suppression of the alternative splicing factor-mediated splicing of $Ca^{2+}$/calmodulin-dependent protein kinase $\delta$," *Clinical and Experimental Pharmacology and Physiology*, vol. 41, no. 12, pp. 976–985, 2014.

[19] M. Dewenter, S. Neef, C. Vettel et al., "Calcium/Calmodulin-Dependent Protein Kinase II activity persists during chronic $\beta$-adrenoceptor blockade in experimental and human heart failure," *Circulation-Heart Failure*, vol. 10, no. 5, article e003840, 2017.

[20] N. Shioda and K. Fukunaga, "Physiological and pathological roles of CaMKII-PP1 signaling in the brain," *International Journal of Molecular Sciences*, vol. 19, no. 1, p. 20, 2018.

[21] J. Mustroph, S. Neef, and L. S. Maier, "CaMKII as a target for arrhythmia suppression," *Pharmacology & Therapeutics*, vol. 176, pp. 22–31, 2017.

[22] L. J. Daniels, R. S. Wallace, O. M. Nicholson et al., "Inhibition of calcium/calmodulin-dependent kinase II restores contraction and relaxation in isolated cardiac muscle from type 2 diabetic rats," *Cardiovascular Diabetology*, vol. 17, no. 1, p. 89, 2018.

[23] P. Zhong, D. Quan, J. Peng et al., "Role of CaMKII in free fatty acid/hyperlipidemia-induced cardiac remodeling both in vitro and in vivo," *Journal of Molecular and Cellular Cardiology*, vol. 109, pp. 1–16, 2017.

[24] J. R. Bell, M. Vila-Petroff, and L. M. D. Delbridge, "CaMKII-dependent responses to ischemia and reperfusion challenges in the heart," *Frontiers in Pharmacology*, vol. 5, p. 96, 2014.

[25] J. R. Bell, J. R. Erickson, and L. M. Delbridge, "$Ca^{2+}$/-calmodulin dependent kinase II: a critical mediator in determining reperfusion outcomes in the heart?," *Clinical and Experimental Pharmacology and Physiology*, vol. 41, no. 11, pp. 940–946, 2014.

[26] P. N. Sanders, O. M. Koval, O. A. Jaffer et al., "CaMKII is essential for the proasthmatic effects of oxidation," *Science Translational Medicine*, vol. 5, no. 195, article 195ra97, 2013.

[27] A. Szobi, T. Rajtik, S. Carnicka, T. Ravingerova, and A. Adameova, "Mitigation of postischemic cardiac contractile dysfunction by CaMKII inhibition: effects on programmed necrotic and apoptotic cell death," *Molecular and Cellular Biochemistry*, vol. 388, no. 1-2, pp. 269–276, 2014.

[28] T. Zhang, Y. Zhang, M. Cui et al., "CaMKII is a RIP3 substrate mediating ischemia- and oxidative stress-induced myocardial necroptosis," *Nature Medicine*, vol. 22, no. 2, pp. 175–182, 2016.

[29] P. Pellicena and H. Schulman, "CaMKII inhibitors: from research tools to therapeutic agents," *Frontiers in Pharmacology*, vol. 5, p. 21, 2014.

[30] Y. Shi, "Serine/threonine phosphatases: mechanism through structure," *Cell*, vol. 139, no. 3, pp. 468–484, 2009.

[31] H. Y. Fang, M. Y. Hung, Y. M. Lin et al., "17$\beta$-Estradiol and/or estrogen receptor alpha signaling blocks protein phosphatase 1 mediated ISO induced cardiac hypertrophy," *PLoS One*, vol. 13, no. 5, article e0196569, 2018.

[32] S. Rebelo, M. Santos, F. Martins, E. F. da Cruz e Silva, and O. A. B. da Cruz e Silva, "Protein phosphatase 1 is a key player in nuclear events," *Cellular Signalling*, vol. 27, no. 12, pp. 2589–2598, 2015.

[33] C. Huang, W. Cao, R. Liao et al., "PP1$\gamma$ functionally augments the alternative splicing of CaMKII$\delta$ through interaction with ASF," *American Journal of Physiology-Cell Physiology*, vol. 306, no. 2, pp. C167–C177, 2014.

[34] N. Brüchert, N. Mavila, P. Boknik et al., "Inhibitor-2 prevents protein phosphatase 1-induced cardiac hypertrophy and mortality," *American Journal of Physiology-Heart and Circulatory Physiology*, vol. 295, no. 4, pp. H1539–H1546, 2008.

[35] D. Y. Chiang, N. Li, Q. Wang et al., "Impaired local regulation of ryanodine receptor type 2 by protein phosphatase 1 promotes atrial fibrillation," *Cardiovascular Research*, vol. 103, no. 1, pp. 178–187, 2014.

[36] H. Aoyama, Y. Ikeda, Y. Miyazaki et al., "Isoform-specific roles of protein phosphatase 1 catalytic subunits in sarcoplasmic reticulum-mediated $Ca^{2+}$ cycling," *Cardiovascular Research*, vol. 89, no. 1, pp. 79–88, 2011.

[37] A. El-Armouche, K. Wittköpper, F. Degenhardt et al., "Phosphatase inhibitor-1-deficient mice are protected from catecholamine-induced arrhythmias and myocardial hypertrophy," *Cardiovascular Research*, vol. 80, no. 3, pp. 396–406, 2008.

[38] Y. Miyazaki, Y. Ikeda, K. Shiraishi et al., "Heart failure-inducible gene therapy targeting protein phosphatase 1 prevents progressive left ventricular remodeling," *PLoS One*, vol. 7, no. 4, article e35875, 2012.

[39] A. N. Carr, A. G. Schmidt, Y. Suzuki et al., "Type 1 phosphatase, a negative regulator of cardiac function," *Molecular and Cellular Biology*, vol. 22, no. 12, pp. 4124–4135, 2002.

[40] H. Sotoud, U. Borgmeyer, C. Schulze, A. El-Armouche, and T. Eschenhagen, "Development of phosphatase inhibitor-1 peptides acting as indirect activators of phosphatase 1," *Naunyn-Schmiedeberg's Archives of Pharmacology*, vol. 388, no. 3, pp. 283–293, 2015.

[41] C. L. Liu, Y. Y. He, X. Li, R. J. Li, K. L. He, and L. L. Wang, "Inhibition of serine/threonine protein phosphatase PP1 protects cardiomyocytes from tunicamycin-induced apoptosis and I/R through the upregulation of p-eIF2$\alpha$," *International Journal of Molecular Medicine*, vol. 33, no. 3, pp. 499–506, 2014.

[42] S. Weber, S. Meyer-Roxlau, and A. El-Armouche, "Role of protein phosphatase inhibitor-1 in cardiac beta adrenergic pathway," *Journal of Molecular and Cellular Cardiology*, vol. 101, pp. 116–126, 2016.

[43] P. Nicolaou, P. Rodriguez, X. Ren et al., "Inducible expression of active protein phosphatase-1 inhibitor-1 enhances basal cardiac function and protects against ischemia/reperfusion injury," *Circulation Research*, vol. 104, no. 8, pp. 1012–1020, 2009.

[44] P. Nicolaou and E. G. Kranias, "Role of PP1 in the regulation of Ca cycling in cardiac physiology and pathophysiology," *Frontiers in Bioscience*, vol. 14, no. 14, pp. 3571–3585, 2009.

[45] M. Xu, Y. Hua, Y. Qi, G. Meng, and S. Yang, "Exogenous hydrogen sulphide supplement accelerates skin wound healing via oxidative stress inhibition and vascular endothelial growth factor enhancement," *Experimental Dermatology*, vol. 28, no. 7, pp. 776–785, 2019.

[46] L. Sun, Y. Chen, H. Luo, M. Xu, G. Meng, and W. Zhang, "$Ca^{2+}$/calmodulin-dependent protein kinase II regulation by inhibitor 1 of protein phosphatase 1 alleviates necroptosis in high glucose-induced cardiomyocytes injury," *Biochemical Pharmacology*, vol. 163, pp. 194–205, 2019.

[47] J. Zhang, J. Yu, Y. Chen et al., "Exogenous hydrogen sulfide supplement attenuates isoproterenol-induced myocardial hypertrophy in a sirtuin 3-dependent manner," *Oxidative Medicine and Cellular Longevity*, vol. 2018, Article ID 9396089, 17 pages, 2018.

[48] L. Tu, C. S. Pan, X. H. Wei et al., "Astragaloside IV protects heart from ischemia and reperfusion injury via energy regulation mechanisms," *Microcirculation*, vol. 20, no. 8, pp. 736–747, 2013.

[49] G. Meng, J. Wang, Y. Xiao et al., "GYY4137 protects against myocardial ischemia and reperfusion injury by attenuating oxidative stress and apoptosis in rats," *Journal of Biomedical Research*, vol. 29, no. 3, pp. 203–213, 2015.

[50] Y. Wang, J. Sun, C. Liu, and C. Fang, "Protective effects of crocetin pretreatment on myocardial injury in an ischemia/-reperfusion rat model," *European Journal of Pharmacology*, vol. 741, pp. 290–296, 2014.

[51] D. T. Chu, Y. Tao, and K. Tasken, "OPA1 in lipid metabolism: function of OPA1 in lipolysis and thermogenesis of adipocytes," *Hormone and Metabolic Research*, vol. 49, no. 4, pp. 276–285, 2017.

[52] H. Zhou, T. Cheang, F. Su et al., "Melatonin inhibits rotenone-induced SH-SY5Y cell death via the downregulation of dynamin-related protein 1 expression," *European Journal of Pharmacology*, vol. 819, pp. 58–67, 2018.

[53] G. Meng, J. Liu, S. Liu et al., "Hydrogen sulfide pretreatment improves mitochondrial function in myocardial hypertrophy via a SIRT3-dependent manner," *British Journal of Pharmacology*, vol. 175, no. 8, pp. 1126–1145, 2018.

[54] S. B. Ong, S. B. Kalkhoran, H. A. Cabrera-Fuentes, and D. J. Hausenloy, "Mitochondrial fusion and fission proteins as novel therapeutic targets for treating cardiovascular disease," *European Journal of Pharmacology*, vol. 763, Part A, pp. 104–114, 2015.

[55] L. H. Kong, X. M. Gu, F. Wu, Z. X. Jin, and J. J. Zhou, "CaMKII inhibition mitigates ischemia/reperfusion-elicited calpain activation and the damage to membrane skeleton proteins in isolated rat hearts," *Biochemical and Biophysical Research Communications*, vol. 491, no. 3, pp. 687–692, 2017.

[56] M. A. Salas, C. A. Valverde, G. Sánchez et al., "The signalling pathway of CaMKII-mediated apoptosis and necrosis in the ischemia/reperfusion injury," *Journal of Molecular and Cellular Cardiology*, vol. 48, no. 6, pp. 1298–1306, 2010.

[57] M. Said, R. Becerra, C. A. Valverde et al., "Calcium-calmodulin dependent protein kinase II (CaMKII): a main signal responsible for early reperfusion arrhythmias," *Journal of Molecular and Cellular Cardiology*, vol. 51, no. 6, pp. 936–944, 2011.

[58] T. Rajtik, S. Carnicka, A. Szobi et al., "Oxidative activation of CaMKII$\delta$ in acute myocardial ischemia/reperfusion injury: a role of angiotensin $AT_1$ receptor-NOX2 signaling axis," *European Journal of Pharmacology*, vol. 771, pp. 114–122, 2016.

[59] C. B. Gray, T. Suetomi, S. Xiang et al., "CaMKII$\delta$ subtypes differentially regulate infarct formation following ex vivo myocardial ischemia/reperfusion through NF-$\kappa$B and TNF-$\alpha$," *Journal of Molecular and Cellular Cardiology*, vol. 103, pp. 48–55, 2017.

[60] S. Watanabe, K. Ishikawa, K. Fish et al., "Protein phosphatase inhibitor-1 gene therapy in a swine model of nonischemic heart failure," *Journal of the American College of Cardiology*, vol. 70, no. 14, pp. 1744–1756, 2017.

[61] G. Wu, J. Marin-Garcia, T. B. Rogers, E. G. Lakatta, and X. Long, "Phosphorylation and hypoxia-induced heme oxygenase-1 gene expression in cardiomyocytes," *Journal of Cardiac Failure*, vol. 10, no. 6, pp. 519–526, 2004.

[62] J. A. MacDonald and K. B. Storey, "Protein phosphatase type-1 from skeletal muscle of the freeze-tolerant wood frog," *Comparative Biochemistry and Physiology Part B: Biochemistry and Molecular Biology*, vol. 131, no. 1, pp. 27–36, 2002.

[63] K. M. Comerford, M. O. Leonard, E. P. Cummins et al., "Regulation of protein phosphatase 1$\gamma$ activity in hypoxia through increased interaction with NIPP1: implications for cellular metabolism," *Journal of Cellular Physiology*, vol. 209, no. 1, pp. 211–218, 2006.

[64] S. Zhang, Y. Zhang, S. Jiang et al., "The effect of hypoxia preconditioning on DNA methyltransferase and PP1$\gamma$ in hippocampus of hypoxia preconditioned mice," *High Altitude Medicine & Biology*, vol. 15, no. 4, pp. 483–490, 2014.

[65] L. Zhao, D. Wu, M. Sang, Y. Xu, Z. Liu, and Q. Wu, "Stachydrine ameliorates isoproterenol-induced cardiac hypertrophy and fibrosis by suppressing inflammation and oxidative stress through inhibiting NF-$\kappa$B and JAK/STAT signaling pathways in rats," *International Immunopharmacology*, vol. 48, pp. 102–109, 2017.

[66] P. Wang, L. Luo, Q. Shen et al., "Rosuvastatin improves myocardial hypertrophy after hemodynamic pressure overload via regulating the crosstalk of Nrf2/ARE and TGF-$\beta$/smads pathways in rat heart," *European Journal of Pharmacology*, vol. 820, pp. 173–182, 2018.

[67] F. Wang, J. C. Liu, R. J. Zhou et al., "Apigenin protects against alcohol-induced liver injury in mice by regulating hepatic CYP2E1-mediated oxidative stress and PPAR$\alpha$-mediated

lipogenic gene expression," *Chemico-Biological Interactions*, vol. 275, pp. 171–177, 2017.

[68] J. Zhang, A. Yang, Y. Wu et al., "Stachydrine ameliorates carbon tetrachloride-induced hepatic fibrosis by inhibiting inflammation, oxidative stress and regulating MMPs/TIMPs system in rats," *Biomedicine & Pharmacotherapy*, vol. 97, pp. 1586–1594, 2018.

[69] X. Zhao, Y. Jin, L. Yang et al., "Promotion of SIRT1 protein degradation and lower *SIRT1* gene expression *via* reactive oxygen species is involved in Sb-induced apoptosis in BEAS-2b cells," *Toxicology Letters*, vol. 296, pp. 73–81, 2018.

[70] C. Wang, X. Nie, Y. Zhang et al., "Reactive oxygen species mediate nitric oxide production through ERK/JNK MAPK signaling in HAPI microglia after PFOS exposure," *Toxicology and Applied Pharmacology*, vol. 288, no. 2, pp. 143–151, 2015.

[71] A. V. Birk, W. M. Chao, C. Bracken, J. D. Warren, and H. H. Szeto, "Targeting mitochondrial cardiolipin and the cytochrome c/cardiolipin complex to promote electron transport and optimize mitochondrial ATP synthesis," *British Journal of Pharmacology*, vol. 171, no. 8, pp. 2017–2028, 2014.

[72] A. P. Halestrap and A. P. Richardson, "The mitochondrial permeability transition: a current perspective on its identity and role in ischaemia/reperfusion injury," *Journal of Molecular and Cellular Cardiology*, vol. 78, pp. 129–141, 2015.

[73] Y. Lu, S. Liu, Y. Wang, D. Wang, J. Gao, and L. Zhu, "Asiatic acid uncouples respiration in isolated mouse liver mitochondria and induces HepG2 cells death," *European Journal of Pharmacology*, vol. 786, pp. 212–223, 2016.

[74] C. Wan, X. Ma, S. Shi et al., "Pivotal roles of p53 transcription-dependent and -independent pathways in manganese-induced mitochondrial dysfunction and neuronal apoptosis," *Toxicology and Applied Pharmacology*, vol. 281, no. 3, pp. 294–302, 2014.

[75] J. Nan, W. Zhu, M. S. Rahman et al., "Molecular regulation of mitochondrial dynamics in cardiac disease," *Biochimica et Biophysica Acta-Molecular Cell Research*, vol. 1864, no. 7, pp. 1260–1273, 2017.

[76] J. Marin-Garcia and A. T. Akhmedov, "Mitochondrial dynamics and cell death in heart failure," *Heart Failure Reviews*, vol. 21, no. 2, pp. 123–136, 2016.

[77] T. MacVicar and T. Langer, "OPA1 processing in cell death and disease – the long and short of it," *Journal of Cell Science*, vol. 129, no. 12, pp. 2297–2306, 2016.

[78] D. A. Patten, J. Wong, M. Khacho et al., "OPA1-dependent cristae modulation is essential for cellular adaptation to metabolic demand," *EMBO Journal*, vol. 33, no. 22, pp. 2676–2691, 2014.

[79] Q. Jin, R. Li, N. Hu et al., "DUSP1 alleviates cardiac ischemia/reperfusion injury by suppressing the Mff-required mitochondrial fission and Bnip3-related mitophagy via the JNK pathways," *Redox Biology*, vol. 14, pp. 576–587, 2018.

Hindawi
Oxidative Medicine and Cellular Longevity
Volume 2019, Article ID 8690746, 15 pages
https://doi.org/10.1155/2019/8690746

*Research Article*

# Plin5/p-Plin5 Guards Diabetic CMECs by Regulating FFAs Metabolism Bidirectionally

**Jin Du,[1] Juanni Hou,[2] Juan Feng,[1] Hong Zhou,[3] Heng Zhao,[4] Dachun Yang,[1] De Li,[1] Yongjian Yang,[1] and Haifeng Pei[1]**

[1]*Department of Cardiology, The General Hospital of Western Theater Command, Chengdu 610083, China*
[2]*Department of Gastroenterology, The General Hospital of Western Theater Command, Chengdu 610083, China*
[3]*Department of Respiration, The General Hospital of Western Theater Command, Chengdu 610083, China*
[4]*Department of Function, Sichuan Petroleum General Hospital, Chengdu 610212, China*

Correspondence should be addressed to Yongjian Yang; yyj10001@126.com and Haifeng Pei; web2010@foxmail.com

Received 12 March 2019; Accepted 23 July 2019; Published 17 October 2019

Guest Editor: Tatjana Bačun



*Background*. Hyper-free fatty acidemia (HFFA) impairs cardiac capillaries, as well as type 2 diabetes mellitus (T2DM). Perilipin 5 (Plin5) maintains metabolic balance of free fatty acids (FFAs) in high oxidative tissues via the states of nonphosphorylation and phosphorylation. However, when facing to T2DM-HFFA, Plin5's role in cardiac microvascular endothelial cells (CMECs) is not defined. *Methods*. In mice of WT or Plin5$^{-/-}$, T2DM models were rendered by high-fat diet combined with intraperitoneal injection of streptozocin. CMECs isolated from left ventricles were incubated with high glucose (HG) and high FFAs (HFFAs). Plin5 phosphorylation was stimulated by isoproterenol. Plin5 expression was knocked down by small interfering RNA (siRNA). We determined cardiac function by small animal ultrasound, apoptotic rate by flow cytometry, microvessel quantity by immunohistochemistry, microvascular integrity by scanning electron microscopy, intracellular FFAs by spectrophotometry, lipid droplets (LDs) by Nile red staining, mRNAs by quantitative real-time polymerase chain reaction, proteins by western blots, nitric oxide (NO) and reactive oxygen species (ROS) by fluorescent dye staining and enzyme-linked immunosorbent assay kits. *Results*. In CMECs, HFFAs aggravated cell injury induced by HG and activated Plin5 expression. In mice with T2DM-HFFA, Plin5 deficiency reduced number of cardiac capillaries, worsened structural incompleteness, and enhanced diastolic dysfunction. Moreover, in CMECs treated with HG-HFFAs, both ablation and phosphorylation of Plin5 reduced LDs content, increased intracellular FFAs, stimulated mitochondrial $\beta$-oxidation, added ROS generation, and reduced the expression and activity of endothelial nitric oxide synthase (eNOS), eventually leading to increased apoptotic rate and decreased NO content, all of which were reversed by N-acetyl-L-cysteine. *Conclusion*. Plin5 preserves lipid balance and cell survival in diabetic CMECs by regulating FFAs metabolism bidirectionally via the states of nonphosphorylation and phosphorylation.

## 1. Introduction

The main features of type 2 diabetes mellitus (T2DM) are hyperglycemia and metabolic disturbance of lipids and proteins [1, 2]. More than 67.1% of T2DM patients have abnormal lipid metabolism [3], such as hyper-free fatty acidemia (HFFA) and hypercholesterolemia. Free fatty acids (FFAs), known as nonesterified fatty acids (NEFAs), are closely related to metabolic syndrome in T2DM patients [4] and serve as an important risk factor in cardiovascular diseases [5]. Moreover, within the body, the metabolic processes of glucose and lipid can interact with each other. Lee et al. even have found that plasma FFAs begin to rise progressively as earlier as two weeks prior to hyperglycemia [6]. It is clear that hyperglycemia aggrandizes the vulnerability of endothelial cells to exogenous stimulus, which can be aggravated by hyperlipidemia. Thus, we cannot ignore the interaction of glucose and lipid in research of diabetic complications. It is well known that microvascular lesions widely occurred in T2DM, resulting in abnormal microcirculation [7, 8]. Microvascular endothelial cells form the basic structure of microvessels, and the pathological changes in cardiac microvascular endothelial

cells (CMECs) occur before the myocardium in the diabetic heart [9]. Recently, coronary microvascular diseases (CMD) have attracted wide attention, such as cardiac X syndrome, coronary slow flow phenomenon, and no-reflow phenomenon. By using coronary angiography, it is believed that microvascular endothelial dysfunction is an important cause of CMD [10]. Therefore, it is an urgent task to explore the molecular mechanism of CMECs injury, which may help develop new target for CMD.

Lipid droplets (LDs) serve as essential organelles for intracellular lipid storage [11]. Perilipin 5 (Plin5) is one of the important members of lipid droplet-associated proteins on the surface of LDs and is highly expressed in high fatty acid oxidation tissues, such as heart, skeletal muscle, liver, and brown fat [12]. Plin5 plays an important role in cellular lipid metabolism by promoting or inhibiting the hydrolysis of neutral fat in LDs. It not only ensures the energy supply of cells but also prevents the lipid toxicity damage caused by fatty acid overload [13]. A large amount of literatures reveal that Plin5 knockout reduces the formation of LDs, enhances the oxidation of FFAs, and causes insulin resistance [14–16]. In vascular endothelial cells, LDs can be quickly formed and decomposed [17]. Plin5 deletion in large arteries of mice can accelerate the progression of atherosclerosis [18]. On the contrary, it is reported that Plin5 overexpression with high cardiac specificity results in myocardial steatosis and mitochondrial dysfunction in mice [19, 20]. However, the concrete role of Plin5 in CMECs has not been well defined yet. More interestingly, the phosphorylation mode of Plin5 (p-Plin5) can promote the hydrolysis of triglyceride (TG) in LDs and enhance the release of FFAs into the cytoplasm [21]. Many studies have shown that protein kinase A (PKA) activation can stimulate the phosphorylation of Plin5 [22, 23], in which serine 155 may be the important site [22, 24]. Moreover, p-Plin5 in the nucleus can also inhibit SIRT1 activity, promote the transcription of peroxisome proliferator-activated receptor gamma coactivator 1-$\alpha$ (PGC-1$\alpha$), and eventually enhance the synthesis and oxidation function of mitochondria [24]. Furthermore, it is reported that increasing the PKA-mediated phosphorylation of Plin5 by atorvastatin can reduce cellular lipid accumulation in hepatocytes [25]. However, the specific action of p-Plin5 in diabetic CMECs remains unclear.

Oxidative stress is caused by excessive production of reactive oxygen species (ROS) and reactive nitrogen (RNS) and/or the reduction of cellular antioxidant capacity [26, 27]. Mitochondria is the most important source of ROS in cells [28], and the $\beta$-oxidation of FFAs can produce a large number of ROS [29, 30]. Many studies show that Plin5 is closely related to oxidative stress, and Plin5 knockout can lead to enhanced mitochondrial $\beta$-oxidation in myocardium and hepatocytes in mice [16, 31]. However, whether oxidative stress mediates the biological function of Plin5/p-Plin5 in diabetic CMECs deserves a thorough study.

The aims of this study are to determine (1) whether Plin5 is disturbed in diabetic CMECs, (2) whether the deficiency and phosphorylation of Plin5 affect the survival of CMECs under the condition of T2DM-HFFA, and, if so, (3) to identify whether oxidative stress participates in those biological effects of Plin5/p-Plin5 in CMECs.

## 2. Material and Methods

*2.1. Preparation of Mice.* Normal mice of wild type (WT; C57BL6/J, male) were obtained from Vital River (Beijing, China) and Plin5$^{-/-}$ mice from Graduate School of Life Science (Hyogo, Japan) for this experiment [14]. The reverse transcription-polymerase chain reaction (RT-PCR) was used to detect the genotypes of mice. Mice were given free access to water and feed and raised under standard conditions at 22-26°C with 12-hour light/12-hour dark cycle. These two genotypes mice were both randomly divided into the control group and type 2 diabetes mellitus with hyper-free fatty acidemia (T2DM-HFFA) group. To prepare animal models of T2DM-HFFA, 6-week-old mice were given high-fat diet (60% from fat, 20% from carbohydrates, and 20% from protein, Research Diets, USA) for 8 weeks and then were fasted for 16 hours and subsequently given intraperitoneal injection of streptozocin (STZ; 30 mg/kg, Sigma, USA). Later, these mice were fed continuously with high-fat diet for 16 weeks [32]. The fasting blood glucose levels ≥11.1 mmol/L and with symptoms of polyuria and polydipsia were confirmed to be successful in modeling [33]. Meanwhile, serum FFAs level ≥3.0 mmol/L was defined HFFA [34]. 24 weeks later, mice with hyperglycemia and HFFA were used for the experiments. All experiments were conducted in adherence with National Institutes of Health Guidelines on the Use of Laboratory Animals and were approved by the Institutional Animal Care and Use Committee in the General Hospital of Western Theater Command.

*2.2. Biochemical Indicator.* The mice were given 12 hours of fasting treatment before experiments. Electronic balance was used to detect body weight of mice. Serum levels of glucose, insulin (INS), free fatty acids (FFAs), triglyceride (TG), and cholesterol (CHOL) were determined by automatic biochemical analyzer (Model 7020, Hitachi, Japan).

*2.3. Scanning Electron Microscope.* Mice were anesthetized with 4% chloral hydrate, and the abdominal aorta was intubated. Heparin saline and acetone butanone mixture was perfused in turn. Then, acrylonitrile butadiene styrene (ABS; 10%) solution was perfused into for 15 mL when perfusion pressure was maintained at about 200 mmHg. After the perfusion was completed, the hearts of mice were placed at room temperature for 24 hours and then corroded by concentrated hydrochloric acid for 1 week. Microvascular casts were obtained by rinsing with water and dried by freeze-drying. After spraying with gold, the microvasculatures were observed by the scanning electron microscope (Model S-3400N, Hitachi, Japan) at 15 kV.

*2.4. Immunohistochemical Staining.* After fixed with formaldehyde, the heart was given treatment of paraffin embedding and finally made into slices with a thickness of 5 $\mu$m. Sections were incubated with hydrogen peroxide ($H_2O_2$; 3%, 25 minutes) to eliminate the endogenous peroxidase. Then, sections were covered with bovine serum albumin

(BSA; 3%, 30 minutes) at room temperature. After the rabbit anti-mouse CD31 primary antibody (1 : 200, CST, USA) was added, sections were kept in the wet box (4°C, overnight). After washed with phosphate-buffered saline (PBS), goat anti-rabbit secondary antibody (1 : 1000, CST, USA) was added and incubated at 37°C for 2 hours. The sections were observed under an optical microscope (DM3000, Leica, Germany). The microvessels were the standard of blood vessel with diameter less than 100 $\mu$m. Each slice was randomly observed for 5 visual fields, and the mean numbers of microvessels were calculated with Image-Pro Plus.

*2.5. Cardiac Function.* The mice were anesthetized with 4% chloral hydrate. VEVO 2100 high-resolution in vivo imaging system (Visual Sonics, Canada) was used to measure the left ventricular early mitral diastolic wave/late mitral diastolic wave (E/A) ratio and the percentage of left ventricular ejection fraction (LVEF). The whole detection process was carried out by an ultrasonic technician who was blinded to the experimental groups, and the detection parameters remained unchanged.

*2.6. Preparation of CMECs.* CMECs were isolated from the hearts as previously described [35, 36]. Briefly, the hearts of experimental mice were washed with precooled PBS at 4°C. After the aorta and atrial tissues were dislodged, the epicardium and endocardium were removed from ventricular tissues which were then cut into slices of 1 $mm^3$ size pieces and incubated in collagenase II (0.2%, Sigma, USA) for 30 minutes. After that, 100 $\mu$m strainer mesh was used to remove the undigested tissues. Finally, cells were cultured in the Dulbecco's modified Eagle's medium (DMEM; HyClone, USA) supplemented with fetal bovine serum (FBS; 15%, Gibco, USA). The cells for transplantation were purified using differential time adherent method. Once cell confluence reaches 80%, cells were digested with trypsin (0.25%, 37°C, 20 minutes; Sigma, USA). The third to fifth generation cells were harvested for the further experiments. CMECs were positively identified by staining of von Willebrand factor (vWF) and CD31. Media were replaced to different conditions 24 hours after cell inoculation: normal glucose medium (normal, 5.5 mmol/L), high glucose medium (HG, 25 mmol/L), high free fatty acids medium (HFFAs; 1 mmol/L, Sigma, USA), and high glucose plus high free fatty acids medium (HG-HFFAs). HFFAs were a mixture of palmitate and oleate, 1 : 2 ($w/w$) [37]. Then, the cells were incubated for another 24 hours. Reagents and drugs used in cell experiments in vitro were as follows: N-acetyl-L-cysteine (NAC; 10 nmol/L, 8 hours; Sigma, USA) and isoprenaline (ISO; 10 $\mu$mol/L, 8 hours; Sigma, USA).

*2.7. Cellular Immunofluorescence.* CMECs were fixed in paraformaldehyde at room temperature for 30 minutes. Triton (0.1%, 5 minutes) was used to broken film. Then, cells were covered with 3% BSA for 30 minutes. Rabbit anti-mouse Plin5 primary antibody (1 : 500, Novus, USA) was added and kept overnight at 4°C. The donkey anti-rabbit fluorescent secondary antibody (1 : 1000, Abcam, USA) was added the next day, and the cells were observed under laser confocal microscopy (LSCM; FV 1000, Olympus, Japan) after cleaning with PBS for 3 times.

*2.8. Cell Apoptosis.* Cell apoptosis was measured by Annexin V-FITC/PI assay kit (BD, USA). After digestion, CMECs were washed 2 times with cooled PBS. Then, cells were suspended with 1× binding buffer and added with Annexin V-FITC and PI 2.5 $\mu$L each. CMECs were incubated under light avoidance conditions at room temperature for 15 minutes. Apoptosis was detected by flow cytometry (Partec, Germany), and data were analyzed by FlowJo software.

*2.9. Nitric Oxide (NO).* When the intervention was completed, CMECs were incubated with DAF-2DA, a kind of fluorescent probe for the detection of NO (5 $\mu$mol/L, 20 minutes; Abcam, England). After washed by PBS for 3 times to remove the unbound DAF-2DA, CMECs were observed under laser confocal microscopy (LSCM; FV 1000, Olympus, Japan) at 488 nm emission wavelengths. In addition, the level of NO in CMECs was also detected by enzyme-linked immunosorbent assay (ELISA) kit (Elixir, Canada) following the instruction [38].

*2.10. Intracellular ROS.* According to the 1 : 1000 ratio, dihydroethidium (DHE; Beyotime, China) was diluted with Hank's balanced salt solution (HBSS; Invitrogen, USA) to make the final concentration (5 $\mu$mol/L). CMECs were incubated with DHE in the incubator of 37°C for 45 minutes. After washed with HBSS, cells were observed under fluorescence microscope (Olympus, Japan). Besides, the content of intracellular ROS was also detected by ELISA kit (Elixir, Canada) following the instruction [39].

*2.11. Gene Expression.* Total RNA was extracted from cells using TRIzol reagent (Invitrogen, USA), quantitated using a NanoDrop 2000 spectrophotometer. Then, the RNA was reverse-transcribed using a kit (TaKaRa, Japan). Quantitative real-time polymerase chain reaction (qRT-PCR) was performed in a CFX96 real-time detection system (Bio-Rad, USA) using SYBR Green PCR kit (TaKaRa, Japan). Relative mRNA levels were quantified using the comparative $\Delta\Delta$CT method with GAPDH as reference gene. The following primer sequences were used for qRT-PCR: GAPDH forward, 5′-AGGTCGGTGTGAACGGATTTG-3′, reverse, 5′-TGTAGACCATGTAGTTGAGGTCA-3′; Plin5 forward, 5′-GAAGTGGGCACAGTGGAGG-3′, reverse, 5′-AAAGAGTGTTCATAGGCGAGAT-3′; and carnitine palmitoyl transferase 1 (CPT-1) forward, 5′-CACTGCAGCTCGCACATTAC-3′, reverse, 5′-CCAGCACAAAGTTGCAGGAC-3′.

*2.12. Western Blot.* CMECs were washed with PBS for 3 times; total protein and nuclear protein were extracted by a kit (Sigma, USA). The concentration of protein was determined with the Bio-Rad protein assay kit (Bio-Rad, USA). Equivalent amounts of total protein (25 $\mu$g) were subjected to SDS-PAGE and transferred to PVDF membranes. The membranes were incubated with specific primary antibodies against Plin5 (1 : 2000, Novus, USA), GAPDH (1 : 3000, Novus, USA), Histone H3 (1 : 2000, CST, USA), and eNOS

(1 : 2000, Novus, USA) for overnight. After incubation with goat anti-rabbit IgG secondary antibody (1 : 2000, 1 hour; Thermo Fisher, USA) at room temperature, proteins were detected with enhanced chemiluminescence and quantified using Image-Pro Plus software [40].

*2.13. Nile Red Staining.* The cells were rinsed 2 times with PBS and fixed by incubating with 2 mL 4% ($w/v$) paraformaldehyde at room temperature for 30 minutes. After that, the cells were washed 3 times with PBS. Nile red stock solution (1 mg/mL, 1 $\mu$L) was added to 10 mL of PBS. Then, the cells were covered with 1 mL Nile red staining solution and incubated for 10 minutes, all of which were protected from ambient light. The cells were washed with PBS 3 times and observed under laser confocal microscopy. The fluorescence intensity was analyzed by ImageJ software.

*2.14. Intracellular FFAs.* CMECs were homogenized in 200 $\mu$L of 1% ($w/v$) Triton X-100 in chloroform solution. The samples were centrifuged at 13,000 g for 10 minutes to remove insoluble material. We collected the organic phases (lower phase) and removed chloroform by air dry at 50°C. The dried lipids were dissolved in 200 $\mu$L fatty acid assay buffer by vortexing extensively for 5 minutes. Then, the concentration of FFAs was determined by a Free Fatty Acid Quantitation Kit (Sigma, USA), according to the instruction.

*2.15. siRNA Transfection.* One day before transfection, the cells were inoculated into 6-well plates and cultured in antibiotic-free medium. Moderate transfection reagent was added Opti-MEM medium and incubated at room temperature for 5 minutes. Small interfering RNA (siRNA), including the control siRNA and Plin5 siRNA (Invitrogen, USA), was added into Opti-MEM medium and blended. Then, the diluted siRNA was gently mixed with the incubated transfection reagent and incubated for 30 minutes at room temperature. Next, we removed the previous medium from the 6-well plates, and added 1.5 ml new antibiotic-free medium and 500 $\mu$l siRNA-transfection reagent in it. The cells were placed in the incubator for 48 hours and then intervened as planned.

*2.16. Statistical Analyses.* Data were shown as means ± standard errors of the means (SEM). The independent sample $t$-test was used in the comparison between the 2 groups. The single-factor *ANOVA* was used in comparison among multiple groups, and pairwise comparison in multiple groups was conducted with LSD $t$-test. $P \leq 0.05$ was considered significant. All statistical tests were performed using GraphPad Prism software version 7.

## 3. Results

*3.1. High FFAs Aggravated Cardiac Microvascular Injury Induced by HG.* We established mouse models of T2DM-HFFA to observe pathological changes in cardiac microvasculature and function. Compared with the control mice, serum levels of glucose, insulin, and FFAs increased significantly in diabetic mice (Table S1), revealing that we prepared the basic platform for our experiments. Echocardiography showed that E/A ratio, but not LVEF percentage, was decreased obviously in diabetic mice (Figures 1(a) and 1(b)), hinting at that T2DM gives rise to ventricular diastolic dysfunction. Moreover, in diabetic mice, the number of cardiac microvessels decreased remarkably (Figure 1(c)), and those remaining microvessels became rough and uneven (Figure 1(d)). In view of the fact that cardiac microvessel is composed of monolayer endothelial cells, CMECs were isolated from neonatal mice. More than 95% of the cells were positively identified by the endothelial cell marker, vWF and CD31 (Figure S1A). HG significantly enhanced CMECs apoptosis and reduced cellular NO content, all of which were further deteriorated by intervention of high FFAs (HFFAs) (Figures 1(e)–1(g)). We also repeated the main experiments on CMECs isolated from the control and T2DM-HFFA mice; the computational data from the T2DM-HFFA modeling largely indicated similar trends with the previous experimental results. T2DM-HFFA not only exacerbated endothelial apoptosis but also further inhibited NO generation (Figure S1B and S1C). These data suggest that disorder of FFAs metabolism is able to aggravate cardiac microvascular injury induced by HG.

*3.2. Plin5 Deletion Increased Intracellular FFAs Content in CMECs.* In order to clarify the concrete role of Plin5 in metabolism of FFAs, immunofluorescence, qRT-PCR and western blots were introduced to judge Plin5 changes in CMECs. As a result, HFFAs, but not HG, enhanced Plin5 expression (Figures 2(a)–2(c)). In addition, RT-PCR was used to detect genotypes in mice (Figure S2), and CMECs were isolated from the WT and Plin5$^{-/-}$ mouse hearts. Nile red staining showed that HG-HFFAs intervention increased intracellular LDs content, and Plin5 deletion significantly reduced intracellular LDs content (Figure 2(d)), whereas, compared with CMECs in WT, Plin5 deficiency had increased intracellular FFAs content under the condition of normal and HG-HFFAs (Figure 2(e)). These results reveal that Plin5 plays a critical role in the FFAs metabolism of CMECs, which may affect the survival and function of CMECs.

*3.3. Plin5 Deficiency Exacerbated CMECs Injury Induced by HG-HFFAs.* Although Plin5 is reported to protect cells from lipid toxicity via preventing excessive FFAs release from TG, its role in lipid metabolism of vascular endothelium has not been investigated. Here, we found that Plin5 knockout had no significant effects on the level of body weight, blood glucose, insulin, and blood lipid (Table S1). Echocardiographic findings suggested that Plin5 ablation had no significant effect on E/A ratio and LVEF under basic condition. However, it exacerbated ventricular diastolic dysfunction in T2DM-HFFA mice (Figures 3(a) and 3(b)). Corresponding to the ultrasound findings, imaging of scanning electron microscopy and immunohistochemistry showed that Plin5 ablation hardly affected the number and integrity of cardiac microvessels under basic condition, whereas Plin5 deletion resulted in less number of cardiac microvessels and worse endothelial junctions between CMECs under T2DM-HFFA condition (Figures 3(c) and 3(d)). Moreover, cell apoptosis and NO production in WT were close to those in Plin5$^{-/-}$ under normal condition. But, Plin5 knockout in CMECs

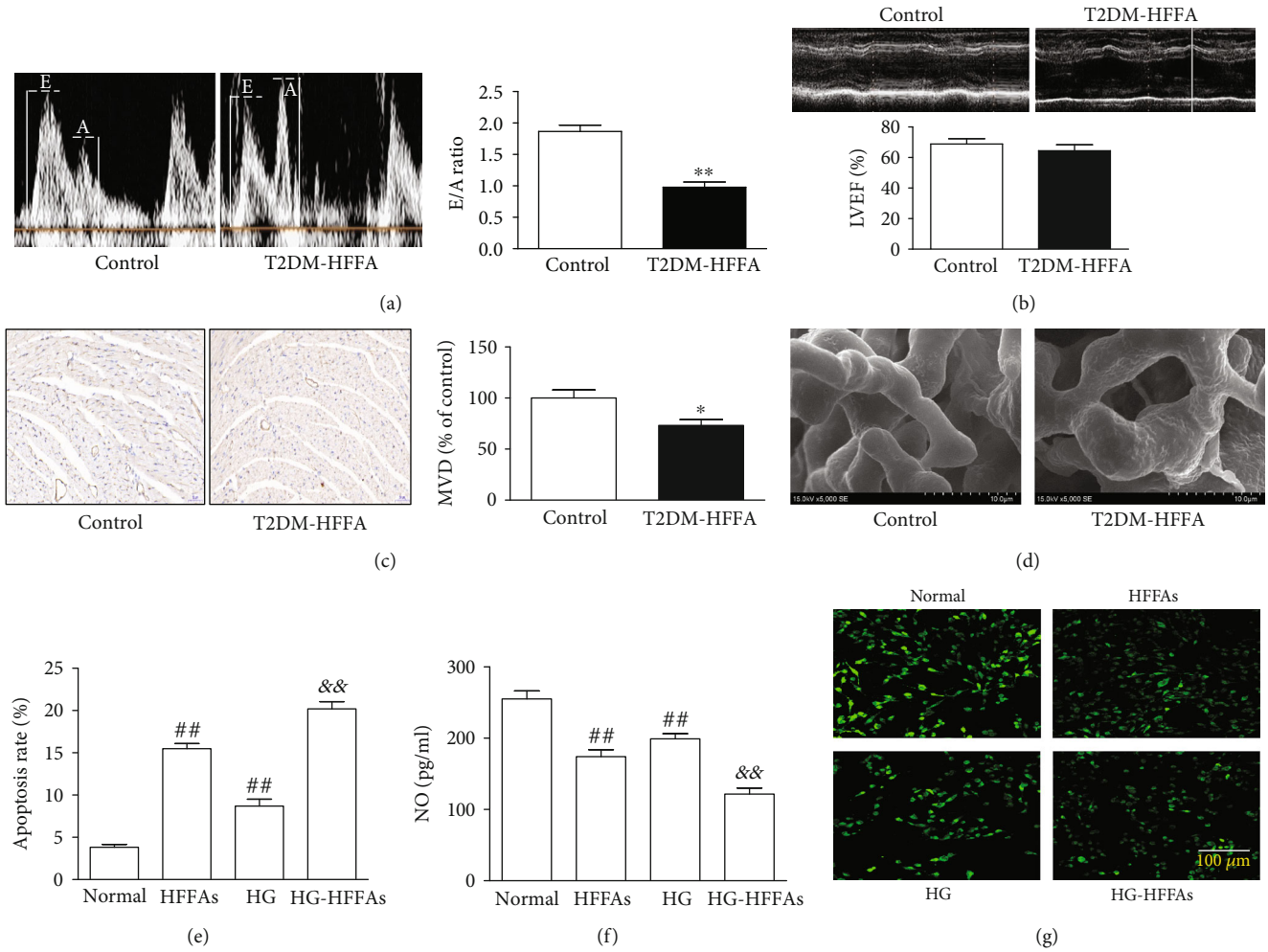


Figure 1: The influence of HG-HFFAs on CMECs. (a) The representative mitral flow patterns detected by cardiac ultrasound (left); the quantification of E/A ratio (right). (b) The percentage of LVEF detected by cardiac ultrasound. (c) The number of cardiac microvessels counted by CD31 immunohistochemical staining (left); the quantification of MVD (right). (d) Cardiac microvascular integrity detected by scanning electron microscope. (e) The apoptosis rate measured by Annexin V-FITC/PI assay kit. (f) NO generation in CMECs measured by ELISA kit. (g) NO production in CMECs detected by staining with DAF-2DA. T2DM-HFFA: type 2 diabetes mellitus with hyper-free fatty acidemia; HG: high glucose; HFFAs: high free fatty acids; HG-HFFAs: high glucose and high free fatty acids; E/A: early mitral diastolic wave/late mitral diastolic wave; LVEF: left ventricular ejection fraction; MVD: microvessel density; ELISA: enzyme-linked immunosorbent assay. Data are expressed as mean ± SEM, $n = 6$-8/group. $^{*}P < 0.05$, $^{**}P < 0.01$ vs. control; $^{\#\#}P < 0.01$ vs. normal; $^{\&\&}P < 0.01$ vs. HG.

exacerbated cell apoptosis and NO reduction induced by HG-HFFAs (Figures 3(e)–3(g)). siRNA was used to knock down the expression of Plin5 in WT; results showed that Plin5 knockdown had no significant effect on the apoptotic rate and NO production in CMECs under normal conditions, and yet it aggravated damage to CMECs under HG-HFFAs conditions (Figure S3A and S3B). In order to explore the mechanism of decreasing NO production, the activity and protein content of endothelial nitric oxide synthase (eNOS) were detected. Under normal conditions, Plin5 knockout had little effect on the activity and protein content of eNOS in CMECs. Nevertheless, under HG-HFFAs conditions, it did reduce the activity and content of eNOS in CMECs (Figure S4A and S4B). Thus, Plin5 serves as an essential molecule in the survival and function of CMECs when facing to the insult of HG-HFFAs.

*3.4. Plin5 Phosphorylation Worsened CMECs Injury Induced by HG-HFFAs.* Plin5 phosphorylation also plays an important role in FFAs metabolism. Here, we introduced ISO to activate the phosphorylation of Plin5. With the western blot technology, we found that ISO intervention added endonuclear Plin5 expression in CMECs under normal and HG-HFFAs conditions (Figure 4(a)), which indirectly indicated that cellular Plin5 phosphorylation was enhanced. Meanwhile, after administration of ISO in CMECs, FFAs level significantly increased and LDs content obviously decreased, under normal and HG-HFFAs conditions (Figures 4(b) and 4(c)). Moreover, ISO intervention also deteriorated cell apoptosis and depressed NO generation in CMECs under HG-HFFAs condition. But it is important to note that ISO intervention had no obvious effect on apoptotic rate and NO production under normal condition (Figures 4(d)–4(f)). Further detection found that ISO intervention had

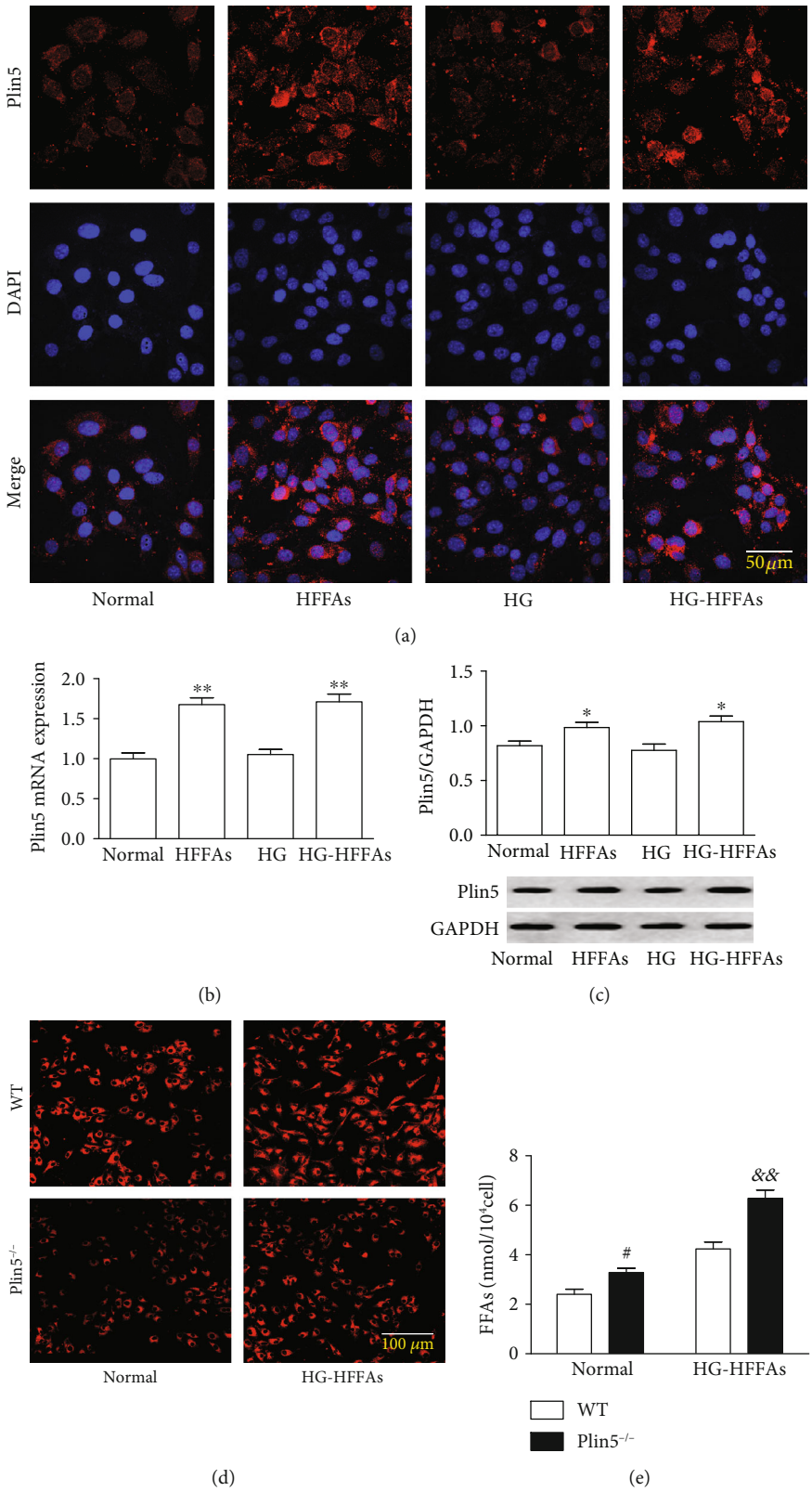


Figure 2: The effects of HG or HFFAs on Plin5 expression in CMECs. (a) Plin5 expression detected by immunofluorescence staining. (b) The mRNA level of Plin5 in CMECs measured by qRT-PCR. (c) The protein level of Plin5 in CMECs determined by western blot. (d) The content of LDs in CMECs detected by Nile red staining. (e) The intracellular level of FFAs in CMECs measured by Free Fatty Acid Quantitation Kit. qRT-PCR: quantitative real-time polymerase chain reaction; HG: high glucose; HFFAs: high free fatty acids; HG-HFFAs: high glucose and high free fatty acids; DAPI: 4′,6-diamidino-2-phenylindole. Data are expressed as mean ± SEM, $n = 6$-8/group. $^{*}P < 0.05$ vs. normal; $^{**}P < 0.01$ vs. normal; $^{\#}P < 0.05$ vs. WT in normal; $^{\&\&}P < 0.01$ vs. WT in HG-HFFAs.

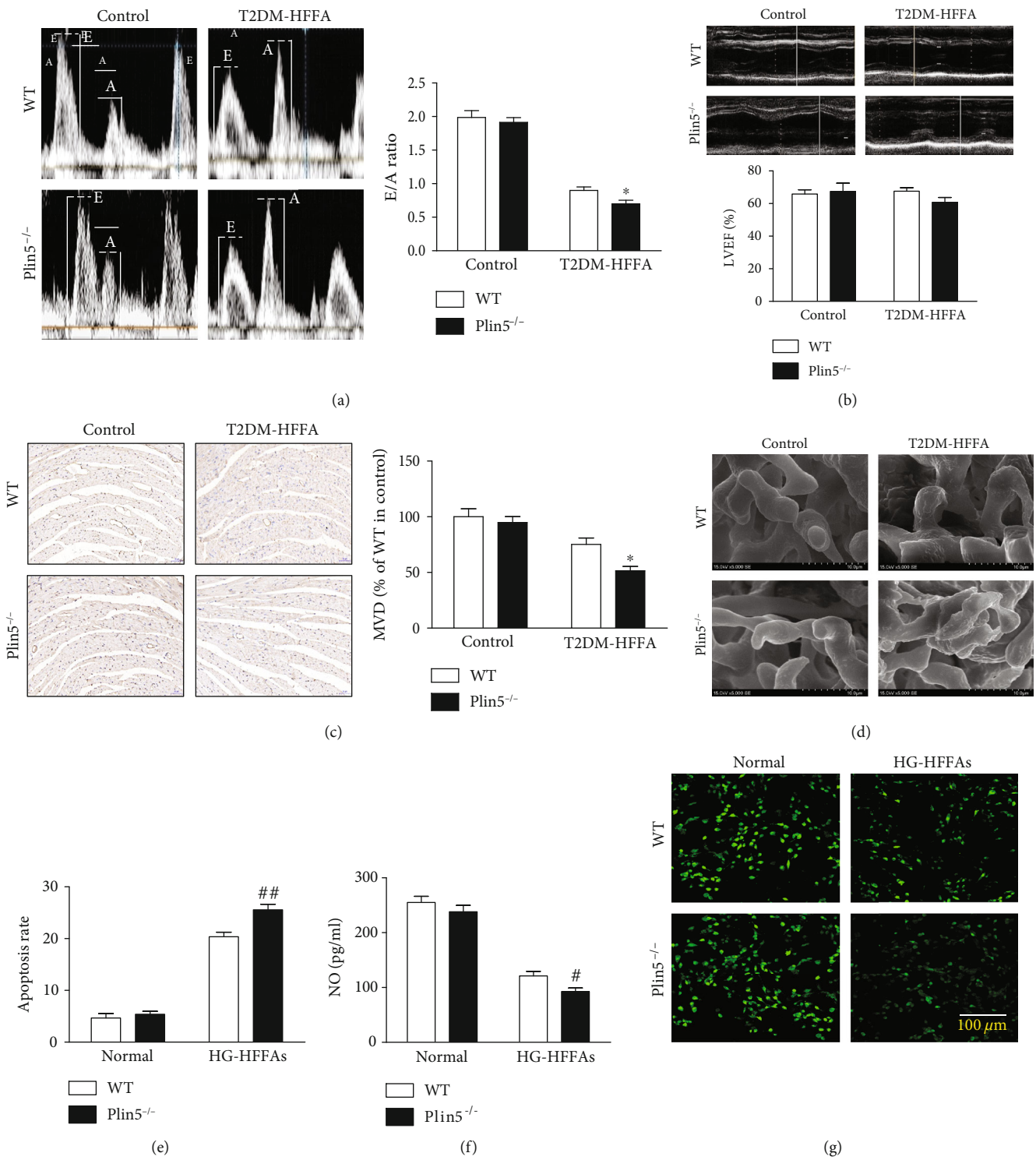


Figure 3: The influence of Plin5 deficiency on CMEC injury induced by HG-HFFAs. (a) The representative mitral flow patterns detected by cardiac ultrasound (left); the quantification of E/A ratio (right). (b) The percentage of LVEF detected by cardiac ultrasound. (c) The number of cardiac microvessels counted by CD31 immunohistochemical staining (left); the quantification of MVD (right). (d) Cardiac microvascular integrity detected by scanning electron microscope. (e) The apoptosis rate measured by Annexin V-FITC/PI assay kit. (f) NO generation in CMECs measured by ELISA kit. (g) NO production in CMECs detected by staining with DAF-2DA. WT: wild type; T2DM-HFFA: type 2 diabetes mellitus with hyper-free fatty acidemia; HG: high glucose; HFFAs: high free fatty acids; HG-HFFAs: high glucose and high free fatty acids; E/A: early mitral diastolic wave/late mitral diastolic wave; LVEF: left ventricular ejection fraction; MVD: microvessel density; ELISA: enzyme-linked immunosorbent assay. Data are expressed as mean ± SEM, $n = 6$-8/group. $^{*}P < 0.05$ vs. WT in T2DM-HFFA; $^{\#}P < 0.05$, $^{\#\#}P < 0.01$ vs. WT in HG-HFFAs.

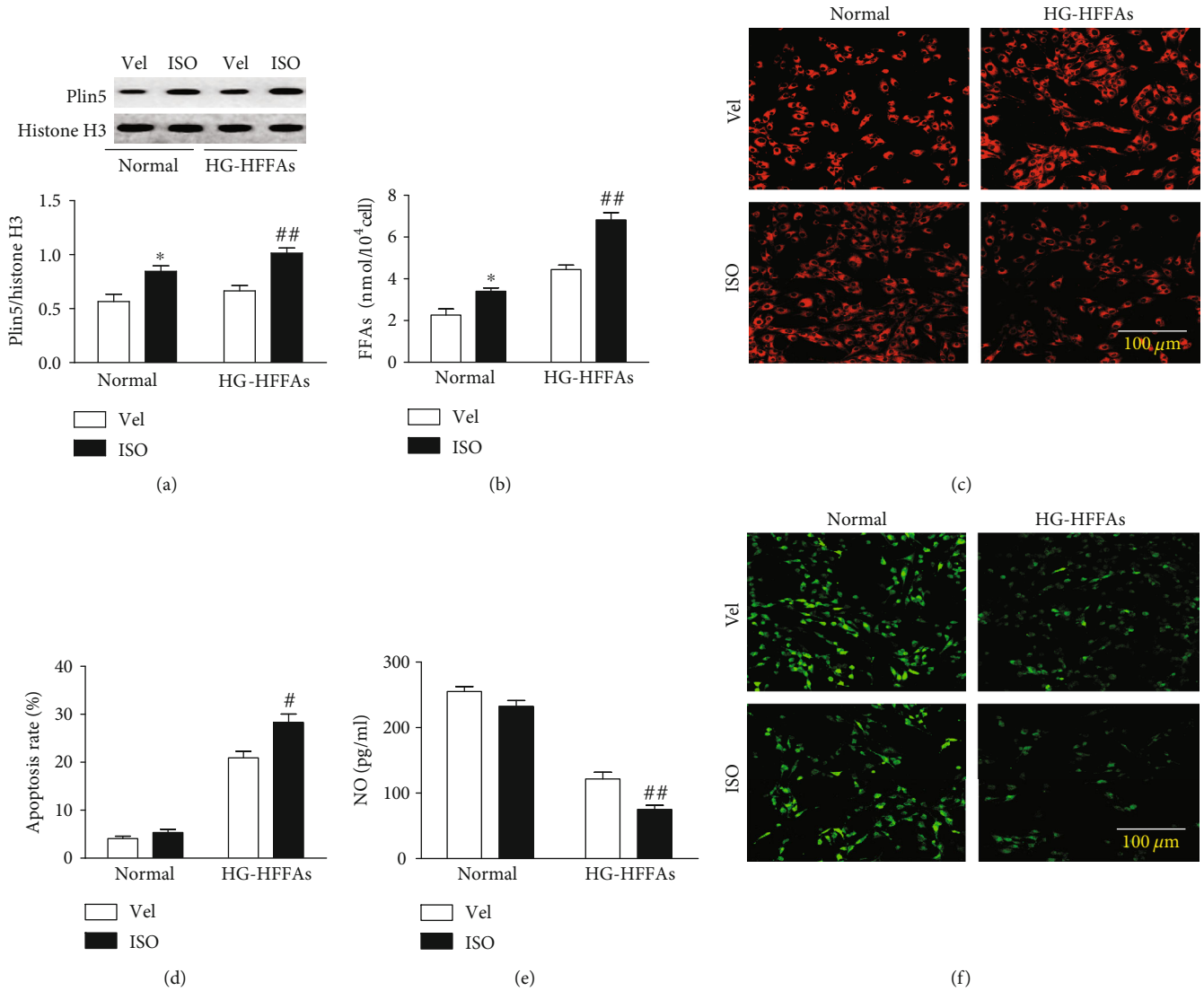


Figure 4: The influence of p-Plin5 on CMECs injury induced by HG-HFFAs. (a) The protein level of Plin5 detected by western blot. (b) The intracellular FFAs content measured by Free Fatty Acid Quantitation Kit. (c) The content of LDs in CMECs determined by Nile red staining. (d) The apoptosis rate. (e) The production of NO measured by ELISA kit. (f) NO generation detected by staining with DAF-2DA in CMECs. Vel: vehicle; ISO: isoproterenol; HG-HFFAs: high glucose and high free fatty acids; ELISA: enzyme-linked immunosorbent assay. Data are expressed as mean ± SEM, $n$ = 6-8/group. $^{*}P < 0.05$ vs. Vel in normal; $^{\#}P < 0.05$, $^{\#\#}P < 0.01$ vs. Vel in HG-HFFAs.

little effect on the activity and protein content of eNOS under normal condition; however, it further reduced the activity and content of eNOS in CMECs under HG-HFFAs conditions (Figure S5A and S5B). In a word, the phosphorylation of Plin5 induced by sympathetic excitement will result in damage to CMECs by enhancing FFAs catabolism.

*3.5. ROS Overload Induced by Disruption in Plin5 Balance Contributed to CMECs Injury under the Condition of HG-HFFAs.* It is well known to all that oxidative stress plays a key role in the development of diabetic cardiovascular complications. ROS, as the main activating factor of oxidative stress, is mainly produced by mitochondria. In this study, we explored whether intracellular ROS was affected by the deletion or phosphorylation of Plin5 in the presence of HG-HFFAs. The experimental results showed that both knockout and phosphorylation of Plin5 in CMECs enhanced ROS generation induced by HG-HFFAs (Figures 5(a) and 5(d), Figure S6A and S6B). Moreover, knockout and phosphorylation of Plin5 enhanced the mRNA expression of CPT-1 (Figure S6C and S6D). In contrast, NAC, a commonly used intracellular antioxidant, partly reversed CMECs injury induced by Plin5 deletion and phosphorylation under HG-HFFAs condition (Figures 5(b) and 5(c), Figures 5(e) and 5(f)). These results suggest that oxidative stress is the underlying mechanism for CMECs injury induced by Plin5 deletion and phosphorylation.

## 4. Discussion

In this study, we established animal models of T2DM-HFFA by introducing WT and Plin5$^{-/-}$ mice to explore the specific

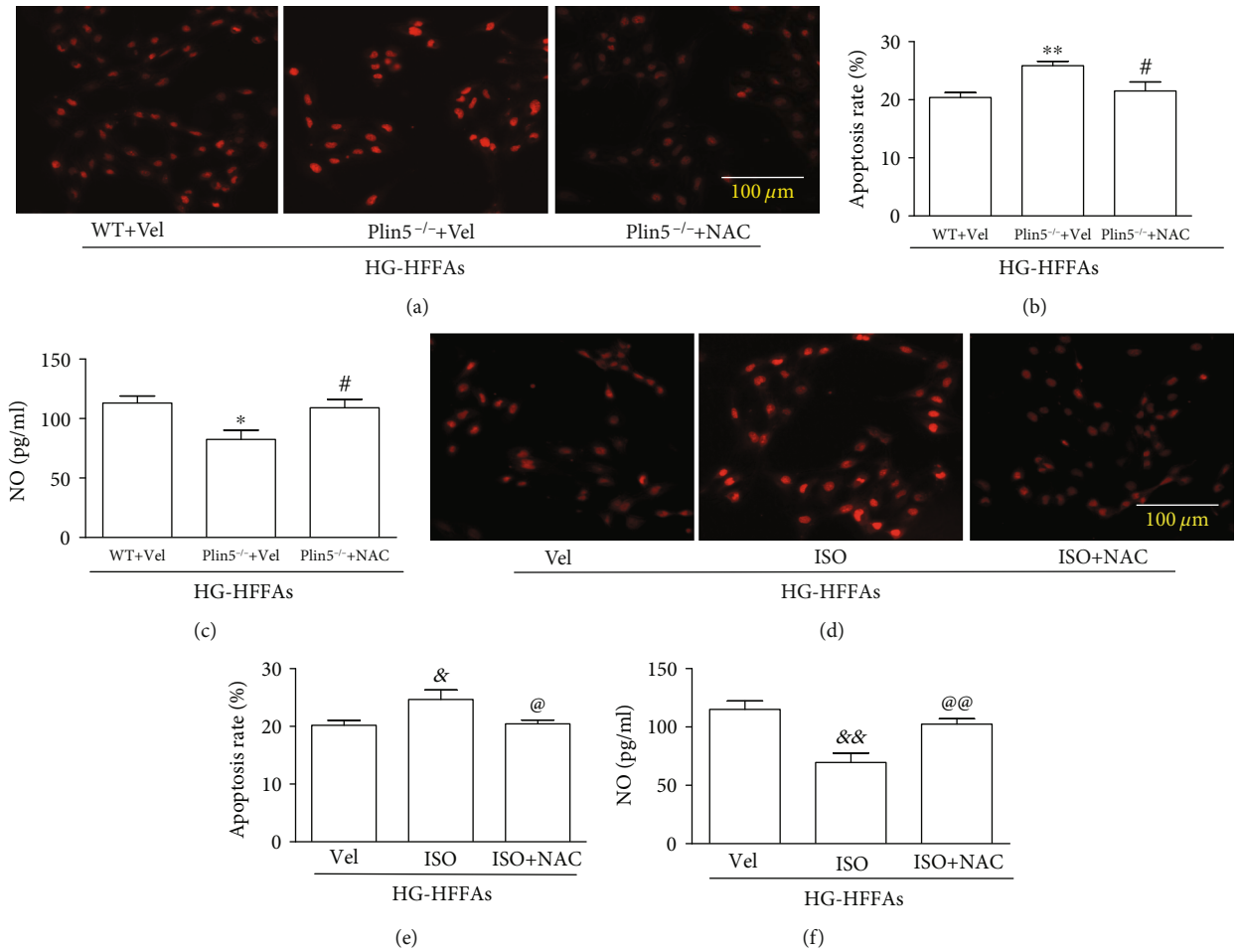


Figure 5: The role of oxidative stress induced by disruption of Plin5 balance in CMECs under the condition of HG-HFFAs. (a, d) ROS in CMECs detected by DHE staining. (b, e) The statistics of apoptosis rate. (c, f) The NO generation in CMECs. ROS: reactive oxygen species; DHE: dihydroethidium; NAC: N-acetyl-cysteine; Vel: vehicle; ISO: isoproterenol; HG-HFFAs: high glucose and high free fatty acid. Data are expressed as mean ± SEM, $n = 6$-8/group. $^{*}P < 0.05$, $^{**}P < 0.01$ vs. WT+Vel; $^{\#}P < 0.05$ vs. Plin5$^{-/-}$+Vel; $^{\&}P < 0.05$, $^{\&\&}P < 0.01$ vs. Vel; $^{@}P < 0.05$, $^{@@}P < 0.01$ vs. ISO.

role of Plin5 in CMECs. We finally observed that both deficiency and phosphorylation of Plin5 aggravated CMECs injury induced by T2DM-HFFA via exacerbating oxidative stress. First, we found that HFFAs, but not HG, could obviously activate Plin5 expression in CMECs; in turn, Plin5 ablation was able to increase intracellular content of FFAs in CMECs. Second, we proved that both deficiency and phosphorylation of Plin5 would deteriorate CMECs injury induced by HG-HFFAs. Third, in the absence or phosphorylated mode of Plin5, intracellular ROS overload would be enhanced to cause worse damage to CMECs under the condition of T2DM-HFFA (Figure 6).

It is estimated that there will be 642 million diabetes mellitus by 2040 [41], most of which will suffer from cardiovascular diseases [42]. As an important category of cardiovascular complications in diabetes, microvascular lesions will result in microcirculation disorder and participate in the pathological process of diabetic multiorgan injuries [43]. Gupta et al. have reported that the incidence of microvascular lesions in asymptomatic T2DM patients is 32.55% [44]. As the basic component of cardiac microvessel, CMECs take part in the pathological process of cardiac microvascular angina by regulating the exchange of energy and substance between cardiomyocyte and blood [45, 46]. In addition, CMECs are the earliest and most vulnerable target of diabetic damage to the heart [47]. According to an epidemiological survey in China, 67.1% of T2DM patients are associated with dyslipidemia. In these T2DM patients, HFFA is one of the most common dyslipidemias that is characterized by excessive FFAs in circulation, which can enhance the inflammatory reaction and oxidative stress in endothelial cells, further induce endothelial apoptosis, and participate in insulin resistance and vascular disease [48–51]. Correction of dyslipidemia can significantly reduce the incidence of cardiovascular complications in T2DM. However, up to now, it is rarely reported about CMECs injury in T2DM-HFFA. In our present study, serum TG, CHOL, INS, and FFAs of T2DM-HFFA mice were significantly increased. Then, our study showed that HFFA reduced the number of microvessels in T2DM-HFFA mice and impaired the integrity of microvessels, which might contribute to the dysfunction of cardiac microvascular barrier and lead to myocardial metabolic

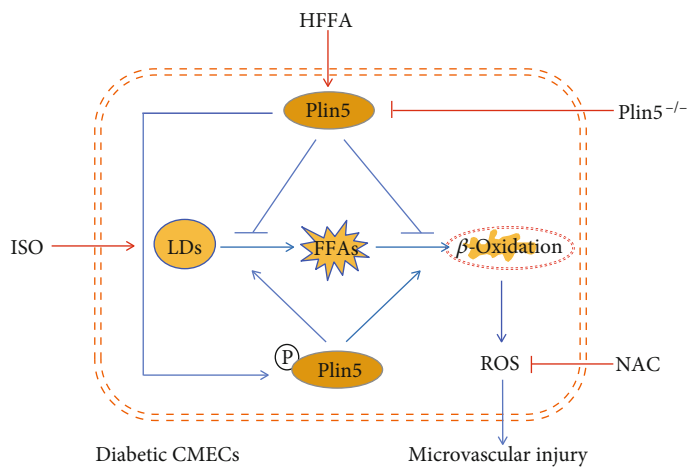


Figure 6: Schematic diagram depicting the bidirectional regulation of Plin5 in the metabolism of intracellular FFAs when facing to T2DM-HFFA. In diabetic CMECs, HFFA, but not hyperglycemia, significantly activates Plin5 expression, and Plin5 is able to inhibit the hydrolysis of LDs to FFAs as well as the mitochondrial $\beta$-oxidation of FFAs, whereas Plin5 ablation promotes the hydrolysis of LDs to FFAs, enhances the mitochondrial $\beta$-oxidation of FFAs, gives rise to the excessive generation of mitochondrial ROS, and finally aggravates CMECs injury induced by T2DM-HFFA. On the other hand, the phosphorylation of Plin5 by ISO also promotes the hydrolysis of LDs to FFAs and the mitochondrial $\beta$-oxidation of FFAs, leading to enhanced oxidative stress and deteriorated CMECs injury. ISO: isoproterenol; LDs: lipid droplets; HFFA: hyper-free fatty acidemia; T2DM-HFFA: type 2 diabetes mellitus with hyper-free fatty acidemia; NAC: N-acetyl-cysteine; ROS: reactive oxygen species; FFAs: free fatty acids.

disorders. Moreover, we found that left ventricular diastolic function was impaired in T2DM-HFFA mice, which might may be related to the disturbance of myocardial energy supply caused by microvascular injury. Furthermore, we also found that HFFAs aggravated cell apoptosis and NO reduction induced by HG in cultured CMECs. In line with our results, Pilz et al. claimed that HFFA increased the risk of ischemic heart disease and the mortality of coronary heart disease [52, 53], and Guo et al. defined HFFA as an independent risk factor for hypertension [54]. Some studies have reported that hyperglycemia and HFFAs induce vascular endothelial cell apoptosis and reduce the synthesis and bioavailability of NO [55–57]. Thus, it is necessary to investigate the specific mechanism of CMECs injury under the condition of HG-HFFAs and explore new targets for clinical intervention.

As mainly formed by central neutral lipids and peripheral phospholipid monolayer, LDs are key regulators for lipid metabolism both in adipose tissues and nonadipose tissues [58]. As an important member of the PAT protein family on the surface of LDs, Plin5 has aroused the enthusiasm of many researchers. Plin5 can inhibit the hydrolysis of neutral lipid in LDs through interaction with lipolytic hydrolase such as hormone-sensitive triglyceride lipase (HSL), adipose triglyceride lipase (ATGL), and comparative gene identification-58 (CGI-58), thus preventing excessive generation and oxidation of FFAs [21, 59]. In our experiments, we simulated T2DM-HFFA state in vitro by giving intervention of glucose and FFAs to cultured CMECs. As last, we found that Plin5 was expressed in CMECs derived from mice. The intervention of HFFAs, but not HG, obviously increased the expression of Plin5 at the mRNA and protein levels. Consistently, many studies proved that exogenous intervention of FFAs stimulated Plin5 expression in many kinds of cultured cells [60–62], and the increase in Plin5 may be generally attributed to the activation of peroxisome proliferator-activated receptors (PPARs) [60, 63]. Some literature even claimed that high-fat diet was able to increase Plin5 expression in the liver and skeletal muscles [16, 64, 65]. It was found that Plin5 knockout could increase the content of FFAs in liver tissue of mice [16]. In our current studies of CMECs, we found that Plin5 ablation could reduce the content of LDs and increase the content of FFAs, suggesting that Plin5 plays an important role in the metabolism of LDs and FFAs in CMECs. Moreover, Plin5 knockout reduced the number of cardiac microvessels and aggravated the injury of microvascular integrity in T2DM-HFFA mice. In addition, Plin5 knockout aggravated cardiac diastolic dysfunction, but had little effects on cardiac systolic function in T2DM-HFFA mice. So, we speculate that the effects of Plin5 deletion on the number and structure of cardiac microvasculature contribute to the deterioration of diastolic dysfunction. The inconformity in changes of cardiac function may be due to differences in the severity of cardiac microvascular and myocardial damage. Consistent with our data, other studies have shown that Plin5 knockout is considered to have no effect on cardiac function in the physiological state [31, 66], but aggravate cardiac dysfunction induced by old age or ischemic stimuli in mice [14]. Furthermore, we found that Plin5 deficiency increased apoptosis rate and decreased NO synthesis in CMECs under the condition of HG-HFFAs. It is well known that eNOS plays a decisive role in the production and utilization of NO in endothelial cells. Studies have confirmed that FFAs can inhibit eNOS mRNA expression and regulate eNOS activity by increasing oxidative stress and inflammatory burden in aortic endothelial cells of rats [56]. Our study also demonstrated that Plin5 deletion reduced eNOS content in CMECs under HG-HFFAs condition, which may contributed to the reduction of NO generation. Similarly, Ibrahim

et al. proved that in patients of obesity, diabetes and nonalcoholic fatty liver, the core of lipid toxicity was the excessive decomposition of TG to FFAs and the accumulation of FFAs [67]. Therefore, Plin5 participates in the metabolism of FFAs in CMECs and its deficiency may aggravate cardiac microvascular injury induced by T2DM-HFFA. Plin5 can be used as a new indicator to predict the occurrence and development of coronary heart disease.

Interestingly, Plin5 overexpression in the heart caused severe cardiac steatosis and left ventricular hypertrophy [19, 20]. Further study found that Plin5 overexpression did not continue to inhibit LDs decomposition in myocardium, which might be associated with p-Plin5-stimulated hydrolysis of LDs under various stressful conditions [22]. Researches in various aspects showed that PAT protein family members participated in cell lipid metabolism via two states which contained nonphosphorylation and phosphorylation. Under basic conditions, Plin5 was bound to ATGL and CGI-58, respectively, to prevent the combination of this two, thus inhibiting the hydrolysis of LDs. Plin5 could also promote FFAs enter into LDs to synthesize neutral fat, thus preventing the excessive oxidation of FFAs [21]. On the other hand, adrenaline, secreted by sympathetic excitability in the case of cold, tension, fear, and so on, is able to activate PKA and increase the phosphorylation of Plin5, which may prompt the incidence of cardiovascular disease, especially in T2DM patients. When adrenergic receptors were activated, Plin5 was phosphorylated by PKA activation and promoted the hydrolysis of LDs. Catecholamine stimulation could increase the lipolysis rate by 50 times in adipose tissues [68]. In addition, p-Plin5 also participated in the transfer of FFAs to mitochondrial for $\beta$-oxidation [13, 22]. The released FFAs from LDs could also increase the transcriptional of PPARs which stimulate gene transcription related to the synthesis and oxidation of mitochondria [21, 24]. At present, there is no specific antibody to detect the phosphorylation of Plin5, but it has been reported that only p-Plin5 can enter into the nucleus to play a corresponding role [24]. Our studies revealed that, in WT group, ISO stimulation increased Plin5 expression in the nucleus. More importantly, ISO enhanced the hydrolysis of LDs, raised the intracellular level of FFAs, reduced intracellular eNOS level, and exacerbated CMECs injury induced by HG-HFFAs. It should be noted that although ISO stimulation increased intracellular FFAs levels in basic condition, it did not cause damage to CMECs which may be related to cellular self-regulation. These results indicated that ISO intervention was able to increase the phosphorylation of Plin5 in CMECs and aggravate CMECs injury induced by HG-HFFAs. In other words, these results suggested that the sympathetic excitement in T2DM-HFFA patients may give rise to functional and structural damage to the cardiac microvasculature, finally leading to sudden cardiac death. Further study of these findings may help uncover the pathological mechanism why strenuous exercise can give rise to angina or even sudden cardiac death.

However, in a study of rats, it was found that the degree in phosphorylation of Plin5 was not consistent with the hydrolysis of LDs in skeletal muscle cells [23]. Interestingly, Kuramoto et al. also proved that in fed condition, Plin5$^{-/-}$ reduced the content of FFAs in the liver, but not in the heart and soleus muscle, whereas in fasted condition, Plin5$^{-/-}$ increased FFAs content in the liver and reduced it in the heart and soleus muscle. This discrepancy may prove again that the concrete roles of Plin5 depend on the species, the tissues, and eating or not.

The generation and removal of free radicals in the body are in equilibrium under normal conditions [69]. But in the pathological condition, the production of free radicals is increased, and the ability of antioxidation in body is decreased, resulting in lipid peroxidation, protein degeneration, and DNA damage [70]. The main marker of oxidative stress is excessive ROS, which is mainly produced from mitochondria. Studies have shown that endothelial cells supply their own energy mainly through glycolysis [71], but it has been reported that endothelial cells still can carry out large amounts of mitochondrial $\beta$-oxidation for energy supply under the stimulation of acute HFFAs [17]. Thus, we believe that mitochondrial ROS produced from $\beta$-oxidation cannot be ignored in the CMECs injury of T2DM-HFFA. Consistently, our studies revealed again that increased intracellular FFAs content led to excessive production of ROS. As well known, CPT-1 is the first speed-limiting enzyme in the process of mitochondrial fatty acid oxidation, and it can catalyze the long-chain fatty acids from the cytoplasm into the mitochondria [72, 73]. In in vitro cell experiment, we found that the deletion and phosphorylation of Plin5 in CMECs increased mRNA expression of CPT-1 and raised intracellular level of ROS under the condition of HG-HFFAs. Consistently, de Barros Reis et al. reported that the increase in CPT-1 activity enhanced FFAs oxidation in islet cells [74]. Moreover, NAC intervention reduced the content of ROS, partly reversed the CMECs injury induced by the deletion and phosphorylation of Plin5. In line with our studies, many previous studies claimed that Plin5 knockout was able to increase the level of FFAs, enhance the $\beta$-oxidation of FFAs, and ultimately increase the production of ROS [14, 31]. In myocardial ischemia-reperfusion injury, it has been reported that Plin5 ablation can increase the content of ROS and malondialdehyde (MDA), but reduce the level of superoxide dismutase (SOD) [31]. Therefore, these results suggest that ROS overload derived from FFAs $\beta$-oxidation contributes to CMECs injury induced by the disruption of Plin5 balance in T2DM-HFFA.

## 5. Conclusion

HFFAs can aggravate HG-induced cardiac microvascular injury; Plin5 in CMECs plays a bidirectionally role in FFAs metabolism via the states of nonphosphorylation and phosphorylation; the deletion or the phosphorylation of Plin5 will break the balance of FFAs metabolism, result in the excessive production of FFAs and the overload of ROS, and eventually aggravate the CMECs injury induced by T2DM-HFFA. This suggests that only appropriate expression and phosphorylation of Plin5 are beneficial to energy supply and fine regulation of FFAs metabolism in CMECs. In short, our study suggests that Plin5 can guard the orderly metabolism of FFAs in CMECs in different states, and it can be explored as a new target for the prevention and treatment of microvascular complications in T2DM-HFFA.

## Abbreviations

HFFA: Hyper-free fatty academia
T2DM: Type 2 diabetes mellitus
Plin5: Perilipin 5
FFAs: Free fatty acids
CMECs: Cardiac microvascular endothelial cells
HG: High glucose
HFFAs: High FFAs
LDs: Lipid droplets
NO: Nitric oxide
ROS: Reactive oxygen species
eNOS: Endothelial nitric oxide synthase
NEFAs: Nonesterified fatty acids
CMD: Coronary microvascular diseases
TG: Triglyceride
PKA: Protein kinase A
PGC-1$\alpha$: Peroxisome proliferator-activated receptor gamma coactivator 1-$\alpha$
RNS: Reactive nitrogen species
STZ: Streptozocin
CHOL: Cholesterol
INS: Insulin
ABS: Acrylonitrile butadiene styrene
BSA: Bovine serum albumin
LVEF: Left ventricular ejection fraction
E/A: Left ventricular early mitral diastolic wave/late mitral diastolic wave
PBS: Phosphate-buffered saline
FBS: Fetal bovine serum
vWF: von Willebrand factor
ISO: Isoprenaline
LSCM: Laser confocal microscopy
ELISA: Enzyme-linked immunosorbent assay
HBSS: Hank's balanced salt solution
qRT-PCR: Quantitative real-time polymerase chain reaction.

## Data Availability

The data used to support the findings of this study are included within the article.

## Consent

The consent to participate was obtained from the participants. Written informed consent for publication of their clinical details and/or clinical images was obtained from the patient. A copy of the consent form is available for review by the editor of this journal.

## Conflicts of Interest

The authors declare that they have no competing interests.

## Authors' Contributions

Yongjian Yang and Haifeng Pei drafted the manuscript. Jin Du, Juanni Hou, and Juan Feng participated in the design of the study and performed the statistical analysis. Dachun Yang, De Li, Hong Zhou, and Heng Zhao conceived the study and participated in its design and coordination and helped to draft the manuscript. All authors read and approved the final manuscript. Jin Du and Juanni Hou equally contributed to this work.

## Acknowledgments

This work was supported by grants from the National Natural Science Foundation of China (Nos. 81970241, 81873477 and 81670419), the Science Fund for Distinguished Young Scholars of Sichuan Province (No. 2017JQ0012), and the China Postdoctoral Science Foundation (No. 2017M613429).

## Supplementary Materials

Table 1: basal physiological parameters in all kinds of mice. Plin5: perilipin 5; BW: body weight; HW: heart weight; GLU: glucose; INS: insulin; TG: triglyceride; FFAs: free fatty acids; CHOL: total cholesterol. Presented values are mean ± SEM, $n$ = 8-10/group. $^{*}P < 0.05$, $^{**}P < 0.01$ vs. WT of the same genotypes. Supplementary Figure 1: identification of cardiac microvascular endothelial cells (CMECs) and T2DM-HFFA caused damage to CMECs. (A) Cell immunofluorescence staining. DAPI: 4′,6-diamidino-2-phenylindole (blue fluorescence); CD31: (green fluorescence); vWF: von Willebrand factor (red fluorescence). (B) The apoptosis rate measured by Annexin V-FITC/PI assay kit. (C) NO generation in CMECs measured by ELISA kit. T2DM-HFFA: type 2 diabetes mellitus with hyper-free fatty acidemia; ELISA: enzyme-linked immunosorbent assay. Data are expressed as mean ± SEM, $n$ = 6-8/group. $^{\theta}P < 0.05$, $^{\theta\theta}P < 0.01$ vs. control. Supplementary Figure 2: identification of mouse genotypes. Polymerase chain reaction was used to identify WT and Plin5$^{-/-}$ mice. Supplementary Figure 3: the impact of Plin5 knockdown on the injury of CMECs induced by HG-HFFAs. (A) The apoptosis rate measured by Annexin V-FITC/PI assay kit. (B) NO generation in CMECs measured by ELISA kit. HG-HFFAs, high glucose and high free fatty acids; Scra siRNA, scrambled siRNA; ELISA, enzyme-linked immunosorbent assay. Data are expressed as mean ± SEM, $n$ = 6-8/group. $^{*}P < 0.05$ vs. HG-HFFAs of Scra siRNA. Supplementary Figure 4: the effect of Plin5 knockout on eNOS in CMECs. (A) The activity of eNOS measured by eNOS Quantitation Kit. (B) The protein level of eNOS in CMECs determined by western blot. WT, wild type; eNOS, endothelial nitric oxide synthase; HG-HFFAs, high glucose and high free fatty acids. Data are expressed as mean ± SEM, $n$ = 6-8/group. $^{**}P < 0.01$ vs. WT of normal; $^{\#\#}P < 0.01$ vs. Plin5$^{-/-}$ of normal; $^{\&}P < 0.05$ vs. WT of HG-HFFAs. Supplementary Figure 5: the effect of Plin5 phosphorylation on eNOS in CMECs. (A) The activity of eNOS measured by eNOS Quantitation Kit. (B) The protein level of eNOS in CMECs determined by western blot. Vel, vehicle; ISO, isoproterenol; eNOS, endothelial nitric oxide synthase; HG-HFFAs, high glucose and high free fatty acids. Data are expressed as mean ± SEM, $n$ = 6-8/group. $^{**}P < 0.01$ vs. Vel of normal; $^{\#\#}P < 0.01$ vs. ISO of normal; $^{\&}P < 0.05$ vs. Vel of HG-HFFAs. Supplementary Figure 6: the effect of Plin5/p-Plin5

on the mRNA expression of CPT-1 and ROS content in CMECs under the condition of HG-HFFAs. (A, B) The production of ROS in CMECs was measured by ELISA kit. (C, D) CPT-1 mRNA expression in CMECs measured by qRT-PCR. CPT-1, carnitine palmitoyltransferase I; HG-HFFAs, high glucose and high free fatty acids; NAC, N-acetylcysteine; Vel, vehicle; ISO, isoproterenol; ELISA, enzyme-linked immunosorbent assay; ROS, reactive oxygen species; qRT-PCR, quantitative real-time polymerase chain reaction. Presented values are mean ± SEM, $n = 6\text{-}8$/group. $^{**}P < 0.01$ vs. WT+Vel; $^{\#\#}P < 0.01$ vs. Plin5$^{-/-}$+Vel; $^{\&\&}P < 0.01$ vs. vehicle; $^{@@}P < 0.01$ vs. ISO. *(Supplementary Materials)*

## References


[1] S. Sharma, H. Singh, N. Ahmad, P. Mishra, and A. Tiwari, "The role of melatonin in diabetes: therapeutic implications," *Archives of Endocrinology and Metabolism*, vol. 59, no. 5, pp. 391–399, 2015.

[2] H. Zheng, J. Wu, Z. Jin, and L. J. Yan, "Potential biochemical mechanisms of lung injury in diabetes," *Aging and Disease*, vol. 8, no. 1, pp. 7–16, 2017.

[3] L. Yan, M. T. Xu, L. Yuan et al., "Prevalence of dyslipidemia and its control in type 2 diabetes: a multicenter study in endocrinology clinics of China," *Journal of Clinical Lipidology*, vol. 10, no. 1, pp. 150–160, 2016.

[4] G. Boden, "Obesity and free fatty acids," *Endocrinology and Metabolism Clinics of North America*, vol. 37, no. 3, pp. 635–646, 2008.

[5] B. M. Egan, E. L. Greene, and T. L. Goodfriend, "Nonesterified fatty acids in blood pressure control and cardiovascular complications," *Current Hypertension Reports*, vol. 3, no. 2, pp. 107–116, 2001.

[6] Y. Lee, H. Hirose, M. Ohneda, J. H. Johnson, J. D. McGarry, and R. H. Unger, "Beta-cell lipotoxicity in the pathogenesis of non-insulin-dependent diabetes mellitus of obese rats: impairment in adipocyte-beta-cell relationships," *Proceedings of the National Academy of Sciences of the United States of America*, vol. 91, no. 23, pp. 10878–10882, 1994.

[7] M. Nyberg, L. Gliemann, and Y. Hellsten, "Vascular function in health, hypertension, and diabetes: effect of physical activity on skeletal muscle microcirculation," *Scandinavian Journal of Medicine & Science in Sports*, vol. 25, Supplement 4, pp. 60–73, 2015.

[8] M. Joshi, S. R. Kotha, S. Malireddy et al., "Conundrum of pathogenesis of diabetic cardiomyopathy: role of vascular endothelial dysfunction, reactive oxygen species, and mitochondria," *Molecular and Cellular Biochemistry*, vol. 386, no. 1-2, pp. 233–249, 2014.

[9] R. S. Rosenson, P. Fioretto, and P. M. Dodson, "Does microvascular disease predict macrovascular events in type 2 diabetes?," *Atherosclerosis*, vol. 218, no. 1, pp. 13–18, 2011.

[10] D. Antoniucci, R. Valenti, A. Migliorini et al., "Direct infarct artery stenting without predilation and no-reflow in patients with acute myocardial infarction," *American Heart Journal*, vol. 142, no. 4, pp. 684–690, 2001.

[11] J. K. Zehmer, Y. Huang, G. Peng, J. Pu, R. G. W. Anderson, and P. Liu, "A role for lipid droplets in inter-membrane lipid traffic," *Proteomics*, vol. 9, no. 4, pp. 914–921, 2009.

[12] K. T. Dalen, T. Dahl, E. Holter et al., "Lsdp5 is a pat protein specifically expressed in fatty acid oxidizing tissues," *Biochimica et Biophysica Acta (BBA) - Molecular and Cell Biology of Lipids*, vol. 1771, no. 2, pp. 210–227, 2007.

[13] H. Wang, U. Sreenivasan, H. Hu et al., "Perilipin 5, a lipid droplet-associated protein, provides physical and metabolic linkage to mitochondria," *Journal of Lipid Research*, vol. 52, no. 12, pp. 2159–2168, 2011.

[14] K. Kuramoto, T. Okamura, T. Yamaguchi et al., "Perilipin 5, a lipid droplet-binding protein, protects heart from oxidative burden by sequestering fatty acid from excessive oxidation," *Journal of Biological Chemistry*, vol. 287, no. 28, pp. 23852–23863, 2012.

[15] R. R. Mason, R. Mokhtar, M. Matzaris et al., "Plin5 deletion remodels intracellular lipid composition and causes insulin resistance in muscle," *Molecular Metabolism*, vol. 3, no. 6, pp. 652–663, 2014.

[16] C. Wang, Y. Zhao, X. Gao et al., "Perilipin 5 improves hepatic lipotoxicity by inhibiting lipolysis," *Hepatology*, vol. 61, no. 3, pp. 870–882, 2015.

[17] A. Kuo, M. Y. Lee, and W. C. Sessa, "Lipid droplet biogenesis and function in the endothelium," *Circulation Research*, vol. 120, no. 8, pp. 1289–1297, 2017.

[18] P.-L. Zhou, M. Li, X.-W. Han et al., "Perilipin 5 deficiency promotes atherosclerosis progression through accelerating inflammation, apoptosis, and oxidative stress," *Journal of Cellular Biochemistry*, vol. 120, no. 11, pp. 19107–19123, 2019.

[19] H. Wang, U. Sreenivasan, D. W. Gong et al., "Cardiomyocyte-specific perilipin 5 overexpression leads to myocardial steatosis and modest cardiac dysfunction," *Journal of Lipid Research*, vol. 54, no. 4, pp. 953–965, 2013.

[20] N. M. Pollak, M. Schweiger, D. Jaeger et al., "Cardiac-specific overexpression of perilipin 5 provokes severe cardiac steatosis via the formation of a lipolytic barrier," *Journal of Lipid Research*, vol. 54, no. 4, pp. 1092–1102, 2013.

[21] R. R. Mason and M. J. Watt, "Unraveling the roles of plin5: linking cell biology to physiology," *Trends in Endocrinology and Metabolism*, vol. 26, no. 3, pp. 144–152, 2015.

[22] N. M. Pollak, D. Jaeger, S. Kolleritsch et al., "The interplay of protein kinase A and perilipin 5 regulates cardiac lipolysis," *Journal of Biological Chemistry*, vol. 290, no. 3, pp. 1295–1306, 2015.

[23] R. E. K. Macpherson, R. Vandenboom, B. D. Roy, and S. J. Peters, "Skeletal muscle plin3 and plin5 are serine phosphorylated at rest and following lipolysis during adrenergic or contractile stimulation," *Physiological Reports*, vol. 1, no. 4, article e00084, 2013.

[24] V. I. Gallardo-Montejano, G. Saxena, C. M. Kusminski et al., "Nuclear perilipin 5 integrates lipid droplet lipolysis with PGC-1α/SIRT1-dependent transcriptional regulation of mitochondrial function," *Nature Communications*, vol. 7, no. 1, article 12723, 2016.

[25] X. Gao, Y. Nan, Y. Zhao et al., "Atorvastatin reduces lipid accumulation in the liver by activating protein kinase A-mediated phosphorylation of perilipin 5," *Biochimica et Biophysica Acta (BBA) - Molecular and Cell Biology of Lipids*, vol. 1862, no. 12, pp. 1512–1519, 2017.

[26] H. Pei, Q. Yu, Q. Xue et al., "Notch1 cardioprotection in myocardial ischemia/reperfusion involves reduction of oxidative/-nitrative stress," *Basic Research in Cardiology*, vol. 108, no. 5, p. 373, 2013.

[27] A. Grindel, B. Guggenberger, L. Eichberger et al., "Oxidative stress, DNA damage and DNA repair in female patients with

diabetes mellitus type 2," *PLoS One*, vol. 11, no. 9, article e0162082, 2016.

[28] H. P. Indo, H. C. Yen, I. Nakanishi et al., "A mitochondrial superoxide theory for oxidative stress diseases and aging," *Journal of Clinical Biochemistry and Nutrition*, vol. 56, no. 1, pp. 1–7, 2015.

[29] M. F. Cury-Boaventura and R. Curi, "Regulation of reactive oxygen species (ROS) production by $C_{18}$ fatty acids in Jurkat and Raji cells," *Clinical Science*, vol. 108, no. 3, pp. 245–253, 2005.

[30] J. Kim, Y. Wei, and J. R. Sowers, "Role of mitochondrial dysfunction in insulin resistance," *Circulation Research*, vol. 102, no. 4, pp. 401–414, 2008.

[31] P. Zheng, Z. Xie, Y. Yuan et al., "Plin5 alleviates myocardial ischaemia/reperfusion injury by reducing oxidative stress through inhibiting the lipolysis of lipid droplets," *Scientific Reports*, vol. 7, no. 1, article 42574, 2017.

[32] H. Lee and Y. Lim, "Tocotrienol-rich fraction supplementation reduces hyperglycemia-induced skeletal muscle damage through regulation of insulin signaling and oxidative stress in type 2 diabetic mice," *The Journal of Nutritional Biochemistry*, vol. 57, pp. 77–85, 2018.

[33] H. T. Pham, W. Huang, C. Han et al., "Effects of Averrhoa carambola L. (Oxalidaceae) juice mediated on hyperglycemia, hyperlipidemia, and its influence on regulatory protein expression in the injured kidneys of streptozotocin-induced diabetic mice," *American Journal of Translational Research*, vol. 9, no. 1, pp. 36–49, 2017.

[34] Y. T. Zhou, P. Grayburn, A. Karim et al., "Lipotoxic heart disease in obese rats: implications for human obesity," *Proceedings of the National Academy of Sciences of the United States of America*, vol. 97, no. 4, pp. 1784–1789, 2000.

[35] J. Li, J. Gong, X. Li, L. Shen, Y. Xie, and R. Zhang, "MicroRNA-34a promotes CMECS apoptosis and upregulate inflammatory cytokines, thus worsening CMECS damage and inhibiting angiogenesis by negatively targeting the Notch signaling pathway," *Journal of Cellular Biochemistry*, vol. 120, no. 2, pp. 1598–1609, 2019.

[36] A. Pavlosky, A. Lau, Y. Su et al., "RIPK3-mediated necroptosis regulates cardiac allograft rejection," *American Journal of Transplantation*, vol. 14, no. 8, pp. 1778–1790, 2014.

[37] Y. Xue, T. Guo, L. Zou et al., "Evodiamine attenuates $P2X_7$-mediated inflammatory injury of human umbilical vein endothelial cells exposed to high free fatty acids," *Oxidative Medicine and Cellular Longevity*, vol. 2018, Article ID 5082817, 10 pages, 2018.

[38] X. Li, J. Hou, J. du et al., "Potential protective mechanism in the cardiac microvascular injury," *Hypertension*, vol. 72, no. 1, pp. 116–127, 2018.

[39] H. F. Pei, J. N. Hou, F. P. Wei et al., "Melatonin attenuates postmyocardial infarction injury via increasing Tom70 expression," *Journal of Pineal Research*, vol. 62, no. 1, 2017.

[40] Q. Xue, H. Pei, Q. Liu et al., "MICU1 protects against myocardial ischemia/reperfusion injury and its control by the importer receptor Tom70," *Cell Death & Disease*, vol. 8, no. 7, article e2923, 2017.

[41] P. Zimmet, K. G. Alberti, D. J. Magliano, and P. H. Bennett, "Diabetes mellitus statistics on prevalence and mortality: facts and fallacies," *Nature Reviews Endocrinology*, vol. 12, no. 10, pp. 616–622, 2016.

[42] T. Mazzone, "Intensive glucose lowering and cardiovascular disease prevention in diabetes: reconciling the recent clinical trial data," *Circulation*, vol. 122, no. 21, pp. 2201–2211, 2010.

[43] M. P. de Boer, R. I. Meijer, N. J. Wijnstok et al., "Microvascular dysfunction: a potential mechanism in the pathogenesis of obesity-associated insulin resistance and hypertension," *Microcirculation*, vol. 19, no. 1, pp. 5–18, 2012.

[44] A. Gupta, A. K. Gupta, and T. P. Singh, "Occurrence of complications in newly diagnosed type 2 diabetes patients: a hospital based study," *Journal of the Indian Medical Association*, vol. 111, no. 4, pp. 245–247, 2013.

[45] Y. Liu, Y. Ma, R. Wang et al., "Advanced glycation end products accelerate ischemia/reperfusion injury through receptor of advanced end product/nitrative thioredoxin inactivation in cardiac microvascular endothelial cells," *Antioxidants & Redox Signaling*, vol. 15, no. 7, pp. 1769–1778, 2011.

[46] Z. Yin, L. Fan, L. Wei et al., "FTY720 protects cardiac microvessels of diabetes: a critical role of S1P1/3 in diabetic heart disease," *PLoS One*, vol. 7, no. 8, article e42900, 2012.

[47] M. Laakso, "Heart in diabetes: a microvascular disease," *Diabetes Care*, vol. 34, Supplement 2, pp. S145–S149, 2011.

[48] A. Virdis, "Endothelial dysfunction in obesity: role of inflammation," *High Blood Pressure & Cardiovascular Prevention*, vol. 23, no. 2, pp. 83–85, 2016.

[49] D. Gao, C. Pararasa, C. R. Dunston, C. J. Bailey, and H. R. Griffiths, "Palmitate promotes monocyte atherogenicity via de novo ceramide synthesis," *Free Radical Biology & Medicine*, vol. 53, no. 4, pp. 796–806, 2012.

[50] J. R. Durrant, D. R. Seals, M. L. Connell et al., "Voluntary wheel running restores endothelial function in conduit arteries of old mice: direct evidence for reduced oxidative stress, increased superoxide dismutase activity and down-regulation of NADPH oxidase," *The Journal of Physiology*, vol. 587, no. 13, pp. 3271–3285, 2009.

[51] S. Wang, A. Ma, S. Song, Q. Quan, X. Zhao, and X. Zheng, "Fasting serum free fatty acid composition, waist/hip ratio and insulin activity in essential hypertensive patients," *Hypertension Research*, vol. 31, no. 4, pp. 623–632, 2008.

[52] S. Pilz, H. Scharnagl, B. Tiran et al., "Free fatty acids are independently associated with all-cause and cardiovascular mortality in subjects with coronary artery disease," *The Journal of Clinical Endocrinology and Metabolism*, vol. 91, no. 7, pp. 2542–2547, 2006.

[53] M. Pirro, P. Mauriège, A. Tchernof et al., "Plasma free fatty acid levels and the risk of ischemic heart disease in men: prospective results from the Québec cardiovascular study," *Atherosclerosis*, vol. 160, no. 2, pp. 377–384, 2002.

[54] S. X. Guo, Y. Z. Yan, L. T. Mu et al., "Association of serum free fatty acids with hypertension and insulin resistance among rural Uyghur adults in far western China," *International Journal of Environmental Research and Public Health*, vol. 12, no. 6, pp. 6582–6590, 2015.

[55] O. Brouwers, P. M. Niessen, G. Haenen et al., "Hyperglycaemia-induced impairment of endothelium-dependent vasorelaxation in rat mesenteric arteries is mediated by intracellular methylglyoxal levels in a pathway dependent on oxidative stress," *Diabetologia*, vol. 53, no. 5, pp. 989–1000, 2010.

[56] A. Ghosh, L. Gao, A. Thakur, P. M. Siu, and C. W. K. Lai, "Role of free fatty acids in endothelial dysfunction," *Journal of Biomedical Science*, vol. 24, no. 1, p. 50, 2017.

[57] H. Li, H. Li, Y. Bao, X. Zhang, and Y. Yu, "Free fatty acids induce endothelial dysfunction and activate protein kinase C and nuclear factor-κB pathway in rat aorta," *International Journal of Cardiology*, vol. 152, no. 2, pp. 218–224, 2011.

[58] S. D. Kohlwein, M. Veenhuis, and I. J. van der Klei, "Lipid droplets and peroxisomes: key players in cellular lipid homeostasisora matter of fat—store 'em up or burn 'em down," *Genetics*, vol. 193, no. 1, pp. 1–50, 2013.

[59] H. Wang, M. Bell, U. Sreenevasan et al., "Unique regulation of adipose triglyceride lipase (ATGL) by perilipin 5, a lipid droplet-associated protein," *Journal of Biological Chemistry*, vol. 286, no. 18, pp. 15707–15715, 2011.

[60] C. Bindesboll, O. Berg, B. Arntsen, H. I. Nebb, and K. T. Dalen, "Fatty acids regulate perilipin5 in muscle by activating PPARδ," *Journal of Lipid Research*, vol. 54, no. 7, pp. 1949–1963, 2013.

[61] E. Grasselli, A. Voci, C. Pesce et al., "Pat protein mRNA expression in primary rat hepatocytes: effects of exposure to fatty acids," *International Journal of Molecular Medicine*, vol. 25, no. 4, pp. 505–512, 2010.

[62] A. M. Hall, E. M. Brunt, Z. Chen et al., "Dynamic and differential regulation of proteins that coat lipid droplets in fatty liver dystrophic mice," *Journal of Lipid Research*, vol. 51, no. 3, pp. 554–563, 2010.

[63] H. Li, Y. Song, L. J. Zhang et al., "LSDP5 enhances triglyceride storage in hepatocytes by influencing lipolysis and fatty acid β-oxidation of lipid droplets," *PLoS One*, vol. 7, no. 6, article e36712, 2012.

[64] R. Rinnankoski-Tuikka, J. J. Hulmi, S. Torvinen et al., "Lipid droplet-associated proteins in high-fat fed mice with the effects of voluntary running and diet change," *Metabolism: Clinical and Experimental*, vol. 63, no. 8, pp. 1031–1040, 2014.

[65] P. M. Badin, I. K. Vila, K. Louche et al., "High-fat diet-mediated lipotoxicity and insulin resistance is related to impaired lipase expression in mouse skeletal muscle," *Endocrinology*, vol. 154, no. 4, pp. 1444–1453, 2013.

[66] K. Kuramoto, F. Sakai, N. Yoshinori et al., "Deficiency of a lipid droplet protein, perilipin 5, suppresses myocardial lipid accumulation, thereby preventing type 1 diabetes-induced heart malfunction," *Molecular and Cellular Biology*, vol. 34, no. 14, pp. 2721–2731, 2014.

[67] S. H. Ibrahim, R. Kohli, and G. J. Gores, "Mechanisms of lipotoxicity in NAFLD and clinical implications," *Journal of Pediatric Gastroenterology and Nutrition*, vol. 53, no. 2, pp. 131–140, 2011.

[68] S. Viswanadha and C. Londos, "Determination of lipolysis in isolated primary adipocytes," *Methods in Molecular Biology*, vol. 456, pp. 299–306, 2008.

[69] B. D'Autreaux and M. B. Toledano, "ROS as signalling molecules: mechanisms that generate specificity in ROS homeostasis," *Nature Reviews Molecular Cell Biology*, vol. 8, no. 10, pp. 813–824, 2007.

[70] G. Bellomo, "Cell damage by oxygen free radicals," *Cytotechnology*, vol. 5, Supplement 1, pp. 71–73, 1991.

[71] O. Culic, M. L. Gruwel, and J. Schrader, "Energy turnover of vascular endothelial cells," *American Journal of Physiology-Cell Physiology*, vol. 273, no. 1, pp. C205–C213, 1997.

[72] J. Kerner and C. Hoppel, "Fatty acid import into mitochondria," *Biochimica et Biophysica Acta (BBA) - Molecular and Cell Biology of Lipids*, vol. 1486, no. 1, pp. 1–17, 2000.

[73] J. D. McGarry and N. F. Brown, "The mitochondrial carnitine palmitoyltransferase system — from concept to molecular analysis," *European Journal of Biochemistry*, vol. 244, no. 1, pp. 1–14, 1997.

[74] M. A. de Barros Reis, V. C. Arantes, D. A. Cunha et al., "Increased L-CPT-1 activity and altered gene expression in pancreatic islets of malnourished adult rats: a possible relationship between elevated free fatty acid levels and impaired insulin secretion," *The Journal of Nutritional Biochemistry*, vol. 19, no. 2, pp. 85–90, 2008.